

ENGINEERED SAFETY FEATURES

6.1 ENGINEERED SAFETY FEATURE MATERIALS

Materials used in the engineered safety feature (ESF) components have been evaluated to ensure that material interactions do not occur which could potentially impair operation of the ESF. Materials have been selected to withstand the environmental conditions encountered during normal operation and postulated accidents.

6.1.1 Metallic Materials

6.1.1.1 Material Selection and Fabrication

6.1.1.1.1 Specifications for Principal ESF Pressure-Retaining Materials

Table 5.2-3 lists the principal pressure retaining materials and the appropriate material specifications for the reactor coolant pressure boundary (RCPB) components. Tables 6.1-1 and 6.1-2 list the principal pressure retaining materials and the appropriate material specifications for the ESFs of the plant.

6.1.1.1.2 ESF Construction Material

All ESF materials are resistant to intergranular stress corrosion cracking (IGSCC) in the atmosphere of the BWR coolant. Piping that may have been susceptible to IGSCC is constructed either from carbon steel or solution heat treated low carbon stainless steel. The injection line for standby liquid control (SLC) and core spray piping from the nozzles to the spargers in the reactor is made from either Type 304L or Type 316L stainless steel. The core spray spargers are Type 304 stainless steel, since the normal operational stress levels are low. The suction lines for the emergency core cooling system (ECCS) and the reactor core isolation cooling (RCIC) system in the suppression pool and in the condensate storage tank are Type 304 stainless steel. However, the operating temperature in the suppression pool and in the condensate storage tank is below 200°F; therefore, these lines are not susceptible to IGSCC.

A conservative corrosion allowance of at least 0.08 in is provided for all exposed surfaces of carbon steel piping. General corrosion on stainless steel is negligible.

Demineralized water, with no additives, is employed in the core cooling water. Following a LOCA, this demineralized water has no detrimental effect on any of the ESF materials.

6.1.1.1.3 Integrity of ESF Components During Manufacturing and Construction

6.1.1.1.3.1 Control of Sensitized Stainless Steel

Controls applied to NSSS supplied ESF components to avoid severe sensitization are the same as the controls applied to RCPB components and are discussed in Section 5.2.3.4. An assessment of compliance with Regulatory Guide 1.44 for the NSSS supplied ESF components may also be found in Section 5.2.3.4.

All non-NSSS supplied ESF components comply with the recommendations of Regulatory Guide 1.44 with the following clarification.

All welding performed on austenitic stainless steel was done to minimize sensitization; however, intergranular corrosion tests have not been performed because of employment of low carbon stainless steel grade or restricted use of Type 304 stainless steel to low temperature piping.

Since severe sensitization is either avoided or material use is restricted by the previously listed safeguards, testing to determine susceptibility to intergranular attack is not performed. Refer to Section 1.8 for the RBS position on Regulatory Guide 1.44.

6.1.1.1.3.2 Cleaning and Contamination Protection Procedures

Specifications for ESF piping and components specify requirements for cleanliness and contamination protection during fabrication, shipment, and storage in the construction phase as recommended by Regulatory Guide 1.44.

Contamination of austenitic stainless steels by compounds that can alter the physical or metallurgical structure and/or properties of the material are controlled or avoided during all stages of fabrication. Painting of stainless steels is prohibited. Grinding is accomplished with wheels that have not previously been used on materials other than stainless steel.

Internal surfaces of completed components are cleaned to produce an item that is clean to the extent that grit, scale, corrosion products, grease, oil, wax, gum, adhered or embedded dirt, or extraneous material are not visible to the unaided eye.

Cleaning agents and demineralized rinse water in contact with austenitic stainless steel contain less than 1 ppm chlorides.

Onsite and preoperational cleaning of ESF components are in accordance with the RBS position on Regulatory Guide 1.37. Refer to Section 1.8 for the position on this regulatory guide.

6.1.1.1.3.3 Cold-Worked Stainless Steel

Austenitic stainless steel with a yield strength greater than 90,000 psi is not used in ESF systems. Cold bending of 2 in and smaller pipe which operates at 200°F and above is allowed using bend radii intended to produce controlled amounts of strain and maintain the yield strength at less than 90,000 psi.

6.1.1.1.3.4 Nonmetallic Insulation

Non-metallic insulation materials in ESF systems comply with Regulatory Guide 1.36 and have the proper ratio of leachable sodium plus silicate ions to leachable chloride plus fluoride ions. Refer to Section 1.8 for the RBS position on this regulatory guide.

6.1.1.1.4 Weld Fabrication and Assembly of Stainless Steel
ESF Components

The recommendations of Regulatory Guide 1.31 for stainless steel filler metal have been followed. Refer to Section 1.8 for the RBS position on Regulatory Guide 1.31.

6.1.1.2 Composition, Compatibility, and Stability of
Containment and Core Spray Coolants

River Bend Station does not employ containment sprays. Demineralized water, with no additives, is employed in the core cooling water and the suppression pool water. The demineralized water maintains a uniform pH during an accident since no additives are introduced into the containment or into systems communicating with the containment. No detrimental effects occur on any of the ESF materials from this demineralized water. In addition, following an accident the containment and drywell atmospheres are maintained below 4 percent (by volume) hydrogen in accordance with Regulatory Guide 1.7.

●→8

6.1.1.3 Austenitic Stainless Steel Piping Welds Sensitive
to IGSCC

Ultrasonic ISI examination of welds in austenitic piping systems that are potentially "service sensitive" to IGSCC are performed in compliance with the requirements of ASME Sections V and XI, along with the recommendations addressed in NRC Generic Letter 88-01. Further guidance for IGSCC related welds are addressed in Section 5.2.4 of the USAR.

8←●

6.1.2 Organic Materials

6.1.2.1 Protective Coatings

All protective coatings used within the primary containment and their approximate quantities are identified in Table 6.1-3. These coatings have been tested to demonstrate that they remain intact on the surface to which they are applied during postulated LOCA conditions. Tests are performed in accordance with Section 4 of ANSI N101.2, Protective Coatings for Light Water Nuclear Reactor Containment Facilities, to meet or exceed the DBA conditions described in Section 6.2.

6.1.2.2 Compliance with Regulatory Guide 1.54

This guide states that ANSI N101.4-1972, in conjunction with ANSI N45.2-1971, provides an adequate basis for complying with quality assurance requirements for protective coatings applied to ferritic steels, aluminum, stainless steel, galvanized steel, concrete, and masonry.

Coatings for NSSS equipment are specified to meet the requirements of this regulatory guide and are qualified using the standard ANSI tests. However, because of the impracticality of using these special coatings on all equipment, certain exemptions are allowed. These exemptions are restricted to small size equipment where, in case of a LOCA, the paint debris would in no way be a safety hazard. Exemptions are for such items as electrical/electronic trim, solenoid valve covers, face plates, valve handles, small size pipe whip restraints, etc. Quality assurance program recommendations stated in Regulatory Guide 1.54 are followed for all non-NSSS supplied major equipment and structures, except for the inspection defined in Section 6.2.4 of ANSI N101.4-1972. Inspection is in accordance with ANSI N5.12-1974, Section 10, "Inspection for Shop and Field Work." The total area coated in accordance with the regulatory guide includes approximately 310,000 sq ft of carbon steel surface and 75,000 sq ft of concrete surface. Miscellaneous coatings applied on electrical equipment, cabinetry, control panels, emergency light cases, and loudspeakers do not meet Regulatory Guide 1.54 recommendations. The surface area covered by such coatings is small as suggested by their volume, as given in Table 6.1-3. Most of these equipment items with miscellaneous coatings are located outside the drywell where LOCA conditions are not severe and, therefore, they are not likely to break down. Also, the total volume of these miscellaneous coatings is so insignificant that if they break down during a LOCA they do not have any adverse effects on the functioning of safety-related equipment. The RBS position on Regulatory Guide 1.54 is given in Section 1.8.

7←• •→8

Miscellaneous site applied and vendor supplied coatings added inside containment after construction are exempt from Regulatory Guide 1.54 requirements. These miscellaneous coatings are applied on piping, structural steel, electrical cabinets, control panels, valve handles, transmitters, and other small equipment. This exemption is limited to small surface areas, and any post LOCA paint debris would have no adverse effects on any safety related equipment.

8←•

6.1.2.3 Other Organic Materials Used in the Primary Containment

Table 6.1-4 gives other organic materials used in the primary containment and their approximate quantities. Further information on electrical cable insulation is provided in Table 6.1-5. These materials have been selected because they have adequate resistance to anticipated radiation exposure and there is no significant degradation of their properties under a normal operating environment as well as under a LOCA environment.

6.2 CONTAINMENT SYSTEMS

●→14

The containment systems include the primary containment (Section 6.2.1), containment heat removal systems (Section 6.2.2), secondary containment and the Fuel Building (Section 6.2.3), containment isolation system (Section 6.2.4), combustible gas control system (Section 6.2.5), and the containment leakage testing system (Section 6.2.6).

14←●

This section provides the design bases, features, and evaluations necessary to demonstrate that the above systems can function within the specified limits throughout the operating lifetime of the plant.

6.2.1 Containment Functional Design

6.2.1.1 Pressure Suppression Containment

The Mark III pressure suppression containment system consists of a drywell, a vapor suppression pool, and a primary containment building. The reinforced concrete cylindrical drywell structure houses the reactor system. The cylindrical, freestanding steel primary containment structure encloses the drywell and the suppression pool which fills the bottom 20 ft of the annular volume outside the drywell. A cylindrical weir wall inside the drywell forms the inner boundary of the suppression pool. A system of submerged horizontal vent openings in the lower portion of the drywell wall are incorporated to direct steam to the suppression pool where condensation (vapor suppression) occurs if a pipe ruptures within the drywell.

6.2.1.1.1 Design Bases

To ensure that the containment system serves its intended function of limiting the release of radioactive fission products to the environment after a LOCA, the following design bases have been employed:

1. The drywell and containment structures have the capability to maintain functional integrity during and following the peak transient pressures and temperatures which result from any loss-of-coolant accident (LOCA). The LOCA analyses which determine the peak transient pressures and temperatures for design assume the most limiting single failure (with regard to containment response) in addition to the pipe break plus the simultaneous occurrence of the safe shutdown earthquake (SSE) and loss of offsite power.

The design basis LOCA analyses are summarized as follows:

•→14

- a. Drywell Internal (Positive) Pressure - The design basis accident (DBA) which gives the maximum calculated internal drywell pressure differential of 20.5 psid (20.7 psid considering the Technical Specification allowable initial conditions) is a main steam line double-ended-rupture (DER) upstream of the first main steam isolation valve. The drywell design internal pressure differential of 25 psid provides a 22 percent margin (21 percent for Technical Specification allowable initial conditions) above the calculated peak value. A detailed discussion of this DBA is contained in Section 6.2.1.1.3.1.4.
- b. Drywell External (Negative) Pressure - The design basis is a bounding calculation of the maximum theoretical external pressure differential -19.4 psid (-19.9 psid considering the Technical Specification allowable initial conditions) as described in Section 6.2.1.1.3.3.1. The drywell design external pressure differential is -20.0 psid.
- c. Containment Internal Pressure - The maximum calculated wetwell (region below HCU floor) internal pressure of 7.9 psig (9.3 psig considering Technical Specification allowable initial conditions) occurs in the short term after a LOCA. The above result is quoted from the short term response to a main steam line DER. For this parameter a margin of 90 percent exists with respect to the design containment internal pressure of 15.0 psig (61 percent margin for Technical Specification initial conditions). The maximum long-term containment pressure of 3.6 psig (5.0 psig considering Technical Specification allowable conditions) is relatively insensitive to the pipe break or location. The detailed discussion of this design parameter is contained in Section 6.2.1.1.3.1.4.

14←•

- d. Containment External Pressure - The design basis event for the external (negative) pressure differential across the containment wall is the accidental cooldown of the containment atmosphere by one unit cooler

under normal operating minimum heat load conditions and with chilled water supplied to the cooler at the minimum temperature of 57°F. This event results in a maximum external pressure differential of -0.43 psid which provides a 40 percent margin with respect to the containment design external pressure differential of -0.6 psid. Further description of this analysis is found in Section 6.2.1.1.3.3.2.

- e. Drywell Temperature - The design basis for drywell atmosphere temperature is a small steam line break assuming no heat transfer to the passive steel and concrete heat sinks in the drywell. This gives a peak calculated drywell temperature of 330°F. Considering the extreme conservatisms assumed, the drywell design temperature was specified to be 330°F. Details of this analysis are provided in Section 6.2.1.1.3.1.7.4.

●→14

- f. Containment Temperature - The peak calculated containment atmosphere temperature of 124°F results from the long term addition of energy to the atmosphere. This long term result is dependent on peak from the suppression pool following a LOCA. suppression pool temperature and is relatively independent of pipe break size. However, the above result is quoted from the long term response to a recirculation pump suction line DER and provides a 61°F margin with respect to the 185°F design value. Section 6.2.1.1.3.1.4.2 gives a detailed discussion of long term accident response for the main steam line break. The long term containment temperature response of the recirculation line break is similar.

14←●

- 2. The design bases for subcompartments within the containment and drywell are given in Section 6.2.1.2.
- 3. The sources of mass and energy considered available for release to the containment (drywell) following any LOCA are:
 - a. The energy stored in the reactor coolant system fluid inventory within the drywell

- b. Decay heat
- c. Fission power coastdown energy
- d. Stored heat in the reactor coolant system metal piping, structures, and core
- e. Metal-water reaction energy
- f. Emergency core cooling system (ECCS) pump heat.

The amounts and post accident time dependence of the mass and energy releases from these sources are addressed in Section 6.2.1.1.3.1.3.

- 4. Energy is removed from the containment after a LOCA by the residual heat removal (RHR) system in the suppression pool cooling mode of operation and by the containment unit coolers of the containment ventilation system. Both systems transfer energy to the standby service water system. The suppression pool cooling mode of the RHR system is designed to limit peak suppression pool temperature after a LOCA to less than 185°F. The containment unit coolers are designed to handle normal plant operating heat loads. The purpose for the system being an ESF is to assist the RHR system in removing heat from the containment for various accidents. Sections 6.2.1.1.3.4 and 6.2.2 describe these engineered safety features in more detail.
- 5. The capability for post-LOCA drywell and containment pressure reduction is not impaired by any single failure. In the short term after a large break LOCA, drywell pressure peaks and is reduced as a result of vent clearing and steam condensation in the suppression pool. In the long term, drywell and containment pressures are reduced by the active containment heat removal systems described above. Each of these systems consists of two independent 100-percent capacity subsystems powered from separate emergency buses so that a single failure does not result in the loss of function of either system. Additional long term pressure reduction capability is afforded by the passive heat sinks (structures) which absorb heat from the drywell and containment atmospheres and from the suppression pool after a LOCA.

6. The capability for post-accident energy removal from the containment under various postulated single failure conditions is mentioned in Item 5 and is discussed in more detail in Section 6.2.2.
7. The containment system is designed to limit fission product leakage following the design basis LOCA. The offsite dose evaluation is based on constant containment leakage at the design rate for the assumed 30-day duration of the accident. No credit is taken for containment depressurization. Therefore, the containment system is not designed for a specific containment depressurization rate. Analyses described in Chapter 15 demonstrate that offsite doses are less than those allowed under 10CFR150.67. [Amendment 132 revised the design basis accident offsite dose limit requirements from 10CFR100 to 10CFR50.67.](#) Leak detection is discussed in Sections 5.2.5 and 7.6.1.2.
8. The containment system is protected from, or designed to withstand, missiles from internal or external sources and excessive motion of pipes which could directly or indirectly endanger containment integrity.
9. The drywell and containment have the capability to withstand jet forces associated with the flow from the postulated rupture of any pipe within them.
10. The containment system is designed to allow for periodically conducted tests at the peak pressure calculated to result from the postulated DBA in order to confirm the leaktight integrity of the containment and its penetrations.
11. The capability for rapid closure or isolation of all pipes or ducts which penetrate the containment is provided (Section 6.2.4) to maintain leakage within permissible limits.
12. The containment system is designed to permit removal of fuel assemblies from the reactor core after a LOCA.

6.2.1.1.2 Design Features

The primary containment system is of the pressure suppression type (Fig. 3.8-1). The primary containment consists of a drywell, a steel containment structure which surrounds the drywell and acts as a pressure suppression chamber through use of a suppression pool which fills the

bottom of the containment, and a connecting vent system for steam flow from the drywell to the suppression pool.

The primary containment system design parameters are given in Table 6.2-1. The drywell and containment volumes were selected on the basis of space required for equipment. The selection of design pressures and temperatures is discussed in Section 6.2.1.1.3, and the design loading considerations are given in Section 3.8. The safety analysis demonstrating primary containment system effectiveness as a radiological barrier is presented in Chapter 15.

The drywell is a 69 ft ID cylindrical reinforced concrete structure surrounding the reactor, the two recirculation loops, and other branch connections of the reactor coolant system. A 64 ft OD cylindrical weir wall, 21.25 ft high and concentric with the lower portion of the drywell wall, forms the inner boundary of the suppression pool. Water in the 30-in annulus between the weir wall and the drywell wall is connected to the main body of the suppression pool by horizontal vent pipes directed radially through the lower portion of the drywell wall. The vents, each 27.5 in ID, are spaced uniformly around the drywell circumference at three elevations. There are 43 vents in each of 3 rows for a total of 129 vents.

The primary containment structure is a free-standing steel cylinder with a torispherical dome, concentric with and outside the drywell. It serves both as a suppression chamber and as a leaktight vapor barrier to protect against release of fission products in the unlikely event of a LOCA. The design leak rate of the freestanding steel containment is 0.325 percent of the total contained free volume per day at the calculated peak containment pressure resulting from the postulated DBA.

The main portion of the suppression pool volume is in the bottom of the containment between the outer surface of the drywell wall and the inner surface of the steel containment structure. Water in the horizontal vents and in the drywell-weir annulus is also part of the total suppression pool volume. The pool functions both as a heat sink for operational transients and postulated accidents and as a reservoir for the ECCS (Section 6.3). Any operational transient which opens the safety/relief valves transfers energy to the suppression pool by means of discharge piping.

The containment structure, internal structures, and engineered safety feature systems are protected from loss of safety function due to the dynamic effects of postulated

accidents. Containment design has provided separation and inclusion of barriers and restraints when required to protect essential structures and safe-shutdown systems and components from internally generated missiles, pipe whip, and jet impingement forces. The detailed criteria, locations, and descriptions of devices used for protection are given in Sections 3.5 and 3.6.

Provision for redundancy and independence of containment system components other than structures are described in the following sections:

- 6.2.2 Containment Heat Removal Systems
- 14
- 6.2.3 Secondary Containment and Fuel Building Functional Design
- 6.2.4 Containment Isolation System
- 6.2.5 Combustible Gas Control in Containment.

Codes and standards applied to the design, fabrication, and erection of the containment and internal structures are discussed in Section 3.8.2.2 for the containment and in Section 3.8.3.2 for the internal structures. Section 3.8.4.2 lists the codes and standards applicable in Section 3.8.3.2. In each case, the codes and standards used are consistent with the equipment safety function.

•→15

Differential pressure transmitters between the shield building annulus and the containment automatically isolate the containment unit coolers and the containment purge exhaust isolation valves (AOV 128 and AOV 166) when containment pressure is reduced to the value of -12 in W.G. This fully redundant, engineered safety feature instrumentation system ensures against the loss of containment integrity due to external pressure loads resulting from inadvertent operation of the containment unit coolers or the containment purge system.

15←•

In the short term after a LOCA, approximately 20,353 cu ft of water accumulates on the drywell floor until the water level reaches the top of the weir wall. The associated short term reduction in suppression pool level is accounted for in the design of the engineered safety feature systems. Water subsequently overflows the weir wall, completing the flow path back to the suppression pool for the long term recirculation phase of the transient. Water does not accumulate in the containment subcompartments because the River Bend Station design does not incorporate a containment spray system to discharge water in the upper regions of the containment.

14←•

●→14

Pressure, temperature, and relative humidity conditions are maintained within design ranges by the containment and drywell ventilation systems described in Sections 9.4.5 and 9.4.6. Both systems function during normal plant operating modes and following a loss of offsite power. The containment ventilation system is an engineered safety feature which also functions after a LOCA, as described in Section 6.2.2.

The containment and drywell purge system (Section 9.4.6) exhausts air from the containment and drywell through the standby gas treatment system (Section 6.2.3).

Materials compatibility considerations are discussed in Section 6.1.

6.2.1.1.3 Design Evaluation

The key design parameters and maximum calculated accident parameters for the pressure suppression containment are listed in Tables 6.2-1, 6.2-2, and 6.2-7.

These parameters are not determined from a single accident event but from an envelope of accident conditions. Therefore, there is no single DBA for the containment system.

Drywell and containment internal design pressures and temperatures are based on the results of an analysis of a spectrum of pipe breaks in the drywell. The maximum drywell pressure occurs during the blowdown phase of a main steam line DER. The most severe drywell temperature condition (peak temperature and duration) occurs for a small steam line break. The maximum long term containment (region above HCU floor) pressure and temperature are approximately the same for all break sizes.

In addition to the LOCA analyses, the pressure suppression containment system has been evaluated for the rupture of unguarded high energy lines in the containment, external pressure, steam bypass of the suppression pool, suppression pool dynamic loads, and asymmetric loads. Each of these aspects of the design evaluation are discussed in detail in the following sections.

6.2.1.1.3.1 Accident Response Analyses

The response of the pressure suppression containment system to postulated pipe breaks in the drywell is analyzed with the M3CPT and SHEX computer programs. These programs, described in

14←●

Section 6.2.1.1.3.7.1, models the reactor system, drywell, vent system, suppression pool, containment, and active and passive heat removal systems.

●→14

The primary results of the accident analyses consist of the transient pressure and temperature responses of the drywell and containment atmospheres and the transient temperature response of the suppression pool.

The analyses assume instantaneous pipe ruptures at worst case initial conditions concurrent with the loss of offsite power. The worst case single active component failure is the failure of one of the two standby diesel generators resulting in minimum containment heat removal capability. This single failure is assumed in all cases.

6.2.1.1.3.1.1 Break Spectrum

To ensure that the containment system design parameters are not exceeded for pipe breaks smaller than the DER of the largest primary system pipe, a spectrum of break sizes are analyzed. The following breaks are considered:

1. An instantaneous guillotine DER of a main steam line
2. An instantaneous guillotine DER of a recirculation pump suction line
3. An intermediate size liquid line rupture
4. A small size steam line rupture.

6.2.1.1.3.1.2 Initial Conditions

The accident response analyses assume that the drywell and containment are initially at the normal operating conditions of pressure, temperature, and relative humidity specified in Table 6.2-3. Parametric studies of these initial conditions over the expected ranges established the Technical Specification allowable values which are presented in Table 6.2-3a.

The peak drywell differential pressure is limited to 20.7 psid to maintain a 21 percent margin relative to the 25 psid design for all combinations of initial pressure, temperature, and humidity (dew point temperature) within the Technical Specification allowable ranges. The specific set of initial conditions which yield the peak differential pressure of 20.7 psid are summarized as follows:

14←●

	<u>Drywell</u>	<u>Containment</u>
Pressure	0.0 psig	+0.3 psig
Temperature	100°F	100°F
Dew Point Temperature	60°F	60°F

•→14

The limiting combination of Technical Specification allowable initial conditions which produce the maximum long-term containment peak pressure of 5.0 psig are:

14←•

	<u>Drywell</u>	<u>Containment</u>
Pressure	1.5 psig	0.3 psig
Temperature	100°F	70°F
Dew Point Temperature	60°F	60°F

The initial temperature of the suppression pool is also assumed to be the maximum normal operating value in order to maximize the suppression pool temperature and containment pressure transients. Similarly, the temperature of the standby service water, which ultimately removes energy from the containment via the RHR heat exchangers and containment unit coolers, is assumed to be the design maximum value throughout the transients.

The reactor is assumed to be operating at 102 percent of rated thermal power just prior to the postulated pipe break accidents. The initial reactor coolant system fluid inventory, pressure, and temperature given in Table 6.2-3 correspond to this power level.

6.2.1.1.3.1.3 Energy Sources

All major sources of energy are considered in the calculation of the mass and energy release to the containment system from each postulated pipe break. The sources of available energy include the following:

1. Stored energy in the reactor coolant system
2. Fission product and heavy element decay heat⁽¹²⁾
3. Fission power coastdown energy
4. Stored energy in the reactor coolant system metal piping, structures, and core
5. Metal-water reaction energy
6. ECCS pump heat.

A description of the models used for the addition of energy from these sources to the reactor coolant is provided in Section 6.2.1.1.3.7.1. The time dependent rates of energy addition to the coolant following a main steam line DER are summarized on Fig. 6.2-11 through 6.2-15.

Reactor feedwater flow is assumed to stop instantaneously at the time of the pipe break for short term analyses of peak drywell pressure. This assumption is conservative in this case because feedwater flow tends to depressurize the reactor pressure vessel, thereby reducing the discharge of steam and water into the drywell.

•→14

For long term effects, such as peak suppression pool temperature and containment pressure, feedwater flow is assumed to continue at the design rate until the conservative inventory of feedwater system mass and energy which maximizes the suppression pool temperature has been added to the reactor.

14←•

6.2.1.1.3.1.4 Main Steam Line Break

The instantaneous DER of a main steam line between the reactor pressure vessel and the flow restrictor results in the maximum discharge of primary system fluid and energy to the drywell. This in turn results in the maximum drywell internal pressure differential.

6.2.1.1.3.1.4.1 Break Area and Mass Energy Release Assumptions

•→14

Fig. 6.2-1 shows the location of the main steam line break. Immediately after the break occurs, the flow from both sides of the break accelerates to the critical flow rate determined by using the Moody flow model with the conservative assumption of zero friction⁽²⁾. The flow from the reactor pressure vessel side of the break is critical in the 2.55-sq ft area main steam line nozzle. Blowdown through the other end of the break occurs because the main steam lines are interconnected upstream of the turbine by the main steam header. This interconnection allows reactor coolant to pass from the three unbroken main steam lines through the header and back into the drywell via the broken line. After the steam inventory in the broken line up to the flow restrictor is discharged, flow from the main steam header is limited to critical flow in the 11.15-in diameter throat of the flow restrictor. Tables 6.2-4 and 6.2-4a summarize the blowdown mass flow rate, the corresponding enthalpy, and the reactor coolant system pressure versus time for the main steam line

14←•

●→14

break with and without the addition of feedwater, respectively. The long-term (with feedwater) blowdown mass flow rate transient is also shown graphically on Figs. 6.2-9a and 6.2-9b.

14←●

The decrease in steam pressure at the turbine inlet initiates closure of the main steam isolation valves within approximately 200 ms after the break occurs (Section 7.3.1.1.2). Also, main steam isolation valve closure signals are generated as the differential pressures across the main steam line flow restrictors increase above isolation set points. The instruments sensing flow restrictor differential pressures generate isolation signals within approximately 0.500 sec after the break occurs.

A reactor scram is initiated as the main steam isolation valves begin to close (Section 7.2.1.1). In addition to the scram initiated from main steam isolation valve closure, voids generated in the reactor coolant during depressurization contribute significant negative reactivity to the core even before the scram is complete.

●→14

After 4.5 sec, the main steam isolation valves in the broken line have closed sufficiently such that the MSIV flow area equals the flow restrictor area. At that time, the critical flow location changes from the flow restrictor to the main steam isolation valve. Subsequent closure of the MSIVs in the broken line terminates flow from this side of the break at 5.5 sec after the postulated failure of the main steam line. Fig. 6.2-2 shows the total effective break area transient.

14←● ●→7

The closing time of the main steam isolation valves is adjustable between 3 and 10 sec by means of a hydraulic control valve. A particular closing time requires the adjustment of the hydraulic control valve and an actual measurement of the valve closure time. The MSIVs are equipped with limit switches at 15 and 90 percent of valve travel, and thus afford a means of accurately measuring the closing time during actuation of the valve. The installed valves are set at cold conditions. Field tests conducted on installed MSIVs, with closing times adjusted from 3 to 5 sec, indicate that the deviation in closing time for a given valve is approximately 1/2 sec or less. MSIVs are therefore adjusted to close in 3.5 to 4.5 sec to ensure a valve closure time of between 3 and 5 seconds.

7←●

Immediately following the break, the steam flow rate leaving the vessel exceeds the steam generation rate in the core. This mismatch causes a depressurization of the reactor

vessel, and the resultant formation of steam bubbles within the reactor vessel liquid causes a rapid rise in water level. When the froth level reaches the vessel steam nozzles and the top of the steam dryers, flow out of the break changes from steam to a two-phase mixture. The two-phase critical flow rates are determined from the Moody model⁽²⁾ with the known values of vessel pressure and mixture enthalpy.

At the time two-phase blowdown starts, the drywell contains superheated steam and air. If instantaneous and complete mixing between the steam, air, and two-phase mixture is assumed, drywell temperature and pressure decrease. This decrease results from heat being transferred from the high temperature steam and air to evaporate the liquid phase of the blowdown. For the sake of conservatism, the assumption of instantaneous homogenous mixing in the drywell is modified for a period immediately following the start of two-phase flow until after peak drywell pressure and temperature occur (except for vent flow calculations where, again to be conservative, a homogenous drywell mixture is always assumed). During this period, it is assumed that the blowdown depressurizes to the drywell total pressure, i.e., pressure flash. The blowdown steam and the steam resulting from the decompressing liquid mix uniformly with drywell air and superheated steam. The unflashed liquid portion of the two-phase blowdown falls to the drywell floor.

6.2.1.1.3.1.4.2 Containment System Response

●→14

Fig. 6.2-4 shows the drywell and containment pressure response for a main steam line DER and Fig. 6.2-6 shows the drywell and containment temperature response for a main steam line DER. A summary of the accident sequence of events is provided in Table 6.2-10. The short-term response (0 - 30 seconds) is calculated with the GE M3CPT computer code. The long-term response is calculated with the GE SHEX computer code. The following paragraphs describe the containment response for the limiting case single active failure of a standby diesel generator unit which results in the minimum, long term containment heat removal capability.

After a main steam line DER, the drywell pressure begins to rise and the water level in the drywell-weir annulus is accelerated downward. At 0.92 sec, the top row of vents clears and a mixture of air, water vapor and entrained liquid is thereby permitted to enter the containment side of the suppression pool. Flow rate through the vents is determined with a homogeneous flow model⁽¹⁾.

At 1.0 sec, the froth level in the reactor vessel reaches the top of the steam dryers, and flow from the break changes
14←●

●→14

to a two-phase mixture. The middle row of vents clears at 1.23 sec, causing the drywell pressure to peak at 20.5 psig. At this time, the drywell internal pressure differential also peaks at 20.5 psid, which is well within the design value of 25 psid (22 percent margin). The bottom row of vents clears at 1.64 sec.

As air flows through the vents into the suppression pool, a bubble is formed at the vent exit. As the bubble grows, it forces the suppression pool to swell upward in a bulk mode, compressing the air above the suppression pool. This air escapes to the upper containment atmosphere by flowing through openings in the hydraulic control unit (HCU) floor (el 114 ft). Due to buoyancy, the bubble rises faster than the suppression pool, breaking through the surface at 1.36 sec. Thereafter, the flow through the HCU floor openings is a mixture of suppression pool liquid and air.

The flow restriction created by the HCU floor causes the vent back-pressure and consequently the drywell pressure to increase. The drywell pressure has a second lesser peak at 1.7 sec and at a value of 20.4 psig. The wetwell (space below HCU floor) pressure reaches a peak of 7.9 psig at 2.47 sec. The maximum calculated pressure differential across the HCU floor is 6.3 psid.

Closure of the MSIV starts to restrict blowdown flow from the main steam header at 4.5. The MSIVs are assumed to close completely at 5.5 sec. As the blowdown proceeds, the reactor coolant system pressure and fluid inventory decrease, resulting in reduced break flow rates. Consequently, the flow rate in the vent system and the pressure differential between the drywell and the containment begin to decrease.

The decrease in drywell - to - containment pressure difference allows the water level in the weir annulus to recover. By 671 seconds all three rows of vents are recovered.

●→13

The high pressure core spray (HPCS) diesel generator unit reaches operating speed and can accept load 13 sec after the accident, and the HPCS pump, which it powers, can pump effectively 14 sec later. Thus, at 27 sec after the accident, water from the suppression pool is sprayed onto the core. At approximately 288 sec, the reactor coolant system pressure has decreased to the drywell pressure, and reactor blowdown is ended.

13←● 14←●

●→14

Emergency injection of suppression pool water into the reactor continues, and at 492 sec the vessel is reflooded to the level of the main steam line nozzles. This ECCS water is heated by decay heat and reactor stored heat to a temperature that is below the saturation temperature of the drywell; i.e., the water is subcooled and thus no steam is formed. After reflood, the subcooled ECCS flow spills from the break onto the drywell floor.

For the long-term analysis, concrete and steel heat sinks are used in SHEX. The sinks cool the drywell by condensation of steam and a slow depressurization results. Reduction of drywell pressure relative to containment pressure causes the level of the suppression pool in the containment to fall. The drywell floor water level, which is at the top of the weir wall because of water spilled from the break, and from suppression pool water overflowing the weir wall, rises above the weir wall at approximately 1150 sec.

The external pressure differential developed is shown on Fig. 6.2-4. This external drywell pressure differential is well within the design value of -20 psid. Section 6.2.1.1.3.3 describes the DBA for external drywell pressure differential.

14←●

The volume of water provided in the suppression pool is such that the submergence of the top row of vents is at least 2 ft whenever the pressure suppression feature is being utilized, i.e., whenever steam is flowing through the vents.

●→16 16←●

●→14

Fig. 6.2-16 shows suppression pool water level for the short term (0-30 sec) which is analyzed with the maximum initial suppression pool height of 20 ft. This provides maximum vent submergence and, consequently, maximum internal drywell pressure differential. Fig. 6.2-16a and 16b show suppression pool water level for the long-term which is analyzed with the minimum initial suppression pool height of 19.5 ft. This provides the minimum heat sink for decay heat and thus the maximum suppression pool temperature.

With the assumptions that offsite power is lost and one of the two standby diesel generators powering RHR pumps fails to start, one of the two suppression pool cooling mode loops with an RHR heat exchanger and pump remains functional and begins operation at 1,800 sec, as does one containment unit cooler. The water pumped in this loop is cooled by 95°F (max) standby service water on the tube side of the RHR heat exchanger and is discharged to the suppression pool. Heat removal from the containment is thereby achieved in the long term as required.

Decay heat from fission products in the core continues to be removed with water supplied by the HPCS pump. The water which overflows through the break and falls to the drywell floor recirculates to the suppression pool by flowing over the weir wall into the drywell-weir annulus and through the vents.

The suppression pool temperature increases as core decay heat is added to it. At approximately 5.5 hr after the LOCA, the RHR heat exchanger in the active suppression pool cooling mode loop is able to remove heat from the suppression pool faster than it is added and the suppression pool temperature decreases. Since the suppression pool temperature is greater than the containment temperature, the suppression pool transfers heat to the containment atmosphere.

14←●

The rate of heat removal from the suppression pool by the RHR heat exchanger is plotted as a function of time in

Fig. 6.2-18. Fig. 6.2-20 shows the rate of heat removal from the containment atmosphere by the containment unit cooler which is automatically actuated by the LOCA signal.

●→14

The passive heat sinks in the drywell and containment that are considered in the analysis are summarized in Table 6.2-6. Figs. 6.2-22 and 22a show the passive heat sink heat removal rates for the drywell and containment.

6.2.1.1.3.1.4.3 Energy Balance

An energy balance for the main steam line break accident showing the energy distribution at various times is given in Table 6.2-8. The times selected include just prior to the break, the time of the maximum drywell internal pressure differential, the time that the suppression pool cooling mode of the RHR system is actuated, and approximately 1 day after the recirculation phase has been in progress. For the purpose of performing the energy balance, the system boundary is defined to be the primary containment. Everything within the system is grouped according to whether it is primarily a heat source or a heat sink, although many items behave as both during the course of the transient. Entries opposite these items represent stored internal energy at a particular time. The reference temperature for stored heat is 32°F. All heat added or removed across the system boundary from time zero is listed as heat input or heat output, respectively.

14←●

6.2.1.1.3.1.5 Recirculation Line Break

The instantaneous DER of a recirculation pump suction line produces a lower peak drywell internal pressure differential than the main steam line DER for the same initial containment and reactor conditions. However, the magnitude of the peak drywell external pressure differential is greater for this break than for the main steam line DER.

6.2.1.1.3.1.5.1 Break Area and Mass Energy Release Assumptions

The location of the recirculation line break is shown schematically on Fig. 6.2-3. Immediately following the rupture of the recirculation line, the flow from both sides of the break is assumed to be the maximum allowed by

critical flow considerations. From the reactor pressure vessel side of the break, flow is limited by the pipe cross-sectional area. Flow from the other side of the break is limited by the area of the 10 jet pump nozzles associated with the broken recirculation pump loop plus the reactor water cleanup cross-tie line area.

The vessel depressurization flow rates are calculated using Moody's critical flow model assuming "liquid only" outflow since this assumption maximizes the energy release to the drywell^(1,2). "Liquid only" outflow implies that all vapor formed in the reactor pressure vessel (RPV) by bulk flashing rises to the surface rather than being entrained in the blowdown. In reality, some of the vapor would be entrained in the break flow which would significantly reduce the RPV discharge flow rates.

●→14

The core decay heat and the sensible heat released in cooling the fuel to 553°F are included in the RPV depressurization calculation. The rate of energy release is calculated using a conservatively high heat transfer coefficient throughout the depressurization period. The resulting high energy release rate causes the RPV to maintain nearly rated pressure for approximately 13 sec (within 10 percent). This high RPV pressure increases the calculated blowdown flow rates, which is again conservative for analysis purposes. The stored energy of the fuel at temperatures below 553°F is released to the vessel fluid along with the stored energy in the vessel and internals as vessel fluid temperatures decrease below 553°F during the remainder of the transient calculation.

14←●

The MSIVs start closing at 0.5 sec after the accident. They are fully closed in the shortest possible time of 3 sec following closure initiation. In actuality, the closure signal for the MSIVs occurs from low reactor water level, so the valves do not receive a signal to close for greater than 4 sec, and the closing time may be as long as 5 sec. By assuming rapid closure of these valves, the RPV is maintained at a high pressure which maximizes the calculated discharge of high energy water into the drywell.

●→14

The recirculation line blowdown mass flow rate, the corresponding enthalpy, and the reactor coolant system pressure transient with and without the addition of feedwater are summarized in Tables 6.2-5 and 6.2-5a, respectively. The long-term (with feedwater) blowdown mass flow rate is also shown graphically on Fig. 6.2-10a.

14←●

6.2.1.1.3.1.5.2 Containment System Response

The calculated containment and drywell pressure and temperature responses for the recirculation line break are shown on Fig. 6.2-5 and 6.2-7, respectively. Following the break, the drywell pressure increases rapidly due to the injection of the recirculation line break flow. The peak drywell pressure occurs during the vent clearing phase of the transient as suppression pool water is being cleared from the vents. Following vent clearing, the drywell pressure decreases as the recirculation line break flow decreases.

The containment is pressurized early in the transient by the carry-over of noncondensables from the drywell. As the transient continues, recirculation line break flow is injected into the suppression pool and the temperature of the suppression pool water increases, causing the containment pressure to increase. At the end of blowdown, the drywell pressure stabilizes at a slightly higher pressure than the containment, the difference being equal to the hydrostatic pressure corresponding to the difference in the water level of the suppression pool in the containment and the drywell-weir annulus. During the RPV depressurization phase, most of the noncondensable gases initially in the drywell are forced into the containment. However, following the depressurization the noncondensables redistribute between the drywell and the containment via the vent system. This redistribution takes place as steam in the drywell is condensed by the drywell passive heat sinks.

The ECCS supplies sufficient core cooling water to control core heatup and limit metal-water reaction to less than 1 percent pursuant to 10CFR50.46. After the RPV is flooded to the height of the jet pump nozzles, the excess flow discharges through the recirculation line break into the drywell. This flow of water (steam flow is negligible) transports the core decay heat out of the RPV, through the broken recirculation line, in the form of hot water which flows into the suppression pool via the drywell-weir annulus and the vent system.

●→14

Table 6.2-7 provides the peak pressure, temperature, and time parameters for the recirculation line break as calculated using the parameters and initial conditions of Tables 6.2-1 through 6.2-3 and in correspondence with Fig. 6.2-5 and 6.2-7. Fig. 6.2-5 also shows the time dependent response of the drywell pressure differential during the first 30 seconds.

14←●

●→14

Figure 6.2-17 shows the suppression pool water level for the first 30 seconds. Figure 6.2-17a shows the long-term suppression pool water level response. Energy removal from the containment system after the recirculation line break is similar to that for the main steam line break. Energy is absorbed throughout the transient by the drywell and containment passive heat sinks and, at 1,800 sec, one containment unit cooler and one loop of the RHR in the suppression pool cooling mode are actuated. This considers the loss of offsite power and single failure of one standby diesel generator.

14←●

The RHR heat exchanger and containment unit cooler heat removal rates are shown as functions of time on Fig. 6.2-19 and 6.2-21, respectively. Fig. 6.2-23 gives the heat absorption rates for the drywell and containment passive heat sinks. The associated surface heat transfer coefficients are shown on Fig. 6.2-25 for the recirculation line break.

A summary of the sequence of events following the recirculation line break is provided in Table 6.2-11.

6.2.1.1.3.1.5.3 Energy Balance

An energy balance for the containment system after the postulated recirculation line break is given in Table 6.2-9. The distribution of energy in the system prior to and at various times throughout the transient is given.

6.2.1.1.3.1.6 Intermediate Size Breaks

The failure of a main steam line results in the most severe internal pressure loading on the drywell structure. However, as part of the containment performance evaluation the consequences of intermediate size breaks are also analyzed. This classification covers those breaks for which the blowdown results in reactor depressurization and operation of the ECCS. This section describes the consequences to the containment and drywell of a 0.1-sq ft break below the RPV water level. This break area is chosen as being representative of the intermediate size break area range. These breaks can involve either steam or liquid blowdown.

Following an intermediate size break, the drywell pressure increases at a sufficiently slow rate, such that the dynamic effect of vent clearing is negligible. The three rows of vents clear sequentially as the drywell-to-containment pressure differential equals the vent submergence hydrostatic pressure for each row.

Approximately 5 sec after the 0.1-sq ft break occurs, air, steam, and water start to flow from the drywell to the suppression pool. The steam is condensed and the air enters the containment atmosphere. The continual discharge of drywell air to the containment results in a gradual pressurization of the containment and drywell to about 4 and 9 psig, respectively. The containment continues to gradually increase in pressure due to the long term suppression pool heatup.

The ECCS is initiated by the 0.1-sq ft break and provides emergency cooling of the core. The operation of these systems is such that the reactor is depressurized in approximately 600 sec. This terminates the blowdown phase of the transient.

In addition, the suppression pool temperature at the end of blowdown is essentially the same as that for the large breaks because the same amount of reactor coolant system energy is released during the blowdown. After reactor depressurization and reflood, water from the ECCS begins to flow out the break. The subsequent long term suppression pool and containment heat-up transient is essentially the same as for the main steam line break.

Based on this analysis, it is concluded that the consequences of an intermediate size break are less severe than from a main steam line DER.

6.2.1.1.3.1.7 Small Size Breaks

6.2.1.1.3.1.7.1 Break Area and Mass Energy Release Assumptions

This section discusses the containment and drywell transients associated with small reactor coolant system blowdowns. The sizes of reactor coolant system ruptures in this category result in blowdowns that do not lead to reactor depressurization due either to loss of reactor coolant or automatic operation of the ECCS equipment. Following the occurrence of a break of this size, it is assumed that the reactor operators initiate an orderly plant shutdown and depressurization of the reactor system.

If the reactor coolant system break is below the RPV water level, the blowdown flow consists of reactor water. The thermodynamic process associated with the blowdown of reactor coolant and vent flow is one of nearly constant enthalpy (adiabatic). Blowdown from reactor pressure to the drywell pressure flashes approximately one-third of this

water to steam and two-thirds remain as liquid. Both phases are at saturation conditions corresponding to the drywell pressure. Thus, if the drywell is at atmospheric pressure, for example, the steam and liquid associated with a liquid blowdown are at 212°F.

If the reactor coolant system rupture is located such that the blowdown flow consists of reactor steam only, the resultant temperature in the drywell is significantly higher than the temperature associated with liquid blowdown. This is because the adiabatic depressurization of high pressure, saturated steam results in superheated steam conditions. For example, decompression of 1,000 psia saturated steam to atmospheric pressure results in 298°F superheated steam (86°F of superheat).

It can be seen that a small reactor steam leak (resulting in superheated steam) imposes the most severe temperature conditions on the drywell structures and the safety equipment in the drywell. For larger main steam line breaks the superheat temperature is nearly the same as for small breaks, but the duration of the high temperature condition for the larger break is less. This is because the larger breaks depressurize the reactor more rapidly than the orderly reactor shutdown that terminates the consequences of the small break.

6.2.1.1.3.1.7.2 Containment System Response

For drywell design considerations, the following sequence of events is assumed to occur. With the reactor and containment operating at the maximum normal conditions (Table 6.2-3), a small break occurs that allows blowdown of reactor steam to the drywell. The resulting pressure increase in the drywell leads to containment isolation. The drywell pressure continues to increase at a rate dependent upon the size of the steam leak. The pressure increase lowers the water level in the drywell-weir annulus until the level sequentially clears the vents. At this time, air and steam enter the suppression pool. The steam is condensed and the air is carried over to the containment atmosphere.

The air carry-over results in a gradual pressurization of the containment at a rate dependent upon the size of the steam leak. Once all the drywell air is carried over to the containment, the short term pressurization of the containment ceases and the containment and drywell reach an equilibrium condition. The drywell contains only superheated steam and continued blowdown of reactor steam condenses in the suppression pool. The suppression pool

temperature continues to increase until the RHR heat exchanger heat removal rate is greater than the decay heat release rate.

6.2.1.1.3.1.7.3 Recovery Operations

The reactor operators are alerted to the incident by the high drywell pressure signal and the reactor scram. For the purposes of evaluating the duration of the superheated steam condition in the drywell, it is assumed that their response is to shut the reactor down in an orderly manner using the RHR heat exchangers or main condenser while limiting the reactor cooldown rate to 100°F per hr. This results in the reactor coolant system being depressurized within 6 hr. At this time, the blowdown flow to the drywell ceases and the superheated steam condition is terminated. If the plant operators elect to cool down and depressurize the reactor coolant system more rapidly than at 100°F per hr in response to indication of a steam bypass condition as described in Section 6.2.1.1.3.4, then the drywell superheated steam condition is shorter.

6.2.1.1.3.1.7.4 Drywell Design Temperature Considerations

For drywell design purposes, it is assumed that there is a blowdown of reactor steam for the 6-hr cooldown period and that the passive heat sinks are neglected. The corresponding design temperature is determined by finding the combination of reactor coolant system pressure and drywell pressure that produces the maximum superheated steam temperature. The maximum drywell temperature occurs when the reactor coolant system is at approximately 450 psia and the drywell pressure is maximum. Thus, for design purposes, it is assumed that the drywell is at 25 psig. This results in a drywell temperature of 330°F.

6.2.1.1.3.2 High Energy Line Rupture Inside Containment

To ensure that the integrity of the containment structure is maintained, the release of high energy fluids must be prevented or limited to an amount that does not result in an unacceptable containment pressure. Several process lines which can contain high energy fluid pass through the containment to the drywell. Guard pipes that vent to the drywell are provided on those process lines which, if broken concurrently with the single active failure of the isolation valve in the drywell, would cause the containment pressure to reach an unacceptable level. Active failure of normally closed check valves within the drywell in such systems as HPCS, LPCS, and the LPCI mode of the RHR is not assumed;

therefore, guard pipes are not provided for these systems. Other process lines with check valves inside the drywell such as RCIC head spray and RHR shutdown cooling have guard pipes because these lines can be used during normal plant operation, after which it could be postulated that the check valve sticks in the open position.

6.2.1.1.3.2.1 Reactor Water Cleanup Break

The current computer code used for High Energy Line Break (HELB) analysis is GOTHIC. This computer code is described in submittals to the NRC dated May 14, 2002, June 27 and July 9, 2003, April 7 and May 12, 2004, as approved in Amendment 139 to NPF-47 dated May 20, 2004.

This computer code includes credit for fluid friction described in the initial submittal and included in the NRC SER, Section 3.4.

Also when performing these analyses, RBS assumes homogenous equilibrium conditions and 100% water entrainment for all breaks unless it is more conservative to not employ these assumptions as in the case of breaks involving fluid which is initially highly subcooled. This analysis is accomplished by disabling the forced equilibrium (i.e., enabling thermal hydraulic non-equilibrium model) and enabling the drop-liquid conversion model in GOTHIC.

The discussions below apply to the design and analyses.

The reactor water cleanup (RWCU) pumps are located outside the containment. RWCU heat exchangers and filter demineralizers are located inside the containment. This system, when operating, is in direct communication with the reactor coolant system, taking suction on the recirculation lines inside the drywell and injecting back into the feedwater lines.

Breaks in this system result in the release of high energy fluid into the containment. The mass loss into the containment is terminated by automatic isolation of the RWCU suction and discharge lines upon detection of the leak. Isolation valves immediately inboard and outboard of the drywell and containment penetrations are provided to perform this function. Check valves in the discharge line prohibit back flow from the feedwater line in the event of a break inside the containment.

•→12

Automatic isolation of the RWCU system in the event of a postulated line break is initiated by two separate leak detection systems. First, leakage is detected by means of flow comparison between RWCU system inlet and outlet. If the inlet flow exceeds the outlet flow by approximately 7 percent of rated flow, an alarm is actuated and an automatic isolation of the system initiated. In addition to the flow comparison method, leakage is detected by means of temperature sensing elements. Redundant temperature sensors are located locally to monitor the ambient temperature in all compartments containing equipment and piping for this system. Signal times to initiate closure of the system isolation valves are on the order of 3 sec for both detection systems described.

12←• •→6 6←•

The postulated DER of the 4-in RWCU pump discharge line between the inboard containment isolation valve and the regenerative heat exchangers is the limiting case for containment pressurization. This break location is shown schematically on Fig. 6.2-26.

Blowdown from the RWCU pump discharge side of the break is initially choked at the restrictor in the pump discharge line. The leak detection signal initiates automatic isolation of the system within 3.7 sec after the break. At 9.3 sec, the isolation valves have closed sufficiently such that the isolation valve flow area equals the flow restrictor area. At that time, the critical flow location changes from the flow restrictor to the isolation valves. Subsequent closure of the valves terminates flow from the RPV at 10.9 sec. Flow from the heat exchanger side of the break is limited to critical flow through the pipe cross-sectional area and is assumed to terminate when the contents of the regenerative heat exchangers are exhausted. For all pipe breaks considered in the RWCU system, the peak subcompartment pressures occur before isolation valve closure begins to limit the blowdown. It should be noted that the valve closure does not influence the blowdown until the valve open area equals the flow restrictor area, as flow is choked at the flow restrictor.

Table 6.2-12 summarizes the 4-in RWCU pump discharge line blowdown used in this analysis. Based on the initial conditions given in Table 6.2-3, this break produces an increase in containment internal pressure of 1.19 psig which is well below the design internal pressure of 15 psig.

6.2.1.1.3.2.2 Instrument Line Break

Instrument lines penetrating the drywell wall are provided with 1/4-in orifices located upstream of the drywell penetrations to preclude containment over-pressurization. In the event of a rupture, containment pressure increases until shortly after the operator starts reactor cooldown. Under the assumption that the operator takes 1/2 hr to detect an instrument line rupture and start reactor cooldown, the rise in containment pressure is only 0.42 psig for a liquid line. For a steam line break, the pressure rise is less.

6.2.1.1.3.3 External Pressure Analyses

Transients that could lead to external (negative) pressure loads on the drywell and containment are described in this section. Vacuum relief devices are not provided for this plant to minimize external pressure loading effects. Drywell depressurization following a LOCA is terminated by reverse vent clearing which allows air to flow from the containment back into the drywell. Containment depressurization due to uncontrolled cooldown by the containment unit coolers is terminated by differential pressure switches which automatically isolate the containment unit coolers at a containment pressure of -12 in of water (-0.43 psig).

6.2.1.1.3.3.1 Drywell External Pressure Differential

Following reactor blowdown, the drywell is filled with steam. The initial drywell air inventory has been discharged through the vents and into the containment. Structural passive heat sinks in the drywell condense the steam, and drywell depressurization occurs.

Reduction of drywell pressure relative to containment pressure causes the suppression pool water level in the containment to fall. When the top row of vents uncovers in the containment (reverse vent clearing), flow of air from the containment to the drywell terminates the drywell depressurization. At this time, the maximum external drywell pressure differential is attained. The change in drywell pressure is slow. The dynamic forces on the suppression pool are negligible and the suppression pool water level is determined by hydrostatic balance. This is described in Section 6.2.1.1.3.1 and for the pressure transients shown on Fig. 6.2-4 and 6.2-5.

For design purposes the following very conservative assumption has been made for drywell external pressure differential. Instead of the slow depressurization process described above, the steam in the drywell instantaneously condenses causing an instantaneous drywell depressurization. This process is assumed to be generated by an infinite heat transfer rate between the ECCS spillover water and the steam environment in the drywell. The calculation is described below.

Between 100 and 600 sec after the LOCA, all of the air initially in the drywell is released into the containment. Subsequent spillover of ECCS water is assumed to condense the steam in the drywell creating an external (negative)

pressure across the drywell wall. To determine the containment pressure at this time, the initial quantities of air in both the drywell and the containment are needed.

The initial mass of air in drywell is given by:

$$M_D = \frac{144(P_{D0} - P_{Dv0})V_D}{RT_{D0}}$$

Where:

$$P_{D0} = \text{Initial pressure in drywell} = 14.7 \text{ psia}$$

$$P_{Dv0} = \text{Initial partial pressure of vapor in drywell} = \phi_{D0} P_{\text{sat}}$$

$$T_{D0} = \text{Initial temperature of drywell} = 135^\circ\text{F} = 595^\circ\text{R}$$

$$R = \text{Gas constant} = 53.34 \text{ ft-lbf/lbm-}^\circ\text{R}$$

$$V_D = \text{Volume of drywell} = 236,196 \text{ cu ft}$$

$$\phi_{D0} = \text{Initial drywell relative humidity} = 0.20$$

$$P_{\text{sat}} = \text{Saturation pressure at } 135^\circ\text{F} = 2.54 \text{ psia}$$

Therefore,

$$M_D = 15,210 \text{ lbm of air}$$

The initial mass of air in containment is given by

$$M_c = \frac{144(P_{c0} - P_{cv0})V_c}{RT_{c0}}$$

Where:

$$P_{c0} = \text{Initial pressure in containment} = 14.7 \text{ psia}$$

$$P_{cv0} = \text{Initial partial pressure of vapor in containment} = \phi_{c0} P_{\text{sat}}$$

$$T_{c0} = \text{Initial temperature of containment} = 70^\circ\text{F} = 530^\circ\text{R}$$

$$R = \text{Gas constant} = 53.34 \text{ ft-lbf/lbm-}^\circ\text{R}$$

RBS USAR

V_c = Volume of containment = 1,191,590 cu ft

ϕ_{c0} = Initial containment relative humidity = 0.20

P_{sat} = Saturation pressure at 70°F = 0.36 psia

Therefore,

M_c = 88,786 lbm of air.

From the above air masses the post-blowdown containment pressure can be calculated:

$$P_{cF} = \frac{\Sigma M(RT_{cF})}{144V_c} + \phi_{cF} P_{sat}$$

Where:

ΣM = Summation of initial air mass in containment and drywell = 103,996 lbm of air

R = Gas constant = 53.34 ft-lbf/lbm-°R

T_{cF} = Final temperature of containment = temperature of suppression pool = 140°F = 600°R

V_c = Containment volume = 1,191,590 cu ft

ϕ_{cF} = Final containment relative humidity = 1.0

P_{sat} = Saturation pressure at 140°F = 2.89 psia

Therefore,

P_{cF} = 22.29 psia

To evaluate the minimum drywell pressure at this time, the following assumptions are made:

1. All steam in the drywell is condensed.
2. ECCS flow out of the reactor vessel is at suppression pool temperature (140°F)
3. All of the air has been released from the drywell.

Using these assumptions, the final drywell pressure is equal to the saturation pressure at 140°F.

$$P_{DF} = P_{sat} = 2.89 \text{ psia}$$

140

Therefore, the external pressure differential across the drywell wall is the difference in the final pressures of the containment and drywell.

$$\begin{aligned} \Delta P_D &= P_{DF} - P_{CF} \\ &= 2.89 - 22.29 \\ &\approx -19.4 \text{ psid} \end{aligned}$$

The above analysis represents a very conservative bounding calculation of the external pressure differential on the drywell wall assuming the following drywell and containment initial conditions:

	<u>Drywell</u>	<u>Containment</u>
Pressure (psig)	0	0
Temperature (°F)	135	70
Relative humidity (%)	20	20

The same analysis revised to reflect the Technical Specification allowable extreme conditions (Table 6.2-3a) summarized below and a pool temperature of 135.6°F at the time of ECCS spillover flow (Figure 6.2-6) results in a maximum predicted external pressure differential of -19.9 psid compared to the -20.0 psid design value.

	<u>Drywell</u>	<u>Containment</u>
Maximum pressure (psig)	1.5	0.3
Minimum temperature (°F)	100	70
Minimum dewpoint temperature (°F)	60	60

6.2.1.1.3.3.2 Containment External Pressure Differential

The design basis event for maximum containment external pressure differential is the accidental cooldown of the containment atmosphere under minimum heat load conditions. This event results from the failure of one of the chilled water control valves to close and isolate the chilled water

supply to one containment unit cooler on low containment atmosphere temperature. Failure of the plant operator to recognize the problem and turn off the containment unit cooler is the assumed single failure.

Supplied with a continuous flow of 57°F (minimum) chilled water, one containment unit cooler continues reducing the containment temperature and pressure. At -12 in W.G. (-0.43 psig) pressure, the chilled water isolation valves are closed automatically by redundant signals from differential pressure transmitters which sense the pressure difference between the containment and the shield building annulus. The containment depressurization transient is thereby terminated and the maximum containment external pressure differential is limited to -0.43 psid, which provides a 40 percent margin relative to the -0.60 psid design value.

Inadvertent containment cooldown occurring during either normal or post-LOCA conditions has been considered. Single failures which could result in continued flow of chilled water to the unit coolers during normal plant conditions or continued flow of standby service water after a LOCA have been analyzed. Table 6.2-47 summarizes single failures analyzed and their consequences. The analysis shows that even with all three 50-percent capacity unit coolers operating, the redundant containment to annulus differential pressure alarms, isolation signals, and isolation valves preclude continued operation of more than one unit cooler.

Six pressure differential transmitters are utilized to provide redundant alarms in the main control room and redundant isolation signals. Transmitters PDT 60A, 60C, and 60E shown in Fig. 9.4-7 develop the Division I isolation signal (based on 2 out of 3 logic) supplied to stop the fan on unit cooler 1A. The Division I signal also closes chilled water isolation valves MOV 127 and 128 (Fig. 7.5-5) as well as standby service water valves MOV 502A and 503A (Fig. 7.3-11). Transmitters PDT 60B, 60D, and 60F develop the Division II signal which stops the fan on unit cooler 1B and closes chilled water isolation valves MOV 102, 129, and 130 and standby service water valves MOV 502B and 503B. These transmitters are powered from separate emergency sources.

Although a direct trip signal is not provided for the nonsafety-related backup unit cooler 1C, cooling water flow to this cooler is terminated by closing the chilled water isolation valves. Either the Division I or Division II containment negative pressure signal effectively isolates unit cooler 1C.

As indicated in Table 6.2-47, operator action is required to isolate unit cooler UC-1A and terminate containment cooldown after a LOCA, assuming the single active failure of a relay in the Division I containment-to-shield building annulus differential pressure logic. The operator is alerted to the need for this action by the Division II alarm at -5 in. W.G. and by the alarm and automatic isolation of unit cooler UC-1B at -12 in. W.G.

A transient analysis was performed to determine the time available for operator action after the -5 in. W.G. alarm. The depressurization transient analysis indicates that the operator would have more than 1.7 hr after the -5 in. W.G. alarm to evaluate the situation and isolate unit cooler UC-1A. In this analysis, it was assumed that the containment air mass remained constant and equal to that corresponding to the normal conditions of 14.7 psia, 90°F, and 50 percent relative humidity prior to the LOCA. To maximize the cooldown rate, it was assumed that both of the ESF unit coolers were operating, with standby service water being supplied for cooling at a temperature of 60°F.

6.2.1.1.3.4 Steam Bypass

The concept of the pressure suppression reactor containment is that any steam released from the reactor coolant system is condensed by the suppression pool and does not have an opportunity to produce a significant pressurization effect on the containment. This is accomplished by channeling the steam into the suppression pool through a vent system. This arrangement forces any steam released from the reactor coolant system to be condensed in the suppression pool.

If a leakage path were to exist between the drywell and the containment, the leaking steam would pressurize the containment. Therefore, the allowable bypass leakage is defined as the amount of steam which could bypass the suppression pool without exceeding the design containment pressure of 15 psig. The allowable bypass leakage is a function of the nature of the leakage path, the duration of the pressure differential across the leakage path, and the rate of condensation of leakage steam inside the containment.

To mitigate the consequences of steam bypass of the suppression pool, a high drywell pressure signal automatically initiates the containment unit coolers which are engineered safety features, as described in Section 6.2.2. The River Bend Station design does not incorporate a containment spray system.

The allowable drywell bypass leakage capacity is expressed in terms of the parameter A/\sqrt{K}

where:

A = Flow area of leakage path, sq ft

K = Geometric and friction loss coefficient.

This parameter is dependent only on the geometry of drywell leakage paths and is a convenient numerical definition of the overall drywell bypass leakage capacity. It results from a consideration of the flow process in the leakage paths. Assuming steady state noncompressible fluid flow theory, (Bernoulli equation) to be applicable to the leakage flow, the pressure loss between the drywell and containment can be written:

$$P_D - P_c = \frac{KV^2}{2g_c v} \frac{1}{144} \text{ psid}$$

where:

P_D = Drywell pressure, psi

P_C = Containment pressure, psi

K = Total geometric and friction loss coefficient of the flow path between the drywell and containment. These losses include entrance, exit, discontinuities, and friction. The latter is somewhat dependent upon the Reynolds Number of the fluid flow, but for drywell leakage considerations, it is considered constant.

V = Velocity of flow, ft/sec

g_c = Conversion factor, 32.2 lbf-ft/lbf-sec²

v = Specific volume of the fluid flowing in the leakage path, cu ft/lbm

If the bypass leakage path flow rate is M (lbm/sec) and the flow area is A (sq ft), the above equation can be rewritten to give:

$$M = \frac{A}{\sqrt{K}} \sqrt{2g_c(P_D - P_c)} \frac{144/v}{\text{sec}} \text{ lbm}$$

Thus, for a given drywell to containment pressure differential, the leakage flow (capacity) is dependent on A/\sqrt{K} and the specific volume of the fluid flowing in the leakage path (which depends on the drywell internal pressure).

•→14

The purpose of the steam bypass analysis is to determine the leakage rate (in terms of bypass leakage capacity, A/\sqrt{K}) that would result in containment pressurization to design pressure for the complete spectrum of line break sizes. The results of the original analysis based on an initial licensed reactor power of 2894 MWt are summarized on Fig. 6.2-27. This figure shows that allowable bypass leakage capacity ranges from approximately 10.3 sq ft for a main steam line DER to 1.21 sq ft for small steam line breaks.

14←•

The size of reactor coolant system break determines the magnitude and duration of the pressure differential across the drywell leakage paths. When a large break occurs, the high mass and energy flow from the reactor coolant system pressurizes the drywell, generating high pressure differential across the assumed leakage paths and producing high leakage flow rates. However, large line breaks rapidly depressurize the reactor, thus quickly terminating the blowdown. When blowdown is over, the pressure differential across the leakage paths dissipates and leakage flow and containment pressurization cease. This very short duration of reactor blowdown gives a large allowable bypass leakage capacity.

Small steam line breaks, on the other hand, result in slow reactor coolant system depressurization. The reactor is scrammed due to the high drywell pressure resulting from the energy and mass released from the reactor coolant system break. The operator brings the reactor down to near atmospheric conditions in an orderly manner to terminate the blowdown.

During this period, the blowdown flow from the reactor coolant system forces the drywell air into the containment. The blowdown steam is condensed in the suppression pool, after the water level in the drywell-weir annulus is depressed to the top of the uppermost row of vents. This results in an essentially continuous internal pressure differential between drywell and containment of 3.1 psid. The allowable bypass leakage capacity for these conditions is an A/\sqrt{K} of 1.0 sq ft.

The bypass leakage analysis is performed assuming that only steam leaks through the bypass paths. This assumption conservatively minimizes the allowable bypass leakage

capacity by maximizing the containment pressurization from the assumed leakage. The results shown on Fig. 6.2-27 are also based on the following assumptions:

1. The passive heat sinks, summarized in Table 6.2-6, absorb energy from the containment and drywell atmospheres. The UCHIDA}20{ convective heat transfer correlation is used.
2. Offsite power is lost and the most limiting single active failure of one onsite standby diesel generator occurs, resulting in the minimum availability of the containment heat removal systems.
3. The one available containment unit cooler is supplied with 95°F standby service water and is operating 10 min after the pipe break.
4. The one available RHR heat exchanger loop is initiated in the suppression pool cooling mode at 30 min after the LOCA.

•→14

5. In the most limiting case of a small steam line break, the plant operator identifies the need for a controlled reactor cooldown and initiates the cooldown 25 min after the pipe break at the rate of 200°F/hr.
6. Initial Reactor Power level at 2952 MWt
(102 * 2894 MWt)

Two of the three containment unit coolers are engineered safety features and operate automatically 10 min after a high drywell pressure signal (Section 6.2.2.2). However, an analysis was performed which assumed one unit cooler actuated 10 min after the pipe break.

The drywell and containment pressure transients for a small steam line break with an area of 0.1 sq ft and bypass leakage (A/√K) of 1.15 sq ft from the original analysis (licensed power of 2894 MWt) are shown on Fig. 6.2-27a. The containment design pressure is approached, but not reached.

14←•

●→14

A confirmatory analysis was performed to demonstrate that the system by pass leakage (A/\sqrt{K}) was still appropriate for the current licensed power level of 3091 MWt. The drywell and containment pressure results are shown in figure 6.2-27b and are based on the assumptions used in the original analysis performed for a licensed power of 2894 MWt, except as noted below:

1. Initial reactor power of 3100 MWt(1.003 x 3091 MWt)
2. Break size of 0.1 sq. ft.
3. Bypass leakage (A/\sqrt{K}) of 0.81 sq. ft.
4. Reactor operator initiates a 200° F/hr reactor cooldown 25 minutes after the start of the event.

The results of the evaluation show that the peak containment pressure is 15.0 psig, which is equal to the 15 psig containment pressure design limit, This demonstrates that the bypass leakage (A/\sqrt{K}) of 0.81 sq. ft is acceptable for the current licensed power level of 3091 MWt.

14←●

To ensure that the drywell conforms to the design bases, a preoperational leak test is conducted at the drywell design internal pressure differential of 25 psid, attained with the drywell internal pressure at 25 psig. The acceptance criterion for this test is that the measured leakage must be less than 10 percent of the leakage corresponding to an equivalent bypass leakage (A/\sqrt{K}) of 0.81 sq ft at the design pressure.

●→12

Low pressure leakage tests of the drywell are conducted periodically at a drywell internal pressure differential of 3 psid, attained with the drywell internal pressure at 3 psig, to simulate the drywell conditions expected to result from a small steam line break. The acceptance criterion for these tests is that the measured leakage must be less than 10 percent of the leakage corresponding to an equivalent bypass leakage (A/\sqrt{K}) of 0.81 sq ft at the drywell internal pressure differential of 3 psid.

12←●

6.2.1.1.3.5 Suppression Pool Dynamic Loads

The containment and internal structures are designed to withstand all suppression pool dynamic effects including safety relief valve (SRV) discharge and LOCA dynamic loads. These loads are discussed in Appendix 6A for the containment and the internal structures.

6.2.1.1.3.6 Asymmetric Containment Loads

Localized pipe forces, earthquake forces, SRV discharge loads, and LOCA loads are asymmetric loads acting on the containment and internal structures.

RBS USAR

The containment and internal structures are designed for asymmetrical loads described in Sections 3.8.3.3 and 3.8.3.4 and Appendix 6A. These loads are included in the applicable load combinations in Sections 3.8.2.3 and 3.8.3.3.

THIS PAGE LEFT INTENTIONALLY BLANK

The maximum LOCA asymmetric pressure loading on the steel containment wall associated with the bubble formation that follows vent clearing is specified as 10 psid⁽³⁾. The basis for this specification is data from the large-scale air blowdown tests that were conducted as part of the Mark III test program. Circumferential variations in this relatively small pressure increase could result from either seismically induced submergence variations or variations in the vent flow composition (air/steam and mixture variations). Increased submergence could lead to an increase in the load. However, pressure suppression test facility (PSTF) data⁽³⁾ shows a very weak relationship between submergence and the containment pressure increase caused by bubble formation. A survey of the PSTF data shows that, for tests having the same drywell pressure at vent clearing, variations of up to 8 ft in submergence lead to variations in the bubble load of 2 to 3 psi. It is concluded that variations in suppression pool depth do not lead to significant asymmetric containment bubble loads.

The bubble loading specification of 10 psid was derived from an air test and is thus the most conservative in terms of vent flow composition. Any steam in the vent flow would be condensed and this would lead to less rapid suppression pool acceleration and thus a reduced pressure load on the containment wall.

Despite strong evidence that circumferential variation in the containment bubble load does not occur, an arbitrary loading combination of 0 psid on one side of the containment with a simultaneous 10 psid load on the other side is considered to account for any uncertainties about asymmetric loading conditions. This conservative asymmetric condition assumes that all air is vented on half of the drywell periphery and steam is vented on the other half.

6.2.1.1.3.7 Analytical Models

6.2.1.1.3.7.1 LOCA Containment Response Model

•→14

The pressure and temperature response of the primary containment and drywell atmospheres and the suppression pool temperature response following a LOCA in the reactor coolant system are determined as functions of time with the GE M3CPT and SHEX computer programs. These programs perform numerical integrations principally of the mass and energy conservation equations, and also of the momentum conservation equation as required to determine flow rates between nodes. These codes simulate behavior of the pressure suppression containment system, the reactor coolant system, the containment heat

14←•

•→14

sources and sinks, and the containment heat removal systems. References 4 and 30 provide a detailed description of the analytical models used and the assumptions employed⁽¹⁾. The analytical models and assumptions incorporated in the M3CPT and SHEX programs to predict conservatively the response of the pressure suppression containment system are summarized in the following paragraphs. In addition, modifications were performed to produce a modified version of the SHEX code with features not present in the standard SHEX code. These modifications include a model for containment coolers and a model which allows reverse vent flow (flow from the containment airspace to the drywell weir annulus) when the vent suppression pool exit is uncovered and containment pressures exceed drywell pressure at the vent exit elevation.

The drywell is modeled as a single volume system, initially containing a homogeneous mixture of air and water vapor. The total energy and mass of air, water vapor, and liquid water inside the drywell are determined at all times by numerical integration of the appropriate flows. The flows included in the M3CPT and SHEX drywell model are the reactor blowdown, the vent flow, and the heat transfer to the containment structures.

14←•

Blowdown from the reactor coolant system causes the drywell pressure to increase and the level of water in the drywell-weir annulus to be depressed until the vents are cleared. A mixture of air, steam, and liquid is then forced through the vents into the containment side of the suppression pool. The liquid and condensed steam are added to the suppression pool inventory while the air from the drywell is added to the wetwell airspace, increasing the wetwell airspace pressure and the pressure at the vent exit. The drywell pressure is dictated by the vent exit pressure, the dynamic pressure losses associated with a given vent flow, the drywell free volume, and the blowdown flow rate. For calculation of flow through the vents into the suppression pool, a homogeneous flow model is employed. This model, in combination with the frictionless Moody flow model used for blowdown calculations, provides a computed flow rate into the drywell that is large and a flow rate out of the drywell that is small; thus, the rate of storage in the drywell is large and the pressure calculated is conservatively high.

In determining the state of the drywell (i.e., pressure and temperature) for a steam line break, the steam mass and enthalpy are added to the drywell atmosphere. Initially, the blowdown consists of saturated steam, but as the reactor vessel pressure drops the water level in the vessel swells. Eventually the froth level reaches the top of the steam dryers, and the blowdown is assumed to change from steam to a two-phase mixture.

At the time the two-phase blowdown starts, the drywell contains superheated steam and air. If instantaneous and

complete mixing between the steam, air, and two-phase mixture is assumed, drywell temperature and pressure decrease. This decrease results from heat being extracted from the high temperature steam and air to evaporate the liquid phase of the blowdown. For the sake of conservatism, the assumption of instantaneous homogenous mixing is modified for the period immediately following the start of two-phase flow until after peak drywell pressure and temperature occur (except for vent flow calculations where, again to be conservative, a homogenous drywell mixture is always assumed).

The modification of the homogeneous mixing assumption is as follows. The steam portion of the blowdown goes directly to the drywell atmosphere. The liquid portion undergoes a pressure flash, where the flashed steam goes directly to the drywell atmosphere and the decompressed liquid falls to the drywell floor. Saturated steam resulting directly from the blowdown and the flashing process mixes uniformly with the existing drywell air and superheated steam.

The thermodynamic state of the drywell atmosphere following a recirculation line break is assumed to always be saturated. The break effluent is homogeneously mixed with the atmosphere and undergoes a pressure flash, with subsequent dropout of the decompressed and unflashed liquid.

•→14

The mode of heat transfer to the drywell and containment heat sinks is determined from the individual heat sink surface temperature and the saturation temperature of the atmosphere adjoining the heat sink surface.

M3CPT incorporates models for vent clearing, vent flow, suppression pool swell, and wetwell pressurization. These models are described in NEDO-20533⁽⁴⁾.

14←•

The sensitivity of drywell and containment pressure response to changes in various parameters is presented in the

●→14

following paragraphs. These sensitivity analyses were performed using the original USAR methods and with an initial reactor power of 2952 MWt. Aside from the parameter under consideration, the same initial conditions and variables are used in this study as were used in the containment integrity analysis described in Section 6.2.1.1.3.1.

14←●

In general, containment peak pressure is sensitive only to those variables that affect the long-term analysis, such as initial suppression pool temperature, decay heat rate, containment unit cooler heat transfer coefficient, RHR heat exchanger heat transfer coefficient, and passive heat sink area. Drywell peak pressure differential is sensitive only to those variables that affect the short-term analysis, such as vent area, submergence, air carry-over rate, blowdown flow rate, and RPV liquid level swell time.

Vent Area

Fig. 6.2-28 shows the effect of vent area changes on peak drywell pressure differential. The nominal area is 532 sq ft and is calculated based on the vent pipe which serves as a liner for the vent. This pipe is 28-in Schedule 10 pipe which has an inside diameter of 27.5-in.

Vent Submergence

Fig. 6.2-29 shows the effect of changes in vent submergence on peak drywell pressure differential. Submergence (measured to centerline of top vent) used in the containment analysis is 7.75 ft. This is the maximum submergence, since the suppression pool height is maintained between 19.5 and 20.0 ft and the centerline height of the top vent is 12.25 ft (submergence ranges from 7.25 to 7.75 ft).

Drywell Air Carry-over Rates to the Containment

Fig. 6.2-30 shows the effect of drywell air carry-over models on peak drywell pressure differential. Nominally, a homogeneous mixture of air, steam, and liquid is assumed for vent flow (i.e., all components have the same velocity). This assumption is inaccurate for high velocity and high void fraction flow, which is characteristic of vent flow, since empirical data reveal the existence of some relative velocity between phases (slip flow)⁽¹⁾. But, the homogeneous assumption reduces vent flow and consequently increases drywell pressure. Thus, the homogeneous flow assumption is conservative.

Blowdown Flow and Energy Rates (Recirculation Pump Suction Line Break)

Fig. 6.2-31 shows the effect of changes in the reactor blowdown flow rate on peak drywell pressure differential. Nominal blowdown (Table 6.2-6) is calculated from the Moody frictionless flow model. The Moody flow rate is about 40 percent above experimental data and is, therefore, conservative^(5,6).

Level Swell Time (Main Steam Line Break)

Fig. 6.2-32 shows the effect of changes in the reactor level swell time on peak drywell pressure differential. Nominal reactor level swell time is 1.05 sec and is calculated by the method described in Reference 1. This method is essentially the same as that given in Appendix B of GE Topical Report NEDO-10329⁽⁷⁾, which agrees with the experimental data contained in the same report.

Initial Suppression Pool Temperature

Fig. 6.2-33 shows the effect of changes in the initial suppression pool temperature on peak containment pressure. The temperature used in the containment analysis is 100°F. Suppression pool temperature is a plant operating parameter that is continuously monitored and subject to a technical specification limit.

Decay Heat Rate

Fig. 6.2-34 shows the effect of changes in the decay heat rate on peak containment pressure. The decay heat rate used in the FSAR analysis is calculated from Branch Technical Position ASB 9-2⁽¹²⁾, with the following positive uncertainties:

<u>Reactor Cooling Time (t)</u>	<u>Uncertainty (%)</u>
$t < 10^3$ sec	+20
10^3 sec $\leq t \leq 10^7$ sec	+10
$t > 10^7$ sec	+10

Containment Unit Cooler Heat Transfer Coefficient

The sensitivity of the peak containment atmosphere pressure to changes in the containment unit cooler heat transfer coefficient is discussed in Section 6.2.2 and shown on Fig. 6.2-35.

RHR Heat Exchanger Heat Transfer Coefficient

The sensitivity of the peak containment pressure to changes in this parameter is discussed in Section 6.2.2 and shown on Fig. 6.2-36.

Passive Heat Sink Area

Fig. 6.2-37 demonstrates the effect of changes in the area of passive heat sinks on the peak containment pressure.

6.2.1.1.3.7.2 Model for High-Energy Line Breaks Inside Containment

The current computer code used for High Energy Line Break (HELB) analysis is GOTHIC. This computer code is described in submittals to the NRC dated May 14, 2002, June 27 and July 9, 2003, April 7 and May 12, 2004, as approved in Amendment 139 to NPF-47 dated May 20, 2004.

This computer code includes credit for fluid friction described in the initial submittal and included in the NRC SER, Section 3.4.

Also when performing these analyses, RBS assumes homogenous equilibrium conditions and 100% water entrainment for all breaks unless it is more conservative to not employ these assumptions as in the case of breaks involving fluid which is initially highly subcooled. This analysis is accomplished by disabling the forced equilibrium (i.e., enabling thermal hydraulic non-equilibrium model) and enabling the drop-liquid conversion model in GOTHIC.

The discussions below apply to the initial design and analyses.

Analyses of the containment response to high-energy line breaks are performed using the subcompartment analysis code, THREED. A detailed description of this code is provided in Appendix 6B.

Mass and energy release rates are manually calculated, assuming Moody critical flow, and are specified as input functions of time to THREED. No credit is taken in the analyses for energy removal by passive heat sinks or containment unit coolers.

6.2.1.1.3.7.3 Model for Steam Bypass Analysis

The analytical model for the steam bypass analysis is described in detail in Section 6.2.1.1.3.4. The same models used in the peak drywell pressure LOCA analysis previously described are employed. Leakage from the drywell to the containment is assumed to be all steam and is a function of the calculated pressure difference across the drywell wall.

Steam leakage causes the containment atmosphere to become saturated immediately after the pipe break. This increases the heat removal capability of the containment unit coolers due to the increase in condensation or latent heat removal from the saturated atmosphere. For the steam bypass analysis, vendor-supplied containment unit cooler heat transfer coefficients based on saturated inlet conditions are used. These coefficients are modified to include a tube-side fouling resistance of 0.0005 hr-sq ft-°F/Btu and are tabulated in Table 6.2-2.

6.2.1.1.3.7.4 Containment Environment Control

The functional capability of the normal containment ventilation system to maintain the temperature, pressure, and humidity in the containment and its subcompartments

within the prescribed limits and the action to be taken if these conditions are exceeded is discussed in Section 9.4.6. The loss of these systems does not result in exceeding the design operating conditions for the safety-related equipment inside the containment. The safety-related containment systems described in Sections 6.2.2 and 6.5 maintain required containment atmosphere conditions after a LOCA.

6.2.1.1.3.7.5 Instrumentation

Refer to Sections 6.2.1.7, 7.2, 7.3, 7.5, and 7.6 for a discussion of instrumentation inside the containment used for monitoring various containment parameters.

6.2.1.2 Containment Subcompartments

6.2.1.2.1 Design Bases

The containment subcompartments are designed in accordance with the following criteria:

1. A pressure response analysis is given for each containment subcompartment containing high energy piping in which breaks are postulated. The definition of high energy piping and the criteria for postulating breaks are outlined in Section 3.6.

The break which, by virtue of its size and location, produced the greatest release of blowdown mass and energy into the subcompartment, during normal operation and hot standby condition, is selected for the design evaluation.

The breaks used in the design evaluations are listed in Section 6.2.1.2.3.

2. All circumferential breaks are considered to be fully double-ended and no credit for limiting blowdown generation is taken due to pipe restraint locations.

The effective cross-sectional flow area of the pipe is used in the jet discharge evaluation for breaks.

3. The design pressure differentials for all subcompartments are higher than the calculated peak pressure differentials resulting from the design basis pipe breaks.

6.2.1.2.2 Design Features

The containment includes the following four subcompartments:

1. Reactor Pressure Vessel-Shield Wall Annulus - The 2 ft thick cylindrical primary shield wall which surrounds the RPV has an outside diameter of 29 ft 10 in and extends from the vessel pedestal to el 147 ft 6 in. Breaks in the recirculation water outlet piping and feedwater piping are analyzed.
- 12
2. Drywell Head - The drywell head is located above the RPV head and surrounds the RPV head, connecting to the drywell bulkhead at el 162 ft 3 in. Five normally open ventilation exhaust hatches are located in the bulkhead at azimuths 30, 75, 165, 225, and 345 deg venting into the drywell. (These hatches are closed only during refueling.) Line Breaks were evaluated for the RCIC head spray line. Although the head spray line was removed, the break analysis will remain in place because the analysis bounds a vessel head vent line break.
- 12←•
3. RWCU Heat Exchanger Room - The RWCU heat exchanger room, located at el 147 ft 3 inches in the containment, vents through the wire door in the south wall and through two 13 ft x 2 ft 2 in openings in the north wall into the containment. RWCU line breaks are analyzed in this room.
 4. RWCU Filter/Demineralizer Rooms - The RWCU filter/demineralizer rooms are located at azimuth 270 deg and el 162 ft 3 in. HVAC ducting and drain lines provide venting to the holding pump room. Special vent paths in one of the plugs separating each of the filter/demineralizer rooms from the refuel floor (el 182 ft 3 in) provide venting to the containment air space.

Drawings depicting piping, equipment, and compartment/venting locations are provided in Section 3.6. The volumes and vent areas are discussed in Section 6.2.1.2.3. The subcompartments described do not incorporate blowout panels. No credit is taken for vent areas that become available after the pipe break occurs.

6.2.1.2.3 Design Evaluation

The current computer code used for High Energy Line Break (HELB) analysis is GOTHIC. This computer code is described in submittals to the NRC dated May 14, 2002, June 27 and July 9, 2003, April 7 and May 12, 2004, as approved in Amendment 139 to NPF-47 dated May 20, 2004.

This computer code includes credit for fluid friction described in the initial submittal and included in the NRC SER, Section 3.4.

Also when performing these analyses, RBS assumes homogenous equilibrium conditions and 100% water entrainment for all breaks unless it is more conservative to not employ these assumptions as in the case of breaks involving fluid which is initially highly subcooled. This analysis is accomplished by disabling the forced equilibrium (i.e., enabling thermal hydraulic non-equilibrium model) and enabling the drop-liquid conversion model in GOTHIC.

The discussions below apply to the initial design and analyses.

The breaks utilized in the design evaluation of the containment subcompartments are listed in Table 6.2-13. The

tables and figures which contain the nodal parameters and results for each analysis are also listed in Table 6.2-13.

•→14

The containment subcompartment design evaluations use the THREED and RELAP4/MOD5⁽⁸⁾ computer codes. Both codes consider two-phase, two-component (steam-water-air) flow through the vents and account for the fluid inertia effects. A detailed description of the THREED analytical model is provided in Appendix 6B. The blowdown mass and energy releases for each of the breaks are provided in the tables which are cross-referenced in Table 6.2-13. For all cases, the blowdown data is based upon conservative methodology developed by GE using the Moody steady-slip flow model with subcooling, as described in Reference 9. The blowdown mass and energy used in the subcompartment calculation are calculated based on 102% of the original reactor power and original reactor pressure. Evaluations performed at 100.3% of current rated power and 1072 psia reactor pressure demonstrated that due to the conservatisms in the methodology, the break mass and energy flows calculated at the original reactor power and pressure remain conservative for application to current rated power conditions.

The assumed initial conditions for the subcompartment volumes are conservatively chosen so as to maximize transient pressure responses. The initial conditions are given in the subcompartment nodal description tables.

The description of and justification for the subsonic and sonic flow model, and the degree of entrainment used in vent flow calculations are given in Appendix 6B.

The piping systems assumed to rupture in the subcompartments are identified in Table 6.2-13. Break locations are discussed in Section 3.6. The need to determine the impact of a RCIC head spray line break inside the drywell head is eliminated with the reroute modification for the RCIC line. Changing the injection line from the reactor spray nozzle to the 'A' feedwater line eliminates the RCIC break in the drywell head as an event and therefore this break does not need to be evaluated.

Although the RCIC break is eliminated with respect to drywell pressurization, another high energy line, the vessel head drain line, is also present in the drywell head. This line is connected between the vessel head and one of the steam lines and is used to purge non-condensable gases from the vessel. A break in this line will result in the discharge of high energy steam to the drywell head and cause pressurization of the drywell head. However, the break area associated with a break in the vessel drain line is significantly smaller than the break area used to calculate the mass and energy release rates applied in the USAR RCIC break calculation. The reduction in break flow rate due to the smaller break area is much more significant than the effect

of increased dome pressure due to power uprate. Consequently, the mass and energy release rates due to a break in the vessel drain pipe are much lower than those assumed for the USAR analysis of the RCIC break. Since the mass and energy release rates used for the USAR RCIC break calculation remain bounding, the existing USAR calculation for drywell head pressurization based on the RCIC break at current power also remains bounding.

Based on the evaluation performed above it is concluded that the USAR drywell head pressurization loads defined using the break mass and energy flow rates of USAR Table 6.2-25 for the RCIC break bound the expected drywell head pressurization loads for a postulated break of the vessel head drain line.

14←•

The subcompartment nodalization schemes are tabulated and provided. The nodalization schemes are selected to maximize pressure differentials across node boundaries. Restrictions resulting from structural components or equipment placement are selected as nodal boundaries for the flow models.

A nodalization sensitivity study ensures that, regarding the feedwater line break in the RPV-shield wall annulus, the maximum pressure loads are predicted by the nodal model. The base model, as depicted on Fig. 6.2-41, consists of 25 volumes or nodes, representing the annulus. The sensitivity nodal model utilizes a 27-node scheme (Fig. 6.2-38) in which volumes 2, 3, 6, and 7 of the base model are divided to create 6 smaller volumes. These particular volumes are chosen because they are located in the immediate vicinity of the break. Any changes in pressurization are more pronounced in this area than at a point farther from the break. The force and moment coordinate system and geometry used in the nodalization sensitivity study are defined in Figure 6.2-74.

THIS PAGE LEFT BLANK INTENTIONALLY

Tables 6.2-48 and 6.2-49 present the projected areas and moment arms applied in the determination of the transient forces and moments for the 27 node model and 25 node model, respectively. The force and moment transients are shown graphically in Figure 6.2-75 for the shield wall and in Figure 6.2-76 for the RPV. The maximum resultant forces and moments are summarized in Table 6.2-50, which shows that the 27-node model yields a maximum force approximately 3 percent higher than the 25-node model and a maximum moment about 7 percent higher.

The pressure response graphs of nodes within each subcompartment model are provided, with the figure numbers listed in Table 6.2-13.

In order to minimize the asymmetric loads resulting from pressurization of the RPV-shield wall annulus, flow diverters are incorporated in the primary shield wall penetration sleeves for the two recirculation water outlet lines. Flow diverters are not provided for the recirculation water inlet lines or feedwater lines. Due to the inclusion of flow diverters into the primary shield wall design, the feedwater line break results in the greatest mass and energy release into the RPV-shield wall annulus. Therefore, the greatest forces upon the RPV and the greatest pressure differentials across the primary shield wall are experienced during this transient.

As part of the RPV-shield wall annulus subcompartment analysis, no credit is taken for any penetrations through the primary shield wall which might allow additional venting out of the annulus. All mass flow from the RPV-shield wall annulus is required to vent through the area at the top of the primary shield wall, except in the case of the flow diverters for the recirculation water outlet line break (discussed above). Additionally, no credit is taken for vent area that might become available due to moveable obstructions to flow such as insulation, ducting, plugs, seals, or doors. Since a finite time is required to develop vent flow out of the annulus, pressure differentials are established across the primary shield wall. As mass flow into the drywell is established, the pressure differentials decrease to values well below the peaks. Vent paths where choked flow occurs are indicated in the vent path description tables for each analysis.

The postulated pipe breaks at the nozzle safe-ends are located between the RPV insulation and the reactor vessel. Since the insulation is not designed to withstand internal pressure buildup, it is assumed that all the RPV insulation

displaces toward the shield wall immediately after the pipe break. This assumption is consistent with the determination of pressure differential across the shield wall rather than simply across the RPV insulation boundary. The insulation is assumed to be compressible; however, the volume occupied by the insulation is conservatively estimated as that of a hollow circular cylinder with a 4-in wall thickness and an outside diameter equal to the inside diameter of the shield wall.

The flow coefficient (C) for a particular geometry is determined as a function of the equivalent head loss coefficient (K_{eff}) for that flow system as follows:

$$C = \frac{1}{\sqrt{K_{eff}}}$$

The value of K_{eff} is simply the sum of the head losses for separate parts of the system. These head losses are defined as follows:

1. Entrance Loss or Contraction - This loss is determined as a function of the ratio of the upstream cross-sectional area to the cross-sectional area of the contraction.
2. Exit Loss or Expansion - This loss is determined as a function of the ratio of the cross-sectional area upstream of the expansion to the cross-sectional area of the expansion.
3. Resistance of Bends to Flow of Fluid - This resistance is determined by the angle and length of the bend.
4. Friction Losses - These losses, although generally very small, are calculated as an fl/d term.
5. Form Losses - These losses are due to objects in the flow path, such as grating, and are included in the vent path description tables with the friction losses. The formulas in Reference 10 are used to calculate the form losses.

The previously listed losses are defined specifically in References 10 and 11. Values for the respective components

are listed in the vent path description table for each break analyzed. The RWCU line break in the RWCU filter/demineralizer room was evaluated using the GOTHIC computer program as described earlier. As this break involves fluid which is initially highly subcooled, the analysis was performed by disabling the forced equilibrium option and enabling the drop-liquid conversion model in GOTHIC.

●→14

6.2.1.3 Mass and Energy Release Analyses for Postulated Loss of Coolant Accidents

The M3CPT and SHEX computer programs are used to calculate the mass and energy released following postulated LOCAs. These codes also calculate the containment system response as described in Section 6.2.1.1.3.7.1. For a description of the mass and energy release models incorporated by M3CPT and SHEX, see Reference 1.

The RBS mass and energy blowdown rates predicted by M3CPT (0-30 sec) and SHEX (long-term) for main steam line and recirculation suction line breaks are given in Tables 6.2, 6.2-4a, 6.2-4b, 6.2-5 and 6.2-5a. In addition, the rates are shown graphically in Figures 6.2-9, 6.2-9a, 6.2-9b, 6.2-10, and 6.2-10a.

14←●

6.2.1.4 PWR - Not Applicable

6.2.1.5 PWR - Not Applicable

6.2.1.6 Testing and Inspection

Two types of tests on the primary containment are performed: the structural acceptance test for verifying structural adequacy of the containment and drywell (Sections 3.8.2.7 and 3.8.3.7); and the tests for verifying that the containment and drywell leakage rate is within allowable limits (Section 6.2.6).

6.2.1.7 Instrumentation Requirements

The following containment parameters are monitored by redundant, safety-related instrumentation (see Fig. 6.2-73a and 6.2-73b):

1. Drywell-to-containment differential pressure
2. Containment-to-shield annulus differential pressure
3. Containment pressure
4. Suppression pool level
5. Suppression pool temperature
6. Containment and drywell area temperatures
7. Containment and drywell hydrogen concentration
8. Containment and drywell ventilation exhaust radiation.

Section 7.2 includes a description of the drywell pressure input to the RPS. Section 7.3 includes a description of containment and drywell pressure and suppression pool level inputs to the ESF systems. Suppression pool temperature monitoring and the ventilation exhaust radiation monitoring system are discussed in Section 7.6. The display instrumentation for containment parameters is discussed in Section 7.5.

6.2.2 Containment Heat Removal Systems

6.2.2.1 Design Bases

The containment heat removal function is performed by the suppression pool cooling mode (SPCM) of the residual heat removal (RHR) system and by the two safety-related containment unit coolers of the containment ventilation system. The systems utilized for post-accident containment heat removal meet the following safety design bases:

1. The systems are designed to limit the long-term bulk temperature of the suppression pool to 185°F when considering the energy additions to the containment following a LOCA, as discussed in Section 6.2.1. The minimum required availability of the containment heat removal systems is also addressed in Section 6.2.1.

2. The systems are designed such that no single failure results in the loss of the safety function.
3. The systems are designed to safety-related requirements including the capability to perform their function following a Safe Shutdown Earthquake (SSE).
4. The systems are qualified for the environmental conditions imposed by a LOCA.
5. Each active component of the systems is capable of being periodically inspected and tested during normal operation of the nuclear power plant.
6. The systems are designed to withstand the dynamic loads resulting from suppression pool hydrodynamic conditions.
7. The systems are designed as Seismic Category I, Safety Class 2.

6.2.2.2 System Design

●→10

When the residual heat removal system is in the suppression pool cooling mode, water is drawn from the suppression pool, pumped through one or both RHR heat exchangers, and returned to the suppression pool. Water from the service water system is pumped through the heat exchanger tube side to exchange heat with the suppression pool water. Two cooling loops are provided, each being mechanically and electrically separate from the other to achieve redundancy. Piping and instrumentation diagrams of the containment heat removal systems are provided in Fig. 5.4-12 and 9.4-7. The plan and elevation drawings of the containment, showing the routing of air flow guidance duct work, are given in Fig. 1.2-9 through 1.2-12. Design and performance data are given in Tables 6.2-2 and 9.4-9.

10←●

The RHR pumps are automatically initiated in the LPCI mode from diverse signals (e.g., vessel water level less than or equal to 1.0 ft above the active core or drywell pressure greater than or equal to 2 psig), and the RHR system is realigned to the SPCM by the plant operator at approximately 1,800 sec after the reactor vessel water level has been recovered. The suppression pool cooling mode of the RHR is manually initiated in loop A or B, as described in Section 7.3.1.1.7.

In the event that a single failure occurs, and the procedure which the plant operator is following does not result in system initiation, the operator places the other, totally redundant loop into operation by following the same initiation procedure. Manual actions are discussed in Section 5.4.7.

•→10 •→7

Each RHR pump takes suction directly from the suppression pool, which does not have a sump. To prevent foreign objects in the suppression pool from entering the ECCS flow path, strainers are located on the RHR suction lines in the suppression pool as shown on Fig. 6A.16-1 and 6A.16-2. The stainless steel strainers extend horizontally from the suction piping at a centerline elevation as follows: RHR "C" is at a centerline of 76' 8 1/4"; RHR A/B are at a center elevation of 75' 4 3/4". The suppression pool floor is at an elevation of 70' 0". The strainer fabrication uses a perforation and/or mesh size of 0.0937 in (3/32 in). The most restrictive component dimension supplied with coolant from the suppression pool is the orifice upstream of the cyclone separators for the RHR pump seals at 0.136 inches. A 0.136 inch particle would be the maximum diameter particle for the ECCS suction strainers to pass.

7←•

Although the suppression pool water quality is monitored and controlled, debris resulting from accident conditions may be postulated to enter the containment side of the suppression pool. To ensure that system function is maintained, the strainers are oversized to minimize pressure drop and flow velocities as the strainer removes suspended debris and becomes partially clogged. The strainer's flow area is a minimum of 200 percent of the suction line flow area.

The fully loaded strainer head loss is ≤ 9.0 ft. The NPSH margin left after accounting for debris, piping, fittings and clean strainer head losses is ≥ 4.0 ft.

10←•

The RHR pump suction strainers located in the containment suppression pool meet the following safety design bases:

1. The strainers are designed to prevent the introduction of objects with diameters greater than 0.094 in into the RHR pump seal cyclone separators.

•→10

2. Adequate net positive suction head to the RHR pumps is provided under design debris loading conditions.
3. The strainers are designed to withstand any loads during suppression pool transients, such as temperature, pressure, and water level.

10←•

THIS PAGE LEFT INTENTIONALLY BLANK

•→10

All strainers and their supports are seismically qualified. The possibility of debris bypassing the strainers has been precluded.

10←•

4. The strainers are designed to accommodate hydrodynamic loads as specified in NUREG-0978. Hydrodynamic loads are further discussed in Appendix 6A.
5. The strainers are designed to permit testing, in conjunction with the periodic RHR testing, to demonstrate strainer operability.

The following types of insulation are used for piping and equipment within the drywell and containment:

1. For piping and equipment which require insulation to minimize heat loss and are located within the drywell, metal-reflective or fiberglass insulation totally encapsulated in fiberglass cloth is used. Two other types of insulation are also used inside the drywell (when the temperature exceeds 150°F) for special and limited application, i.e., "Min-k" insulation and "Temp-Mat" insulation.

Reactor bottom head and the drywell-to-containment penetration metal-reflective insulation is an all-metal construction-type insulation which has a stainless steel inside and outside jacket which encapsulates multiple layers of stainless steel or aluminum insulation material.

Encapsulated fiberglass insulation may consist of high temperature fiberglass panel, flexwrap, or pipe covering, which is totally encapsulated in fiberglass cloth. Once installed, the insulation is encased with a stainless steel jacket.

"Min-k" is a powder-type insulation used where space is limited and is encapsulated so as to be watertight using a silicone impregnated fiberglass cloth.

"Temp-Mat" is a borated, spun glass, blanket-type insulation used where it is necessary to lower the neutron flux, i.e., at the primary shield wall penetration, and is also encapsulated in fiberglass cloth.

2. Stainless steel-jacketed foamed plastic insulation is used in cases where sweating of cool pipes could occur.
3. Metal-jacketed fiberglass insulation is used for hot piping and equipment outside of the drywell.

Metal-reflective insulation is installed in sections with overlapping edges secured with sheet metal screws. Fiberglass insulation is installed in sections and secured with self-adhering tabs or impaled on insulation pins. Metal-jacketed fiberglass insulation is installed in sections and secured with wire or metal bands. Metal-jacketed foam plastic antisweat insulation is installed in sections and secured with a contact-type adhesive. Metal jacketing is installed over pipe insulation in approximately 3-ft overlapping sections with metal bands, self taping screws, or quick release latches with keepers.

The mechanism for transport of any insulation debris from the drywell into the containment side of the suppression pool following an accident involves a series of unlikely occurrences, as discussed below.

●→10

In the event of a postulated pipe break (LOCA), insulation from a relatively large zone of influence is assumed to be removed by jet impingement. Some of this debris will be transported into the suppression pool during the initial blow-down of air and steam. An additional quantity of the debris will be small enough to bypass the meshes and gratings, to flow into the pool formed by the drywell floor and the weir wall. Due to the drywell turbulence, a fraction of this debris is assumed to be transported by break flow over the wier wall into the suppression pool. The insulation debris which reaches the suppression pool could then be transported to the ECCS suction strainers, and thereby, increase the strainer head losses. The optimized stacked-disk suction strainers are conservatively designed to process the insulation and other miscellaneous debris which may be present in the suppression pool following a LOCA. The strainer design complies with Regulatory Guide 1.82, Revision 2, Criteria C.2.2 and C.2.3, and satisfies Option 1 of NRC Bulletin 96-03.

The suction strainer design analysis conservatively assumes that (1) only 3 of the 5 ECCS pumps are available (i.e., a Division 1 or Division 2 diesel generator failure), (2) 600 ft³ (1800/3ft³) of fiberglass insulation is transported to each strainer, (3) 167 lbs. (500/3lbs) of corrosion products debris, and (4) 50 lbs (150/3lbs) of dirt and dust, (5) 28.3 lbs (85/3lbs) of paint, (6)16.7 (50/3lbs) of rust, and (7) bulk suppression pool temperature of 185°F. For all three ECCS pump types (HPCS, LPCS, & LPCI) the minimum NPSH margin remains at least 4 feet, which is greater than the NPSH values for the ECCS - core coolant flows assumed in the safety analyses.

10←●

●→10

10←●

●→7

The containment unit coolers are automatically initiated on high drywell to containment differential pressure with an interlock to delay initiation until 10 minutes after the high drywell pressure signal. The 10-minute delay minimizes the short-term break load on the standby diesel generators. Automatic initiation is provided to protect the containment in the event of suppression pool steam bypass leakage, as described in Section 6.2.1.1.3.4.

7←●

Two of the three containment unit coolers are safety related. The coolers are sized for normal operating conditions and normally are supplied with coolant from the chilled water system. During an accident, standby service water is used for cooling water. One containment unit cooler is powered from the Division I standby bus and one from the Division II standby bus. Thus, at least one containment unit cooler is available if any one standby diesel generator fails to start. Cooling water is supplied from the standby service water system (Section 9.2.7) at a maximum of 95°F and at a flow rate through each containment unit cooler of 540 gpm.

On this basis, the containment unit coolers supplement the condensing capability of the passive heat sinks and provide an active means for condensation of steam in the unlikely event that a direct path for steam bypass of the suppression

pool exists after a LOCA. The containment unit coolers are not required to mitigate the effects of a LOCA except in the case of steam bypass.

Seismic supports are used to maintain the integrity of the ductwork during an SSE. Codes and standards used for design purposes are addressed in Sections 5.4.7 and 9.4.6. Environmental qualification of the containment heat removal systems is discussed in Section 3.11.

6.2.2.3 Design Evaluation

The design basis accident (DBA) for containment pressure and also for the containment heat removal system is a double-ended rupture (DER) of a recirculation pump suction line, which, in the long-term, is similar to the DER of a main steam line, described in detail in Section 6.2.1.1.3.1. In the event that such an accident occurs, the short-term (prior to actuation of the RHR heat exchangers) energy released from the reactor coolant system will be absorbed by the suppression pool, and the suppression pool temperature will increase, as discussed in Section 6.2.1.1.3.1.

In the long-term, fission product decay heat continues to be absorbed by the suppression pool. Unless this energy is removed from the suppression pool, an unacceptably high containment pressure eventually results. The suppression pool cooling mode of the RHR system is used to remove heat from the suppression pool and to limit the long-term, post-LOCA containment internal pressure and suppression pool temperature to less than 15 psig and 185°F, respectively.

In order to evaluate the adequacy of the RHR system, the following sequence of events is assumed to occur:

•→14

1. With the reactor initially at 100.3 percent of rated thermal power (3100 MWt), a recirculation pump suction line DER occurs.

14←•

2. A loss of offsite power occurs and one standby diesel generator fails to start and remains out of service during the entire transient. This is the most limiting single failure.
3. Only three ECCS pumps are functional following the postulated loss of offsite power and standby diesel generator failure. The Division II standby diesel generator supplying two of the LPCI pumps is assumed to have failed, so that the three operating

pumps serve the LPCS, LPCI, and the HPCS. Section 6.3 describes the ECCS equipment.

4. After 30 minutes, the plant operators actuate the RHR heat exchanger in the active suppression pool cooling loop in order to start containment heat removal.

Once the suppression pool cooling mode has been established, no further operation action is required.

• →4

When calculating the long-term, post-LOCA containment pressure and suppression pool temperature, it is assumed that the initial suppression pool and RHR standby service water temperature are at 100°F and 95°F, respectively. This assumption maximizes the heat sink temperature to which the containment heat is rejected and thus maximizes the suppression pool temperature and containment pressure responses.

In addition, the RHR heat exchanger and containment unit cooler are assumed to be in a fully fouled condition during the transient. This is also conservative since it minimizes their heat removal capability. The overall heat transfer coefficient for the RHR heat exchanger which is input to the containment heat removal evaluation includes a tube side fouling resistance of 0.001 hr-ft²-°F/Btu and a shell side fouling resistance of 0.0005 hr-ft²-°F/Btu. The containment unit cooler heat transfer coefficients supplied by the manufacturer are modified to include a tube side fouling resistance of 0.0005 hr-ft²-°F/Btu.

Analysis for containment heat removal capability is done with SHEX as discussed in Section 6.2.1. The resultant containment pressure and temperature responses are described in Section 6.2.1.1.3.1 and shown on Fig. 6.2-5 and 6.2-7. Even with the very degraded conditions outlined above, the peak containment pressure does not exceed the containment design pressure of 15 psig and the peak pool temperature does not exceed the design pool temperature of 185°F. The failure modes and effects analyses for both of the containment heat removal systems (RHR and the containment unit coolers portion of the reactor plant ventilation system) are provided in the FMEA document.

14←•

The available NPSH for the RHR pumps is calculated based on the regulatory position of Regulatory Guide 1.1 as shown in Section 6.3.2.2.

When the RHR system is in the suppression pool cooling mode, the pump draws water from the suppression pool, passes it through the RHR heat exchanger, and returns it to the suppression pool. By the time the RHR system is switched to the suppression pool cooling mode, enough water has spilled from the reactor to flood the drywell floor above the weir wall, thus establishing a closed flow path back to the suppression pool.

The general arrangement of the closed flow path is shown on Fig. 6.2-56 and 6.2-57. This general arrangement results in adequate mixing in the suppression pool in the following ways. Mixing is promoted in the drywell when the water flowing from the reactor is mixed as the level rises above the drywell floor. The water is then equally distributed to all quadrants of the suppression pool as it flows over the weir wall. To promote circumferential mixing in the suppression pool, the return lines for the RHR A and B pumps are located remotely from the suction lines.

The return lines are also separate from each other. To promote radial mixing of the suppression pool, the suction lines are located near the suppression pool outer diameter and the weir wall overflow is located at the suppression pool inner diameter. To promote vertical mixing, the return lines (colder water) are located near the surface of the suppression pool and the suction lines (hotter water) are located near the suppression pool bottom. At a flow rate of 5,050 gpm, the entire suppression pool volume of about 10^6 gal is circulated at least 7 times per day. This recirculation rate and the provisions for mixing result in adequate mixing of the suppression pool volume. To prevent foreign objects in the suppression pool from entering the flow path, strainers are provided on the suction lines in the suppression pool.

Figures and tables showing the calculated performance of the following variables as functions of time following occurrence of a design basis LOCA, assuming minimum safeguards are provided:

1. Containment pressure on Fig 6.2-5.
2. Containment and suppression pool temperatures on Fig. 6.2-7.
3. RHR heat exchanger duty on Fig. 6.2-19.
4. The integrated energy content of the containment atmosphere and recirculation water in Table 6.2-9.

5. The integrated energy absorbed by the structural, passive heat sinks and removed by the containment unit cooler and/or RHR heat exchanger in Table 6.2-9.
6. The heat removal rate of the containment unit cooler on Fig. 6.2-21.

6.2.2.4 Tests and Inspections

Testing and inspection of the containment heat removal systems are performed periodically during normal plant operation and after each plant shutdown. Functional testing is performed on all active components and controls. The system reference characteristics will be established during preoperational testing to be used as base points for checking measurements obtained from the system tests during normal plant operation.

A design flow functional test of the RHR main system pumps is performed for each pump during normal plant operation by taking suction from the suppression pool and discharging through the test line back to the suppression pool.

Each pump is tested individually for flow and pressure measurements while the other pumps remain on standby for emergency core cooling. The discharge valves to the feedwater system and injection nozzles remain closed during this test.

RHR heat exchangers are checked for effectiveness by measuring inlet and outlet temperatures at the tube and shell sides. Also, samples of the process water are taken from the line downstream of each heat exchanger, in order to check the conductivity of the water.

All motor- and air-operated valves required to operate to perform safety-related functions are capable of being exercised periodically during normal power operation. The layout and arrangement of critical equipment, such as drywell wall penetrations, piping, and valves, are designed to permit access for appropriate equipment used in testing and inspecting system integrity.

Periodic inspection and maintenance of the RHR main system pumps, pump motors, and heat exchangers are conducted in accordance with the manufacturer's instructions to ensure reliable system performance.

During normal plant operation, the pumps, heat exchangers, valves, piping, instrumentation, wiring, and other components inside and outside the containment can be inspected visually at any time. Testing frequencies are generally correlated with testing frequencies of the associated controls and instrumentation. When a pump or valve control is tested, the operability of that pump or valve and its associated instrumentation is tested by the same action. When a system is tested, operation of the components is indicated by installed instrumentation. Relief valves are either removed for bench tests and setting adjustments or tested in place for setpoint verification, as scheduled, at refueling outages.

●→14

Operational sequencing of the LPCI mode of the RHR system is tested after the reactor is shut down and the RHR system has been drained and flushed.

14←●

Further information on the testing and inspection of the components of the containment heat removal systems may be found in Sections 5.4.7.4, and 9.4.6.4 and in Chapter 14.

6.2.2.5 Instrumentation Requirements

The details of the instrumentation are provided in Sections 7.3.1.1.6, 7.3.1.1.7, and 9.4.6.5.1. The suppression pool cooling mode of the RHR system is manually initiated from the main control room.

●→14

6.2.3 Secondary Containment and Fuel Building Functional Design

●→8

The secondary containment consists of the shield building and the auxiliary building. The secondary containment and fuel building are provided with leakage and filtration systems and is subjected to individual tests in accordance with the procedures specified in the Technical Specification/Requirements Manual. The secondary containment and fuel building structures house the refueling equipment, safety-related equipment required for safe shutdown of the plant, and equipment, components, piping, cables, and instrumentation necessary for power generation. The secondary containment and fuel building are of Seismic Category I design. Refer to Section 3.8.4 for a discussion of secondary containment and fuel building structural design. The containment/drywell purge system (Section 9.4.6) is provided for purging the containment and drywell volumes during normal operation and shutdown. The annulus (shield building primary containment annulus) pressure control system (Section 9.4.6) maintains the annulus at negative pressure during normal operation. The standby gas treatment system (SGTS) (Section 6.5) maintains the annulus and auxiliary

8←● 14←●

• -14

building at a negative pressure and provides cleanup of the potentially contaminated annulus and auxiliary building volumes during high radiation conditions and following a design basis accident (DBA). The fuel building charcoal filtration system (Section 9.4.2) maintains the fuel building at negative pressure and filters the effluent following a fuel handling accident (FHA) and during high radiation conditions.

6.2.3.1 Design Bases

1. The secondary containment, in conjunction with the operation of the SGTS, is designed to limit the thyroid dose and the whole body dose to within the guidelines of 10CFR50.67 at the site boundary and the low population zone, and the main control room operator doses during a DBA. Amendment 132 revised the design basis accident main control room dose limit requirements to incorporate the limits of 10CFR50.67. The limits of 10CFR50 Appendix A, General Design Criteria 19, also remain applicable to the RBS design basis.

The primary function of the SGTS is to maintain a negative pressure in the annulus and auxiliary building and to process potentially contaminated air from the annulus. It is also designed to process exhaust air from the auxiliary building shielded compartments (Section 9.4.3) in the post-accident mode and from the containment/drywell purge system during normal operation for fast entry.

2. The secondary containment, in conjunction with the operation of the SGTS, is designed to achieve and maintain an external post-LOCA pressure of at least -1/2 in W.G. in the annulus and at least -1/4 in W.G. in the auxiliary building relative to the outside atmosphere, and prevents exfiltration at wind speeds less than or equal to 17.5 mph.

14←•

3. The secondary containment is designed to provide a dilution and holdup volume for fission products which may leak from the primary containment following a postulated accident.

4. The secondary containment is designed and constructed in accordance with the structural design criteria presented in Section 3.8.4, and provides for low leakage during reactor operation.

•→14 •→10

5. The fuel building is designed and constructed in accordance with the structural design criteria presented in section 3.8.4. The fuel building in conjunction with the HVF system are designed to maintain an internal fuel building pressure of - 1/4 in W.G. during movement of recently irradiated fuel and to limit the off site dose of a FHA to well within 10CFR50.67 limits. [Amendment 132 revised the design basis accident offsite dose limit requirements from 10CFR100 to 10CFR50.67.](#)

10←• 14←•

6. The main steam positive leakage control system controls and minimizes the fission products which could leak through the main steam isolation valves and main steam drain lines that terminate in untreated areas.
7. The secondary containment isolation signals, isolation valves for the ventilation systems, the SGTS, the fuel building charcoal filtration system, and the annulus mixing system are all designed to Seismic Category I requirements and powered from emergency power buses.

•→14

8. The secondary containment and fuel building are designed to permit periodic inspections and functional tests of all penetrations (including automatic isolation).

6.2.3.2 System Design

The secondary containment consists of the shield building and the auxiliary building. The fuel building has similar construction as secondary containment, but is not considered part of secondary containment. The boundary region of the secondary containment and the fuel building is shown on the following figures:

14←•

<u>Figure</u>	<u>Title</u>
1.2-9 through 1.2-12	General Arrangement Reactor Building Plans and Sections
1.2-13 through 1.2-19	General Arrangement Auxiliary Building Plans and Sections
1.2-20 through 1.2-23	General Arrangement Fuel Building Plans and Sections

•→14

A tabulation of the design and performance data of the secondary containment and fuel building structures are given in Tables 6.2-32, 6.2-33, and 6.2-34. Codes and standards used in the design of the secondary containment and fuel building are listed in Section 3.8.4.

The performance objective of the secondary containment is to provide a volume which can be used to hold up, filter, and dilute fission products that might otherwise leak to the environment following a DBA. The exhaust air required to maintain the negative pressure in the annulus and auxiliary building is discharged through the SGTS charcoal filter train(s). The exhaust air required to maintain a negative pressure during a fuel handling accident in the fuel building is discharged through the fuel building charcoal filtration system.

In order to minimize the amount of radioactive material that leaks to the secondary containment following a DBA, all primary containment penetrations are provided with redundant, ASME, Section III, Class 2, Seismic Category I isolation valves in accordance with General Design Criteria (GDC) 54, 55, 56, and 57. The containment isolation system is discussed in Section 6.2.4. The program for leakage rate testing of the primary containment structure and containment components is described in Section 6.2.6.

14←•

The secondary containment structure, in conjunction with the following systems, provides the means of controlling and minimizing leakage from the primary containment to the environment.

6.2.3.2.1 Standby Gas Treatment System

Regulatory Guide 1.52 is used as a basis of design for the SGTS. See Table 6.5-1 for a compliance summary. For a detailed description of the SGTS components and the SGTS fission product removal capability, see Section 6.5 and Fig 6.2-58.

The configuration of the SGTS filter trains is shown on Fig. 1.2-14, and design data of principal components is listed in Table 6.5-2. The SGTS consists of two identical 100 percent, parallel, physically separated air filtration assemblies (filter trains) of 12,500 cfm design capacity. Each assembly is capable of handling the design cfm flow rates. Each exhaust fan is capable of delivering 12,500

●→13

cfm. During normal operation, the annulus pressure control system maintains the annulus at negative pressure (Section 9.4.6). The SGTS also serves as a backup non-ESF system to the annulus pressure control system (APCS) during normal operation. Upon loss of the APCS, a high radiation signal from one of two radiation monitors located in the annulus airstream, or an ESF signal (i.e., LOCA), the annulus air and air from the shielded compartments in the auxiliary building are automatically diverted through the SGTS filter train.

13←●

If the SGTS filter trains are not treating the annulus atmosphere or the exhaust air of the shielded compartments in the auxiliary building, the containment and drywell purge can be manually diverted through both SGTS filter trains. By utilizing both SGTS filter trains, a maximum of 25,000 cfm of containment/drywell purge air can be processed by the filter trains (Section 9.4.6).

●→14

The SGTS is designed to maintain a negative pressure of at least -0.50 in W.G. in the annulus during post-LOCA operation. With the annulus at a negative pressure, any potential leakage is directed inward (away from the shield building). Therefore, if a primary containment DBA occurs, airborne radioactivity which exfiltrates the steel primary containment is collected and passed through a filter train of the SGTS before being released.

14←● ●→10

Potential paths exist for bypass of the annulus mixing system and the SGTS. Potential leakage paths and measures taken to mitigate their consequences are discussed in Sections 6.7. The inleakage rates for the MS-PLCS valves are provided in the Technical Specifications, and discussed in Section 6.7.5.

●→12

Since the annulus and the auxiliary building are exhausted via the SGTS filter train following a LOCA, the only leakage considered to bypass the SGTS is that which leaks to areas other than those previously mentioned. This would be from systems listed in Table 6.2-40 with leakage classification listed as SCB.

12←●

The primary containment and penetration valve leakage are monitored during the periodic tests of the containment and during the tests to measure local leakage, as discussed in Section 6.2.6.

10←●

The integral welded design of the guard pipes precludes leakage from the drywell into the containment portion of the main steam tunnel (see Fig. 3.8-4 for the sleeved penetration design). The electrical penetrations in the primary containment can leak only into the annulus and this leakage is treated by the SGTS.

The maximum inleakage rate across the shield building barrier when the annulus is at a pressure of -3 in W.G. is 2,000 cfm. During normal operation, the annulus inleakage approximately equals the exhaust capability of the annulus pressure control system. The exhaust air is not diverted through the SGTS unless it is radioactive. If the leak rate is actually less than 2,000 cfm, the initial pressure is at a value lower than -3 in W.G. (e.g., -4 in W.G.).

●→13

Two full-capacity SGTS exhaust fans are provided, each powered by a separate standby diesel generator. The DBA is assumed to occur with the annulus at its maximum normal operating conditions, namely, -3 in W.G. and 2,000 cfm inleakage. If a DBA occurs along with loss of offsite power and assuming the single failure of a standby diesel generator, the SGTS fan will reach rated speed within 48 seconds (i.e., 10 seconds diesel start time, plus 30 seconds until SGTS is loaded, and 8 seconds for the fan to get up to speed.). The design flow rate of the SGTS in the post-accident mode is 12,500 cfm, which is equal to the maximum estimated flow rate being exhausted from the annulus and the shielded compartments in the auxiliary building during a DBA.

13←●

6.2.3.2.2 Annulus Mixing System (Disabled)

●→14 14←●

6.2.3.2.3 Fuel Building Charcoal Filtration System

●→14

The fuel building charcoal filtration system is designed to limit the release of airborne radioactivity to the environment and maintain the building at a pressure of at least -0.25 in W.G. following a fuel handling accident. Regulatory Guide 1.52 is used as a basis of design for the fuel building charcoal filtration system. See Table 6.5-1 for a compliance summary. For a detailed description of the fuel building charcoal filtration system and its components, see Section 9.4.2.

14←●

●→10

6.2.3.2.4 Deleted

10←●

6.2.3.2.5 Main Steam Positive Leakage Control System

●→14

The main steam positive leakage control system is designed to prevent the release of fission products from the main steam isolation valves and main steam drain lines which could bypass the SGTs after a design basis LOCA. This is accomplished by two independent inboard and outboard systems. For a detailed description of operating modes and components, see Section 6.7.

14←●

6.2.3.2.6 Potential Bypass Leakage Paths

●→10

Penetration 1KJB*Z35 (valves 1DFR*AOV101 and 1DFR*AOV102) is considered a potential bypass leakage path since the reactor building floor drain (DFR) discharge line terminates in the radwaste building. Similarly, penetration 1KJB*Z38 (valves 1DER*AOV126 and 1DER*AOV127) is considered a potential bypass leakage path, since the reactor building equipment drain (DER) discharge lines terminate in the turbine and radwaste buildings. The DER and DFR lines are both seismically supported inside containment and are protected against the effects of pipe whip and jet impingement. Therefore, these lines are not postulated to crack or break, and a bypass leakage path through the pipe is not postulated due to a pressure boundary failure. Additionally, these lines originate in the drain sumps located in the bottom of the drywell, which are flooded by the water released during a LOCA, thereby establishing a water seal at the point of origin of these lines.

10←●

All other process lines that penetrate the containment that could act as a containment bypass leakage path following a

●→10

containment isolation due to a LOCA are controlled by the main steam-positive leakage control system (MS-PLCS) or the standby gas treatment system (SGTS). For the postulated post-LOCA leakage paths to the outside atmosphere, see Table 6.2-39.

10←● ●→14

6.2.3.2.7 Openings to Secondary Containment and the Fuel Building

●→5

Openings leading to the secondary containment and the fuel building are equipped with alarms. Doors leading to the secondary containment have alarm capability to the security areas in the normal switchgear buildings and primary access point (PAP) facility, which are manned 24 hr a day by security personnel.

5←●

6.2.3.3 Design Evaluation

The SGTS maintains the secondary containment at a negative pressure with respect to environment following a design basis LOCA, ensuring that any leakage from the primary containment to secondary containment does not escape to the environment.

The SGTS and fuel building charcoal filtration system incorporate two 100 percent capacity exhaust fans. The redundant fans and dampers are connected to separate standby buses which are capable of being supplied from either normal or standby power sources. The two redundant, full capacity filter trains of the SGTS ensure that no fission products released into the secondary containment escape directly to the environment. Temperature monitors and differential pressure gauges warn of filter failure. All equipment is designed to Seismic Category I, Safety Class 2 and 3 criteria and is housed in Seismic Category I structures. The equipment is located in areas accessible to maintenance personnel.

The fuel building filtration system incorporates two 100 percent capacity exhaust fans. The redundant fans and dampers are connected to separate standby buses which are capable of being supplied from either normal or standby power sources. This system is not required to mitigate the consequence of a LOCA. The fuel building filtration system does ensure that any fission products released during a FHA involving recently irradiated fuel is not released directly to the environment. All equipment is designed to Seismic Category I, Safety Class 2 and 3 criteria and is housed in Seismic Category I structures. The equipment is located in areas accessible to maintenance personnel.

14←●

Radiation monitors are provided in the annulus exhaust duct to continuously monitor the radiation level of the discharged air. During normal operation, the annulus is exhausted through the annulus pressure control system. However, the annulus exhaust is automatically lined up to the standby gas treatment system, upon the following contingencies:

1. Occurrence of high-high radiation in the annulus exhaust air.
2. Receipt of the high drywell pressure, or low reactor water level signal, or both.

Provisions are made to enable the main control room operators to manually divert the annulus exhaust through the standby gas treatment system.

•→14

The contaminated air from the shielded compartments in the auxiliary building is exhausted through the SGTS filter train, thereby precluding any potential release of contaminated air from the auxiliary building in excess of 10CFR50.67 limits.

14←•

The system controls also have capability for manual actuation of the SGTS filter trains. The required alignment of system dampers and startup of the SGTS are discussed in Section 7.3.

All equipment is designed to meet Seismic Category I requirements and is housed in a Seismic Category I structure. Equipment is located in areas accessible to maintenance personnel.

Radiation monitors are also provided in the fuel building exhaust duct to continuously monitor the radiation level of the discharged air. During normal operation, the fuel building is exhausted through normal exhaust system. However, the exhaust system is automatically lined up to the charcoal filtration system, upon the following contingencies:

1. Occurrence of high-high radiation in the exhaust air.
2. Receipt of the high drywell pressure, or low reactor water level signal, or both. For a detailed safety evaluation of fuel building charcoal filtration system, see Section 9.4.2.

•→14

The results of the post-LOCA pressure response of the secondary containment system are shown on Fig. 6.2-61a and 6.2-61b for the annulus and auxiliary building, respectively. Initial conditions for these analyses are listed in Table 6.2-32.

14←•

The assumptions used in the pressure transient analysis for the annulus and the auxiliary building are as follows:

1. External wind speed is zero.
2. Offsite power is lost simultaneously with LOCA.
3. The single active failure is the failure of one standby diesel generator to start.
4. System frictional pressure losses are 21.5 in W.G. at 12,500 cfm flow.
5. The SGTS centrifugal exhaust fan characteristic is shown on Fig. 6.2-59.

•→14 •→10

6. The annulus exhaust rate at a 21.5 in W.G. pressure loss is 2,500 cfm and the auxiliary building exhaust rate is 6,300 cfm, with the SGTS exhaust fan operating at 48 sec.

•→13

Results of the analysis of the annulus and the auxiliary building indicate that a pressure of -0.25 in W.G. is attained in 216 and 102 sec, respectively. A bounding value of 1800 seconds is used to determine the post-LOCA dose consequences (See Section 15.6.5).

10←• 13←• 14←•

•→14 •→13

14←• •→10

Fig. 6.2-61a indicates that there is a period following a LOCA during which a gauge pressure greater than -0.25 in W.G. exists in the annulus. This period begins approximately 20.5 sec after the LOCA and lasts for approximately 195.5 sec. The dose rate analysis during this period indicates that release of contaminated air from the secondary containment is within the limits of 10CFR50.67. Amendment 132 revised the design basis accident offsite dose limit requirements from 10CFR100 to 10CFR50.67.

10←• 13←• •→14

The amount of heat transferred to the secondary containment atmosphere (annulus) has no detrimental effect, since no safety equipment is located inside the annulus. No heat transfer is assumed to the environment. The walls of the shield building are reinforced concrete, 2'-6" thick, and do not offer a contribution of heat into the auxiliary building during the transient. The analysis for the drawdown time considered all possible heat loads inside the auxiliary building. The cubicles containing equipment (e.g., the ECCS pumps and heat exchangers) that operate during post-LOCA operations are provided with recirculation-type-unit coolers. The unit coolers have been conservatively designed to remove the heat at the rate at which it is being generated during full operation of the equipment.

A bounding time-dependent heat load is determined for input to the auxiliary building analysis based on the assumption that a LOCA coincident with a loss of off-site power occurs, all equipment which is supplied divisional power is operating. Heat removal by the safety related unit coolers is assumed to occur once power is supplied to both the unit cooler fans and the standby service water system. The single failure assumption is that one train of SGTS is assumed to fail. The resulting net positive heat load is provided in Table 6.2-32.

•→13 13←• 14←•

6.2.3.4 Tests and Inspection

Tests and inspections of the containment isolation system are discussed in Sections 6.2.4, 6.2.6, and 7.3.1. Tests and inspections of the SGTS and fuel building charcoal filtration system are discussed in Sections 6.5 and 9.4.2, respectively. Primary containment leak rate testing is discussed in Section 6.2.6.

•→8

Containment isolation system SGTS, and fuel building charcoal filtration system preoperational testing is discussed in Section 14.2. Doors and hatches are provided with sufficient instrumentation and/or administrative controls to assure that they are normally closed and have no adverse impact on the operation of the SGTS or the fuel building charcoal filtration system. Periodic testing of SGTS, charcoal filter units and secondary containment, including drawdown time, will be performed as indicated in the Technical Specifications/ Requirements Manual.

●→14 ●→13

13←● 14←●

6.2.3.4 Tests and Inspection

Tests and inspections of the containment isolation system are discussed in Sections 6.2.4, 6.2.6, and 7.3.1. Tests and inspections of the SGTS and fuel building charcoal filtration system are discussed in Sections 6.5 and 9.4.2, respectively. Primary containment leak rate testing is discussed in Section 6.2.6.

●→8

Containment isolation system SGTS, and fuel building charcoal filtration system preoperational testing is discussed in Section 14.2. Doors and hatches are provided with sufficient instrumentation and/or administrative controls to assure that they are normally closed and have no adverse impact on the operation of the SGTS or the fuel building charcoal filtration system. Periodic testing of SGTS, charcoal filter units and secondary containment, including drawdown time, will be performed as indicated in the Technical Specifications/ Requirements Manual.

8←●

In order to maintain uniform negative pressures in the secondary containment structures, exhaust rates are properly apportioned in various areas. Preoperational testing includes system airflow balancing to assure proper flow distribution for uniformity of negative pressure. The pressure sensors monitoring the annulus and auxiliary building pressure are located in the auxiliary building.

6.2.3.5 Instrumentation Requirements

Refer to Section 6.5.1.5 for a description of the instrumentation for the SGTS. Design details and logic of the SGTS are described in Section 7.3.1.1.4.

Section 9.4.6 describes the instrumentation for the containment/drywell purge system, annulus pressure control system, and the annulus mixing system. Design details and logic of the annulus mixing system are described in Section 7.3.1.1.6.

Refer to Section 9.4.2.5 for a description of the instrumentation for the fuel building charcoal filtration system.

Section 9.3.6.5 describes the instrumentation for the penetration valve leakage control system. Design details

and logic of the penetration valve leakage control system are described in Section 7.6.1.6.

Section 6.7.4 describes the instrumentation for the main steam positive leakage control system. Design details and logic of the MS-PLCS are described in Section 7.3.1.1.3.

6.2.4 Containment Isolation System

The containment isolation system (CIS) has isolation provisions to assure conformance to General Design Criteria (GDC) 54, 55, 56, and 57 for preventing or limiting the escape of fission products that are present in the primary containment after a LOCA.

6.2.4.1 Design Bases

6.2.4.1.1 Safety Objective

The purpose of the CIS is to prevent the release of significant amounts of radioactive materials from the fuel, the reactor coolant pressure boundary (RCPB), and the steel primary containment by automatically isolating appropriate lines in the nuclear steam supply system (NSSS), auxiliary systems, and support systems which penetrate the primary containment.

The CIS is automatically actuated when monitored system variables exceed pre-established limits. It is neither necessary nor desirable that every containment isolation valve close simultaneously upon a containment isolation signal. Pre-determined plant design allows selected valves in those systems which are essential to mitigate the effects of an event to remain in or move to their open positions.

The governing conditions for containment isolation are presented in Section 7.3.1 in discussions of initiating circuits, isolation functions and settings, logics, and redundancy. Section 7.3.1.1.2 presents a discussion of variables which input to the containment and reactor vessel isolation control system (CRVICS) logics for reactor vessel, drywell, and containment isolation.

The CIS isolates fluid penetrations of systems not required for emergency operation. Valves attached to penetrations supporting engineered safety feature (ESF) systems are remote manual actuation and are capable of being operated from the main control room. The pre-selected containment isolation valves close upon receipt of an isolation signal.

Isolation signals for each valve are specified in Table 6.2-40.

The leakage detection system detects possible leakage from lines inside/outside containment and provides the operator in the main control room with information required to isolate fluid systems equipped with remote manual isolation valves. Parameters used to detect leakage are high radiation, high area temperature, high sump level, and reactor pressure vessel level and pressure, as discussed in Sections 5.2.5.1.3, 7.6.1.2, and 12.3.4.1. System parameters such as flow, pressure, and temperature are indicated and/or alarmed in the main control room. These enable the operator to detect degraded system performance attributable to system leakage and take appropriate action to isolate systems that are potential leakage paths.

The only exception to this is the chilled water and standby service water system piping associated with the containment unit coolers inside the containment, which do not have leak detection capabilities. However, during an accident any leakage through these penetrations would flow into the containment since the pressure in the service water system at the penetration during normal and degraded modes of operation is greater than the calculated peak containment pressure. Therefore, it is not possible for containment atmosphere to leak outside the containment.

6.2.4.1.2 Identification of Safety Criteria

The piping systems which penetrate the primary containment are designed with capabilities for leak detection, isolation, and valving arrangements which satisfy the requirements of General Design Criteria 54, 55, 56, and 57. The capability of testing isolation valve operability as well as the means to determine leakage rates of containment isolation valves is considered in valve selection and piping configurations. Redundancy and physical separation are provided in the mechanical design to ensure that no single failure in the CIS prevents the system from performing its design function.

Compliance with other Regulatory Guides is described in Section 1.8. The containment isolation valves and systems conform to the guidelines of Regulatory Guide 1.141.

The containment isolation valves and system piping, including the penetrations within the primary containment boundary, are classified as Seismic Category I. Qualification and documentation procedures used for Seismic

Category I equipment and systems are identified in Sections 3.10A and 3.10B.

The containment isolation valves are designed to ASME Code Section III, Class 1 or 2 as applicable. Valves, other than manually or process operated, are designed to fulfill their system-intended functions while meeting applicable sections of 10CFR50.67 and industry codes. [Amendment 132 revised the design basis accident offsite dose limit requirements from 10CFR100 to 10CFR50.67.](#)

A discussion of associated instrumentation and control equipment design for containment isolation valves is presented in Section 7.3.

Protection from damage due to missiles and dynamic effects of pipes is described in Sections 3.5, 3.6A, and 3.6B.

6.2.4.2 System Design

Fig. 6.2-63 through 6.2-65 schematically represent the valve information summarized in Tables 6.2-35 through 6.2-38 of Sections 6.2.4.3.1 through 6.2.4.3.4. These figures show the containment isolation valve locations relative to the primary containment.

Table 6.2-39 describes two phases of postulated post-LOCA leakage paths to the environs. Phase I concerns systems containing no leakage control system. This phase includes drain systems and ventilation purge systems. The drain system lines are permanently routed to a drain sump, and the lines and sump are normally kept filled with water.

●→10

Phase II concerns systems provided with a leakage control system. Phase II contains only the main steam lines system. Additional details regarding the main steam positive leakage control system are given in Section 6.7.

10←●

Table 6.2-40 provides design information relative to containment isolation provisions for fluid systems lines and fluid instrument lines penetrating the primary containment including containment penetration numbering by sequence. Note that not all of the containment penetrations have their penetrations going through the steel primary containment.

In addition to providing isolation capabilities for all fluid lines penetrating the primary containment, isolation valving is provided for lines which penetrate the drywell only. For lines which comprise part of the RCPB, this

•→10

valving is provided to isolate the reactor pressure vessel (RPV) and to minimize the possibility of direct blowdown to the containment in case of the unlikely event of pipe rupture. For lines which communicate with drywell free space and have the potential to adversely affect drywell bypass, isolation valving is provided to prevent bypassing the suppression pool resulting in direct blowdown to primary containment free air space. Closed systems penetrating only the drywell are provided with isolation valves to complete isolation of all fluid lines passing through the drywell wall. Table 6.2-51 provides information relative to drywell isolation provisions for fluid system lines and fluid instrument lines penetrating the drywell.

10←• •→14

The closure time for the containment isolation valves is based on the guidelines in 10CFR50.67 for the purpose of limiting the leakage of fission products from the primary containment. Amendment 132 revised the design basis accident offsite dose limit requirements from 10CFR100 to 10CFR50.67. A discussion of valve closure time relative to systems not terminating within the secondary containment and the fuel building is provided in Section 15.

14←•

A discussion of compliance assessment for Regulatory Guides 1.26 and 1.29 is presented in Section 1.8.

Section 5.2.5 describes the RCPB leakage detection system and Section 6.2.6 discusses the containment leakage testing system.

The design of the CIS considers the possibility of internally generated missiles during a LOCA. Appropriate protection is provided for isolation system components.

Based on the assumption of failure of all bonnet bolts there is a potential for valve bonnets to become missiles. This requires instantaneous clean severance of all bolts, with no overturning motion. The damage potential is dependent upon the size of the valve and the system in which the valve is located. When it is necessary to locate valves where protection of the isolation system is required, several solutions to the problem are available, such as welding the bonnets, providing deflector plates, and adding braces or keepers.

In addition to the considerations with which equipment is oriented with regard to missiles, special care is taken in arranging system components so that, within a system, a failure associated with one subsystem cannot cause the failure of another subsystem.

Also, care is taken to ensure that the failure of any component which would bring about the need for safety

RBS USAR

systems does not render the entire system incapable of achieving its design objective.

Further discussion of protection for components against damage from missiles and dynamic effects of pipe rupture is provided in Sections 3.5, 3.6A, and 3.6B.

Operability of the CIS under accident conditions is provided through qualification of components to endure the environmental conditions existing during an accident at the component location. The environmental design criteria are discussed in Section 3.11.

Containment isolation valves and associated piping and penetrations meet the requirements of the ASME Boiler and Pressure Vessel Code, Section III, Classes 1 or 2 (for Class 2, Class MC impact testing is also added), as applicable. Where necessary, a dynamic system analysis, as discussed in Sections 3.9A and 3.9B, including the impact effect of rapid valve closures under operating conditions, is included in piping systems which require containment isolation valves.

●→14

Power-operated containment isolation valves are equipped with limit switches which give position indication in the main control room. Loss of power to each motor-operated valve is detected and annunciated. Air-operated containment isolation valves are designed to fail in a safe position upon loss of service air. Power for valves used in series originates from physically independent Class 1E sources to ensure that no single event could interrupt motive power to both closure devices. Containment isolation valves are either automatically actuated by the various signals shown in Table 6.2-40 or are of remotely manual operation, as appropriate. Sealed closed barriers used in place of automatic isolation valves are under administrative control to assure that they cannot be opened inadvertently. This administrative control includes mechanical devices to seal or lock the valve closed, or to prevent power from being supplied to the valve operator. Instrument lines that penetrate the primary containment and monitor containment post accident pressure are provided with manual isolation valves that remain in the locked open position following an accident. Relief valves that are used as containment isolation valves have set points that are at least 1 1/2 times the containment design pressure. Some containment isolation check valves are provided with air operators which are used for testing purposes. These valves are identified in Table 6.2-40. All containment isolation valves are located as shown in Fig. 6.2-63 through 6.2-65.

14←●

Each structure is of Seismic Category I design and is protected against damage from missiles, as discussed in Section 3.5.

6.2.4.3 Design Evaluation

As stated in Section 6.2.4.1, the design of isolation valving for fluid lines penetrating the primary containment conforms to General Design Criteria 54 through 57. An evaluation against these criteria is detailed here in the following sections.

The capability of the instrumentation and control portion of the containment isolation system to perform its intended function is discussed in Section 7.3.2. The design criteria and post-LOCA operation of the reactor plant ventilation systems are described in Section 9.4.6.

6.2.4.3.1 General Design Criterion 54 - Piping Systems Penetrating Primary Containment

Fluid piping systems penetrating the primary containment are provided with leak detection and isolation capabilities as required by General Design Criterion 54 of 10CFR50, Appendix A. These systems are redundant as discussed in Section 6.2.4.2 and are tested periodically after the initial testing as discussed in Section 6.2.4.4.

6.2.4.3.2 General Design Criterion 55 - Reactor Coolant Pressure Boundary Lines Penetrating Primary Containment

Design

●→10

The RCPB (as defined in 10CFR50, Section 50.2 (v)) consists of the RPV, pressure-retaining appurtenances attached to the vessel, and valves, pumps, pipes, and supports which extend from the RPV up to and including the outermost containment isolation valve. The outermost containment isolation valve is designed to meet the requirements of General Design Criterion 55. The lines of the RCPB which penetrate the primary containment are capable of isolating the primary containment, thereby, precluding any significant release of radioactivity. Similarly, for lines which do not penetrate the primary containment but which form a portion of the RCPB, the design ensures that isolation from the RCPB can be achieved.

10←●

●→10

Fig. 6.2-63 schematically represents Criterion 55 isolation valves.

10←●

Influent Lines

Influent lines which penetrate both the primary containment and drywell are equipped with at least two isolation valves, one inside the drywell or primary containment area and the other as close to the external side of the steel containment as possible. Each valve requiring electric power is fed from a Class 1E power source. Protection of the environment is provided by these isolation valves. Additional (not all lines have GP) protection of the containment from pressurization in the case of a pipeline rupture outside the drywell along the section of pipe between the drywell and primary containment penetration is further ensured by extending the drywell in the form of guard pipes up to and including the primary containment penetration. These guard pipes encase the pipeline together with the isolation valves and ensure protection against pressurization of the containment area in the event of pipe rupture between the drywell and the primary containment.

Table 6.2-35 lists those influent pipes that comprise the RCPB. This table summarizes the design of each line as it satisfies the requirements imposed by General Design Criterion 55. The paragraphs referenced in the table describe compliance with General Design Criterion 55. Fig. 6.2-63 schematically represents the information given in Tables 6.2-35 and 6.2-36.

Effluent Lines

Effluent lines which form part of the RCPB and penetrate primary containment, drywell, or both are equipped with at least two isolation valves: one inside the drywell, and the other outside the containment and located as close to the containment as possible. Each valve requiring electric power is fed from a Class 1E power source. Additional protection of the containment from pressurization in the case of a pipeline rupture outside the drywell along the section of pipe between the drywell and primary containment penetration is further ensured by extending the drywell in the form of guard pipes up to and including the primary containment penetration. Together with the isolation valves, these guard pipes encase the pipeline and ensure protection against pressurization of the containment area in the event of a failure between the drywell and the primary containment.

Table 6.2-36 lists those effluent lines that comprise the RCPB and that penetrate the primary containment, the drywell, or both.

Summary

In order to assure protection against the consequences of accidents involving the release of radioactive material, pipelines which form the RCPB are shown to provide adequate isolation capabilities on a case-by-case basis. In all cases, a minimum of two barriers is shown to protect against the release of radioactive materials. Where necessary to protect the containment from overpressurization, guard pipes around the lines between the primary containment and the drywell are shown.

In addition to meeting the isolation requirements stated in General Design Criterion 55, the pressure-retaining components which comprise the RCPB are designed to meet other appropriate requirements which minimize the probability or consequences of an accidental rupture. The quality requirements for these components ensure that they are designed, fabricated, and tested to the highest quality standards of all reactor plant components. The components which comprise the RCPB are designed in accordance with the ASME Boiler and Pressure Vessel Code, Section III, Class 1.

•→10

10←•

It can therefore be concluded that the design of piping systems which comprise the RCPB satisfies General Design Criterion 55.

6.2.4.3.3 General Design Criterion 56 - Primary Containment Isolation Design

General Design Criterion 56 requires that lines which penetrate the containment and communicate with the containment interior must have two isolation valves, one inside the containment and the other outside. It should be noted that this criterion does not reflect consideration of the BWR suppression pool design. For instance, those lines which connect to the suppression pool do not have an isolation valve located inside the primary containment, as this would necessitate placement of the valve underwater. In effect, this would result in introducing a potentially

unreliable valve in a highly reliable system, thereby compromising design.

General Design Tables 6.2-37 and 6.2-38 list those lines that penetrate the primary containment. These tables summarize the design of each line as it satisfies the requirements imposed by General Design Criterion 56. The paragraphs referenced in these tables describe compliance with General Design Criterion 56. Figures 6.2-64 and 6.2-65 schematically represents these lines and their isolation valves.

Both influent and effluent lines are isolated by automatic or remote manual isolation valves which are located as close as possible to the containment boundary. Certain lines not used during power operation are isolated by locked closed manual valves located on each side of the primary containment penetration.

Lines having relief valves located outside the containment utilize the relief valves themselves for containment isolation and have set points which are greater than 1.5 times the containment design pressure.

Summary

To ensure protection against the consequences of accidents involving the release of significant amounts of radioactive materials, lines penetrating the steel containment are designed to provide isolation capability meeting the isolation requirements of General Design Criterion 56. The pressure-retaining components of these systems meet the same quality standards as the primary containment.

Accordingly, it can be concluded that lines that penetrate the primary containment and connect directly to the primary containment atmosphere or lines which fail to meet the closed system criteria of General Design Criterion 57 satisfy General Design Criterion 56 and conform to the guidelines of Regulatory Guide 1.11 (instrumentation lines).

6.2.4.3.4 General Design Criterion 57 - Closed System Isolation Valves Design

Lines penetrating the primary containment for which neither General Design Criterion 55 nor General Design Criterion 56 governs comprise the closed system isolation valve group. River Bend Station has no containment penetrations classified according to the criteria of General Design Criterion 57.

6.2.4.3.5 Conformance to Regulatory Guide 1.11

Instrument piping, connecting to the reactor coolant pressure boundary and leaving the drywell, terminates at instruments located within the primary containment. These lines have manual isolation valves located in the primary containment. These valves are not considered containment isolation valves since the lines do not penetrate the primary containment.

The River Bend Station (RBS) position for Regulatory Guide 1.11 is provided in Table 1.8-1. RBS design complies with Regulatory Guide 1.11 except for containment and drywell pressure and differential pressure monitoring lines. Each line is safety related and is designed in accordance with ASME III. Each line has one normally locked open manual valve between the instrument and the containment, and one normally locked closed manual valve with a capped nipple downstream of the transmitter which is used for calibration and testing of the instrument. The intent of this arrangement is to ensure that the highest reliability possible is provided commensurate with the safety function performed by these instruments. The instruments in question are shown on revised Figure 6.2-71, and on Figures 6.7-1 and 9.4-7, and perform the following functions:

<u>Figure</u>	<u>Instrument No.</u>	<u>Function</u>
•→7 6.2-71	1CMS*PT 2A,B	Drywell pressure for post-accident monitoring
	1CMS*PT 4A,B	Containment pressure for post-accident monitoring
	1CMS*PDT 29A,B	Drywell/containment differential pressure for post-accident monitoring. This information is also used by the operator to manually relieve negative pressure in the drywell/containment through the purge system.
7←•		

RBS USAR

<u>Figure</u>	<u>Instrument No.</u>	<u>Function</u>
●→14●→12 6.7-1	●→7 ILVS*PT 21A,B	Drywell pressure set point. Used as input to computer point for operator information
7←● 12←● 9.4-7	HVR*PDT 60A,B,C,D,E,F	Annulus and containment differential pressure for the automatic shutdown of the containment unit coolers to aid in preventing containment negative pressure. Also, this information is used by the operator to manually relieve negative pressure in the containment through the purge system.

14←●
Providing a remote manually operated valve in these lines will reduce overall reliability and degrade the safety function provided by the above instruments due to inadvertent or spurious isolation events resulting in false indications and signals. The locked open valves are accessible for manual closure.

6.2.4.3.6 Failure Analysis

One of the basic purposes of the containment system is to provide the minimum of one protective barrier between the reactor core and the environs subsequent to a postulated accident involving failure of the piping components of the reactor coolant system. To fulfill its role as a barrier, the containment is designed to remain intact before, during, and subsequent to a LOCA. The process system and the containment are considered as separate systems, but where process lines penetrate primary containment, the penetration design achieves the same integrity as the primary containment structure itself. The process line isolation valves are designed to achieve the containment function inside the process lines, when required.

Since a rupture of a large line penetrating the primary containment and connecting to the reactor coolant system may

be postulated, an isolation barrier for that line is required to be located within the containment boundary. An isolation valve in each line is required to be closed automatically on various indications of reactor coolant loss. Reliability is added when a second valve, located outboard or inboard of the containment as close as practical, is included. This second valve also closes automatically. If failure involves one valve, the second valve is available to function as the containment barrier. By physically separating the two valves, there is less likelihood that a failure of one valve would cause a failure of the second. Power sources are given in Table 6.2-40. The consequences for the CIS active component failures are presented in the Failure Modes and Effects Analysis (FMEA).

6.2.4.3.7 Conformance to NUREG 0737, Item II.E.4.2 Containment Isolation Dependability

All lines that penetrate the reactor containment are designed to conform to the seven positions of NUREG 0737, Item II.E.4.2. Compliance of the Containment Isolation System with Item II.E.4.2 is as follows:

1. Position 1 requires diverse parameters for the initiation of containment isolation. Diverse parameters are sensed to detect a loss-of-coolant accident (LOCA) and other design basis accidents (DBA). The preferred containment isolation diverse signals are low reactor vessel water level or high drywell pressure. The containment isolation design does comply with the recommendations of SRP 6.2.4 in that there is diversity in the parameters sensed for the initiation of containment isolation.

Diverse signal groups to detect LOCA and other DBAs are listed below. These include containment isolation and process isolation signals.

<u>Group No.</u>	<u>Isolation Signal Code</u>	<u>Description</u>
1	B	Reactor Vessel Low Water Level 2
	K	High Drywell Pressure
•→6		
2	W	Reactor Pressure Low
	X(Note 1)	RCIC Isolation Signals
3	W	Reactor Pressure Low (Note 2)
	K	High Drywell Pressure (Note 2)
6←•		

RBS USAR

<u>Group No.</u>	<u>Isolation Signal Code</u>	<u>Description</u>
4	Y	MS-PLCS Air Line Header Flow High
	Z	MS-PLCS Air Line Header & Steamline Differential Pressure Low
●→12		
5	C	Reactor Vessel Low Water Level 3
	L	High Reactor Pressure
	R	RHR System Equipment Area High Ambient Temperature
●→16 ●→8		
6	A	Reactor Vessel Low Water Level 1
	D	High Main Steam Line Flow
	F	Main Steam Line Low Pressure (Reactor Mode Switch in Run Only)
	G	Low Main Condenser Vacuum
	H	High Main Steam Line Tunnel Ambient Temperature
8←● 16←●		
7	B	Reactor Vessel Low Water Level 2
	H	High Main Steam Line Tunnel Ambient Temperature
	M	Standby Liquid Control System Actuated
	N	High Nonregenerative Heat Exchanger Outlet Temperature (RWCU System)
	O	RWCU System High Differential Flow
	P	RWCU System Equipment Area High Ambient Temperature
12←●		
8	B	Reactor Vessel Low Water Level 2
	K	High Drywell Pressure
	T	Containment High Gaseous Radiation
9	B	Reactor Vessel Low Water Level 2
	E	High Main Steam Line Radiation

RBS USAR

<u>Group No.</u>	<u>Isolation Signal Code</u>	<u>Description</u>
10	A	Reactor Vessel Low Water Level 1
	K	High Drywell Pressure
11*	B	Reactor Vessel Low Water Level 2
	K	High Drywell Pressure
●→8		
12*	B	Reactor Vessel Low Water Level 2
	K	High Drywell Pressure
	U	Reactor Building Annulus Ventilation Radiation High
	AA	Reactor Building Annulus Pressure High (Loss of Vacuum)
8←●		
13*	B	Reactor Vessel Low Water Level 2
	K	High Drywell Pressure
	V	Fuel Building Ventilation Exhaust Radiation High
●→12		
14	C	Reactor Vessel Low Water Level 3
	K	High Drywell Pressure
	R	RHR System Equipment Area High Ambient Temperature
15	B	Reactor Vessel Low Water Level 2
	H	High Main Steam Line Tunnel Ambient Temperature
	O	RWCU System High Differential Flow
	P	RWCU System Equipment Area High Ambient Temperature
16	B	Reactor Vessel Low Water Level 2
	H	High Main Steam Line Tunnel Ambient Temperature
	M	Standby Liquid Control System Actuated
	O	RWCU System High Differential Flow
	P	RWCU System Equipment Area High Ambient Temperature

●←12

*For secondary containment isolation only.

RBS USAR

<u>Group No.</u>	<u>Isolation Signal Code</u>	<u>Description</u>
•→12		
12←••→10		
17	A	Reactor Vessel Low Water Level 1
	C	Reactor Vessel Low Water Level 3
	K	High Drywell Pressure
	R	RHR System Equipment Area High Ambient Temperature
10←•		
•→6		

NOTE 1: RCIC isolation signals (Code X) are comprised of any of the following:

- 6←•
 - a. RCIC pipe route area high temperature.
 - b. Equipment area high temperature.
 - c. Turbine exhaust diaphragm high pressure.
 - d. Steam line high differential pressure or instrument break.

•→6
NOTE 2: Both signals must be present to initiate isolation

- 6←•
 - 2. Position 2 establishes a requirement to define essential and nonessential systems and to classify, in accordance with these definitions, all systems that contain piping which penetrate the containment as essential or nonessential.

The definitions for essential and nonessential listed below, as they pertain to containment isolation systems and system lines, are based on the review of the GE Report NEDO-24782, NUREG 0737, NUREG-0800, SRP 6.2.4, and R.G. 1.141. System and line classifications are detailed in Table 6.2-40.

- a. Essential systems and lines:

Those systems and lines that are required to either provide coolant or monitor containment atmosphere during emergency conditions, through containment, while preserving containment boundary to prevent or limit release of fission products from postulated accidents. The containment isolation valves for these essential systems and lines are open to perform their intended function. However, these valves may be closed either remote manually, if they are not required, or by process signals to preserve the containment boundary.

b. Nonessential systems:

Those systems that are not required to either provide coolant or monitor containment atmosphere during emergency conditions, through containment, but are required to preserve containment boundary to prevent or limit release of fission products from postulated accidents. The containment isolation valves for these nonessential systems either are automatically closed or are locked closed and are under administrative control.

c. Nonessential lines:

Those lines in an essential or nonessential system that are not required to either provide coolant or monitor containment atmosphere during emergency conditions, through containment, and therefore are required to automatically isolate to preserve containment boundary to prevent or limit release of fission products from postulated accidents. The containment isolation valves for these nonessential lines operate the same as those for the nonessential systems above.

3. Position 3 requires all nonessential systems to be automatically isolated by the containment isolation signal.

Containment isolation valves in nonessential loss-of-coolant accident, or the isolation is not initiated by diverse containment isolation signals, are identified and justifications for the design are provided in Section 6.2.4.3.7.2. Essential instrument lines that are not provided with isolation valves capable of automatic operation in accordance with Regulatory Guide No. 1.11, paragraph C.1c are identified and justifications for this design are provided in Section 6.2.4.3.7.2.

4. Position 4 requires automatic containment isolation valves to remain closed after the isolation is reset. Deliberate operator action is required to reopen a containment isolation valve after the isolation is reset. Gang reopening is not

RBS USAR

acceptable following reset of containment isolation signal or single operator action.

All automatic containment isolation valves remain closed after the isolation is reset.

5. Position 5 requires the reduction of high drywell pressure trip point setting, used for containment isolation to the minimum compatible with normal operating conditions.

The design basis used to develop the minimum containment set point pressure complies with the NRC requirements.

6. Position 6 requires containment supply or exhaust lines that do not satisfy the operability criteria set forth in Branch Technical Position (BTP) CSB 6-4 or the Staff Interim Position of October 23, 1979, to be sealed closed during operational modes of power operation, startup, hot standby, and hot shutdown.

The containment supply and exhaust lines are designed in accordance with the operability criteria set forth in BTP CSB 6-4 during the above operational modes. However, the containment purge system differs from the explicit requirements set forth in the Branch Technical Position. Detailed findings and justifications are given for the system lines in Section 6.2.4.3.7.2.

7. Position 7 requires all containment purge supply and exhaust isolation valves to close on a high radiation signal.

The containment purge supply and exhaust lines are automatically isolated on high radiation. This isolation signal is required in addition to isolation on diverse containment isolation signals (Position 1).

6.2.4.3.7.1 Systems in Full Compliance

The following systems comply with all of the applicable positions of NUREG-0737, Item II.E.4.2.

1. Main Steam - Positive Leakage Control System
2. High Pressure Core Spray

3. Low Pressure Core Spray
4. Fuel Pool Cooling and Cleanup
5. Reactor Building Equipment Drains
6. Feedwater System
7. Reactor Building Floor Drains
8. Reactor Plant Component Cooling
- 10
9. Deleted
- 10←•
10. Standby Service Water
11. Ventilation Chilled Water
12. Reactor Plant Ventilation
13. Service Air
14. Instrument Air
15. Condensate Makeup
16. Fire Protection Water

•→6

6←•

6.2.4.3.7.2 Systems in Less Than Full Compliance

The following summaries contain detailed findings and justifications for those systems in which less than full compliance with applicable NRC positions exists.

1. Main Steam Lines and Line Drains

The Main Steam Lines and Line Drains comply with all applicable portions of NUREG-0737 Item II.E.4.2, except:

a. Position 1:

These are nonessential lines that do not receive the preferred diverse containment isolation signal, i.e., high drywell pressure. However, these lines provide a heat sink path for the reactor pressure vessel. It is desirable to keep the main

RBS USAR

steam isolation valves open for this function during postulated small leaks or breaks. Therefore, high drywell pressure has been deliberately omitted from isolation of main steam lines. These lines do isolate on the parameters identified as Group 6 in Section 6.2.4.3.7 and via remote manual operation.

2. Residual Heat Removal System

The Residual Heat Removal System complies with all applicable portions of NUREG-0737, Item II.E.4.2, except:

a. Position 1:

The RHR automatic isolation valves in the nonessential lines listed below do not receive the high drywell pressure signal.

<u>Penetration</u>	<u>Title</u>	<u>Valve No.</u>
1KJB*Z3A	RHR Shutdown Cooling Injection	1E12*MOVF053A
1KJB*Z3B	RHR Shutdown Cooling Injection	1E12*MOVF053B
•→12 12←•		
1KJB*Z20	RHR Shutdown Cooling Supply	1E12*MOVF008 1E12*MOVF009
1KJB*Z21A	Coolant to Sparger in Reactor Vessel	1E12*MOVF037A
1KJB*Z21B	Coolant to Sparger in Reactor Vessel	1E12*MOVF037B

The high drywell pressure (Signal K) has been deliberately omitted from the isolation initiation logic for these line valves to avoid the loss of the RHR shutdown cooling mode for small breaks or leaks.

b. Positions 1 and 3:

The following manually operated containment isolation valves are closed during normal, shutdown, and postaccident conditions.

<u>Penetration</u>	<u>Title</u>	<u>Valve No.</u>
1KJB*Z21A	Coolant to Fuel Storage Area	1E12*VF099A
	Flushing Water Supply to RHR System	1E12*VF044A
1KJB*Z21B	Coolant to Fuel Storage Area	1E12*VF099B
●→4	Flushing Water Supply to RHR System	1E12*VF044B
4←●		

For the above manually operated valves (inside containment), administrative control includes mechanical devices to seal or lock the valve closed. Valve position and locking devices are checked each time the containment is secured. The opening of these valves is performed only by use of specific procedures. These procedures ensure that the operator is aware that the RHR LPCI function cannot be performed effectively in the event of a LOCA if these valves are open.

3. Reactor Water Cleanup System

The reactor water cleanup system complies with all applicable portions of NUREG-0737, Item II.E.4.2, except:

a. Position 1:

High drywell pressure (Signal K) is not an isolation signal for the following valves:

<u>Penetration</u>	<u>Title</u>	<u>Valve No.</u>
1KJB*Z4	RWCU Discharge to Main Condenser	1G33*MOVF028 1G33*MOVF034

RBS USAR

<u>Penetration</u>	<u>Title</u>	<u>Valve No.</u>
●→3 KJB*Z6	RWCU Return to FWS	1G33*MOVF040 1G33*MOVF039
1KJB*Z7	RWCU Pumps Suction	1G33*MOVF001 1G33*MOVF004
3←● 1KJB*Z129	RWCU Pumps Discharge	1G33*MOVF053 1G33*MOVF054

High drywell pressure is deliberately omitted to avoid inadvertent isolation of the above lines in order to keep the capability of continuously cleaning the reactor vessel coolant. This system incorporates break detection logic in conjunction with leak detection systems which automatically isolate on an unbalanced flow or high temperature.

4. Control Rod Drive

The Control Rod Drive System complies with all applicable portions of NUREG-0737, Item II.E.4.2 except:

a. Positions 1 and 3:

Remote manually operated containment valve 1C11*MOVF083 (outside containment) in nonessential penetration 1KJB*Z29 is open during normal operation and closed during shutdown. However, in the postaccident position, this valve is open to direct the water to the accumulators to recharge them in order to preclude the possible loss of the scram condition. Then the valve is closed by the operator.

The CRD System provides cooling to the RPV by way of the control rod assemblies. This CRD design is significant enough to warrant leaving this system line open. Also, a check valve 1C11*F122 is installed inside containment to support isolation of this line.

RBS USAR

5. Reactor Plant Ventilation (Containment Purge System Portion)

The Reactor Plant Ventilation System complies with an applicable portion of NUREG-0737, Item II.E.4.2, except:

a. Position 6:

RBS complies with Branch Technical Position (BTP) CSB6-4 with the following exceptions:

- (1) BTP CSB 6-4 Position B.1.c: The containment/drywell purge system supply and exhaust lines are each 36 in in diameter in contrast to the 8 in in diameter recommended size in the technical position.

Justification: The size of the containment/drywell purge system supply and exhaust lines exceeds 8 in in diameter because restriction to 8 in in diameter limits air flow rate to approximately 850 cfm. This limitation of flow rate permits a containment air change only once in 22 hr, which is contradictory to the commitment to maintain satisfactory conditions for operating personnel during periods of required access to the containment. The larger diameter lines allow for a complete change or recirculation of containment air every 3 hr on a continuous basis, and every 1.5 hr at periodic, required intervals. This combination provides the operational capabilities necessary for access to the containment. Further, the analysis performed to demonstrate compliance with the Branch Technical Position B.5.a

shows that the use of the larger diameter lines is acceptable. The offsite dose calculation used to determine the radiological consequences, assuming a loss-of-coolant accident (recirculation line break) and isolation of the containment purge supply and exhaust valves, showed that the valves are well within 10CFR50.67 guideline values. Amendment 132 revised the design basis accident offsite dose limit requirements from 10CFR100 to 10CFR50.67.

- (2) BTP CSB 6-4 Position B.3: The containment atmosphere cleanup system filters are located in the auxiliary building, not within the containment. The containment ventilation system includes a recirculation feature which processes containment atmosphere through charcoal filters for cleanup. Use of the recirculation feature minimizes the need for purging and reduces the frequency of discharging filtered exhaust to the environment. The filters are located in the auxiliary building and not within the containment for the following reasons:
- (a) The filters must remain accessible for inspection, testing, and maintenance.
 - (b) Containment space is not available for installation of such large equipment without possible interference with the suppression pool functional requirements.

(c) The auxiliary building air is filtered and controlled following an accident.

(d) Analysis has determined mixing of the annulus volume is not required, recirculation system (Annulus Mixing System) is disabled.

•→10

(3) BTP CSB 6-4 Position B.4: The leakage rate testing of the isolation valves is performed in accordance with the primary containment leak rate testing program for the Type C tests, and is, therefore, considered to satisfy the intent of the technical position requirement for leakage rate testing. The system complies with this technical position for testing the availability of the valve isolation function. Leak tightness and testing in accordance with 10CFR50, Appendix J, are considered to satisfy the intent of the branch technical position requirement for leakage rate testing.

10←•

(4) BTP CSB 6-4 Position B.5.c: The ECCS back pressure requirement is not applicable to BWR containment.

Demonstration of the operability of the containment purge valves and their ability to close during a design basis accident is summarized in Table 6.2-52. A detailed report has been submitted to the NRC under separate cover⁽²⁷⁾. The report verifies that the valve actuator's torque capability has sufficient margin to overcome the torques and forces that resist closure when stroking from the initial open position to full seated in the time limit specified following a design basis LOCA.

6. Containment Hydrogen Purge

The Containment Hydrogen Purge System complies with all applicable portions of NUREG-0737, Item II.E.4.2, except:

a. Positions 1 and 3:

Manually operated containment isolation valves in the nonessential penetrations listed below are closed during normal, shutdown, and postaccident operation.

<u>Penetration</u>	<u>Title</u>	<u>Valve No.</u>
1KJB*Z31	Containment Hydrogen Purge Supply Line	1CPP*SOV140
1KJB*Z33	Containment Hydrogen Purge Return Line	1CPP*MOV104 1CPP*MOV105

For these motor-operated and solenoid-operated valves, administrative control includes mechanical devices to seal or lock the valve closed or to prevent power from being supplied to the valve operator. Valve position and locking devices are checked each time the containment is secured. In addition, the seal or lock is verified intact at least every 31 days. The position indication lights in the control room allow the operator to verify proper valve position. The opening of these valves is performed only by use of specific procedures. These procedures ensure that the operator is aware that primary containment integrity cannot be achieved in the event of a LOCA if these valves are open.

7. Containment Leakage Monitoring

The Containment Leakage Monitoring System complies with all applicable portions of NUREG-0737, Item II.E.4.2, except:

a. Position 3:

The manual containment isolation valves in the nonessential instrument line

penetrations listed below are locked closed during normal operation.

<u>Penetration</u>	<u>Title</u>	<u>Valve No.</u>
1KJB*Z603A	Drywell Leakage Monitoring Pressure	1LMS*V14 1LMS*V12
1KJB*Z603C	Drywell Leakage Monitoring Pressure	1LMS*V7 1LMS*V16

For these manually operated valves, administrative control includes mechanical devices to seal or lock the valve closed. Valve position and locking devices are checked each time the containment is secured. In addition, the seal or lock is verified intact at least every 31 days. The opening of these valves is performed only by use of specific procedures. These procedures ensure that the operator is aware that primary containment integrity cannot be achieved in the event of a LOCA if these valves are open.

8. Containment Atmospheric Monitoring

The Containment Atmospheric Monitoring System complies with all applicable portions of NUREG-0737, Item II.E.4.2.

The containment hydrogen monitoring system is a closed system outside containment required for use during an accident. It was determined that the system piping is Safety Class 2 and meets ASME III except for the piping inside containment up to the inboard containment isolation valves (piping is optionally upgraded to non-safety, requirement of ASME Section XI, Table IWC-2500-1. Visual Examination does not apply), and the hydrogen monitor. The hydrogen monitor, which is an instrument to monitor containment hydrogen, is designed to withstand the containment environment, qualified to Seismic Category I standards, and protected from missiles. This monitor meets the ASME III requirements, including the material certification for traceability, but does not have the required N-stamp. Based on the hydrogen monitor's stringent design requirements, the containment hydrogen system design ensures that the containment integrity is maintained during normal and accident conditions.

RBS USAR

9. Instrument Lines

The Instrument Lines comply with all applicable portions of NUREG-0737, Item II.E.4.2, except:

Each essential line listed below has one normally locked-open valve between the containment and the transmitter and one normally locked-closed manual valve with a capped end downstream of the transmitter. This valve arrangement does not comply with Regulatory Guide 1.11, paragraph C.1.c, isolation valve capable of automatic operation.

<u>Penetration</u>	<u>Title</u>	<u>Valve No.</u>
1KJB*Z602A	Containment to Annulus Differential Pressure	1HVR*V8
1KJB*Z602B	Containment to Annulus Differential Pressure	1HVR*V10
1KJB*Z602D	PVLCS Reactor Drywell Pressure	1LSV*V64
1KJB*Z602F	Containment to Annulus Differential Pressure	1HVR*V12
1KJB*Z605A	Containment Pressure	1CMS*V2
1KJB*Z605B	Containment Pressure	1CMS*V3
1KJB*Z606A	Containment to Annulus Differential Pressure	1HVR*V14
1KJB*Z606B	Containment to Annulus Differential Pressure	1HVR*V16
1KJB*Z606C	Drywell Pressure	1CMS*V16
1KJB*Z606D	Containment Pressure	1CMS*V15
1KJB*Z606E	PVLCS Reactor Drywell Pressure	1LSV*V65
1KJB*Z606F	Containment to Annulus Differential Pressure	1HVR*V18

Instrument line function reliability is assured by redundant lines with environmentally and seismically qualified I&C devices, with associated

piping and tubing systems designed to guidelines for safety-grade systems. The instrument line breaks have essentially zero differential pressure across the containment wall a short time after the accident, which would limit leakage to the secondary containment. Any leakage would be treated by safety-grade filtration systems prior to discharge to the environment. Based on an engineering technical evaluation, the instrument line design and associated filtration system availability limits the potential offsite exposure below the guidelines of 10CFR50.67. Amendment 132 revised the design basis accident offsite dose limit requirements from 10CFR100 to 10CFR50.67.

•→6

10. Reactor Core Isolation Cooling

Reactor core isolation cooling system containment isolation valves comply with all applicable portions of NUREG-0737, Item II.E.4.2, except:

•→13

Group 3 valves, E51-F077 and E51-F078, require high drywell pressure coincident with low reactor pressure to automatically initiate containment isolation of the RCIC turbine exhaust vacuum breaker piping.

13←•

Vacuum breaking reliability, and thus RCIC reliability, is assured during all non-accident conditions by only initiating containment isolation when an accident condition has been confirmed (coincident high drywell pressure and low reactor pressure).

Automatic isolation of these valves is only initiated when (1) the RCIC system is no longer able to perform its injection function (reactor pressure low signal) and (2) an accident has occurred requiring containment isolation (high drywell pressure).

6←•

6.2.4.4 Testing and Inspection

Testing of isolation system valves of the following systems is presented in the sections listed below:

<u>System</u>	<u>Section</u>
•→14	
Control rod drive system	4.6.3
Main steam isolation valves	5.4.5
Residual heat removal system	5.4.7
Reactor water cleanup system	5.4.8
Feedwater system	5.4.9
Main steam line drain system	5.4.9
Secondary containment functional design	6.2.3
Containment isolation valve leakage rate test	6.2.6
Emergency core cooling systems	6.3
Inservice inspection of ASME code, Class 2 and 3 components	6.6

14←•

All motor- and air-operated valves in the remaining systems are capable of being exercised periodically during plant operation. The system layout permits access for appropriate equipment used in testing and inspecting system integrity.

During plant operation, the valves, piping, instrumentation, wiring, and other components outside the drywell can be inspected visually. Components inside the drywell can be inspected when the drywell is open for access. Testing frequencies are correlated with the testing frequencies of the associated controls and instrumentation. When a valve control is tested, the operability of that valve and its associated instrumentation is tested by the same action.

For systems in service during plant operation, operability of the containment isolation valves in those systems can be demonstrated during operation of the system. For systems not normally in operation, regularly scheduled operational tests are performed.

6.2.5 Combustible Gas Control in Containment

●→5

The combustible gas control system is designed to monitor and control the concentration of hydrogen which may be released in the drywell and containment as a result of a postulated LOCA. Subsystems are provided for the drywell and containment to measure the hydrogen concentrations (hydrogen analyzer), to mix the atmospheres (hydrogen mixing), and to reduce hydrogen concentrations without relying on purging to the environment (hydrogen recombiners). In addition, a backup containment hydrogen purge system is provided to aid in long-term, post-LOCA cleanup. A hydrogen igniter system has also been provided to mitigate degraded core hydrogen generation events.

●→7

RBS is a member of the BWR/6 Mark III Containment Hydrogen Control Owners' Group (HCOG) which was formed to address the hydrogen control issue (10CFR50.44) on a generic basis for BWR/6 plants.

7←● ●→12

Results of the evaluations and studies performed under the auspices of the HCOG were used to develop a River Bend Station-specific hydrogen control program. In addition to the HCOG evaluation and study results, RBS-specific analyses and reports were submitted under separate cover in accordance with the final rule.

12←●

6.2.5.1 Design Bases

The RBS design basis LOCA evaluation is not based on a single accident event but on an envelope of accident conditions. These conditions encompass large, intermediate, and small breaks in the drywell. All of the accident scenarios assume that the reactor core is recoverable and that all ECCS systems are operable for high volume reflooding of the reactor pressure vessel (RPV).

5←●

•→8 •→5

The high volume reflooding of the RPV is the primary difference between the LOCA and the hydrogen generation event (HGE). 10CFR50.44 requires that hydrogen production equivalent to 5 times the calculated metal-water reaction (MWR) rate be addressed as a result of a design basis LOCA, or to be the amount that would result from reaction of all the metal in the outside surfaces of the cladding cylinders surrounding the fuel to a depth of 0.00023 inch, whichever amount is greater. Because of the high volume reflooding of the RPV during the LOCA, the generation of hydrogen is but a fraction of the total hydrogen generated during an HGE.

The combustible gas control system is designed in accordance with the following criteria:

1. Sizing of the combustible gas control subsystems (hydrogen mixing, hydrogen recombiners, and hydrogen purge) is based on limiting the drywell and containment hydrogen concentrations after a LOCA to 4 volume percent. Hydrogen generation and accumulation from 5 times the calculated active core cladding metal-water reaction rate radiolysis, and metal corrosion is in accordance with the assumptions specified by Regulatory Guide 1.7, Rev. 2.

8←•

The igniter system is designed to mitigate the hydrogen release from degraded core accidents involving metal-water reaction of up to 75 percent of the fuel cladding surrounding the active fuel region, in accordance with the requirements of 10CFR50.44.

2. The capability to uniformly mix the drywell atmosphere with the containment atmosphere in the long term after a LOCA is provided by the hydrogen mixing subsystem described in Section 6.2.5.2.1. Prior to initiation of this subsystem, the drywell and containment atmospheres are segregated. During this time, both the drywell and containment atmospheres are assumed to be uniformly mixed due to natural convection and molecular diffusion. Mixing of the containment atmosphere is further promoted by operation of the engineered safety feature containment unit coolers, which are automatically actuated early in the post-accident sequence of events.

•→14

3. The containment atmosphere monitoring system incorporates hydrogen analyzers and provides the capability to sample and measure the hydrogen concentration in the drywell and containment during normal and post-accident conditions. Alarms in the main control room, indicating greater than or equal to a minimum detectable hydrogen concentration, as recommended by the Hydrogen Control Owner's Group (HCOG) Emergency Procedure Guideline (EPG) [Ref. 28 & 29], at any 1 of the 12 drywell and containment sample point locations, alert the operator to the need for initiation of hydrogen control equipment.

5←• 14←•

●→5

4. The subsystems meet the requirements of 10CFR50, Appendix A, General Design Criterion 41, with respect to their capability to control the concentration of hydrogen following postulated accidents.

●→14

5. Design of the Safety Class 2 combustible gas control system is such that no single failure results in the loss of function of any of the subsystems for monitoring, mixing, or controlling hydrogen concentration after an accident. The backup containment hydrogen purge system, which is nonnuclear safety class and nonseismic, is not required to meet this design criterion, except for those portions serving a containment isolation function which are Safety Class 2.

6. Protection from postulated missiles and pipe whip is provided as required to ensure proper system operation. All active components of the hydrogen mixing system and hydrogen recombiner system are located in the primary containment outside the drywell. The hydrogen igniters distributed throughout the drywell and containment are designed for or shielded from LOCA pool swell loads. The effect of local jet impingement loads due to a LOCA are evaluated to ensure igniter system function in accordance with Appendix 3C. The major system components and associated performance data are listed in Table 6.2-41. The piping and instrumentation of the hydrogen mixing system are shown on Fig. 6.2-66.

14←●

7. All components of the combustible gas control system are of Seismic Category I design and are capable of withstanding the transient environmental conditions of temperature, pressure, humidity, and radiation to which they are exposed following a LOCA, with the exceptions previously noted.

8. The combustible gas control system is designed to meet General Design Criterion 42 with respect to testing and General Design Criterion 43 with respect to inspection. Section 6.2.5.4 provides a further discussion of the periodic tests and inspections performed on the system.

5←●

•→5

9. The system does not rely on equipment shared with another unit. Two permanently installed thermal recombiners are located on opposite sides of the containment refueling floor (el 186 ft-3 in). This location precludes the need for shielding around the recombiners, since the containment is not readily accessible after a LOCA.

10. As a backup to the redundant hydrogen recombiner systems and to comply with Regulatory Guide 1.7, the containment hydrogen purge system provides the capability to purge the containment and drywell through the shield building annulus and standby gas treatment system (SGTS) to the atmosphere.

•→12

11. Initiation of the hydrogen mixing system, the recombiners, and igniters is based on manual actuation from the main control room. The hydrogen control systems are manually initiated as directed by Emergency Operating Procedures and Severe Accident Procedures when hydrogen concentration reaches a minimum detectable level, as recommended by the HCOG EPG, or reactor water level reaches the top of active fuel or cannot be determined.

12←•

6.2.5.2 System Design

The appropriate subsystems of the combustible gas control system provide effective control of the hydrogen generated following a LOCA or degraded core hydrogen generation event. The system consists of the following features:

•→8

1. A hydrogen mixing system which operates to mix the drywell atmosphere with the containment atmosphere approximately 30 minutes after the design basis LOCA, so that the hydrogen concentration in the drywell does not reach the 4 volume percent limit in the short term.

8←• •→14

2. A hydrogen recombiner system which is initiated approximately 12.5 days after the design basis LOCA, to limit the hydrogen concentration in both the drywell and containment to less than 4 volume percent.

•→12 14←•

3. A containment hydrogen purge system is also provided as a backup in accordance with Regulatory Guide 1.7. Its use is also defined by Emergency Operating Procedures and Severe Accident Procedures.

12←•

• -13 • -5

4. A hydrogen analyzer system for measuring the amount of hydrogen in the drywell and containment atmospheres. The concentration of hydrogen in the drywell and containment is measured during LOCA conditions and is displayed in the main control room. Piping and instrumentation for this system is shown on Fig. 6.2-71. Safety-related display instrumentation for containment and drywell monitoring is listed in Table 7.5-1.

13←• • -12

5. A hydrogen control system (igniters) distributed throughout the drywell and containment. The igniters are operated in accordance with plant Emergency Operating Procedures (EOPs) and Severe Accident Procedures (SAPs) which implement the HCOG Emergency Procedure Guidelines for hydrogen control.

12←•

6. All controls for operating the hydrogen mixing system, the hydrogen recombiner system, and the igniter system are located in the main control room. The controls for operation of the containment hydrogen purge system are local.
7. A tabulation of the design and performance data for each system component is listed in Table 6.2-41.
8. Environmental qualification information for safety-related equipment, as required by Regulatory Guide 1.7, is given in Section 3.11.
9. Electrical requirements for equipment associated with this system are in accordance with the appropriate IEEE standards, as referenced in Section 8.1.

6.2.5.2.1 Hydrogen Mixing System

The primary function of the hydrogen mixing system is to mix the drywell atmosphere with the primary containment atmosphere. The zirconium-water reaction which is assumed to occur in the reactor core results in a higher hydrogen concentration in the drywell than in the primary containment in the short term after the design basis LOCA. The hydrogen mixing system uses the larger, essentially hydrogen-free containment atmosphere to dilute the drywell atmosphere. This tends to equalize the hydrogen concentration in the drywell and containment.

5←•

●→5

As shown on Fig. 6.2-66, the hydrogen mixing system consists of two independent, 100-percent capacity trains located in the containment. Each train consists of one hydrogen mixing fan and associated piping, valving, and instrumentation. All components of the hydrogen mixing system are capable of sustaining normal as well as seismic loads; temperature, pressure, and humidity transients; and radiation resulting from an emergency situation. Environmental qualification of system equipment is discussed in Section 3.11.

●→12

The EOPs and SAPs require actuation of the hydrogen mixing system when the drywell hydrogen concentration reaches a minimum detectable level and the RPV pressure drops below 30 psig. The hydrogen recombiners are placed in operation if the containment hydrogen concentration is between 0.7 and 6 volume percent.

12←●

When the hydrogen mixing system is actuated, the air from the primary containment enters the drywell through two openings. These openings are located diametrically opposite each other on the circumference of the drywell, just above the suppression pool. The drywell atmosphere is exhausted into the larger primary containment volume through two penetrations located at the top of the drywell by means of two recirculating fans. Thus, the air from the primary containment which is relatively free of hydrogen is mixed with the air in the drywell and dilutes the drywell atmosphere.

There are several mechanisms which ensure mixing of hydrogen in the drywell and containment atmospheres. Prior to operation of the hydrogen mixing system, the drywell atmosphere is segregated from the containment atmosphere. During this time, each of these volumes is assumed to experience uniform mixing. In the drywell, turbulence is created by reactor coolant cascading out of the pipe break. In addition, natural convection and diffusion are assumed to mix the air, steam and combustible gases within the drywell. In the containment, natural convection and diffusion are also expected prior to hydrogen mixing operation.

When the hydrogen mixing system is activated, the drywell atmosphere will be in direct communication with the containment atmosphere. Containment air will be drawn into the drywell and drywell atmosphere will be exhausted into containment. This forced mixing dilutes the hydrogen, steam, and air mixture in the drywell; and increases the containment hydrogen concentration. Turbulence and entrainment due to this forced mixing and recirculation further redistributes the gases in containment. In the

5←●

- -5

subcompartments, there is little or no hydrogen generation. Therefore, the rate of subcompartment hydrogen buildup is very small and cannot exceed the concentration of the surrounding atmosphere.

- -8

Assuming a design basis LOCA, metal-water reaction and hydrogen production due to zinc corrosion and radiolysis increases the drywell hydrogen concentration to 3.5 volume percent at approximately 30 minutes after the accident. The hydrogen production rate at 30 minutes is approximately 11 scfm. Operation of one hydrogen mixing fan at its design flow rate of 600 cfm (513 scfm) removes 21 cfm (17.9 scfm) of hydrogen from the drywell if the hydrogen concentration is 3.5 volume percent.

- 8←•

Initiation of the hydrogen mixing system requires an operator first to energize an inlet valve in the line connecting the drywell and containment. Opening of the valve equalizes drywell and containment pressures if they are different. An interlock is provided to prevent opening of the outlet valves before the inlet valves are fully opened. The operator then manually opens the outlet valves and, with the valves in their fully opened position, starts the hydrogen mixing fan (Fig. 7.3-8). Limitation on the initiation of the hydrogen mixing system due to pressure differentials between the drywell and containment is 3 psi because of the hydrogen mixing valve design. These valves will operate (i.e., open against 3 psi differential pressure) for up to 180 days after an accident.

- -8

Using extremely conservative assumptions, hydrogen mixing system initiation is not required until at least 30 minutes following the LOCA; that is, when hydrogen concentration reaches 3.5 volume percent. An alarm is sounded in the main control room when hydrogen concentration at any of the four drywell sample points is determined by the analyzer to be greater than or equal to a minimum detectable level as prescribed by the HCOG EPG. This alarm signals the operator to manually initiate the hydrogen mixing system at the earliest practical time in order to reduce the chances of exceeding a combustible gas concentration during a degraded core accident hydrogen generation event; this will be described in more detail under separate cover as previously mentioned. The hydrogen mixing system valves close on a LOCA signal which can be overridden by the operator upon verifying that an actual LOCA does not exist. The

- 5←• 8←•

•→5

requirement for manual operation ensures that spurious signals do not prematurely actuate the system and, therefore, do not result in inadvertent steam bypass leakage from the drywell to the primary containment. The valve interlock previously described ensures that a single operator error does not result in initiation of the hydrogen mixing fans. Although a single operator error could result in the opening of one 6 in hydrogen mixing system inlet path, the allowable steam bypass leakage capacity for the River Bend Station drywell ($A/\sqrt{K} = 0.81 \text{ ft}^2$) exceeds the bypass leakage capacity of this leakage path ($A/\sqrt{K} = 0.2 \text{ ft}^2$) as discussed in Section 6.2.1.1.3.4.

Drywell and containment conditions of pressure, temperature, and hydrogen concentration are continuously monitored and are available to the main control room operators.

5←•

6.2.5.2.2 Hydrogen Recombiner System

The long-term control of hydrogen below the 4 percent by volume flammable limit is achieved by means of thermal hydrogen recombiners located in the primary containment. The hydrogen recombinder system is fully redundant and consists of two 100 percent capacity hydrogen recombiners. Each hydrogen recombinder has controls located in the main control room and a power supply cabinet in the auxiliary building. The hydrogen recombinder is located on the operating deck of the primary containment. Air flows by natural convection through the hydrogen recombinder unit. The recombinder is a completely passive device.

Each hydrogen recombinder unit incorporates the following design features:

1. The hydrogen recombinder unit consists of an inlet preheater section, a heater-recombination section, and an exhaust chamber. The unit is completely enclosed except for the inlet and outlet ports, which are louvered.
2. The heater section consists of 4 banks of vertically stacked electric heaters with each bank containing 60 individual U-type heaters.
3. A mixing chamber which mixes and dilutes the hot effluent with primary containment air to lower the temperature of the discharge stream.
4. An orifice plate regulates the rate of air flow through the unit.
5. Except for electrical power, there is no need of any plant service.
6. The hydrogen recombinder units are designed for all normal and accident loads, including seismic, temperature, and pressure transients following a LOCA.

Air and its contained hydrogen enter the hydrogen recombinder and flow up through a heated vertical duct and out the top by natural convection. As it rises, replacement air is drawn through intake louvers downward through a preheater section which heats the air and lowers its relative humidity. The preheated air then flows through an orifice plate, sized to maintain 100 scfm flow rate, to the heater section. The air flow is heated to the hydrogen-oxygen

reaction temperature (approximately 1,150°F). After passing through the heater section, the flow enters a mixing section where the hot gases are mixed and cooled with primary containment atmosphere before the gases are discharged directly into the primary containment atmosphere.

Tests verify that the hydrogen-oxygen recombination is not a catalytic surface effect associated with the heaters. Recombination occurs because of the increased temperature of the process gases. Since the phenomenon is not a surface effect, poisoning of the hydrogen recombiner unit by fission products or other post-LOCA products is not a problem. There are no differences between the hydrogen recombiner system on which the qualification tests were conducted and the hydrogen recombiner system which is used at River Bend Station. Results of tests performed on prototype and production electric hydrogen recombiners are given in References 13 through 16.

6.2.5.2.3 Containment Hydrogen Purge System

The containment hydrogen purge system is shown on Fig. 6.2-66.

The purge air is supplied by the service air system and enters the primary containment through the piping of the containment and drywell purge system (Section 9.4.6). The purge fan, located in the containment, discharges the purge air into the annulus through the piping of the containment and drywell purge system. From there, the purge air enters the annulus (Fig. 9.4-7) and is treated by the SGTS (Fig. 6.2-58). The flow passes through the charcoal filter beds and high-efficiency particulate air filters of the SGTS to minimize the release of radioactivity. If neither recombiner is operated, hydrogen control can be achieved by actuating the purge system.

6.2.5.2.4 Hydrogen Analyzer System

As discussed in Section 6.2.5.1, the limiting parameter for control is the hydrogen concentration. The hydrogen concentration is measured in the drywell and primary containment by two fully independent hydrogen analyzer trains. The redundant system design assures that the volumes are sampled in the event of the functional failure of one of the analyzer trains. The location of sample points within the drywell and primary containment is shown on Fig. 6.2-71.

For each independent train, samples are derived from 1 of 12 sources (10 in the containment and 2 in the drywell) and are

●→13

returned to the drywell. Two manually selected sample sources (any one of 10 in the containment and any one of 2 in the drywell) are automatically monitored by an automatic/manual sequencer that controls the opening and closing of the respective solenoid-operated valves in the sample lines. Prior to day 11 of post accident operation, each operating hydrogen analyzer will be placed in the manual mode of operation to prevent automatic sequencing between the drywell and containment. This is necessary to preserve the environmental qualifications of the solenoid-operated valves in each of the sample lines. The hydrogen analyzers will be aligned to continuously sample from either the drywell or containment, or a combination of both, for the remainder of the event. The hydrogen concentration level displayed on the main control room hydrogen analyzer recorders is accurate to within $\pm 0.5\%$ H₂ over the entire range (0-10%) and the ninety percent response time to sample the hydrogen concentration is 60 seconds or less.

13←●

All tests conducted to demonstrate the performance capability of the analyzers are referred to in Section 14.2.12.1.24.

6.2.5.2.5 Hydrogen Control System (Igniters)

●→5

The RBS hydrogen igniter system has been designed to meet the 10CFR50.44 requirement to address the generation of hydrogen during a hydrogen generation event (HGE). The hydrogen ignition system design has been substantiated by an extensive program of testing and analysis. The system is capable of maintaining the hydrogen concentration at safe levels (i.e., near the lower flammability limit of 4 percent by volume) during an event leading to considerable hydrogen production.

5←●

The design of the HCS is based on the concept of providing distributed ignition sources so that hydrogen combustion is accomplished in a controlled manner. The HCS consists of a total of 104 igniters, which are powered by two physically separate and electrically independent divisions each containing 52 igniters (see Section 7.3.1.1.5 for the electrical description of the HCS).

●→12

Per the EOPs and SAPs, the hydrogen igniter system would be manually initiated before significant hydrogen generation occurs. Actuation is directed when containment or drywell hydrogen concentration is greater than or equal to 0.7 volume percent.

If drywell hydrogen concentration exceeds 9 volume percent, then the EOPs and SAPs direct the operators to secure and prevent operation of the drywell igniters. If containment hydrogen volume percent exceeds the hydrogen deflagration overpressure limit (HDOL) for the containment pressure, then the EOPs direct the operators to secure and prevent operation of containment hydrogen igniters, hydrogen mixing, and hydrogen recombiners.

12←●

•→5 •→8

The combustible gas control system was originally designed to control the hydrogen generated during a design basis LOCA. The design basis of hydrogen mixing system and the hydrogen recombiner system enables these two systems to handle the amount of hydrogen generated as a result of 5 times the calculated metal-water reaction (MWR) rate. As a consequence of the Hydrogen Control Rule (10CFR50.44), the hydrogen igniter system was installed to conform with hydrogen control requirements for 75 percent MWR scenarios. Because it is designed to mitigate the consequences of a hydrogen generation event more severe than a design basis LOCA, operation of the hydrogen igniter system is not affected by availability of the hydrogen mixing or hydrogen recombiner systems. In this respect the hydrogen igniter system bounds the DBA scenario used in sizing the hydrogen mixing and recombiner systems.

8←•

The hydrogen igniters are located in accordance with the following criteria:

1. Hydrogen can be released to the containment atmosphere through the safety relief valves or through the drywell vents. In both cases hydrogen exhausts through the suppression pool. Therefore, igniter assemblies are located in a ring above the suppression pool as well as at other locations throughout the containment.
2. Hydrogen can be released to the drywell atmosphere through a pipe break in the drywell. Therefore, igniter assemblies are located throughout the drywell.
3. In open areas of the containment and the drywell, igniter assemblies are located in accordance with the following criteria:
 - a. Assuming only one Class 1E divisional power supply is functional following an accident, a

5←•

RBS USAR

THIS

PAGE

LEFT

INTENTIONALLY

BLANK

RBS USAR

maximum distance of 60 ft exists between the operable igniters.

- b. Assuming both Class 1E divisional power supplies are functional following an accident, a maximum distance of 30 ft exists between the operable igniters.
4. Igniters are located in all enclosed volumes/areas within the containment subject to possible hydrogen accumulation and pocketing. At least two igniters are located in each volume/area and are powered from separate Class 1E divisional power sources.
5. Hydrogen has a very large difference between the upward and downward flame propagation limits (4.1 percent hydrogen by volume for upward, 9 percent for downward, and 6 percent for horizontal). Refer to NUREG/CR-2530 (SAND82-0218) draft report "Review of the Grand Gulf Igniter System," Sandia National Laboratory. Igniter assemblies at RBS are positioned so that they can burn out large volumes of lean mixtures with upward propagation of flames (with the exception of igniters which are located close to the surface of the containment dome because of lack of structural supports in the dome). Igniters are located near or below the mid-plane regions of volumes/areas being protected and, where possible, away from large, solid surfaces, including surfaces above the igniters (i.e., ceilings or other structures).
6. In open spaces in the containment and the drywell, igniter assembly locations at the same elevation are alternated with respect to their Class 1E divisional power source. In addition, igniter assemblies are symmetrically staggered in azimuth positions with respect to those located on the next lower and higher elevations in order to maximize the number of likely hydrogen ignition points.
7. Two igniters, powered from separate Class 1E divisional power sources, are located within 30 ft of each hydrogen mixing system inlet terminal. Two igniters are located within 30 ft of each hydrogen mixing system fan exhaust and each of these two igniters is powered from separate Class 1E divisional power source

8. Igniters are located in the chimneys (hoist space and staircases at azimuth positions 150°, 225°, and 315°) at each floor elevation and powered by either Class 1E divisional power sources.

Table 6.2-53 gives the approximate igniter locations. All enclosed regions within the containment are served by redundant igniters.

6.2.5.3 Design Evaluation

Calculations are performed to determine the hydrogen generated in the post-LOCA environment, the resultant drywell and primary containment hydrogen concentrations as a function of time if uncontrolled, and the consequent functional requirements of the combustible gas control system to maintain the hydrogen concentration within limits. The consequences of combustible gas control system active component failures are presented in the Failure Modes and Effects Analysis (FMEA).

•→5

The following paragraphs describe the evaluation of the combustible gas control system (hydrogen mixing, hydrogen recombiners, and hydrogen purge) relative to its performance in controlling hydrogen concentrations under design basis LOCA (Regulatory Guide 1.7) conditions. The design adequacy and performance of the hydrogen igniters is being fully addressed for RBS by the Hydrogen Control Owners' Group (HCOG).

5←•

6.2.5.3.1 Accident Description

A complete description of the post-LOCA conditions is found in Sections 6.2.1 and 6.3. The following is a brief description of events associated with the DBA for hydrogen generation and control:

1. Complete severance of a recirculation pump suction line with the worst single active failure of a standby diesel generator is assumed to occur at time zero.
2. Drywell pressurization causes noncondensables in the drywell to be swept into the suppression pool, from which they rise to the primary containment atmosphere. For conservatism, all hydrogen generated in the drywell is assumed to remain in the drywell until the hydrogen mixing system is initiated.

•→8

3. Metal-water reaction occurs during the first 2 minutes, and a fraction of cladding equivalent

8←•

●→8 ●→5

to 5 times the value calculated for core-wide hydrogen generation in ECCS analyses is assumed to react.

8←●

4. Radiolysis begins to occur in the core water on the drywell floor and in the suppression pool.

Hydrogen and oxygen produced by incore radiolysis flow out through the break and into the drywell atmosphere. Hydrogen and oxygen produced by radiolysis of the water on the drywell floor rise to the drywell atmosphere. Hydrogen and oxygen produced in the suppression pool rise to the primary containment atmosphere.

●→12 ●→8

5. The drywell hydrogen concentration approaches 3.5 volume percent approximately 30 minutes after the LOCA. For this classic LOCA analysis the hydrogen mixing system is then initiated by the operator which results in dilution of hydrogen in the drywell to less than 1.4 volume percent. Note that plant EOPs and SAPs provide actual system operating guidance. The above hydrogen concentrations are conservative DBA assumptions. However, as previously mentioned, the high hydrogen alarm and concurrent manual actuation of hydrogen control equipment will occur at a minimum detectable hydrogen concentration to minimize the possibility of a hydrogen generation containment failure.

8←● ●→14

6. Radiolysis continues to increase the hydrogen concentration in both the drywell and the primary containment. When the hydrogen-monitoring instrumentation indicates that the concentration again reaches 3.5 volume percent, the hydrogen recombiners are started. Note that plant EOPs and SAPs provide actual system operating guidance. The above hydrogen concentrations are conservative DBA assumptions. With the conservative assumptions used for analysis purposes, hydrogen recombiner initiation would be required about 12.5 days following the LOCA, as shown on Fig. 6.2-68.

12←● 14←●

6.2.5.3.2 Sources of Hydrogen

6.2.5.3.2.1 Short-Term Hydrogen Generation

●→8

The combustible gas control system is designed for a metal-water reaction of five times the maximum calculated reaction given in Sections 6.3 and 4B. The reaction is assumed to occur over a period of 2 min.

5←● 8←●

6.2.5.3.2.2 Long-Term Hydrogen Generation

The generation of hydrogen due to radiolysis begins immediately following the LOCA, but proceeds at a much slower rate than the metal-water reaction.

Three regions are considered for radiolysis. Radiolysis of water in the reactor vessel and on the drywell floor contributes hydrogen to the drywell; the suppression pool radiolysis contributes hydrogen directly to the primary containment.

Incore radiolysis results from fission products remaining in the core, while suppression pool radiolysis occurs from fission products swept into the suppression pool. Hydrogen generation rate due to suppression pool and core radiolysis is taken from Reference 17. Gamma energy from incore fission products, attenuated by a factor of 0.1, is used to calculate the radiolysis of coolant adjacent to the core.

In addition, the gamma and beta energy from released halogens is used to calculate radiolysis in both the core region and the suppression pool. In all cases, a constant hydrogen radiolytic generation rate $G(\text{H}_2)$ of 0.5 molecule/100 eV absorbed and a constant, oxygen radiolytic generation rate $G(\text{O}_2)$ of 0.25 molecule/100 eV absorbed are used.

The quantity of hydrogen initially contained within the reactor coolant system is negligibly small and hence is neglected.

•→8

For aluminum and zinc, the corrosion rates are obtained from References 18 and 19, and are given in Table 6.2-42. The surface areas of aluminum and zinc are included in Table 6.2-43. Hydrogen production from corrosion of zinc-fabricated and zinc-coated items within the drywell is considered in the analysis. Aluminum corrosion in post-LOCA BWR conditions is insignificant. Reference 18 shows that aluminum is resistant to corrosion in distilled water (<2 mils/yr) up to 414°F. Hence, hydrogen production from aluminum corrosion is neglected. There is no mechanism for corrosion of aluminum in the primary containment, as the temperature of the atmosphere in the primary containment is much lower than that which would be necessary to promote corrosion; also, there are no containment sprays at River Bend Station.

5←• 8←•

• →5

6.2.5.3.3 Analysis

Based on the preceding hydrogen generation sources and the accident description, the hydrogen concentration in the drywell and primary containment are obtained as a function of time. To calculate the redistribution of hydrogen between the drywell and primary containment, a two-region computer model of the containment system is used. This model takes into consideration hydrogen generation from the metal-water reaction, radiolysis, metal corrosion in the drywell, mixing, and recombination. The calculation determines the inventory, partial pressure, and mole fraction of each atmospheric constituent in both regions as a function of time. All of the generated hydrogen is assumed to remain in the drywell until the hydrogen mixing system is initiated.

• →8

Tables 6.2-44 and 6.2-45 present the parameters used in the analysis of hydrogen buildup in the drywell. Fig. 6.2-68 presents the hydrogen concentration transients in the drywell and primary containment for the two cases of full and partial system availability. At approximately 30 minutes after the accident, the drywell hydrogen concentration reaches 3.5 volume percent. The hydrogen mixing system, for the purposes of this analysis, is started at this time. This results in reducing the concentration of hydrogen in the drywell by mixing the drywell atmosphere with the primary containment atmosphere.

8←• • →4

The hydrogen recombiners are started approximately 12.5 days after the LOCA, at which time the second peak in hydrogen concentration occurs. The zinc surface area provided in Table 6.2-43 has included the contribution from permanent shielding. The added zinc surface area from the permanent shielding increases the total hydrogen generation less than 0.5% and has no impact on the hydrogen recombiner start time. Thermal recombination of the hydrogen and oxygen in the primary containment atmosphere maintains the hydrogen concentration at safe levels. The hydrogen generation from all sources as a function of time after the LOCA is given on Fig. 6.2-69.

14←•

It should be reiterated that the hydrogen mixing system will actually be started at a minimum detectable hydrogen concentration as recommended by the HCOG EPG. This recommendation resulted from the Mark III Containment Hydrogen Control Owner's Group Topical Report HGN-112-NP, Appendix B.

5←•

•→5

6.2.5.3.4 Controlled Purge Site Doses

In the event of a design basis LOCA, the redundant hydrogen mixing and recombiner systems of the combustible gas control system operate so that containment hydrogen purging is not required. Eventually, however, the primary containment must be purged of the residual combustible gases and fission products prior to reentry by personnel.

Since the controlled containment hydrogen purge would not be initiated until some time in excess of 30 days after the LOCA, site boundary and low-population zone doses resulting from a controlled purge would be very small in comparison to that which is calculated for containment leakage following the LOCA (Chapter 15).

6.2.5.4 Testing and Inspection

Each active component of the combustible gas control system that is provided to operate after the DBA is testable during normal operation. The hydrogen mixing system, recombiners, and containment hydrogen purge system are periodically tested to ensure that the combustible gas control system operates in the unlikely event of a line break.

5←•

RBS USAR

THIS PAGE LEFT INTENTIONALLY BLANK

Preoperational tests of the combustible gas control system during the final stages of plant construction prior to plant startup (Section 14.2) ensure correct functioning of all controls, instrumentation, fans, recombiners, piping, and valves. System reference characteristics, such as pressure differentials and flow rates, are documented during the preoperational tests and are used as base points for measurements in subsequent operational tests.

During normal operation, the hydrogen mixing system fans, piping, recombiners, valves, instrumentation, wiring, and other components outside the drywell can be inspected visually at any time.

6.2.5.5 Instrumentation Requirements

6.2.5.5.1 Hydrogen Mixing System

Control switches are provided in the main control room for manually opening and closing the hydrogen mixing inlet and outlet valves. Interlocks prevent the outlet valves from opening unless the associated inlet valves are fully open. The hydrogen mixing system valves close on a LOCA signal which can be overridden by the operator upon verifying that an actual LOCA does not exist.

Control switches are provided in the main control room for manually starting and stopping the hydrogen mixing fans. Interlocks prevent the fans from running unless the associated inlet and outlet valves are fully open. Hydrogen mixing system inoperative alarms are provided in the main control room.

6.2.5.5.2 Hydrogen Recombiner System

Pushbutton controls are provided in the main control room for operation of the hydrogen recombiner feeder breakers.

On-off control switches and raise-lower potentiometers are provided in the main control room to operate the hydrogen recombiner electric heaters. Wattmeters and temperature indicators are provided in the main control room for monitoring the power to the heaters and the temperature of the gas stream. Hydrogen recombiner system inoperative alarms and breaker auto-trip alarms are provided in the main control room

6.2.5.5.3 Containment Hydrogen Purge System

Local control switches and pushbutton controls are provided for manual operation of the containment hydrogen purge fan and associated discharge valve, respectively. Local push-button controls are also provided for the containment hydrogen purge discharge valve to annulus.

Containment hydrogen purge fan discharge flow is maintained at its set point by modulating an air-operated flow control valve. A local indication of flow is provided.

Inoperative alarms are provided for the containment hydrogen purge system isolation valves.

A local control switch is provided for manually opening and closing the containment hydrogen purge supply solenoid-operated valve. Interlocks prevent the containment hydrogen purge supply valve from opening unless the containment hydrogen purge discharge to annulus valve is fully open.

Prior to operation of local switches from panel 1CPP*PNL102, portable and local ventilation will be provided if required to maintain local ambient temperatures below 107°F to ensure that environmental qualification of the panel is maintained.

6.2.5.5.4 Hydrogen Analyzer System

The analyzer containment isolation valves are manually controlled from the main control room.

●→13

The containment/drywell hydrogen concentration is recorded in the main control room. The redundant recorders operate in conjunction with the associated sequence programmer which selects the sample point to be analyzed. A pushbutton is provided in the main control room to override the sequence programmer and manually select the sample point. The post-accident hydrogen recorders automatically start recording when a manual or automatic containment isolation signal is present. Prior to day 11 of post accident operation, each operating hydrogen analyzer will be placed in the manual mode of operation to prevent automatic sequencing between the drywell and containment. This is necessary to preserve the environmental qualifications of the solenoid-operated valves in each of the sample lines. The hydrogen analyzers will be aligned to continuously sample from either the drywell or containment, or a combination of both, for the remainder of the event. The hydrogen analyzers are located in the auxiliary building. A high containment/drywell hydrogen concentration activates an alarm in the main control room.

13←●

6.2.5.5.5 Hydrogen Control System (Igniters)

The instrumentation and controls for the hydrogen control system are described in Section 7.3.1.1.5.

6.2.6 Containment Leakage Testing

•→10

This section presents the testing program for determination of the primary reactor containment integrated leakage rates (Type A tests), primary containment penetration leakage rates (Type B tests), and containment isolation valve leakage rates (Type C tests). The containment testing program complies with the primary containment leak rate testing program. This section also presents the testing program for determination of the drywell bypass leakage rate.

10←•

6.2.6.1 Containment Integrated Leakage Rate Test

•→8

Upon completion of construction of the primary reactor containment, including installation of all portions of mechanical, fluid, electrical, and instrumentation systems penetrating containment associated with containment integrity, and upon satisfactory completion of the structural integrity tests described in Section 3.8.2.7, the preoperational containment integrated leakage rate test is performed to verify that the actual measured containment (L_{am}) leakage rate does not exceed the design limit (L_d).

8←•

The preoperational containment integrated leakage rate test is performed at pressure P_a (7.6 psig) to measure the leakage rate L_{am} , which is required to be less than 0.75 times the maximum allowable leakage rate (L_a). River Bend Station is based upon an allowable leakage rate, L_a , equal to the design leakage limit, L_d , of 0.325 percent per day.

•→10

Prior to the performance of any Type A test, a general inspection of the accessible interior and exterior surfaces of the primary containment structure is performed to discover any evidence of structural deterioration which may affect either the containment structural integrity or leaktightness. If there is evidence of structural deterioration, the Type A test is not to be performed until corrective action is taken in accordance with repair procedures, nondestructive examinations, and tests as specified in the construction codes discussed in Section 3.8. Any corrective action taken is reported in accordance with the requirements of the primary containment leak rate testing program and 10CFR50.34. During the period between the completion of one Type A test and the initiation of the containment inspection for the subsequent Type A test, repairs may be made, if necessary, to assure that leakage through the containment isolation barriers does not exceed design limits.

10←•

•→8 •→6

The periodic Type A tests are conducted using the Absolute Method described in ANSI/ANS 56.8-1994. The containment leakage rate calculations are based on either the Total Time method of BN-TOP-1 or the Mass Point Analysis Method of ANSI/ANS 56.8-1994. Values of primary containment atmosphere drybulb temperature, dewpoint temperature (water vapor pressure), and pressure are used in the leakage rate calculations. A statistical linear regression analysis of the data is performed using the method of least squares to calculate the leakage rate and associated 95-percent confidence interval. The calculated leakage rate and upper 95-percent confidence limit (UCL) are reported in accordance with the requirements of the Technical Specifications/Requirements.

8←•

The quantity and types of sensors associated with primary containment integrated leakage rate instrumentation are selected to meet the leakage testing requirements of 10CFR50, Appendix J.

6←•

Prior to commencement of any Type A test, the following pretest requirements are met:

1. The closure of containment isolation valves is accomplished by normal operation and without any preliminary exercising or adjustments (e.g., no tightening of valve with manual handwheel after closure by valve motor). Valve closure malfunctions or valve position adjustments necessary to reduce containment leakage are reported in conjunction with the Type A test final report.
2. The fluid systems are aligned in accordance with 10CFR50, Appendix J, Option B. Those fluid lines which are vented and drained to ensure exposure of the system containment isolation valves to the containment atmosphere and the full differential pressure during the Type A test are identified in Table 6.2-40. Those systems that remain filled for the Type A test and whose isolation valves are not subjected to Type A test pressure, but are later subjected to Type C tests, are also identified in Table 6.2-40. As permitted by regulations, fluid lines (pathways) which are Type B or C tested within the previous 24 calendar months need not be vented or drained during the Type A test. The as-found and as-left leakage rate for all Type B or C pathways that are not drained and vented must be added to the Type A leakage rate Upper Confidence Limit (UCL).
3. The primary reactor containment atmosphere is allowed to stabilize for a minimum of 4 hr after

reaching test pressure prior to the start of the Type A test. The containment atmosphere is considered stabilized when the stabilizing requirements of BN-TOP-1 or ANSI/ANS 56.8-1994 are met. The relative humidity, temperature, and absolute pressure of the containment atmosphere are monitored so that vapor pressure correction can be made.

4. The preoperational ILRT duration will be 24 hr to allow for diurnal (cyclic) effects and ISG effects, if any, to be observed and evaluated.

Upon completion of the Type A test, a verification test is performed to confirm the capability of the integrated leakage rate instrumentation to satisfactorily determine the containment integrated leakage rate. The verification test is accomplished using the superimposed leak method. As an alternate to the superimposed leak method, the mass step change method is used.

If, during the performance of a Type A test, excessive leakage occurs through locally testable penetrations or isolation valves to the extent that it interferes with the satisfactory completion of the test, these leakage paths are isolated and the Type A test continued to full test period. Local leakage tests are then performed before and after the repair of each isolated leakage path. The sum of the post-repaired leakage rates shall be added to the measured leakage rate and the UCL. This total is required to be less than 75 percent of the maximum allowable leakage rate, L_a (where L_a is equal to L_d , or 0.325 percent per day). Local leakage rates are not subtracted from the Type A test results to determine the acceptability of a test. Test results are reported with both the pre- and post-repaired leakage rates.

6.2.6.2 Containment Penetration Leakage Rate Test

Containment penetrations for which design incorporates resilient seals, gaskets, or sealant compound, air lock door seals, and the equipment and access doors with resilient or inflatable seals or gaskets, and other such penetrations receive a preoperational and periodic Type B leak test in accordance with Appendix J of 10CFR50.

These Type B tests are conducted at a test pressure of P_a (7.6 psig). 10 CFR 50 Appendix J defines P_a as the "calculated peak containment internal pressure related to the design basis accident and specified either in the technical specification or associated bases." The containment pressure response is shown in RBS USAR Figures 6.2-4 for main steam line breaks and 6.2-5 for reactor coolant recirculation line breaks. These figures show the pressure rise in containment and the wetwell. The containment is the air space above the hydraulic control unit (HCU) floor while the wetwell is the region between the HCU floor and the surface of the suppression pool. The wetwell pressure is initially the same as the containment pressure. At about 2 seconds, the wetwell pressure increases rapidly while the containment pressure increases gradually. At about 5 to 6 seconds, the wetwell pressure decreases to the same pressure as the containment pressure. After this point, both the wetwell and containment pressure increase in unison to an eventual peak of 3.6 psig.

The short-term localized pressure spike in wetwell pressure (9.3 psig, considering Technical Specification allowable initial conditions) is not appropriate to use for P_a , as that value is not representative of the long-term potential leakage for the containment as a whole. Accordingly, RBS was granted an exemption to the Appendix J definition of P_a by NRC.

The following is a list of containment penetrations receiving a Type B test:

1. Fuel transfer tube blind flange and expansion bellows
2. Containment vessel control rod drive removal hatch
3. Containment vessel personnel air locks
4. Containment vessel equipment hatch
5. All piping penetrations fitted with expansion bellows
6. Containment electrical penetrations.

For the containment personnel locks, the lock design incorporates provisions for testing between the door seals and the door (Fig. 6.2-72). These provisions include:

• →4

1. Testing of annulus between seals - A test connection has been provided on each door. The annulus between the seals can be pressurized and the pressure decay monitored to calculate the leaktight integrity of the seals.

14←•

2. Overall lock pressure test - A test connection has been provided on the outer face of each bulkhead. The entire lock interior can be pressurized and the pressure decay monitored to calculate the overall lock leakage.
3. Shafts and view ports penetrating doors or bulkheads - A test connection has been provided to permit pressurization between seals.

The combined leakage rate for all penetrations and valves subject to Type B and C tests is required to be less than $0.60 L_a$ (where L_a is equal to L_d , or 0.325 percent per day).

6.2.6.3 Containment Isolation Valve Leakage Rate Test

Any valve that is intended to provide a barrier between the containment environment and the outside environment and which must be in a closed condition to effect containment

integrity receives a preoperational and a periodic leak test in accordance with Appendix J of 10CFR50.

Those containment isolation valves that receive a Type C test are indicated in Table 6.2-40. Those containment isolation valves that are not required to receive a Type C test and the basis for their exclusion from Type C testing are also indicated in Table 6.2-40.

•→8

Test taps for leakage rate testing have been provided on the lines associated with the containment isolation valves. They are classified as double-isolated sealed-pipe test connections consisting of a locked closed isolation valve in series with a pipe cap. Administrative controls and Technical Specification requirements are established to assure proper isolation of the test taps used for leakage rate testing.

8←•

The test pressure for all Type C tested containment isolation valves is 7.60 psig.

•→10 •→8

The main steam isolation valve leakage will be excluded from the summation for the local leak tests since it is supplied with the positive pressure MSPLCS seal system. Secondary containment bypass leakage paths will also not be included in the computation of $0.60 L_a$. Secondary containment bypass leakage paths are required to meet a leakage rate limit specified in Technical Specifications. This leakage limit is included in the offsite radiological dose assessment as leakage in addition to $0.60 L_a$.

8←• 10←•

The test fluids used to conduct Type C tests will be water, instrument air, and nitrogen.

The total acceptable leakage from Type B and C tests is required to be less than $0.60 L_a$ (where L_a is equal to L_d , or 0.325 percent per day).

6.2.6.4 Scheduling and Reporting of Periodic Tests

The periodic leakage rate tests are conducted at the intervals described in the Primary Containment Leakage Rate Testing Program.

•→8

Types B and C tests may be conducted at any time during normal plant operations or during shutdown periods as long as the time interval between any individual Type B or C test does not exceed the maximum allowable interval specified in the Primary Containment Leakage Rate Testing Program. Each time a Type B or C test is completed, the overall total leakage rate for all

8←•

●→8

required Types B and C tests are updated to reflect the most recent test results. Types A, B, and C test results must be documented and available for inspection.

6.2.6.5 Special Testing Requirements

6.2.6.5.1 Drywell Bypass Leakage Test

●→8A

On a schedule consistent with the drywell structural integrity test described in Section 3.8.3.7, a preoperational drywell bypass leakage test is performed at drywell design pressure. Preoperational and periodic drywell leakage tests at a reduced pressure, defined in the technical specifications/requirements, are performed in addition to the preoperational and periodic Type A tests previously described. These drywell leakage tests verify that, over the design life of the plant, no paths for gross leakage from the drywell to the containment air space bypassing the pressure suppression feature exist. The combination of the design pressure and reduced pressure leakage tests also verifies that the drywell can perform adequately for the full range of postulated coolant system break sizes. The basis for the drywell leakage limits are described in Section 6.2.1.

8←● 8A←●

Drywell bypass leakage tests are performed with the drywell isolated from the containment. The containment air space external to the drywell is vented to the atmosphere via the reactor plant ventilation system. The horizontal vents are capped for the preoperational tests to achieve the design drywell internal pressure, but the reduced periodic test pressure is less than that required to cause drywell air to flow through the horizontal vents to the wetwell. The drywell atmosphere is allowed to stabilize for a period of 1 hr after attaining test pressure. Leakage rate tests commence after the stabilization period. The bypass leakage tests are conducted for a minimum of 1 hr to determine actual leakage rates. If at the end of 1 hr, leakage rates are well established and less than allowable values, the test is terminated; otherwise, leakage testing is continued for a minimum of 4 hr or until reaching atmospheric pressure, whichever occurs first.

The test method is based on drywell atmosphere pressure observations and the known drywell free air volume. The leakage rate is calculated from pressure data, drywell free air volume, and elapsed time.

•→8

The periodic drywell bypass leakage test pressures and acceptance criteria are specified in the Technical Specification requirements. Periodic drywell structural inspections are performed at intervals specified in the technical specifications.

8←•

The preoperational drywell leakage is required to be no greater than the maximum allowable leakage rate of 7824 scfm at drywell design pressure (25 psig) test and maximum allowable leakage rate of 3248 scfm at drywell reduced pressure (3 psig) test. Preoperational drywell leakage tests are performed as late as is practical in the construction sequence, but before initial plant operation.

•→10 •→8

Preoperational tests of the main steam positive leakage control system shall be performed to ensure that these systems meet the requirements of 10CFR50, Appendix J. The basis for the acceptable fluid leakage rates is established in the Technical Specifications Bases. The main steam positive leakage control system can deliver seal fluid sufficient to assure the sealing function for at least 30 days at a pressure of 1.10 P_a.

8←• 10←•

References - 6.2

1. Models Used in LOCTVS - A Computer Code to Determine Pressure and Temperature Response of Vapor Suppression Containments Following a Loss-of-Coolant Accident, SWECO 8101, March 1981.
2. Moody, F. J. Maximum Two-Phase Vessel Blowdown from Pipes, APED-4827, April 1965.
3. GE Design Report, Containment Loads Report (CLR) Mark III Containment, 22A4365, Rev. 4, January 1980 (including Class III Proprietary Supplement).
4. Bilanin, W. J. The General Electric Mark III Pressure Suppression Containment System Analytical Model, NEDO-20533, June 1974 (including Supplement, NEDO-20533-1, September 1975).
5. Slater, C. E. Comparison of Predictions from the Reactor Primary System Decompression Code (RELAP 3) with Decompression Data from the Semiscale Blowdown and Emergency Core Cooling (ECC) Project, IN-1444, December 1970.
6. Allemann, R. T., et al. High-Enthalpy-Water Blowdown Tests from a Simple Vessel through a Side Outlet, BNWL-1470, February 1971.
7. Slifer, B. C. and Hench, J. E. Loss-of-Coolant Accident and Emergency Core Cooling Models for General Electric Boiling Water Reactors, NEDO-10329, April 1971.
8. RELAP4/MOD5 A Computer Program for Transient Thermal-Hydraulic Analysis of Nuclear Reactors and Related Systems User's Manual, ANCR-NUREG-1335, September 1976.
9. Sharma, D. F. Technical Description Annulus Pressurization Load Adequacy Evaluation, NEDO-24548, January 1979.
10. Idel'Chik, I. E. Handbook of Hydraulic Resistance Coefficients of Local Resistance and of Friction, U.S. AEC-TR-6630, 1966.
11. Crane Co. Flow of Fluids through Valves, Fittings, and Pipe, Technical Paper No. 410, 1969.

RBS USAR

12. NRC Branch Technical Position ASB 9-2, Residual Decay Energy for Light Water Reactors for Long-Term Cooling, Rev. 1, Attached to Standard Review Plan Section 9.2.5.
13. WCAP 7709-L Supplement 1, Electric Hydrogen Recombiner for PWR Containments, April 1972.
14. WCAP 7709-L Supplement 2, Electric Hydrogen Recombiner for PWR Containments Equipment Qualification Report, September 1972.
15. WCAP 7709-L Supplement 3, Electric Hydrogen Recombiner for PWR Containments Long Term Tests, January 1974.
16. WCAP 7709-L Supplement 4, Electric Hydrogen Recombiner for PWR Containments, April 1974.
17. ANS draft ANSI 5/N275, Containment Hydrogen Control, June 1976.
18. Corrosion Data Survey, Fifth Edition, compiled by N. E. Hammer, National Association of Corrosion Engineers (Publishers), 1981.
19. Van Rooyen, D. Hydrogen Release From Zinc Corrosion. Brookhaven National Laboratory Memorandum, February 8, 1978.
20. Uchida, H.; Oyama, A.; and Togo, Y. Evaluation of Post-Incident Cooling Systems of Light-Water Power Reactors, Proceedings of the Third International Conference on the Peaceful Uses of Atomic Energy held in Geneva, Switzerland August 31 to September 9, 1964, Vol. 13, New York, NY, United Nations, 1965, p 93-104, (A/Conf. 28/p 436).
21. NUREG 0737, Clarification of TMI Action Plan Requirements, November 1980, Item II.E.4.2, Attachment 1, dated October 23, 1979, Interim Position for Containment Purge and Vent Valve Operation Pending Resolution of Isolation Valve Operability.
22. Branch Technical Position (BTP), Containment System Branch (CSB) 6-4, Containment Purging During Normal Plant Operations.
23. NUREG 0578, TMI-2 Lessons Learned, Task Force Status Report and Short-Term Recommendations, July 1979.

RBS USAR

24. Regulatory Guide 1.141, Containment Isolation Provisions for Fluid Systems, April 1978.
25. Regulatory Guide 1.11, Instrument Lines Penetrating Primary Containment, March 10, 1971; supplement, February 17, 1972.
26. BWR Owners' Group, NUREG 0578, Implementation Analyses and Positions for Plan-Unique Submittals NEDO-24782, BONED006 Class I, August 1980.
27. Transmittal Letter RBG-19,385, from J. E. Booker to H. R. Denton dated November 8, 1984.
●→5
28. HGN-122, Revision 3 to Mark III Combustible Gas Emergency Procedure Guideline.
29. HGN-112-NP, Mark III Containment Hydrogen Control Owner's Group Topical Report.
5←●
●→14
30. NEDO-10320, "The GE Pressure Suppression Containment System Analytical Model," April 1971.
14←●

6.3 EMERGENCY CORE COOLING SYSTEMS

6.3.1 Design Bases and Summary Description

Section 6.3.1 provides the design bases for the emergency core cooling systems (ECCS) and a summary description of the systems as an introduction to the more detailed design descriptions provided in Section 6.3.2 and the performance analysis provided in Section 6.3.3.

6.3.1.1 Design Bases

6.3.1.1.1 Performance and Functional Requirements

●→16 ●→15

The ECCS is designed to provide protection against postulated loss-of-coolant accidents (LOCA) caused by ruptures in primary system piping. The functional requirements (for example, coolant delivery rates) specified in detail in Table 6.3-2 are such that the system performance under all LOCA conditions postulated in the design satisfies the requirements of Paragraph 50.46, "Acceptance Criteria for Emergency Core Cooling System for Light Water Cooled Nuclear Power Reactors," of 10CFR50. These requirements, the most important of which is that the post-LOCA peak cladding temperature (PCT) is limited to 2,200°F, are summarized in Section 6.3.3.2. In addition, the ECCS is designed to meet the following requirements:

15←● 16←●

1. Protection is provided for any primary system line break up to and including the double ended rupture (DER) of the largest line.
2. Two independent cooling methods (flooding and spraying) are provided to cool the core.

●→10

3. One high pressure cooling system is provided which is capable of maintaining water level above the top of the core and preventing automatic depressurization system (ADS) actuation for breaks of lines less than 1 inch nominal diameter.
4. No operator action is required for at least 20 min after an accident to allow for operator assessment and decision.

10←●

5. The ECCS is designed to satisfy all criteria specified in Section 6.3 for any normal mode of reactor operation.

6. A sufficient water source and the necessary piping, pumps, and other hardware are provided so that the containment and reactor core can be flooded for possible core heat removal following a LOCA.

6.3.1.1.2 Reliability Requirements

The following reliability requirements apply:

1. The ECCS must conform to all licensing requirements and good design practices of isolation, separation, and common mode failure considerations.
2. In order to meet the above requirements, the ECCS network has built-in redundancy so that adequate cooling can be provided, even in the event of specified failures. As a minimum, the following equipment makes up the ECCS:
 - a. High pressure core spray (HPCS)
 - b. Low pressure core spray (LPCS)
 - c. Low pressure coolant injection (LPCI) loops
 - d. Automatic depressurization system (ADS)
3. The system is designed so that a single active or passive component failure, including power buses, electrical and mechanical parts, cabinets, and wiring does not disable the ADS.
4. In the event of a break in a pipe that is not a part of the ECCS, no single active component failure in the ECCS prevents automatic initiation and successful operation of less than the following combination of ECCS equipment:
 - a. 3 LPCI loops, the LPCS and the ADS (i.e., HPCS failure); or
 - b. 2 LPCI loops, the HPCS and the ADS (i.e., LPCS diesel generator failure); or
 - c. 1 LPCI loop, the LPCS, the HPCS, and ADS (i.e., LPCI diesel generator failure).
5. In the event of a break in a pipe that is a part of the ECCS, no single active component failure in the ECCS prevents automatic initiation and successful

operation of less than the following combination of ECCS equipment:

- a. 2 LPCI loops and the ADS; or
- b. 1 LPCI loop, the LPCS, and the ADS; or
- c. 1 LPCI loop, the HPCS, and the ADS; or
- d. The LPCS, the HPCS, and ADS.

These are the minimum ECCS combinations which result after assuming any failure (from 4 above) and assuming that the ECCS line break disables the affected system.

●→10

- 6. Long term (once level has been recovered and PCT has dropped significantly) cooling requirements call for the removal of decay heat via the standby service water system. In addition to the break which initiated the loss of coolant event, the system must be able to sustain one failure, either active or passive, and still have at least one ECCS pump (LPCI, HPCS, or LPCS) operating putting water into the vessel and an RHR heat exchanger operating with 100 percent standby service water flow.

10←●

- 7. Offsite power is the preferred source of power for the ECCS network and precautions are made to assure its availability. However, onsite emergency power is provided with sufficient diversity and capacity so that all the above requirements can be met if offsite power is not available.
- 8. The onsite diesel fuel reserve is in accordance with IEEE-308 (1974) criteria.
- 9. Diesel-load configuration is as follows:
 - a. 1 LPCI loop (with heat exchanger) and the LPCS connected to a single diesel generator.
 - b. 2 additional LPCI loops (1 loop with heat exchanger) connected to a single diesel generator.
 - c. The HPCS connected to a single diesel generator.

10. Systems which interface with, but are not part of, the ECCS are designed and operated such that failure(s) in the interfacing systems does not propagate to and/or affect the performance of the ECCS.
11. Non-ECCS systems interfacing with the ECCS buses are automatically shed and/or inhibited from the ECCS buses when a LOCA signal exists and offsite ac power is not available.
12. No more than one storage battery is connectable to a Class 1E dc power bus.
13. Each system of the ECCS including flow rate and sensing networks is capable of being tested during shutdown. All active components are capable of being tested during plant operation, including logic required to automatically initiate component action.
14. Provisions for testing the ECCS network components (electronic, mechanical, hydraulic, and pneumatic, as applicable) are installed in such a manner that they are an integral and nonseparable part of the design.

6.3.1.1.3 ECCS Requirements for Protection from Physical Damage

The ECCS piping and components are protected against damage from movement, from thermal stresses, from the effects of the LOCA, and the safe shutdown earthquake (SSE).

The ECCS is protected against the effects of pipe whip, which might result from piping failures up to and including the design basis event LOCA. This protection is provided by separation, pipe whip restraints, or energy absorbing materials if required. One of these three methods is applied to provide protection against damage to piping and components of the ECCS which otherwise could result in a reduction of ECCS effectiveness to an unacceptable level.

The ECCS piping and components located outside the reactor building are protected from internally and externally generated missiles by the Seismic Category I structure of the auxiliary building ECCS pump rooms. In addition, the watertight construction of the ECCS pump rooms protects against mass flooding of redundant ECCS pumps.

The RBS design employs an ECCS valve crescent area between the separate watertight ECCS equipment rooms and the suppression pool. The ECCS suction lines and the isolation valves within the crescent area are Safety Class 2. The systems' design/operating pressures and temperatures are 100 psig 212°F/25 psig 185°F, and the minimum piping design pressure and temperatures are 235 psig 212°F. The valves are designed to preclude leakage and no seals or gaskets are installed between the containment penetrations and the isolation valves.

- →6

Each ECCS equipment room is provided with a safety-related level transmitter, to detect a rising water condition which annunciates an alarm and provides level indication in the control room. Also, these rooms each contain a sump with a high level alarm and duplex pumps.

- 16←•

The crescent area contains a sump with high level alarm and duplex pumps with operating indication in the main control room. In addition, periodic surveillance of this area ensures that leakage is detected.

Suppression pool leakage into the ECCS equipment rooms and crescent area can also be detected by safety-related suppression pool low level alarms and indications in the main control room.

If leakage is detected by instruments and/or operator surveillance, the pump suction isolation valve is remote-manually closed from the main control room. This isolation occurs such that the suppression pool water level does not fall below the minimum allowable vent coverage level.

Mechanical separation outside the drywell is achieved as follows:

1. The ECCS is separated into three functional groups:
 - a. HPCS
 - b. LPCS + 1 LPCI + 100 percent service water and heat exchanger
 - c. 2 LPCI pumps + 100 percent service water and heat exchanger

2. The equipment in each group is separated from that in the other two groups. In addition, the HPCS and reactor core isolation cooling (RCIC) system (which is not part of the ECCS) is physically separated.
3. Separation barriers are constructed between the functional groups as required to assure that environmental disturbances such as fire, pipe rupture, falling objects, etc, affecting one functional group do not affect the remaining groups. In addition, separation barriers are provided as required to assure that such disturbances do not affect both the RCIC and the HPCS.

6.3.1.1.4 ECCS Environmental Design Basis

Each ECCS and the RCIC system have a safety related injection/isolation testable check valve located in piping within the drywell. In addition, the RCIC system has an isolation valve in the drywell portion of its steam supply piping. All valves are located above the highest water level expected in the drywell during any accident. The valves are qualified for the applicable envelope-of-accident environmental conditions.

The portions of ECCS and RCIC piping and equipment located outside the drywell and within the secondary containment are qualified for the applicable envelope-of-accident environmental conditions.

6.3.1.2 Summary Descriptions of ECCS

The ECCS injection network comprises a high pressure core spray (HPCS) system, a low pressure core spray (LPCS) system, and the low pressure coolant injection (LPCI) mode of the residual heat removal (RHR) system. These systems are briefly described here as an introduction to the more detailed system design descriptions provided in Section 6.3.2. The ADS which assists the injection network under certain conditions is also briefly described. A comparison of ECCS designs of other boiling water reactors (BWR) is provided in Table 1.3-3.

6.3.1.2.1 High Pressure Core Spray

The HPCS pumps water through a peripheral ring spray sparger mounted above the reactor core. Coolant is supplied over the entire range of system operating pressures. The primary purpose of HPCS is to maintain reactor vessel coolant

inventory after small breaks which do not depressurize the reactor vessel. HPCS also provides spray cooling heat transfer following larger breaks.

6.3.1.2.2 Low Pressure Core Spray

The LPCS is an independent loop similar to the HPCS. The primary difference is that the LPCS delivers water over the core at relatively low reactor pressure. The primary purpose of the LPCS is to provide coolant inventory makeup and spray cooling following large breaks. Following a small break and ADS initiation, LPCS provides coolant inventory makeup and spray cooling heat transfer.

6.3.1.2.3 Low Pressure Coolant Injection

LPCI is an operating mode of the RHR system. Three pumps deliver water from the suppression pool to the bypass region inside the shroud through three separate reactor vessel penetrations to provide inventory makeup following large pipe breaks. Following a small break and ADS initiation, LPCI provides coolant inventory makeup.

6.3.1.2.4 Automatic Depressurization System

The ADS utilizes 7 of 16 safety relief valves to reduce reactor pressure following small breaks in the event of HPCS failure. When the vessel pressure is reduced to within the capacity of the low pressure systems (LPCS and LPCI), they provide inventory makeup to maintain acceptable post-accident temperatures.

6.3.2 System Design

A more detailed description of the individual systems including individual design characteristics of the systems are covered in detail in Sections 6.3.2.1 through 6.3.2.4.

The following discussion provides details of the combined systems; in particular, those design features and characteristics which are common to all systems.

6.3.2.1 Schematic Piping and Instrumentation Diagrams

●→10

The P&IDs for the ECCS are identified in Section 6.3.2.2.

10←●

6.3.2.2 Equipment and Component Descriptions

●→16 ●→15 ●→12

The starting signal for the ECCS comes from at least two independent and redundant sensors of drywell pressure and low reactor water level. The ECCS is automatically actuated and requires no operator action during the first 20 min following the accident. A time sequence for starting of the systems is provided in Table 6.3-1.

12←●15←●16←●

Electric power for operation of the ECCS is from normal ac power sources. Upon loss of the regular power, operation is from onsite standby ac power sources. Standby sources have sufficient diversity and capacity so that all ECCS requirements are satisfied. The HPCS is powered from one ac supply bus. The LPCS and one LPCI are powered from a second ac supply bus and the two remaining LPCIs are powered from a third and separate ac supply bus. The HPCS has its own diesel generator as its alternate power supply. The LPCS and one LPCI loops switch to one standby diesel generator and the other two LPCI loops switch to a second standby diesel generator. Section 8.3 contains a more detailed description of the power supplies for the ECCS.

Suction piping for the ECCS pumps is conservatively designed to eliminate the potential for local flashing and cavitation. The limiting condition for NPSH available occurs for all of the ECCS pumps when suction is taken from the suppression pool.

Regulatory Guide 1.1, Rev. 0 prohibits design reliance on pressure and/or temperature transients expected during a LOCA for assuring adequate net positive suction head (NPSH). The requirements of this Regulatory Guide are applicable to the HPCS, LPCS, and LPCI pumps. The BWR design conservatively assumes 0 psig containment pressure and maximum expected temperatures of the pumped fluids. Thus no reliance is placed on pressure and/or temperature transients to assure adequate NPSH. The limiting condition for NPSH available occurs for all of the ECCS pumps when suction is taken from the suppression pool. In addition to the requirements of Regulatory Guide 1.1, the following design features/criteria were applied to calculations of NPSH available for ECCS suction piping from the suppression pool:

●→10

1. Suppression pool level is assumed to be at its post-LOCA minimum level of 83 ft 3 in.
2. The maximum expected suppression pool temperature is 185°F.

●→11 10←●11←●

•→10

4. Pumps are assumed to be operating at maximum run-out flow.
5. The minimum pump NPSH available is designed to be 5 ft at a point 2 ft above the pump mounting flange.
6. All ECCS pump suction lines are run from their points of origin in the suppression pool to their respective pump suction flanges. Liquid continuity is ensured throughout the entire length of the piping.

The HPCS and LPCS suppression pool suction strainer centerline elevation is at 77' 8 7/16". A minimum ECCS suction strainer submergence of greater than 3 ft is maintained to preclude vortex formation.

The following discussion demonstrates that the available NPSH at all points in ECCS pump suction is adequate to preclude local flashing and pump cavitation under worst postulated conditions.

10←•

HPCS

The HPCS pump can take suction from the condensate storage tank or the suppression pool. However, the combination of minimum static head, maximum fluid vapor pressure, and frictional losses in piping and fittings make suction from the suppression pool the limiting condition of NPSH available.

•→10

10←•

RBS USAR

THIS PAGE HAS BEEN DELETED

LPCS

The LPCS pump takes suction from either the suppression pool or the RHR system. However, suction from the RHR system is used only during shutdown for test purposes and does not constitute the limiting condition for NPSH available. The combination of minimum static head, maximum fluid vapor pressure, and frictional losses in piping and fittings make suction from the suppression pool the limiting condition of NPSH available.

●→10

10←●

LPCI

●→10

This ECCS mode of RHR system operation constitutes the limiting condition of NPSH available for the RHR pumps. With all other conditions equal the NPSH available for RHR pump A is the least of the three due to the greatest equivalent length of suction piping and fittings. The ECCS mode of operation is the worst case based upon the fluid velocity. Accordingly, the NPSH calculation is for this pump only while performing its ECCS function.

Pump characteristic curves are given in Fig. 6.3-3 (HPCS), 6.3-6 (LPCS), and 6.3-7 (LPCI).

●→2

The NPSH calculations use a reference elevation of 2 ft above the pump mounting flange and a desired NPSH available of ≥ 5 ft since these requirements are specified diagrams in the respective systems' process to allow for some design margin. The ≥ 5 -ft value of NPSH available does not relate to actual pump performance requirements.

10←● 2←●

The graphs of NPSH required shown on Figures 6.3-3, 6.3-6, and 6.3-7 are based on performance tests conducted by

the pump manufacturer. The comparison table below demonstrates that all the ECCS pumps have adequate margin of NPSH available over actual NPSH required:

<u>Pump</u>	<u>NPSH Margin Adjusted to a Reference Elevation 3 Ft Above Pump Mounting Flange (ft)</u>	<u>NPSH Required 3 Ft Above Pump Mounting Flange Based on Performance Test by Pump Vendor (ft)</u>
•→10		
HPCS	>5	1.00
LPCS	>5	0.30
RHR (LPCI)	>5	0.30

10←•

6.3.2.2.1 High Pressure Core Spray (HPCS) System

•→10

The HPCS system consists of a single motor-driven centrifugal pump located outside the primary containment, a spray sparger in the reactor vessel located above the core (separate from the LPCS sparger), and associated system piping, valves, controls, and instrumentation. The system is designed to operate from normal offsite auxiliary power or from a diesel generator supply if offsite power is not available. The P&ID, Fig. 6.3-1 for the HPCS, shows the system components and their arrangement.

10←• •→12

The principal active HPCS equipment is located outside the primary containment. Suction piping is provided from the condensate storage tank and the suppression pool. Such an arrangement provides the capability to use reactor grade water from the condensate storage tank when the HPCS system functions to back up the RCIC system. In the event that the condensate storage water supply becomes exhausted or is not available, automatic switchover to the suppression pool water source assures a closed cooling water supply for continuous operation of the HPCS system. HPCS pump suction is also automatically transferred to the suppression pool if the suppression pool water level exceeds a prescribed value. The condensate storage tank reserves a maximum of 125,000 gal of water just for use by the HPCS and RCIC.

12←•

After the HPCS injection piping enters the vessel, it divides and enters the shroud at two points near the top of the shroud. A semicircular sparger is attached to each outlet. Nozzles are spaced around the spargers to spray the water radially over the core and into the fuel assemblies.

●→3●→13

The HPCS discharge line to the reactor is provided with two isolation valves. One of these valves is a manually testable check valve located inside the drywell as close as practical to the reactor vessel. HPCS injection flow causes this valve to open during LOCA conditions (i.e., no power is required for valve actuation during LOCA). If the HPCS line should break outside the containment, the check valve in the line inside the drywell prevents the loss of reactor coolant outside the containment. The other isolation valve (which is also referred to as the HPCS injection valve) is a motor operated gate valve located outside the primary containment as close as practical to HPCS discharge line penetration into the containment. This valve is capable of opening with the maximum differential pressure across the valve expected for any system operating mode including HPCS pump shutoff head. The valve opens sufficiently to provide rated flow to the vessel within 12 sec following receipt of a signal to open provided power is available. This valve is normally closed to back up the inside testable check valve for containment integrity purposes. A test connection/drain line is provided between the two isolation valves and is normally closed with two valves to assure containment integrity.

3←●13←●

Remote controls for operating the motor operated components and diesel generator are provided in the main control room. The controls and instrumentation of the HPCS system are described, illustrated, and evaluated in Section 7.3.1.1.

The system is designed to pump water into the reactor vessel over a wide range of pressures. For small breaks that do not result in rapid reactor depressurization, the system maintains reactor water level and depressurizes the vessel. For large breaks the HPCS system cools the core by a spray.

If a LOCA should occur, two signals indicating low water level or high drywell pressure initiate the HPCS and its support equipment. The system can also be placed in operation manually.

The HPCS system is capable of delivering rated flow into the reactor vessel within 27 sec following receipt of an initiation signal.

When a high water level in the reactor vessel is signaled, the HPCS is automatically stopped by a signal to the injection valve to close. The HPCS system also serves as a backup to the RCIC system in the event the reactor becomes isolated from the main condenser during operation and feedwater flow is lost.

If normal auxiliary power is not available, the HPCS pump motor is supplied by its own standby diesel generator. The HPCS diesel generator is discussed in Section 8.3.

When the system is started, initial flow rate is established by primary system pressure. As vessel pressure decreases, flow increases. When vessel pressure reaches 200 psid (psid = differential pressure between the reactor vessel and the suction source) the system reaches rated core spray flow. The HPCS motor size is based on peak horsepower requirements.

●→10

The elevation of the HPCS pump is sufficiently below the water level of both the condensate storage tank and the suppression pool to provide a flooded pump suction and to meet NPSH requirements with the containment at atmospheric pressure, and the suction strainer at the design debris loading condition. (Refer to Section 6.3.2.2 for strainer pressure drop.) The available NPSH has been calculated in accordance with Regulatory Guide 1.1 as shown in Section 6.3.2.2.

10←●

A motor operated valve is provided in the suction line from the suppression pool. The valve is located as close to the suppression pool penetration as practical. This valve is used to isolate the suppression pool water source when HPCS system suction is from the condensate storage system and to isolate the system from the suppression pool in the event a leak develops in the HPCS system.

The HPCS pump characteristics of head, flow, horsepower, and required NPSH are shown in Fig. 6.3-3.

●→10

The design pressure and temperature of the system components are established based on the ASME Section III Boiler and Pressure Vessel Code.

10←●

A check valve, flow element, and restricting orifice are provided in the HPCS discharge line from the pump to the injection valve. The check valve is located below the minimum suppression pool water level and is provided so the piping downstream of the valve can be maintained full of water by the discharge line fill system (Section 6.3.2.2.5). The flow element is provided to measure system flow rate during LOCA and test conditions, and for automatic control of the minimum low flow bypass gate valve. The measured flow is indicated in the main control room. The restricting

orifice is sized during the preoperational test of the system to limit system flow to acceptable values as described on the HPCS system process diagram.

A low flow bypass line with a motor-operated gate valve connects to the HPCS discharge line upstream of the check valve on the pump discharge line. The line bypasses water to the suppression pool to prevent pump damage due to overheating when other discharge line valves are closed. The valve automatically closes when flow in the main discharge line is sufficient to provide required pump cooling.

To assure continuous core cooling, signals to isolate the containment do not operate any HPCS valves.

The HPCS system incorporates relief valves to protect the components and piping from overpressure conditions. One relief valve, set to relieve at 1,560 psig, is located on the discharge side of the pump downstream of the check valve to relieve thermally expanded fluid. A second relief valve is located on the suction side of the pump and is set at 100 psig with a capacity of >10 gpm @ 10 percent accumulation.

The HPCS components and piping are positioned to avoid damage from the physical effects of design-basis accidents (DBA), such as pipe whip, missiles, and high temperature, pressure, and humidity.

●→12

The HPCS equipment and support structures are designed in accordance with Seismic Category I criteria (Chapter 3), except for a portion of the pump suction and test return piping (reference Table 3.2-1, Sheet 5 of 34). The system is assumed to be filled with water for seismic analysis.

12←●

Provisions are included in the HPCS system which permit the HPCS system to be tested. These provisions are:

1. All active HPCS components are testable during normal plant operation.
2. A full flow test line is provided to route water from and to the condensate storage tank without entering the reactor pressure vessel (RPV). The suction line from the condensate storage tank also provides reactor grade water to fully test the HPCS including injection into the RPV during shutdown.

3. A full flow test line is provided to route water from and to the suppression pool without entering the RPV.
4. Instrumentation is provided to indicate system performance during normal test operations.
5. All motor-operated valves are capable of either local or remote manual operation for test purposes.
6. System relief valves are removable for bench-testing during plant shutdown.

6.3.2.2.2 Automatic Depressurization System (ADS)

If the reactor water level cannot be maintained at high pressure, the ADS, which is independent of any other ECCS, reduces the reactor pressure so that flow from LPCI and LPCS enters the reactor vessel in time to cool the core and limit fuel cladding temperature.

The ADS employs seven nuclear system pressure relief valves to relieve high pressure steam to the suppression pool. The design, location, description, operational characteristics, and evaluation of the pressure relief valves are discussed in detail in Section 5.2.2. The instrumentation and controls for the ADS are discussed in Section 7.3.1.1.1.2.

6.3.2.2.3 Low Pressure Core Spray (LPCS) System

●→10

The LPCS consists of: a centrifugal pump that can be powered by normal auxiliary power or the standby ac power system; a spray sparger in the reactor vessel above the core (separate from the HPCS sparger); piping and valves to convey water from the suppression pool to the sparger; and associated controls and instrumentation. Fig. 6.3-4, the LPCS system P&ID, presents the system components and their arrangement.

10←●

When low water level in the reactor vessel or high pressure in the drywell is sensed, and with reactor vessel pressure low enough, the LPCS system automatically starts and sprays water into the top of the fuel assemblies to cool the core. The LPCS injection piping enters the vessel, divides and enters the core shroud at two points near the top of the shroud. A semicircular sparger is attached to each outlet.

Nozzles are spaced around the sparger to spray the water radially over the core and into the fuel assemblies.

●→16 ●→15

The LPCS is designed to provide cooling to the reactor core only when the reactor vessel pressure is low, as is the case for large LOCA break sizes. However, when the LPCS operates in conjunction with the ADS, then the effective core cooling capability of the LPCS is extended to all break sizes because the ADS rapidly reduces the reactor vessel pressure to the LPCS operating range.

15←●16←●

The LPCS pump and all motor operated valves can be operated individually by manual switches located in the main control room. Operating indication is provided in the main control room by a flowmeter and valve indicator lights.

To assure continuity of core cooling, signals to isolate the containment do not operate any LPCS system valves.

●→12

The LPCS discharge line to the reactor is provided with two isolation valves. One of these valves is a testable check valve located inside the drywell as close as practical to the reactor vessel. LPCS injection flow causes this valve to open during LOCA conditions (i.e., no power is required for valve actuation during LOCA). If the LPCS line should break outside the containment, the check valve in the line inside the drywell prevents loss of reactor coolant outside the containment.

12←●

The other isolation valve (which is also referred to as the LPCS injection valve) is a motor operated gate valve located outside the primary containment as close as practical to LPCS discharge line penetration into the containment. This valve is capable of opening with the maximum differential across the valve expected for any system operating mode. The valve is capable of opening against a differential pressure equal to normal reactor pressure minus the minimum LPCS system shutoff pressure. The valve is capable of opening within 40 sec following a maximum recirculation line break accident. This valve is normally closed to back up the inside testable check valve for containment integrity purposes. A test connection/drain line is provided between the two isolation valves and is normally closed with a locked closed valve to assure containment integrity.

The LPCS system components and piping are arranged to avoid unacceptable damage from the physical effects of DBAs, such

as pipe whip, missiles, and high temperature, pressure, and humidity.

All principal active LPCS equipment is located outside the primary containment.

A check valve, flow element, and restricting orifice are provided in the LPCS discharge line from the pump to the injection valve. The check valve is located below the minimum suppression pool water level and is provided so the piping downstream of the valve can be maintained full of water by the discharge line fill system (Section 6.3.2.2.5). The flow element is provided to measure system flow rate during LOCA and test conditions and for automatic control of the minimum low flow bypass gate valve. The measured flow is indicated in the main control room. The restricting orifice is sized during the preoperation test of the system to limit system flow to acceptable values as described on the LPCS system process diagram.

The LPCS pump (pump performance test results) characteristics of head, flow, horsepower, and required NPSH are shown in Fig. 6.3-6.

A low flow bypass line with a motor-operated gate valve connects to the LPCS discharge line upstream of the check valve on the pump discharge line. The line bypasses water to the suppression pool to prevent pump damage due to overheating when other discharge line valves are closed or reactor pressure is greater than the LPCS system discharge pressure following system initiation. The valve automatically closes when flow in the main discharge line is sufficient to provide required pump cooling.

LPCS flow passes through a motor-operated pump suction valve that is normally open. This valve can be closed by a remote manual switch (located in the main control room) to isolate the LPCS system from the suppression pool should a leak develop in the system. This valve is located in the low pressure core spray pump suction line as close to the suppression pool as practical. Because the LPCS conveys water from the suppression pool, a closed loop is established for the spray water escaping from the break.

●→10

The design pressure and temperature of the system components are established based on the ASME Section III Boiler and Pressure Vessel Code.

10←●

●→10

The LPCS pump is located in the auxiliary building sufficiently below the water level in the suppression pool to assure a flooded pump suction and to meet pump NPSH requirements with the containment at atmospheric pressure and the suction strainers at the design debris loading condition. (Refer to Section 6.3.2.2 for strainer pressure drop.) A pressure gauge is provided to indicate the suction head. The LPCS pump characteristics are shown in Fig. 6.3-6. The available NPSH has been calculated in accordance with Regulatory Guide 1.1 as shown in Section 6.3.2.2.

10←●

The LPCS system incorporates relief valves to prevent the components and piping from overpressure conditions. One relief valve, located on the pump discharge, is set at 570 psig with capacity of 100 gpm at 10 percent accumulation. The second relief valve is located on the suction side of the pump and is set for 100 psig at a capacity of ≥ 10 gpm @ 10 percent accumulation.

The LPCS system piping and support structures are designed in accordance with Seismic Category I criteria (Chapter 3). The system is assumed to be filled with water for seismic analysis.

Provisions are included in the LPCS system which permit the LPCS system to be tested. These provisions are:

1. All active LPCS components are testable during normal plant operation.
2. A full flow test line is provided to route water from and to the suppression pool without entering the RPV.
3. A suction test line supplying reactor grade water is provided to test pump discharge into the RPV during normal plant shutdown.
4. Instrumentation is provided to indicate system performance during normal and test operations.
5. All motor-operated valves and check valves are capable of operation for test purposes.
6. Relief valves are removable for bench-testing during plant shutdown.

6.3.2.2.4 Low Pressure Coolant Injection (LPCI)

LPCI is an operating mode of the RHR system. The LPCI mode system is automatically actuated by low water level in the reactor or high pressure in the drywell and uses the three RHR motor-driven pumps to draw suction from the suppression pool and inject cooling water flow into the reactor core and accomplish cooling of the core by flooding. Each loop has its own suction and discharge piping and separate vessel nozzle which connects with the core shroud to deliver flooding water on top of the core. In this mode, the RHR system is a high volume core flooding system.

●→16 ●→15

The LPCI, like the LPCS system, is designed to provide cooling to the reactor core only when the reactor vessel pressure is low, as is the case for large LOCA break sizes. However, when the LPCI operates in conjunction with the ADS then the effective core cooling capability of the LPCI is extended to all break sizes because the ADS rapidly reduces the reactor vessel pressure to the LPCI operating range.

15←● 16←● ●→10

The RHR pumps receive power from ac power buses having standby power source backup supply. Two RHR pump motors and the associated automatic motor-operated valves receive ac power from one bus, while the LPCS pump and the other RHR pump motor and valves receive power from another bus (Section 8.3).

10←●

The pump, piping, controls, and instrumentation of the LPCI loops are separated and protected so that any single physical event, or missiles generated by rupture of any pipe in any system within the drywell, cannot make all loops inoperable.

To assure continuity of core cooling, signals to isolate the primary containment do not operate any RHR system valves which interfere with the LPCI mode of operation.

●→12 ●→1

Each LPCI discharge line to the reactor is provided with at least two isolation valves. A testable check valve is provided inside the drywell and a normally closed motor-operated gate valve is provided either outside the drywell (loops A and B) or outside the containment (loop C). No power is required to operate the check valve inside of the drywell; rather, it opens as a result of LPCI injection flow. If a break were to occur outboard of the check valve

1←● 12←●

it would shuttle close to isolate the reactor from the line break.

The motor-operated valve outside of the drywell is called the LPCI injection valve and is located as close as practical to the drywell wall. It is capable of opening against the maximum differential pressure expected for the LPCI mode; i.e., normal reactor pressure minus the upstream pressure with the RHR pump running at minimum flow. LPCI loops A and B also have a normally open motor-operated valve located as close as practical to the containment.

The valve opens within 37 sec following an accident signal, including time to start emergency power sources.

●→14

The P&ID, Fig. 5.4-12, indicates a great many flow paths are available other than the LPCI injection line. However, the low water level or high drywell pressure signals which automatically initiate the LPCI mode are also used to isolate all other modes of operation and revert other system valves to the LPCI lineup. Inlet and outlet valves from the heat exchangers receive no automatic signals as the system is designed to provide rated flow to the vessel whether they are open or not.

14←●

A check valve in the pump discharge line is used together with a discharge line fill system (Section 6.3.2.2.5) to prevent water hammer resulting from pump start against a potential shutoff condition. A flow element in the pump discharge line is used to provide a measure of system flow and to originate automatic signals for control of the pump minimum flow valve. The minimum flow valve permits a small flow to the suppression pool in the event that either no discharge valve is open, or in the case of a LOCA, vessel pressure is higher than the pump shutoff head.

Using the suppression pool as the source of water for LPCI establishes a closed loop for recirculation of LPCI water escaping from the break.

●→10

10←●

LPCI pumps and equipment are described in detail in Section 5.4.7, which also describes the other functions served by the same pumps if not needed for the LPCI function. The RHR heat exchangers are not associated with the emergency core cooling function. The heat exchangers

are discussed in Section 6.2.2. The portions of the RHR required for accident protection including support structures are designed in accordance with Seismic Category I criteria (Chapter 3). The available NPSH was calculated in accordance with Regulatory Guide 1.1 as shown in Section 6.3.2.2. The LPCI pump characteristics are shown in Fig. 6.3-7.

The LPCI system incorporates a relief valve on each of the pump discharge lines which protects the components and piping from overpressure conditions. These valves are set to relieve pressure at 500 psig.

Provisions are included in the LPCI system to permit testing of the system. These provisions are:

1. All active LPCI components are designed to be testable during normal plant operation.
 2. A discharge test line is provided for the three pumps to route suppression pool water back to the suppression pool without entering the RPV.
 3. A suction test line, supplying reactor grade water, is provided to test loop C discharge into the RPV during normal plant shutdown.
 4. Instrumentation is provided to indicate system performance during normal and test operations.
 5. All motor-operated valves, air-operated valves, and check valves are capable of manual operation for test purposes.
- 10
6. Shutdown lines taking suction from the recirculation system are provided for loops A and B to test pump discharge into the RPV after normal plant shutdown and to provide for shutdown cooling. Loop C interfaces with the SPC system to provide an alternate decay heat removal method during normal plant shutdown. The SPC interface valves, RHS-AOV62, AOV63, and AOV64 are equipped with administratively controlled, keylocked isolation bypass switches to minimize the potential for inadvertent loss of decay heat removal.
- 10←●
7. All relief valves are removable for bench-testing during plant shutdown.

6.3.2.2.5 ECCS Discharge Line Fill System

A requirement of the emergency core cooling system is that cooling water flow to the reactor vessel be initiated rapidly when the system is called on to perform its function. This quick-start system characteristic is provided by quick-opening valves, quick-start pumps, and standby ac power sources. The lag between the signal to

RBS USAR

THIS

PAGE

LEFT

INTENTIONALLY

BLANK

start the pump and the initiation of flow into the RPV can be minimized by keeping the ECCS pump discharge lines full. Additionally, if these lines were empty when the systems were called for, the large momentum forces associated with accelerating fluid into a dry pipe could cause physical damage to the piping. Therefore, the ECCS discharge line fill system is designed to maintain the pump discharge lines in a filled condition.

Since the ECCS discharge lines are elevated above the suppression pool, check or stop-check valves are provided near the pumps to prevent back flow from emptying the lines into the suppression pool. Past experience has shown that these valves leak slightly, producing a small back flow that eventually empties the discharge piping. To ensure that this leakage from the discharge lines is replaced and the lines are always kept filled, a water leg pump is provided for each of the three ECCS divisions. The power supply to these pumps is Class 1E. Indication is provided in the main control room as to whether these pumps are operating, and alarms indicate low discharge line pressure.

6.3.2.3 Applicable Codes and Classifications

The applicable codes and classification of the ECCS are specified in Section 3.2. All piping systems and components (pumps, valves, etc) for the ECCS comply with applicable codes, addenda, code cases, and errata in effect at the time the equipment is procured. The piping and components of each ECCS within the containment and out to and including the pressure retaining injection valve are Safety Class 1. The remaining piping and components are Safety Class 2, 3, or NNS as indicated in Section 3.2, and as indicated on the individual system P&ID. The equipment and piping of the ECCS are designed to the requirements of Seismic Category I. This seismic designation applies to all structures and equipment essential to the core cooling function. IEEE codes applicable to the controls and power supplies are specified in Section 7.1 and 8.3, respectively.

6.3.2.4 Materials Specifications and Compatibility

Materials specifications and compatibility for the ECCS are presented in Sections 6.1 and 3.2. Nonmetallic materials such as lubricants, seals, packings, paints and primers, and insulation, as well as metallic materials, etc, are selected as a result of an engineering review and evaluation for compatibility with other materials in the system and the surroundings with concern for chemical, radiolytic, mechanical, and nuclear effects. Materials used are

reviewed and evaluated with regard to radiolytic and pyrolytic decomposition and attendant effects on safe operation of the ECCS.

6.3.2.5 System Reliability

A single failure analysis shows that no single failure prevents the starting of the ECCS when required, or the delivery of coolant to the reactor vessel. No individual system of the ECCS is single failure proof with the exception of the ADS. The consequences of the most severe single failures are shown in Table 6.3-6. The most severe effects of single failures with respect to loss of equipment occur if the LOCA occurs in combination with an ECCS pipe break coincident with a loss of offsite power.

6.3.2.6 Protection Provisions

Protection provisions are included in the design of the ECCS. Protection is afforded against missiles, pipe whip, and flooding. Also accounted for in the design are thermal stresses, loadings from a LOCA, and seismic effects.

The ECCS piping and components located outside the drywell are protected from internally and externally generated missiles by the reinforced concrete structure of the ECCS pump rooms. The watertight construction of these ECCS pump rooms also protects the equipment against flooding. The pump rooms layout and protection is covered in Section 3.6.

The ECCS is protected against the effects of pipe whip, which might result from piping failures up to and including the design basis event LOCA. This protection is provided by separation, pipe whip restraints, and energy absorbing materials. These three methods are applied to provide protection against damage to piping and components of the ECCS which otherwise could result in a reduction of ECCS effectiveness to an unacceptable level. See Section 3.6 for criteria on pipe whip.

The component supports which protect against damage from movement and from seismic events are discussed in Section 5.4.14. The methods used to provide assurance that thermal stresses do not cause damage to the ECCS are described in Section 3.9.3.

6.3.2.7 Provisions for Performance Testing

Periodic system and component testing provisions for the ECCS are described in Section 6.3.2.2 as part of the individual system descriptions.

6.3.2.8 Manual Actions

●→10

The ECCS is actuated automatically and requires no operator action during the first 20 min following the accident. During the long term cooling period (after 10 min), the operator actions are as specified in Section 6.2.

10←●

The operator has multiple instrumentation available in the main control room to assist him in assessing the post-LOCA conditions. This instrumentation provides reactor vessel pressures, water levels, containment pressure, temperature and radiation levels as well as indicating the operation of the ECCS. ECCS flow indication is the primary parameter available to assess proper operation of the system. Other indications such as position of valves, status of circuit breakers, and essential power bus voltage are also available to assist him in determining system operating status. The electrical and instrumentation complement to the ECCS is discussed in detail in Section 7.3. Other available instrumentation is listed in the P&IDs for the individual systems. Monitoring instrumentation available to the operator is discussed in Chapter 5 and Section 6.2.

6.3.3 ECCS Performance Evaluation

●→16 ●→15 ●→10

This section provides evaluation of the systems that protect against the postulated loss-of-coolant accidents (LOCA) and is applicable to the reload core.

15←● 16←●

The performance of the ECCS is determined through application of the 10CFR50 Appendix K evaluation models and then showing conformance to the acceptance criteria of 10CFR50.46. NEDE-23785 provides a complete description of the methods used to perform the calculations. These methods are summarized herein. A summary description of the LOCAs is also provided herein. For a complete description of the LOCA events see Reference 3.

10←●

The ECCS performance is evaluated for the entire spectrum of break sizes for postulated LOCAs. The accidents, as listed in Chapter 15, for which ECCS operation is required are:

- 15.2.8 Feedwater line break
- 15.6.4 Steam system piping break outside containment
- 15.6.5 Loss-of-coolant accidents (inside containment)

Chapter 15 provides the radiological consequences of the above listed events.

6.3.3.1 ECCS Bases for Technical Specifications

The maximum average planar linear heat generation rates calculated in this performance analysis provide the basis for technical specifications designed to ensure conformance with the acceptance criteria of 10CFR50.46. Minimum ECCS functional requirements are specified in Sections 6.3.3.4 and 6.3.3.5, and testing requirements are discussed in Section 6.3.4. Limits on minimum suppression pool water level are discussed in Section 6.2.

6.3.3.2 Acceptance Criteria for ECCS Performance

- ~~10~~

The applicable acceptance criteria, extracted from 10CFR50.46, are listed and for each criterion applicable parts of Section 6.3.3, where conformance is demonstrated, are indicated. A detailed description of the methods used to show compliance are shown in Reference 3.

Criterion 1, Peak Cladding Temperature

- ~~16~~ • ~~15~~ • ~~1~~

"The calculated maximum fuel element cladding temperature shall not exceed 2,200°F." Conformance to Criterion 1 is shown in Table 6.3-3 (details in References 7 and 9).

Criterion 2, Maximum Cladding Oxidation

"The calculated total local oxidation of the cladding shall nowhere exceed 0.17 times the total cladding thickness before oxidation." Conformance to Criterion 2 is shown in Table 6.3-3 (details in References 7 and 9).

Criterion 3, Maximum Hydrogen Generation

"The calculated total amount of hydrogen generated from the chemical reaction of the cladding with water or steam shall not exceed 0.01 times the hypothetical amount that would be generated if all the metal in the cladding cylinder surrounding the fuel, excluding the cladding surrounding the plenum volume, were to react." Conformance to Criterion 3 is shown in Table 6.3-3 (details in References 7 and 9).

- ~~4~~ 1←• 4←• 10←• 15←• 16←•

Criterion 4, Coolable Geometry

"Calculated changes in core geometry shall be such that the core remains amenable to cooling." As described in Reference 2, Section III, conformance to Criterion 4 is demonstrated by conformance to Criteria 1 and 2.

Criterion 5, Long-Term Cooling

●→10

"After any calculated successful initial operation of the ECCS, the calculated core temperature shall be maintained at an acceptably low value and decay heat shall be removed for the extended period of time required by the long-lived radioactivity remaining in the core." Conformance to Criterion 5 is demonstrated generically for GE BWRs in Reference 2, Section III.A. Briefly summarized, the core remains covered to at least the jet pump suction elevation and the uncovered region is cooled by spray cooling. A spray cooling system (HPCS or LPCS) must be available for long-term cooling following large recirculation line breaks (when core is only covered up to the jet pump suction).

10←●

During long-term cooling following a small LOCA, no operator actions are required to control system pressure to preclude overpressurizing the pressure vessel after it has been cooled off. The system is always protected by relief valve capacity that is more than adequate to handle decay heat energy generation.

6.3.3.3 Single Failure Considerations

The functional consequences of potential operator errors and single failures (including those which might cause any manually controlled electrically operated valve in the ECCS to move to a position which could adversely affect the ECCS), and the potential for submergence of valve motors in the ECCS are discussed in Section 6.3.2. There it was shown that all potential single failures are no more severe than one of the single failures identified in Table 6.3-6 (see also Appendix 15A).

●→14

It is, therefore, only necessary to consider each of these single failures in the ECCS performance analyses. For large breaks, failure of the Division III (HPCS) diesel generators is in general the most severe failure. For small breaks, the failure of the HPCS is the most severe failure.

●→10

A single failure in the ADS (one ADS valve) results in only a small increase in the calculated PCT following small breaks and has no effect on large breaks. As a matter of calculational convenience, it is assumed in all calculations that two ADS valves are non-functioning in addition to the identified single failure. This

10←● 14←●

assumption reduces the number of calculations required in the performance analysis and bounds the effects of one ADS valve failure and HPCS failure by themselves.

6.3.3.4 System Performance During the Accident

In general, the system response to an accident can be described as

1. Receiving an initiation signal,
2. A small lag time (to open all valves and have the pumps up to rated speed), and
3. Finally the ECCS flow entering the vessel.

Key ECCS actuation setpoints and time delays for all the ECCSs are provided in Table 6.3-2. The minimization of the delay from the receipt of signal until the ECCS pumps have reached rated speed is limited by the physical constraints on accelerating the diesel-generators and pumps. The delay time due to valve motion in the case of high pressure system provides a suitably conservative allowance for valves available for this application. In the case of the low pressure system, the time delay for valve motion is such that the pumps are at rated speed prior to the time the vessel pressure reaches the pump shutoff pressure.

The flow delivery rates analyzed in Section 6.3.3 can be determined from the head-flow curves in Fig. 6.3-3, 6.3-6, and 6.3-7 and the pressure versus time plots discussed in Section 6.3.3.7. Simplified piping and instrumentation and functional control diagrams for the ECCS are provided in Section 6.3.2. The operational sequence of ECCS for the DBA is shown in Table 6.3-1.

Operator action is not required, except as a monitoring function, during the short term cooling period following the LOCA. During the long term cooling period, the operator takes action as specified in Section 6.2.2.2 to place the containment cooling system into operation.

6.3.3.5 Use of Dual Function Components for ECCS

With the exception of the LPCI system, the systems of the ECCS are designed to accomplish only one function: to cool the reactor core following a loss of reactor coolant. To this extent, components or portions of these systems (except for pressure relief) are not required for operation of other systems which have emergency core cooling functions, or vice

versa. Because either the ADS initiating signal or the overpressure signal opens the safety relief valve, no conflict exists.

•→12 •→4

The LPCI mode, however, uses the RHR pumps and some of the RHR valves and piping. When the reactor water level is low, the LPCI mode has priority through the valve control logic over the other RHR modes for suppression pool cooling and shutdown cooling. Following receipt of a LOCA signal, the RHR system is directed to the LPCI mode.

4←• 12←•

•→8

8←•

6.3.3.6 Limits on ECCS Parameters

The limits on the ECCS parameters are discussed in Sections 6.3.3.1 and 6.3.3.7.1.

Any number of components in any given system may be out of service, up to and including the entire system. The maximum allowable out-of-service time is a function of the level of redundancy and the specified test intervals as discussed in Section 15A.5.

6.3.3.7 ECCS Analyses for LOCA

6.3.3.7.1 LOCA Analysis Procedures and Input Variables

•→10

The procedures approved for LOCA analysis conformance calculations are described in detail in References 2 and 3. These procedures were used in the calculations documented in Section 6.3.3. The LOCA analysis for RBS was done for an initial nominal power of 3039 MWt and a nominal vessel pressure of 1080 psia in Reference 4. The licensing (10CFR50 Appendix-K) results in the Reference 4 analysis were confirmed bounding for a core nominal power increase of 1.7% (3091 MWt) at constant pressure in the Reference 6 general disposition evaluations. The nominal PCT calculations (SAFER/GESTR Upper Bound PCT criteria) were confirmed in the Reference 6 evaluation to have ample margin to the Upper Bound to accommodate a PCT change of 10°F due to a 1.7% power increase at constant pressure. The PCT values for the fuel types in the current reload are referenced Appendix 15B.

Reference 4 documents the base SAFER/GESTR-LOCA evaluation performed for GE11 fuel. Results from Reference 4 are summarized in Figure 6.3-10. Reference 9 supplements Reference 4 with SAFER/GESTR-LOCA evaluations applicable to GNF2 fuel. Key inputs and results from References 7 and 9 are summarized in Tables 6.3-1, 6.3-2, 6.3-3 and 6.3-6. For convenience, the four computer codes are briefly described below. The interfaces between the codes are shown schematically in Figure 1-2 Volume II of Reference 3. The major interfaces are briefly noted below.

Short-term Thermal Hydraulic Model (LAMB)

The LAMB code is a model which is used to analyze the short-term thermodynamic and thermal-hydraulic behavior of the coolant in the vessel during a postulated LOCA. In particular, LAMB predicts the core flow, core inlet enthalpy and core pressure during the early stages of the reactor vessel blowdown. For a detailed description of the model

and a discussion regarding sources of input to the model refer to the "LAMB Code Documentation," Section II.A.3 of Reference 2.

●→10

Transient Critical Power (SCAT/TASC)

The SCAT code is used to evaluate the short-term thermal-hydraulic response of the coolant in the core during a postulated LOCA. For GE11 and later fuel types an improved SCAT model, designated TASC, is used. SCAT/TASC receives input from LAMB and analyzes the convective heat transfer process in the thermally limiting fuel bundle. For a detailed description of the SCAT model and a discussion regarding sources of input to the model refer to the "SCAT Code Documentation," Section II.A.4 of Reference 2. For a detailed description of the TASC model see Reference 5.

Fuel Rod Thermal Performance (GESTR-LOCA)

The GESTR-LOCA code provides parameters to initialize the fuel stored energy and fuel rod fission gas inventory at the onset of a postulated LOCA for input into SAFER. GESTR-LOCA also establishes the transient pellet-cladding gap conductance for input to both SAFER and SCAT/TASC. The GESTR code incorporates the effects of fuel/cladding thermal expansion, fuel/cladding creep and fuel irradiation swelling, densification, relocation, and fission gas release as they affect pellet-cladding thermal conductance, and fuel rod internal pressure. For a detailed description of the model and a discussion regarding sources of input refer to Volume I of Reference 3.

Long-term Inventory Model (SAFER)

The SAFER code is a model which is used to analyze the long-term thermodynamic behavior of the coolant in the vessel. The SAFER code calculates the long-term system response of the reactor over a complete spectrum of hypothetical break sizes and locations. SAFER calculates the core and vessel water levels, system pressure response, ECCS performance, and other primary thermal-hydraulic phenomena occurring in the vessel as a function of time. SAFER realistically models all regimes of heat transfer in the core and calculates PCT.

For a detailed description of the model refer to Volume II of Reference 3.

6.3.3.7.2 Accident Description

A detailed description of the LOCA calculation is provided in Reference 3. For convenience, a short description of the major events during the DBA is included here.

10←●

• →0

Immediately after the postulated double-ended recirculation line break, vessel pressure and core flow begin to decrease. The initial pressure response (Fig. 6.3-12) is governed by the closure of the main steam isolation valves (MSIV) and the relative values of energy added to the system by decay heat and energy removed from the system by the initial blowdown of fluid from the downcomer. The initial core flow decrease is rapid because the recirculation pump in the broken loop ceases to pump almost immediately because it has lost suction. The pump in the intact loop coasts down relatively slowly. This pump coastdown governs the core flow response for the next several seconds. When the jet pump suction uncovers, calculated core flow decreases to near zero. When the recirculation pump suction nozzle uncovers, the energy release rate from the break increases significantly and the pressure begins to decrease more rapidly. As a result of the increased rate of vessel pressure loss, the initially subcooled water in the lower plenum saturates and flashes up through the core, increasing the core flow. This lower plenum flashing continues at a reduced rate for the next several sec.

Heat transfer rates on the fuel cladding during the early stages of the blowdown are governed primarily by the core flow response. Nucleate boiling continues in the high power plane until shortly after jet pump uncover. Boiling transition follows shortly after the core flow loss that results from jet pump uncover. Film boiling heat transfer rates then apply, with increasing heat transfer resulting from the core flow increase during the lower plenum flashing period. Heat transfer then slowly decreases until the high power axial plane uncovers. At that time, convective heat transfer is assumed to cease.

Water level inside the shroud (Fig. 6.3-11a, 6.3-11b & 6.3-11c) remains high during the early stages of the blowdown because of flashing of the water in the core. After a short time, the level inside the shroud has decreased to uncover the core. Several seconds later the ECCS is actuated. As a result the vessel water level begins to increase. Some time later, the lower plenum is filled, and the core is subsequently rapidly recovered.

A rapid, short duration cladding heatup follows the time of boiling transition (which is assumed to occur very early into the LOCA) when film boiling occurs and the cladding temperature approaches that of the fuel. This heat up is recovered as the saturation temperature of the coolant decreases. The subsequent heatup is slower, being

10←•

•→10

governed by decay heat and core spray heat transfer. Finally the heatup of the reactor fuel is terminated when the core is either recovered by the accumulation of ECCS water or the core cooling heat transfer exceeds the decay heat of the fuel.

6.3.3.7.3 Break Spectrum Calculations

A complete spectrum of postulated break sizes and locations is considered in the evaluation of ECCS performance. The general analytical procedures for conducting break spectrum calculations are discussed in Reference 2 and Volume III of Reference 3.

A summary of the results of the break spectrum calculations, for Appendix K runs only, is shown graphically in Fig. 6.3-10. Details of Nominal and Appendix K runs are given in Reference 4. Conformance to the acceptance criteria ($PCT \leq 2200F$, local oxidation ≤ 17 percent, and core wide metal-water reaction ≤ 1 percent) is demonstrated in table 6.3-3. Details of calculations for specific breaks are included in subsequent paragraphs.

10←•

•→16 •→10

6.3.3.7.4 Recirculation Line Break Calculations

Important variables from the analyses of the limiting large and small break DBA events are shown in Fig. 6.3-11c through 6.3-18c for the GNF2 fuel type. These variables are:

16←•

1. Water level inside and outside the shroud,
2. Reactor vessel pressure,
3. Peak cladding temperature (PCT),
4. ECCS Flow Rate

•→4 •→1

1←• 4←•

6.3.3.7.5 Deleted

6.3.3.7.6 Deleted

6.3.3.7.7 Calculations for Other Break Locations

The HPCS line break, the LPCI line break, the feedwater line break, and the main steam line break inside the containment (2.55 sq ft) were analyzed using SAFER/GESTR-LOCA.

SAFER/GESTR-LOCA analysis was also done for the main steam line break outside the containment (2.66 sq ft). The results of these analyses show the other break locations result in significantly lower PCTs than the recirculation line results. Details of these analyses can be found in Reference 4.

6.3.3.8 Alternate Operating Mode Considerations

6.3.3.8.1 Increased Core Flow (ICF)

•→4 •→1

The impact on LOCA results due to increased core flow (ICF) operation (corresponding to 107% of rated core flow) was evaluated for a thermal power level of 3039 MWth using the same ECCS parameters used for rated conditions. The limiting LOCA event, a DBA recirculation line break with a Division III (HPCS) diesel generator failure, was analyzed for ICF conditions, using both nominal and Appendix K assumptions. The nominal and Appendix K results show that there is small difference in the PCTs between the ICF cases and the rated core flow cases.

1←• 4←• 10←•

●→10 ●→4 ●→2 2←● 4←●

6.3.3.8.3 Feedwater Heater Out-of-Service

The impact on LOCA analysis due to a 100°F reduction in feedwater temperature was evaluated using the same ECCS parameters as used for nominal feedwater temperature. The limiting LOCA event, a DBA recirculation suction line break with a HPCS diesel generator failure, was analyzed with a 100°F reduction in feedwater temperature using both nominal and Appendix K assumptions. The nominal and Appendix K results show that there is small difference in the PCTs between the reduced feedwater cases and the rated feedwater cases.

6.3.3.8.4 Single-Loop Operation (SLO)

The impact of SLO on the LOCA analyses was evaluated using the same parameters as used for Two Loop Operation. The difference is that the SLO cases assume an earlier boiling transition (dry out) time due to the immediate loss of all forced circulation. A multiplier on MAPLHGR limits is applied for SLO operation which ensures that the SLO LOCA results are bounded by the Two Loop Operation results. The MAPLHGR multiplier is located in the Core Operating Limits Report.

6.3.3.8.5 Maximum Extended Load Line Limit (MELLL)

The impact on LOCA analysis due to operation at MELLL conditions was evaluated using the same ECCS parameters as used for nominal core flow conditions. The limiting LOCA event, a DBA recirculation line break with a HPCS diesel generator failure, was analyzed at MELLL conditions using both nominal and Appendix K assumptions. The nominal and Appendix K results show that there is small difference in the PCTs between the reduced feedwater cases and the rated feedwater cases.

6.3.3.9 LOCA Analysis Conclusions

●→16 ●→15 ●→4 ●→1

Having shown compliance with applicable acceptance criteria of Section 6.3.3.2, it is concluded that the ECCS will perform its function in an acceptable manner and meet all of the 10CFR50.46 acceptance criteria, given operation at or below the MAPLHGR limits specified in the Core Operating Limits Report. The applicability of the LOCA analysis is confirmed on a cycle specific basis in Appendix 15B.

10←● 15←● 16←●

6.3.4 Tests and Inspections

6.3.4.1 ECCS Performance Tests

All systems of the ECCS are tested for their operational ECCS function during the preoperational and/or startup test program.

1←●

RBS USAR

Each component is tested for power source, range, direction of rotation, set point, limit switch setting, torque switch setting, etc. Each pump is tested for flow capacity for comparison with vendor data. (This test is also used to verify flow measuring capability.) The flow

THIS PAGE INTENTIONALLY LEFT BLANK

tests involve the same suction and discharge source; i.e., suppression pool or condensate storage tank.

All logic elements are tested individually and then as a system to verify complete system response to emergency signals including the ability of valves to revert to the ECCS alignment from other positions.

Finally the entire system is tested for response time and flow capacity taking suction from its normal source and delivering flow into the reactor vessel. This last series of tests is performed with power supplied from both offsite power and onsite emergency power.

See Chapter 14 for a thorough discussion of preoperational testing for these systems.

6.3.4.2 Reliability Tests and Inspections

The average reliability of a standby (nonoperating) safety system is a function of the duration of the interval between periodic functional tests. The factors considered in determining the periodic test interval of the ECCS are: the desired system availability (average reliability), the number of redundant functional system success paths, the failure rates of the individual components in the system, and the schedule of periodic tests (simultaneous versus uniformly staggered versus randomly staggered). For the ECCS the above factors were used to determine test intervals utilizing the methods described in Reference 1.

All of the active components of the HPCS system, ADS, LPCS, and LPCI systems are designed so that they may be tested during normal plant operation. Full flow test capability is provided by a test line back to the suction source. The full flow test is used to verify the capacity of each ECCS pump loop while the plant remains undisturbed in the power generation mode. In addition, each individual valve may be tested during normal plant operation. Input jacks are provided such that by racking out the injection valve breaker, each ECCS loop can be tested for response time.

All of the active components of the ADS except the safety/relief valves and their associated solenoid valves are designed so that they may be tested during normal plant operation. The safety/relief valves and associated solenoid valves are all tested at least once each 24 months during plant startup following a refueling outage. Safety/relief valves and their associated solenoid valves which have been

overhauled during a plant outage are tested during the startup following that outage.

Testing of the initiating instrumentation and controls portion of the ECCS is discussed in Section 7.3.2. The emergency power system, which supplies electrical power to the ECCS in the event that offsite power is unavailable, is tested as described in Section 8.3. The frequency of testing is specified in Chapter 16. Visual inspections of all the ECCS components located outside the drywell can be made at any time during power operation. Components inside the drywell can be visually inspected only during periods of access to the drywell. When the reactor vessel is open, the spargers and other internals can be inspected.

6.3.4.2.1 HPCS Testing

The HPCS can be tested at full flow with condensate storage tank water at any time during plant operation except when the reactor vessel water level is low, or when the condensate level in the condensate storage tank is below the reserve level, or when the valves from the suppression pool to the pump are open. If an initiation signal occurs while the HPCS is being tested, the system returns automatically to the operating mode. The two motor-operated valves in the test line to the condensate storage system are interlocked closed when the suction valve from the suppression pool is open.

A design flow functional test of the HPCS over the operating pressure and flow range is performed by pumping water from the condensate storage tank and back through the full flow test return line to the condensate storage tank.

The suction valve from the suppression pool and the discharge valve to the reactor remain closed. These two valves are tested separately to ensure their operability.

●→10

10←●

6.3.4.2.2 ADS Testing

The ADS valves are fully tested during the time when the reactor is at reduced pressure prior to or following a refueling outage. This testing includes simulated automatic actuation of the system throughout its emergency operating sequence. Each individual ADS valve is manually actuated.

During plant operation the ADS system can be checked as discussed in Section 7.3.2.1.3.

6.3.4.2.3 LPCS Testing

●→10

The LPCS pump and valves are tested periodically during reactor operation. With the injection valve closed and the return line open to the suppression pool, full flowing pump capability is demonstrated. The injection valve and the check valve are tested in a manner similar to that used for the LPCI valves.

6.3.4.2.4 LPCI Testing

Each LPCI loop can be tested during reactor operation. During plant operation, this test does not inject cold water into the reactor because the injection line check valve is held closed by vessel pressure, which is higher than the pump pressure. The injection line portion is tested with reactor water when the reactor is shut down and when a closed system loop is created. This prevents unnecessary thermal stresses.

10←●

To test an LPCI pump at rated flow, the test line valve to the suppression pool is opened, the pump suction valve from the suppression pool is opened (this valve is normally open), and the pumps are started using the remote/manual switches in main control room. Correct operation is determined by observing the instruments in the main control room.

If an initiation signal occurs during the test, the LPCI system returns to the operating mode. The valves in the test bypass lines are closed automatically to assure that the LPCI pump discharge is correctly routed to the vessel.

6.3.5 Instrumentation Requirements

Design details including redundancy and logic of the ECCS instrumentation are discussed in Section 7.3.

All instrumentation required for automatic and manual initiation of the HPCS, LPCS, LPCI, and ADS is discussed in Section 7.3.2 and is designed to meet the requirements of IEEE 279 and other applicable regulatory requirements. The HPCS, LPCS, LPCI, and ADS can be manually initiated from the main control room.

The HPCS, LPCS, and LPCI are automatically initiated on low reactor water level or high drywell pressure. (See Table 6.3-2 and Section 7.3.2 for specific initiation levels for each system.) The ADS is automatically actuated by sensed variables for reactor vessel low water level and drywell high pressure plus indication that at least one LPCI or LPCS pump is operating. The HPCS, LPCS, and LPCI automatically return from system flow test modes to the emergency core cooling mode of operation following receipt of an automatic initiation signal. The LPCS and LPCI system injection into the RPV begin when reactor pressure decreases to system discharge shutoff pressure.

HPCS injection begins as soon as the HPCS pump is up to speed and the injection valve is open since the HPCS is capable of injecting water into the RPV over a pressure range from 1,177 psid to 0 psid (psid = differential pressure between RPV and pump suction source).

References - 6.3

1. Hirsch, H. M. Methods for Calculating Safe Test Intervals and Allowable Repair Times for Engineered Safeguard Systems. January 1973 (NEDO-10739).
2. General Electric Company Analytical Model for Loss-of-Coolant Analysis in Accordance with 10CFR50, Appendix K, NEDO-20566P, November 1975.
●→12 ●→10
3. The GESTR-LOCA and SAFER Models for the Evaluation of the Loss-of-Coolant-Accident, NEDE-23785-1-PA, Volumes I and II, December 1981 and Volume III, October 1984.
12←● ●→14
4. River Bend Station SAFER/GESTR-LOCA, Loss-of-Coolant-Accident Analysis With Relaxed ECCS Parameters, NEDC-32922P, December 1999.
14←●
5. GE11 Compliance with Amendment 22 of NEDE-20411-P-A (GESTAR-II), NEDE-31917P, April 1991.
10←●
6. Entergy Operations Incorporated River Bend Station Thermal Power Optimization, GE-NE-0000-0000-1850-02, Rev. 1, March 2002.
7. DELETED
8. DELETED
9. GEH-0000-0100-8682-R0, "River Bend Station GNF2 ECCS-LOCA Evaluation," September 2010. (River Bend Station Report # RBS-SA-10-00003, Revision 0).

6.4 HABITABILITY SYSTEMS

The [main control room](#) habitability systems are provided to ensure that the main control room operators can remain in the main control room and take actions to operate the plant safely under normal conditions and to maintain it in a safe condition under all accident conditions.

The main control room habitability systems include missile protection, radiation shielding, radiation monitoring, air filtration and ventilation systems, [emergency lighting](#), [food, water, kitchen, sleeping, sanitary facilities](#), [fire protection](#), personnel and administrative support.

Detailed descriptions of the various habitability systems and provisions are discussed in the following sections:

- | | | |
|-----|--|-------------------------------|
| 1. | Evaluation of Potential Accidents | Section 2.2.3 |
| 2. | Conformance with NRC General Design Criteria | Section 3.1 |
| 3. | Wind and Tornado Loadings | Section 3.3 |
| 4. | Water Level (Flood) Design | Section 3.4 |
| 5. | Missile Protection | Section 3.5 |
| 6. | Protection against Dynamic Effects Associated with the Postulated Rupture of Piping | Section 3.6A |
| 7. | Seismic Qualification of Seismic Category I Instrumentation and Electrical Equipment | Section 3.10A |
| 8. | Environmental Design of Mechanical and Electrical Equipment | Section 3.11 |
| 9. | Radiation Protection | Section 12.3,
Chapter 15.0 |
| 10. | Control Building Chilled Water System | Section 9.2.10 |
| 11. | Control Building Ventilation System | Section 9.4.1 |
| 12. | Fire Protection System | Section 9.5.1,
Appendix 9A |

13.	Lighting Systems	Section 9.5.3
14.	Electric Power	Chapter 8
15.	Radiation Instrumentation and Monitoring	Sections 7.6, 12.3.4, 11.5
16.	Instrumentation and Controls Main Control Room Ventilation System	Section 7.3

Equipment and systems are discussed in this section only as necessary to describe their connection with main control room habitability. References to other sections are made where appropriate.

6.4.1 Design Basis

The main control room is designed so that it provides a location from which the reactor may be safely operated during all modes of plant operation. This includes a 30-day period following the design basis accident (DBA). The main control room habitability systems:

1. Provide the capability to detect and limit the introduction of radioactive material and smoke into the main control room.
2. Provide the occupants with fresh, filtered breathing air and a comfortable working atmosphere.
3. Provide suitable food, water, medical supplies, sanitary, hygienic, and sleeping facilities for an emergency team of five persons to sustain them during the DBA.
4. Provide the occupants with fire protection warning and firefighting equipment.
5. Maintain temperature and humidity conditions within equipment design ranges.
6. Provide the occupants with respiratory, eye, and skin protection for emergency use within areas of the main control room pressure boundary.
7. The habitability systems are capable of performing their safety functions assuming a single active component failure coincident with a loss of offsite power.

The main control room envelope or pressure boundary includes all instrumentation and controls necessary for safe shutdown of the plant and is limited to those areas requiring operator access during and after a DBA.

The radiation exposure of main control room personnel through the duration of any one of the postulated DBAs discussed in Chapter 15 does not exceed the guidelines set by 10CFR50.67. Amendment 132 revised the design basis accident main control room dose limit requirements to incorporate the limits of 10CFR50.67. The limits of 10CFR50 Appendix A, General Design Criteria 19, also remain applicable to the RBS design basis.

•→9 •→3

The main control room air conditioning system is designed to provide temperature and humidity conditions of 80°F and 70 percent maximum, respectively. This temperature and humidity is based upon optimum room conditions for personal comfort as described by the American Society of Heating, Refrigeration and Air Conditioning Engineers. These parameters are also within the 104°F maximum [control room ambient](#) temperature limit to support the 122°F equipment design temperature.

3←• 9←•

All components of the HVAC systems serving the main control room that are required to ensure main control room habitability and essential equipment operations are redundant, Seismic Category I, powered from Class 1E buses, and Safety Class 3.

If there is a loss of offsite power, power to the main control room air conditioning equipment is interrupted for 60 sec. No significant temperature rise within the main control room is possible before the system is returned to operation via emergency power from the standby diesel generators.

•→3

Four 100-percent-capacity water chiller units (1HVK*CHL1A and C on Division I, and 1HVK*CHL1B and D on Division II), feed two 100-percent air supply systems. One pre-selected chiller unit of Division II starts automatically, i.e., 1HVK*CHL1B or 1D. If the chiller fails to start, a pre-selected chiller of Division I starts automatically, i.e., 1HVK*CHL1A or 1C. The two not pre-selected chillers one on each Division will not start automatically. The failed chiller unit or the failed air supply circuit is annunciated in the control room. The control building chilled water system is described in detail in Section 9.2.10.

3←•

Instrumentation is provided to warn the operators of any dangerous condition which could affect their lives and safety. Firefighting equipment is also supplied. Maintaining a positive pressure in the main control room provides a continuous purge of the main control room and also protects the operators against infiltration of smoke, toxic chemicals or airborne radioactivity from the surrounding areas. Cables and pipes penetrating the main control room pressure boundary are sealed. This aids in the pressurization of the main control room and also limits the spread of fire and smoke that may enter pipe or cable chases.

6.4.2 System Design

6.4.2.1 Definition of the Main Control Room Envelope

•→14 •→7

The main control room envelope consists of all rooms located on the main control room elevation 135 ft 0 in and main control room HVAC equipment room located on elevation 115 ft 0 in. Included in the envelope, served by the main control room HVAC system, are the main control room, shift superintendent office, kitchen, toilet, and HVAC equipment room. Airtight doors are provided at the access points and from the main control room envelope. The enclosed volume of the main control room envelope is 240,700 cu ft. An outline of the main control pressure boundary is shown in Figure 6.4-2.

7←• 14←•

6.4.2.2 Control Room Air Conditioning System Design

The design, construction, and operation of the main control room system are described in detail in Section 9.4.1. Fig. 9.4-1 shows system flow diagram with major components and instrumentation. A description of the major component flow rates, capacities, and major design parameters is in Section 9.4.1.

Fig. 6.4-1 shows the plant layout, including the location of potential radiological release points with respect to the main control room air intakes.

Elevation and plan drawings showing building dimensions and equipment locations are given on Fig. 1.2-24 through 1.2-26. Potential sources of toxic gas release are identified in Section 2.2.

A description of the main control room instrumentation for monitoring of radioactivity is given in Sections 12.3.4. and 11.5.

Protection of the main control room HVAC from internally generated missiles is discussed in Section 3.5.

•→15 •→14

A dedicated control building smoke removal system is provided to purge the control room, switchgear rooms, cable vault, cable chases, and general areas in the event of an accidental fire.

14←• 15←•

Smoke removal in the battery rooms, inverter charger rooms, and chiller equipment room is achieved by manually operating the exhaust systems serving those areas.

Removal of radioiodines from the main control room ventilation outside air supply during a DBA is accomplished through use of charcoal filter trains. To comply with 10CFR50.67, two 100-percent redundant charcoal filter trains are provided. Amendment 132 revised the design basis accident main control room dose limit requirements to incorporate the limits of 10CFR50.67. The limits of 10CFR50 Appendix A, General Design Criteria 19, also remain applicable to the RBS design basis. The main control room charcoal filter trains are designed in accordance with requirements of Regulatory Guide 1.52 (with the exceptions noted in Table 6.5-1). Both filter trains and associated air handling equipment, designed to Seismic Category I, are located within the main control room pressure boundary.

Each train has an air handling capacity to deliver 4,000 cfm of outdoor and return air. Outdoor air is supplied from the outside air intake. Separate intakes (local and remote) are furnished to provide alternative sources of outdoor air with the capability of selecting either source from the main control room. Redundant radiation monitors in each of the main control room air supply duct system monitor the radioactivity level of the outside supply air.

Each charcoal filter train consists of the following principal components:

1. A demister (moisture separator) to remove at least 99 percent by weight of the entrained moisture in an airstream containing 0.005 lb of entrained moisture per cu ft and at least 99 percent by count of the 1- to 10-micron diameter droplets without visible carryover at rated (4,000 cfm) to twice rated capacity.
2. An electric heating coil powered from a standby bus to limit the relative humidity of the incoming air to 70 percent at design flow during post-LOCA conditions.
3. Prefilters upstream of the first bank of high efficiency particulate air (HEPA) filters to remove coarse particles from the airstream. The prefilters have 80-percent efficiency based on the National Bureau of Standards dust spot test.
4. A bank of HEPA filters to remove virtually all fine airborne particulates from the airstream. The filters are of water-repellent and fire-resistant construction. The HEPA filters are tested to a

minimum efficiency of 99.97 percent for 0.3-micron diameter homogeneous particulates of dioctylphthalate (DOP). These tests are performed in accordance with MIL-STD-282⁽¹⁾.

5. A minimum of 4-in deep bank of charcoal adsorber filters. Filters are of an all welded, gasketless design and are sized for a maximum air velocity of 40 fpm through the charcoal at rated airflow. The adsorber media is activated coconut shell charcoal impregnated with potassium iodide (KI).
6. A second bank of HEPA filters, identical to item 4 above, to capture charcoal particles which may escape from the charcoal filters.

All of these components are mounted in an all-welded steel housing. Each charcoal filter train is provided with an integrally mounted, water spray, fire extinguishing system consisting of discharge nozzles and distribution piping. A thermistor detection system is installed in the charcoal beds. The detection panels are integrated into the main control room panel to annunciate an alarm in the event of fire. Housing floor drains are provided for the demister condensate, the occasional washdown required for decontamination, and the deluge water sprays, in the event of a fire in accordance with recommendations of ERDA 76-21⁽²⁾. The drains are sized to draw water at the same rate as the rate at which the deluge system supplies it, without backup of water in the housing.

●→15

A centrifugal-type fan with 4,000 cfm capacity is provided downstream of each filter unit. The fan is a direct-drive type with a single speed motor. The decay heat produced by radioactive materials in the inactive charcoal filtration unit is removed by a 100-cfm centrifugal fan. Cool air from the equipment room passes through the filter unit and warm air is discharged from the filter unit back to the equipment room.

15←●

Filter train component sizing is governed by the following flow parameters:

1. High Efficiency Particulate Air Filters - Both HEPA filter banks are designed so that airflow through any standard 24 x 24 x 11 1/2-in cell does not exceed 1,000 cfm.
2. Charcoal Filter Bank - The effective face area of the charcoal filter is designed so that the average air velocity through the charcoal bed does not

exceed 40 ft/min when the filter train is operating at 4,000 cfm. Gas residence time in the charcoal bed is a minimum of 0.25 sec per 2 in of bed depth. The adsorption capability of a charcoal filter bank is more than 2.5 mg of total iodine (radioactive plus stable) per gram of activated carbon. There are 2,400 lb of activated carbon material in each of the charcoal filter trains to meet the gas flow and minimum residence time established herein.

Filter train components are fully accessible by means of access doors located at each filter bank. Filter cabinets are designed with space between components to permit access for filter inspection, testing, and maintenance.

HEPA filters are capable of removing a minimum of 99.95-percent thermally generated DOP particulate of uniform 0.3-micron diameter droplet size at the design flow rate of 4,000 cfm.

The charcoal filter bed is capable of removing 98 percent of airborne radioactive iodine (I_2) and methyl iodide (CH_2I) at the design flow rate.

The electric cable to and from the power generation control complex units and the computer is routed through a false floor 12 in deep. The floor sections are protected with a Halon 1301 fire protection system. In these floor sections smoke and thermal detectors are placed. These detectors annunciate and alarm on a control board in the main control room. Operators manually activate the fire protection system as required. Portable fire extinguishers are provided to extinguish fires that occur above the main control room floor. The cable vault located at el 70 ft 0 in of the main control building and cable chases through the entire height are protected by automatic sprinkler systems. Smoke detection is installed in all other areas of the control building. For further description of fire protection system see Section 9.5.1.

There are no items of equipment which, when operating under their design conditions, produce any noxious gases. Electrical cables are constructed of materials which do not support combustion; however, during a fire, melting cables and electrical equipment would produce noxious gases. Smoke removal is provided by a separate system.

6.4.2.3 Leak Tightness

The main control room envelope boundary is designed with low leakage construction to minimize the potential for the infiltration of air into the main control room. The walls, floor, and roof are constructed of poured-in-place reinforced concrete which is essentially leak tight. The access doors are of airtight design with self-closing devices which shut the doors automatically following the passage of personnel. All cable and air duct penetrations are provided with a fire retardant seal which provides leak tight construction.

The pressurization system that pressurizes the main control room under all operating conditions has a maximum pressurization rate of one volume change per hour. A periodic test (every 24 months) is performed to verify that the makeup air and recirculation air for main control room pressurization is ± 10 percent of the design value.

The control room dose rate calculations assumed an unfiltered in-leakage rate of 300 CFM. The baseline tracer gas test was performed in May, 2004 based on methodology recommended by NEI 99-3⁽²⁾, Appendix I, described in ASTM Standard E2029-99, and ASTM E-741. Air in-leakage into the control room envelope and corresponding fresh air makeup flow rates were measured with control room fresh air system operating in two pressurization modes (Local Intake and Remote Intake). The test results confirmed the measured in-leakage into the control room envelope is significantly less than the analytical in-leakage of 300 CFM.

The control room habitability analysis⁽⁴⁾ determined that the control room habitability is based on maximum vapor concentration in the main control room due to postulated releases of toxic chemicals. This analysis used very conservative assumptions and determined there is no credible MCR habitability threats onsite or offsite as a result of analysis of postulated releases of the toxic chemicals reported in USAR Table 2.2-7 and 2.2-8. The main control room air intake header can be manually isolated in the event of a toxic gas release.

6.4.2.4 Interaction with Other Zones and Pressure-Containing Equipment

The main control room air conditioning system is provided with radiation detectors.

A high radiation or LOCA signal automatically diverts air flow from local air intake through charcoal filter and shuts down kitchen and toilet exhaust fans. The main control room operator can manually switch over to remote air intake if the radiation level at the local air intake is above the permissible level.

Once the main control room isolation signal is activated, the following actions occur automatically:

1. All open outside air makeup isolation dampers close.
2. The main control room utility exhaust fans in toilet and kitchen shut down, and the associated isolation dampers close.
3. If the main control room smoke exhaust line isolation dampers are open, they are closed; a resulting signal shuts down the operating smoke removal fan.

If a smoke detection signal is received during the main control room isolation, an alarm is given, but the air conditioning units continue to operate and the smoke removal system isolation dampers remain closed. This prohibits possible spurious smoke detector signals from compromising system operation under emergency conditions. Portable respirators are available for emergency needs.

6.4.2.5 Shielding Design

Floor plans of the main control room and lower levels are provided on Fig. 1.2-24 through 1.2-26.

The main control room shielding, air supply system, and administrative control procedures limit the amount of radiation received by personnel to 5 rem whole body or 30 rem thyroid dose for the duration of the accident.

For further description of the main control room radiological considerations, see Chapter 15. Section 12.3.2 discusses the design objectives of shielding provided for the main control room envelope.

Shielding is provided by reinforced concrete floors and walls of the following thicknesses:

<u>Structure</u>	<u>Envelope Boundary</u>	<u>Thickness</u>
Walls	All exterior walls of control building	2'-0"
	Interior walls	1'-0"
Floor slabs	Main control room, floor el 135' and 115' (envelops lower boundary)	0'-11" (includes 2" corrugated steel decking)
	Control building roof, el 156' (envelops upper boundary)	2'-3" (includes 3" corrugated steel decking)

6.4.2.6 Portable Self-Contained Air Breathing Units

Ten full face, pressure demand self-contained breathing apparatuses (SCBA), complying with NIOSH requirements, are provided for main control room use. Additionally, at least three spare air bottles are available for each SCBA. Each SCBA is sized to supply an operator for approximately 1 hr during moderate exertion. Routine replenishment is available through a cascade system located onsite with offsite replenishment available through compressed gas suppliers in the Baton Rouge area. Operator training is provided in donning and operating this equipment such that a trained operator can be breathing air supplied by these units within 30 sec. Maintenance is provided for the SCBAs monthly and after each use to ensure their availability.

Ten full-face respirators with high-efficiency particulate filters are also provided in the main control room.

•→3

3←•

6.4.3 System Operational Procedures

As summarized in Section 6.4.2 and described in detail in Section 9.4.1, the response of the main control room habitability systems to a LOCA condition is fully automatic. During normal and emergency operation, the main control room operator selects the air handling unit which operates to maintain design temperatures in the main control room. Periodically the operating unit is stopped and the standby unit is started so that the service time of both units is approximately equal. In the event the operating unit fails, the standby unit starts automatically.

The response of the main control room habitability system to airborne radioactivity from outside air intake is automatic. On receipt of a high radiation signal, airflow is diverted through the emergency charcoal filtration unit, and kitchen and toilet exhaust fans are shut down.

6.4.4 Design Evaluation

6.4.4.1 Radiological Protection

Under normal plant conditions, outside air enters the main control room through the local outside air intake located on the roof of the control building. During accident conditions, fresh air may be drawn in through the remote air intake. Measurements taken from the radiation monitor in the air supply duct allow operators to select the least radioactive air intake. During a LOCA, the outside air supply is automatically diverted through the main control room charcoal filter as a precaution regardless of outside air quality. All habitability systems are designed to meet the single-failure criterion.

6.4.4.2 Toxic Gas Protection

The effects on main control room habitability resulting from postulated releases of offsite toxic chemicals, including chlorine and ammonia, are discussed in Section 2.2. Consideration of the human odor detection threshold is

appropriate since the time difference between detection and incapacitation is equal to or greater than 120 sec.

The main control room operators are provided with self-contained breathing apparatus for protection in the event of a toxic gas release. Each operator is taught to distinguish the odor of chlorine and ammonia, and practice drills are conducted to ensure that each operator can don breathing apparatus within 2 min. The main control room air intake header can be manually isolated in the event of a toxic gas release.

The protection of main control room operators and analysis of hazardous chemicals, as discussed in Section 2.2, is in compliance with the guidance outlined in Regulatory Guide 1.78.

6.4.4.3 Compliance with Regulatory Guide 1.52

A detailed description of compliance with positions C.2.a through C.2.f and C.2.k of Regulatory Guide 1.52 is provided as follows:

C.2.a

The ESF atmosphere cleanup systems for the main control room are redundant and consist of the following components: 1) demister, 2) electric heater, 3) prefilters, 4) HEPA filters, 5) iodine absorber (impregnated activated carbon), 6) HEPA filters.

C.2.b

The redundant ESF atmosphere cleanup system filtration units in the control building are physically separated by 1-ft thick reinforced concrete wall at the fans' locations.

C.2.c

All components of the control building ESF atmosphere cleanup system are designated as Seismic Category I.

C.2.d

The control building ESF atmosphere cleanup system is not subjected to pressure surges.

C.2.e

The effects of radiation are considered for all organic-containing materials that are necessary for operation during a postulated DBA.

C.2.f

The volumetric airflow rate through a single cleanup unit for the main control room is 4000 ft³ /min. The filter layout for the main control room is two HEPA filters high and two wide.

C.2.k

•→15

Outdoor air intake openings are equipped with security grating and bird screens.

15←•

6.4.5 Testing and Inspection

The equipment that maintains the habitability of the main control room is thoroughly tested in a program consisting of the following classification:

1. Predelivery and component qualification tests
2. Post-delivery acceptance tests
3. Post-operation surveillance tests.

The factory and component qualification tests consist of the following:

1. All equipment is factory inspected and tested in accordance with the applicable equipment specifications, codes, and quality assurance requirements. System ductwork and erection of equipment is inspected during various construction stages for quality assurance. Construction tests are performed on all mechanical components, and the system is balanced for the design air and water flows and system operating pressures. Controls, interlocks, and safety devices are checked, adjusted, and tested to ensure the proper sequence of operation. Test results are recorded and maintained in auditable files.
2. The environmental qualification of Class 1E equipment is discussed in Section 3.11.

3. The preoperational tests are performed as described in Chapter 14.

•→8

4. Operational surveillance testing is described in the Technical Specifications/Requirements Manual.

8←•

6.4.5.1 Main Control Room Charcoal Filter Trains

Initial performance verification and periodic surveillance tests are conducted to ensure operability and performance of both charcoal filter train units to the specified efficiencies. HEPA filters are shop tested prior to installation in accordance with MIL-STD-282 at 100 percent and at 20 percent of rated flow. Charcoal adsorber banks are leak tested using R-11, or equivalent, in accordance with test procedures described in ERDA 76-21 (Reference 3), Paragraph 8.3.2, p 194 through 198.

Impregnated activated carbon is tested prior to installation in accordance with the methods specified in RDT-M16-1T for apparent density, CCl activity, percent hardness, percent moisture, particle size distribution, and ash content and meet the intent of Regulatory Guide 1.52.

The program of preoperational testing performed on the charcoal filter trains is presented in Chapter 14.

6.4.5.2 Water Chillers

Design and Operating Codes

The water chiller packages are designed, installed, and tested in accordance with the following standards and codes:

1. ASME Boiler and Pressure Vessel Code, Section III - Construction of chiller heat exchanger watersides is in compliance with this code.
2. ANSI B31.5 and B31.5a, Code for Pressure Piping - The chiller refrigerant piping is in compliance with this code.
3. ANSI B9.1, Safety Code for Mechanical Refrigeration - The chillers are installed and operated in compliance with this code.
4. NEMA MG1 - The routine tests are performed on each motor in accordance with this standard.

5. IEEE-323-1974 - All electrical components are fabricated and qualified in compliance with this code as applicable.

Certification Testing

The water chiller rotors are subjected to an overspeed spin test and static and dynamic balancing. Material certification for all parts subjected to pressure is required. The chiller package is seismically analyzed to meet postulated acceleration forces.

6.4.5.3 Fans

Certification Testing

The fan impellers are subjected to an overspeed spin test and static and dynamic balancing. A performance test or manufacturers' certified ratings in accordance with Air Moving and Conditioning Association (AMCA) standards are required. Material certification for fan shaft and impeller is required. The fan units are seismically analyzed to meet postulated acceleration forces. Seismic qualification testing is discussed in Section 3.10A.

6.4.5.4 Air Handling Units

Certification Testing

The air handling unit impellers are subjected to an overspeed spin test and static and dynamic balancing. Every air handling unit is given a shop running test. The cooling coils are hydrostatically air pressure and leak tested. A performance test or manufacturer's certified ratings in accordance with AMCA or Air Conditioning and Refrigeration Institute standards are required. Material certification for fan shaft, blade, and cooling coil is required. The air handling units are seismically analyzed to meet postulated acceleration forces. Seismic qualification testing is discussed in Section 3.10A.

6.4.5.5 Pumps

Certification Testing

Each chilled water pump is tested in accordance with ASME PTC 8.2-1965, Power Test Code - Centrifugal Pumps, which establishes the pump performance characteristics. Seismic qualification testing is discussed in Section 3.9A.

6.4.5.6 Valves

Certification Testing

All valves associated with the main control room HVAC system are factory leak tested to a minimum of 75 psig using the halogen diode detector method. The test is repeated after cycling the valve three times. The test is in accordance with ASME Section V, Article 10, Paragraph T-1040. Seismic qualification testing is addressed in Section 3.9A.

6.4.6 Instrumentation Requirements

The instrumentation requirements for the main control room area ventilation system are described in Section 9.4.1.5.1. The instrumentation requirements for the chilled water system which supplies chilled water to the main control room air conditioning units is described in Section 9.2.10.5.

The ESFs for the main control room area ventilation and chilled water systems are described in Section 7.3.1.

Conformance with NRC General Design Criterion 19 [and 10CFR50.67](#) | is described in Section 3.1.2.19.

References - 6.4

1. MIL-STD-282-1974, Filter Units, Protective Clothing, Gas-Mask Components and Related Products: Performance-Test Methods, Military Standard.
2. NEI 99-03 Revision 1, Nuclear Energy Institute Control Room Habitability Guidance.
3. ERDA 76-21, Nuclear Air Cleaning Handbook, Oak Ridge National Laboratory.
4. G13.18.2.1*090, Control Room Habitability Analysis: Postulated Accidental Release of Onsite and Offsite Toxic Chemicals.

6.5 FISSION PRODUCT REMOVAL AND CONTROL SYSTEMS

6.5.1 Engineered Safety Feature (ESF) Filter Systems

•→14

The ESF filter systems consist of the main control room emergency fresh air filter system, fuel building charcoal filtration system (fuel handling accident only), and standby gas treatment system (SGTS). These three air filtration systems are required to perform safety-related functions following a design basis accident (DBA). The main control room air-conditioning subsystem is discussed in Sections 6.4 and 9.4.1. The fuel building charcoal filtration system is discussed in Section 9.4.2 and the SGTS is described in this section.

14←•

The nonsafety-related filter systems include the radwaste building exhaust air filter and tank vent charcoal filter trains (Section 9.4.3), the continuous containment and drywell purge charcoal filter trains (Section 9.4.6), and the air removal mechanical vacuum pump charcoal filter trains (Section 9.4.4).

6.5.1.1 Design Basis

The SGTS limits release to the environment of radioisotopes which may leak from the primary containment, ECCS systems, and other potentially radioactive sources to the secondary containment under accident conditions. The SGTS has the following safety design bases:

1. The SGTS is of Seismic Category I design.
2. The SGTS is designed with sufficient redundancy to meet the single-failure criterion. Each of the two SGTS trains is separated and housed in an independent cubicle so that damage to one train does not cause damage to the other train.
3. The SGTS redundant equipment is connected to separate buses to allow uninterrupted operation of the system in the event of the loss of offsite power.
4. The SGTS is designed to limit the thyroid and the whole body doses to within the limits of 10CFR50.67 at the site boundary (exclusion area boundary) and the low-population zone outer boundary. [Amendment 132 revised the design basis accident offsite dose limit requirements from 10CFR100 to 10CFR50.67.](#)
5. The SGTS charcoal filter trains are designed in accordance with Regulatory Guide 1.52 except as noted in Table 6.5-1.

6. The sizing of the SGTS equipment and components is based on results of an infiltration analysis of the auxiliary building and the annular space between the primary containment and shield building (annulus).
- 14
7. The SGTS is designed to maintain a negative pressure of at least -0.50 in W.G. in the annulus and a negative pressure of at least -0.25 in W.G. in the auxiliary building.
- 14←•
8. The SGTS components are located in Seismic Category I structures and are protected against outside missiles and dynamic effects of tornado and wind pressure.

6.5.1.2 System Design

6.5.1.2.1 General System Description

The configuration of the SGTS filter trains is shown in Fig. 1.2-14 and design data of principal components are listed in Table 6.5-2.

The SGTS consists of two identical, 12,500 cfm 100-percent capacity parallel, physically separated, charcoal filter trains with associated ductwork, dampers, controls, and centrifugal exhaust fans. The discharge from the two fans is connected to a common exhaust duct. The air is drawn from the annulus mixing system (Section 9.4.6) recirculation ductwork and exhausted or recirculated through the SGTS filters.

During post-accident operation the primary function of the SGTS is to process exhaust air from the annulus and the auxiliary building. During normal operation it serves as a backup to the containment and drywell purge system.

•→14 •→10 •→8

During normal operation, the annulus pressure control system maintains the annulus at negative pressure (Section 9.4.6). Upon receipt of a LOCA, high-radiation signal (from one of the two radiation monitors located in the annulus), or loss of APCS flow, the annulus air is automatically diverted through the SGTS filter trains and the exhaust air from the shielded compartments in the auxiliary building is also automatically diverted through SGTS filter trains. On a high-radiation condition in the shielded compartments of the auxiliary building, the SGTS is manually started to process the contaminated air and maintain a negative pressure of at least -0.25 in W.G.

8←• 10←• 14←•

If the SGTS filter trains are not processing the annulus atmosphere and the exhaust air of the shielded compartments in the auxiliary building, the containment and drywell purge can be manually diverted through the two SGTS filter trains (Section 9.4.6). By utilizing both SGTS filter trains, a maximum of 25,000 cfm of exhaust air can be processed. All controls for the SGTS are located in the main control room.

●→14

The SGTS is designed to maintain a negative pressure of at least -0.50 in W.G. in the annulus during post-LOCA operation. With the annulus at a negative pressure, any leakage is directed inward (away from the shield building) and primary containment leakage is collected and passed through a filter train of the SGTS before being released to the environs.

14←●

The SGTS can also be manually started for annulus and auxiliary building exhaust air purification, as needed.

The SGTS units are automatically started in the event of any of the following four isolation signals:

1. High radiation in the annulus exhaust
2. High pressure in the drywell
3. Reactor vessel low water level

●→10 ●→8

4. Loss of annulus pressure control flow

8←● 10←●

The plant operator can stop one of the SGTS filter trains from the main control room after system initiation is completed. In consideration of the possibility of iodine desorption and charcoal ignition at elevated temperatures, a water spray system is provided for the charcoal adsorber section of the SGTS filter trains. In order to detect any abnormal temperature rise at the outlet of the charcoal adsorber, each charcoal bed is provided with a thermistor detection system. When the temperature exceeds a pre-determined set point, there is an alarm in the main control room, the exhaust fan is manually stopped and, if warranted, the spray system is manually initiated.

The decay heat produced by radioactive materials in the inactive SGTS filter train is removed by a 100-cfm capacity centrifugal fan, taking air from the equipment rooms and exhausting to the main plant exhaust duct.

In addition to the instrumentation previously described, the filter trains are instrumented to indicate pressure differentials across each element of the filter train. A

low flow condition (high pressure differential) in the charcoal filter unit automatically initiates the redundant filter train.

There are 5,000 lbm of activated carbon material in each of the two charcoal filter banks. The adsorption capability of each charcoal filter bank is more than 2.5 mg of total iodine (radioactive and stable) per gram of activated carbon as required by Regulatory Guide 1.52.

The sizing of the SGTS components is governed by the following flow parameters:

1. Demister (moisture separator) - The demister is designed to remove at least 99 percent by weight of the entrained moisture in an airstream containing 0.005 lbm of entrained moisture per cu ft and at least 99 percent by count of the 1 to 10 micron diameter droplets without visible carry-over when operating at rated (12,500 cfm) capacity to twice rated capacity.
2. Prefilters - Prefilters are designed so that airflow through any standard 24" x 24" x 11 1/2" cell does not exceed 2,000 cfm.
3. High Efficiency Particulate Air Filters - Both HEPA filter banks are designed so that airflow through any standard 24" x 24" x 11 1/2" cell does not exceed 1,000 cfm.
4. Charcoal Filter Bank - The effective face area of charcoal filter is designed so that the average air velocity through the charcoal bed does not exceed 40 ft/min when the filter train is operating at 12,500 cfm. Gas residence time in the charcoal bed is a minimum of 0.25 sec per 2 in of absorbent bed. Five thousand lbm of activated carbon material similar in type to Barnaby Cheney 727 is provided for each filter train to meet the gas flow and minimum residence time established herein.

6.5.1.2.2 System Component Description

The SGTS is shown in Fig. 6.2-58. Principal system components with their performance parameters are listed in Table 6.5-2. The system consists of two 100-percent capacity filter trains, each of which consists of the following components in series:

RBS USAR

1. A demister (moisture separator) to remove entrained water particles in the incoming air stream.
2. An electric heating coil powered from a standby bus to limit the relative humidity of the incoming air to 70 percent at design flow during post-LOCA conditions.
3. Prefilters upstream of the first bank of high efficiency particulate air (HEPA) filters to remove coarse particles from the airstream. The prefilters have an 80-percent efficiency, based on the National Bureau of Standards dust spot test.
4. A bank of HEPA filters to remove virtually all fine airborne particulates from the airstream. The HEPA filters are of water-repellant and fire-resistant construction and are tested to a minimum efficiency of 99.97 percent for 0.3 micron diameter homogeneous particulates of dioctylphthalate (DOP). These tests are performed in accordance with MIL-STD-282⁽¹⁾.
5. A 4-in minimum depth bank of charcoal adsorber filters. Filters are of an all-welded, gasketless design and are sized for a maximum air velocity of 40 fpm through the charcoal at rated airflow. The adsorber media is activated coconut shell charcoal, impregnated with potassium iodide (KI).
6. A second bank of HEPA filters, identical to item 4 above, to capture charcoal particles which may escape from the charcoal filters.

All the preceding components are mounted in an all-welded steel housing. Each charcoal filter train is provided with an integrally mounted, water spray, fire-extinguishing system, consisting of discharge nozzles and distribution piping. The thermistor detection system panels are integrated into the main control room panel to annunciate in the event of a fire. Housing floor drains are provided for the demister condensate, the occasional washdown required for decontamination, and the deluge water sprays in the event of a fire, in accordance with recommendations of ERDA 76-21⁽²⁾. The drains are sized to draw water at the same rate as the deluge system supplies it, without backup of water in the housing.

A centrifugal-type fan with 12,500-cfm capacity is provided downstream of each filter train. The fan is a direct-drive

type with a single speed motor. The decay heat produced by radioactive materials in the inactive charcoal filter train is removed by a 100-cfm centrifugal fan, taking air from the equipment rooms and exhausting to the main plant exhaust duct.

The SGTS charcoal filter trains are located in the auxiliary building at el 141 ft.

The design of the SGTS assemblies and appurtenances conforms to the requirements of Regulatory Guide 1.52, with the exceptions listed in Table 6.5-1. All assemblies and appurtenances are designed to withstand operational and environmental conditions specified in Tables 9.4-1 and 3.11-1.

Access doors are provided to give complete accessibility to all components for servicing. The doors are airtight, fitted with locking devices, and have provisions for opening inside the housing, as recommended in ERDA 76-21, Section 4.5⁽²⁾.

The SGTS is designed in accordance with ALARA considerations to minimize the radiation exposures to personnel changing filters and devices under possible radiation conditions. The system is designed to provide enough space for handling used and new filters without releasing radioactivity associated with the used filters or the housing.

6.5.1.3 Design Evaluation

Continued operation of system components during all modes of plant operation is assured by the following features for which the system is designed:

1. The SGTS is designed to Seismic Category I requirements, as specified in Section 3.2. The components and supporting structures of any system, equipment, or structure that is not Seismic Category I, and whose collapse could result in loss of the safety function of the ESF filter systems through either impact or flooding, are analytically checked (and upgraded if necessary) to assure that they do not collapse when subjected to seismic loading.
2. The SGTS is designed and constructed to be consistent with the recommendations of Regulatory Guide 1.52, with the exceptions listed in Table 6.5-1.

3. The SGTS is designed to prevent the release of contaminated air from the annulus or from the auxiliary building following an accident or abnormal occurrence.
4. During loss of offsite power, all active components such as motors, damper operators, controls, and instrumentation receive power from their respective independent standby power supplies.
5. The SGTS consists of two 100-percent capacity, physically separated filter trains. Should any component in one train fail, filtration can be performed by the other redundant train. The consequences of SGTS active component failures are presented in the Failure Modes and Effects Analysis (FMEA).
6. The SGTS is designed to limit the release of airborne radioactivity resulting from a postulated accident to values within the guidelines of 10CFR50.67. [Amendment 132 revised the design basis accident offsite dose limit requirements from 10CFR100 to 10CFR50.67.](#)

6.5.1.4 Tests and Inspection

The SGTS and its components are thoroughly tested in a program consisting of the following classifications:

1. Pre-delivery tests and component qualification tests
2. Post-delivery acceptance tests
3. Post-operation surveillance tests.

All pre-delivery, post-delivery, and post-operation tests are performed to meet the objectives of Regulatory Guide 1.52, with the exceptions listed in Table 6.5-1.

6.5.1.4.1 Preoperational Testing

The SGTS charcoal filter train housings are pressure tested to demonstrate a leakage of less than 0.2 cfm per 1,000 cfm of system flow at a pressure differential of 1.5 times the system pressure. The housing leak test is performed in accordance with ANSI N510, Section 6⁽³⁾.

HEPA filters are shop tested prior to installation, in accordance with MIL-F-51068 and MIL-STD-282, at 100 percent and 20 percent of rated flow^(1,6).

Impregnated activated carbon is tested prior to installation in accordance with the methods specified in RDT Standard MI6-IT for apparent density, carbon tetrachloride activity, percent hardness, percent moisture, particle size distribution, and ash content, and meets the intent of Regulatory Guide 1.52.

Elemental and methyl iodine removal and retention capabilities are measured at postulated accident conditions in accordance with RDT Standard M16-IT⁽⁴⁾. Impregnate content, leachout, and charcoal ignition temperature are also determined.

HEPA filter banks are tested in place prior to operation to verify the efficiency of at least 99.97 percent with cold-generated DOP.

The charcoal filter banks are freon leak-tested prior to operation to verify less than 0.05 percent bypass. In addition, a laboratory test of a representative sample of the impregnated activated carbon is performed to verify iodine removal efficiencies.

The program of preoperational testing performed on the ESF filter systems is presented in Chapter 14.

6.5.1.4.2 Inservice Testing

●→8A

Inservice testing of the SGTS is conducted in accordance with the surveillance requirements given in the Technical Specifications/Requirements.

8A←●

6.5.1.5 Instrumentation Requirements

●→10 ●→8

Pushbutton controls are provided in the main control room for either manual or automatic operation of the redundant SGTS exhaust fans. Startup of each fan is monitored by the plant computer. Pushbutton controls are also provided for lining up the SGTS with the annulus exhaust (Section 9.4.6.5.5) and the auxiliary building exhaust (Section 9.4.3.5.1). During normal operation a high annulus exhaust radiation signal, a LOCA signal, or a loss of annulus pressure control flow automatically lines up both the annulus exhaust and the auxiliary building exhaust with the SGTS. The annulus exhaust radiation monitors are described in Section 12.3.4.

Automatic startup of both SGTS exhaust fans occurs when either a LOCA signal, a loss of annulus pressure control flow, or high high radiation conditions is present in the

8←● 10←●

annulus exhaust (Table 12.3-2). The fans also start up when the manual initiation pushbuttons in the main control room are actuated. After stopping one of the fans (and an automatic signal is present), control logic is provided to start the fan automatically when an SGTS filter train low air flow signal exists due to the failure of the operating fan. An SGTS fan automatic restart alarm is provided in the main control room. After a time delay, a low flow condition in an operating train activates an alarm in the main control room. The fans are interlocked with their respective inlet and outlet isolation dampers so that the dampers are open when the fan is running and closed when the fan stops running. Fully open position of the inlet isolation damper is a permissive for the fan to start. The outlet isolation damper is open when the fan is running and closed when the fan stops running.

●→11

11←●

SGTS inoperative alarms are provided in the main control room for each division.

Pushbutton controls are provided in the main control room for manual operation of the SGTS filter train electric heating coils.

The temperature differential between the SGTS heating coils discharge air and the inlet air (auxiliary building, annulus exhaust, containment and drywell purge air temperature) is maintained at its setpoint by modulating a multi-step sequence controller. The heating coil is automatically deenergized when either the associated SGTS fan circuit breaker is opened or the heater high temperature cutout (manual or automatic) is activated. An alarm is activated in the main control room when a heating coil breaker automatically trips.

●→4

A control switch is provided in the main control room for either automatic or manual operation of the SGTS filter train decay heat removal fans. When operating in the automatic mode, the decay heat removal fan starts up after the SGTS inlet isolation damper has been open for a definite period of time and then fully closed. The fans are interlocked with their respective inlet isolation damper so that the damper is open when the fan is running and closed when the fan is not running.

4←●

SGTS decay heat removal fan inoperative alarms are provided in the main control room.

The SGTS filter train is monitored by the plant computer for any abnormal conditions, such as high filter pressure differentials. Charcoal filter bed inlet temperature is monitored in the main control room. A high charcoal filter bed outlet temperature alarm is provided in the main control room. An SGTS filter train trouble alarm is provided in the main control room for each division.

•→10

A control switch is provided in the main control room for opening and closing the SGTS recirculation damper. Interlocks are provided so that the damper opens automatically when its associated exhaust fan is running, the damper control switch is in auto, and either a high radiation in the annulus exhaust signal, a LOCA signal, or a loss of APCS signal is received (the recirculation damper will not open on a manual start) The recirculation damper closes when the fan stops running.

10←•

SGTS effluent radiation levels are recorded in the main control room. A high radiation level alarm is provided in the main and auxiliary control rooms. The SGTS exhaust radiation monitoring system is described in Section 7.6.1.

6.5.1.6 Materials

The housings and all framing materials of the SGTS filter trains are fabricated of steel alloys and, as such, are nonflammable. Each of the materials is compatible with the normal and accident environments postulated for the area in which the equipment is located, as well as the areas served by the return air ductwork. The following is a list of the materials used in the various components of the ESF filter units.

•→7

1. Demisters - The demister (moisture separator) section of each ESF filter system consists of a number of nonwoven mats in series, separated by grid assemblies with media retaining pins. The frame is made from 16 gauge (minimum) stainless steel formed into channel cross sections with welded corners. The demisters are designed, constructed, and tested in accordance with the recommendations of ANSI N509⁽⁵⁾ and meet the Underwriter's Laboratory (UL) Class 1 requirements.

7←•

2. Heater - The electric heating coil is provided upstream of the prefilters to reduce the relative humidity from 100 percent to less than 70 percent.

A heating element is integrally mounted in the filter train and connected to a terminal box. Heating elements are of the finned tubular type with carbon steel sheaths and copper plated steel fin material painted with high temperature aluminum paint. Heater frame, terminal box, and element support brackets are constructed of 14 gauge aluminized steel in accordance with ASTM A463; internal brackets, bridges, etc, are of 18 gauge (minimum) aluminized steel in accordance with ASTM A463.

3. Prefilters - Prefilters are of the Group III (high efficiency), extended medium, dry type with pleated media and full depth rigid frames. The media is American Air Filter (AAF) Vericel 90, UL Class 1. The filter media is contained in a fire-resistant exterior-grade plywood encased in a steel frame.
4. HEPA Filters - There are two banks of HEPA filters, one before and one after the charcoal filter bank, on each ESF filter system. The filters are AAF No. 5A25J6TI and consist of UL Class 1 fiberglass media in cadmium-plated frames with aluminum separators. The HEPA filters are designed, constructed, and tested in accordance with Regulatory Guide 1.52.
5. Charcoal Filter Bank - Each charcoal cell, including all components touching the charcoal, are fabricated of austenitic stainless steel. Stainless steel adsorbent bed screens are No. 26 U.S. gauge (minimum). The charcoal material is coconut shell AAF No. 2701 and has minimum ignition temperature of 340°C.

The housing for the entire filter train consists of 3/16-in HRS plate ASTM A-36, with the exception of charcoal filter section housing which is 3/16-in stainless steel plate ASTM A-240.

The SGTS is not exposed to accident environments of extreme temperature or radiation that could potentially produce pyrolytic or radiolytic decomposition of filter materials; thus filter train decomposition products are not present. A fire from external sources, which could cause pyrolytic decomposition of construction materials of the charcoal filters, is not postulated to occur simultaneously with any other plant accident which could require the operation of the filters for radioiodine removal credit. Therefore, fire

is not a credible event which could adversely affect the operation of the filter trains.

6. Ductwork and Accessories - All ductwork and accessories are designed and constructed in accordance with the recommendations of Section 5.10 of ANSI N509⁽⁵⁾, with the exceptions listed in Table 6.5-1. All dampers are designed and constructed in accordance with Section 5.9 of ANSI N509, with the exceptions listed in Table 6.5-1.

6.5.2 Containment Spray Systems

Not applicable to River Bend Station.

6.5.3 Fission Product Control Systems

●→14

The release of fission products to the environment in the event of a LOCA is largely controlled passively by the leaktight integrity of the primary and secondary containments and actively by the SGTS. Leakage into the fuel building from primary containment is assumed to be released directly to the environment since fuel building integrity is not required during a LOCA.

The SGTS filters the effluent from the auxiliary building and the annular space between the primary containment and the shield building. For detailed discussions of the primary and secondary containment structural and functional design and of the containment systems, refer to the following sections:

14←●

Design of Seismic Category I Structures	3.8
Containment Systems	6.2
Reactor Plant Ventilation System	9.4.6

6.5.3.1 Primary Containment

The primary containment consists of a steel vessel in the form of a cylinder anchored at its base to the concrete mat and closed at the top by a torispherical dome, forming a continuous, leaktight membrane. Details of the primary containment structural design are discussed in Section 3.8.2. The primary containment pressure suppression concept is the GE Mark III design. Layouts of the primary containment structure and the combustible gas control system are given in the equipment location drawings of Section 1.2.

The primary and secondary containment walls, mechanical penetrations, isolation valves, hatches, and locks, in

conjunction with the ESF filter systems, function to limit the release of radioactive materials, subsequent to postulated accidents, so that the resulting offsite doses are less than 10CFR50.67 limits. Amendment 132 revised the design basis accident offsite dose limit requirements from 10CFR100 to 10CFR50.67. Primary containment parameters affecting fission product release analyses are given in Table 6.5-3.

Long-term primary containment pressure response to the DBA is discussed in Section 6.2.1.

The combustible gas control system (consisting of a redundant hydrogen mixing system, redundant hydrogen recombiners, and containment hydrogen purge system) required to control the short and long term hydrogen concentration is discussed in Section 6.2.5.

During normal operation, the primary containment can be purged by SGTS filter trains upon detection of higher than normal radioactivity concentrations (Section 9.4.6). The containment and drywell purge system penetrations are automatically isolated in response to LOCA signals (high drywell pressure or low reactor water level). The penetrations are, for the most part, provided with redundant, Seismic Category I, air-operated, fail-closed, ASME Section III, Class 2 butterfly valves, which assure prompt and tight closure of the openings (Table 6.2-40). In the event that the primary containment is being purged at a higher than normal rate through the SGTS filter trains, prompt and tight closure of these penetrations is also assured by similar containment isolation valves. Refer to Section 9.4.6 for a description of the containment ventilation system.

●→14

6.5.3.2 Secondary Containment and the Fuel Building

The secondary containment and fuel building boundary region for which ESF filter systems are provided is as follows:

1. The annular space between the primary containment and the shield building
2. The volume enclosed by the exterior walls and roof of the auxiliary building
3. The volume enclosed by the exterior walls and roof of the fuel building.

This boundary region of the secondary containment and fuel building are shown in the following figures:

14←●

<u>Figure</u>	<u>Title</u>
1.2-9 through 1.2-12	General Arrangement-Reactor Building Plans and Sections
1.2-13 through 1.2-19	General Arrangement-Auxiliary Building Plans and Sections
1.2-20 through 1.2-23	General Arrangement-Fuel Building Plans and Sections

The primary containment is discussed in Section 6.5.3.1. The shield building protects the steel primary containment from tornado winds and missiles. It also provides biological shielding in the event of a LOCA. It is a right circular cylinder capped with a torispherical segment dome and supported on the reactor building mat. The shield building is a reinforced concrete structure. The details of the shield building structural design are discussed in Section 3.8.4.

•→14

The secondary containment, in conjunction with other containment systems, provides the means for controlling and minimizing leakage from the primary containment and ECCS systems in the auxiliary building to the outside atmosphere during a LOCA and from the refueling facilities in containment. The fuel building provides a means of controlling and minimizing leakage during normal refueling activities involving recently irradiated fuel and Fuel Handling Accidents (FHA) in the fuel building.

Dose analysis of postulated radiological releases involving the site boundary and low-population zone are given in Chapter 15. Radiation exposures resulting from these occurrences are within the limits of 10CFR50.67. Amendment 132 revised the design basis accident offsite dose limit requirements from 10CFR100 to 10CFR50.67.

The annulus pressure control system (Section 9.4.6) maintains a uniform negative pressure of at least -3 in W.G. in the annulus at all times during normal operation. Following a LOCA or high radiation conditions in the annulus exhaust duct, a negative pressure of at least -0.50 in W.G. is maintained by SGTS (Section 6.5.1). Loss of negative pressure in the annulus is alarmed in the main control room. The secondary containment and fuel building functional designs are discussed in Section 6.2.3.

14←• •→10

6.5.4 Ice Condenser as a Fission Product Cleanup System

Not Applicable to River Bend Station

10←•

●→10

6.5.5 Pressure Suppression Pool as a Fission Product Cleanup System

Standard Review Plan (SRP) 6.5.5, "Pressure Suppression Pool as a Fission Product Cleanup System," allows credit for the pressure suppression pool as a fission product cleanup system. The guidance in this SRP replaces the guidance provided in Regulatory Guide 1.3 Position C.1.f. In accordance with the guidance provided in this SRP, suppression pool scrubbing credit is allowed if:

- a. The drywell and its penetrations are designed to ensure that, even with a single active failure, all releases from the reactor core must pass into the suppression pool, except for a small bypass fraction.
- b. The bypass leakage assumed for purposes of evaluating fission product retention must be demonstrated in periodic tests by the licensee technical specifications.
- c. For plants with a construction permit, the iodine retention calculated using SRP 6.5.5 must not be used to justify the removal of the standby gas treatment or other filtered exhaust system from status as an engineered safety feature.
- d. Any change in plant design, proposed testing, surveillance or maintenance must be supported by considerations of lowered operator dose and other projected benefits.
- e. Charcoal filters must be at least maintained to the minimum level of Table 2 of Regulatory Guide 1.52, Revision 2.
- f. Acceptance criteria for containment leakage and engineered safety features atmospheric cleanup systems must be unchanged.
- g. A decontamination factor (DF) of 10 for elemental and particulate iodine is allowed without additional calculational support for Mark III containments.

As noted above, SRP 6.5.5 allows a factor of 10 reduction in elemental and particulate iodine passing through the suppression pool without calculation provided certain design and operational conditions are met. RBS meets these conditions as discussed below and credit is taken in the design basis analysis for suppression pool scrubbing. The design of the RBS drywell and its penetrations ensures all releases from the reactor core

10←●

•→10

except for a small bypass fraction pass through the suppression pool even with consideration of a single failure. The allowable drywell bypass leakage is demonstrated by performance of periodic testing in accordance with RBS Technical Specifications.

In the event of a large break LOCA, the suppression pool functions as a fission product filter to mitigate offsite doses. At the time of the LOCA, the activity released from the damaged core is assumed to enter the drywell. Transfer from the drywell to the containment is either through the suppression pool, where a decontamination factor (DF) of 10 is taken, or through drywell leakage which bypasses the suppression pool. The bypass flow which enters the containment atmosphere and the activity leaving the suppression pool are assumed to be uniformly mixed in the containment atmosphere. Suppression pool scrubbing with a DF of 10 is assumed to remain effective as long as there is flow from the drywell into the suppression pool. See Section 15.6.5.

10←•

References - 6.5

1. MIL-STD-282-1974, Filter Units, Protective Clothing, Gas-Mask Components, and Related Products: Performance - Test Methods, Military Standard.
2. ERDA 76-21, Nuclear Air Cleaning Handbook, Oak Ridge National Laboratory.
- 8
3. ANSI N510-1989, Testing of Nuclear Air Cleaning Systems, American National Standards Institute.
- 8←●
4. RDT Standard M16-IT-1977, Gas-Phase Adsorbents for Trapping Radioactive Iodine and Iodine Compounds, United States Nuclear Regulatory Commission, Division of Reactor Development and Technology.
5. ANSI N509-1976, Nuclear Power Plant Air Cleaning Units and Components, American National Standards Institute.
6. MIL-F-51068-1974, Filter, Particulate, High-Efficiency, Fire Resistant, Military Specification.
7. AMCA 201-1973, Fan Application Manual, Air Moving and Conditioning Association.
8. ANSI/ASME N509-1980, Nuclear Power Plant Air Cleaning Units and Components.
9. ASTM D3809-89, Standard Test Method for Nuclear - Grade Activated Carbon.

6.6 INSERVICE INSPECTION OF ASME CODE CLASS 2 AND CLASS 3 COMPONENTS

●→8

6.6.1 Components Subject to Examination

Inservice inspection (ISI) and testing (IST) of ASME Class 2 and 3 pressure retaining components, such as vessels, piping, pumps, valves, welds, bolting and supports will comply with ASME Section XI as required by the Code of Federal Regulations (10CFR50.55a (g)). Exceptions have been documented in requests for relief pursuant to 10CFR50.55 (g) (6) (i).

The initial preservice inspection (PSI) of ASME Class 2 and 3 components has been performed in accordance with ASME Section XI. The 1974 Edition, up to and including Winter 1975 Addenda was used for Emergency Core Cooling systems (ECCS) and Residual Heat Removal system (RHS) and the 1977 Edition, up to and including Winter 1978 Addenda was used for the remaining systems. Augmented examinations are established in accordance with regulatory and industry documents, such as Regulatory Guides, Bulletins, Generic Letters and vendor recommendations. Requests for Relief from ASME Section XI requirements that were identified during PSI were submitted to the USNRC and were approved in NUREG-0989, Supplement 3.

●→11

ISI will be in accordance with an approved ASME Section XI code. Exceptions to this will be identified in the ISI Program plan. IST is addressed in Section 3.9.6A of the USAR.

11←●

Details of ISI are contained in the River Bend Station ISI Program Plan. This plan defines ASME Class 1, 2 and 3 components subject to inspection, extent and frequency of examinations, exemptions and requests for relief. The initial plan is submitted to the USNRC for review and acceptance.

Components and supports within the ASME Section III, Class 2 boundaries are subject to the requirements of ASME Section XI, Subarticles IWA, IWC, and IWF.

Components and supports within the ASME Section III, Class 3 boundaries are subject to the requirements of ASME Section XI, Subarticles IWA, IWD, and IWF.

8←●

●→8

6.6.2 Accessibility

For accessibility requirements of ASME Class 2 and 3 components, the same requirements are addressed in Sections 5.2.4.2.1 and 5.2.4.2.3 of the USAR.

6.6.3 Examination Techniques and Procedures

For examination technique and procedure requirements of ASME Class 2 and 3 components, the same requirements are addressed in Section 5.2.4.3 of the USAR.

6.6.4 Inspection Intervals

As defined in ASME Section XI, Subarticle IWA-2400, the inspection interval is ten years, unless otherwise approved by the USNRC. The interval may be extended by as much as one year to permit inspections to be concurrent with planned outages.

The inspection schedule is in accordance with IWC-2400 and IWD-2400 for ASME Class 2 and 3 piping, respectively. ISI examinations are performed during plant operation and planned or unplanned outages occurring during the inspection interval.

6.6.5 Examination Categories and Requirements

●→14

The extent and frequency of examinations performed and methods used for ASME Class 2 and 3 components comply with the requirements of ASME Section XI, Tables IWC-2500-1 and IWD-2500-1, respectively. The examination categories and requirements for ASME Class 2 and 3 component supports comply with ASME Section XI, Table IWF-2500-1. In addition, PSI for ASME Class 2 and 3 components meet the requirements of IWC-2200 and IWD-2200, respectively.

14←●

6.6.6 Evaluation of Examination Results

For evaluation requirements of ASME Class 2 and 3 components, the same requirements are addressed in Section 5.2.4.6 of the USAR.

6.6.7 System Pressure Tests

System pressure tests comply with ASME Code, Section XI, Subarticles IWC-5000 and IWD-5000 for ASME Class 2 and 3 components, respectively.

8←●

●→8

6.6.8 Augmented Inservice Inspection to Protect Against Postulated Class 2 Piping Failures

High energy ASME Class 2 pipe welds located between the first moment limiting restraints, outboard of the isolation valves, are subject to the following additional inspection requirements.

Nonexempt circumferential welds greater than four inches nominal pipe size (NPS) are volumetrically examined each inspection interval as defined in Section 6.6.4 [in accordance with Section 3.6.2.1.5.2.1A.2.g.](#)

8←●

•→8

THIS PAGE LEFT INTENTIONALLY BLANK

8←•

6.7 MAIN STEAM POSITIVE LEAKAGE CONTROL SYSTEM (MS-PLCS)

The MS-PLCS prevents the release of fission products, in the event of leakage, through the closed main steam isolation valves (MSIV) and main steam drain lines (MSDL) after a design-basis LOCA. The system establishes a pressurized volume in the main steam lines by maintaining a pressure of at least 10 percent over the prevailing post LOCA reactor vessel pressure which could otherwise instigate leakage to the environment.

6.7.1 Design Bases

6.7.1.1 Safety Criteria

The following criteria correspond to the positions provided in Regulatory Guide 1.96 and represent system design, safety and performance requirements:

1. The MS-PLCS and interface are designed in accordance with Seismic Category I and Safety Class 2 requirements, with the exception of any portion of the MS-PLCS piping that connects to the main steam system piping between the inner and outer containment isolation valves. Piping, up to and including the first isolation valve in the inboard MS-PLCS, is designed in accordance with Seismic Category I and Safety Class 1 requirements supplemented by NRC Branch Technical Position APCSB 6-1, Appendix A.
2. The MS-PLCS is capable of performing its safety function, when necessary, considering effects from a LOCA, including: a) missiles that may result from equipment failures; b) dynamic effects associated with pipe whip and jet forces from LOCA; and c) normal operating and accident-caused local environmental conditions consistent with the design-basis event. Further, the portion of the MS-PLCS which is Safety Class 1 is protected from missiles, pipe whip, and jet force effects originating outside of the containment to assure containment integrity.
3. The MS-PLCS is capable of performing its safety function following a LOCA and any assumed single-active failure (including failure of any MSIV to close).

4. The MS-PLCS is designed so that effects resulting from a single-active component failure do not affect the integrity or operability of the main steam system or the MSIVs or contribute to an overpressurization of the containment.
5. The MS-PLCS is capable of performing its safety function following a loss of offsite power, coincident with a postulated design-basis LOCA.
6. The MS-PLCS is designed to prevent leakage from the main steam lines, as necessary, to maintain containment integrity for up to 30 days.
7. The MS-PLCS is manually initiated and is designed to permit actuation within 20 min after a design-basis LOCA. This time period is consistent with loading requirements of the emergency electrical buses, and with reasonable times for operator action.
8. The MS-PLCS, including instrumentation and circuits necessary for the functioning of the system, is designed to standards applicable to an engineered safety feature.
9. The MS-PLCS controls include interlocks to prevent inadvertent operation of the system. In particular, interlocks are provided to prevent damage to the MS-PLCS, or to the main steam system, due to accidental opening of any system isolation valves when the pressure in the connecting main steam piping exceeds MS-PLCS operating pressure. All such controls and interlocks are activated from appropriately designed safety systems or circuits.
10. The MS-PLCS is designed to permit testing of the operability of controls and actuating devices during power operation to the extent practical, and complete testing of system function during plant shutdowns.
11. The MS-PLCS is designed so that: a) thermal stresses and pressures associated with flashing and thermal deformations, under the loading conditions associated with the activated system do not affect the structural integrity or operability of the main steam system or MSIVs; and b) any deformation of isolation valve internals does not induce leakage

of the MSIV beyond the capacity or capability of the MS-PLCS.

12. Equipment is provided (as part of the MS-PLCS) to prevent the release of valve stem packing leakage to the environment from MSIVs outside the containment.

6.7.2 System Description

6.7.2.1 General Description

●→10 ●→8 ●→6

The source of air for the MS-PLCS is the penetration valve leakage control system (PVLCS) air compressors, one for the outboard system and one for the inboard system. Each air compressor is a nuclear safety-related air supply source for the MS-PLCS, and the main steam safety/relief valve system. Each compressor assembly contains an accumulator which is sized to accommodate the initial post-accident requirements of the three above listed systems with the long term requirements being met with the function of the air compressor. (However, as stated in Section 5.2.2.4, main steam safety/relief valve accumulators used for ADS must be pressurized to a minimum of 131 psig prior to the start of an accident.) The air compressors are equipped for water cooling and are designed to run for 100 days after an accident. The design temperature and pressure for the compressor assemblies are 150°F and 200 psig, respectively. Each compressor assembly delivers sufficient volume of compressed air to meet the maximum post LOCA demand (long and short term) of 36 scfm from MS-PLCS, and main steam safety/relief valve system (SVV). Refer to Section 9.3.6 for a complete description of the PVLCS.

6←● 8←● 10←●

Two independent systems (outboard and inboard) are provided to accomplish the leakage control function. The leakage control barrier is established by pressurizing the isolated volumes in the main steam line between the inboard and outboard isolation valves and the main steam shutoff valves. The pressurized volume eliminates out-leakage through the closed MSIVs and main steam drain lines such that any leakage which does occur is inward from the pressurized volume into the reactor pressure vessel (RPV) or containment. Both systems are connected to the offsite as well as onsite emergency power.

●→10

The MS-PLCS is shown in Fig. 6.7-1. The outboard system is connected to each of the main steam shutoff valves, drain lines (inboard and outboard MSIV), and outboard MSIV stem packing leak-off lines. The inboard system is connected to the outboard MSIV body (inlet side), and to the inboard MSIV drain lines located outside the containment.

10←●

The MS-PLCS is categorized in three sections: 1) an injection section, consisting of a system connection to the penetration valve leakage control system, maintenance valve, pressure control valve (PCV), bypass valve including the restricting orifice, flow measuring device, pressure relief valve, swing-free disc check valve, and the air injection valve; 2) an isolation section, consisting of the two isolation valves, maintenance valves, and including the process line connected to the main steam system; and 3) a header section, which is a portion of the system between the isolation and injection section up to and including the drain valve.

The drain line, equipped with a normally open valve, is connected to the MS-PLCS header section (process line low point) which provides the means to continuously release condensate that may collect in the system process lines during normal power operation.

6.7.2.2 System Operation

The inboard and outboard systems are remote-manually initiated in the main control room. Operation of both systems is initiated after it has been ascertained that a design-basis LOCA has occurred (as evidenced by high drywell pressure and low reactor water level indications in the main control room). Either one of the two systems is sufficient to establish the necessary barrier between the containment and the environs. As a prerequisite to the operator's action in actuating the system, the motor-operated valves within the main steam system scope, considered as an integral part of a successful MS-PLCS operation, must be cycled to the closed position using their respective remote manual switches (RMS).

The initiating RMS do not activate the system unless the air supply and reactor vessel pressures are within the permissive interlock set points.

The initiating RMS provide the circuit to activate the bypass valve to open and the drain valve to close. The same circuit activates the pressure controller, which normally keeps the diaphragm valve in a closed position while the plant is at normal power operation. When the drain valve is closed, as established through the valve-closed position switch, the injection valve and isolation valves receive an activation signal to open.

The MS-PLCS isolation valves remain closed if the main steam line pressure is higher than the pressure interlock set point. When the interlock is cleared, air is admitted to raise the pressure of the steam lines to 8.5 psi above the reactor vessel pressure to establish the containment leakage barrier. Once the valves have cycled open, the pressure interlock function is disarmed and only a system isolation trip signal or the initiating RMS turned to "off" position can actuate reclosure. A pressure-control valve maintains the required pressure differential of 8.5 psi between the reactor vessel and the pressurized portion of the main steam line.

●→7

A 5-min timer is activated when closure of the drain valve is completed. During this time air is injected via a line which bypasses the pressure-control valve in order to provide an initial high flow at low differential pressure to rapidly pressurize the main steam line volume. When the 5-min timer cycle is completed, the bypass flow is isolated and the system air flow is reduced to that required for steady-state operation. If high flow or low differential pressure persists either after the timer cycle is completed or system initiation logic de-energizes and the system is not tripped, an alarm is annunciated in the main control room. Further increase of flow, or continuous reduction of differential pressure to a specified set point, result in an automatic isolation of the respective MS-PLCS.

7←●

The bypass valve automatically closes on either timer set point duration, or upon establishing the required pressure differential between the main steam system and the reactor vessel.

6.7.2.3 Equipment

The following equipment is provided to accomplish system operation:

●→10

1. Piping - Process piping is carbon/stainless steel pipe throughout the system. The portion of the system piping, connected to the main steam piping between MSIVs, up to and including the first MS-PLCS isolation valve, is designed and constructed to ASME Section III, Class 1. The remainder is designed and constructed to ASME Section III, Class 2. The equipment and piping installation is designed to withstand Seismic Category I loads.

10←●

2. Valves - Motor- or solenoid-operated valves provide the required isolation and/or process control following system initiation. The valves are

constructed to ASME Section III code class appropriate to the piping in which they are installed.

3. Instrumentation - Instrumentation and circuits necessary for a satisfactory MS-PLCS operation are designed in accordance with standards applicable to engineered safeguard components (Class 1E).
4. Penetration Valve Leakage Control (PVLCS) - The PVLCS is designed to provide the required volume of air for MS-PLCS operation.

6.7.3 System Evaluation

The following discussions are evaluations of the MS-PLCS capability in preventing the release of radioactivity from the main steam lines following a design basis LOCA.

6.7.3.1 Functional Protection Features

The inboard and outboard divisions of the MS-PLCS are physically separated. The equipment is designed to operate under the post-LOCA environmental conditions appropriate to the equipment location.

The MS-PLCS is arranged so as to minimize the exposure of the system equipment to missiles, pipe deformations, and jet forces caused by the LOCA event. The equipment is located outside the containment to minimize any possible effects of a design basis recirculation line break. Furthermore, system equipment is located outside the steam tunnel, wherever practical, in order to minimize equipment exposure to steam line break although the MS-PLCS is not needed for any safety function in a steam line break event.

The use of onsite emergency power assures system operation during the loss of offsite power.

6.7.3.2 Effects of Single Active Failures

The MS-PLCS function following an active component failure (including failure of any one MSIV to close) is assured by the provision of both an inboard and an outboard MS-PLCS, either of which is sufficient to perform the system's containment function. The function of the air supply to the MS-PLCS is similarly assured by the provision of an inboard and an outboard PVLCS. The systems are independently powered from two separate divisions of the emergency power supply. Redundant isolation valves in series are provided

which are electrically and mechanically separated and are operated by separate sensors and controls to ensure that no single active failure can affect the integrity of the main steam lines.

6.7.3.3 Effects of Seismic-Induced Failures

The MS-PLCS is designed to operate following the application of Seismic Category I design loads in conjunction with operating loads associated with the post-LOCA event.

The MS-PLCS is also designed to perform its safety function following a design-basis loss-of-coolant accident (LOCA), including the consideration of effects associated with: a) internally generated missiles; b) the dynamic effects associated with pipe whip and jet forces from postulated pipe break events; c) environmental conditions consistent with the design basis event; and d) internal and external flooding.

6.7.3.4 Isolation Provisions

The MS-PLCS valves are expected to maintain containment integrity by virtue of a series of operating checkpoints and pressure interlocks. Unless the interlock set points are satisfied, the system isolation valves remain in a closed position. Two isolation valves are provided. One out of two valves satisfies isolation requirements. In addition, the valve electrical circuit cannot be activated unless the initiating keylocked remote manual switch is in the operate position.

6.7.3.5 Leakage Protection Evaluation

The MS-PLCS is designed to prevent the release of radioactive materials to the environment following a design-basis LOCA. The system provides a positive seal, thereby eliminating any out-leakage through the closed MSIVs directly to the environment. The allowable leakage on the MSIVs does not have a radiological consequence, but is a function of the permissible in-leakage pressurization of the containment. Excessive MSIV in-leakage is prevented by automatic system isolation.

The MS-PLCS is manually initiated and is designed to permit actuation 20 min following the postulated design-basis LOCA. This actuation time is consistent with the NRC Branch Technical Position APCSB 6-1 and with loading requirements of the emergency buses and allows for reasonable times for operator information, decision, and action. In the time

period following the postulated LOCA and prior to MS-PLCS initiation, leakage is not a significant contributor to the 2-hr site boundary dose, since conservative allowances for transport delay effects indicate that actual transport times are well in excess of the 20-min sealing system start time.

6.7.3.6 Failure Mode and Effects Analysis

The consequences of component malfunctions are shown in Table 6.7-1. System level qualitative Type A analysis is provided in Appendix 15A.

6.7.3.7 Influence on Other Safety Features

●→10

The use of MS-PLCS as a positive leakage barrier results in in-leakage and gradual pressure buildup within the containment. As previously stated, the total allowable MSIV in-leakage rate does not have radiological consequences. The total allowable air inleakage rate from the MSIVs is limited such that containment pressurization does not exceed 50 percent of the design value in a 30-day period due to these sources. System design includes the use of instruments to continuously monitor in-leakage rate and trip the system to isolate whenever recorded leak rate is in excess of the allowable level.

10←●

Instrumentation necessary for control and status indication are adequately provided to assist the operator to initiate appropriate action, if necessary.

6.7.4 Instrumentation Requirements

The instrumentation necessary for control and status indication of the MS-PLCS are designed and qualified in accordance with applicable IEEE Standards to function under Seismic Category I and LOCA environmental loading conditions. The control circuits are designed to satisfy the mechanical and electrical separation criteria (see Section 7.3.1.1.3 for a control and instrumentation description).

6.7.5 Inspection and Testing

Preoperational tests for the MS-PLCS are discussed in Chapter 14. During plant operation, valves, piping, instrumentation, electrical circuits, and other components outside the steam tunnel can be inspected visually at any time. Complete system functional testing is performed only

during extended reactor shutdown or plant refueling. This precludes inadvertent steam discharge.

•→10

Since the MS-PLCS establishes a containment leakage barrier, direct MSIV out-leakage to the environment is eliminated. Therefore, the only concern regarding MSIV leak rate is possible containment pressurization when the MS-PLCS is in operation. The MS-PLCS allowable leak rate is provided in the Technical Specifications and established such that the total air inleakage from valves served by the MS-PLCS does not contribute greater than 50 percent of the containment design pressure in a 30-day period.

10←•

APPENDIX 6A

CONTAINMENT DYNAMIC LOADING ASSESSMENT

RBS USAR

APPENDIX 6A

CONTAINMENT DYNAMIC LOADING ASSESSMENT

6A.0	PURPOSE	6A.0-1
PART I - CONTAINMENT DYNAMIC LOAD DEFINITION		6A.1-1
6A.1	INTRODUCTION	6A.1-1
6A.1.1	Confirmatory Testing	6A.1-1
6A.1.2	Definition of LOCA	6A.1-1
6A.1.3	Design Margins	6A.1-1
6A.2	REVIEW OF PHENOMENA	6A.2-1
6A.2.1	Design Basis Accident (DBA)	6A.2-1
6A.2.2	Intermediate Break Accident (IBA)	6A.2-2
6A.2.3	Small Break Accident (SBA)	6A.2-3
6A.2.4	Safety Relief Valve Actuation	6A.2-3
6A.2.5	Other Considerations	6A.2-3
6A.3	DYNAMIC LOAD TABLE	6A.3-1
6A.4	DRYWELL STRUCTURE	6A.4-1
6A.4.1	Drywell Loads During a Large Break Accident	6A.4-1
6A.4.1.1	Sonic Wave	6A.4-1
6A.4.1.2	Drywell Pressure	6A.4-1
6A.4.1.3	Hydrostatic Pressure	6A.4-1
6A.4.1.4	Loads on the Drywell Wall During Pool Swell	6A.4-1
6A.4.1.5	Condensation Oscillation Loads	6A.4-1
6A.4.1.6	Fallback Loads	6A.4-1
6A.4.1.7	Negative Load During ECCS Flooding	6A.4-1
6A.4.1.8	Chugging	6A.4-2
6A.4.1.9	Loads Due to Chugging	6A.4-2
6A.4.2	Drywell Loads During Intermediate Break Accident	6A.4-2
6A.4.3	Drywell Loads During a Small Break Accident	6A.4-2
6A.4.3.1	Drywell Temperature	6A.4-2

APPENDIX 6A

TABLE OF CONTENTS (Cont)

<u>Section</u>	<u>Title</u>	<u>Page</u>
6A.4.3.2	Drywell Pressure	6A.4-2
6A.4.3.3	Chugging	6A.4-2
6A.4.4	Safety Relief Valve Actuation	6A.4-3
6A.4.5	Drywell Environmental Envelope	6A.4-3
6A.4.6	Top Vent Temperature (Cycling) Profile During Chugging	6A.4-3
6A.4.7	Drywell Multicell Effects	6A.4-3
6A.5	WEIR WALL	6A.5-1
6A.5.1	Weir Wall Loads During a Design Basis Accident	6A.5-1
6A.5.1.1	Sonic Wave	6A.5-1
6A.5.1.2	Outward Load During Vent Clearing	6A.5-1
6A.5.1.3	Outward Load Due to Vent Flow	6A.5-1
6A.5.1.4	Chugging Loads	6A.5-1
6A.5.1.5	Inward Load Due to Negative Drywell Pressure	6A.5-1
6A.5.1.6	Suppression Pool Fallback Loads	6A.5-1
6A.5.1.7	Hydrostatic Pressure	6A.5-2
6A.5.1.8	Safety Relief Valve Loads	6A.5-2
6A.5.1.9	Condensation	6A.5-2
6A.5.2	Weir Wall Loads During an Intermediate Break Accident	6A.5-2
6A.5.3	Weir Wall Loads During a Small Break Accident	6A.5-2
6A.5.4	Weir Wall Environment Envelope	6A.5-2
6A.5.5	Weir Annulus Multicell Effects	6A.5-2
6A.6	CONTAINMENT	6A.6-1
6A.6.1	Containment Loads During a Large Steam Line Break (DBA)	6A.6-1
6A.6.1.1	Compressive Wave Loading	6A.6-1
6A.6.1.2	Water Jet Loads	6A.6-1
6A.6.1.3	Initial Bubble Pressure	6A.6-1
6A.6.1.4	Hydrostatic Pressure	6A.6-2
6A.6.1.5	Local Containment Loads Resulting from Structures at or Near the Pool Surface	6A.6-2
6A.6.1.6	Containment Load Due to Pool Swell at the HCU Floor	6A.6-4
6A.6.1.7	Fallback Loads	6A.6-4

APPENDIX 6A

TABLE OF CONTENTS (Cont)

<u>Section</u>	<u>Title</u>	<u>Page</u>
6A.6.1.8	Post Pool Swell Waves	6A.6-5
6A.6.1.9	Condensation Oscillation Loads	6A.6-5
6A.6.1.10	Chugging	6A.6-5
6A.6.1.11	Long-Term Transient	6A.6-5
6A.6.1.12	Containment Environmental Envelope	6A.6-5
6A.6.2	Containment Loads During an Intermediate Break Accident	6A.6-5
6A.6.3	Containment Loads During a Small Break Accident	6A.6-5
6A.6.4	Safety Relief Valve Loads	6A.6-6
6A.6.5	Suppression Pool Thermal Stratification	6A.6-6
6A.7	SUPPRESSION POOL BASEMAT LOADS	6A.7-1
6A.8	LOADS ON STRUCTURES IN THE SUPPRESSION POOL	6A.8-1
6A.8.1	Design Basis Accident	6A.8-1
6A.8.1.1	Vent Clearing Jet Load	6A.8-1
6A.8.1.2	Drywell Bubble Pressure and Drag Loads Due to Pool Swell	6A.8-1
6A.8.1.3	Fallback Loads	6A.8-1
6A.8.1.4	Condensation Loads	6A.8-1
6A.8.1.5	Chugging	6A.8-1
6A.8.1.6	Compressive Wave Loading	6A.8-1
6A.8.1.7	Safety Relief Valve Actuation	6A.8-1
6A.9	LOADS ON STRUCTURES AT THE POOL SURFACE	6A.9-1
6A.10	LOADS ON STRUCTURES BETWEEN THE POOL SURFACE AND THE HCU FLOORS	6A.10-1
6A.10.1	Impact Loads	6A.10-1
6A.10.2	Drag Loads	6A.10-3
6A.10.3	Fallback Loads	6A.10-4
6A.11	LOADS ON EXPANSIVE STRUCTURES AT THE HCU FLOOR ELEVATION	6A.11-1

APPENDIX 6A

TABLE OF CONTENTS (Cont)

<u>Section</u>	<u>Title</u>	<u>Page</u>
6A.12	LOADS ON STRUCTURES AT AND ABOVE THE HCU FLOOR ELEVATION	6A.12-1
6A.13	DYNAMIC RESPONSE OF PRIMARY STRUCTURES TO HYDRODYNAMIC LOADS	6A.13-1
6A.13.1	Structural Response Due to Safety Relief Valve Discharge Loads	6A.13-1
6A.13.1.1	Method of Analysis	6A.13-1
6A.13.1.2	Application of Loads	6A.13-3
6A.13.2	Structural Response Due to Loss of Coolant Accident Loads	6A.13-3
6A.13.2.1	Method of Analysis	6A.13-3
6A.13.2.2	Application of Loads	6A.13-3
PART II - CONTAINMENT DYNAMIC LOAD ASSESSMENT		
6A.14	ASSESSMENT OF CONTAINMENT STRUCTURES FOR HYDRODYNAMIC LOADS	6A.14-1
6A.14.1	Introduction	6A.14-1
6A.14.2	Description of Structures	6A.14-1
6A.14.3	Design Criteria and Loads	6A.14-1
6A.14.4	Method of Analysis and Design	6A.14-1
6A.14.5	Summary of Results	6A.14-2
6A.14.5.1	Containment Structures and Foundation Basemat, Internal Forces, and Moments	6A.14-2
6A.14.5.2	Amplified Response Spectra Curves	6A.14-2
6A.14.6	Conclusions	6A.14-2
6A.15	CONTAINMENT SYSTEM ASSESSMENT	6A.15-1
6A.15.0	General	6A.15-1
6A.15.1	Basemat Liner	6A.15-1
6A.15.1.1	Load Sources and Design Criteria	6A.15-2
6A.15.1.1.1	Load Sources	6A.15-2
6A.15.1.1.2	Design Criteria	6A.15-2
6A.15.1.1.3	Basemat Embedments Design Criteria	6A.15-3
6A.15.1.2	Basemat Liner Analysis	6A.15-3
6A.15.1.2.1	Assumptions	6A.15-3
6A.15.1.2.2	Strain-Displacement Relationships	6A.15-3
6A.15.1.2.3	Basemat Liner Static Analysis	6A.15-4
6A.15.1.2.4	Basemat Liner Anchorage System	6A.15-4

APPENDIX 6A

TABLE OF CONTENTS (Cont)

<u>Section</u>	<u>Title</u>	<u>Page</u>
6A.15.1.3	Basemat Liner Evaluation Summary	6A.15-5
6A.15.1.3.1	Basemat Liner Strain Evaluation	6A.15-5
6A.15.1.3.2	Basemat Liner Instability Evaluation	6A.15-5
6A.15.1.3.3	Basemat Liner Fatigue Evaluation	6A.15-6
6A.15.1.3.4	Basemat Liner Embedment Evaluation	6A.15-6
6A.15.2	Containment Vessel	6A.15-7
6A.15.2.1	Load Sources and Design Criteria	6A.15-7
6A.15.2.1.1	Load Sources	6A.15-7
6A.15.2.1.2	Design Criteria	6A.15-7
6A.15.2.2	Containment Vessel Analysis	6A.15-8
6A.15.2.2.1	Assumptions	6A.15-8
6A.15.2.2.2	Containment Vessel Static Analysis	6A.15-8
6A.15.2.2.3	Containment Vessel Dynamic Analysis	6A.15-9
6A.15.2.2.4	Containment Vessel Discontinuity Analysis	6A.15-10
6A.15.2.2.5	Containment Vessel Attachment Analysis	6A.15-11
6A.15.2.2.6	Containment Penetration Analysis	6A.15-11
6A.15.2.3	Containment Vessel Evaluation Summary	6A.15-11
6A.16	PIPING AND PIPE SUPPORTS LOAD ASSESSMENT	6A.16-1
6A.16.1	Introduction	6A.16-1
6A.16.2	Analysis of Piping Systems for Indirect (Inertia) Loads	6A.16-1
6A.16.2.1	Load Cases	6A.16-1
6A.16.2.2	Method of Analysis	6A.16-2
6A.16.2.3	Effects of Parameter Variations on Floor Response Spectra	6A.16-3
6A.16.2.4	Modeling Considerations	6A.16-3
6A.16.2.5	Determination of the Number of Cycles	6A.16-4
6A.16.2.6	Avoidance of Response Spectrum Peaks	6A.16-4
6A.16.2.7	Differential Displacements	6A.16-4
6A.16.2.8	Loading at Containment Penetrations	6A.16-4
6A.16.3	Analysis of Piping Systems for Direct Hydrodynamic Loading	6A.16-5

RBS USAR

APPENDIX 6A

TABLE OF CONTENTS (Cont)

<u>Section</u>	<u>Title</u>	<u>Page</u>
6A.16.3.1	Introduction	6A.16-5
6A.16.3.2	Load Cases and Load Combinations for Pipe Stress Analysis	6A.16-5
6A.16.3.3	Special Considerations	6A.16-6
6A.16.3.4	Piping Subjected to Hydrodynamic Loads	6A.16-7
6A.16.3.5	Pipe Stress Analysis Procedure for Piping Subjected to Hydrodynamic Loads	6A.16-7
6A.17	ASSESSMENT OF EQUIPMENT QUALIFICATION	6A.17-1
6A.17.1	INTRODUCTION	6A.17-1
6A.17.2	DYNAMIC LOADS	6A.17-1
6A.17.2.1	DESCRIPTION	6A.17-1
6A.17.2.2	DEVELOPMENT OF RESPONSE SPECTRA	6A.17-2
6A.17.2.3	MAGNITUDES AND FREQUENCY CONTENT	6A.17-2
6A.17.2.4	NUMBER OF EVENTS AND STRESS CYCLES	6A.17-2
6A.17.3	QUALIFICATION ACCEPTANCE CRITERIA	6A.17-2
6A.17.4	QUALIFICATION PROCEDURES	6A.17-3
6A.17.4.1	QUALIFICATION BY ANALYSIS	6A.17-3
6A.17.4.1.1	STATIC ANALYSIS	6A.17-3
6A.17.4.1.2	DYNAMIC ANALYSIS	6A.17-3
6A.17.4.2	QUALIFICATION BY TESTING	6A.17-4
6A.17.4.3	PUMP AND VALVE OPERABILITY PROGRAM	6A.17-4

TABLE OF CONTENTS (Cont)

<u>Attachment</u>	<u>Title</u>
A	NUMERICAL INFORMATION FOR SAFETY RELIEF VALVE DISCHARGE LOADS
B	Refer to GESSAR.
C	Refer To GESSAR.
D	Refer to GESSAR.
E	SUPPRESSION POOL SEISMIC INDUCED LOADS
F	Refer To GESSAR.
G	DRYWELL NEGATIVE PRESSURE CALCULATION
H	CONTAINMENT ASYMMETRIC LOADS
I	Refer To GESSAR.
J	Refer To GESSAR.
K	Refer to GESSAR.
L	SUBMERGED STRUCTURE LOADS DUE TO LOCA AND SRV ACTUATIONS
M	POOL SWELL VELOCITY
N	MULTIPLE SAFETY/RELIEF VALVE ACTUATION FORCING FUNCTION METHODS
O	SUPPRESSION POOL TEMPERATURE RESPONSE TO SAFETY RELIEF VALVE DISCHARGE EVENTS

APPENDIX 6A

LIST OF TABLES

<u>Table Number</u>	<u>Title</u>
•→15 6A-1	DELETED
6A-2	DELETED
6A-3	DELETED
6A-4	DELETED
15←• 6A.1-1	SUMMARY OF SPECIFIED AND REALISTIC DESIGN VALUES
6A.14-1	DEFINITION OF INTERNAL FORCES AND MOMENTS
6A.14-2	DEFINITION OF INTERNAL STRESSES
6A.14-3	MAXIMUM FORCES, MOMENTS, AND STRESSES DUE TO SRV
6A.14-4	MAXIMUM FORCES, MOMENTS, AND STRESSES DUE TO LOCA
6A.15-1	CYCLIC STRESS DATA
6A.15-2	BASEMAT LINER STRAIN SUMMARY
6A.16-1	MAXIMUM STRESS AND ALLOWABLE STRESS IN PIPING SYSTEMS CRITICALLY LOADED BY DYNAMIC SUPPRESSION POOL EVENTS
6A.16-2	PIPE STRESS SUMMARY (UPSET AND FAULTED) FOR PIPING SUBJECTED TO DIRECT WATER LOADS

RBS USAR

APPENDIX 6A

LIST OF FIGURES

<u>Figure Number</u>	<u>Title</u>
●→14 6A.4-1	DRYWELL-LOADING CHART FOR DBA
6A.4-2	DRYWELL-LOADING CHART FOR DBA
6A.4-3	DRYWELL-LOADING CHART FOR IBA
6A.4-4	MAXIMUM DESIGN DRYWELL ATMOSPHERE BULK TEMPERATURE AND PRESSURE ENVELOPE
6A.4-4a	DRYWELL PRESSURE ENVELOPE M3CPT & SHEX (3100 MWt)
6A.4-4b	DRYWELL TEMPERATURE ENVELOPE M3CPT & SHEX (3100 MWt)
6A.5-1	WEIR WALL-LOADING CHART FOR DBA
6A.5-2	WEIR WALL-LOADING CHART FOR SBA
6A.5-3	WEIR WALL-LOADING CHART FOR IBA
6A.6-1	CONTAINMENT-LOADING CHART FOR DBA
6A.6-2	CONTAINMENT-LOADING CHART FOR IBA
6A.6-3	CONTAINMENT-LOADING CHART FOR SBA
6A.6-4	CONTAINMENT ATMOSPHERE BULK TEMPERATURE AND PRESSURE DESIGN ENVELOPE FOR ALL BREAKS
6A.6-4a	CONTAINMENT PRESSURE ENVELOPE M3CPT & SHEX (3100 MWt)
6A.6-4b	CONTAINMENT TEMPERATURE ENVELOPE M3CPT & SHEX (3100 MWt)
14←● 6A.6-5	DYNAMIC LOADS ASSOCIATED WITH INITIAL BUBBLE FORMATION IN THE POOL
6A.6-6	DRAG LOADS ON PROTRUDING STRUCTURES DUE TO POOL SWELL
6A.6-7	IMPACT FORCE (PER UNIT LENGTH) ON WEDGE-SHAPED PROTRUSIONS FROM THE CONTAINMENT WALL
6A.6-8	IMPACT PRESSURE ON HORIZONTAL LEDGES ATTACHED TO CONTAINMENT WALL
6A.6-9	CONTAINMENT LOADING DUE TO FLOW P ACROSS HCU FLOOR
6A.8-1	STRUCTURES WITHIN SUPPRESSION POOL- LOADING CHART FOR DBA

APPENDIX 6A

LIST OF FIGURES (Cont)

<u>Figure Number</u>	<u>Title</u>
6A.9-1	THE TIP DRIVE PLATFORM AT AZIMUTH 55° OVER SUPPRESSION POOL
6A.10-1	THE STRUCTURES AT AZIMUTH 225° OVER SUPPRESSION POOL
6A.10-2	PROFILE OF IMPACT LOADS ON SMALL STRUCTURES WITHIN 18 FEET OF THE POOL SURFACE
6A.10-3	SUMMARY OF POOL SWELL LOADING SPECIFICATIONS FOR SMALL STRUCTURES IN THE CONTAINMENT ANNULUS (NOT APPLICABLE TO THE STEAM TUNNEL OR EXPANSIVE HCU FLOORS)
6A.10-4	PRESSURE DROP DUE TO FLOW ACROSS GRATING WITHIN 18 FEET OF THE POOL SURFACE FOR 40 FT/SEC POOL SWELL
6A.10-5	DRAG LOAD ON SOLID STRUCTURES WITHIN 18 FEET OF THE POOL SURFACE
6A.10-6	DRAG LOADS FOR VARIOUS GEOMETRICS (SLUG FLOW)
6A.10-7	REDUCTION IN PULSE DURATION FOR RADIAL STRUCTURES CLOSER THAN 6 FEET TO THE POOL SURFACE
6A.10-8	REDUCTION IN PULSE DURATION FOR RADIAL STRUCTURES SHORTER THAN 4 FEET
6A.10-9	REDUCTION IN PULSE DURATION FOR CIRCUMFER- ENTIAL TARGETS CLOSER THAN 6 FEET TO THE POOL SURFACE
6A.11-1	LOADS ON HCU FLOOR DUE TO POOL-SWELL FROTH IMPACT AND TWO-PHASE FLOW
6A.12-1	FROTH IMPACT PRESSURE - PEAK AMPLITUDE
6A.13-1	SUPPRESSION POOL GEOMETRY

APPENDIX 6A

LIST OF FIGURES (Cont)

<u>Figure Number</u>	<u>Title</u>
6A.13-2	FINITE ELEMENT MODEL OF REACTOR BUILDING
6A.13-3	HORIZONTAL ANALYTICAL MODEL FOR HYDRODYNAMIC LOADS ANALYSIS (5 Sheets)
6A.13-4	LOADS APPLIED TO MODEL
6A.14-1	POSITIVE SIGN CONVENTION FOR INTERNAL FORCES AND MOMENTS
6A.14-2	POSITIVE SIGN CONVECTION FOR INTERNAL STRESS
6A.14-3	RADIAL ARS PLOT AT A DRYWELL LOCATION DUE TO SRV DISCHARGE
6A.14-4	VERTICAL ARS PLOT AT A SHIELD BUILDING WALL LOCATION DUE TO SRV DISCHARGE
6A.14-5	TANGENTIAL ARS PLOT AT A DRYWELL LOCATION DUE TO SRV DISCHARGE
6A.14-6	RADIAL ARS PLOT AT A DRYWELL LOCATION DUE TO CONDENSATION OSCILLATION (LOCA)
6A.14-7	VERTICAL ARS PLOT AT A DRYWELL LOCATION DUE TO CONDENSATION OSCILLATION (LOCA)
6A.14-8	VERTICAL ARS PLOT AT PEDESTAL BASEMAT JUNCTION DUE TO CONDENSATION OSCILLATION (LOCA)
6A.15-1	BASEMAT LINER GEOMETRY AND DETAILS
6A.16-1	SUPPRESSION POOL PIPING PLAN VIEW
6A.16-2	SUPPRESSION POOL PIPING DEVELOPED ELEVATION

6A.0 PURPOSE

The purpose of this River Bend Station Containment Load Report is to address the concerns regarding suppression pool hydrodynamic loads. River Bend Station has utilized the parameters, methods, assumptions, and concepts recommended by GE in Appendix 3B of GESSAR II, (hereinafter referred to as GESSAR).

Differences between the River Bend Station and the GESSAR-238 plant, upon which GESSAR is based, are accounted for in plant unique analyses. These analyses are conducted for River Bend Station in accordance with GESSAR and are described in this Appendix. The River Bend Station has a 218-in diameter reactor vessel, a thermal power rating of 2,894 MWT, 16 safety relief valves (SRV), and slightly different suppression pool dimensions. The loads specified in GESSAR are developed specifically for the GESSAR-238 design which has a 238-in diameter reactor vessel, a reactor thermal power rating of 3,579 MWT, and 19 SRVs.

This Appendix is organized in two parts. Dynamic loads are defined in Part I which consists of Sections 6A.1 through 6A.12 corresponding directly to GESSAR Sections 3B.1 through 3B.12. In Part I, plant specific differences are discussed where applicable and sections of GESSAR are incorporated by reference to GESSAR where the generic loads are being applied for River Bend Station. The table and figure numbers in Part I also reference GESSAR numbers where applicable. Figures and tables that are identical to those in GESSAR and referenced in sections which are identical to those in GESSAR are not included herein. Part II of this Appendix, consisting of Sections 6A.13 through 6A.16, describes the River Bend Station assessment of the loads defined in Part I.

This Appendix, in conjunction with GESSAR, represents the River Bend Station Containment Dynamic Loads Report.

References - Appendix 6A

1. GESSAR II, General Electric Standard Safety Analysis Report, BWR/6 Nuclear Island Design, Appendix 3B.
2. Ghosh, S. and Wilson, E. Dynamic Stress Analysis of Axisymmetric Structures Under Arbitrary Loading. Received from the University of California at Berkley (Report EERC-69-10). Modified by Stone & Webster Engineering Corporation as Computer Program ST-200, September 1973.
3. NRC Staff Report, NUREG 0484, Revision 1, Methodology for Combining Dynamic Responses, May 1980.
4. McIntyre, T.R., et al. Mark III Confirmatory Test Program, One-third Scale Pool Swell Impact Tests (Test Series 5805), General Electric Company, August 1975 (NEDE-13,426-P).
5. Not used.
6. NRC Staff Report, NUREG-0978, Issued for Comments, Mark III LOCA-Related Hydrodynamic Load Definition, February 1984.
7. NRC Staff Report, NUREG-0661, Safety Evaluation Report, Mark I Containment Long Term Program, July 1980.
8. NRC Staff Report, NUREG-0802, Safety/Relief Valve - Quencher Loads Evaluation Report - BWR Mark II and III Containments
- 10
9. GE Report NEDE-21730 Class III, Dec. 1977, Mark II Pressure Suppression Containment Systems - Loads on Submerged Structures, An Application Memorandum.
- 10←●

RBS USAR

PART I CONTAINMENT DYNAMIC LOAD DEFINITION

6A.1 INTRODUCTION

This report describes loss of coolant accident (LOCA) and safety relief valve (SRV) dynamic loads, based upon GE pressure suppression and safety relief valve test programs. General Electric has concluded the confirmatory test program for the Mark III containment configuration. These tests support and confirm the pressure suppression loads that result from the postulated LOCA and from SRV operation. The confirmation program includes a series of scaled multivalent tests that demonstrate no significant vent interaction effects for the LOCA process. The Caorso tests are also considered in specifying the SRV loads.

During a loss-of-coolant accident and events such as SRV actuation, the structures forming the containment system and other structures within the reactor building experience dynamic phenomena. The report provides numerical information on the dynamic loads that these phenomena impose on the River Bend Station containment system structures.

The loading information is based on either observed test data or conservatively calculated peak values. The LOCA loading combinations are presented in the form of bar charts for each of the containment system structures. In addition to defining the timing of the LOCA related loads, the bar charts identify other loading conditions such as seismic accelerations, dead-weight, etc.

To provide a better understanding of the various dynamic loads and their inter-relationships, Section 6A.2 contains a qualitative description of sequential events for a wide range of postulated accidents.

•→14

The LOCA hydrodynamic loads defined in Appendix 6A and associated attachments are based on conservatively applied test data and analytical approaches described in Appendix 3B of GESSAR. Application of the GESSAR load definition methods to define the River Bend hydrodynamic loads originally considered the containment thermal hydraulic response to postulated LOCA events assuming an initial reactor thermal power of 2952 MWt and an initial reactor pressure of 1060 psia. Subsequent calculations of the LOCA containment pressure and temperature response with an initial reactor

14←•

●→14

thermal power of 3100 MWt (100.3% of current rated thermal power) and an initial reactor pressure of 1072 psia demonstrated that the LOCA Loads defined in Appendix 6A are valid with the current rated thermal power.

In addition, the SRV Loads analyses documented in Appendix 6, including the loads defined in Attachments A, L, and N to Appendix 6A, were based on the original set of SRV relief valve and safety valve setpoints shown in Figure A.6A.4-3. Subsequent to these analyses, the nominal relief valve setpoints were raised by 30 psi. In addition, the maximum analytical value of the safety valve opening setpoints was increased to 1246 psig, which includes a 30 psi increase in the nominal SRV opening set point and an increase in the tolerance relaxation to 3%.

Evaluations were performed to evaluate the impact of these changes on the SRV loads defined in Appendix 6A. It was demonstrated by these evaluations that the conservatism in the GESSAR SRV air clearing load methodology used for River Bend is significantly larger than the changes introduced by the SRV valve setpoint changes. This conservatism was demonstrated by a comparison of SRV test data to predictions obtained with the GESSAR methodology. This comparison is documented in Attachment O to GESSAR Appendix 3B. Therefore, the SRV loads defined in Appendix 6A remain bounding with the current SRV setpoints.

14←●

6A.1.1 Confirmatory Testing

As described in Reference 1 (Section 3B.1.1).

6A.1.2 Definition of LOCA

As described in Reference 1 (Section 3B.1.2).

6A.1.3 Design Margins

Table 6A.1-1 summarizes the loads due to a LOCA for the containment structures for River Bend Station.

RBS USAR

TABLE 6A.1-1

SUMMARY OF SPECIFIED AND REALISTIC DESIGN VALUES
(Reference: GESSAR Table 3B-2)

Load	Specified for Design	Engineering Estimate	Design Basis		Section	Comments
			Analysis	GE PSTF Test		
<u>Structure: Drywell</u>						
<u>Break size: Large</u>						
●→14 Drywell pressurization	25 psig	18 psig	LOCTVS		6A.4.1.2	Peak calculated 20.7 psig (M3CPT) ⁽⁴⁾
Hydrostatic pressure	pH	pH	Standard analytical techniques		6A.4.1.3	
Bubble formation	0 → 21.8 psid	18 psid	Max pressure equal D.W. pressure		6A.4.1.4	
Wetwell pressurization	11 psid	3-5 psid	LOCTVS	5801, 5802 5803, 5804	6A.12.1	Test shows pressure differential in the 3 to 5 psi range PEAK CALCULATED VALUE 6.3 psig (M3CPT) ⁽⁴⁾
Pool swell 14←●						
Slug impact load	115 psi	60 psi		5706, 5801 5802, 5805	6A.12.1	Applies to small flat structures attached to D.W. (Fig. 6A.10-3)
Froth impingement load	21 psi max	15 psi		5706, 5801 5802, 5805		Applies to small struc- tures attached to D.W. (Fig. 6A.10-3)
Velocity for computing drag loads (slug flow)		30ft/sec	Bounding calculation		6A.9.0 6A.10.2	
Condensation for oscillation loads	±7 psid (mean)	±4 psid		5702, 5703 5801, 5807	6A.4.1.5	See GESSAR Fig. 3B-17 pressure distribution
Fallback velocity for drag loads	35 ft/sec	20 ft/sec	Bounding calculation		6A.4.1.6	
Negative load during ECCS flooding	-20 psid	-15 psid	Bounding calculation		6A.4.1.7	Assumes no vacuum relief due to reverse vent clearing

RBS USAR

TABLE 6A.1-1 (Cont)

Load	Specified for Design	Engr'g Estimate	Design Basis		Section	Comments
			Analysis	GE PSTF Test		
Chugging						
Gross structure	±2 psid	±1 psid		5801, 5802 5803, 5804	6A.4.1.8	Design pressures are ±25 psig and -20 psid
Loading within top vent					6A.4.1.9	
1. Pre-chug under- pressure	-15.0 psid (peak) -9.0 psid (mean)	-12 psid (peak) -8 psid (mean)		5707	6A.4.1.9	
2. Pulse (spike)	540 psid (peak) 214 psid (mean)	500 psid (peak) 180 psid (mean)		5707	6A.4.1.9	Local and global pulse train specified
3. Net force	250 kips (peak) 91 kips (mean)	250 kips (peak) 75 kips (mean)		5707	6A.4.1.9	Local and global net upward vertical load
Loading on drywell I.D.					6A.5.1.4	Same as weir wall specification
Loading on drywell O.D.				5707	6A.4.1.9	See GESSAR Table 3B-4 for duration and frequency
1. Pre-chug under- pressure	-5.8 psid (peak) -2.65 psid (mean)	-4.0 psid (peak) -1.0 psid (mean)				
2. Pulse (spike)	100 psid (peak) 24 psid (mean)	75 psid (peak) 20 psid (mean)				
3. Post-chug oscillation	±6.5 psid ±2.2 psid (mean)	±4.0 psid ±1.1 psid (mean)				

RBS USAR
TABLE 6A.1-1 (Cont)

Load	Specified for Design	Engr'g Estimate	Design Basis		Section	Comments
			Analysis	GE PSTF Test		
<u>Structure: Drywell</u>						
<u>Break size: Intermediate</u>						
ADS					6A.4.2	See Attachment A
Chugging					6A.4.1.8- 6A.4.1.9.2	Same as large break specification
<u>Structure: Drywell</u>						
<u>Break size: Small</u>						
Temperature	330°F/310°F	330°F/ 310°F	Bounding calculation		6A.4.3.1	3 hr at 330°F initially, next 3 hr at 310°F
Chugging					6A.4.1.8- 6A.4.1.9.2	Same as large break specification
<u>Structure: Weir Wall</u>						
<u>Break size: Large⁽¹⁾</u>						
Outward load due to vent clearing	10 psig	5 psig	Model in GESSAR Ref. 5		6A.5.1.2 6A.5.1.3	First 30 sec of blowdown
Chugging				5707	6A.5.1.4	Local and global loading specified
1. Pre-chug under- pressure	-2.15 psid (peak) -0.98 psid (mean)	-2.0 psid (peak) -0.5 psid (mean)				
2. Peak spike of pulse train	43 psid (peak) 15 psid (mean)	35 psid (peak) 13 psid (mean)				
Inward load due to negative drywell pressure differential	12,800 lbf (top vent) 9,800 lbf (mid) 7,200 lbf (bottom)	8000 lbf (top vent) 6000 lbf (mid) 4000 lbf (bottom)	Bounding calculation		6A.5.1.5	

RBS USAR
TABLE 6A.1-1 (Cont)

Load	Specified for Design	Engr'g Estimate	Design Basis		Section	Comments
			Analysis	GE PSTF Test		
Hydrostatic pressure	pH	pH	Standard analytical techniques		6A.5.1.7	
<u>Structure: Weir Wall</u>						
<u>Break size: Intermediate</u> ⁽¹⁾						
ADS						
<u>Structure: Weir Wall</u>						
<u>Break size: Small</u> ⁽¹⁾						
Temperature	330°F/310°F		Bounding calculation		6A.5.4	330°F for initial 3 hr, 310°F for next 3 hr
<u>Structure: Containment</u>						
<u>Break size: Large</u>						
Water jet	<1 psig	0 psig	Attachment L	5706	6A.6.1.2	Measured pressure is small and is obscured by bubble pressure
Bubble formation	10 psid	8 psid		5701, 5702 5703, 5705 5706	6A.6.1.3	
Hydrostatic pressure	H	H	Standard analytical techniques		6A.6.1.4	
Pool swell loads for attached structures at pool surface	10 psid (bubble)	8 psid	D.W. bubble pressure		6A.6.1.5	Only large structures see bubble pressure
	50 ft/sec (max drag velocity)	30ft/sec	Bounding calculation		6A.6.1.5	
Pool swell near the HCU floor elevation	21 psi max (froth impingement)	10 psi		5706	6A.6.1.6	

RBS USAR

TABLE 6A.1-1 (Cont)

Load	Specified for Design	Engr'g Estimate	Design Basis		Section	Comments
			Analysis	GE PSTF Test		
•→14	11 psi (flow ΔP)	3-5 psi	LOCTVS	5801, 5802 5803, 5804	6A.6.1.6	Test shows pressure differential in the 3 to 5 psi range PEAK CALCULATED 6.3 psid (M3CPT) ⁽⁴⁾
14←• Fallback velocity for drag loads	35 ft/sec	20 ft/sec	Bounding calculation		6A.6.1.7	
Post pool swell waves	2 ft	2 ft		PSTF tests	6A.6.1.8	Negligible load
Condensation oscillation loads	±1 psid (mean)	±0.6		5807, 5701 5702	6A.6.1.9	
Chugging				5707	6A.4.1.9	See GESSAR Table 3B-4 for duration and frequency
1. Pre-chug-under-pressure	-1.3 psid (peak) -1.0 psid (mean)	-0.8 psid (peak) -0.3 psid (mean)				
2. Pulse (spike)	3.0 psid (peak) 0.7 psid (mean)	2.2 psid (peak) 0.6 psid (mean)				
3. Post-chug	±1.7 psid (peak) ±1.0 psid (mean)	±1.5 psid (peak) ±0.5 psid (mean)				
•→14 Pressurization	15 psig	5 psig	LOCTVS		6A.6.1.11	Peak Calculated 6.3 psid (M3CPT) ⁽⁴⁾
Temperature	185°F ⁽²⁾	<150°F	LOCTVS		6A.6.1.11	Peak Calculated Suppression Pool Temperature is 170.7 °F (SHEX) ⁽⁴⁾
14←• <u>Structure: Containment</u>						
<u>Break size: Intermediate</u>						
Pressurization	15 psig	5 psig	Bounding calculation		6.2	

RBS USAR
TABLE 6A.1-1 (Cont)

Load	Specified for Design	Engr'g Estimate	Design Basis		Section	Comments
			Analysis	GE PSTF Test		
ADS					6A.6.2	See Attachment A
Chugging					6A.4.1.8- 6A.4.1.9.2	Same as large break specification
<u>Structure: Containment</u>						
<u>Break size: Small</u>						
Temperature stratification (dome)	220°F	185°F	Bounding calculation		6A.6.3	Local temperatures of 300°/250°F are possible in the event of reactor steam/liquid blowdowns to containment.
Pressure	2 psig	1 psig	Bounding calculation		6A.6.3	Typical value
Chugging					6A.4.1.8- 6A.4.1.9.2	Same as large break specification
<u>Structure: Basemat</u>						
<u>Break size: Large</u>						
Hydrostatic	pH	pH	Standard analytical techniques			
Bubble formation	10 → 21.8 psid	18 psid	Peak equal to D.W. pressure	5706/4	6A.7.0	10 psi over 1/2 pool assumed to increase linearly to 21.8 psi. See GESSAR Fig. 3B-68
Condensation oscillation load	±1.7 psid	±1.0 psid		5807, 5702 5701	6A.7.0	See Section 6A.4

RBS USAR
TABLE 6A.1-1 (Cont)

Load	Specified for Design	Engr'g Estimate	Design Basis		Section	Comments
			Analysis	GE PSTF Test		
Chugging				5707	6A.4.1.9.2	See GESSAR Table 3B-4 for duration and frequency See GESSAR Fig. 3B-28 through 3B-31 for basemat attenuation
1. Pre-chug under-pressure	-1.8 psid (peak) -1.34 psid (mean)	-1.5 psid (peak) -0.7 psid (mean)				
2. Pulse (spike)	10 psid (peak) 2.4 psid (mean)	7.5 psid (peak) 2 psid (mean)				
3. Post-chug oscillation	±2.1 psid (peak) ±1.3 psid (mean)	±2.0 psid (peak) ±1.0 psid (mean)				
<u>Structure: Basemat</u>						
<u>Break size: Intermediate</u>						
ADS					6A.7.0	See Attachment A
Chugging					6A.4.1.9	Same as large break specification
<u>Structure: Basemat</u>						
<u>Break size: Small</u>						
Chugging					6A.4.1.9	Same as large break specification
<u>Structure: Submerged structures</u>						
<u>Break size: Large⁽³⁾</u>						
LOCA water jet loads						Attachment L
LOCA air bubble load		8.2 psid				Attachment L

RBS USAR

TABLE 6A.1-1 (Cont)

<u>Load</u>	<u>Specified for Design</u>	<u>Engr'g Estimate</u>	<u>Design Basis</u>		<u>Section</u>	<u>Comments</u>
			<u>Analysis</u>	<u>GE PSTF Test</u>		
Velocity for computing drag loads	50 ft/sec (maximum)	30 ft/sec	Bounding calculation			See Attachment M
Fall back velocity for drag loads	35 ft/sec	20 ft/sec	Bounding calculation		L.6A.2.4	
LOCA condensation oscillation loads		0.7 psid	Attachment L		Attachment L	
LOCA chugging loads		1.9 psid	Attachment L		Attachment L	
X-Quencher water jet load		Negligible	Attachment L		Attachment L	Load is negligible outside a sphere circumscribed by the quencher arms
X-Quencher air bubble load		0.5 psid	Attachment L		Attachment L	
<u>Structure: Submerged Structures</u>						
<u>Break size: Intermediate</u> ⁽³⁾						
ADS						See Attachment L
<u>Structure: Submerged Structures</u>						
<u>Break size: Small</u> ⁽³⁾						
No additional loads generated						
<u>Structure: Structures at pool surface</u>						
<u>Break size: Large</u>						
Bubble formation						
•→14 Drywell	21.8 psid	18 psi	Equal to D.W. Pressure		6A.9.0	Large structures only PEAK CALCULATED D.W. Pressure is 20.5 psid (M3CPT) ⁽⁴⁾
14←• Containment	10.0 psid		Attenuated			

RBS USAR
TABLE 6A.1-1 (Cont)

<u>Load</u>	<u>Specified for Design</u>	<u>Engr'g Estimate</u>	<u>Design Basis</u>		<u>Section</u>	<u>Comments</u>
			<u>Analysis</u>	<u>GE PSTF Test</u>		
Velocity for computing drag loads	40 ft/sec	30 ft/sec	Bounding calculation		6A.9.0	
Fallback velocity for drag loads	35 ft/sec	20 ft/sec	Bounding calculation		6A.4.1.6	
<u>Structure: Structures at pool surface</u>						
<u>Break size: Intermediate</u>						
ADS						See Attachment A
<u>Structure: Structures at pool surface</u>						
<u>Break size: Small</u>						
No additional loads generated						(See large break tabulation)
<u>Structure: Structures between pool surface and HCU floor</u>						
<u>Break size: Large</u>						
Slug Impact Loads						
Small flat structures	115 psi	60 psi		5801, 5802 5805, 5706	6A.10.1	
Piping	60 psi	30 psi		5801, 5802 5805, 5706	6A.10.1	
Froth impingement loads	Varies			5706	6A.10.1	See Fig. 6A.12-1
Velocity for computing drag loads	50 ft/sec	30 ft/sec	Bounding calculation		6A.10.2	See Fig. 6A.10-4 for grating loads
Fallback velocity for drag loads	35 ft/sec	20 ft/sec	Bounding calculation		6A.10.3	

RBS USAR

TABLE 6A.1-1 (Cont)

Load	Specified for Design	Engr'g Estimate	Design Basis		Section	Comments
			Analysis	GE PSTF Test		
<u>Structure: Structures between pool surface and HCU floor</u>						
<u>Break size: Intermediate</u>						
No additional loads generated						(See large break tabulation)
<u>Structure: Structures between pool surface and HCU floor</u>						
<u>Break size: Small</u>						
No additional loads generated						(See large break tabulation)
<u>Structure: Expansive Structures at HCU floor elevation</u>						
<u>Break size: Large</u>						
Wetwell pressurization	11 psig (3-4 sec)	3-5 psig (1-2 sec)	LOCTVS	5801, 5802 5803, 5804	6A.11.0	
Froth impingement	Varies	10 psig		5801, 5802	6A.11.0	
•→14				5805, 5706		
Flow pressure differential	11 psig	3-5 psig	LOCTVS	5801, 5802 5803, 5804	6A.12.0	Test shows pressure differential of 3 to 5 psi PEAK CALCULATED VALUE 6.3 psid (M3CPT) ⁽⁴⁾
14←•						
Fallback and water accumulation	1 psi	0.5 psi	Bounding calculation		6A.12.0	Based on water flow through HCU floor
<u>Structure: Expansive Structures at HCU floor elevation</u>						
<u>Break size: Intermediate</u>						
No additional loads generated						See large break tabulation
<u>Structure: Expansive Structures at HCU Floor elevation</u>						
<u>Break size: Small</u>						
No additional loads generated						See large break tabulation

RBS USAR

TABLE 6A.1-1 (Cont)

Load	Specified for Design	Engr'g Estimate	Design Basis		Section	Comments
			Analysis	GE PSTF Test		
<u>Structure: Small Structures at HCU elevation</u>						
Froth impingement	Varies	10 psid		5801, 5802 5805, 5706	6A.12.0	See Fig. 6A.12-1
No additional loads generated						See large break tabulation
<u>Structure: Expansive Structures at HCU Floor elevation</u>						
<u>Break size: Small</u>						
No additional loads generated						See large break tabulation
<u>Structure: Small Structures at HCU elevation</u>						
Froth impingement	Varies	10 psid		5801, 5802 5805, 5706	6A.12.0	See Fig. 6A.12-1
•→14 Flow pressure differential	11 psid	3-5 psid	LOCTVS	5801, 5802 5803, 5804	6A.12.0	Test shows pressure differential of 3 to 5 psi PEAK CALCULATED VALUE
14←• Fallback and water accumulation	1 psid	0.5 psid	Bounding calculation		6A.12.0	6.3 psid (M3CPT) ⁽⁴⁾ Based on water flow through HCU floor

NOTES: 1. Where S/R valve loads are specified in the applicable bar charts, refer to Attachment A, Section 6A.5.6 for margin discussion.

2. Not all loads for IBA and SBA are tabulated. Generally the large break load condition governs.

(1) Chugging loads on weir wall are the same for large, intermediate, and small break accidents.

(2) See Section 6A.6.1.11.

(3) Chugging loads are the same for large, intermediate, and small break accidents.

•→14

(4) M3CPT and SHEX calculated values based on an MSLB with 3100 MWT initial reactor thermal power and 1072 psig initial reactor pressure.

14←•

6A.2 REVIEW OF PHENOMENA

The purpose of this section is to qualitatively review the sequence of events that could occur during the course of the design basis accident (DBA), an intermediate break accident (IBA), a small break accident (SBA), and during SRV actuation. The objective of this review is to provide an understanding of the various pool dynamic loads and their interrelationships, and to define the dynamic loading terminology.

6A.2.1 Design Basis Accident (DBA)

●→14

Fig. 6.2-4 and 6.2-5 show the containment pressure transients for a double-ended rupture (DER) of a 24-in main steam line and for a 20-in recirculation pump suction line, respectively. Both results are based on the assumption that the reactor and containment are operating at maximum normal conditions at the time of the accident. Thus, the reactor thermal power is considered to be initially at 3100 MWt (100.3 percent nuclear boiler rated power), and the drywell and containment temperatures are taken as 145°F and 90°F, respectively. The summary of peak conditions is presented in Table 6.2-7. The GE M3CPT computer code described in Section 6.2.1.1.3.7 is used to determine the containment response following a postulated loss-of-coolant accident (LOCA).

In the context of this section of the Appendix, the DBA is considered to be the main steam line DER which is the LOCA that produces the maximum drywell wall positive pressure differential. The accident chronology for a main steam line DER is given in Table 6.2-10.

The peak calculated drywell pressure is 20.7 psig for River Bend Station as described in Section 6.2.1. However, the value of 21.8 psig specified in GESSAR is conservatively assumed for the vent clearing bubble pressure load evaluation.

14←●

The post-DBA negative drywell pressure resulting from condensation of steam in the drywell is evaluated according to the method outlined in Attachment G of GESSAR. This analysis is presented in Section 6.2.1.1.3.3. The River Bend Station drywell is designed for a negative or external pressure of 20 psid and does not utilize a vacuum relief system. Drywell negative pressure is terminated by reverse vent clearing and return flow of air from the containment.

The reverse vent clearing due to drywell depressurization is relatively quiescent compared to forward vent clearing following a LOCA. Drywell depressurization is a slow process driven by condensation of steam onto the drywell passive heat sinks and condensation and cooling resulting from spilling ECCS water from the break following vessel reflood.

●→14

Therefore, the dynamic loads resulting from liquid during reverse vent clearing are negligible compared to those for forward vent clearing.

14←●

The potential for flooding of equipment and components in the drywell due to reverse vent flow following a LOCA is not of concern because the lower levels of the drywell are expected to be flooded before reverse vent flow. Therefore, no safety-related equipment is located in this area.

●→14

The maximum suppression pool temperature after a DBA is calculated to be 107.7°F which occurs in the long term containment cooling phase of the transient. It should be noted that neither containment nor drywell sprays are provided in the River Bend Station design. Long term heat removal is accomplished by the RHR system suppression pool cooling mode and the containment unit coolers.

14←●

6A.2.2 Intermediate Break Accident (IBA)

As described in Reference 1 (Section 3B.2.2).

6A.2.3 Small Break Accident (SBA)

As described in Reference 1 (Section 3B.2.3).

6A.2.4 Safety Relief Valve Actuation

As described in Reference 1 (Section 3B.2.4).

6A.2.5 Other Considerations

As described in Reference 1 (Section 3B.2.5).

6A.3 DYNAMIC LOAD TABLE

As described in Reference 1 (Section 3B.3).

6A.4 DRYWELL STRUCTURE

The drywell structure experiences loads during both the design basis LOCA (see Fig. 6A.4-1) and during a small steam break accident (see Fig. 6A.4-2). Loads occurring during an IBA (see Fig. 6A.4-3) are less severe than those associated with the large and small break. Other dynamic loads such as pipe whip, jet impingement, and missiles are considered in the design and are discussed in Section 3.8.3.

6A.4.1 Drywell Loads During a Large Break Accident

As described in Reference 1 (Section 3B.4.1).

6A.4.1.1 Sonic Wave

As described in Reference 1 (Section 3B.4.1.1).

6A.4.1.2 Drywell Pressure

•→14

During the vent clearing process, the drywell reaches a peak calculated pressure differential of 20.5 psid. Fig. 6.2-4 shows the drywell pressure during the DBA. It includes the HCU floor pool swell interference effects. The computer code M3CPT is used to calculate these values.

14←•

6A.4.1.3 Hydrostatic Pressure

As described in Reference 1 (Section 3B.4.1.3).

6A.4.1.4 Loads on the Drywell Wall During Pool Swell

As described in Reference 1 (Section 3B.4.1.4).

6A.4.1.5 Condensation Oscillation Loads

As described in Reference 1 (Section 3B.4.1.5).

6A.4.1.6 Fallback Loads

As described in Reference 1 (Section 3B.4.1.6).

6A.4.1.7 Negative Load During ECCS Flooding

Somewhere between 100 and 600 sec following a LOCA (the time is dependent on break location and size), the ECCS system refills the reactor pressure vessel (RPV). ECCS spillover from the break and the drywell passive heat sinks condense the steam in the drywell. The drywell pressurization produced by this condensation draws noncondensable gas from

the containment free space via the vents. It is during this drywell depressurization transient that the maximum drywell negative pressure occurs. However, for design purposes a conservative bounding end point calculation is performed which assumes that drywell depressurization occurs instantaneously before any air can return to the drywell via the vents. This theoretical conservative calculation yields a drywell external pressure differential of -19.4 psid (Section 6.2.1.1.3.3.1).

6A.4.1.8 Chugging

Chugging consists of pressure pulse trains of about 0.1 sec duration, occurring every 1 to 5 sec. During vent chugging, drywell pressure fluctuations result if significant quantities of suppression pool water are splashed into the drywell when the returning water impacts the weir wall. This can result in a differential pressure on the drywell as shown in GESSAR, Fig. 3B-20. The maximum values of this load (+2.0, -0.7 psid) are negligible when compared to the design drywell pressure differentials of +25.0, -20.0 psid.

For further information regarding test data, refer to GESSAR.

6A.4.1.9 Loads Due to Chugging

As described in Reference 1 (Section 3B.4.1.9).

6A.4.2 Drywell Loads During Intermediate Break Accident

As described in Reference 1 (Section 3B.4.2).

6A.4.3 Drywell Loads During a Small Break Accident

As described in Reference 1 (Section 3B.4.3).

6A.4.3.1 Drywell Temperature

As described in Reference 1 (Section 3B.4.3.1).

6A.4.3.2 Drywell Pressure

As described in Reference 1 (Section 3B.4.3.2).

6A.4.3.3 Chugging

As described in Reference 1 (Section 3B.4.3.3).

6A.4.4 Safety Relief Valve Actuation

As described in Reference 1 (Section 3B.4.4).

6A.4.5 Drywell Environmental Envelope

●→14

Figures 6A.4-4a and 6A.4-4b show an envelope of the drywell pressure and temperature based on the results of analyses performed with the GE M3CPT and SHEX codes with an initial reactor thermal power of 3100 MWt.

The peak drywell airspace temperature calculated for the DBA-LOCA MSLB does exceed the drywell structural design value of 330 °F. However, this peak drywell temperature is calculated using the GE M3CPT computer code which does not model drywell or containment structural passive heat sinks. The original USAR containment analysis for the DBA-LOCA MSLB for River Bend included heat sinks. This modeling difference explains, at least in part, the difference between the peak MSLB drywell temperature using the GE M3CPT code and the peak drywell temperature reported in the USAR.

Since River Bend is licensed to take credit for heat sinks in containment analyses of the DBA LOCA MSLB, the effect of using heat sinks is quantified. To quantify the effect of using heat sinks, sensitivity analyses are performed with the GE SHEX computer code for the DBA-LOCA MSLB. The GE SHEX code has the capability to model heat sinks. It is, however, not used to calculate the initial drywell pressure and temperature response for the MSLB LOCA since this code does not include a model for inertial dynamic vent clearing that occurs during the first seconds of a DBA-LOCA. That model is only present in the GE M3CPT model.

However, with appropriate adjustments to the SHEX vent model inputs, SHEX produces drywell temperatures and drywell pressures during the first seconds that are very similar to those obtained with M3CPT. The results of these calculations can then be used to explore the sensitivity of drywell temperature to the use of heat sinks. SHEX sensitivity analyses are performed with and without heat sinks which demonstrates that with heat sinks, the peak drywell atmospheric temperature for the MSLB is reduced by 3 °F. When this effect is applied to the M3CPT peak drywell temperature prediction of 332.8 °F, the peak drywell airspace temperature is reduced to below the 330 °F design limit.

14←●

Fig. 6A.4-4 shows the design envelope of drywell atmospheric pressures and temperatures for the spectrum of postulated LOCAs. Fig. 6A.4-4 defines only the drywell atmospheric condition; separate analyses are required to evaluate the transient structural response to these conditions. The high-pressure and

high-temperature conditions shown for the first 45 sec cannot occur simultaneously and need not be considered in combination.

6A.4.6 Top Vent Temperature (Cycling) Profile During Chugging

As described in Reference 1 (Section 3B.4.6).

6A.4.7 Drywell Multicell Effects

As described in Reference 1 (Section 3B.4.7).

STRUCTURE: DRYWELL
 ACCIDENT: LARGE STEAM LINE BREAK (DBA)

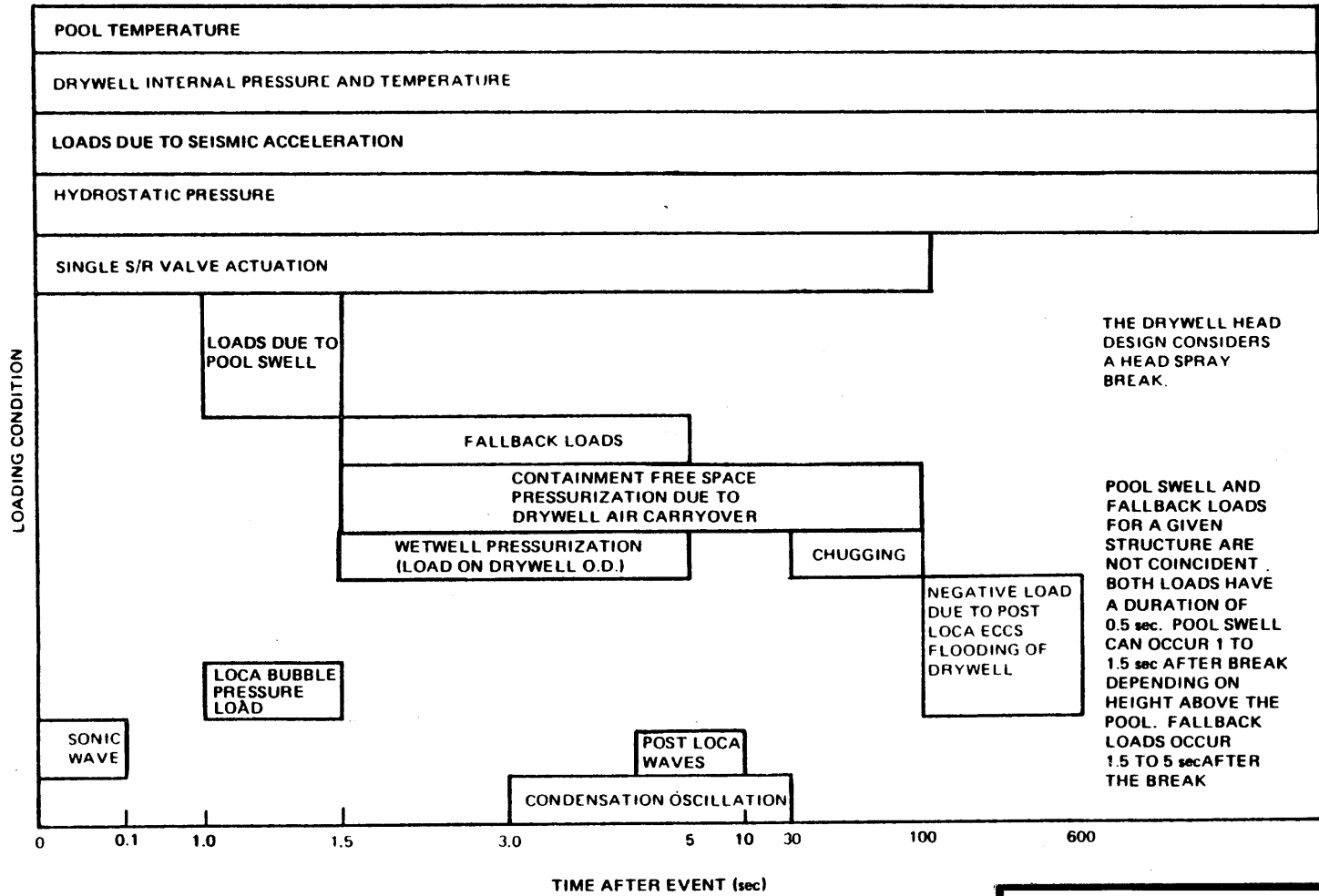


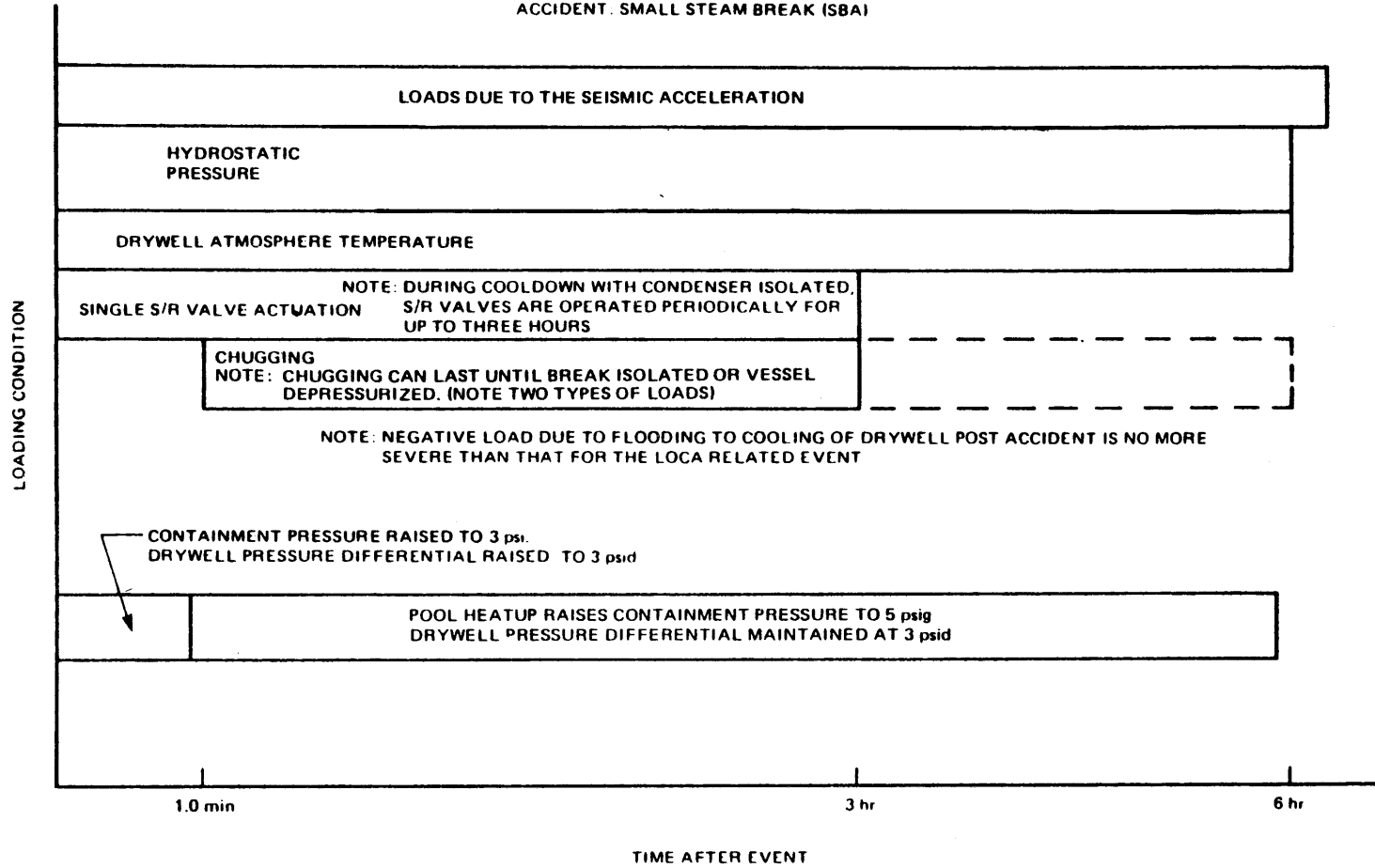
FIGURE 6A.4-1

DRYWELL-LOADING CHART FOR DBA

RIVER BEND STATION
 UPDATED SAFETY ANALYSIS REPORT

REF.: GESSAR FIG. 3B-9

STRUCTURE: DRYWELL
ACCIDENT: SMALL STEAM BREAK (SBA)

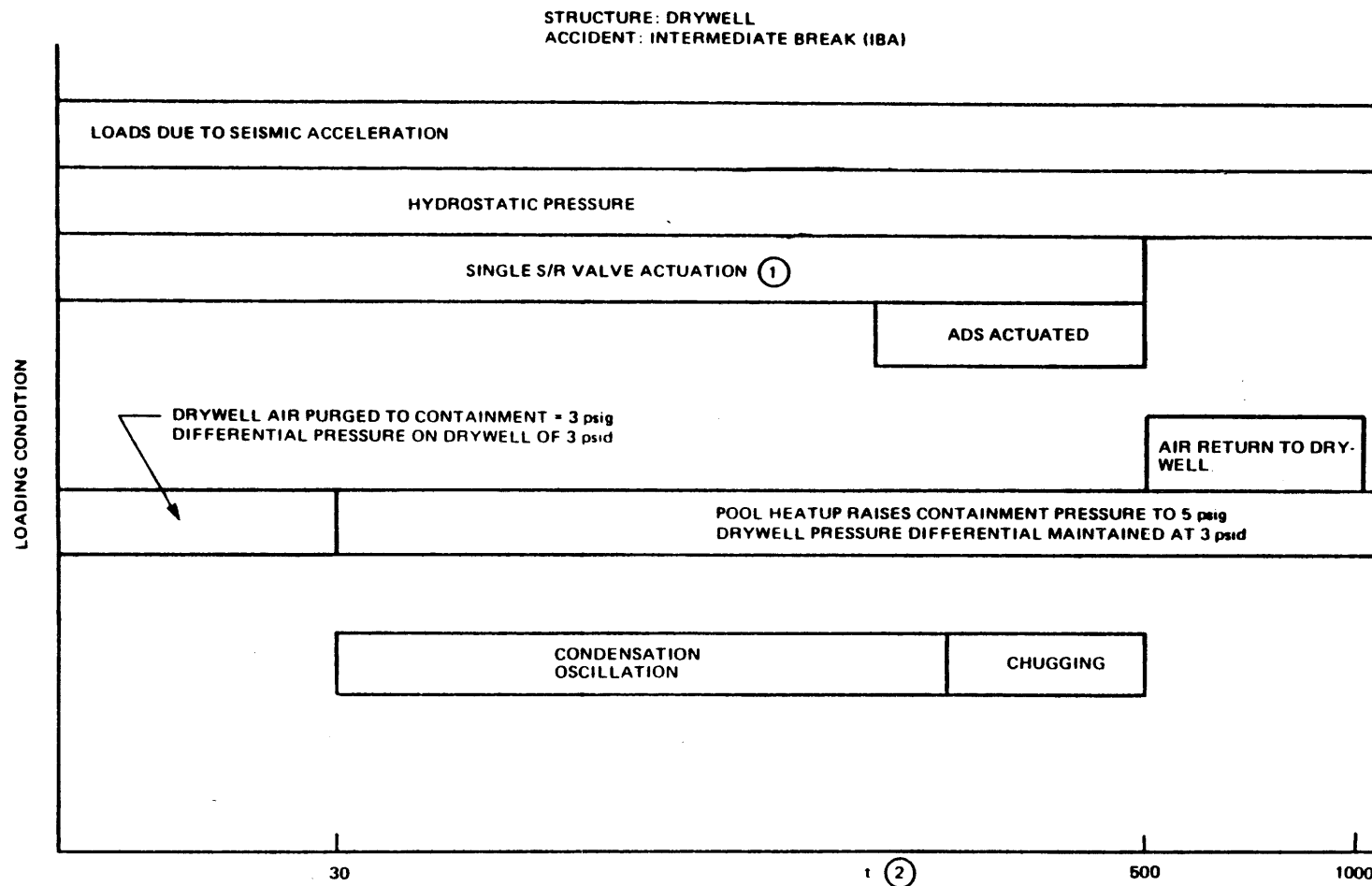


REF.: GESSAR FIG. 3B-37

FIGURE 6A.4-2

DRYWELL-LOADING CHART FOR SBA

RIVER BEND STATION
UPDATED SAFETY ANALYSIS REPORT



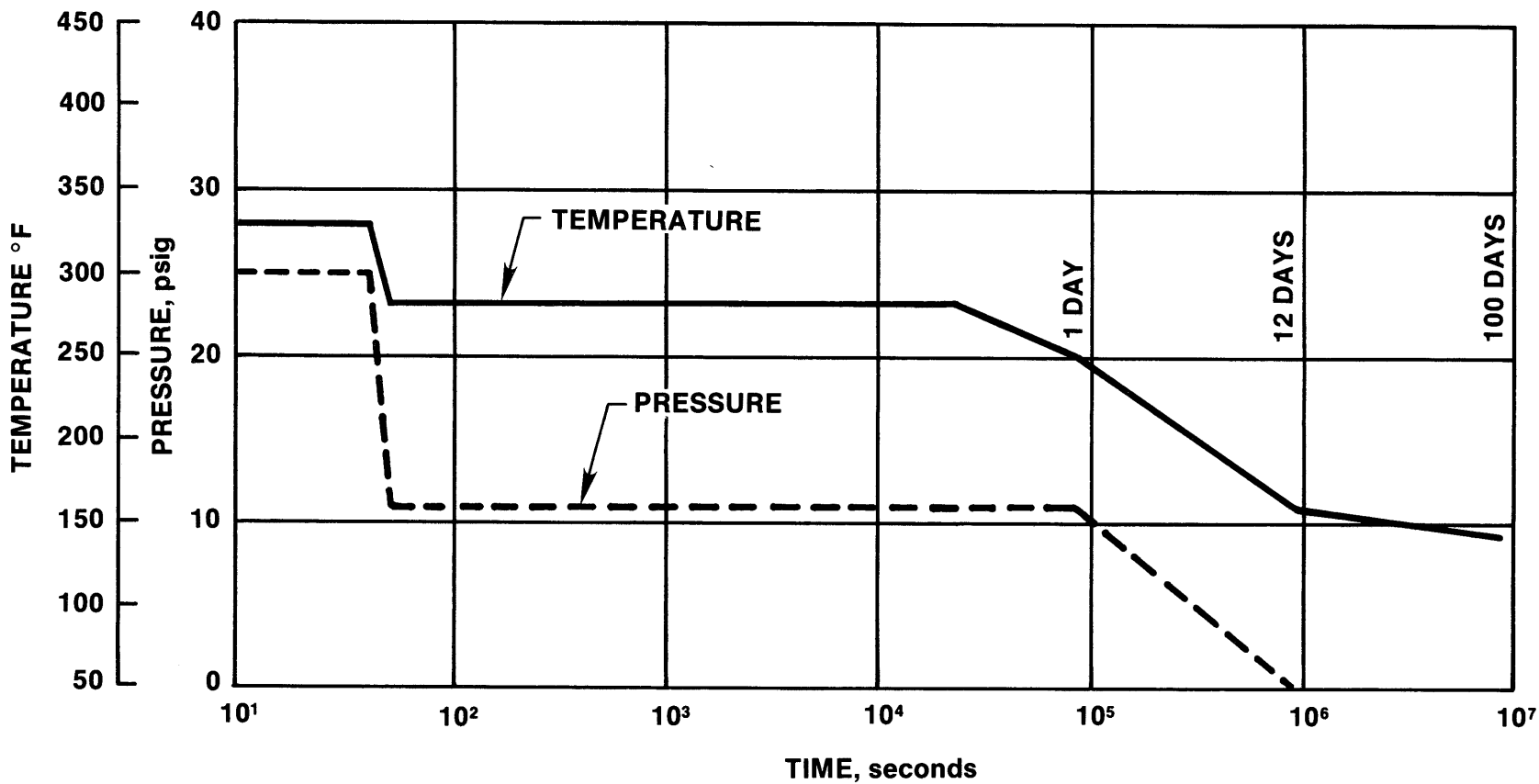
- ① SINGLE SRV LOADS DO NOT COMBINE WITH OTHER SRV LOADS
- ② TIME SCALE DEPENDENT UPON BREAK SIZE, MINIMUM VALUE OF $t \approx 2$ min

REF.: GESSAR FIG. 3B-36

FIGURE 6A.4-3

DRYWELL-LOADING CHART FOR IBA

RIVER BEND STATION
UPDATED SAFETY ANALYSIS REPORT



NOTE:

1. DRYWELL NEGATIVE PRESSURE DURING ECCS FLOODING NOT SHOWN

FIGURE 6A.4-4

MAXIMUM DESIGN DRYWELL
ATMOSPHERE BULK TEMPERATURE AND
PRESSURE ENVELOPE

RIVER BEND STATION

UPDATED SAFETY ANALYSIS REPORT

M3CPT & SHEX (3100 MWT)

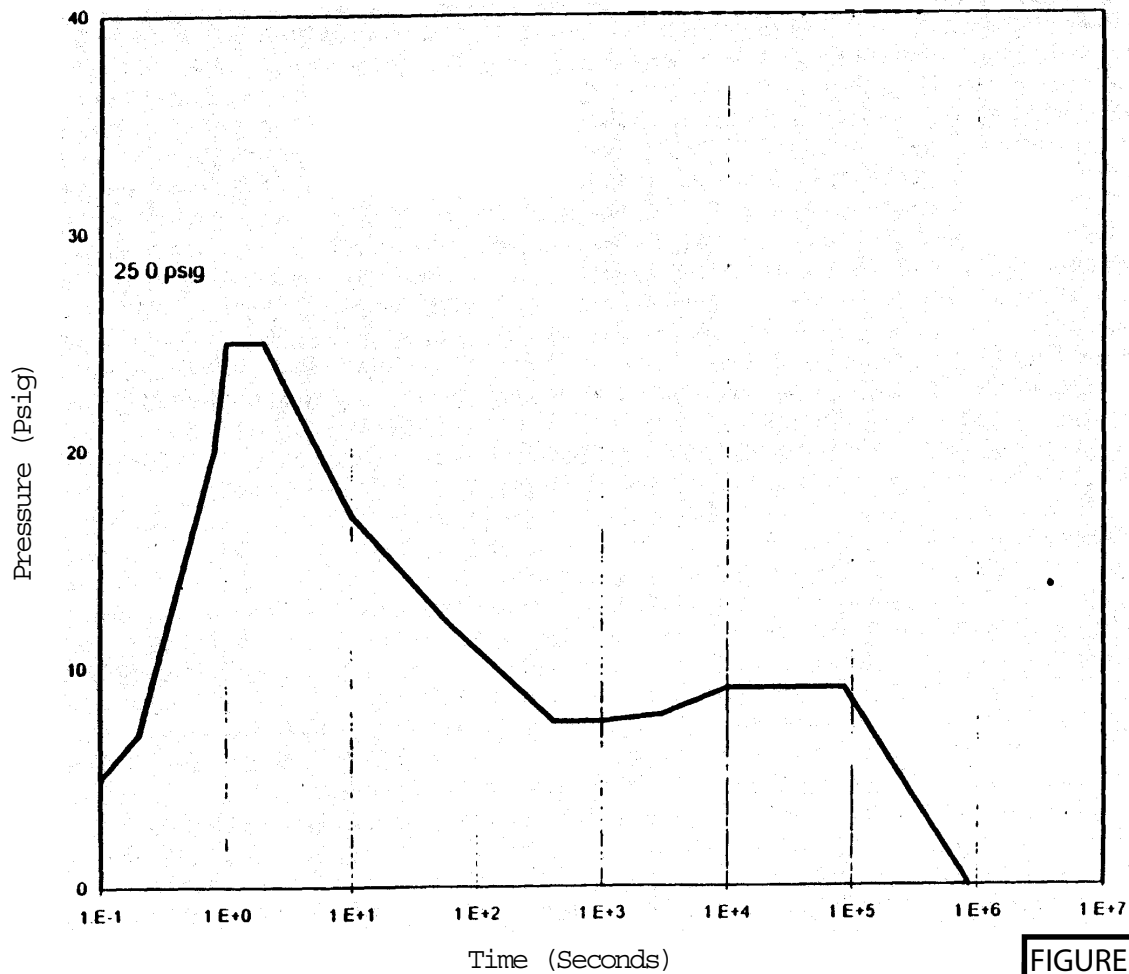


FIGURE 6A.4-4a

DRYWELL PRESSURE ENVELOPE

RIVER BEND STATION
UPDATED SAFETY ANALYSIS REPORT

M3CPT & SHEX (3100 MWT)

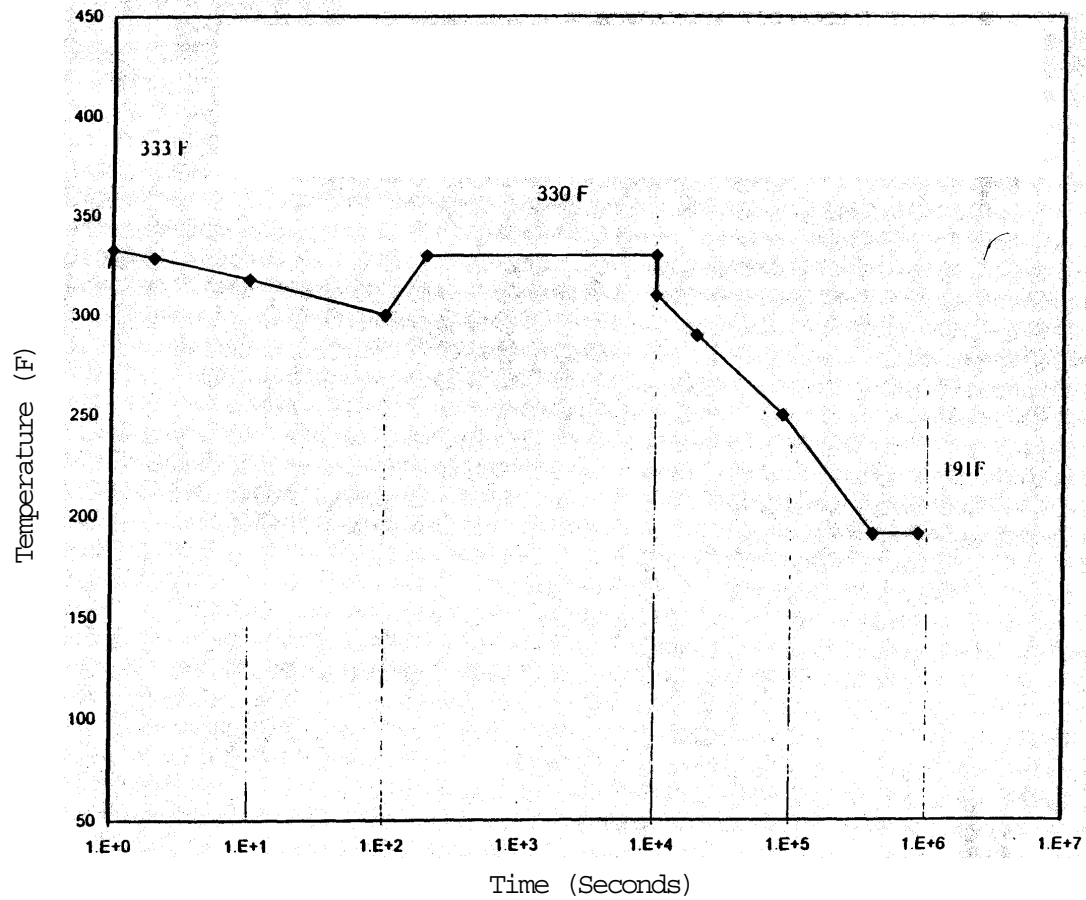


FIGURE 6A.4-4b

DRYWELL TEMPERATURE ENVELOPE

RIVER BEND STATION
UPDATED SAFETY ANALYSIS REPORT

6A.5 WEIR WALL

The weir wall experiences loading conditions during both the design basis LOCA and during a small steam break accident. Fig. 6A.5-1 and 6A.5-2 are the bar charts for these two cases. The intermediate break loads are less severe than those associated with the large and small break. Fig. 6A.5-3 is the bar chart for this case.

6A.5.1 Weir Wall Loads During a Design Basis Accident

6A.5.1.1 Sonic Wave

As described in Reference 1 (Section 3B.5.1.1).

6A.5.1.2 Outward Load During Vent Clearing

As described in Reference 1 (Section 3B.5.1.2).

6A.5.1.3 Outward Load Due to Vent Flow

As described in Reference 1 (Section 3B.5.1.3).

6A.5.1.4 Chugging Loads

As described in Reference 1 (Section 3B.5.1.4).

6A.5.1.5 Inward Load Due to Negative Drywell Pressure

As described in Reference 1 (Section 3B.5.1.5), except as follows:

1. For radial structures within 1-ft of the top of the weir wall, the stresses are increased by a multiplier. This multiplier is 1.0 when the natural frequency of the structure is less than 200 Hz, and 1.8 when the natural frequency is greater than 500 Hz with a linear ramp between these values.
2. Impact loads on structures located within 3 in of the top of the weir wall are calculated based on Section 2.7 of Appendix A of NUREG-0661, using an impact velocity of 4 ft/sec.

6A.5.1.6 Suppression Pool Fallback Loads

As described in Reference 1 (Section 3B.5.1.6).

6A.5.1.7 Hydrostatic Pressure

As described in Reference 1 (Section 3B.5.1.7).

6A.5.1.8 Safety Relief Valve Loads

As described in Reference 1 (Section 3B.5.1.8).

6A.5.1.9 Condensation

As described in Reference 1 (Section 3B.5.1.9).

6A.5.2 Weir Wall Loads During an Intermediate Break
Accident

As described in Reference 1 (Section 3B.5.2).

6A.5.3 Weir Wall Loads During a Small Break Accident

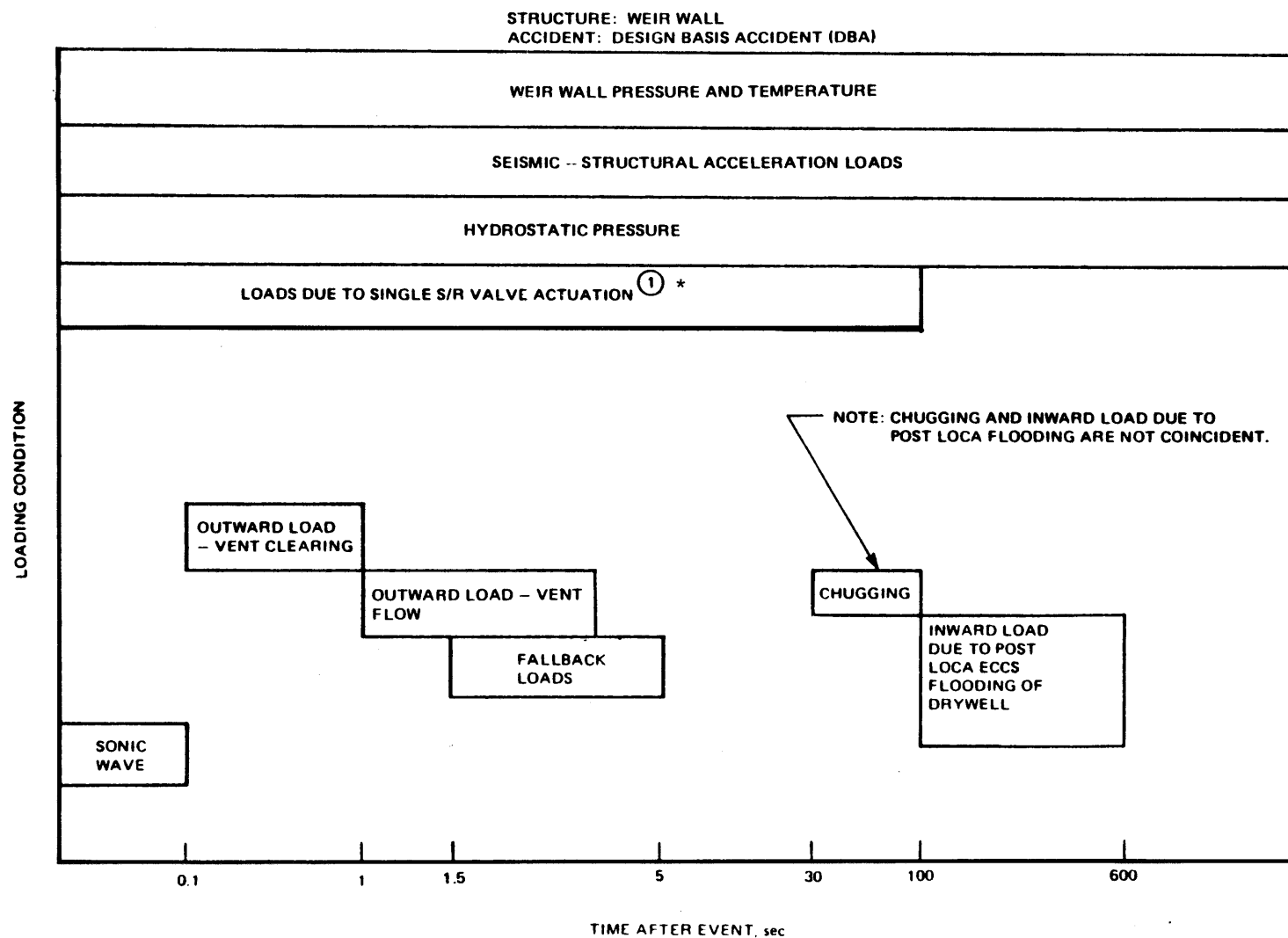
As described in Reference 1 (Section 3B.5.3).

6A.5.4 Weir Wall Environment Envelope

As described in Reference 1 (Section 3B.5.4).

6A.5.5 Weir Annulus Multicell Effects

As described in Reference 1 (Section 3B.5.5).



① APPLIES TO BOTTOM 2 VENTS ONLY
* ADD S/R DYNAMIC LOAD TO STATIC LOAD DUE TO DRYWELL AIR PURGED TO CONTAINMENT

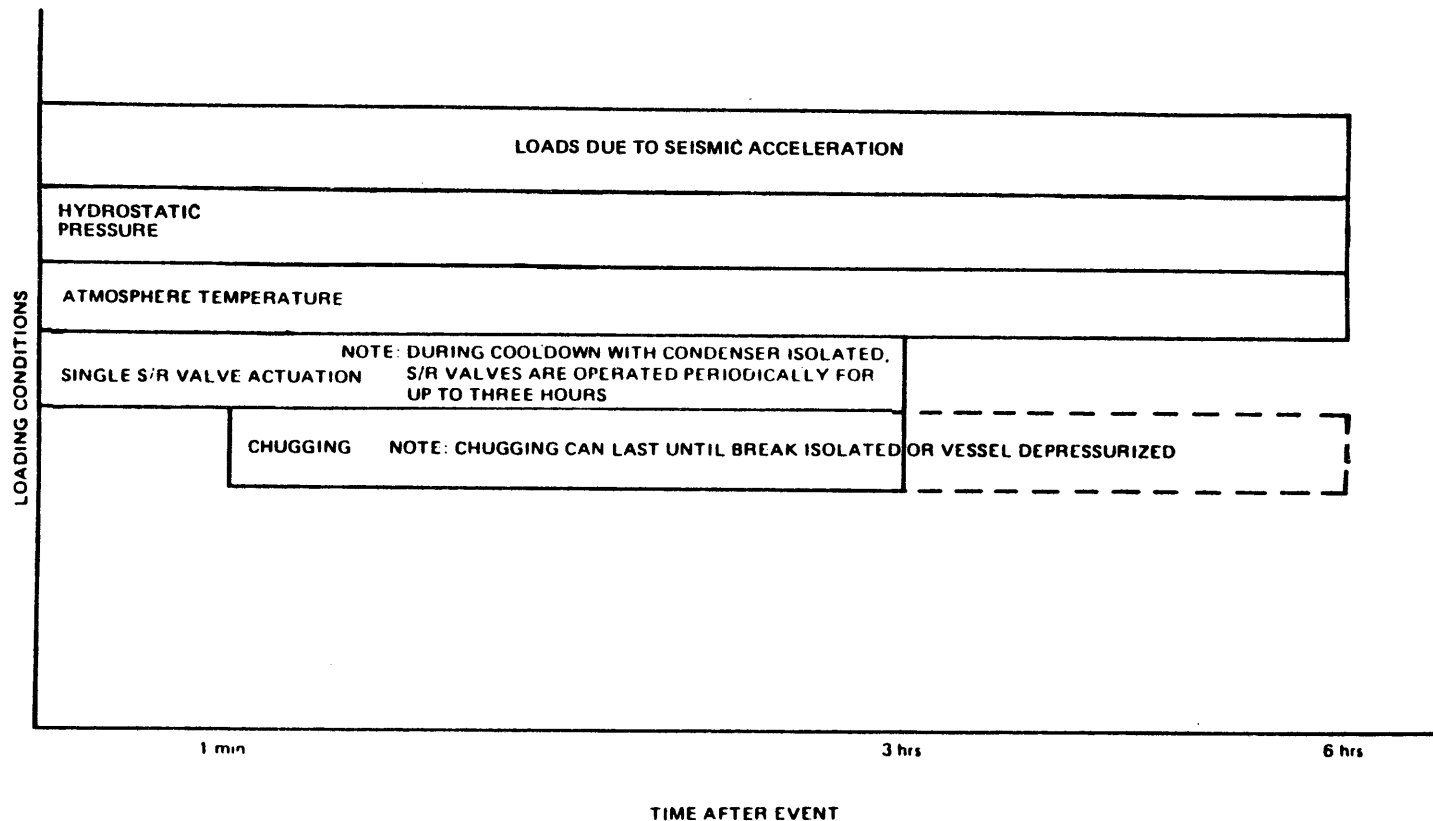
REF.: GESSAR FIG. 3B-42

FIGURE 6A.5-1

WEIR WALL-LOADING CHART FOR DBA

RIVER BEND STATION
UPDATED SAFETY ANALYSIS REPORT

STRUCTURE: WEIR WALL
ACCIDENT: SMALL BREAK ACCIDENT (SBA)

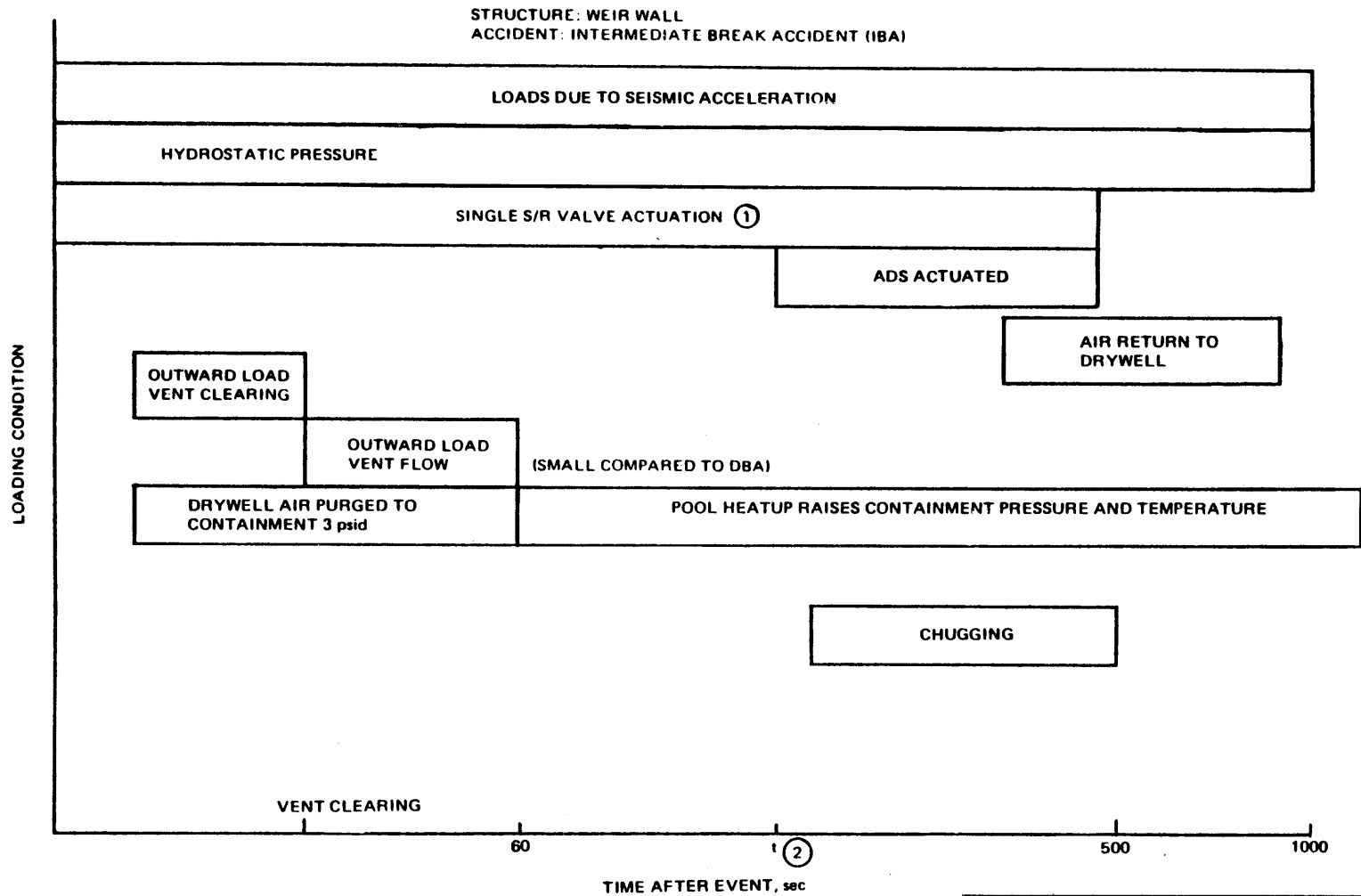


REF.: GESSAR FIG. 3B-43

FIGURE 6A.5-2

WEIR WALL-LOADING CHART FOR SBA

RIVER BEND STATION
UPDATED SAFETY ANALYSIS REPORT



- ① SINGLE SRV LOADS DO NOT COMBINE WITH OTHER SRV LOADS
- ② TIME SCALE DEPENDENT UPON BREAK SIZE, MINIMUM VALUE OF $t \approx 2.0$ min

REF.: GESSAR FIG. 3B-44

FIGURE 6A.5-3

WEIR WALL-LOADING CHART FOR IBA

RIVER BEND STATION
UPDATED SAFETY ANALYSIS REPORT

6A.6 CONTAINMENT

The containment experiences dynamic loadings during all three classes of LOCAs.

6A.6.1 Containment Loads During a Large Steam Line Break (DBA)

Fig. 6A.6-1 is the bar chart showing the loading conditions that the containment structure experiences during the DBA LOCA. Design loads for the various structures in the containment annulus are presented in Sections 6A.7 through 6A. 12.

6A.6.1.1 Compressive Wave Loading

Very rapid compression of the drywell air could, theoretically, result in a compressive wave being generated in the weir annulus water. This wave could then travel down the weir annulus, through the vents, and across the pool to the containment wall. This phenomenon, evaluated at the PSTF, is not specifically included in the containment design conditions on the basis that the approximately 20 psi/sec pressure rate in the drywell is not sufficiently rapid to generate a compressive wave in the water. In addition, even if a 20 psi/sec wave were generated at the weir annulus surface, the very significant attenuation as the wave crosses the 20.5-ft-wide suppression pool would lead to insignificant containment wall loads. This phenomenon has never been observed in any GE pressure suppression test.

6A.6.1.2 Water Jet Loads

As described in Reference 1 (Section 3B.6.1.2).

6A.6.1.3 Initial Bubble Pressure

The PSTF air test data for runs 3 and 4 have been examined for evidence of bubble pressure loading of the suppression pool wall opposite the vents. These tests were chosen because the drywell pressure at the time of vent clearing was comparable to that expected in a full-scale Mark III (i.e., approximately 20 psid) and because the vent air flow rates and associated pool dynamics were more representative than the large-scale steam blowdown tests. The maximum bubble pressure load on the containment observed during PSTF testing was 10 psid (GESSAR Fig. 3B-18). GESSAR Fig. 38-56 is a summary of all the peak containment wall pressure observed in PSTF tests during the bubble formation phase of

the blowdown. The RBS design load which is based on these tests is shown in Fig. 6A.6-5.

The magnitude of the containment pressure increase following vent clearing is dependent upon the rate at which the drywell air bubble accelerates the suppression pool water. Circumferential variations in the air flow rate may occur due to drywell air/steam mixture variations, but negligible variations result in the containment bubble pressure load (Attachment H).

The conservative asymmetric condition assumes that air is vented on half of the drywell periphery and steam is vented on the other half.

For evaluation of the containment, the worst-case asymmetric loads are assumed to be those specified for the symmetric case but applied to only a 180-deg arc of the containment, drywell, and basemat.

6A.6.1.4 Hydrostatic Pressure

In addition to the hydrostatic load due to the suppression pool water, the data presented in Attachment E is used to determine the hydrostatic pressure loads on the containment during an earthquake. During periods of horizontal accelerations, there is an asymmetric distribution around the circumference of the containment.

6A.6.1.5 Local Containment Loads Resulting from Structures at or Near the Pool Surface

Any structures in the containment annulus that are at or near the suppression pool surface experience upward loads during pool swell. If these structures are attached to the containment wall, then the upward loads are transmitted into the containment wall. Sections 6A.9 and 6A.10 discuss the types of loads that will be transmitted.

Localized loads on the containment wall resulting from the pressure losses associated with water flowing past a body are depicted on Fig. 6A.6-6. Data presented in this figure are based on drag-type calculations and must be multiplied by $(V/40)^2$ if the pool swell velocity is greater than 40 ft/sec as calculated in Section 6A.10.1.

In addition, there will be impact forces on these attached structures unless the lower surface is immersed in the pool before pool swell. The half-wedge protrusion has an applied impact load time history as shown on Fig. 6A.6-7. The

velocity of impact (V) (from Section 6A.10.1) is taken to the height where the wedge is first fully submerged, i.e., upper surface. If the lower surface is initially submerged, the abscissa of Fig. 6A.6-7 is replaced by (Vt/h), where h is the unsubmerged height of the wedge. If the wedge angle is not 45 deg, the following ratios are used when applying Fig. 6A.6-7:

$$\frac{F_{\beta}}{F_{45}} = \left[\frac{(\beta)}{(90 - \beta)} \right]^2 \cot \beta$$

$$\frac{\tau_{\beta}}{\tau_{45}} = \cot \beta$$

For horizontal ledges, the impact forces are calculated in the following manner: ~

1. The force will have a triangular shape as shown in Fig. 6A.6-8.
2. The hydrodynamic mass of impact (per unit area) for flat targets from Fig. 6-8 of Reference 4 using b (not b/2) for target width.
3. Calculate the impulse using the following equation:

$$I_p = \frac{M_H}{A} V \cdot \frac{1}{(32.2) (144)}$$

Where:

I_p = Impulse per unit area, psi-sec

$\frac{M_H}{A}$ = Hydrodynamic mass per unit area, lbm/ft,
from (2) above

V = Impact velocity, ft/sec, determined according to Section 6A.10.1

4. Calculate the pulse duration from the equation:

$$\tau = 0.02 H/V (b/2)$$

Where:

τ = Pulse duration, sec

H = Height above pool, ft

b/2 =Width of ledge, ft

V = Impact velocity, ft/sec. determined according to Section 6A.10.1

5. The value of P_{\max} will be obtained using the following equation:

$$P_{\max} = 2 I_p / t$$

Where:

P_{\max} =Peak pressure, psi

6A.6.1.6 Containment Load Due to Pool Swell at the HCU Floor

This structure is approximately 22 ft above the pool surface and is 10 ft above the point where breakthrough occurs. Froth reaches the HCU floor approximately 1/2 sec after top vent clearing and generates both impingement loads on the structures and a flow pressure differential as it passes through the restricted annulus area at this elevation.

The impingement results in vertical loads on the containment wall from any structures attached to it, and the flow pressure differential results in an outward pressure loading on the containment wall at this location. For design, impingement loads as described in Sections 6A.11 and 6A.12 are applied; the containment wall sees an 11 psi discontinuous pressure loading at this elevation. Fig. 6A.6-9 shows details of the 11 psi pressure loading.

When evaluating the containment response to the pressure differential at the HCU floor, any additional loads transmitted to the containment via HCU floor supports (beam seats, etc) are assumed to occur simultaneously. These loads are based on the assumption that there is approximately 1,500 sq ft of vent area reasonably distributed around the annulus at this elevation. The question of circumferential variations in the pressure underneath the HCU floor is addressed in Section 6A.12 and Attachment K.

6A.6.1.7 Fallback Loads

As described in Reference 1 (Section 3B.6.1.7)

6A.6.1.8 Post Pool Swell Waves

As described in Reference 1 (Section 3B.6.1.8).

6A.6.1.9 Condensation Oscillation Loads

As described in Reference 1 (Section 3B.6.1.9).

6A.6.1.10 Chugging

As described in Reference 1 (Section 3B.6.1.10).

6A.6.1.11 Long-Term Transient

●→14

The discussion of the long-term transient given in GESSAR is applicable to River Bend Station except that the model used to simulate the long-term post-LOCA containment heatup transient is the SHEX model described in Sections 6.2.1.1.3.1 and 6.2.1.1.3.7.

6A. 6.1.12 Containment Environmental Envelope

Fig. 6A.6-4 is a diagram showing the maximum design containment pressure and temperature envelope for any size of credible primary system rupture. The calculated long-term containment pressure and temperature following a DBA are shown on Fig. 6.2-4 and 6.2-6, respectively.

Figures 6A.6-4a and 6A.6-4b show an envelope of the containment pressure and temperature based on the results of analyses performed with the GE M3CPT and SHEX codes with an initial thermal power of 3100 MWt.

14←●

6A.6.2 Containment Loads During an Intermediate Break Accident

As described in Reference 1 (Section 3B.6.2).

6A.6.3 Containment Loads During a Small Break Accident

No containment loads are generated by a small break in the drywell that are any more severe than the loads associated with the intermediate break. Fig. 6A.6-3 is the bar chart for this case.

There are unguarded reactor water cleanup (RWCU) lines in the containment that can release steam to the containment free space in the event of a rupture. The RWCU isolation valves and flow limiter for this system are designed to terminate the blowdown before significant containment pressurization can occur. A 0.53 psi pressure increase is predicted for RBS.

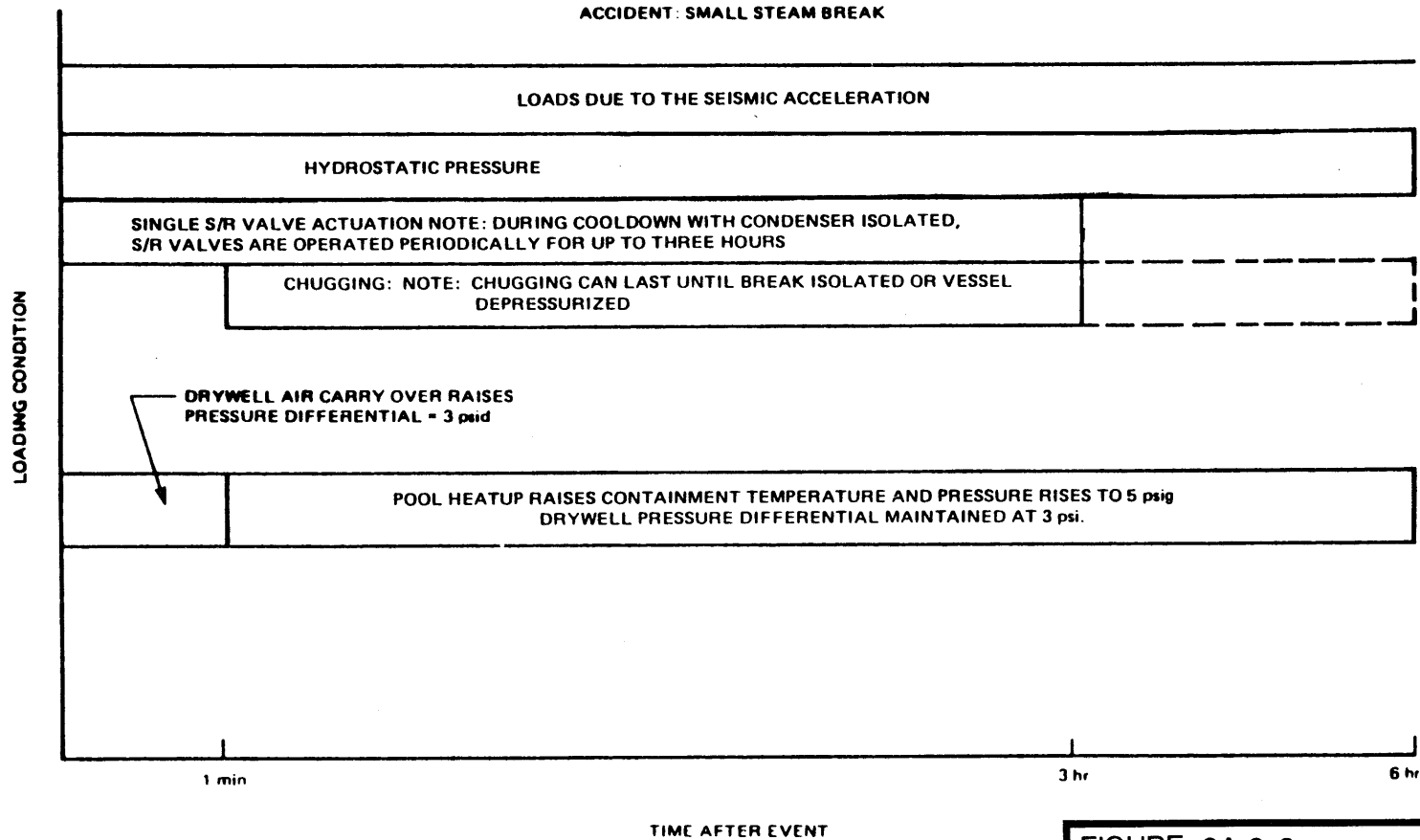
6A.6.4 Safety Relief Valve Loads

River Bend Station safety relief valve loads are discussed in Attachment A.

6A.6.5 Suppression Pool Thermal Stratification

The temperature profile given in GESSAR Fig. 3B-40 is for the standard plant, but is considered applicable also to River Bend Station.

**STRUCTURE: CONTAINMENT WALL
ACCIDENT: SMALL STEAM BREAK**



REF.: GESSAR FIG. 3B-67

FIGURE 6A.6-3

CONTAINMENT-LOADING
CHART FOR SBA

RIVER BEND STATION
UPDATED SAFETY ANALYSIS REPORT

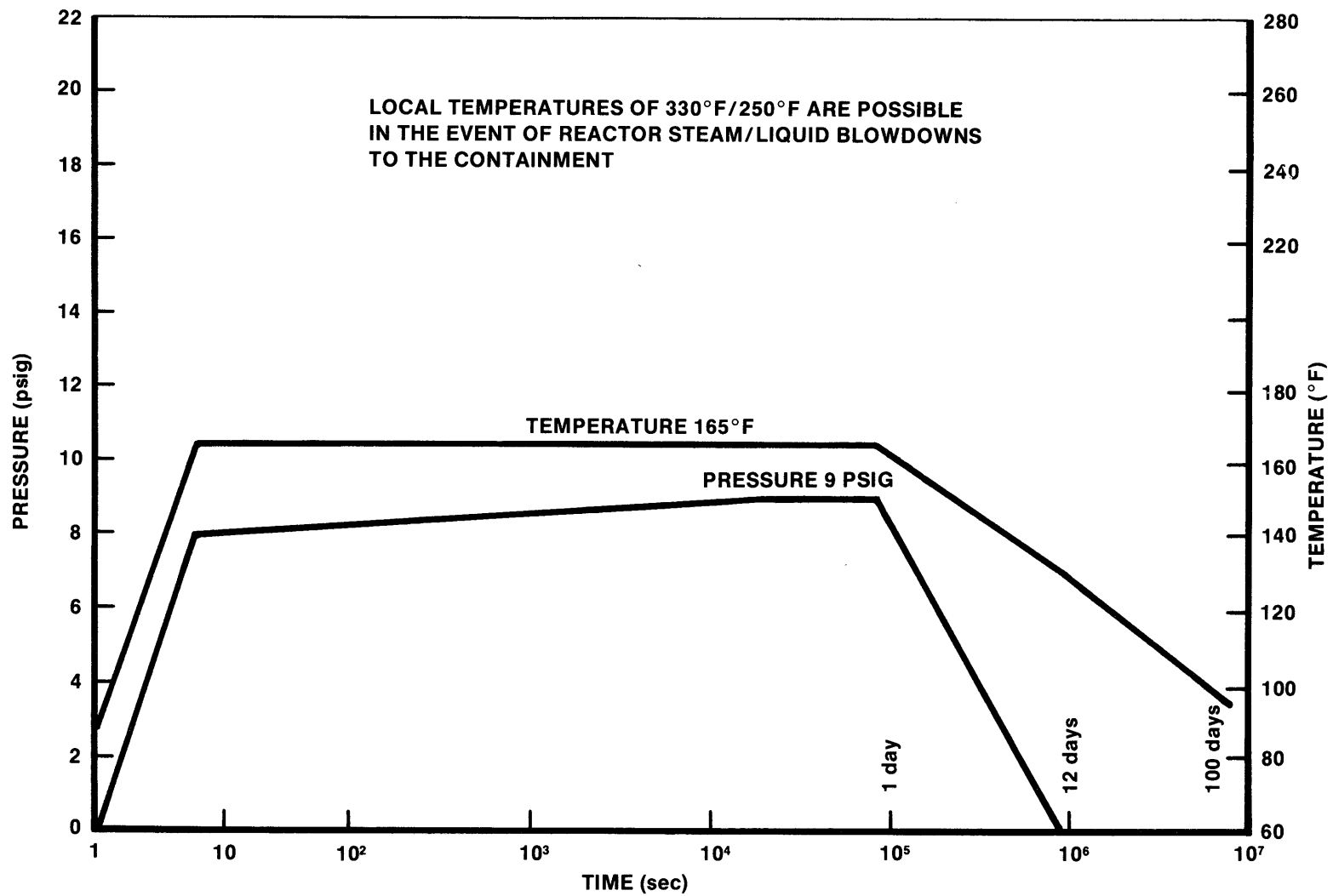


FIGURE 6A.6-4

CONTAINMENT ATMOSPHERE BULK
TEMPERATURE AND PRESSURE DESIGN
ENVELOPE FOR ALL BREAKS

RIVER BEND STATION
UPDATED SAFETY ANALYSIS REPORT

M3CPT & SHEX (3100 MWT)

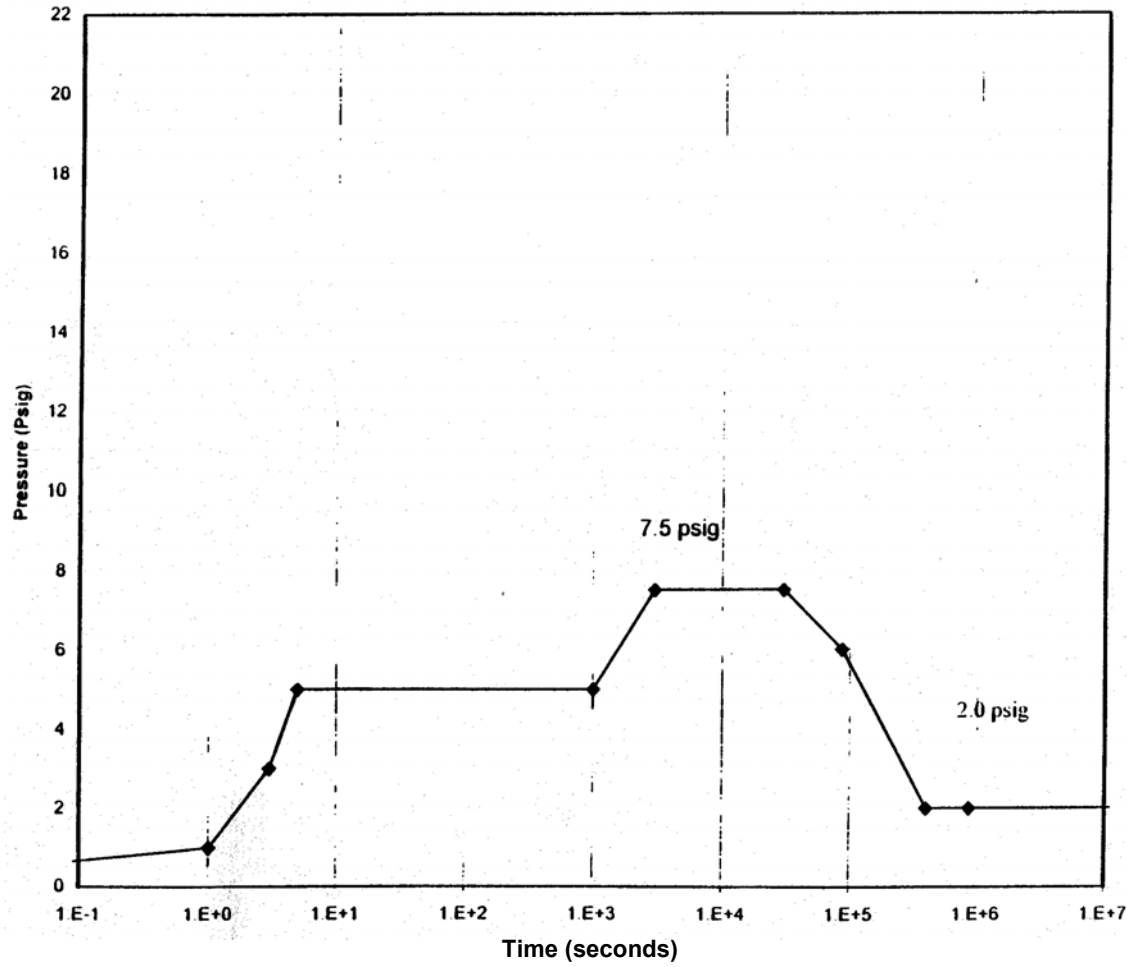


FIGURE 6A.6-4a

CONTAINMENT PRESSURE ENVELOPE

RIVER BEND STATION
UPDATED SAFETY ANALYSIS REPORT

M3CPT & SHEX (3100 MWT)

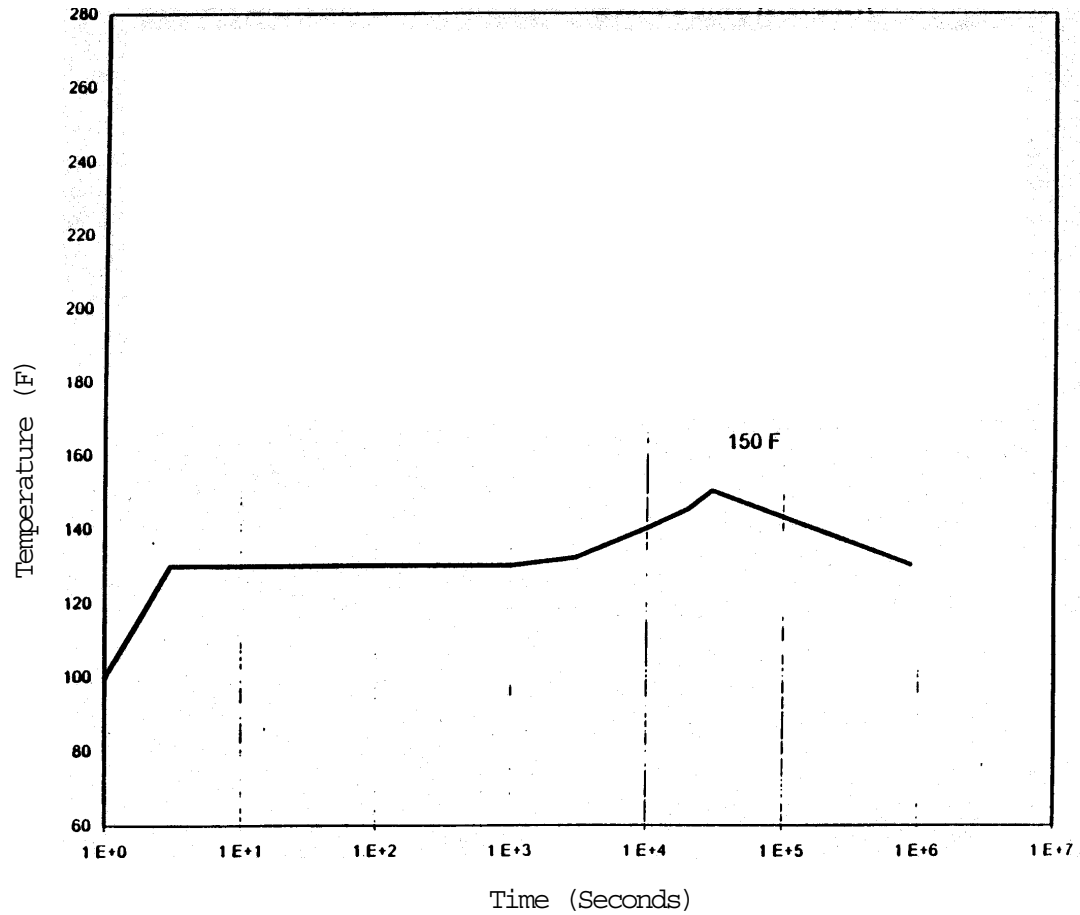
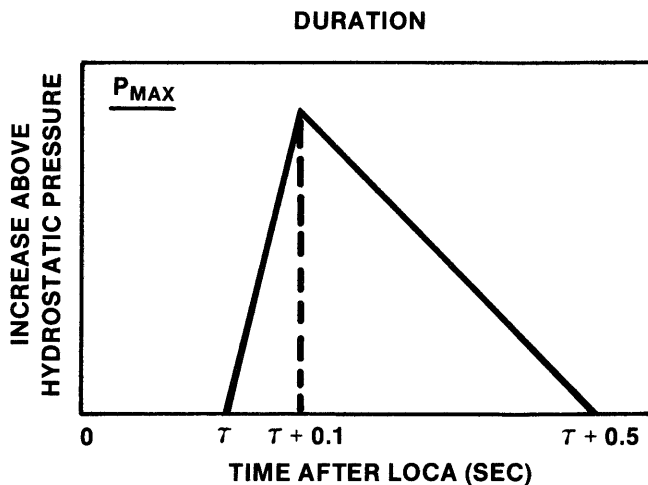
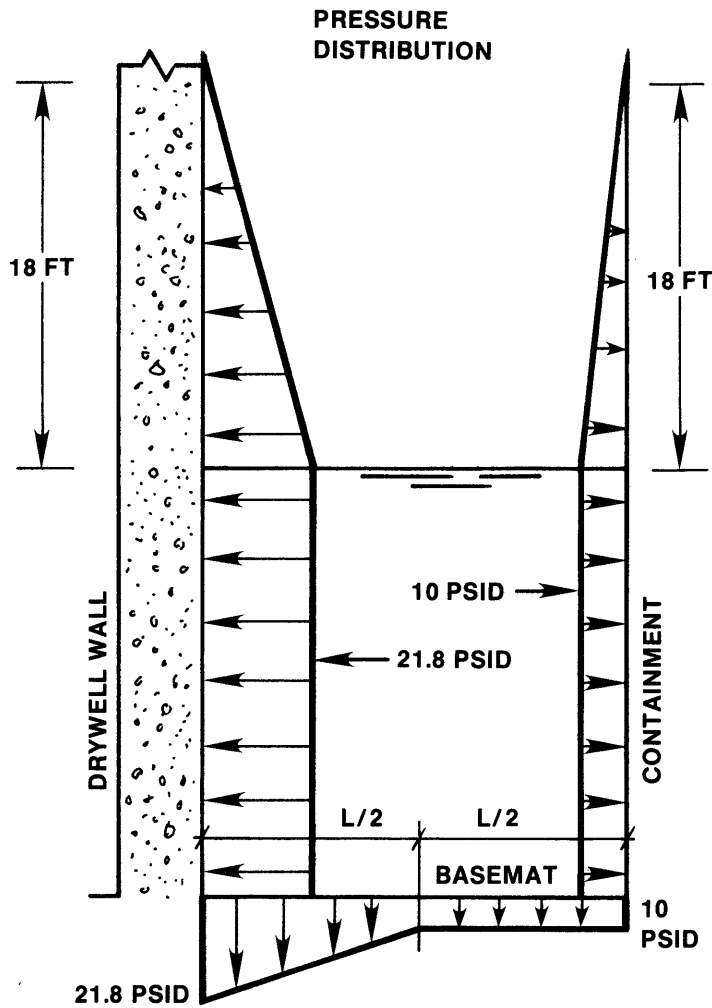


FIGURE 6A.6-4b

CONTAINMENT TEMPERATURE ENVELOPE

RIVER BEND STATION
UPDATED SAFETY ANALYSIS REPORT



FOR $Y < Y_0$, $\tau = 1.0$ SEC
 FOR $Y > Y_0$, $\tau = 1.0 + (Y - Y_0)$

WHERE

τ = DELAY DUE TO FINITE POOL SWELL VELOCITY

Y = HEIGHT ABOVE BASEMAT, FT.

Y_0 = INITIAL POOL DEPTH, FT
 (BASED UPON 40 FPS POOL SWELL VELOCITY)

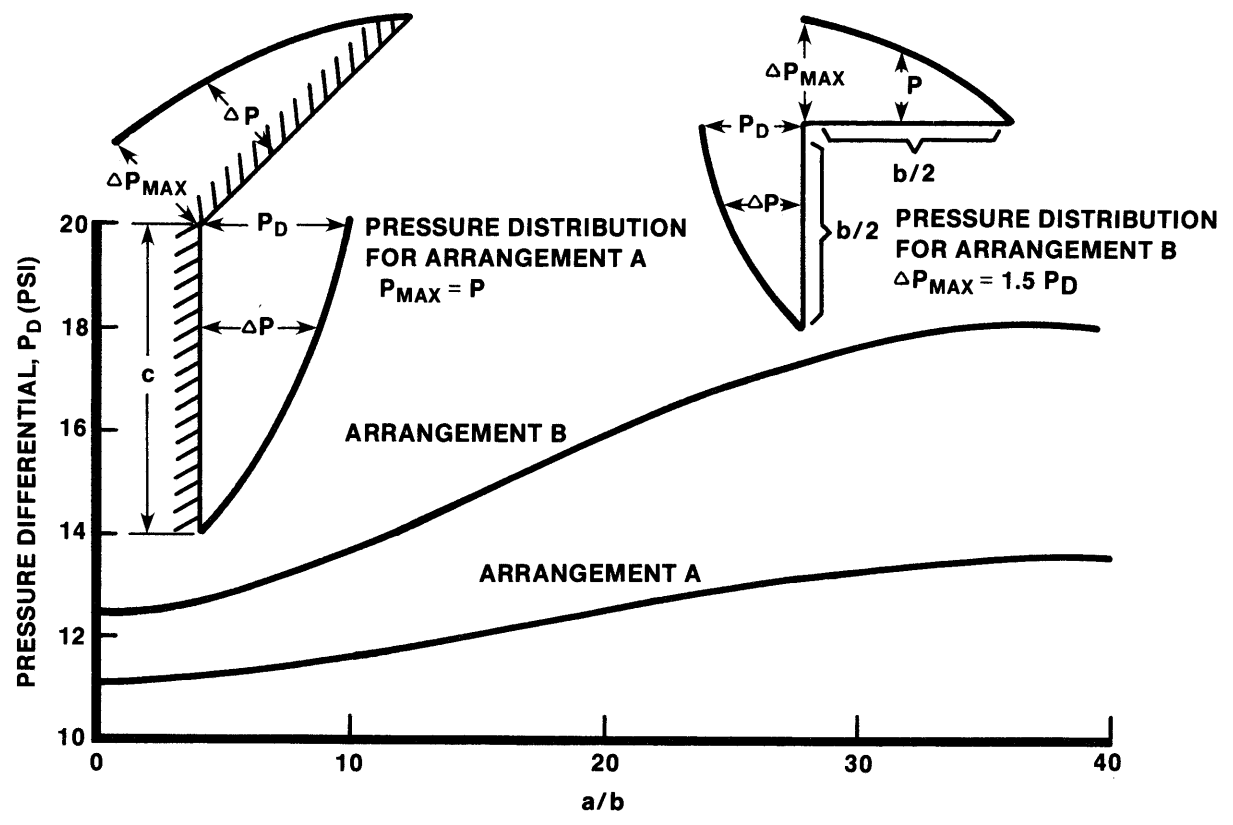
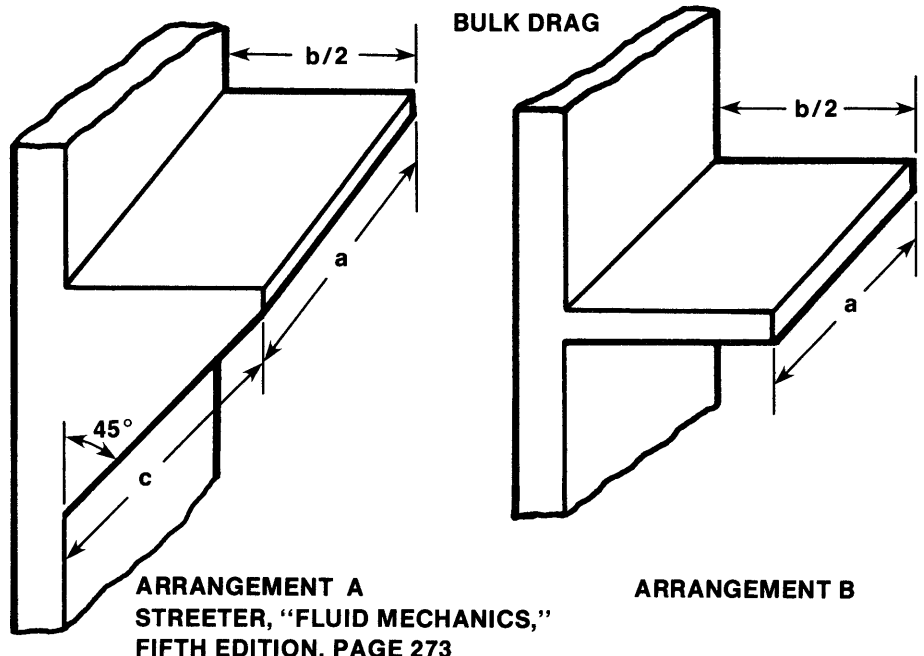
$Y_{MAX} = Y_0 + 18$ FT

REF.: GESSAR FIG. 3B-11

FIGURE 6A.6-5

DYNAMIC LOADS ASSOCIATED WITH INITIAL BUBBLE FORMATION IN THE POOL

RIVER BEND STATION
 UPDATED SAFETY ANALYSIS REPORT



REF.: GESSAR FIG. 3B-57

FIGURE 6A.6-6

DRAG LOADS ON PROTRUDING
STRUCTURES DUE TO POOL SWELL

RIVER BEND STATION
UPDATED SAFETY ANALYSIS REPORT

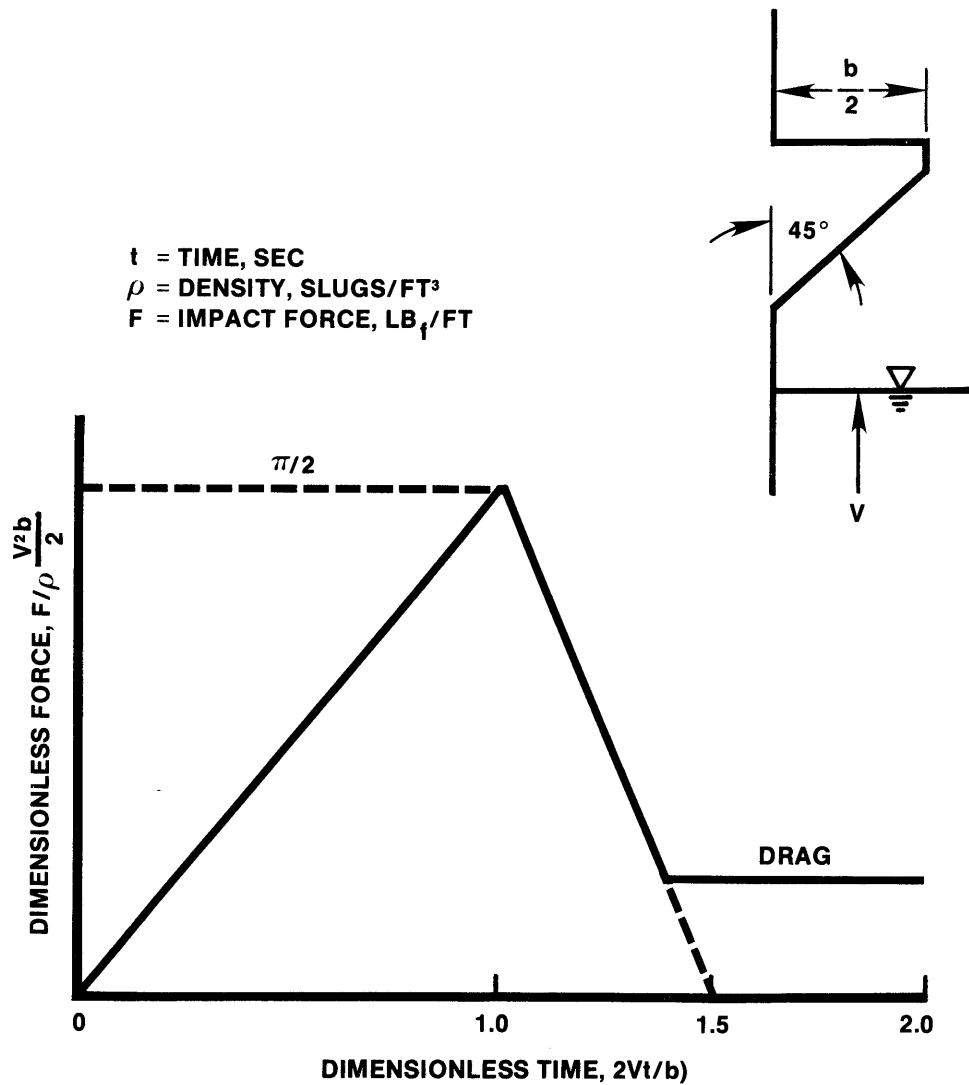


FIGURE 6A.6-7

IMPACT FORCE (PER UNIT LENGTH)
 ON WEDGE-SHAPED PROTRUSIONS FROM
 THE CONTAINMENT WALL

RIVER BEND STATION
 UPDATED SAFETY ANALYSIS REPORT

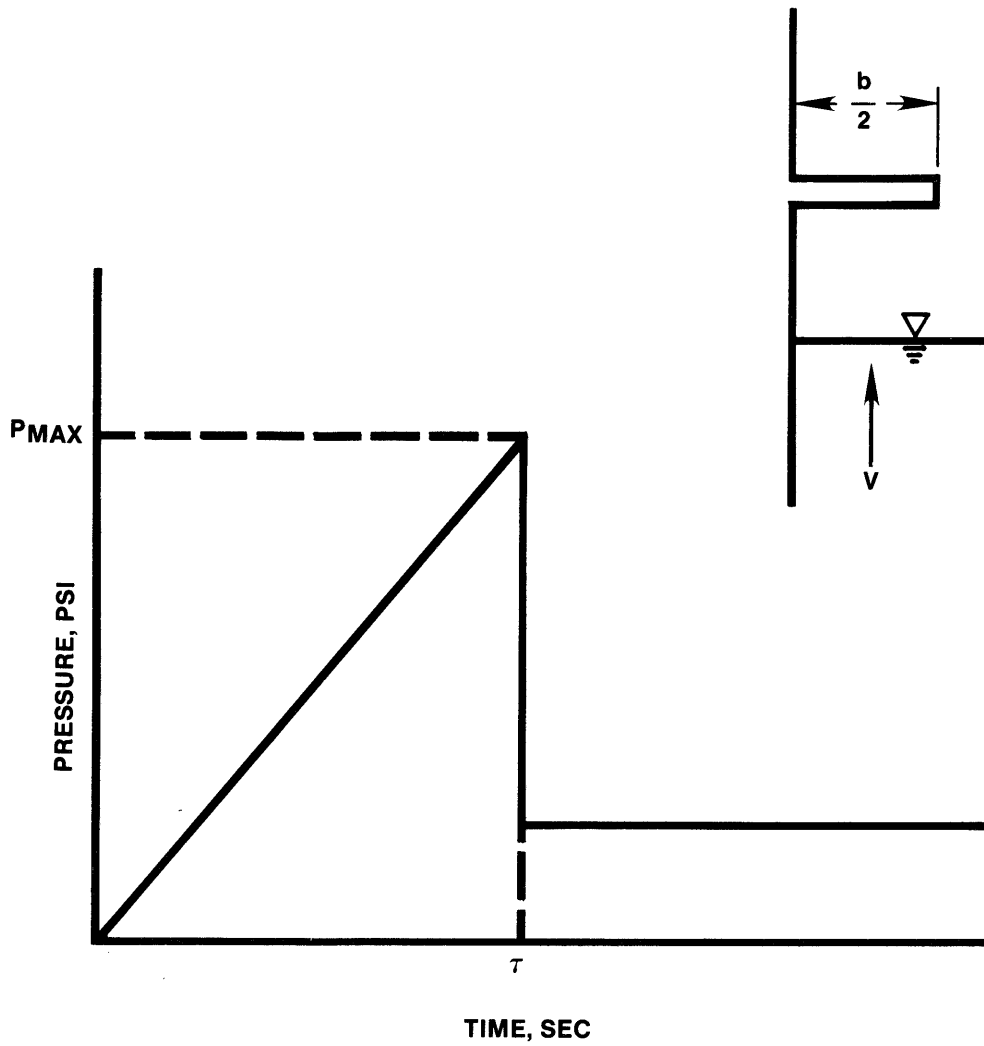
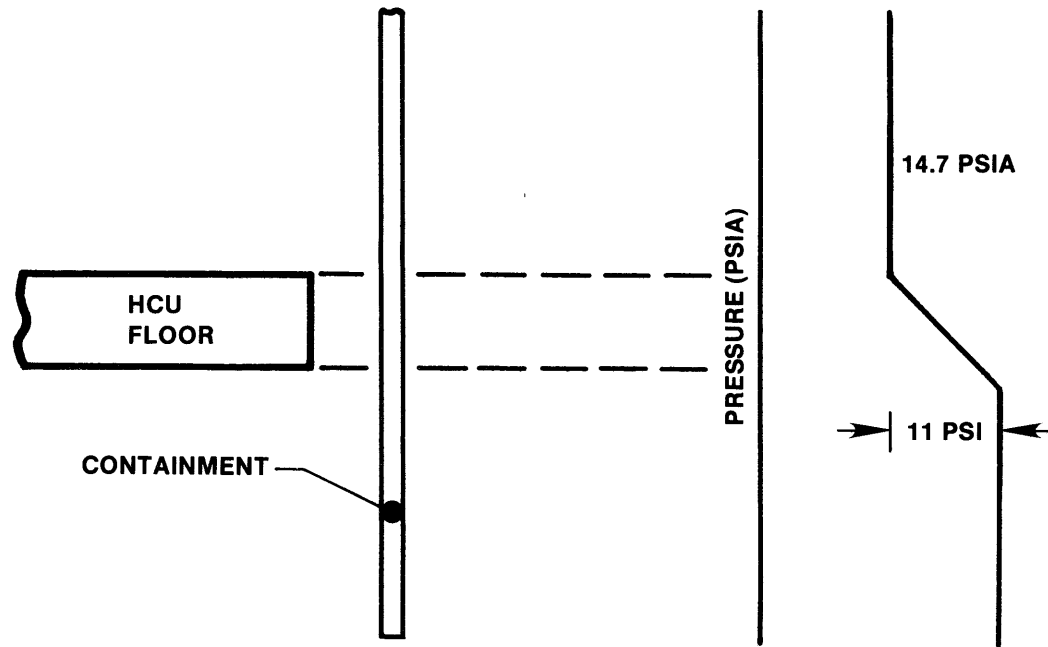


FIGURE 6A.6-8

IMPACT PRESSURE ON HORIZONTAL
LEDGES ATTACHED TO
CONTAINMENT WALL

RIVER BEND STATION
UPDATED SAFETY ANALYSIS REPORT



REF.: GESSAR FIG. 3B-58

FIGURE 6A.6-9

CONTAINMENT LOADING DUE TO FLOW
 ΔP ACROSS HCU FLOOR

RIVER BEND STATION
 UPDATED SAFETY ANALYSIS REPORT

6A.7 SUPPRESSION POOL BASEMAT LOADS

As decribed in Reference 1 (Section 3B.7).

6A.8 LOADS ON STRUCTURES IN THE SUPPRESSION POOL

There are certain structures within the suppression pool which experience dynamic loads during both LOCA and/or SRV actuation.

6A.8.1 Design Basis Accident

Fig. 6A.8-1 is the bar chart that defines the loads that structures in the suppression pool experience during the LOCA.

6A.8.1.1 Vent Clearing Jet Load

During the initial phase of the DBA, the drywell air space is pressurized and the water in the weir annulus vents is expelled to the pool, inducing a flow field in the suppression pool. This induced flow field creates a dynamic load on structures submerged in the pool. However, this dynamic load is less (Attachment L) than the load induced by the LOCA air bubble which forms after the water is expelled, except in the quencher strut. Vent clearing jet load on the strut is discussed in Section L.6A.2.2.

6A.8.1.2 Drywell Bubble Pressure and Drag Loads Due to Pool Swell

As described in Reference 1 (Section 3B.8.1.2).

6A.8.1.3 Fallback Loads

As described in Reference 1 (Section 3B.8.1.3).

6A.8.1.4 Condensation Loads

As described in Reference 1 (Section 3B.8.1.4).

6A.8.1.5 Chugging

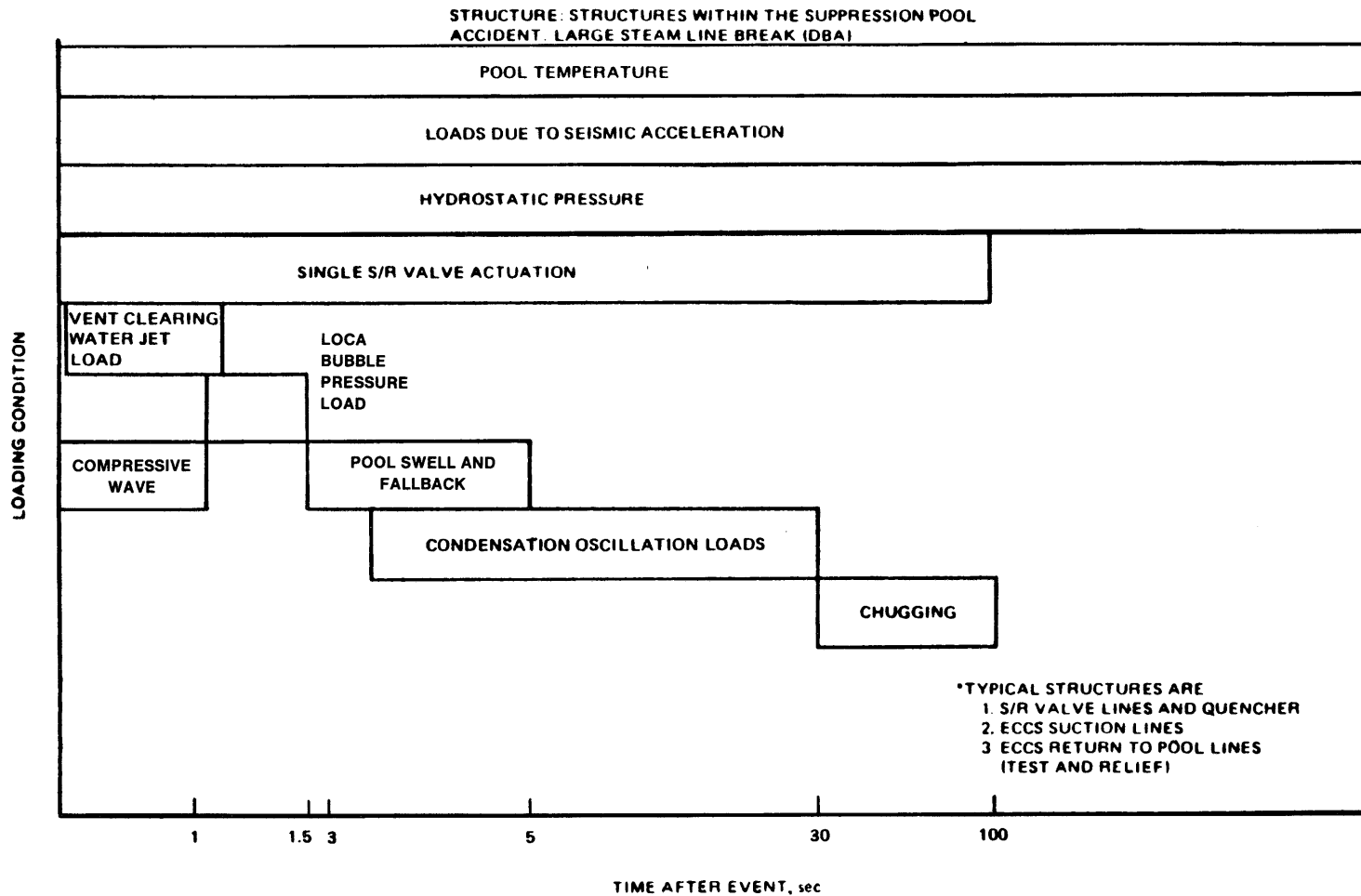
As described in Reference 1 (Section 3B.8.1.5).

6A.8.1.6 Compressive Wave Loading

As described in Reference 1 (Section 3B.8.1.6).

6A.8.1.7 Safety Relief Valve Actuation

As described in Reference 1 (Section 3B.8.1.7).



REF.: GESSAR FIG. 3B-69

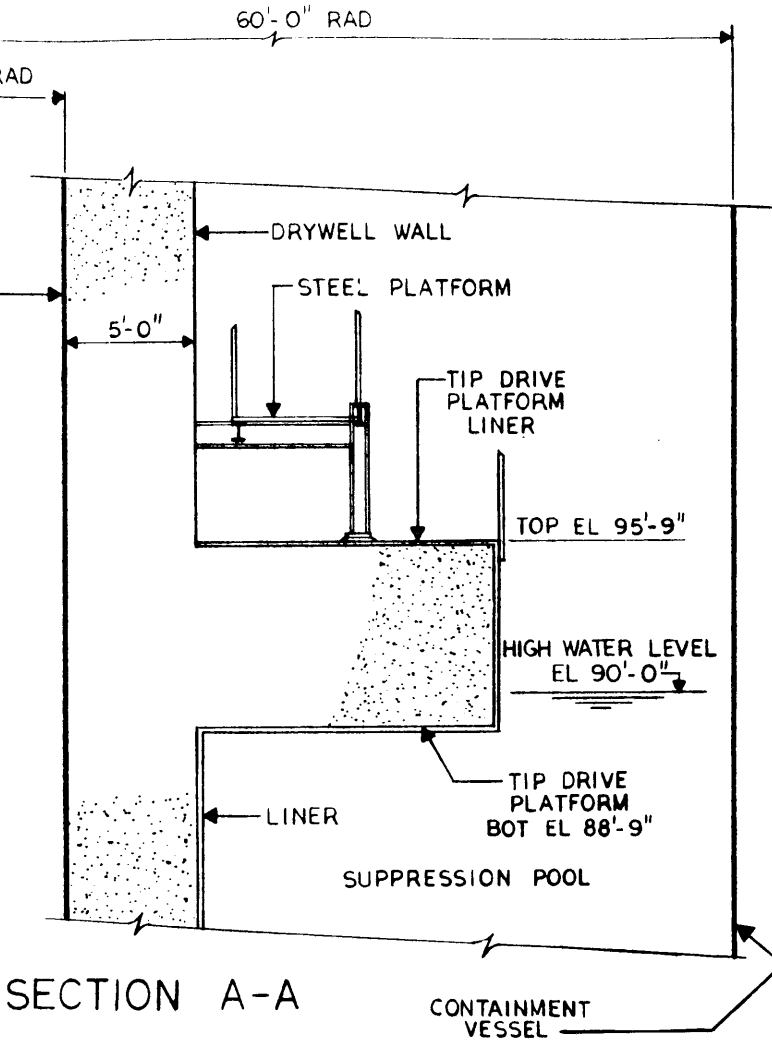
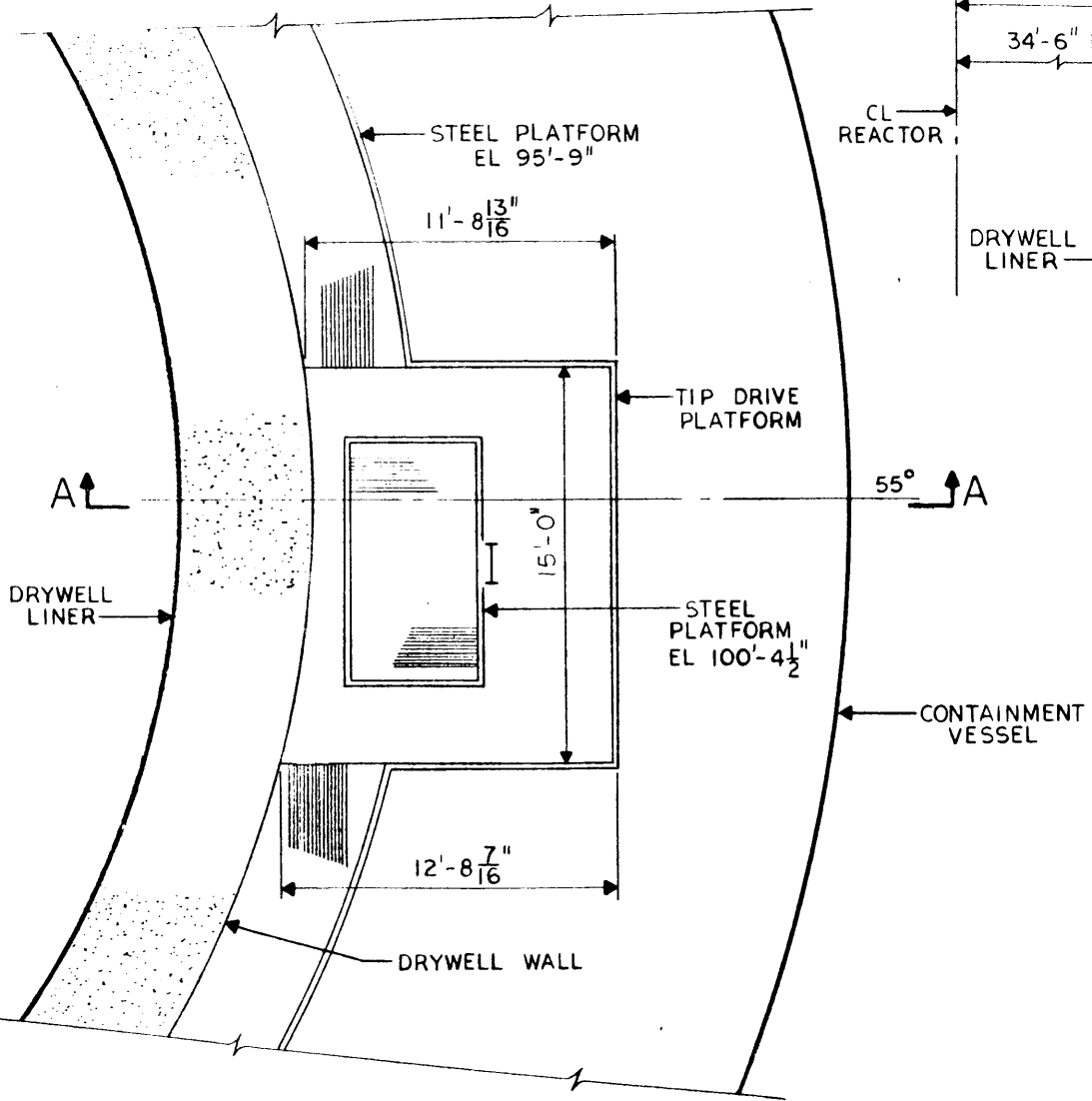
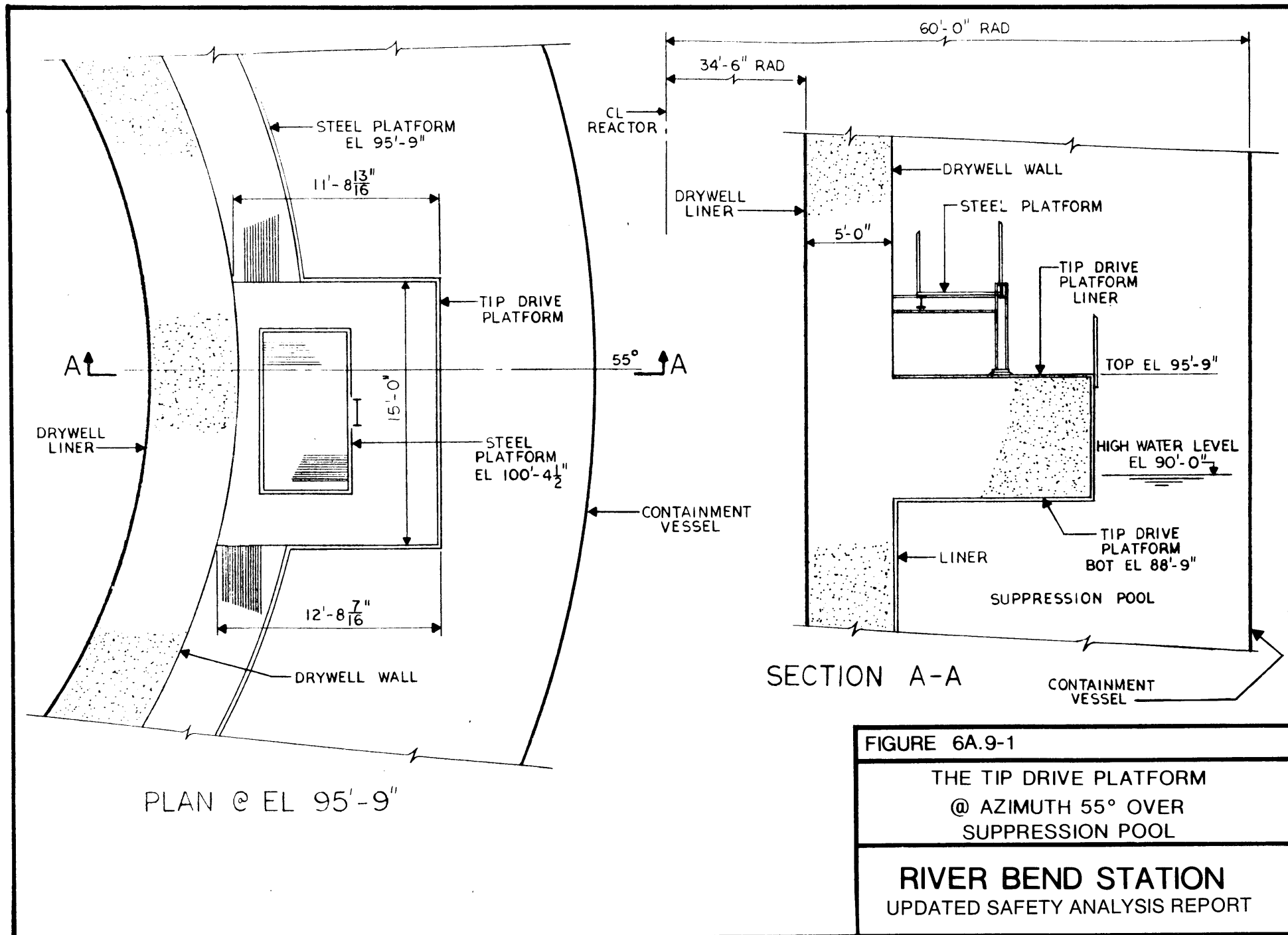
FIGURE 6A.8-1

STRUCTURES WITHIN SUPPRESSION
POOL-LOADING CHART FOR DBA

RIVER BEND STATION
UPDATED SAFETY ANALYSIS REPORT

6A.9 LOADS ON STRUCTURES AT THE POOL SURFACE

As described in Reference 1 (Section 3B.9).



6A.10 LOADS ON STRUCTURES BETWEEN THE POOL SURFACE AND THE HCU FLOORS

As described in Reference 1 (Section 3B.10).

6A.10.1 Impact Loads

•→10

All structures (e.g., beams and pipes) in the annulus above the suppression pool within 18 ft above the pool have widths less than 20 in. Impact loads due to bulk pool swell on these structures are as shown in Fig. 6A.10-2. For structures with impacted surface located less than 10 ft above the pool surface, the impact pressure can be reduced by:

$$\frac{p'}{P_{\max}} = (V/50)^2$$

where V is the slug velocity at the moment of impact in feet/sec.

All beams and pipes experiencing these impact loads fall within the conservative range as defined in GESSAR Fig. 3B.33-1 through Fig. 3B.33-4, with the pulse duration and pressure amplitude adjusted as follows:

1. Radial-oriented structures
 - a. For structures with impacted surfaces located within 6 ft of the pool surface, pulse duration τ_1 is given in Fig. 6A.10-7.
 - b. For structures less than 4 ft in length, the pulse duration τ_2 is given in Fig. 6A.10-8.
 - c. For structures both less than 4 ft in length and with surface impacted within 6 ft of the pool surface, the pulse duration is given by:

$$= (\tau_1 \times \tau_2) / 0.007$$
 - d. The value of τ need not be less than that calculated by:

Cylindrical targets

$$\tau = 0.0468 D/V$$

10←•

Flat targets

$$\tau = 0.011 W/V \text{ for } V \geq 7 \text{ ft/sec}$$

$$\tau = 0.0016 W \text{ for } V < 7 \text{ ft/sec}$$

where:

τ = Pulse duration

D = Diameter of target (ft)

W = Width of flat structure (ft)

V = Impact velocity (ft/sec)

- e. The pressure load is increased if the duration is less than 0.007 seconds. This increase is given by:

$$p = p' (0.007/\tau)$$

where:

p' = Peak pressure shown in Fig. 6A.10-2, adjusted as noted above for structures within 10 ft of the pool surface.

2. Circumferential-oriented structures

•→10

- a. For structures with impacted surface located within 6 ft of the pool surface, the pulse duration is given in Fig. 6A.10-9.
- b. For structures with impacted surface located greater than 6 ft above the pool surface, the pulse duration of Fig. 6A.10-2 is used as long as the criteria of GESSAR Fig. 3B.33-3 and 3B.33-4 are met.
- c. The value of τ need not be less than that calculated by:

Cylindrical targets

$$\tau = 0.0468 D/V$$

10←•

Flat targets

$$\tau = 0.011 W/V \text{ for } V \geq 7 \text{ ft/sec}$$

$$\tau = 0.0016 W \text{ for } V < 7 \text{ ft/sec}$$

where τ , D, W, and V are defined as above.

- d. If τ is less than 0.007 sec, the pressure amplitude is increased by:

$$p = p' (0.007/\tau)$$

where p' is defined as above.

There are no impact loads on gratings. The width of the grating surfaces does not sustain an impact load.

For structures between 18 and 19 ft above the pool surface, the impact load is interpolated between the values described above and the froth impact loading described in Section 6A.12. The duration is also interpolated from 0.007 sec at 18 ft to 0.100 sec at 19 ft. Fig. 6A.10-3 demonstrates this transition.

Impact loads on structures attached to the containment wall are described in Section 6A.6.

•→10

Impact loads acting on structures are based on a pool swell velocity at the moment of impact which varies with height above the pool surface. This variation is given by:

$$\begin{aligned} V &= 5H (2.6 - 0.506 \sqrt{H}) && \text{for } H < 10 \text{ ft}^* \\ V &= 50 \text{ ft/sec} && \text{for } 20 \geq H \geq 10 \text{ ft} \\ V &= \sqrt{3788 - 64.4 H} && \text{for } 30 \geq H > 20 \text{ ft} \end{aligned}$$

Where H is the distance of the impacted surface of structure above the pool surface for calculation of P'.

6A.10.2 Drag Loads

The drag load on grating is based on Fig. 6A.10-4. The drag load found from this figure is multiplied by $(V/40)^2$ if V is greater than 40 ft/sec where V is the maximum pool swell velocity found at the geometric center of the structure.

For drag loads on flat plates, Fig. 6A.10-5 is used. If the velocity is greater than 40 ft/sec, the drag load is multiplied by $(V/40)^2$. If the shorter side (b) is attached to the containment or drywell wall, the abscissa in Fig. 6A.10-5 becomes $2(a/b)$ instead of a/b .

For other shapes, Fig. 6A.10-6 is used to calculate the pressure for 40 ft/sec. If the pool swell velocity, V, is

10←•

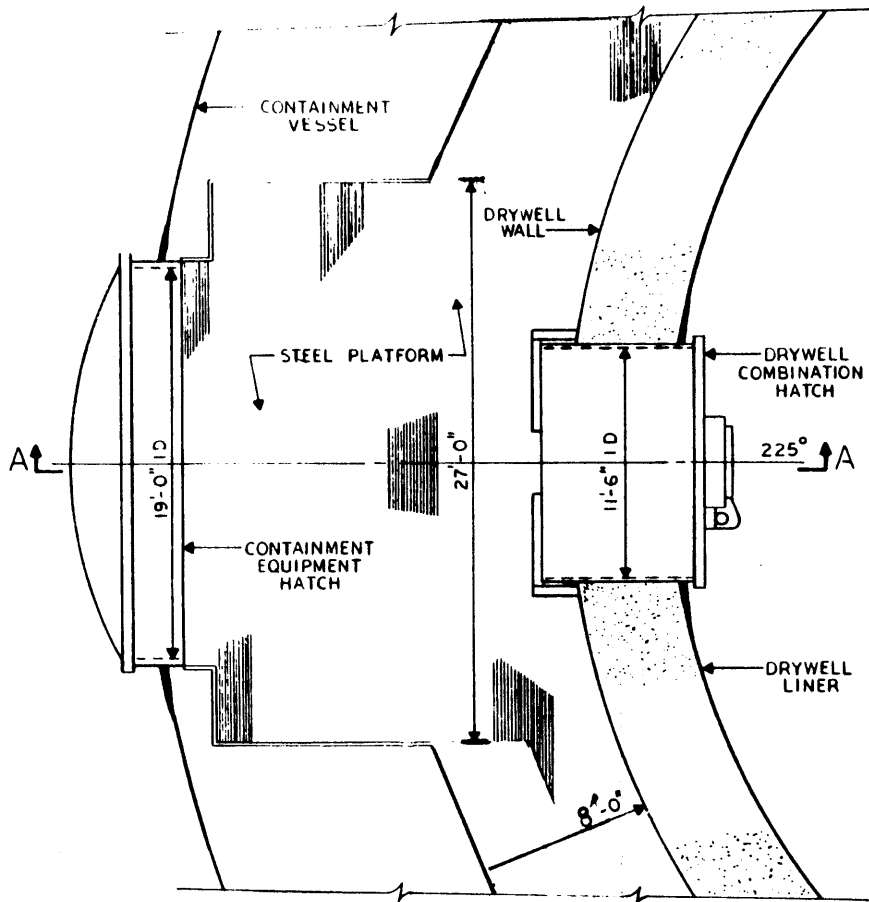
*V less than 20 ft/sec shall not be used.

greater than 40 ft/sec, the pressure is multiplied by $(V/40)^2$.

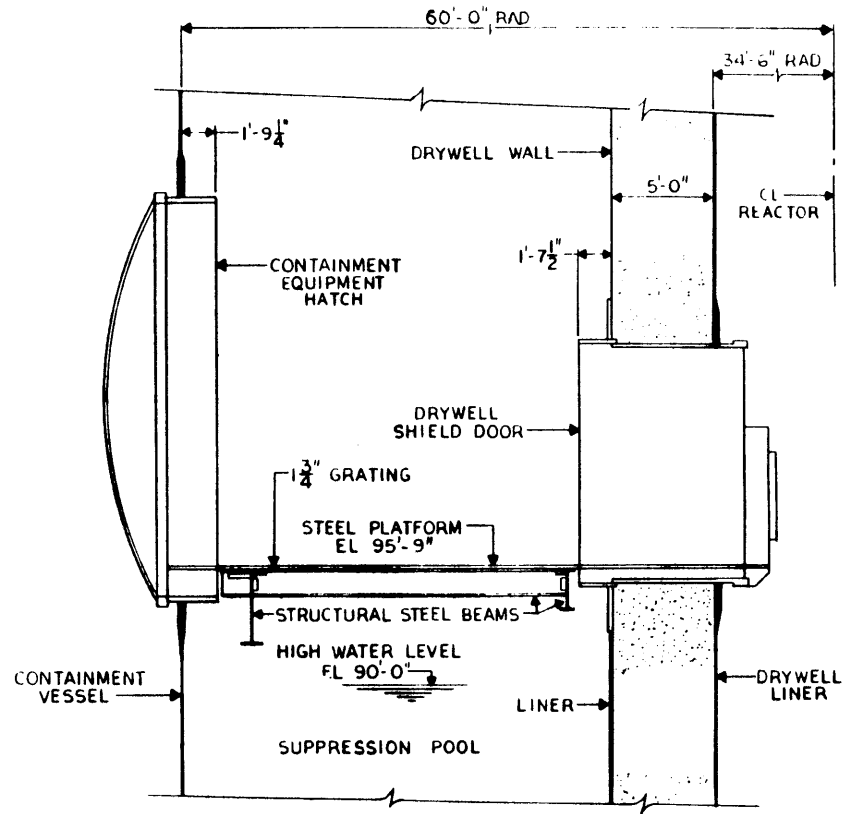
For all drag loads, the duration is 0.5 sec.

6A.10.3 Fallback Loads

As described in Reference 1 (Section 3B.10.3).



PLAN @ EL 95'-9"

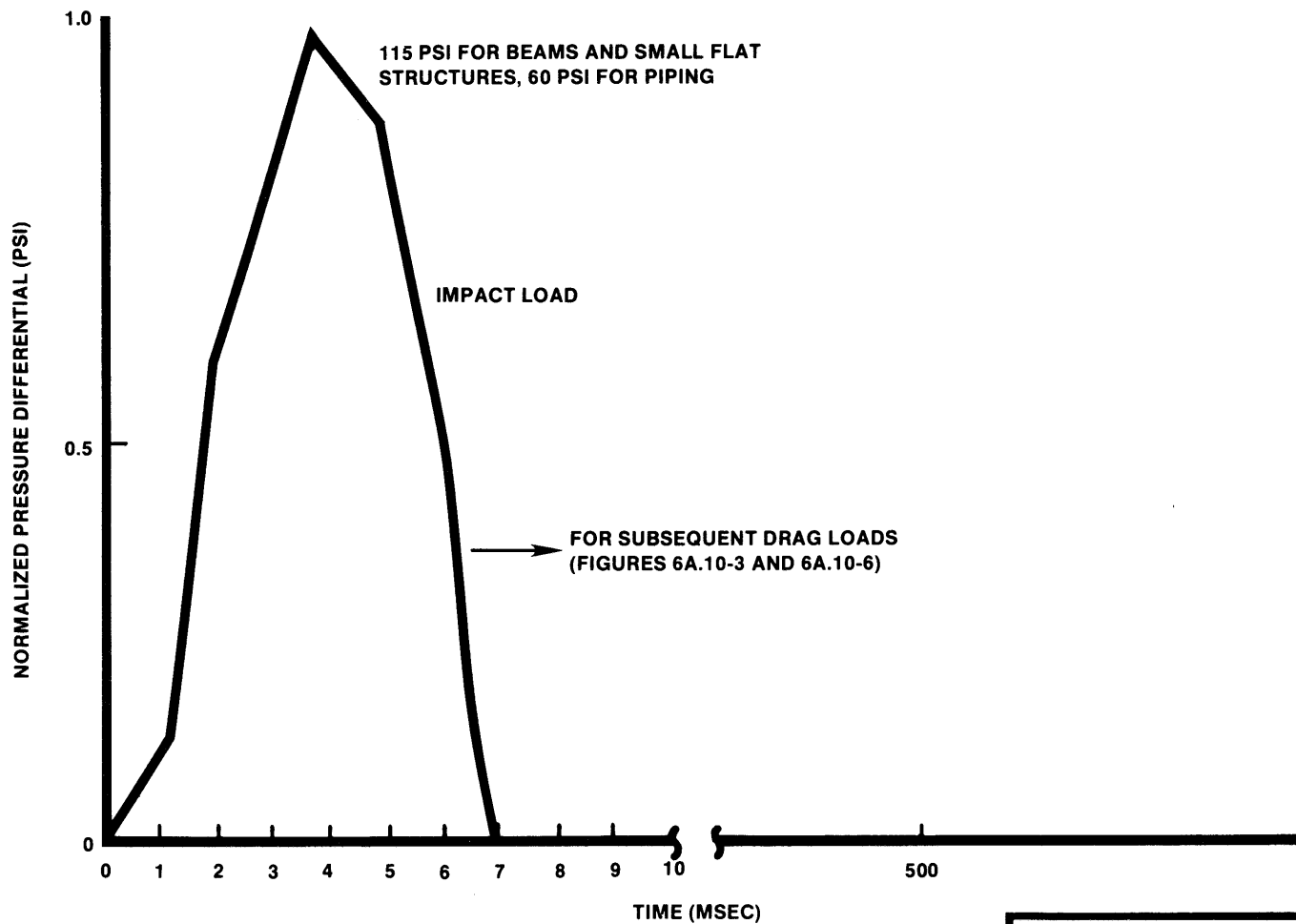


SECTION A-A

FIGURE 6A.10-1

THE STRUCTURES
@ AZIMUTH 225°
OVER SUPPRESSION POOL

RIVER BEND STATION
UPDATED SAFETY ANALYSIS REPORT



REF.: GESSAR FIG. 3B-72

FIGURE 6A.10-2
PROFILE OF IMPACT LOADS ON SMALL STRUCTURES WITHIN 18 FEET OF THE POOL SURFACE
RIVER BEND STATION UPDATED SAFETY ANALYSIS REPORT

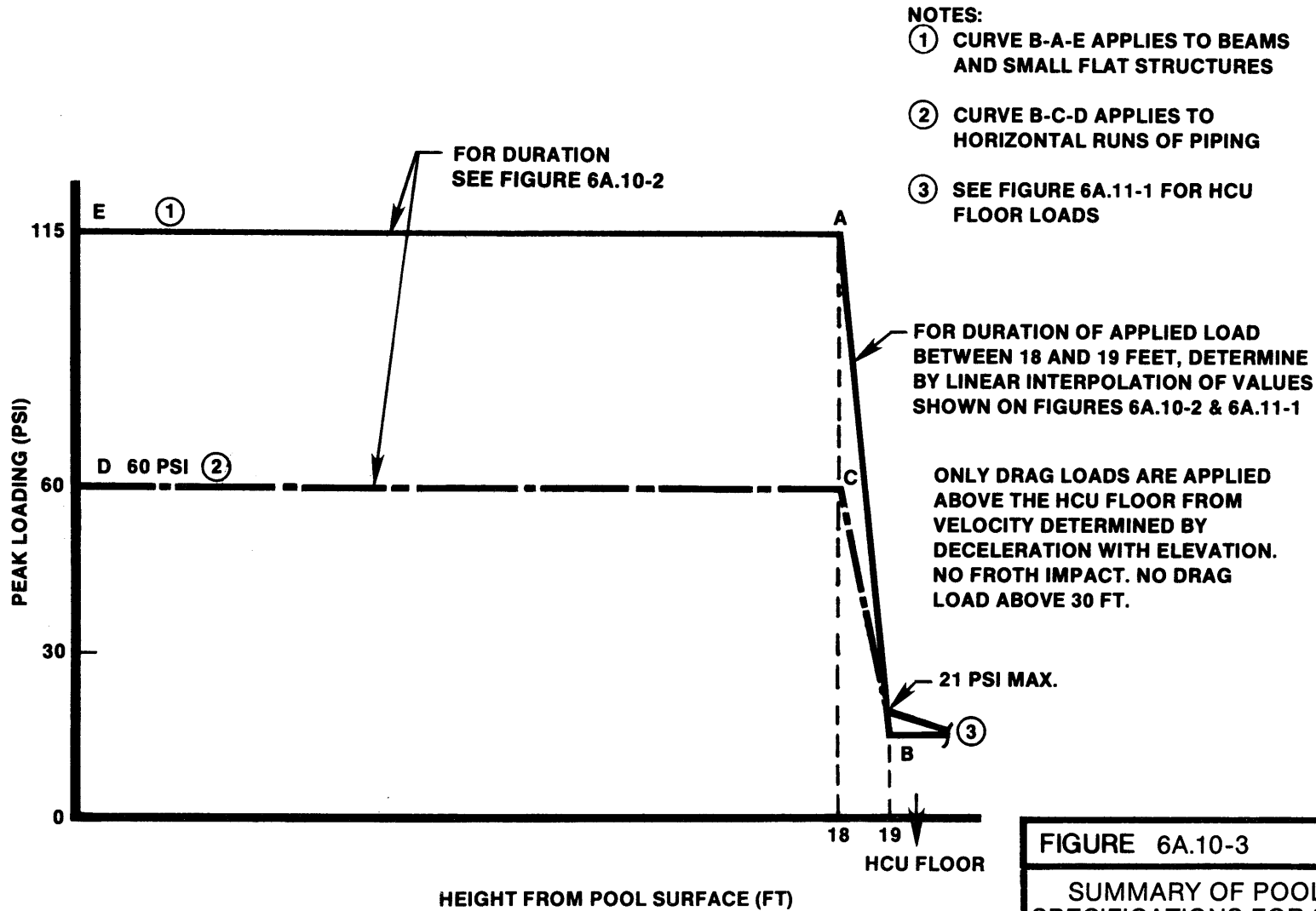
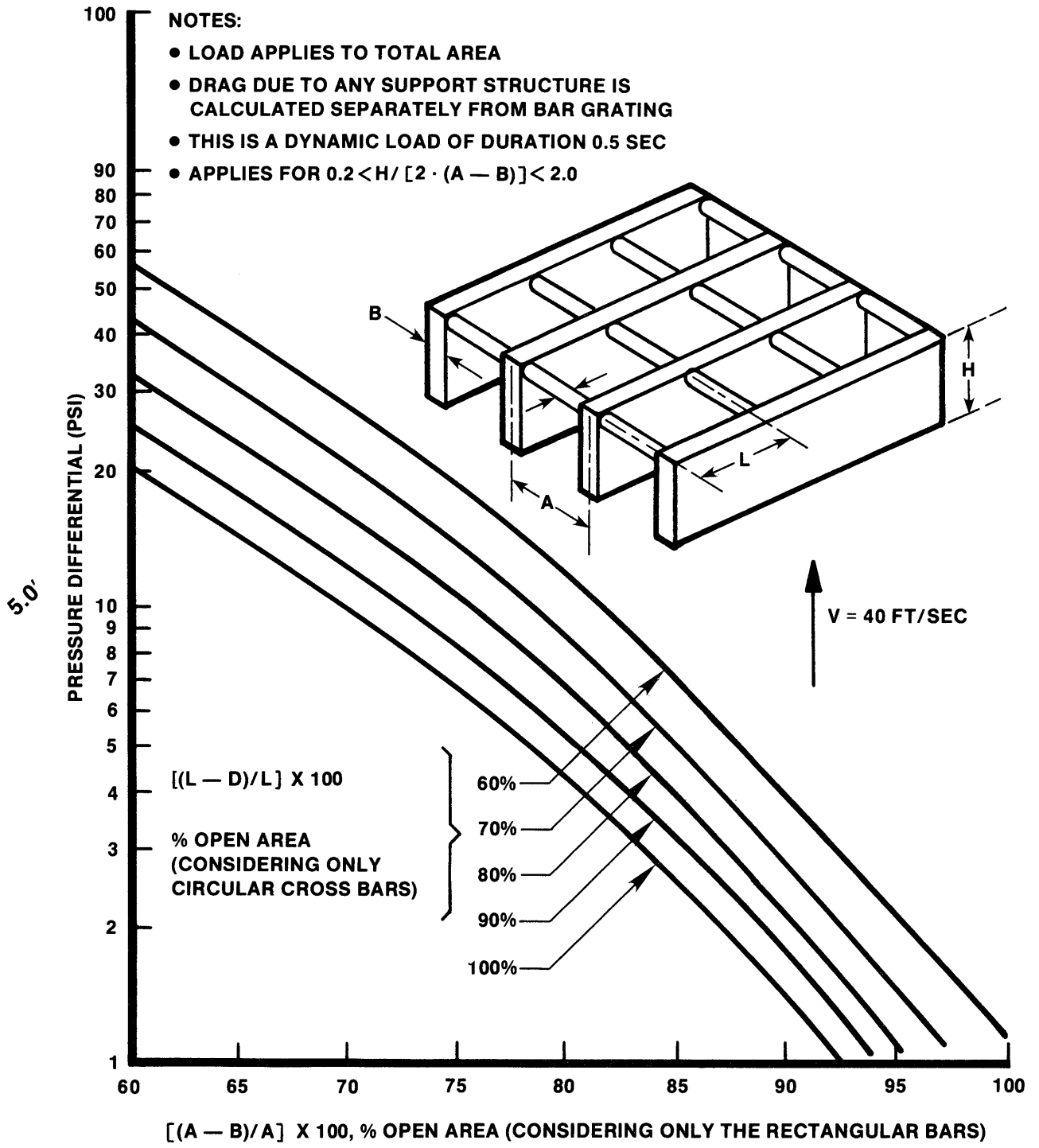


FIGURE 6A.10-3

SUMMARY OF POOL SWELL LOADING SPECIFICATIONS FOR SMALL STRUCTURES IN THE CONTAINMENT ANNULUS (NOT APPLICABLE TO THE STEAM TUNNEL OR EXPANSIVE HCU FLOORS)

RIVER BEND STATION
 UPDATED SAFETY ANALYSIS REPORT

REF.: GESSAR FIG. 3B-75

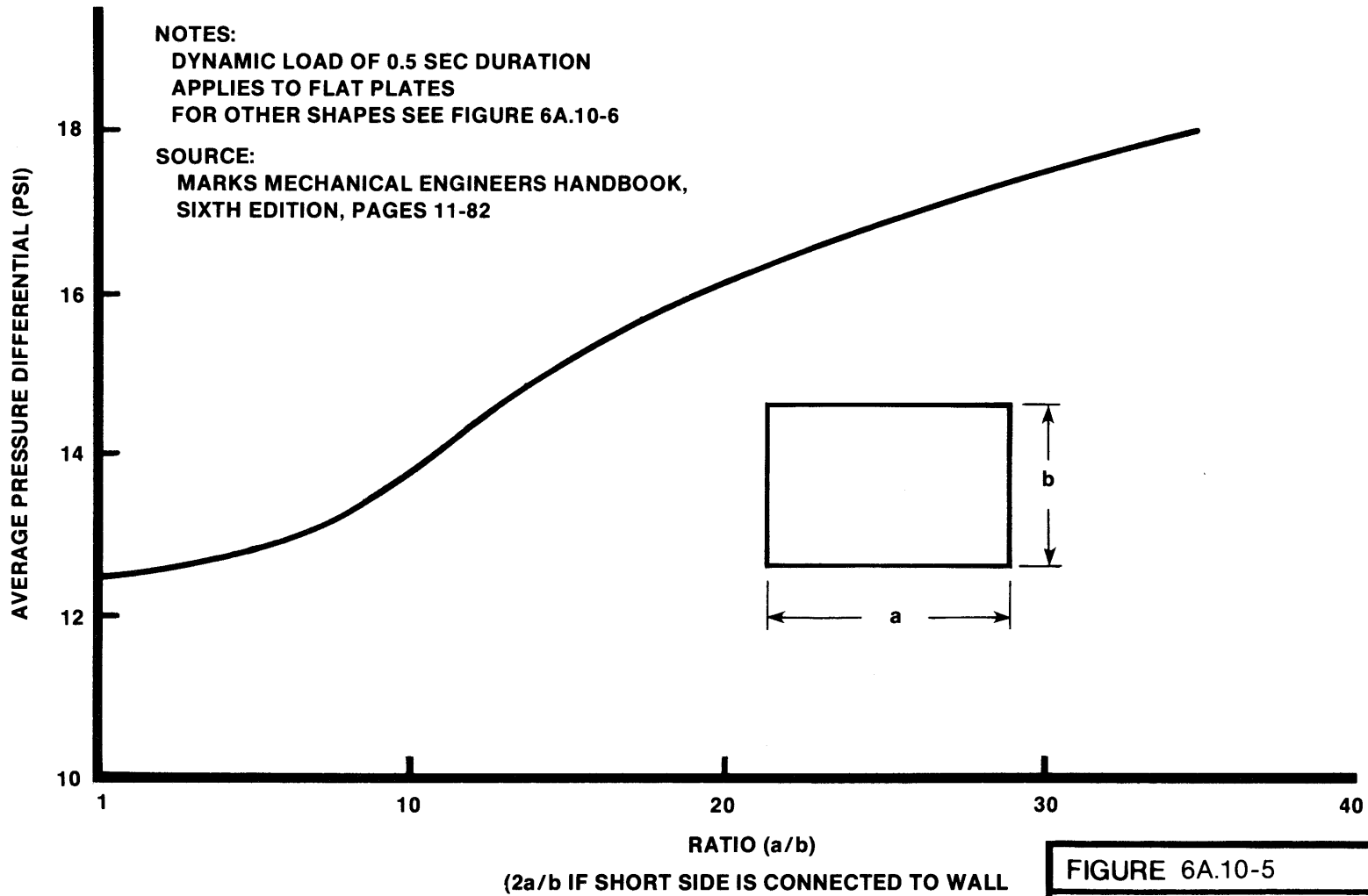


REF.: GESSAR FIG. 3B-73

FIGURE 6A.10-4

PRESSURE DROP DUE TO FLOW ACROSS GRATING WITHIN 18 FEET OF THE POOL SURFACE FOR 40 FT/SEC. POOL SWELL

RIVER BEND STATION
UPDATED SAFETY ANALYSIS REPORT



REF.: GESSAR FIG. 3B-76

FIGURE 6A.10-5
 DRAG LOAD
 ON SOLID STRUCTURES WITHIN
 18 FEET OF THE POOL SURFACE

RIVER BEND STATION
 UPDATED SAFETY ANALYSIS REPORT

(REF: FLUID MECHANICS, VICTOR L STREETER, FIFTH EDITION MCGRAW HILL)

BODY SHAPE	DRAG COEFFICIENT* C_D		BASED ON $V=40$ fps PRESSURE DIFFERENTIAL (psi)	BASED ON $V=35$ fps PRESSURE DIFFERENTIAL (psi)
CIRCULAR CYLINDER	1.2		13	10
CIRCULAR CYLINDER (UPRIGHT)	0.99		$L/D \leq 7$ 11	8.5
ELLIPTICAL CYLINDER	0.6		2:1 7	8
ELLIPTICAL CYLINDER	0.32		4:1 4	3
ELLIPTICAL CYLINDER	0.29		8:1 3	2
SQUARE	2.0		22	17
TRIANGLE	2.0		120° 22	17
TRIANGLE	1.72		120° 19	14
TRIANGLE	2.15		90° 23	18
TRIANGLE	1.6		90° 17	13
TRIANGLE	2.2		60° 24	18
TRIANGLE	1.39		60° 15	12
TRIANGLE	1.8		30° 19	15
TRIANGLE	1.0		30° 11	8
SEMITUBULAR	2.3		25	19
SEMITUBULAR	1.12		12	9

*These drag coefficients are conservative because they are for low Reynold's Number flow conditions (10^4 - 10^5 Range).
Use of lower values may be used if its applicability can be demonstrated.

REF GESSAR FIG. 3B-19
GE REPORT NEDE-21730

FIGURE 6A.10-6

DRAG LOADS FOR VARIOUS GEOMETRIES
(SLUG FLOW)

RIVER BEND STATION
UPDATED SAFETY ANALYSIS REPORT

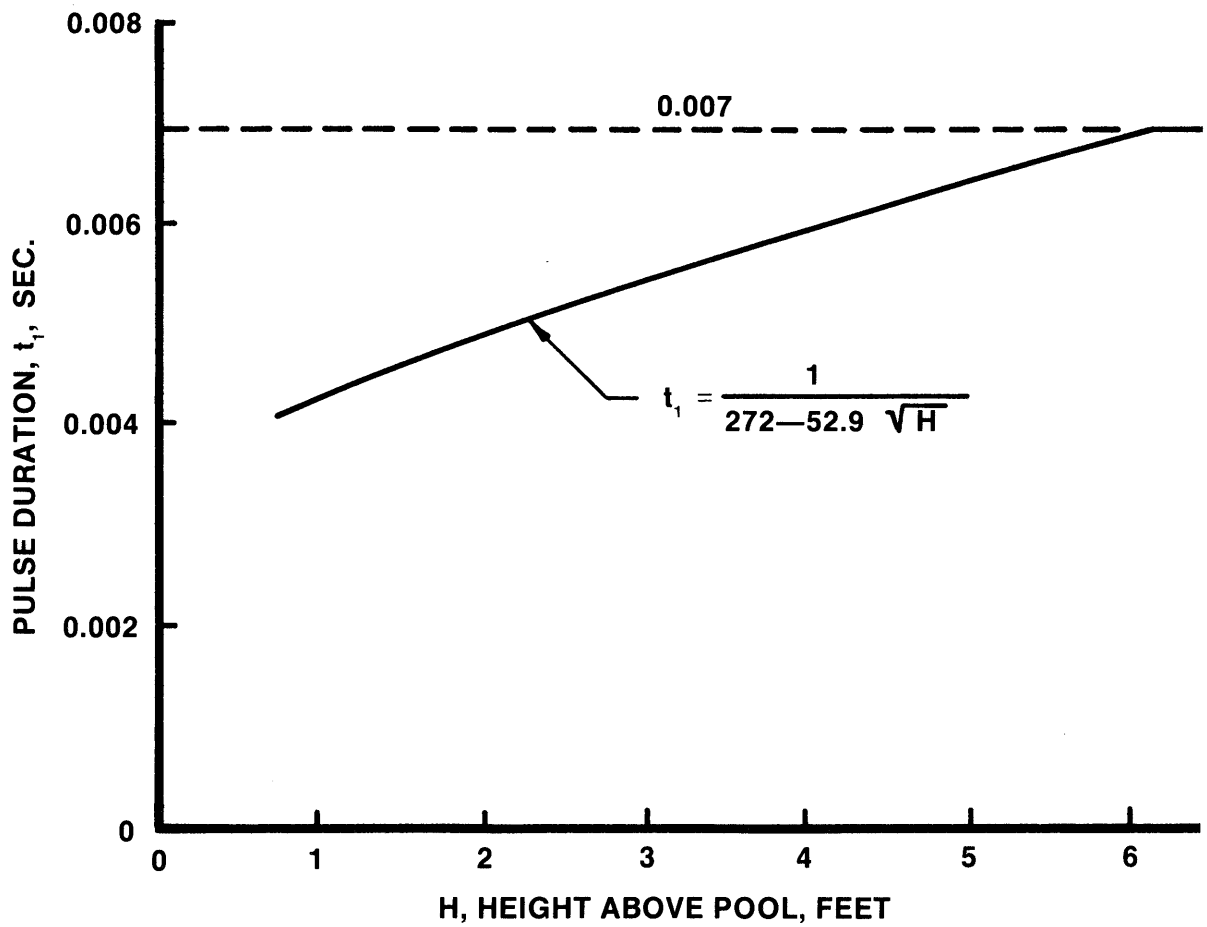


FIGURE 6A.10-7

REDUCTION IN PULSE DURATION FOR
RADIAL STRUCTURES CLOSER THAN
6 FEET TO THE POOL SURFACE

RIVER BEND STATION
UPDATED SAFETY ANALYSIS REPORT

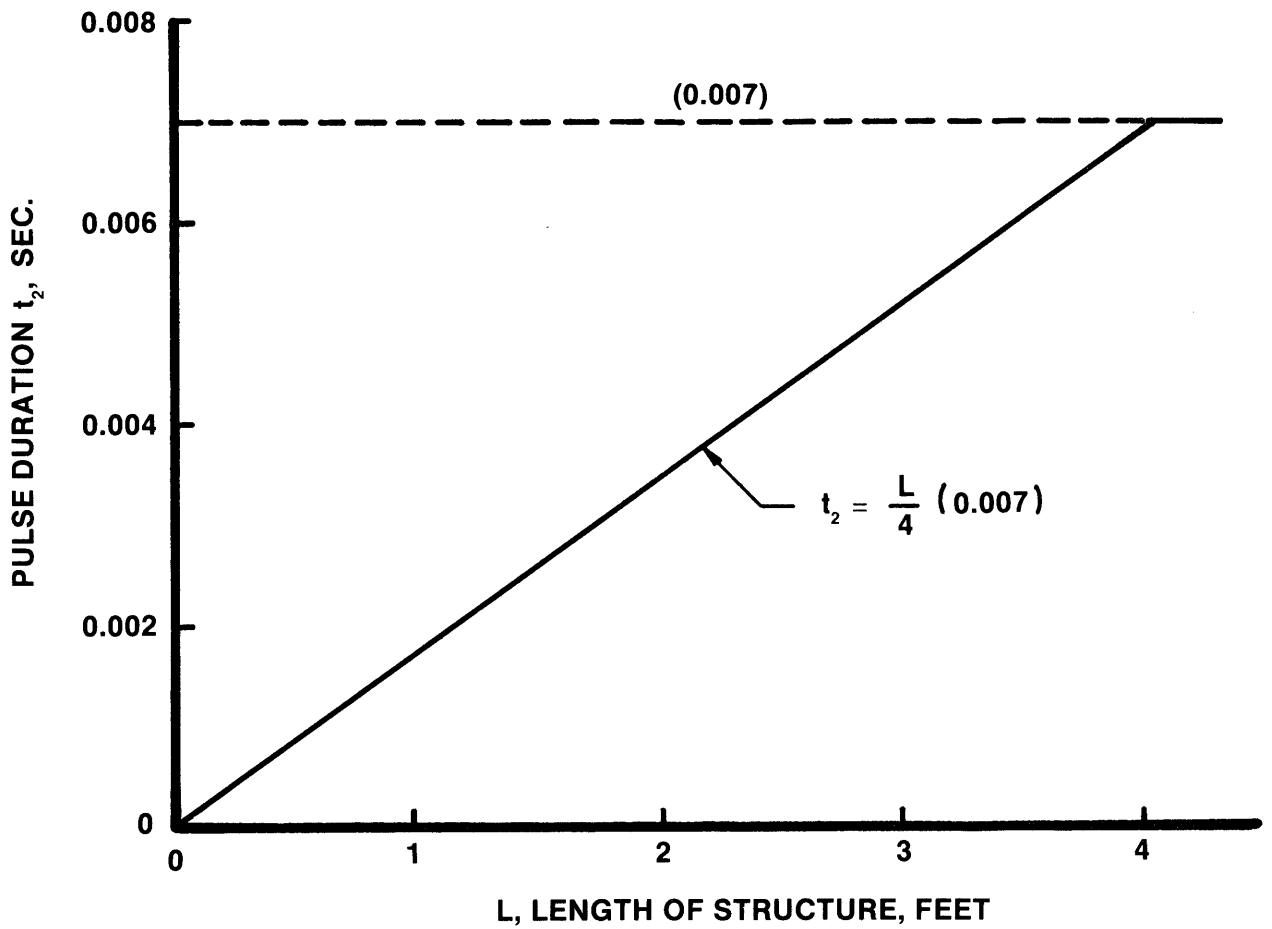


FIGURE 6A.10-8

REDUCTION IN PULSE DURATION FOR
RADIAL STRUCTURES SHORTER THAN
4 FEET

RIVER BEND STATION
UPDATED SAFETY ANALYSIS REPORT

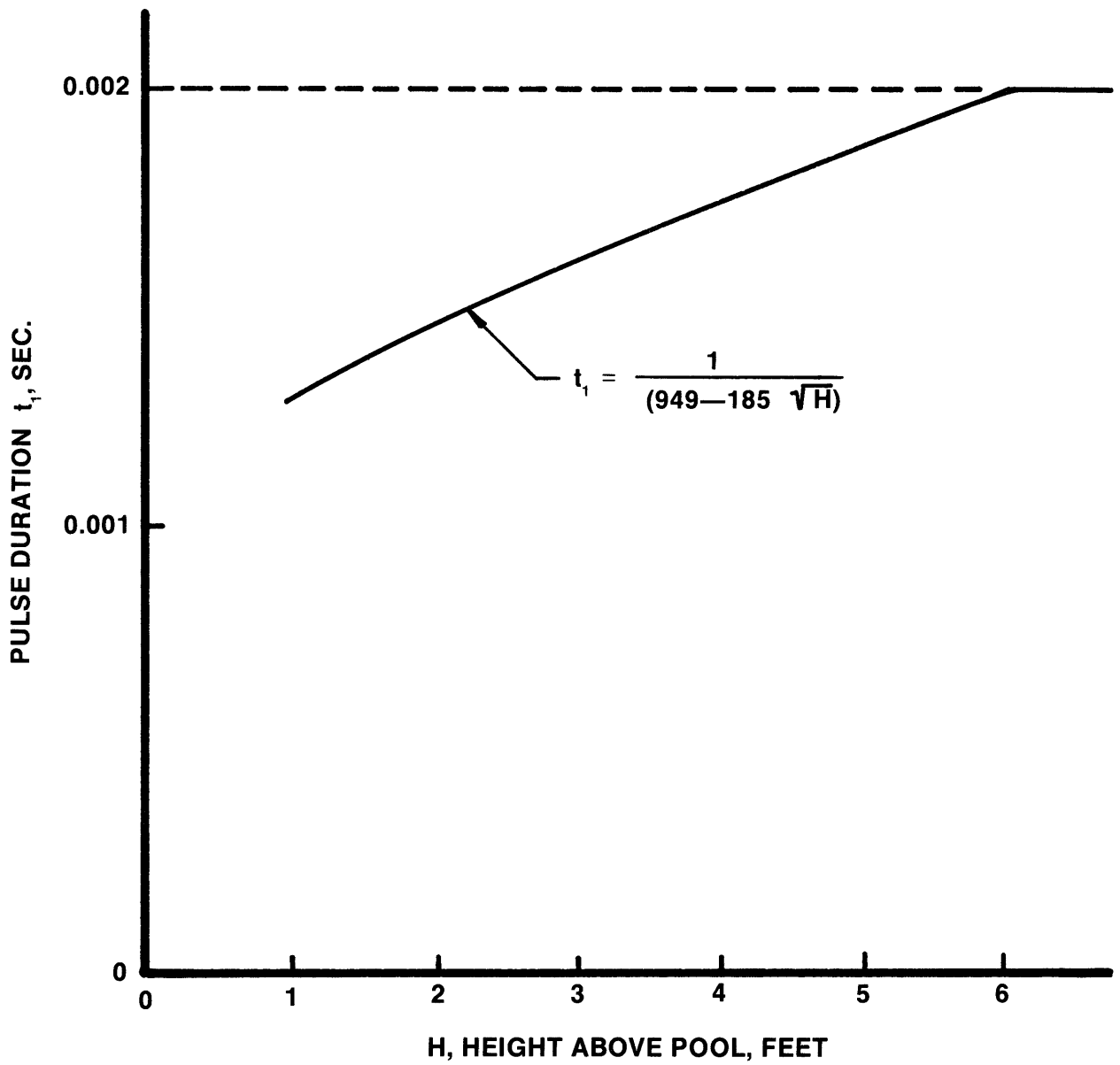


FIGURE 6A.10-9

REDUCTION IN PULSE DURATION FOR
CIRCUMFERENTIAL TARGETS CLOSER
THAN 6 FEET TO THE POOL SURFACE

RIVER BEND STATION
UPDATED SAFETY ANALYSIS REPORT

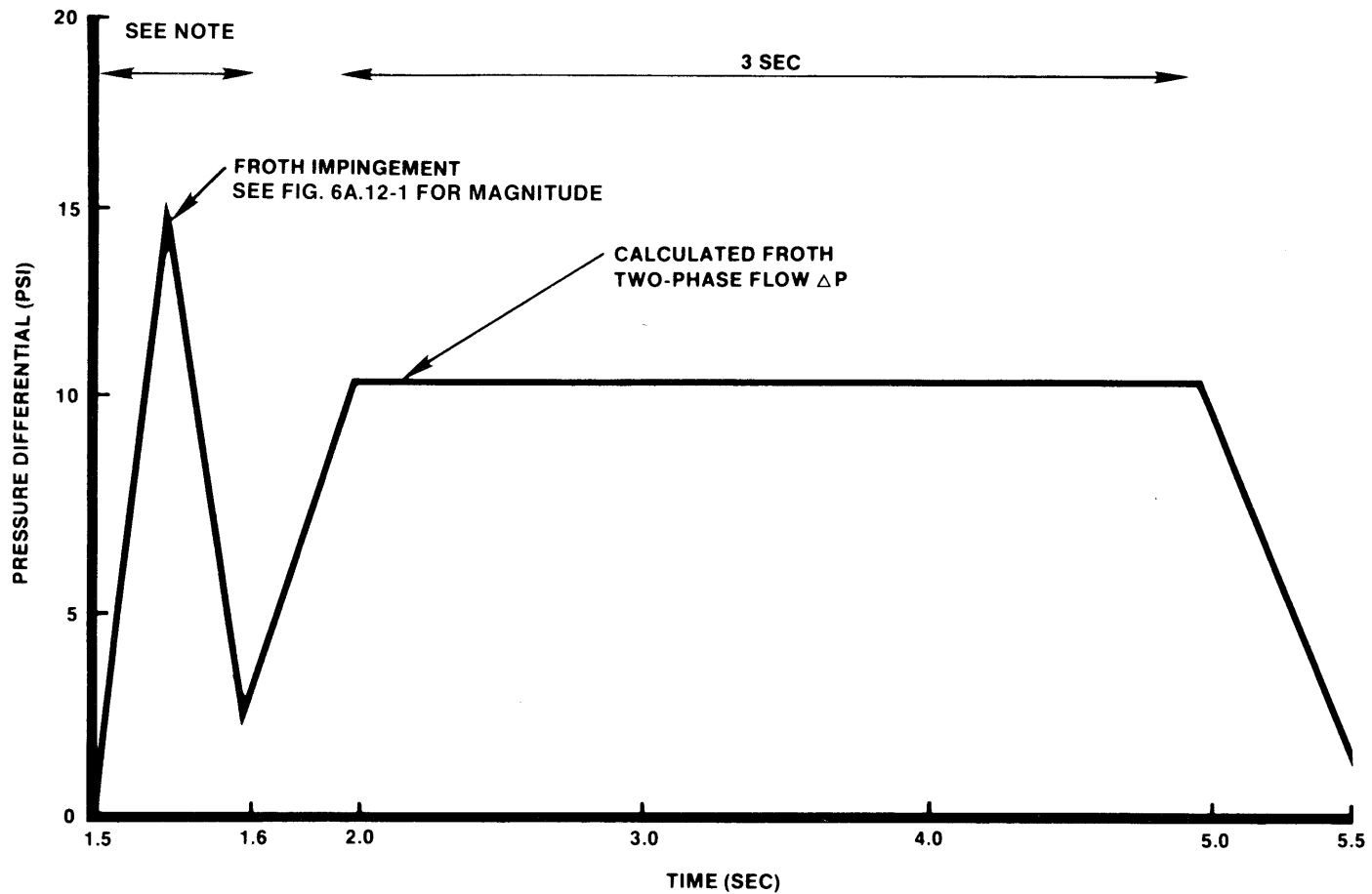
6A.11 LOADS ON EXPANSIVE STRUCTURES AT THE HCU FLOOR ELEVATION

At the HCU floor elevation (el 114 ft) there are portions of the floor which are comprised of beams and grating and other portions that are solid expansive structures. The bottom of the steam tunnel is at approximately the same elevation (el 110 ft). The small structure portion (beams and grating) of the HCU floor is discussed in Section 6A.12.

The expansive structures at this elevation experience an impulsive loading followed by an 11 psi pressure differential. The impulsive load is due to the momentum of the froth which is decelerated by the expansive structure. The 11 psi pressure differential is based on an analysis of the transient pressure in the space between the pool surface and the HCU floor resulting from the froth flow through the 1,500 sq ft vent area at this elevation (Section 6A.6.1.6). Fig. 6A.11-1 shows the loading history.

The 11 psi froth flow pressure differential lasting for 3 sec is based on an analysis of the transient pressure in the space between the pool surface and the HCU floor. The value of 11 psi is from the GESSAR analysis that assumes that the density of the flow through the annulus restriction is the homogeneous mixture of the top 9 ft of the suppression pool (i.e., 18.8 lbm/cu ft). Supplement 1 to GESSAR Reference 5 describes the analytical model used to simulate the HCU floor flow pressure differential and presents a comparison of model predictions with test data. This is a conservative density assumption confirmed by the PSTF 1/3 scale tests which show average densities of approximately 10 lbm/cu ft. GESSAR Reference 11 indicates that the HCU floor pressure differential is in the 3 to 5 psi range. The River Bend Station analysis conducted with the LOCTVS analytical model predicts a froth flow pressure differential of 3.4 psi.

The potential for circumferential variations in the pressure transient in the wetwell region beneath the HCU floor has been examined, and on the basis of bounding calculations, it is included that the pressure variation is less than 0.5 psid.



REF: GESSAR FIG. 3B-74

NOTE: IMPACT DURATION CHOSEN TO GIVE THE MAXIMUM DYNAMIC LOAD FACTOR, BUT NOT LESS THAN 50 MSEC FOR EXPANSIVE STRUCTURES

FIGURE 6A.11-1

LOADS ON HCU FLOOR
DUE TO POOL-SWELL FROTH IMPACT
AND TWO-PHASE FLOW

RIVER BEND STATION
UPDATED SAFETY ANALYSIS REPORT

6A.12 LOADS ON STRUCTURES AT AND ABOVE THE HCU FLOOR ELEVATION

Structures at the HCU floor elevation experience "froth" pool swell which involves both impingement and drag type forces. GESSAR Fig. 3B-12 shows the loading sequences. Only structures in the line of sight of the pool experience froth pool swell loads.

The froth impingement load is applicable to structures between 19 ft above the initial pool surface and at and above the HCU floor. The forcing function is an isosceles triangle with a maximum amplitude shown on Fig. 6A.12-1. The pulse duration is chosen so as to give the maximum dynamic load factor for a triangular pulse. For elongated structures (i.e., pipes and beams) that span the entire pool, pulse durations less than 50 milliseconds need not be considered. Gratings are not subjected to these impingement loadings.

As discussed in Section 6A.6.1.6, following the initial froth impingement there is a period of froth flow through the annulus restriction at this elevation.

•→14

The froth flow pressure differential load (i.e., drag type force) specification of Fig. 6A.11-1 is based on an analysis of the transient pressure in the space between the pool surface and the HCU floor. The value of 11 psi is from the GESSAR analysis that assumes that the density of the flow through the annulus restriction is the homogenous mixture of the top 9 ft of the suppression pool water and the free air between the HCU floor and the pool (i.e., 18.8 lbm/cu ft). This is a conservative density assumption confirmed by the PSTF 1/3 scale tests which show an average density of approximately 10 lbm/cu ft. Representative tests of the expected Mark III froth conditions at the HCU floor are the 5-ft submergence tests of Series 5801, 5802, 5803, and 5804. GESSAR Reference 11 indicates the HCU floor pressure differential during these tests was in the 3 to 5 psi range (drag load on HCU floor). The River Bend Station analysis conducted with the M3CPT analytical model predicts a froth flow pressure differential of 6.3 psi.

14←•

Structures above open areas at the HCU floor also experience loads. The impingement loads described above apply to an elevation 26 ft above the initial pool surface for flat structures and to 28.5 ft above for pipes. These impingement loads may be reduced by the ratio of grating open area to total area for structures above grated areas. The drag-type loads apply to structures

up to 30 ft above the initial pool surface. The drag force can be reduced for structures more than 20 ft above the pool surface by multiplying by $(V/50)^2$, where V is the velocity as described in Section 6A.10.

The potential for circumferential variations in the pressure transient in the wetwell region beneath the HCU floor has been examined, and on the basis of bounding calculations it is concluded that the pressure variation is less than 0.5 psid.

The HCU floor has been designed to withstand loads from a pool swell event. CRD piping is capable of withstanding the vibratory responses due to all hydrodynamic loadings.

For the pool swell froth impact load, the loading, as shown in Fig. 6A.11-1 was applied to a finite element model of a segment of the HCU floor where HCUs are located. Dynamic responses of the floor were generated in the form of amplified response spectra (ARS) and maximum displacements at various locations on the floor for evaluation of HCUs and the frame structure supporting the HCUs.

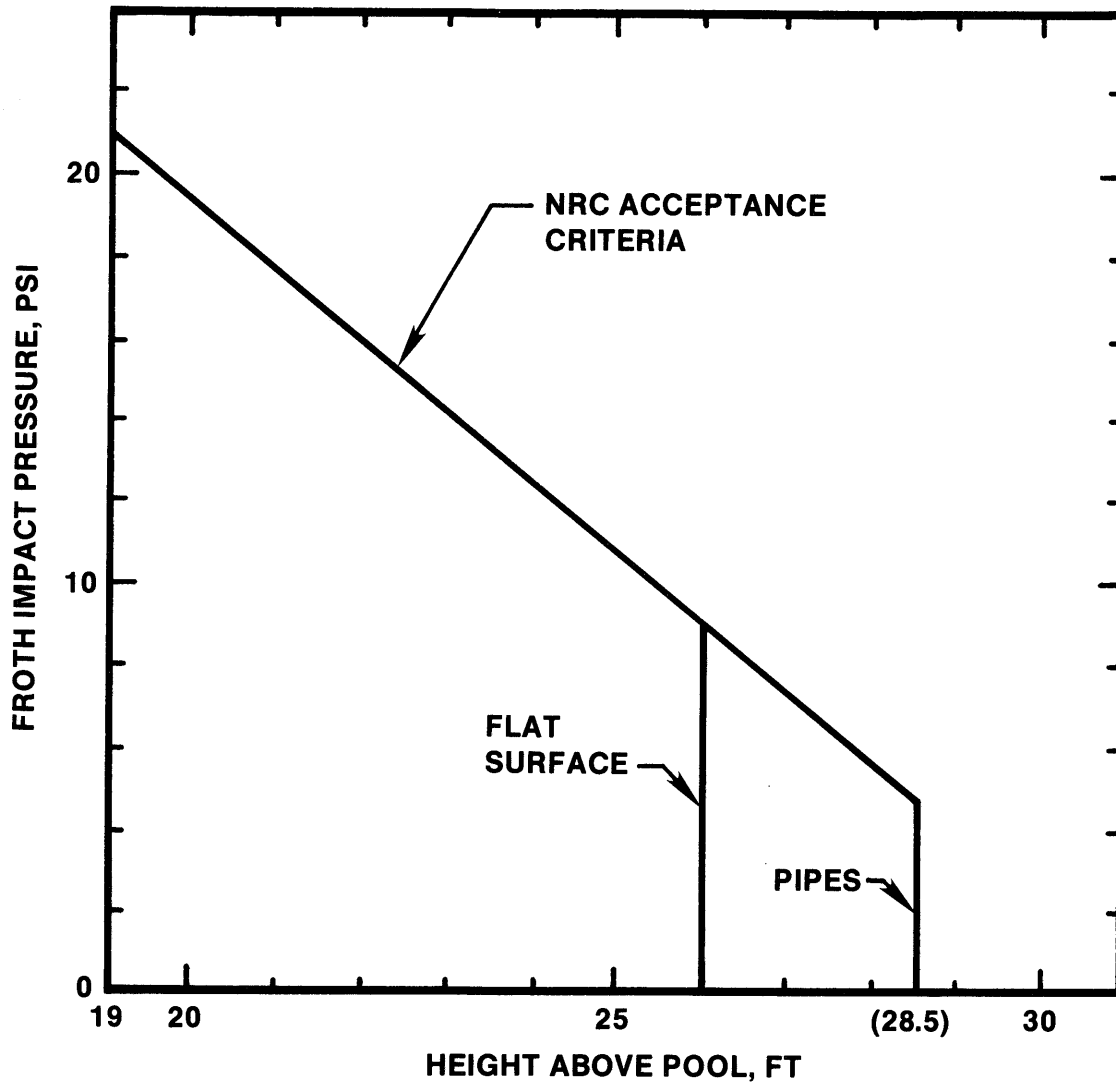


FIGURE 6A.12-1

FROTH IMPACT PRESSURE —
PEAK AMPLITUDE

RIVER BEND STATION
UPDATED SAFETY ANALYSIS REPORT

6A.13 DYNAMIC RESPONSE OF PRIMARY STRUCTURES TO HYDRODYNAMIC LOADS

The objective of Sections 6A.13.1 and 6A.13.2 is to provide a description of the behavior of the containment structures when subjected to hydrodynamic loads, i.e., safety relief valve discharge loads, and loss of coolant accident dynamic loads, in the suppression pool. Maximum responses, in terms of internal forces and stresses and resultant structural acceleration time histories, at specific locations in the foundation basemat, drywell wall, steel containment, shield building, reactor support pedestal, weir wall and primary shield wall are generated through the dynamic analysis. Plots and tables of these results are provided in Section 6A.14.

For each particular location in the containment structures, acceleration time history responses are obtained from the time history analysis. Amplified response spectra (ARS) plots are generated from these acceleration time histories. ARS are defined as plots of the maximum response of single-degree-of-freedom damped oscillators as a function of period (or natural frequency) to a specified acceleration time history at their support.

The suppression pool arrangement is shown in Fig. 6A.13-1.

6A.13.1 Structural Response Due to Safety Relief Valve Discharge Loads

Internal forces, moments, and stresses due to the safety relief valve discharge loads are combined with other internal forces and moments, as described in the load combination tables provided in Section 3.8. ARS curves are generated for evaluation of subsystems.

6A.13.1.1 Method of Analysis

The dynamic response of the containment structures when subjected to safety relief valve discharge loads is determined by the finite element-based computer program (GHOSH). A description of this program is given in Appendix 3A.

The structural models used in the analysis represent the containment structures (i.e., drywell wall, steel containment, shield building, reactor pedestal, the primary shield wall), the reactor pressure vessel, the foundation basemat, and the soil foundation using axisymmetric thin shell/plate and solid finite elements. Two separate

axisymmetric finite element models of the structures (Fig. 6A.13-2 and 6A.13-3) were used to generate maximum internal stress resultants (forces and moments), acceleration time histories (T-H), and ARS curves. Both models use solid elements to represent the soil foundation and the concrete fill. The foundation radius and depth are taken as twice that of the basemat diameter to ensure that the response at the boundaries is very small. The remaining containment structures and the reactor pressure vessel were represented by axisymmetric thin shell/plate elements.

The model shown in Fig. 6A.13-2 was used to generate the acceleration time histories and ARS curves. Vertical and horizontal models for the reactor pressure vessel (RPV) and its internals, provided by General Electric, are used when analyzing the symmetric and asymmetric loads, respectively.

The analytical model shown in Fig. 6A.3-3 was used to find the internal forces, moments, and stresses. In this model the basemat is represented largely by shell elements except in the region adjoining the concrete fill area where solid elements were employed. Only the horizontal model properties of the RPV and its internals were incorporated in this model.

A time history analysis, with the equations of motion solved numerically by direct integration, is performed for each load case, and the maximum values of the structural response are established for use in the design. Resultant acceleration time history responses are generated, and the corresponding amplified response spectra curves are calculated. A time step of 0.001 sec is used in the numerical integration scheme.

Mass properties of the structures are assumed to be uniform within each element. This leads to a consistent mass matrix for the structural system. The effects of structural damping have been included in the dynamic analysis. The Rayleigh damping technique is utilized in such a way that the damping matrix is assumed to be linearly proportional to the mass and stiffness matrix:

$$[C] = \alpha[M] + \beta[K]$$

The constants of proportionality (i.e., α and β) are chosen such that damping of 4 percent of critical damping is not exceeded between frequencies of 10 and 70 Hz. These limits are selected in order to encompass the range of frequencies in which significant dynamic response occurs.

6A.13.1.2 Application of Loads

The loads applied to the suppression pool boundaries due to the SRV loads are described in Attachment A.

The SRV loads are pressure time histories with circumferential and meridional variation. For the purpose of analysis, the circumferential variation is resolved into Fourier coefficients at each time step in the time history analysis. The continuous pressure profiles in the meridional direction are replaced by a series of nodal forces and moments, as shown in Fig. 6A.13-4.

A detailed analysis of the structure is performed for the following three SRV discharge conditions: 1) single-valve subsequent actuation, 2) two adjacent valve first actuation, and 3) all valves simultaneous actuation. The single valve first actuation and the first actuation of the automatic depressurization systems (ADS) cases were not analyzed since they are bounded by the single valve subsequent actuation and all valve first actuation cases, respectively. The bounding cases are substituted for these cases when evaluating structures and equipment. The analysis includes the SRV steam condensation oscillation phase (SRV CO) of the discharge, based on the pressure trace shown in Fig. A.6A.8-1.

6A.13.2 Structural Response Due to Loss of Coolant Accident Loads

Internal forces, moments, and stresses produced by loss of coolant accident dynamic loads in the suppression pool are combined with other internal forces and moments, as described in the load combination tables presented in Section 3.8. Acceleration time histories and ARS curves are generated for equipment and piping evaluations.

6A.13.2.1 Method of Analysis

The analytical models and procedures described in Section 6A.13.1.1 for the SRV loads analysis are applicable to the analysis of the LOCA loads.

6A.13.2.2 Application of Loads

The loads applied to the suppression pool boundaries due to the loss of coolant accident dynamic loads are described in Sections 6A.4 and 6A.5.

The significant dynamic loads experienced by the suppression pool boundary structures (i.e., drywell wall, steel containment, weir wall, and basemat) during a loss of coolant accident caused by a large steam break or a reactor water recirculation line break (DBA) are: chugging loads, condensation oscillation loads, and pool swell/vent clearing loads.

The method of applying these loads to the analytical model is similar to the application of the SRV loads as described in Section 6A.13.1.2.

The time step used in the integration scheme for the chugging loads is taken as 0.0005 sec due to the short duration of the individual chugs (5 msec for first spike). For the post-chugging oscillation component of the forcing function, frequencies of 10, 11, and 12 Hz are considered. The variation of the frequency from 10 to 12 Hz does not affect the results considerably, because the major contribution comes from the pre-chug underpressure and pulse components. For this reason the internal forces, moments, and stresses were obtained using the time history with the dominant frequency of 10 Hz.

The duration of the load for condensation oscillation is taken as 5.3 sec. The total response of the structures for a pulsating force is obtained with this duration. The weir wall is not loaded during the condensation oscillation phase.

The pool swell/vent clearing loads are applied in accordance with that method described in Section 6A.13.1.2. The loads are defined in Section 6A.4.

The time step used in the integration scheme for the condensation oscillation loads and pool swell/vent clearing loads is 0.001 sec.

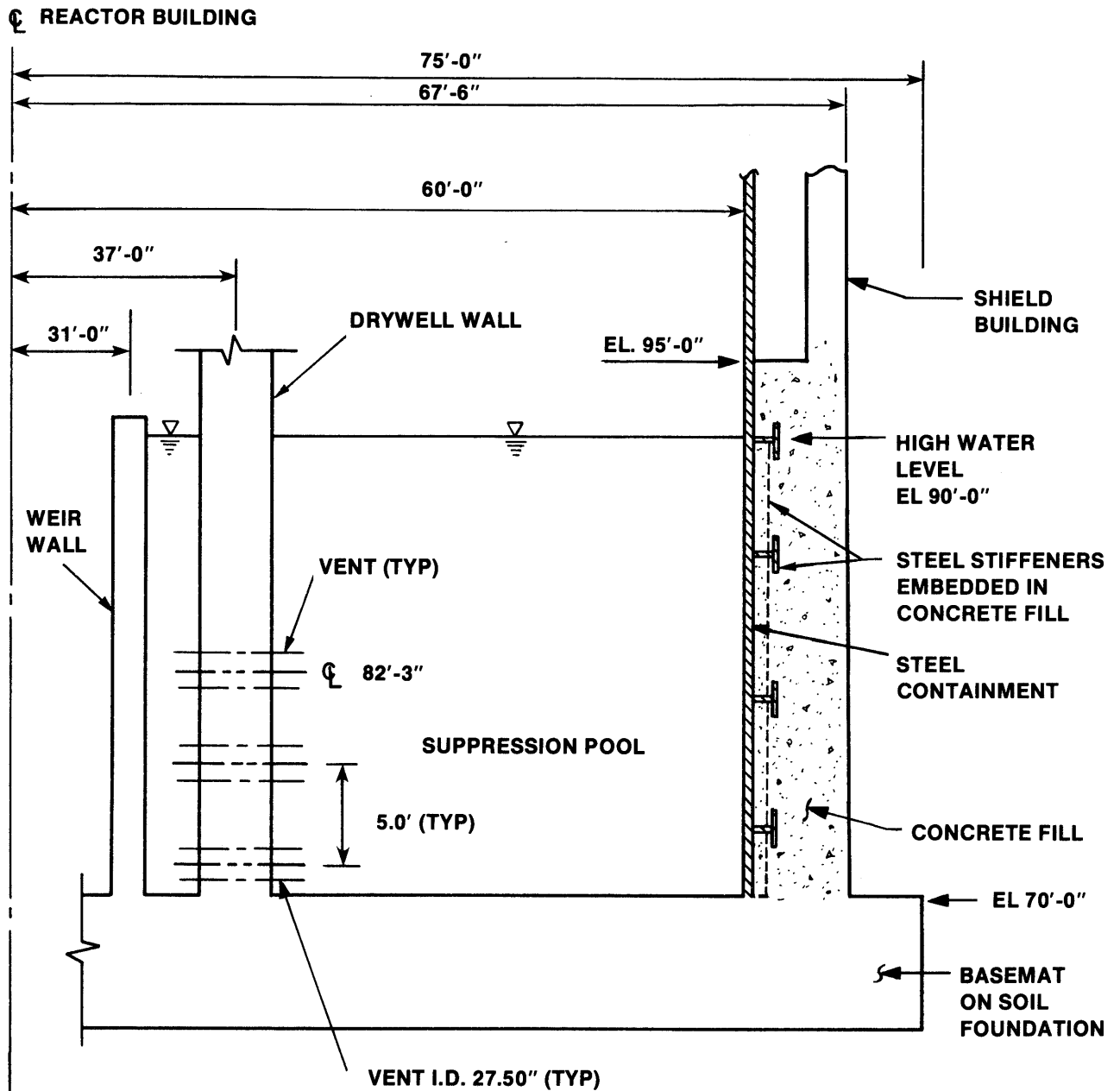


FIGURE 6A.13-1

SUPPRESSION POOL GEOMETRY

RIVER BEND STATION
 UPDATED SAFETY ANALYSIS REPORT

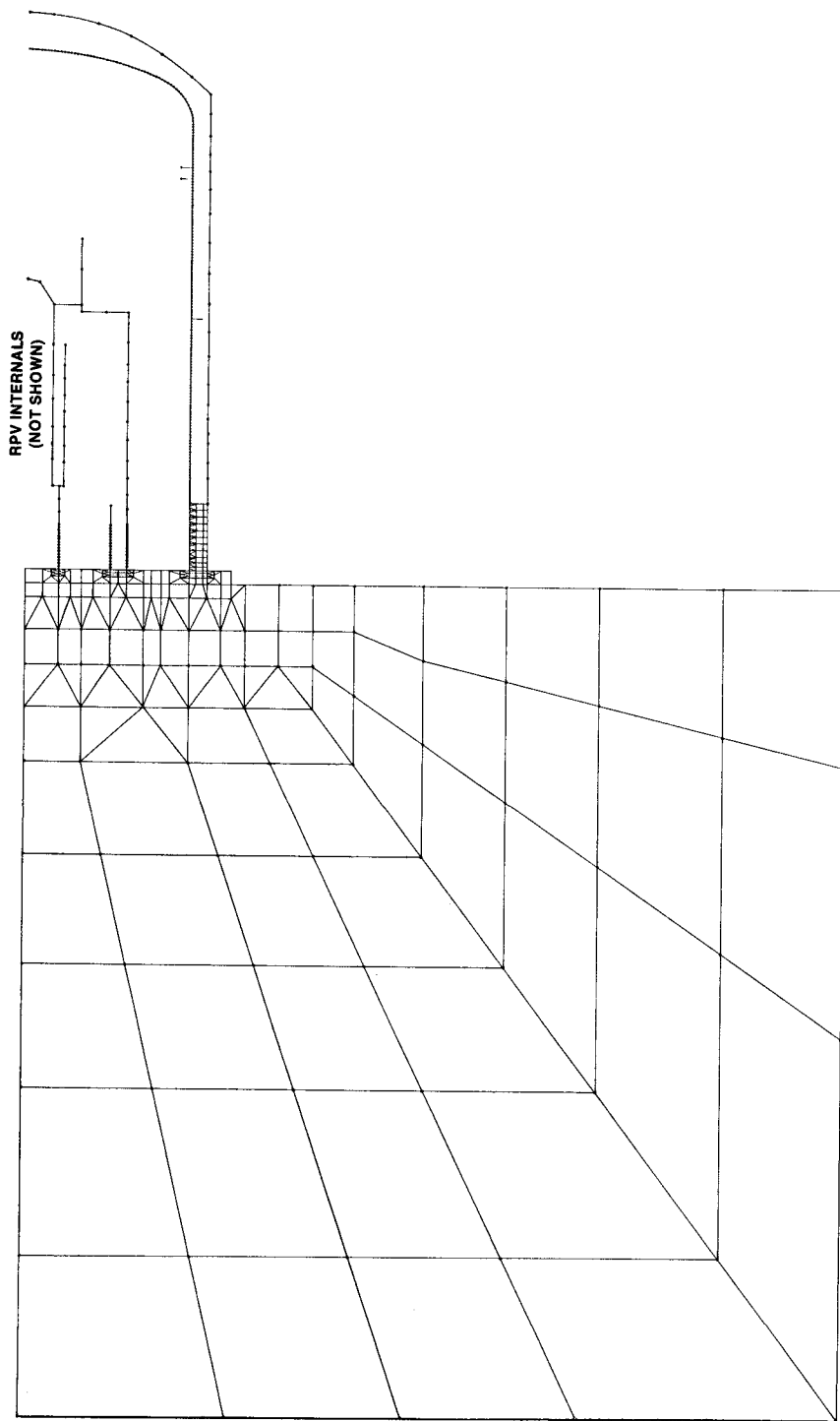


FIGURE 6A.13-2

FINITE ELEMENT MODEL
OF REACTOR BUILDING

RIVER BEND STATION
UPDATED SAFETY ANALYSIS REPORT

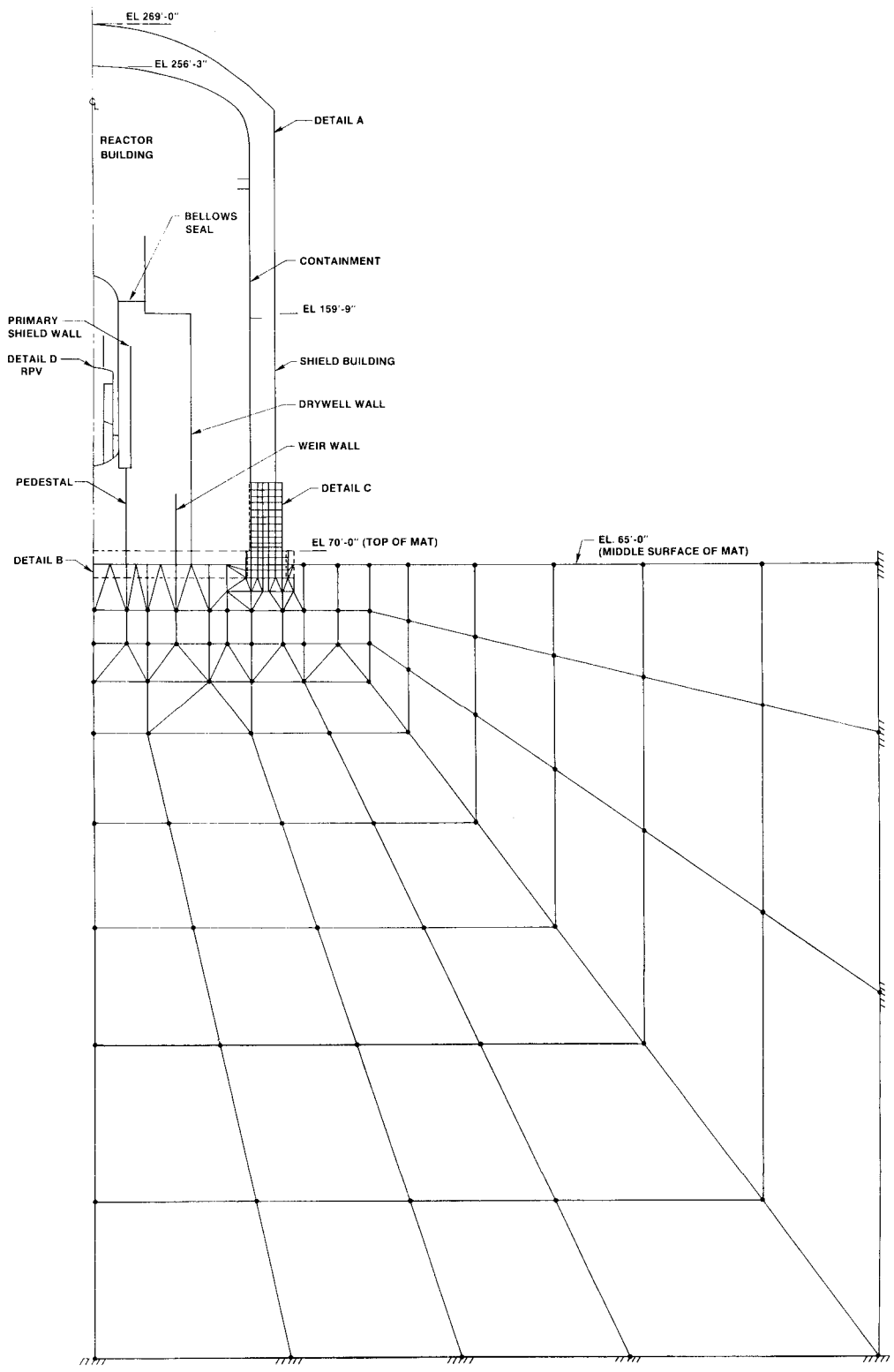
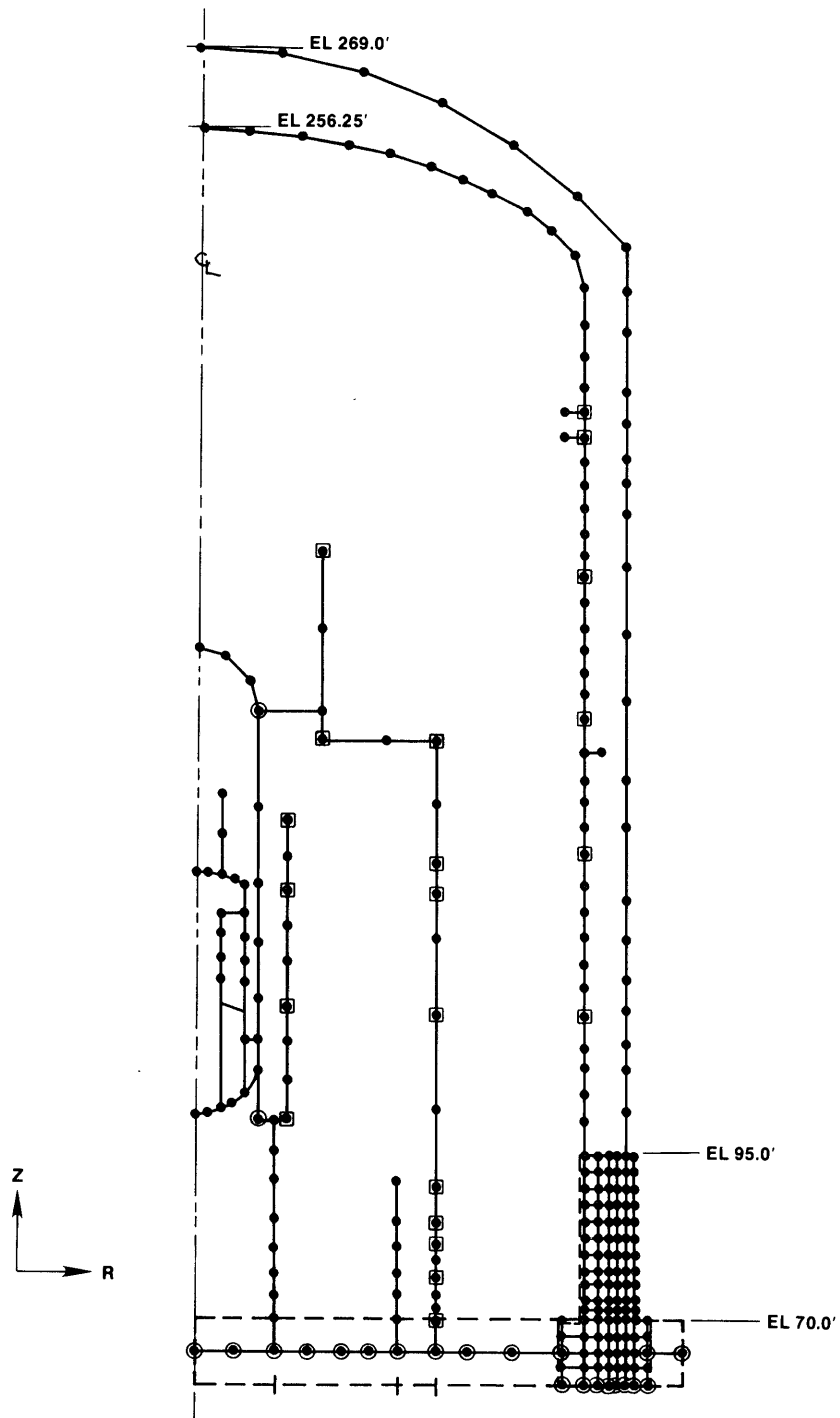


FIGURE 6A.13-3
 HORIZONTAL ANALYTICAL MODEL
 FOR HYDRODYNAMIC LOADS ANALYSIS
 SHEET 1 OF 5
RIVER BEND STATION
 UPDATED SAFETY ANALYSIS REPORT

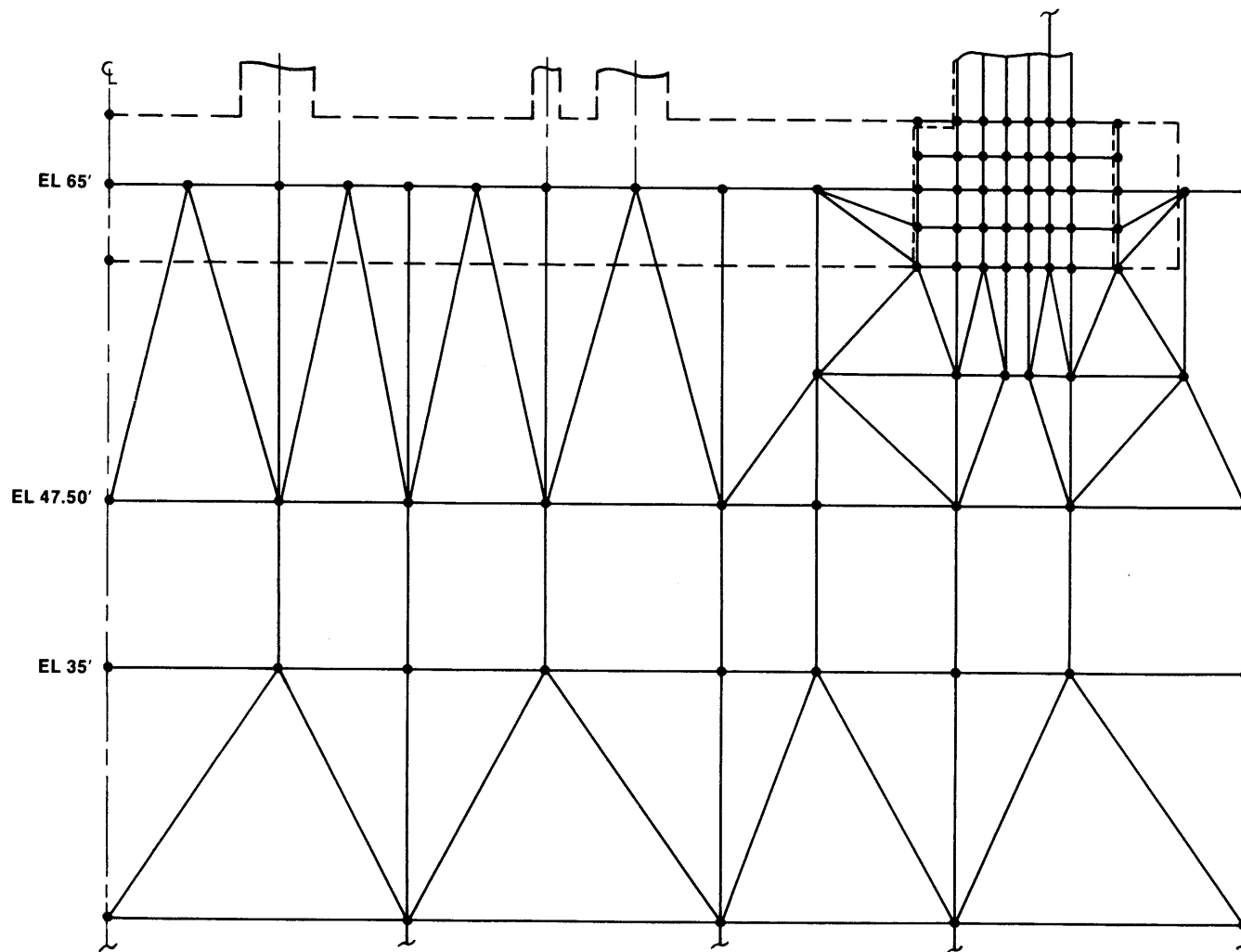


DETAIL A
REACTOR BUILDING

FIGURE 6A.13-3

HORIZONTAL ANALYTICAL MODEL
FOR HYDRODYNAMIC LOADS ANALYSIS
SHEET 2 OF 5

RIVER BEND STATION
UPDATED SAFETY ANALYSIS REPORT

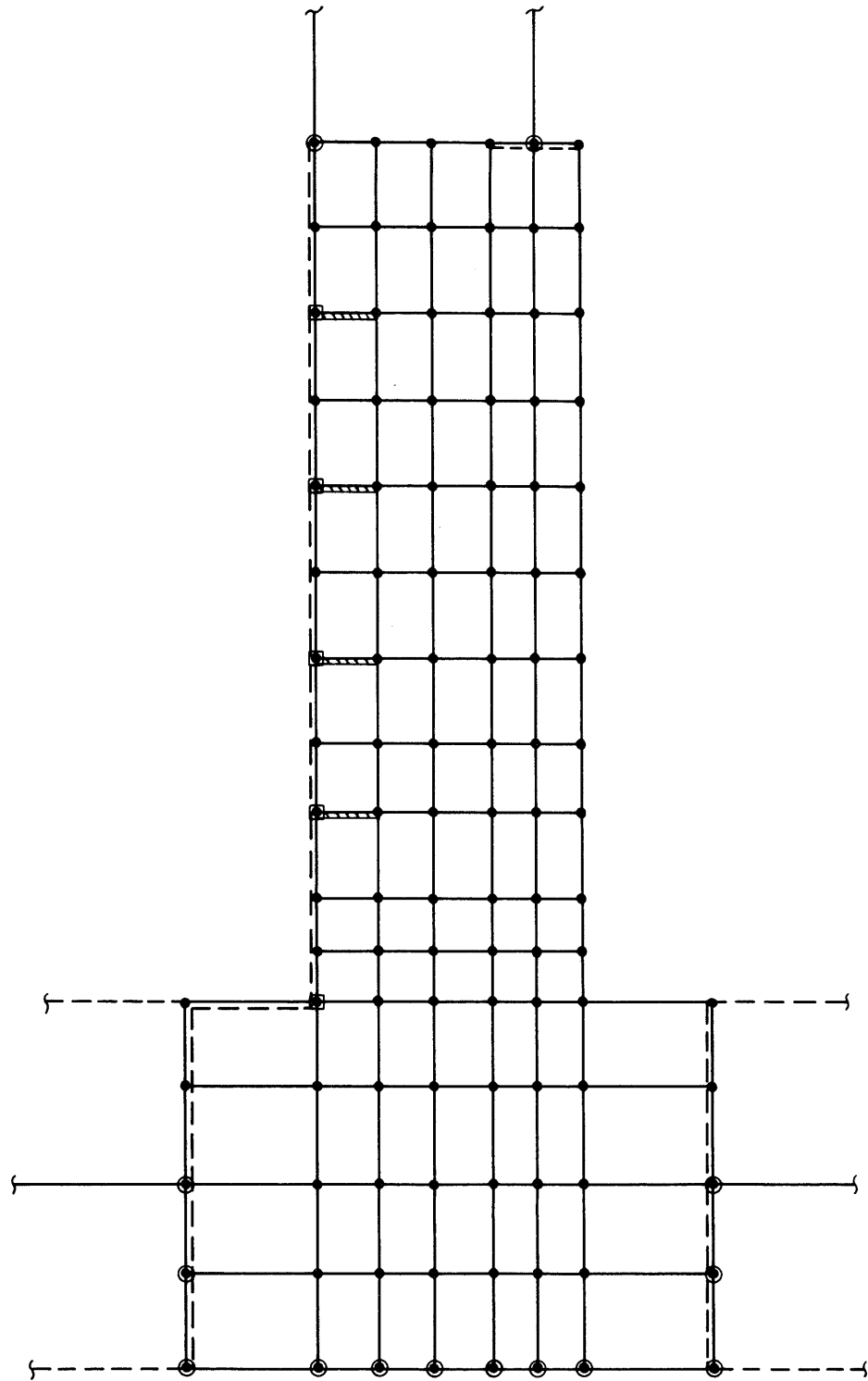


DETAIL B
MAT

FIGURE 6A.13-3

HORIZONTAL ANALYTICAL MODEL
FOR HYDRODYNAMIC LOADS ANALYSIS
SHEET 3 OF 5

RIVER BEND STATION
UPDATED SAFETY ANALYSIS REPORT

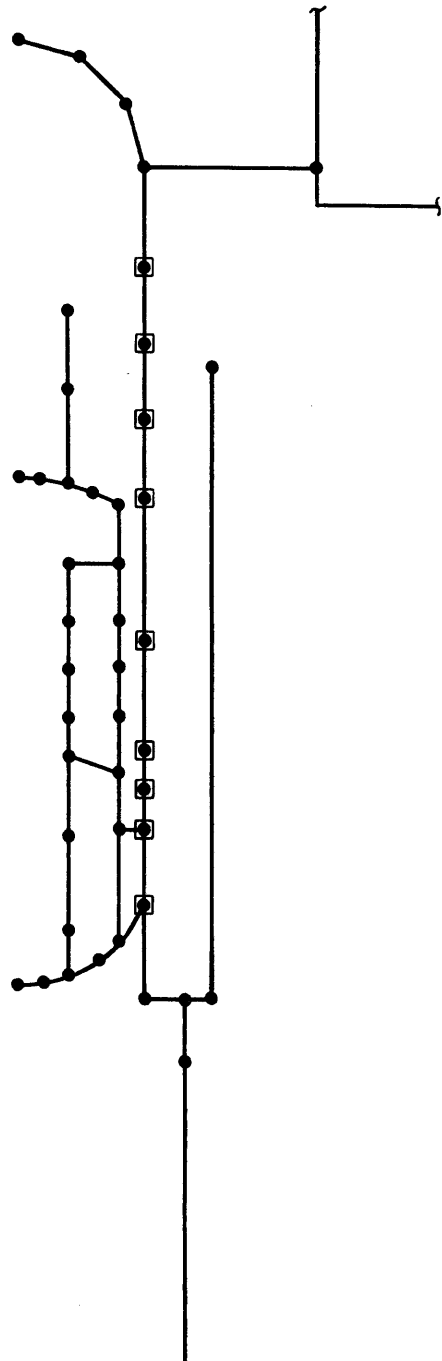


**DETAIL C
CONCRETE FILL**

FIGURE 6A.13-3

**HORIZONTAL ANALYTICAL MODEL
FOR HYDRODYNAMIC LOADS ANALYSIS
SHEET 4 OF 5**

**RIVER BEND STATION
UPDATED SAFETY ANALYSIS REPORT**

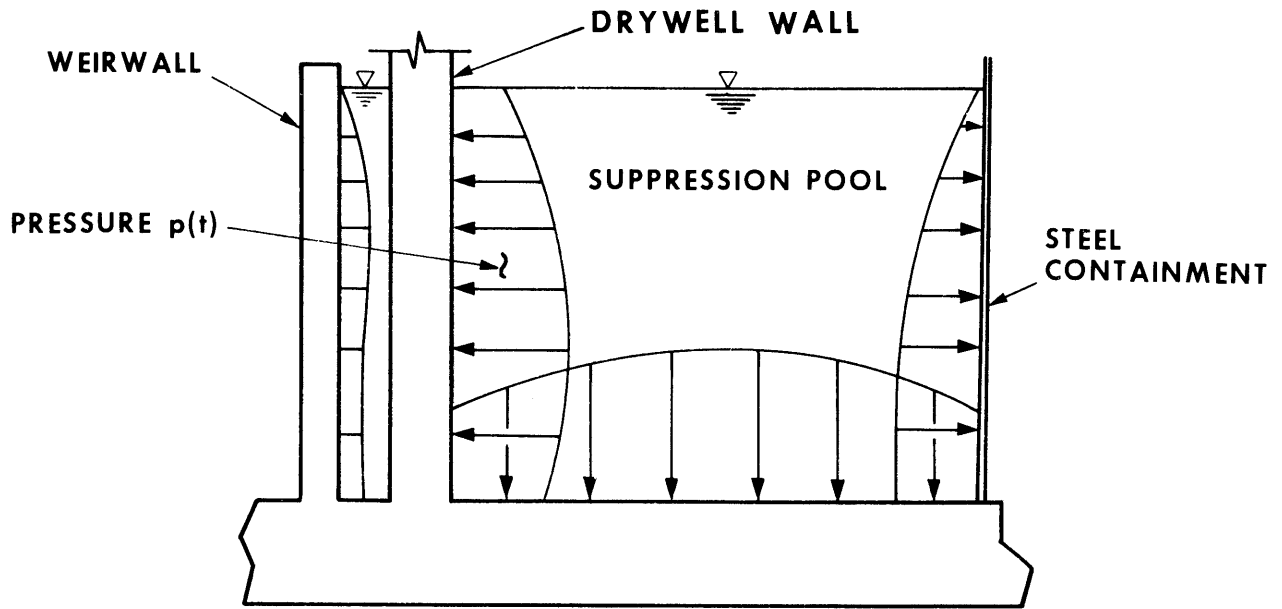


**DETAIL D
REACTOR PRESSURE VESSEL**

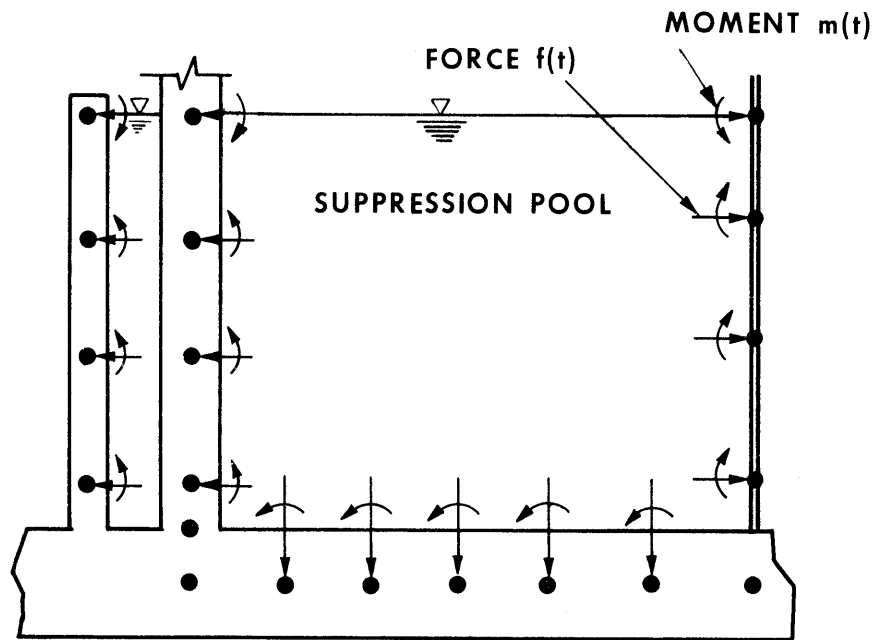
FIGURE 6A.13-3

**HORIZONTAL ANALYTICAL MODEL
FOR HYDRODYNAMIC LOADS ANALYSIS
SHEET 5 OF 5**

**RIVER BEND STATION
UPDATED SAFETY ANALYSIS REPORT**



MERIDIONAL PRESSURE PROFILE



IDEALIZED NODAL FORCES AND MOMENTS

FIGURE 6A.13-4

LOADS APPLIED TO MODEL

RIVER BEND STATION
 UPDATED SAFETY ANALYSIS REPORT

RBS USAR

PART II
CONTAINMENT DYNAMIC LOAD ASSESSMENT

6A.14 ASSESSMENT OF CONTAINMENT STRUCTURES FOR HYDRODYNAMIC LOADS

6A.14.1 Introduction

This section presents an evaluation of the capacity of the containment structures to withstand the hydrodynamic loads: safety relief valve discharge loads, and LOCA loads. The assessment for the containment is discussed in Section 6A.15. The remaining structures (i.e., drywell wall, reactor pedestal, shield building, primary shield wall, weir wall, and foundation basemat) are evaluated in this section for their abilities to resist the loads described in the load combination tables given in Section 3.8, which include SRV loads and LOCA loads.

The assessment is accomplished by providing tables of maximum internal forces, moments, and stresses and ARS plots at specific locations in the containment structures just listed due to the hydrodynamic loads. These tables and plots are also provided for the steel containment.

6A.14.2 Description of Structures

A description of the containment structures is provided in Section 3.8.

6A.14.3 Design Criteria and Loads

The containment structures are designed to withstand the hydrodynamic loads described in Section 6A.13 combined with other loads as indicated in load combination tables given in Section 3.8.

Applicable codes and standards used in designing the containment structures are listed in Section 3.8.

Material properties of the containment structures are given in Section 3.8.

6A.14.4 Method of Analysis and Design

As indicated in Section 6A.13.1.2, the response of the containment structures to the hydrodynamic loads (SRV and LOCA loads) is determined using the finite element computer program GHOSH (see Appendix 3A). The internal forces, moments, and stresses obtained from the dynamic analysis are combined as specified in Section 3.8. Steel reinforcement stresses and concrete compression stresses resulting from the bending moments and in-plane forces are obtained for

each load combination at a number of specific locations in the containment structures. Shear stresses are also calculated. These stresses are compared with allowable stresses to check the adequacy of the sections.

6A.14.5 Summary of Results

6A.14.5.1 Containment Structures and Foundation Basemat, Internal Forces, and Moments

Definitions of the internal forces, moments, and stresses shown on Fig. 6A.14-1 and 6A.14-2 are given in Tables 6A.14-1 and 6A.14-2, respectively. Values of these forces, moments, and stresses at specific locations in the containment structures are given in the following tables:

<u>Table No.</u>	<u>Description</u>
6A.14-3	Maximum values of dynamic forces, moments, and stresses due to SRV loadings
6A.14-4	Maximum values of dynamic forces and moments in the containment structures due to LOCA loadings

6A.14.5.2 Amplified Response Spectra Curves

Typical plots of amplified response spectra curves are shown in Fig. 6A.14-3 through 6A.14-8.

Such curves are utilized in Section 6A.16 for assessment of piping and mechanical systems.

6A.14.6 Conclusions

An evaluation of the structural capacity of the containment structures to resist the loads described in this section in combination with other design loads as described in Section 3.8 indicates that the design is adequate.

RBS USAR

TABLE 6A.14-1

DEFINITION OF INTERNAL FORCES AND MOMENTS

The positive sign convention of the stress resultants shown on Fig. 6A.14-1 are defined as follows:

- N
SS = force/length in axial (or meridional) direction
(k/ft)
- N
TT = force/length in circumferential direction (k/ft)
- N
ST = in-plane shear/length (k/ft)
- M
SS = moment/length along axial (or meridional)
direction
(k-ft/ft)
- M
TT = moment/length along circumferential direction
(k-ft/ft)
- M
ST = twisting moment/length (kt/ft)
- Q
S = flexural shear/length in axial direction (k/ft)
- Q
T = flexural shear/length in circumferential
direction
(k/ft)

TABLE 6A.14-2

DEFINITION OF INTERNAL STRESSES

The positive sign convention of the solid element stresses (ksf) shown on Fig. 6A.14-2 are defined as follows:

σ_{RR} = normal stress in radial direction

σ_{ZZ} = normal stress in axial direction

σ_{TT} = normal stress in circumferential direction

σ_{RZ} = shear stress in R-Z plane

τ_{RT} = shear stress in the plane normal to Z-axis

τ_{ZT} = shear stress in the plane normal to R-direction

RBS USAR

TABLE 6A.14-3

MAXIMUM FORCES, MOMENTS, AND STRESSES DUE TO SRV
(ALL VALUES ARE ±)

Basemat - El 65.00 ft

Radius (ft)	Moments (k-ft/ft)			Forces (k/ft)			Shears (k/ft)	
	M-SS	M-TT	M-ST	N-SS	N-TT	N-ST	Q-S	Q-T
6.04	73.00	75.00	4.41	10.90	10.70	5.93	4.44	0.85
12.08 (I)	62.40	69.30	0.15	10.90	10.90	6.26	3.28	2.42
12.08 (O)	171.00	85.30	0.15	7.99	9.57	7.24	20.70	2.57
16.75	88.40	84.20	4.96	9.35	7.34	7.38	14.90	0.81
26.25	39.40	56.20	2.91	11.70	6.83	8.11	12.60	0.80
31.00 (I)	77.20	39.40	1.11	12.60	6.83	8.36	10.70	1.14
31.00 (O)	55.60	43.50	1.11	9.03	7.28	5.92	11.80	1.36
37.00 (I)	101.00	31.60	0.57	9.65	5.39	6.29	9.88	1.57
37.00 (O)	141.00	53.90	0.57	16.80	8.49	6.30	22.50	3.64
43.00	52.20	45.10	6.47	15.20	4.89	5.16	19.30	1.19
49.00	49.90	35.70	4.58	12.50	4.67	3.92	7.90	1.36
55.00	13.00	28.70	4.29	11.20	5.17	3.39	6.67	0.38

(I) Point just inside adjoining shell structure.

(O) Point just outside adjoining shell structure.

Basemat - Adjoining Concrete Fill

El (ft)	Radius (ft)	Normal Stresses (ksf)			Shear Stresses (ksf)		
		σ_{RR}	σ_{ZZ}	σ_{TT}	τ_{RZ}	τ_{RT}	τ_{ZT}
61.25	57.50	0.51	0.14	0.93	0.41	0.55	0.03
63.75	57.50	1.46	0.24	0.66	0.34	0.36	0.02
66.25	57.50	1.34	0.58	0.66	1.86	0.19	0.04
68.75	57.50	0.54	1.11	0.69	1.91	0.06	0.15
61.25	69.25	0.43	0.17	0.71	0.23	0.26	0.03
63.75	69.25	0.31	0.26	0.49	0.11	0.19	0.03
66.25	69.25	0.42	0.48	0.42	0.47	0.12	0.04
68.75	69.25	0.76	0.82	0.68	0.85	0.19	0.06

TABLE 6A.14-3 (Cont)

Concrete Fill

<u>El (ft)</u>	<u>Radius (ft)</u>	<u>Normal Stresses (ksf)</u>			<u>Shear Stresses (ksf)</u>		
		<u>σ_{RR}</u>	<u>σ_{ZZ}</u>	<u>σ_{TT}</u>	<u>τ_{RZ}</u>	<u>τ_{RT}</u>	<u>τ_{ZT}</u>
70.75	60.83	1.22	2.56	0.97	1.50	0.40	0.42
70.75	62.50	0.77	0.98	0.77	1.04	0.25	0.24
70.75	64.17	0.55	0.90	0.80	0.78	0.17	0.20
70.75	65.63	0.66	1.69	0.89	0.68	0.12	0.23
70.75	66.88	0.89	3.62	1.13	1.03	0.10	0.30
76.50	60.83	0.50	1.45	1.12	0.68	0.03	0.32
76.50	62.50	0.50	1.08	1.19	0.87	0.06	0.28
76.50	64.17	0.27	1.21	1.27	0.88	0.05	0.26
76.50	65.63	0.10	1.82	1.34	0.64	0.04	0.30
76.50	66.88	0.02	2.45	1.41	0.26	0.01	0.35

Pedestal - Radius = 12.08 ft

<u>El (ft)</u>	<u>Moments (k-ft/ft)</u>			<u>Forces (k/ft)</u>			<u>Shears (k/ft)</u>	
	<u>M-SS</u>	<u>M-TT</u>	<u>M-ST</u>	<u>N-SS</u>	<u>N-TT</u>	<u>N-ST</u>	<u>Q-S</u>	<u>Q-T</u>
70.00	48.10	7.28	0.53	18.20	15.80	1.59	12.10	0.39
73.42	15.40	2.16	0.30	18.20	18.20	1.37	6.93	0.28
76.80	0.87	1.17	0.47	17.50	11.90	1.44	2.75	0.17
81.08	5.39	0.98	0.26	17.50	3.97	1.50	0.18	0.10
85.00	3.90	0.58	0.39	16.50	0.71	1.41	0.60	0.09
91.67	1.62	0.28	0.19	16.50	1.21	1.29	0.79	0.08

RPV Support - Radius = 9.33 ft

<u>El (ft)</u>	<u>Moments (k-ft/ft)</u>			<u>Forces (k/ft)</u>			<u>Shears (k/ft)</u>	
	<u>M-SS</u>	<u>M-TT</u>	<u>M-ST</u>	<u>N-SS</u>	<u>N-TT</u>	<u>N-ST</u>	<u>Q-S</u>	<u>Q-T</u>
100.67	1.03	0.03	0.00	9.39	2.29	0.69	0.89	0.00
107.75	1.17	0.02	0.00	9.39	4.69	0.95	1.18	0.00

Weir Wall - Radius = 31.00 ft

<u>El (ft)</u>	<u>Moments (k-ft/ft)</u>			<u>Forces (k/ft)</u>			<u>Shears (k/ft)</u>	
	<u>M-SS</u>	<u>M-TT</u>	<u>M-ST</u>	<u>N-SS</u>	<u>N-TT</u>	<u>N-ST</u>	<u>Q-S</u>	<u>Q-T</u>
70.00	12.70	1.85	0.08	5.08	4.76	3.00	3.41	0.75
73.42	2.79	0.41	1.23	3.95	5.09	3.61	3.11	0.12
81.08	4.28	2.35	0.90	1.32	7.24	2.58	0.89	0.35
85.00	2.55	2.48	0.57	0.54	5.79	1.52	0.36	0.30

RBS USAR

TABLE 6A.14-3 (Cont)

Bio-Shield Wall - Radius = 13.92 ft

<u>El (ft)</u>	<u>Moments (k-ft/ft)</u>			<u>Forces (k/ft)</u>			<u>Shears (k/ft)</u>	
	<u>M-SS</u>	<u>M-TT</u>	<u>M-ST</u>	<u>N-SS</u>	<u>N-TT</u>	<u>N-ST</u>	<u>Q-S</u>	<u>Q-T</u>
100.67	1.54	0.42	0.07	5.92	0.74	0.56	0.40	0.06
106.53	0.37	0.08	0.06	5.92	0.61	0.72	0.10	0.01
112.37	0.16	0.07	0.02	5.13	0.76	0.76	0.07	0.01
118.23	0.97	0.21	0.02	5.13	1.46	0.80	0.43	0.01
124.08	0.10	0.05	0.01	3.52	0.99	0.86	0.19	0.01
129.93	0.10	0.07	0.01	3.52	0.77	0.83	0.15	0.00

Drywell Wall - Radius = 37.00 ft

<u>El (ft)</u>	<u>Moments (k-ft/ft)</u>			<u>Forces (k/ft)</u>			<u>Shears (k/ft)</u>	
	<u>M-SS</u>	<u>M-TT</u>	<u>M-ST</u>	<u>N-SS</u>	<u>N-TT</u>	<u>N-ST</u>	<u>Q-S</u>	<u>Q-T</u>
70.00	115.00	16.50	0.83	15.70	10.20	7.91	24.80	4.74
71.08	88.20	12.80	3.06	15.00	11.90	8.19	24.60	3.58
73.42	45.90	7.14	8.21	13.80	12.70	8.72	21.30	1.44
81.08	36.80	15.90	7.33	13.50	18.60	7.89	2.60	2.17
83.42	40.50	17.90	4.97	13.50	19.90	6.97	3.44	2.41
90.00	21.00	13.50	3.64	13.00	16.40	4.94	5.15	1.47
101.00	9.08	9.78	4.29	13.00	6.23	3.95	1.50	0.92
114.00	12.70	11.20	2.65	11.40	3.15	3.96	1.71	1.40

Stiffened Shell - Radius = 60.00 ft

<u>El (ft)</u>	<u>Moments (k-ft/ft)</u>			<u>Forces (k/ft)</u>			<u>Shears (k/ft)</u>	
	<u>M-SS</u>	<u>M-TT</u>	<u>M-ST</u>	<u>N-SS</u>	<u>N-TT</u>	<u>N-ST</u>	<u>Q-S</u>	<u>Q-T</u>
70.00	5.51	1.68	0.03	7.72	2.69	0.74	3.48	0.06
71.50	0.60	0.18	0.06	7.72	2.84	0.74	3.55	0.01
75.50	0.86	0.26	0.05	3.45	1.73	0.44	0.20	0.01
77.50	0.88	0.27	0.05	3.44	1.94	0.44	0.24	0.01
82.50	1.14	0.34	0.04	1.48	1.64	0.39	0.19	0.01
85.00	0.80	0.24	0.04	1.48	1.83	0.38	0.15	0.01
90.00	0.03	0.00	0.05	1.65	2.33	0.23	0.06	0.00
92.50	0.01	0.01	0.08	1.65	2.54	0.26	0.04	0.00

RBS USAR

TABLE 6A.14-3 (Cont)

Steel Containment Wall - Radius = 60.00 ft

<u>El (ft)</u>	<u>Moments (k-ft/ft)</u>			<u>Forces (k/ft)</u>			<u>Shears (k/ft)</u>	
	<u>M-SS</u>	<u>M-TT</u>	<u>M-ST</u>	<u>N-SS</u>	<u>N-TT</u>	<u>N-ST</u>	<u>Q-S</u>	<u>Q-T</u>
95.00	0.10	0.01	0.00	3.48	3.45	1.16	0.11	0.00
100.00	0.02	0.02	0.00	3.48	0.60	1.20	0.01	0.00
111.00	0.01	0.00	0.00	3.40	0.33	1.19	0.01	0.00
114.00	0.01	0.00	0.00	3.40	0.28	1.19	0.01	0.00
132.00	0.01	0.00	0.00	3.06	0.33	1.13	0.01	0.00
141.00	0.01	0.00	0.00	3.06	0.35	1.12	0.01	0.00
158.00	0.01	0.00	0.00	1.94	0.51	0.91	0.01	0.00
162.00	0.01	0.00	0.00	1.94	0.36	0.89	0.01	0.00
230.21	0.05	0.00	0.00	0.56	1.96	0.45	0.06	0.00
234.02	0.05	0.00	0.00	0.61	1.78	0.40	0.06	0.00
254.29	0.05	0.01	0.00	1.51	1.62	0.20	0.04	0.00
255.39	0.06	0.01	0.00	1.63	1.62	0.21	0.06	0.00

Shield Building - Radius = 66.25 ft

<u>El (ft)</u>	<u>Moments (k-ft/ft)</u>			<u>Forces (k/ft)</u>			<u>Shears (k/ft)</u>	
	<u>M-SS</u>	<u>M-TT</u>	<u>M-ST</u>	<u>N-SS</u>	<u>N-TT</u>	<u>N-ST</u>	<u>Q-S</u>	<u>Q-T</u>
95.00	1.85	0.26	0.06	7.13	4.37	1.67	0.35	0.02
101.00	1.11	0.17	0.10	7.13	4.32	1.66	0.29	0.01
117.00	0.88	0.21	0.05	7.08	2.84	1.62	0.18	0.02
122.00	1.00	0.23	0.10	7.08	2.75	1.62	0.17	0.02
134.00	1.09	0.25	0.09	7.06	2.68	1.61	0.21	0.01
144.00	1.07	0.26	0.08	7.06	2.55	1.56	0.21	0.13
185.00	1.08	0.23	0.08	6.49	2.02	1.66	0.22	0.01
210.50	1.20	0.19	0.07	5.60	1.37	1.87	0.19	0.01

RBS USAR

TABLE 6A.14-4

MAXIMUM FORCES, MOMENTS, AND STRESSES DUE TO LOCA
(ALL VALUES ARE \bar{E} AND ARE THE MAXIMUM OF CHUGGING
AND CONDENSATION OSCILLATION)

Basemat - El 65.00 ft

<u>Radius (ft)</u>	<u>Moments (k-ft/ft)</u>			<u>Forces (k/ft)</u>			<u>Shears (k/ft)</u>	
	<u>M-SS</u>	<u>M-TT</u>	<u>M-ST</u>	<u>N-SS</u>	<u>N-TT</u>	<u>N-ST</u>	<u>Q-S</u>	<u>Q-T</u>
6.04	19.80	23.60	0.00	6.92	6.92	0.00	3.50	0.00
12.08 (I)	9.05	15.00	0.00	6.56	6.66	0.00	2.62	0.00
12.08 (O)	24.60	17.92	0.00	5.13	6.48	0.00	6.36	0.00
16.75	13.40	13.20	0.00	5.45	6.11	0.00	4.59	0.00
26.25	19.00	10.90	0.00	3.32	4.71	0.00	3.55	0.00
31.00 (I)	26.50	11.70	0.00	3.27	4.24	0.00	3.00	0.00
31.00 (O)	37.40	12.22	0.00	4.10	4.31	0.00	4.44	0.00
37.00 (I)	40.50	15.80	0.00	3.87	3.96	0.00	3.72	0.00
37.00 (O)	49.60	11.70	0.00	4.39	3.38	0.00	3.75	0.00
43.00	30.60	11.10	0.00	4.15	2.82	0.00	3.22	0.00
49.00	14.80	9.87	0.00	3.65	2.88	0.00	2.72	0.00
55.00	2.02	7.87	0.00	3.57	2.97	0.00	2.42	0.00

(I)=Point just inside adjoining shell structure.
(O)=Point just outside adjoining shell structure.

Basemat - Adjoining Concrete Fill

<u>El (ft)</u>	<u>Radius (ft)</u>	<u>Normal Stresses (ksf)</u>			<u>Shear Stresses (ksf)</u>		
		<u>σ_{RR}</u>	<u>σ_{ZZ}</u>	<u>σ_{TT}</u>	<u>τ_{RZ}</u>	<u>τ_{RT}</u>	<u>τ_{ZT}</u>
61.25	57.50	0.24	0.03	0.34	0.17	0.00	0.00
63.75	57.50	0.51	0.05	0.33	0.25	0.00	0.00
66.25	57.50	0.42	0.11	0.34	0.30	0.00	0.00
68.75	57.50	0.11	0.23	0.37	0.33	0.00	0.00
61.25	69.25	0.25	0.06	0.30	0.14	0.00	0.00
63.75	69.25	0.25	0.09	0.29	0.07	0.00	0.00
66.25	69.25	0.17	0.17	0.27	0.15	0.00	0.00
68.75	69.25	0.24	0.28	0.25	0.27	0.00	0.00

RBS USAR

TABLE 6A.14-4 (Cont)

Concrete Fill

<u>El (ft)</u>	<u>Radius (ft)</u>	<u>Normal Stresses (ksf)</u>			<u>Shear Stresses (ksf)</u>		
		<u>σ_{RR}</u>	<u>σ_{ZZ}</u>	<u>σ_{TT}</u>	<u>τ_{RZ}</u>	<u>τ_{RT}</u>	<u>τ_{ZT}</u>
70.75	60.83	0.25	0.50	0.33	0.26	0.00	0.00
70.75	62.50	0.18	0.17	0.30	0.20	0.00	0.00
70.75	64.17	0.15	0.22	0.29	0.19	0.00	0.00
70.75	65.63	0.21	0.53	0.29	0.20	0.00	0.00
70.75	66.88	0.28	1.21	0.40	0.32	0.00	0.00
76.50	60.83	0.13	0.31	0.37	0.14	0.00	0.00
76.50	62.50	0.11	0.21	0.38	0.17	0.00	0.00
76.50	64.17	0.06	0.26	0.39	0.18	0.00	0.00
76.50	65.63	0.02	0.39	0.41	0.13	0.00	0.00
76.50	66.88	0.06	0.55	0.42	0.05	0.00	0.00

Pedestal - Radius = 12.08 ft

<u>El (ft)</u>	<u>Moments (k-ft/ft)</u>			<u>Forces (k/ft)</u>			<u>Shears (k/ft)</u>	
	<u>M-SS</u>	<u>M-TT</u>	<u>M-ST</u>	<u>N-SS</u>	<u>N-TT</u>	<u>N-ST</u>	<u>Q-S</u>	<u>Q-T</u>
70.00	9.08	1.38	0.00	5.80	2.55	0.00	2.09	0.00
73.42	3.47	0.50	0.00	5.80	3.54	0.00	1.15	0.00
76.80	0.59	0.08	0.00	6.14	2.60	0.00	0.68	0.00
81.08	0.92	0.18	0.00	6.14	1.22	0.00	0.07	0.00
85.00	0.84	0.15	0.00	6.39	0.51	0.00	0.13	0.00
91.67	1.50	0.19	0.00	6.39	1.05	0.00	0.55	0.00

RPV Support - Radius = 9.33 ft

<u>El (ft)</u>	<u>Moments (k-ft/ft)</u>			<u>Forces (k/ft)</u>			<u>Shears (k/ft)</u>	
	<u>M-SS</u>	<u>M-TT</u>	<u>M-ST</u>	<u>N-SS</u>	<u>N-TT</u>	<u>N-ST</u>	<u>Q-S</u>	<u>Q-T</u>
100.67	0.85	0.02	0.00	3.66	2.03	0.00	0.75	0.00
107.75	0.52	0.02	0.00	3.66	1.31	0.00	0.40	0.00

Weir Wall - Radius = 31.00 ft

<u>El (ft)</u>	<u>Moments (k-ft/ft)</u>			<u>Forces (k/ft)</u>			<u>Shears (k/ft)</u>	
	<u>M-SS</u>	<u>M-TT</u>	<u>M-ST</u>	<u>N-SS</u>	<u>N-TT</u>	<u>N-ST</u>	<u>Q-S</u>	<u>Q-T</u>
70.00	13.80	2.15	0.00	1.90	1.42	0.00	3.23	0.00
73.42	3.89	0.62	0.00	1.90	5.30	0.00	3.42	0.00
81.08	8.28	1.17	0.00	1.22	22.10	0.00	2.66	0.00
85.00	11.00	1.58	0.00	1.22	21.20	0.00	2.15	0.00

RBS USAR

TABLE 6A.14-4 (Cont)

Bio-Shield Wall - Radius = 13.92 ft

<u>El (ft)</u>	<u>Moments (k-ft/ft)</u>			<u>Forces (k/ft)</u>			<u>Shears (k/ft)</u>	
	<u>M-SS</u>	<u>M-TT</u>	<u>M-ST</u>	<u>N-SS</u>	<u>N-TT</u>	<u>N-ST</u>	<u>Q-S</u>	<u>Q-T</u>
100.67	1.28	0.35	0.00	3.65	0.36	0.00	0.25	0.00
106.53	0.37	0.08	0.00	3.65	0.57	0.00	0.07	0.00
112.37	0.12	0.05	0.00	3.39	0.72	0.00	0.07	0.00
118.23	0.81	0.17	0.00	3.39	1.21	0.00	0.36	0.00
124.08	0.09	0.04	0.00	2.55	0.87	0.00	0.16	0.00
129.93	0.10	0.05	0.00	2.55	0.54	0.00	0.11	0.00

Drywell Wall - Radius = 37.00 ft

<u>El (ft)</u>	<u>Moments (k-ft/ft)</u>			<u>Forces (k/ft)</u>			<u>Shears (k/ft)</u>	
	<u>M-SS</u>	<u>M-TT</u>	<u>M-ST</u>	<u>N-SS</u>	<u>N-TT</u>	<u>N-ST</u>	<u>Q-S</u>	<u>Q-T</u>
70.00	45.60	7.11	0.00	2.90	4.50	0.00	7.28	0.00
71.08	37.70	5.88	0.00	2.90	5.41	0.00	7.35	0.00
73.42	20.70	3.24	0.00	2.93	7.84	0.00	7.38	0.00
81.08	23.90	3.69	0.00	3.13	20.50	0.00	1.93	0.00
83.42	28.90	4.47	0.00	3.13	23.20	0.00	2.91	0.00
90.00	22.40	2.97	0.00	3.45	20.30	0.00	5.49	0.00
101.00	19.80	3.25	0.00	3.45	15.60	0.00	3.40	0.00
114.00	13.00	2.10	0.00	3.50	2.20	0.00	1.50	0.00

Stiffened Shell - Radius = 60.00 ft

<u>El (ft)</u>	<u>Moments (k-ft/ft)</u>			<u>Forces (k/ft)</u>			<u>Shears (k/ft)</u>	
	<u>M-SS</u>	<u>M-TT</u>	<u>M-ST</u>	<u>N-SS</u>	<u>N-TT</u>	<u>N-ST</u>	<u>Q-S</u>	<u>Q-T</u>
70.00	0.85	0.26	0.00	1.51	0.50	0.00	0.45	0.00
71.50	0.20	0.07	0.00	1.51	0.54	0.00	0.45	0.00
75.50	0.22	0.07	0.00	0.79	0.47	0.00	0.06	0.00
77.50	0.20	0.06	0.00	0.79	0.51	0.00	0.06	0.00
82.50	0.23	0.06	0.00	0.57	0.50	0.00	0.04	0.00
85.00	0.23	0.07	0.00	0.57	0.53	0.00	0.04	0.00
90.00	0.01	0.00	0.00	0.19	0.58	0.00	0.01	0.00
92.50	0.01	0.00	0.00	0.19	0.58	0.00	0.01	0.00

RBS USAR

TABLE 6A.14-4 (Cont)

Steel Containment Wall - Radius = 60.00 ft

<u>El (ft)</u>	<u>Moments (k-ft/ft)</u>			<u>Forces (k/ft)</u>			<u>Shears (k/ft)</u>	
	<u>M-SS</u>	<u>M-TT</u>	<u>M-ST</u>	<u>N-SS</u>	<u>N-TT</u>	<u>N-ST</u>	<u>Q-S</u>	<u>Q-T</u>
95.00	0.01	0.00	0.00	0.42	0.67	0.00	0.02	0.00
100.00	0.01	0.00	0.00	0.42	0.25	0.00	0.01	0.00
111.00	0.00	0.00	0.00	0.38	0.22	0.00	0.00	0.00
114.00	0.01	0.00	0.00	0.38	0.24	0.00	0.01	0.00
132.00	0.01	0.00	0.00	0.35	0.19	0.00	0.01	0.00
141.00	0.00	0.00	0.00	0.35	0.18	0.00	0.01	0.00
158.00	0.01	0.00	0.00	0.39	0.25	0.00	0.01	0.00
162.00	0.01	0.00	0.00	0.39	0.22	0.00	0.01	0.00
230.21	0.01	0.00	0.00	0.16	0.56	0.00	0.02	0.00
234.02	0.02	0.00	0.00	0.17	0.55	0.00	0.02	0.00
254.29	0.01	0.00	0.00	0.35	0.35	0.00	0.01	0.00
255.39	0.01	0.00	0.00	0.36	0.36	0.00	0.01	0.00

Shield Building - Radius = 66.25 ft

<u>El (ft)</u>	<u>Moments (k-ft/ft)</u>			<u>Forces (k/ft)</u>			<u>Shears (k/ft)</u>	
	<u>M-SS</u>	<u>M-TT</u>	<u>M-ST</u>	<u>N-SS</u>	<u>N-TT</u>	<u>N-ST</u>	<u>Q-S</u>	<u>Q-T</u>
95.00	0.60	0.09	0.00	0.89	1.18	0.00	0.17	0.00
101.00	0.32	0.05	0.00	0.89	0.92	0.00	0.11	0.00
117.00	0.43	0.07	0.00	0.81	0.42	0.00	0.07	0.00
122.00	0.28	0.04	0.00	0.81	0.28	0.00	0.06	0.00
134.00	0.46	0.07	0.00	0.85	0.34	0.00	0.08	0.00
144.00	0.48	0.07	0.00	0.85	0.28	0.00	0.08	0.00
185.00	0.36	0.05	0.00	0.73	0.24	0.00	0.06	0.00
210.50	0.35	0.05	0.00	0.82	0.21	0.00	0.08	0.00

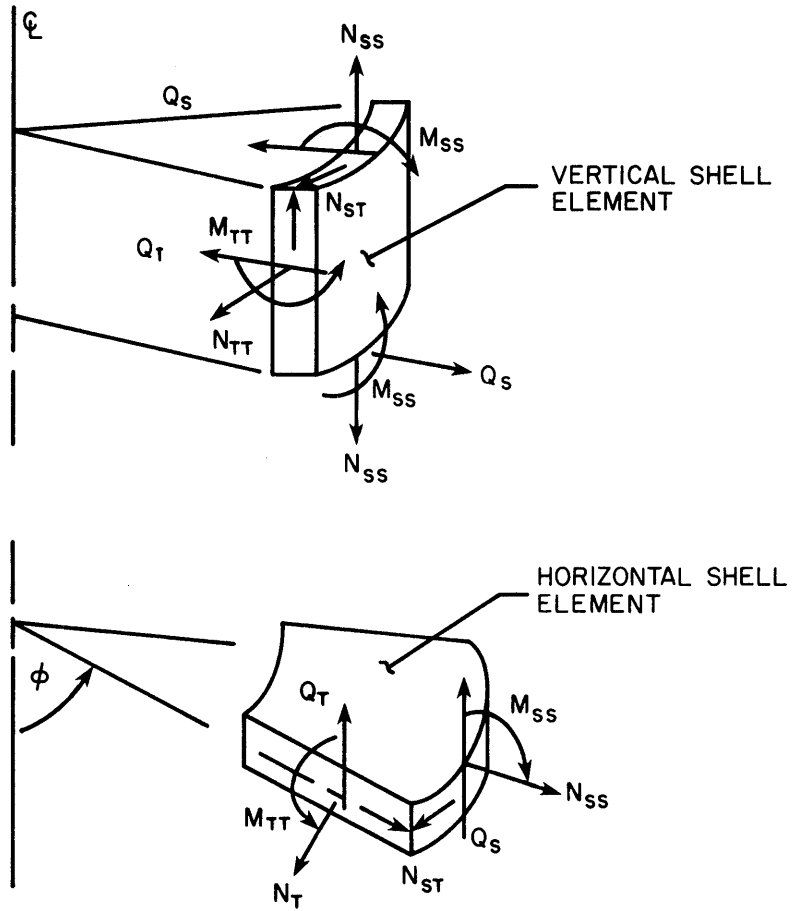


FIGURE 6A.14-1

POSITIVE SIGN CONVENTION FOR
INTERNAL FORCES AND MOMENTS

RIVER BEND STATION
UPDATED SAFETY ANALYSIS REPORT

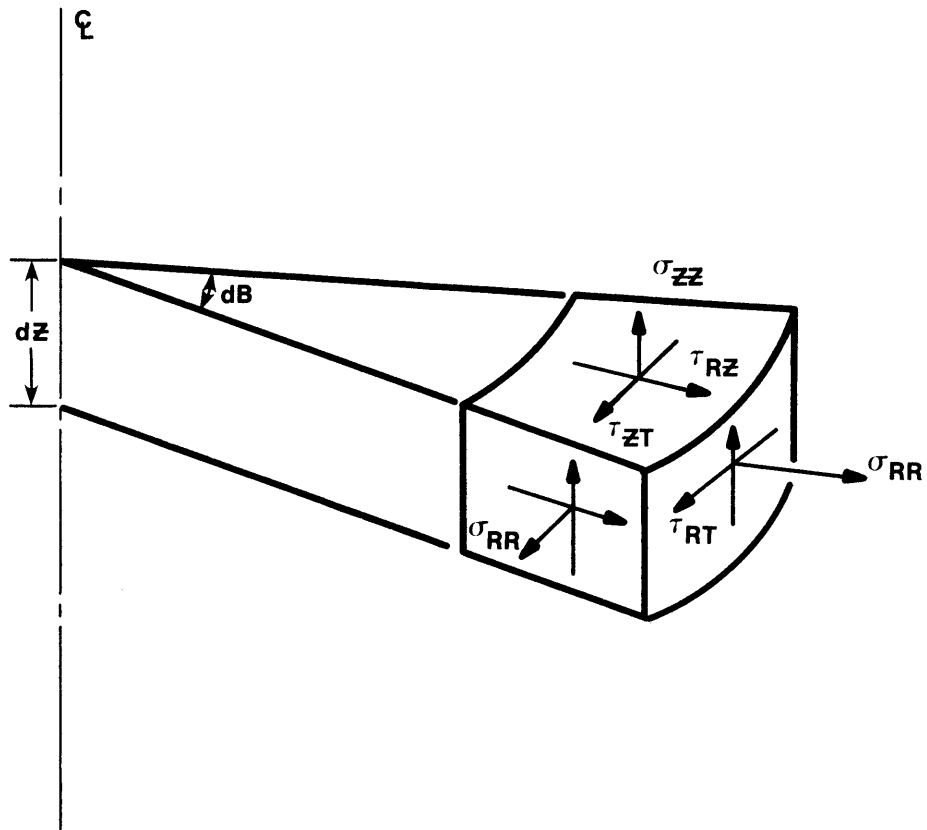


FIGURE 6A.14-2

POSITIVE SIGN CONVENTION FOR
INTERNAL STRESSES

RIVER BEND STATION
UPDATED SAFETY ANALYSIS REPORT

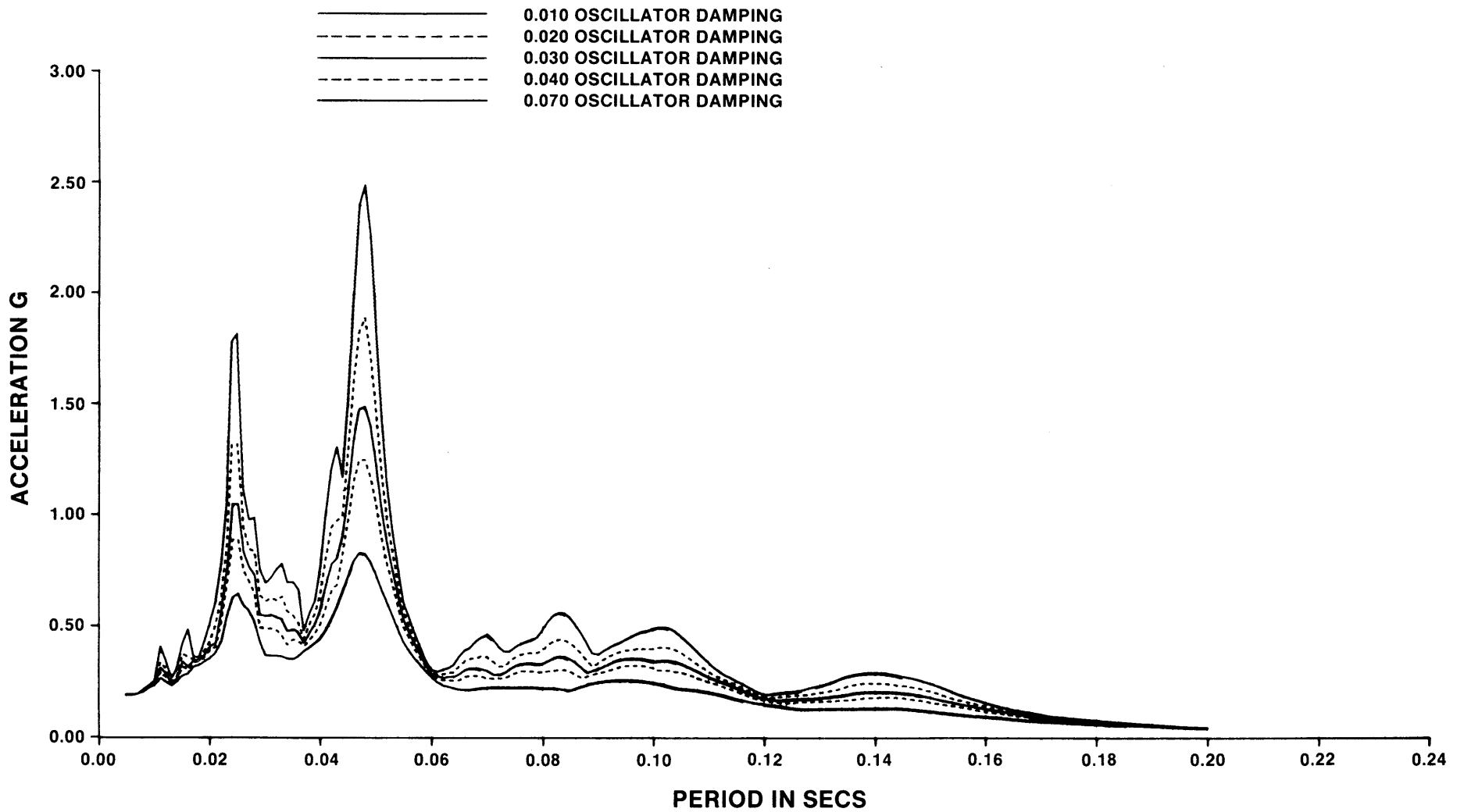


FIGURE 6A.14-3

RADIAL ARS PLOT AT A DRYWELL
LOCATION DUE TO SRV DISCHARGE

RIVER BEND STATION
UPDATED SAFETY ANALYSIS REPORT

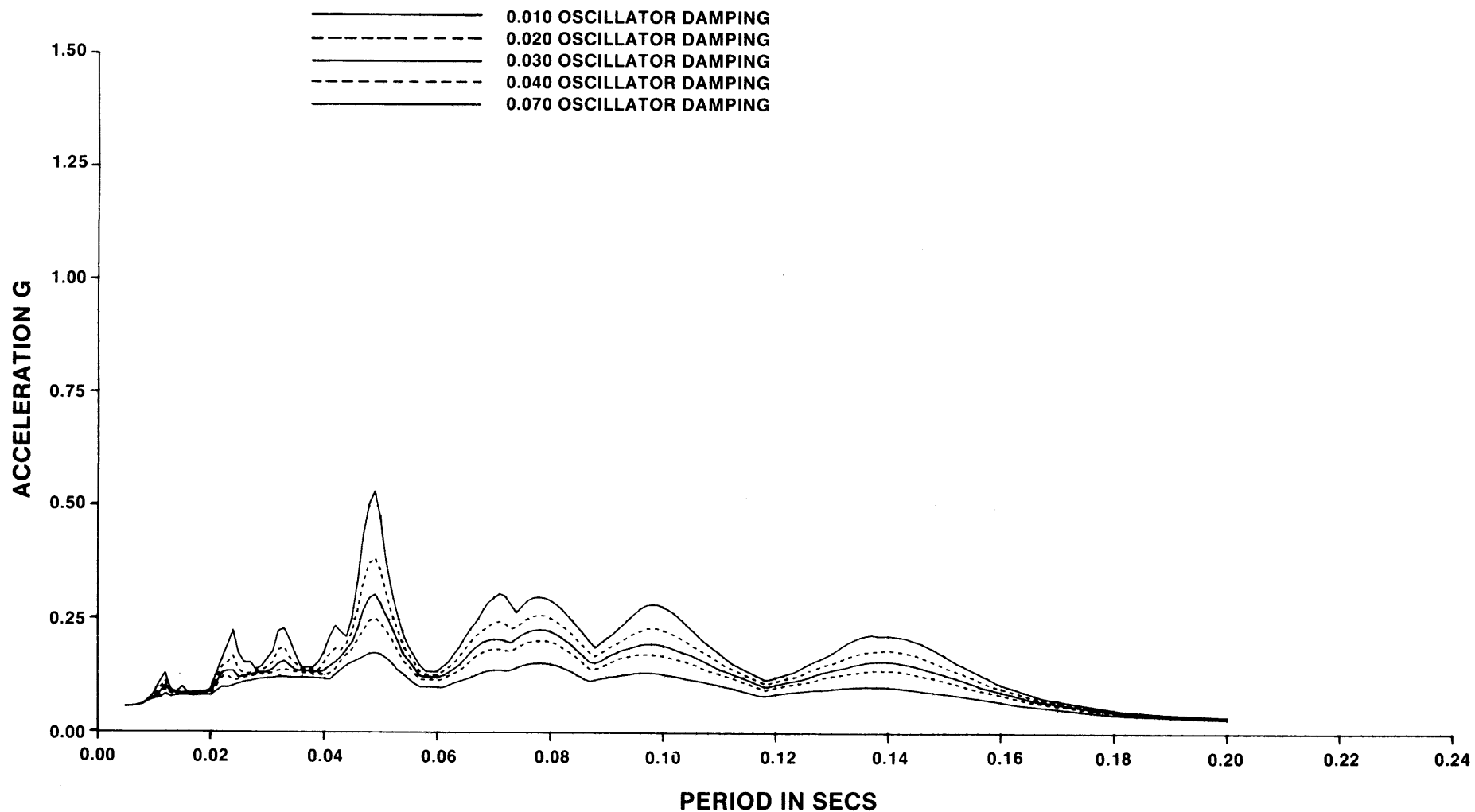


FIGURE 6A.14-4
 VERTICAL ARS PLOT AT A SHIELD
 BUILDING WALL LOCATION DUE TO
 SRV DISCHARGE
RIVER BEND STATION
 UPDATED SAFETY ANALYSIS REPORT

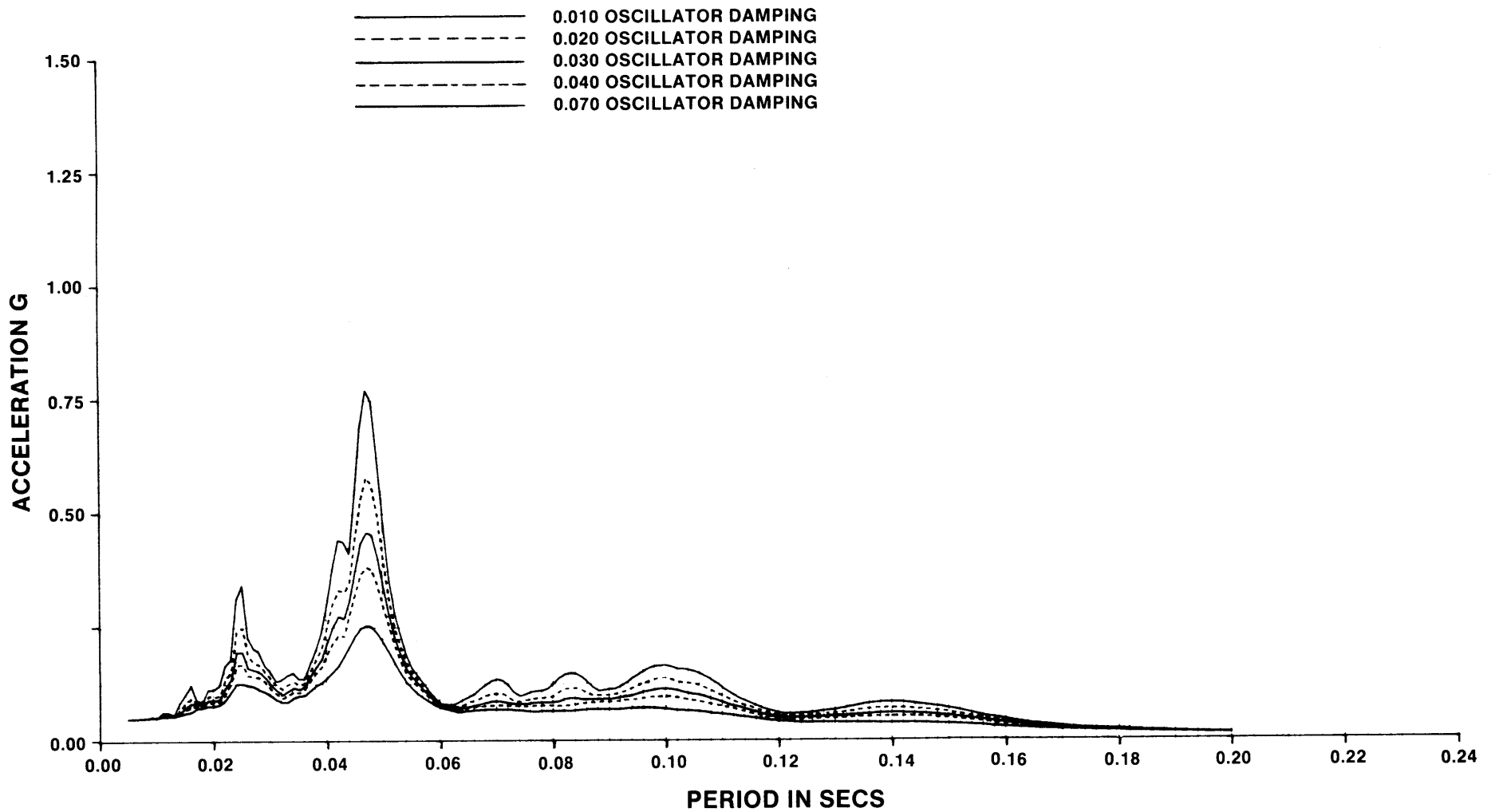


FIGURE 6A.14-5

TANGENTIAL ARS PLOT AT A DRYWELL
LOCATION DUE TO SRV DISCHARGE

RIVER BEND STATION
UPDATED SAFETY ANALYSIS REPORT

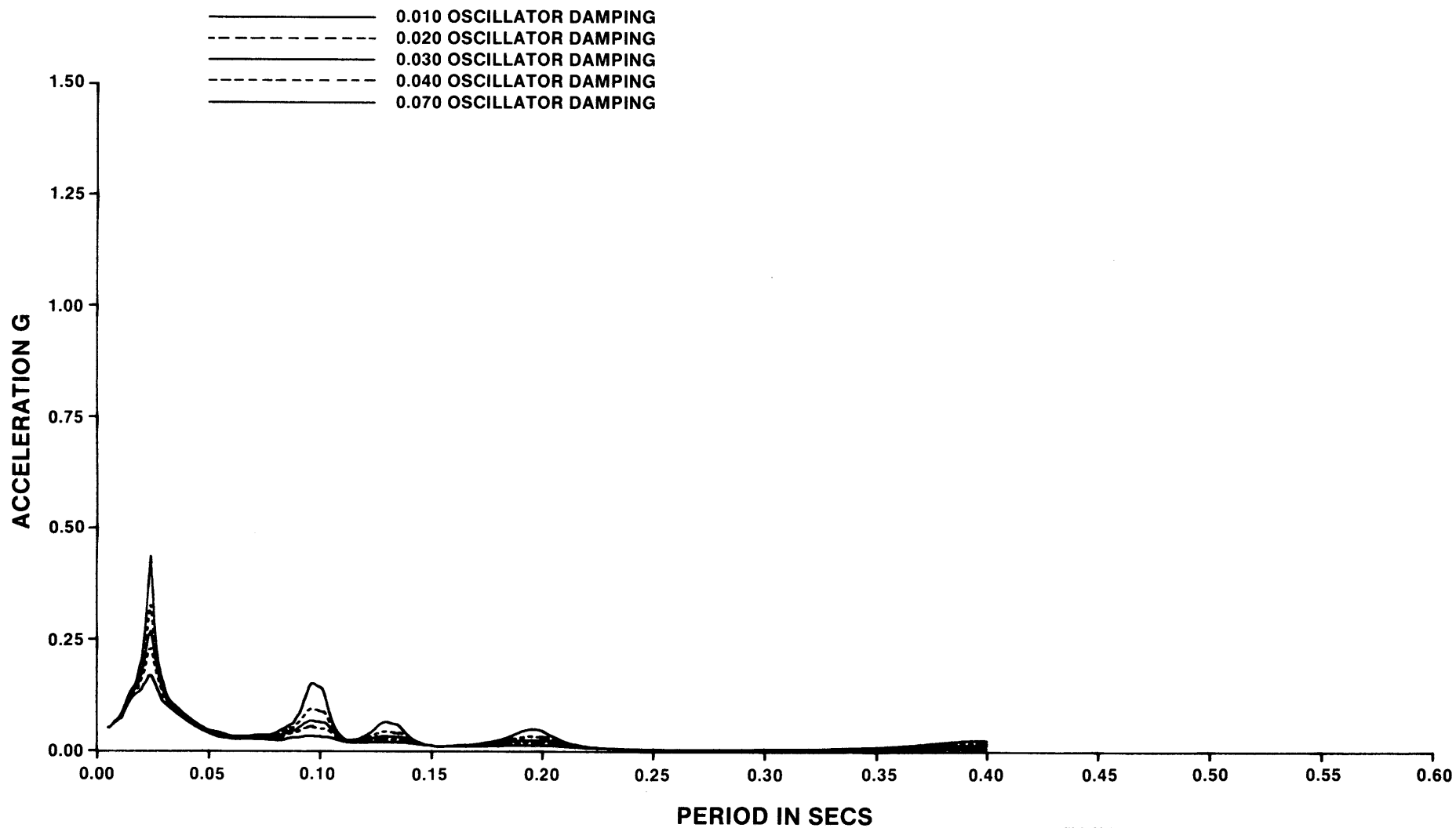


FIGURE 6A.14-6

RADIAL ARS PLOT AT A DRYWELL
LOCATION DUE TO CONDENSATION
OSCILLATION (LOCA)

RIVER BEND STATION
UPDATED SAFETY ANALYSIS REPORT

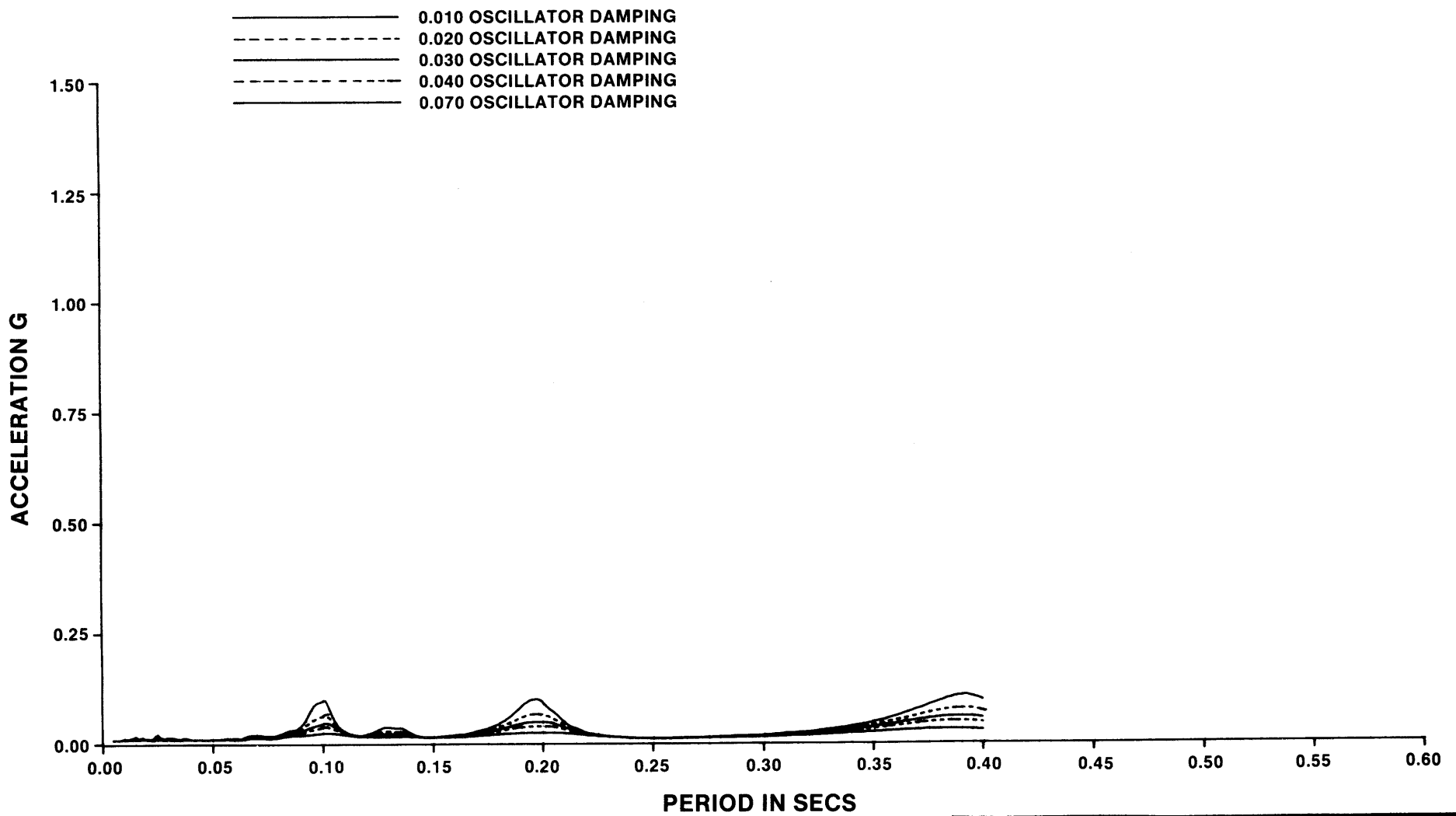


FIGURE 6A.14-7

VERTICAL ARS PLOT AT A DRYWELL
LOCATION DUE TO CONDENSATION
OSCILLATION (LOCA)

RIVER BEND STATION
UPDATED SAFETY ANALYSIS REPORT

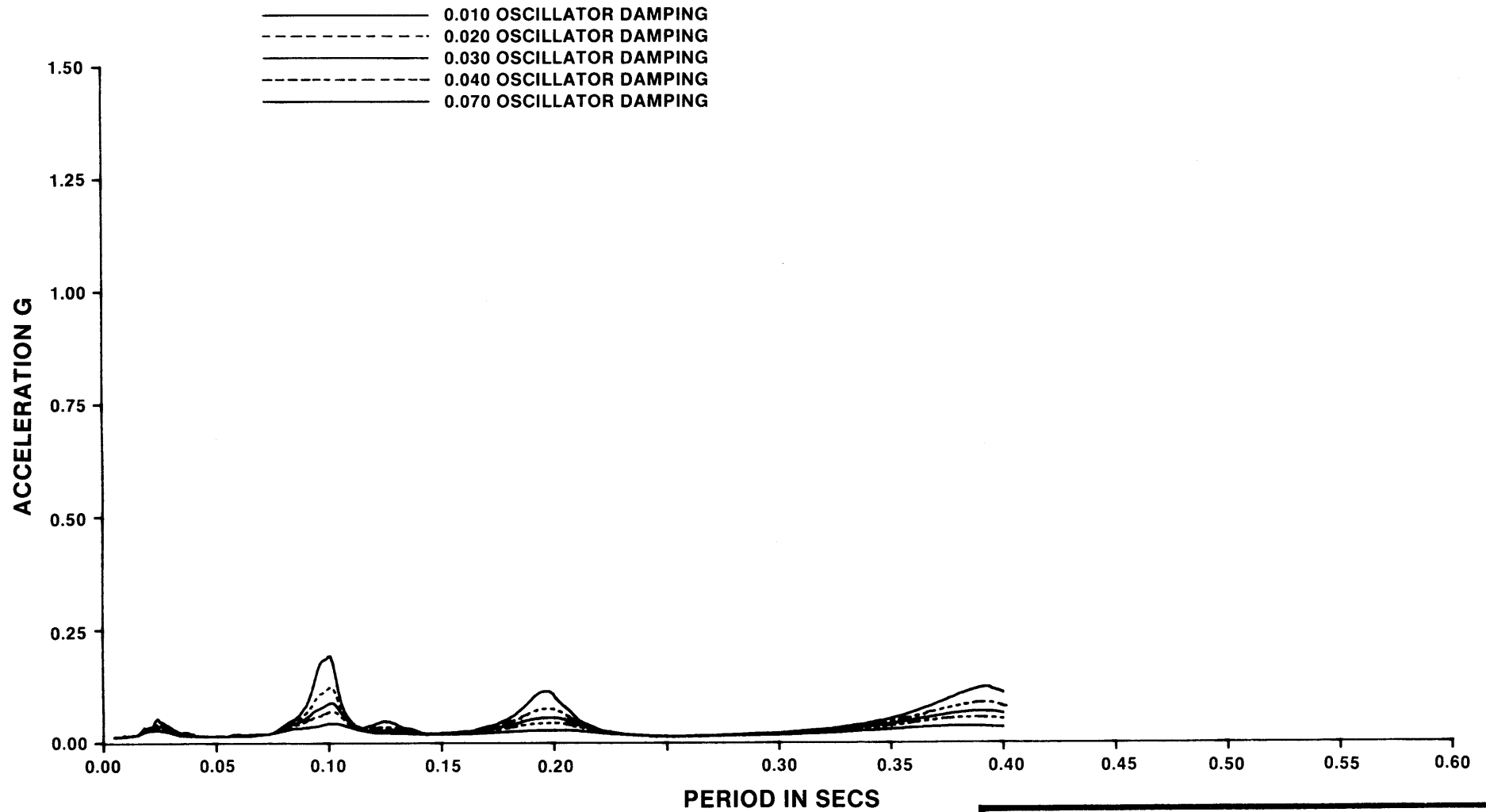


FIGURE 6A.14-8

VERTICAL ARS PLOT AT PEDESTAL—
BASEMENT JUNCTION DUE TO
CONDENSATION OSCILLATION (LOCA)

RIVER BEND STATION
UPDATED SAFETY ANALYSIS REPORT

6A.15 CONTAINMENT SYSTEM ASSESSMENT

6A.15.0 General

The containment system is assessed in two parts. Section 6A.15.1 discusses the assessment of the basemat liner and its associated anchorage system. Section 6A.15.2 discusses the assessment of the steel containment vessel. References to the description of loads affecting the containment system, including hydrodynamic SRV and LOCA loads, are included in each of the sections as applicable.

6A.15.1 Basemat Liner

The basemat liner consists primarily of three types of elements: liner plates, bridging bars, and embedment plates. The liner plates are constructed of flat 3/8-in thick steel plates with their edges welded to bridging bars and embedment plates as shown in Fig. 6A.15-1. Bridging bars provide anchorage to the concrete mat at each radial plate edge. Embedment plates are used in areas within the containment where reinforced concrete walls must be anchored to the concrete mat (drywell, weir wall, and reactor pedestal walls). Embedment plates are made from flat 1 1/2-in thick steel plate. A corner transition section provides continuity between the cylindrical containment vessel and the basemat liner plates. Each basemat liner plate connection is made with full penetration welds. Details of each of the above are given in Fig. 3.8-2.

The 3/8-in thick basemat liner between the weir wall and reactor pedestal wall is covered by an 11 ft-1 3/4-in thick reinforced concrete slab. The 3/8-in thick basemat liner inside the reactor pedestal wall is covered by a 3 ft-1/4-in thick reinforced concrete slab. Both slabs will remain in continuous contact with their respective liners under all plant conditions. Therefore, the primary analysis of the basemat liner is restricted to the areas where the liner is exposed to the internal containment environment. This occurs for the mat liner between the weir wall and drywell wall (in the weir annulus), and between the outer drywell wall and containment vessel, under the suppression pool.

A test member exists at each mat liner weld detail. The test member is either a channel or an angle, welded over the liner connection. The details of these members are shown in Fig. 3.8-2.

6A.15.1.1 Load Sources and Design Criteria

6A.15.1.1.1 Load Sources

The history and background of loads imparted upon containment structures, including the basemat liner, caused by hydrodynamic loading conditions as a result of a LOCA are described in detail in Appendix 6A, Sections 6A.1 through 6A.12. The background of loads caused by the SRV discharge phenomenon are described in Appendix 6A, Attachment A. Additionally, elevated suppression pool temperatures during normal operation and accident conditions cause stresses in the suppression pool basemat liner.

Loads from other sources are also present. Among these are dead and hydrostatic loads, containment internal pressures, and loads associated with seismic events, including water sloshing. However, as the liner is continuously backed by concrete, positive pressure loads do not govern the design of the basemat liner. The governing loading conditions result from a net negative pressure developed in the suppression pool by hydrodynamic forces during SRV, LOCA, and seismic events.

6A.15.1.1.2 Design Criteria

The design criteria for the containment basemat liner, including the effects of LOCA and SRV discharge, are the same as the applicable liner load combination tables as shown in Section 3.8.2. The liner is evaluated using the unfactored load combinations given in Table 3.8-2, and compared with the strain allowables listed in the table. The 1977 ASME Section III, Division 2, Subsection CC has been used as a guide in the development of the basemat liner strain allowable limits. In the evaluation of the liner, strains generated by the various effects are combined to yield the maximum tensile or compressive values, in accordance with the proper loading combination, and are then compared to their respective allowables.

A fatigue analysis of the basemat liner is performed to verify that the cumulative usage factor, due to cyclic load application, is less than unity (1.0). The fatigue analysis uses the load combinations as given in Table 3.8-2 and the methods as prescribed in ASME Section III, Division I, Subsection NE-3222.4(e).

Stress concentration factors are considered at each weld location in the liner plates to obtain the maximum peak stresses. These peak stresses are then used in the fatigue

analysis of the basemat liner, in accordance with ASME Section III, Division I, Subsection NE requirements.

6A.15.1.1.3 Basemat Embedments Design Criteria

The design criteria for the containment basemat liner embedments is similar to that of the basemat liner. The embedments are evaluated using the load combinations given in Table 3.8-2. Allowables for the embedment design are based on ACI Standard 318-71 for concrete shear stress and on the ASME Section III, Division 2, Subsection CC for steel embedment force and displacement allowable limits.

6A.15.1.2 Basemat Liner Analysis

6A.15.1.2.1 Assumptions

The following assumptions are made in the analysis of the basemat liner plates:

1. The basemat liners under the reactor pedestal and weir wall are covered with thick concrete. Therefore, liners in these areas are assumed to be continuously backed by concrete from both sides.
2. The basemat liner instantaneously assumes the temperature of the water in the suppression pool. No thermal gradient exists in the liner plate.
3. Liner segments are analyzed as rectangular plates, fixed along their boundaries. Small plate curvatures and angular deviations are neglected.
4. The liner material stress-strain curve is modeled with a linear-elastic linear plastic distribution. The plastic modulus of elasticity (E_p) is assumed to have a slope equal to one-tenth of that of the elastic modulus (E_e); i.e., $E_p = 0.10 E_e$.

6A.15.1.2.2 Strain-Displacement Relationships

The displacements and rotations of the concrete basemat resulting from the analysis discussed in Section 6A.14 are included in the analysis of the strain levels in the basemat liner. The hoop and radial strains at the top of the concrete basemat are used as an equivalent uniform strain through the depth of the liner.

Strains from temperature effects are determined by considering a fully restrained two-dimensional plate. In

this respect, strong consideration is given to the time period associated with specified loading combinations, as short-term and long-term suppression pool temperatures may vary widely.

Stresses and strains due to plate bending are determined by classical plate theory. Bending is caused by negative pressure distributions in the suppression pool during the occurrence of a LOCA or SRV discharge, pulling the liner away from the concrete basemat. As pressure distributions in the suppression pool are time-dependent during normal operation and accident conditions, due consideration is given when combining these loads in accordance with Table 3.8-2.

When stresses above the material yield stress are encountered, a linear plastic stress and strain approach is used. The results are then compared to the allowable limits as defined in Table 3.8-2.

In the fatigue evaluation, the strains used in evaluating the basemat liner are converted to stresses and multiplied by a stress concentration factor to account for peak stress effects, as discussed in Section 6A.15.1.1.2. The fatigue analysis performed uses the cyclic data shown in Table 6A.15-1. A conservative stress concentration factor of 4.0 is used to represent the local increase in secondary membrane stresses in the basemat liner at each weld location in the plate.

6A.15.1.2.3 Basemat Liner Static Analysis

The basemat liner is analyzed for static load application. Dynamic loads are converted to equivalent static loads using acceleration profiles (ARS) generated as described in Section 6A.13.

As discussed previously, the maximum liner stresses and strains are governed by negative pressure distributions. Therefore, the basemat liner static analysis is based on a constant peak negative pressure in conjunction with thermal stresses and strains.

6A.15.1.2.4 Basemat Liner Anchorage System

The basemat liner is anchored to the concrete basemat with bridging bars, as described in Section 6A.15.1. The bars transmit loads from the liners into the concrete. Tension on the embedments, as a result of the liner uplift, is resisted by the formation of "shear failure cones" in the

concrete. The maximum allowable shear loads are calculated in accordance with ACI Code 318-71.

6A.15.1.3 Basemat Liner Evaluation Summary

6A.15.1.3.1 Basemat Liner Strain Evaluation

The critical loading combinations, as determined by the basemat liner analysis, occur during the normal operation mode, and during the abnormal/extreme environment design condition (Table 3.8-2). Note that for the abnormal/extreme environment, the worst case liner loads are associated with a long-term SBA. Strains are summarized in Table 6A.15-2, for two regions on the basemat liner:

1. In the weir annulus, between the drywell wall and weir wall
2. Under the suppression pool, between the outer drywell wall and the containment vessel. Strains are evaluated at the center of the liner plate and at its supporting edge in this region.

In many cases, the summation of bending plus membrane strain is greater than the material yield strain. Therefore, a plastic analysis is performed. In all cases, however, strains are less than the allowable limits as defined in Table 3.8-2. See Table 6A.15-2 for this strain summary.

6A.15.1.3.2 Basemat Liner Instability Evaluation

The basemat liners in the weir annulus and under the suppression pool are both analyzed for instability.

In each case, analysis shows that the critical stress is greater than the calculated liner stress. However, as shown in Section 6A.15.1.3.1, in many cases liner strains occur in the plastic range. Therefore, a modified plastic instability analysis, based on strain approach, is used.

The results of the basemat liner instability analysis are as follows:

1. For the liner in the weir annulus, the equivalent critical strain is 0.003 in/in. The maximum strain is 0.0014 in/in.
2. For the liner between the drywell and containment vessel, the equivalent critical strain is 0.003 in/in. The maximum strain is 0.0016 in/in.

6A.15.1.3.3 Basemat Liner Fatigue Evaluation

The load combination Table 3.8-2 is used in conjunction with the stress cycle Table 6A.15-1 in order to perform a fatigue analysis. The analysis shows the following results:

1. For the basemat liner in the weir annulus, the cumulative usage factor is $0.85 < 1.0$. The analysis is performed in accordance with ASME Section III, Division I, Subsection NE. The option of analysis in the elastic shakedown region is being utilized.
2. For the basemat liner between the drywell wall and containment vessel, the cumulative usage factor is $0.034 < 1.0$.

From Table 6A.15-1, it can be seen that 1,800 SRV events are expected in the plant life of 40 yr. The fatigue design analysis is calculated based upon 4,200 SRV events. Therefore, both basemat liner fatigue analyses show a significant margin of safety.

6A.15.1.3.4 Basemat Liner Embedment Evaluation

The analysis of the basemat liner embedments shows the following results:

1. Maximum embedment uplift force on any embedment is 290 lb per linear in. The stresses in the steel members are very small in comparison to the allowable limits.
2. Maximum calculated concrete shear stress is 17 lb/sq in. Allowable concrete shear stress, in accordance with ACI Standard 318-71, is 253 lb/sq in.

Therefore, all embedments show a significant margin of safety against failure.

6A.15.2 Containment Vessel

The containment vessel is a structure constructed of 1 1/2-in (nominal) thick steel plate. The vessel consists of a 120-ft diameter cylindrical shell enclosed at the top by a torispherical dome. The lower 20 ft of the cylindrical shell is stiffened both vertically and circumferentially by steel stiffeners welded to the vessel and is backed by structural concrete placed to elevation 94 ft 8 in. in the annulus between the containment and shield building.

Openings are provided in the containment shell for penetrations, locks, and hatches. Where required, additional reinforcement is provided around such openings. There are other structures attached to the containment shell. These include beam seats, polar crane supports, etc. In each case, additional shell reinforcing is provided as required. The geometry and layout of the containment vessel is shown in Fig. 3.8-1.

6A.15.2.1 Load Sources and Design Criteria

6A.15.2.1.1 Load Sources

The history and background of hydrodynamic loadings on the containment vessel are similar to those discussed in Section 6A.15.1.1.1 for the basemat liner. Positive pressure loads, in combination with other loads including those caused by hydrodynamic loads, result in significant stress levels. However, as for the basemat liner, negative pressure distributions in the suppression pool govern the containment vessel design in this region.

6A.15.2.1.2 Design Criteria

The design criteria for the containment vessel above elevation 94 ft 8 in, including the effects of SRV discharge and LOCA, are the same as the applicable containment vessel stress comparisons as shown in Section 3.8.2, and meet the requirements of ASME III, Division 1, Subsection NE. The vessel is evaluated using the unfactored load combinations given in Table 3.8-1 and compared with the applicable stress allowables listed in Table 3.8-1. These allowables are in accordance with the stress limits as given in ASME Section III, Division I, Subsection NE-3220.

The design criteria is applicable to all containment vessel stress comparisons, including, but not limited to:

1. Static stress analysis, including stresses resulting from instability analysis (buckling) of the containment vessel
2. Dynamic analysis
3. Discontinuity analysis at the shell to basemat junction, shell to dome junction, and at openings in the vessel
4. Analysis at attachments to the containment vessel

5. Containment penetration analysis.

The applicable codes and standards used in designing the containment vessel are listed in Section 3.8.2.2.1.

6A.15.2.2 Containment Vessel Analysis

6A.15.2.2.1 Assumptions

The following assumptions are made in the analysis of the containment vessel:

1. The containment vessel is modeled as a linear axisymmetric thin shell of revolution.
2. The analysis of the containment vessel is based on linear-elastic material behavior.

6A.15.2.2.2 Containment Vessel Static Analysis

Two methods of static analysis are evaluated in the design of the containment vessel. The first is an overall vessel stress analysis. The second is an instability (buckling) analysis of the containment vessel. For each method of analysis, loads are combined in accordance with Table 3.8-1. Stress comparisons for each loading combination are also given in Table 3.8-1. Both loading combinations and stress comparisons are in accordance with ASME Section III, Division 1, Subsection NE.

Overall Static Stress Analysis

The containment vessel is modeled as an orthotropic thin shell of revolution, using the SHELL 1 (Appendix 3A) finite difference computer program. Static loads (such as dead, live, and pressure loads) are input into the model. Output from the SHELL 1 computer runs includes forces and moments and/or stresses at specified elevations on the containment model. For the containment vessel region backed by the concrete fill, the SHELL 1 analysis is checked with a Ghosh Wilson analysis using a model similar to the one shown on Fig. 6A.13-3. Forces and moments due to hydrodynamic SRV and LOCA loads are generated by the Ghosh-Wilson finite element computer program, as described in Sections 6A.13 and 6A.14. For containment vessel regions above the suppression pool, hydrodynamic forces and moments are converted to stresses and added directly to the stress output from SHELL 1 in accordance with Table 3.8-1. For the containment vessel regions backed by the concrete fill, hydrodynamic forces and moments are added to the static

forces and moments prior to the conversion to stresses. The calculation of stresses in the suppression pool region accounts for the modified section modulus of the stiffened containment vessel.

Instability Static Stress Analysis

Stresses resulting from instability of the containment vessel (buckling analysis) are evaluated two ways. The first considers the negative pressure distributions generated in the suppression pool region during SRV discharge and LOCA. Calculations are done in accordance with ASME Section III, Division 1, Subsection NE formulas and criteria. Stress comparisons of maximum compressive stresses are given in Table 3.8-1, based on ASME, Section III, Division 1, Subsection NE.

Compressive stresses along the containment due to mechanical loads are also considered in the containment vessel design. Included in this analysis are load components induced into the containment shell from floor beam seats, crane supports, etc, during hydrodynamic events. Instability analysis is done in accordance with ASME Code Case N-284.

6A.15.2.2.3 Containment Vessel Dynamic Analysis

A representation of the containment vessel is included as part of the multi-structure model described in Section 6A.13. The model is used in the dynamic analysis to determine the response of reactor building structures to the applied dynamic loadings associated with SRV discharge and LOCA. Amplified Response Spectra (ARS) plots are then generated for each of the reactor building structures, at various elevations, as described in Section 6A.14. An example of a containment vessel ARS plot is shown in Fig. 6A.14-6. Additionally, this analysis provides forces and moments in the containment vessel due to the applied dynamic loadings.

The information generated by the above analysis is then incorporated in the containment vessel calculations in accordance with Table 3.8-1.

6A.15.2.2.4 Containment Vessel Discontinuity Analysis

Discontinuity stresses in the containment vessel are determined at the shell-to-basemat junction, at the shell-to-containment dome junction, and at openings in the containment vessel provided for personnel lock and equipment hatches.

Vessel-to-Basemat Junction

Discontinuity stresses at the shell-to-basemat junction are determined in the following manner:

The shell-to-basemat junction is modeled into the SHELL 1 and Ghosh-Wilson computer models as previously described. Secondary stresses from each of the load cases, including those created by hydrodynamics, are included in the output from the computer analysis at this region. Therefore, the primary plus secondary stress output need only be properly combined and checked against the allowable stress limits.

Vessel-to-Dome Junction

Discontinuity stresses at the shell-to-dome junction are determined in the following manner:

The shell-to-dome junction is modeled into the SHELL 1 and Ghosh-Wilson computer models as previously described. Secondary stresses from each of the load cases, including those created by hydrodynamics, are included in the output from the computer analysis at this region. Therefore, the primary plus secondary stress output need only be properly combined and checked against the allowable stress limits.

Openings in the Vessel

Discontinuity stresses at openings in the containment vessel, provided for personnel locks and equipment hatches, are determined in the following manner:

A finite element model of the local region around the lock or hatch is generated, using one of the computer programs listed in Appendix 3A. Loads are applied on the appropriate boundaries of the finite element model. The applied loads are extracted from the SHELL 1 and Ghosh-Wilson computer analyses previously discussed, at the applicable elevation for a particular lock or hatch. The primary plus secondary stresses are then generated by the finite element computer program.

For each of the discontinuity analyses described above, input loads are combined in accordance with the combinations of Table 3.8-1, and the primary plus secondary stresses are compared to the appropriate allowable stress limits listed in Table 3.8-1. Loading combinations and stress comparisons

are in accordance with ASME, Section III, Division 1, Subsection NE.

6A.15.2.2.5 Containment Vessel Attachment Analysis

Stresses at attachments to the containment vessel from floor beam seats, polar crane supports, and pipe supports are determined in the following manner:

Equivalent static loads at floor beam seats and crane supports are determined from the steel floor and polar crane dynamic analyses, respectively. For pipe support attachments, the forces and moments are obtained from the pipe stress analysis. The stresses in the containment shell due to these loads are determined by "Stresses from Local Loading in Cylindrical Pressure Vessels," by P. P. Bylaard, Transactions of the ASME, August 1955. These stresses are then added to the stresses caused by other containment loads in accordance with Table 3.8-1.

6A.15.2.2.6 Containment Penetration Analysis

Analysis methods and criteria for containment vessel penetrations are discussed in Section 3.8.2.

6A.15.2.3 Containment Vessel Evaluation Summary

Containment vessel stresses and stress comparisons are summarized in the containment stress report.

Note that the stress comparisons given in these tables are due to combinations of hydrodynamic load as well as other load components, in accordance with the loading combinations of Table 3.8-1.

TABLE 6A.15-1
CYCLIC STRESS DATA

<u>Load/Event Cycle</u>	<u>Number of Cycles per Event</u>
Design Basis Accident (DBA) 1 Event/40 yr	1
Seismic	
1 SSE/40 yr	20
5 OBE/40 yr	20
Safety Relief Valve (SRV) 1,800 Events/40 yr	8*
Small or Intermediate Break Accident (SBA/IBA) 1 Event/40 yr (assumed)	1

*Assumed number of negative-positive pressure cycles that affect basemat liner.

TABLE 6A.15-2

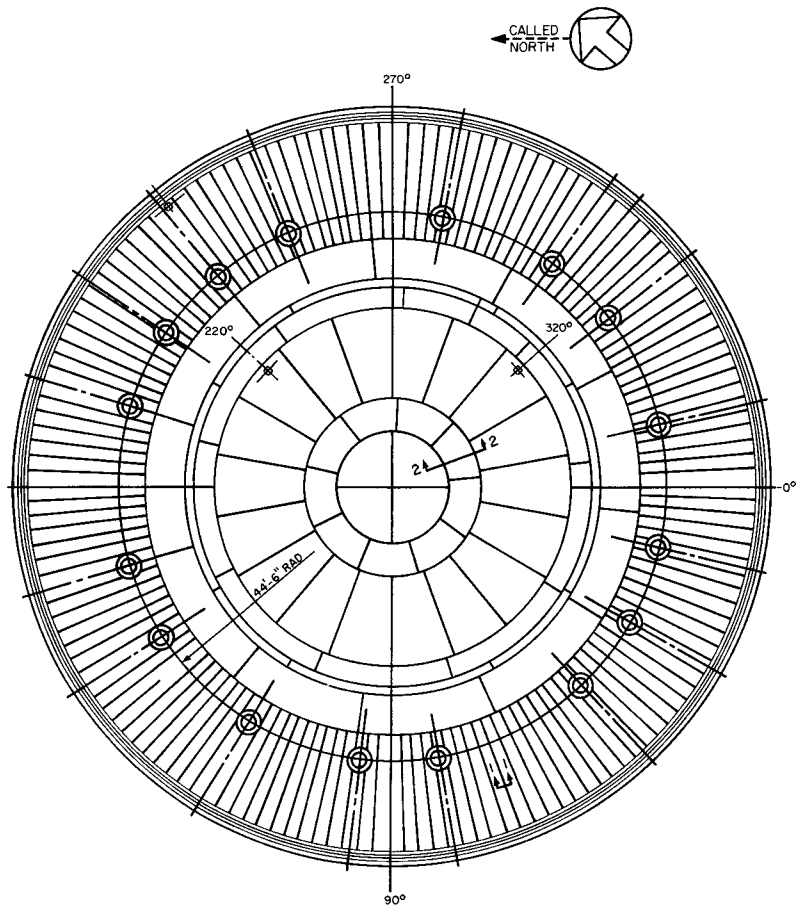
BASEMAT LINER STRAIN SUMMARY

<u>Location</u>	<u>Elastic Analysis</u>			<u>Yield Strain</u>	<u>Plastic ϵ_{m+b} (If Reqd)</u>	<u>Allowables</u>	
	ϵ_m	ϵ_b	ϵ_{m+b}			ϵ_m	ϵ_{m+b}
<u>Normal Operation</u>							
W	0.00079	0.00020	0.00099	0.00089	0.0024	0.002	0.004
S ₁	0.00046	0.00019	0.00066	0.00089	-	0.002	0.004
S ₂	0.00077	0.00013	0.00090	0.00089	-	0.002	0.004
<u>Abnormal/Extreme (Long-Term SBA)</u>							
W	0.00141	>yield		0.00089	0.0093	0.005	0.014
S ₁	0.00128	>yield		0.00089	0.0032	0.005	0.014
S ₂	0.00159	>yield		0.00089	0.0029	0.005	0.014

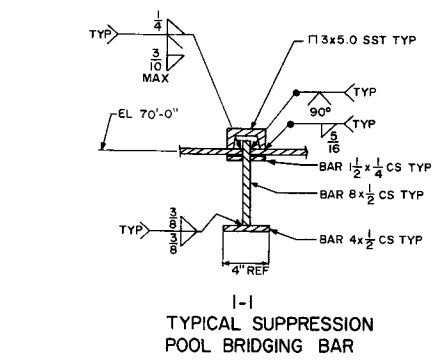
Key:

W = Inside weir annulus
 S₁ = Under suppression pool at midspan
 S₂ = Under suppression pool at supporting edge

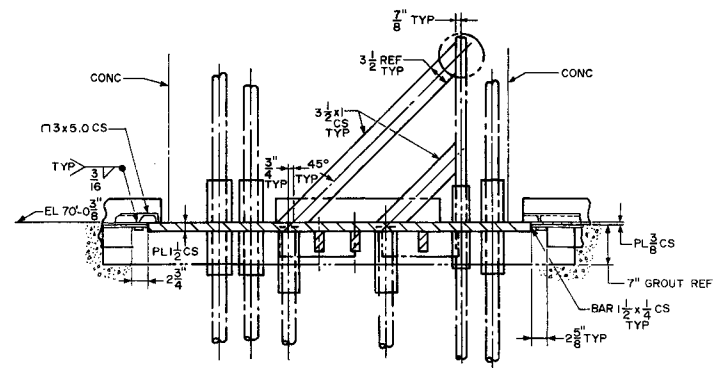
ϵ_m = Membrane strain
 ϵ_b = Bending strain
 ϵ_{m+b} = Membrane + bending strain



PLAN VIEW OF BASEMAT LINER PLATE LAYOUT
EL. 70'-0³/₈"



1-1
TYPICAL SUPPRESSION
POOL BRIDGING BAR



2-2
TYPICAL EMBEDMENT PLATE

FIGURE 6A.15-1
BASEMAT LINER GEOMETRY
AND DETAILS
RIVER BEND STATION
UPDATED SAFETY ANALYSIS REPORT

6A.16 PIPING AND PIPE SUPPORTS LOAD ASSESSMENT

6A.16.1 Introduction

Piping and its supports experience two types of dynamic loadings resulting from suppression pool events: direct loads from water flowing past or impinging the component, and indirect loads imposed by the vibratory response of the building walls and floors on the piping through its restraints.

Only a few lines are directly exposed to water or water spray. But all piping in the reactor building and outside up to the first anchor in other buildings is affected indirectly by the vibratory response of the reactor building.

This section describes the method of analysis of piping systems for the direct as well as the indirect loads, and it lists the highest stress in piping which runs in or near the suppression pool and in piping where the vibration transmitted through the supports to the piping is critical.

First, the analysis of the indirect loads is discussed. Since the piping experiences these loads in the same way as seismic loads, the analysis is analogous to the seismic analysis, with certain qualifications. Therefore the criteria discussed in Section 3.7 under seismic analysis are reviewed below in view of the suppression pool-induced vibrations. The methods for calculation of loads on small subsystems, such as piping, in or near the suppression pool are given in Sections 6A.5.1.5, 6A.8, 6A.9, 6A.10, and Attachments E and L.

6A.16.2 Analysis of Piping Systems for Indirect (Inertia) Loads

6A.16.2.1 Load Cases

Tables 3.9A-2 and 3.9A-3 list the load cases associated with the reactor building and specify their combination with each other and with other loads. These load cases are:

SRV_{max} = Maximum of responses to individual SRV cases, i.e., to 1V, 2V, 7V, 16V, and 1V subsequent actuation, including SRVCO.

The 7-valve case is bounded by the 16-valve case. Therefore, only the following peak-

spread SRV floor response spectra are used to form SRV_{max} :

1V2V = ENV (1V, 2V, SRVCO 2V)

16V = ENV (16V, SRVCO 16V)

Chug/CO = Response to envelope of response spectra for chugging and condensation oscillation due to LOCA

PS = Pool swell bubble formation (vent air clearing) due to a main steam or recirculation line break (DBA) only

AP_{max} = Maximum of responses to the individual annulus pressurization cases (main steam - AP MSB, feedwater - AP FWB, and recirculation line breaks - AP RCB)

6A.16.2.2 Method of Analysis

All load cases except the SRV cases are analyzed via the response spectrum method. For the SRV cases, the response spectrum method or the time history method is used.

The generation of response spectra and time histories for selected points of the building model is described in Section 6A.13. All these spectra are given in cylindrical coordinates, and their radial, tangential, and vertical components are the envelopes of the spectra of all azimuth angles. The time histories describe a realistic situation but can only describe one configuration at a time. They, too, are given in cylindrical coordinates.

The 16-valve SRV case, chugging, and condensation oscillation are considered axisymmetric load cases. They have no tangential component.

Since all other load cases with which the responses to the suppression pool cases have to be combined later are analyzed in the global cartesian coordinate system, the response spectra in the cylindrical coordinate system are applied conservatively as described in the following paragraphs:

The envelope of the radial and tangential spectra applying to a support is used as both the X- and the Z-direction input, and the vertical spectrum forms the Y-input. At some containment penetrations where the

stresses near the penetration are critical, this conservatism is eliminated by rotating the global cartesian coordinate system about its vertical axis so that the X-axis is parallel to the radial direction outward of the penetration, applying the radial spectrum in the new X-direction and the tangential spectrum in the new Z-direction.

In the case where piping runs inside the reactor building or from the reactor building to another building, the multiple support response spectrum method is used as an alternate method whenever the stresses are close to the allowables. This method permits different spectra for several groups of supports. NUPIPE (Appendix 3A) is used for these analyses.

6A.16.2.3 Effects of Parameter Variations on Floor Response Spectra

The smoothed floor response spectra of the suppression pool-induced load cases and of annulus pressurization are peak-spread -13/+18 percent in the period scale from the peak so that the broadened peaks are bounded on each side by lines that are parallel to the lines of the smoothed original spectrum. This is in conformance with the intent of Regulatory Guide 1.122, as clarified in Section 1.8, which stipulates a maximum spread of ± 15 percent in the frequency scale.

When the time history method is used, the envelope of the responses to the same time history data with three different time intervals is formed, as described in Section 3.7.2.9A. These intervals are $W t$ and $(1 \pm 0.15) W t$. The time history analysis is based on two or more sets of independent support motion. NUPIPE (Appendix 3A) is used for these analyses.

6A.16.2.4 Modeling Considerations

The suppression pool events have response spectra with peaks at much higher frequencies than the earthquakes. This requires a more detailed dynamic description of the piping system than the seismic analysis. The requirements for placement of mass nodes given in Section 3.7.3.8A for seismic analysis result in an adequate number of mass nodes between supports even for the above-mentioned cases. Therefore, the number of modes used for the analysis is increased from the natural frequency limit for OBE and SSE to 100 Hz for suppression pool events.

The equations of motion and their solution in terms of eigenvalues and mode shapes are the same as for earthquakes.

6A.16.2.5 Determination of the Number of Cycles

Fatigue analysis is performed only on ASME Code Class 1 systems. The applicable significant suppression pool events are the SRV discharge cases (combined 1-valve/2-valve case and 16-valve case used) and chugging. All other dynamic cases have insignificant amplitudes for fatigue considerations. Based on the number and types of SRV discharge events listed in Section A.6A.9, the 1800 total SRV discharges can be split into approximately 1500 single subsequent and 300 multiple discharges.

The number of load cycles (equivalent number of stress reversals at peak amplitude) per SRV discharge actuation and per chugging event depends on the event and on the piping system characteristics in the vicinity of the point considered. It is discussed for equipment in Section 6A.17.2.4. The same is applicable to piping. In noncritical cases, the following numbers of cycles are used: SRV 1V2V-8775, SRV 16V-1515, Chug-5410.

Annulus pressurization is a shock-type event, producing less than 25 significant cycles.

6A.16.2.6 Avoidance of Response Spectrum Peaks

The suppression pool events are characterized by amplified response spectra with peaks in the 30- to 80-Hz range before peak spreading, with a possible second peak range for SRV cases between 10 and 30 Hz. Because of this wide range of spectrum peaks and the high frequency content, generally no attempt is made to influence the piping system characteristics.

6A.16.2.7 Differential Displacements

Differential displacements are applicable only under normal and upset conditions, i.e., to the SRV discharge cases. They are so small that they were not included.

6A.16.2.8 Loading at Containment Penetrations

For all piping penetrations of either drywell, steel containment, or shield building, the highest stress and the allowable stress in the piping at or near the penetration are listed in Table 6A.16-1.

6A.16.3 Analysis of Piping Systems for Direct Hydrodynamic Loading

6A.16.3.1 Introduction

Loads on piping in the suppression pool are described in Sections 6A.8, 6A.9, and 6A.10. LOCA bubble, CO, and chugging loads and SRV actuation loads on submerged structures are developed in Attachment L. The loads on piping affected by weir wall swell are described in Section 6A.5.1.5. OBE and SSE sloshing loads on the submerged part of the pipe are discussed in Attachment E.

The application of these loads in accordance with the ASME Code criteria for pipe stress is discussed as follows. The load combination tables, Tables 3.9A-2 and 3.9A-3, show the combination of direct and of indirect loads for the various conditions to be analyzed. On each pipe segment that is subject to direct hydrodynamic loads, the direct and indirect loads from a given event are combined by the SRSS method.

6A.16.3.2 Load Cases and Load Combinations for Pipe Stress Analysis

Under normal and upset conditions, all piping in the suppression pool is subjected to SRV discharge loads (Section 6A.2.4) and simultaneous OBE sloshing loads. Any of the SRV cases can occur; therefore, SRV_{max} (the envelope of the responses to all significant SRV discharge cases) is applied.

Under emergency conditions the plant may experience an SBA or an IBA simultaneously with an OBE. The effects of SBA and IBA on loads in the suppression pool are the same. The SBA/IBA produces condensation oscillation (CO) and chugging (Chug) sequentially. Under emergency conditions, any of the SRV cases can occur, or, if the emergency condition is associated with an intermediate or small line break, the single SRV case, including 1-valve subsequent actuation (1VSUB) or the 7-valve case (ADS), is postulated in Section 6A.2.2 to occur simultaneously with chugging or with condensation oscillation. By assuming SRV_{max} combined with the larger of chugging and condensation oscillation, a slight degree of conservatism is introduced.

●→4

4←●

•→4

4←•

The following faulted conditions are considered: SSE with normal or upset or emergency conditions other than LOCA, SSE with SBA/IBA, SSE with DBA, and SSE with RHR discharge. Since the pool experiences without SBA/IBA only SRV discharge, and with SBA/IBA, SRV discharge combined with condensation oscillation or with chugging, the first condition is bounded by the second condition. SSE produces SSE sloshing loads (same function as OBE sloshing, but with twice the amplitude).

The DBA has several phases, illustrated in the bar charts of Sections 6A.6 through 6A.12. The DBA produces sequentially the following loads in the RPV annulus: annulus pressurization in or above the suppression pool, vent-clearing water jet overlapping with pool swell bubble formation, then bulk pool swell, impingement, froth, fallback overlapping with condensation oscillation, and then chugging.

The SRV 1-valve discharge event is postulated to occur simultaneously with the following DBA phenomena: vent clearing, pool swell bubble formation, pool swell impact and drag, fallback, and condensation oscillation. Tables 3.9A-2 and 3.9A-3 conservatively specify SRV_{max} instead.

Piping in the zone from water level up to 14 ft above the top of the weir wall in the weir annulus is subjected to impingement and drag loads upward, and fallback loads downward from weir well water in the reverse vent-clearing event produced by a DBA. (There is no piping in the weir well.) Simultaneously, the impinged piping may be subject to SSE inertia loads. The applied loads are based on GESSAR and Reference 6 and are described in Section 6A.5.1.5.

6A.16.3.3 Special Considerations

In the first phase of the DBA, the annulus between the reactor vessel and the biological shield wall is pressurized asymmetrically. This event produces only one peak-load cycle immediately following the break. Therefore, it is assumed realistically that this loading will not combine with the single-valve, first actuation SRV case.

Upward bulk pool swell drag loads can act on all submerged components that offer resistance to vertical flow. Post-

impact swell drag loads on components above the pool surface may exceed loads between water level and 10 ft above.

Fallback loads in the suppression pool annulus above the water surface are bounded by impingement loads. Fallback loads below the water surface ($V=35$ ft/s) are experienced by all horizontal pipe segments and components above the bottom vent (el 72.25 ft), including strainers and SRV discharge lines.

RHR chugging is bounded by RHR condensation oscillation, so that an envelope need not be formed.

RHR water jet loads are experienced only by segments of piping in two small regions. The RHR discharge loads, except for the water jet loads in these regions, are much smaller than the combined loads of SRV and CO/Chug, so that for but these segments, the condition SSE with RHR is bounded by the phase SSE with SRV and CO/Chug of the condition SSE with DBA.

The two RHR discharge lines, in addition to the discharge loads listed above, are subjected to lateral loads concurrently with RHR chugging loads.

6A.16.3.4 Piping Subjected to Hydrodynamic Loads

The affected piping is shown on Fig. 6A.16-1 and 6A.16-2 for piping in or above the suppression pool and in Fig. A.6A.10-2 for piping above and near the weir well. The most critically loaded points in each line are listed in Table 6A.16-2 with their stresses and stress allowables.

Linear (vertical) pipe supports with pinned-pinned connections were avoided in the design of piping above the suppression pool surface due to pool swell impact drag loads. Only the short horizontal segment of ECCS piping at the penetration elevation, within 25 ft above the suppression pool surface, is subjected to pool swell impact.

6A.16.3.5 Pipe Stress Analysis Procedure for Piping Subjected to Hydrodynamic Loads

All piping near or below the suppression pool surface is ASME Code Class 2, and therefore is analyzed like any other Class 2 piping by means of NUPIPE. Under normal and upset conditions, ASME Section III, Subsection NC Equation 9 for primary stresses and Equation 10 for secondary stresses or alternately for Equation 10, Equation 11 for primary sustained and secondary stresses must be satisfied.

Under emergency and faulted conditions, only Equation 9 for primary stresses, with appropriate stress limits, must be satisfied. The damping values under emergency and faulted conditions are higher than under normal and upset conditions.

For combination of the inertia loads, the phases of the DBA event after AP can be lumped into one load combination case, since pool swell, chugging, and condensation oscillation do not overlap.

The hydrodynamic loads consist of dynamic velocity drag and acceleration drag line loads normal to the pipe axis. These are simulated as forces at an adequately spaced number of node points. Pool swell bubble formation drag is analyzed as a time history case. For other drag loads and impact loads, a static analysis is performed with a bounding load distribution in each of two orthogonal directions normal to the pipe axis, and the responses of the static analysis are multiplied by a dynamic load factor based on the characteristics of the forcing function and the lowest natural frequency of the piping system before combination with other load cases.

TABLE 6A.16-1

MAXIMUM STRESS AND ALLOWABLE STRESS IN PIPING SYSTEMS
CRITICALLY LOADED BY DYNAMIC SUPPRESSION
POOL EVENTS⁽¹⁾

System	Line Number	Containment Penetration		Calc. AX-	Node Point	Location	Upset Condition		Faulted Condition	
		Azimuth (deg)	Elevation				Max. Stress Equation 9 (lb/sq in)	Allowable Stress (lb/sq in)	Max. Stress Equation 9 (lb/sq in)	Allowable Stress (lb/sq in)
FWS	1-FWS-020-67-1	0	122'-0"	17E	150	Elbow	14,165	29,670	20,492	59,340
ICS	1-ICS-008-1-1	0	122'-5 3/8"	2G	347	Elbow	23,110	26,790	38,396	53,580
RHS	1-RHS-010-68-2	330	121'-5 1/2"	71H	37	Valve jct.	14,263	18,000	15,414	36,000
SWP	1-SWP-012-118-2	331.5	148'-4"	19A	17	Valve jct.	10,174	18,000	9,583	36,000
WCS	1-WCS-004-185-2	0	118'-9"	74E	20	Penet. jct.	10,406	18,000	10,494	36,000

⁽¹⁾ Typical highest stress in piping at or near penetration; five samples listed.

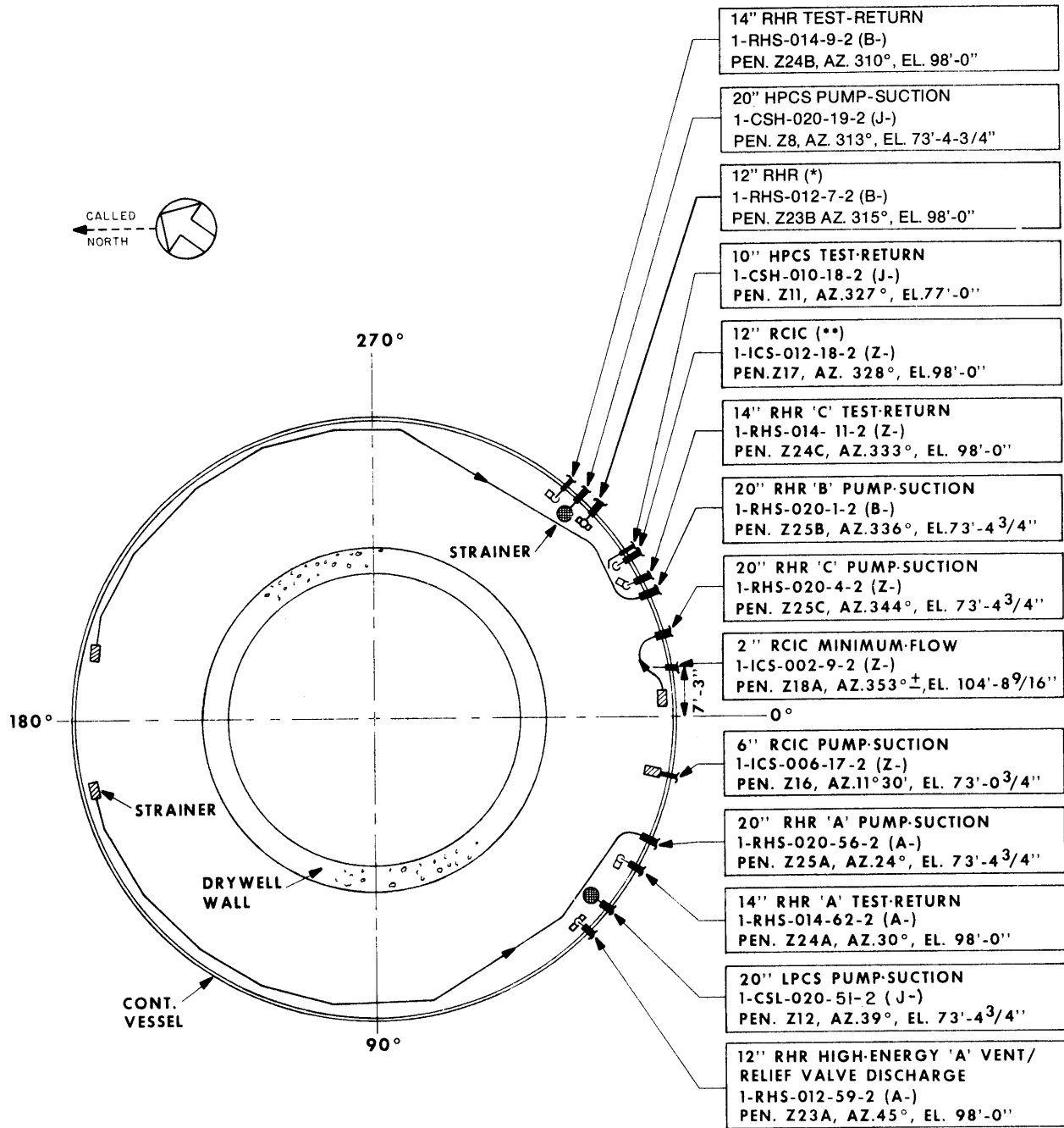
RBS USAR

TABLE 6A.16-2

PIPE STRESS SUMMARY (UPSET AND FAULTED) FOR PIPING
SUBJECTED TO DIRECT WATER LOADS⁽¹⁾

System	AX Number	Containment Penetration		Upset Condition				Faulted Condition			
		Azimuth (deg)	Elevation	Node Point	Type	Max. Stress Equation 9 (lb/sq in)	Allowable Stress (lb/sq in)	Node Point	Type	Max. Stress Equation 9 (lb/sq in)	Allowable Stress (lb/sq in)
ICS	13D	328	98'-0"	165	Run	4,547	20,640	100	Elbow	17,770	36,000
RHS	71AJ	24	73'-4 3/4"	320	Run	4,875	21,540	320	Run	8,709	43,080
RHS	71AR	45	98'-0"	30	Run	2,892	19,488	30	Run	18,906	38,976
CSL	78D	39	73'-4 3/4"	290	Elbow	12,118	21,540	290	Elbow	14,093	43,080
CSH	83D	313	73'-4 3/4"	200	Elbow	11,373	21,540	200	Elbow	12,250	43,080

⁽¹⁾ Typical highest stress at suppression pool side; five samples listed.



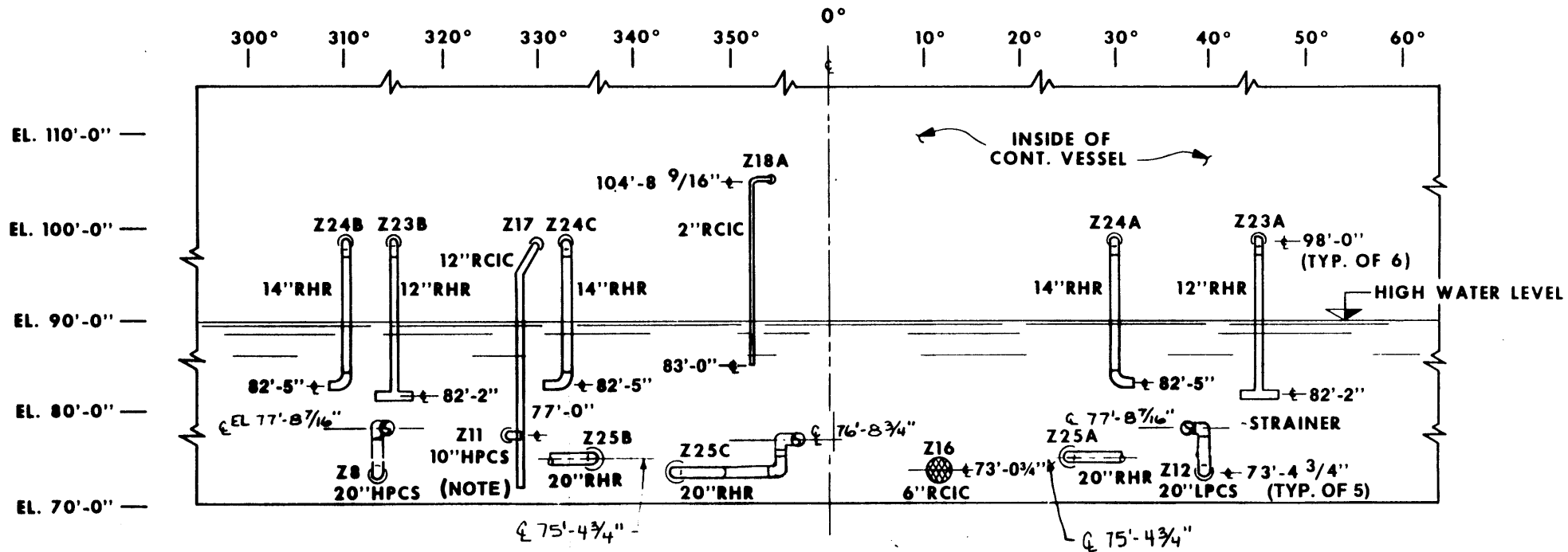
NOTE : SRV DISCHARGE LINES AND QUENCHERS NOT SHOWN HERE.

- (*) = HIGH ENERGY 'B' VENT RELIEF VALVE DISCHARGE
- (**) = TURBINE EXHAUST/ CONDENSING SPARGER

FIGURE 6A.16-1

**SUPPRESSION POOL
PIPING PLAN VIEW**

**RIVER BEND STATION
UPDATED SAFETY ANALYSIS REPORT**



NOTE: SEE FIGURE 5.4-9a FOR DETAILS OF SPARGER ON THIS 12" RCIC LINE

FIGURE 6A.16-2

SUPPRESSION POOL PIPING
DEVELOPED ELEVATION

RIVER BEND STATION
UPDATED SAFETY ANALYSIS REPORT

6A.17 ASSESSMENT OF EQUIPMENT QUALIFICATION

6A.17.1 Introduction

Safety-related equipment is qualified for the combined effects of seismic and hydrodynamic vibrations. This combined qualification is required for equipment located inside the reactor building. The description of the hydrodynamic loads and the methods of accomplishing the required qualification are discussed below. The summary of results for equipment affected by the combined seismic and hydrodynamic loads are provided in the appropriate tables in Sections 3.9 and 3.10.

6A.17.2 Dynamic Loads

6A.17.2.1 Description

The hydrodynamic loads that are considered in the qualification of equipment are caused by the events identified below:

SRV_{max} = Envelope of individual SRV discharge load cases, i.e., the 2-valve, 7-valve, 16-valve, and 1-valve first and subsequent actuations.

Chugging = Chugging due to LOCA

CO = Condensation oscillation due to LOCA

PS = Pool swell due to LOCA

AP = Annulus pressurization due to high energy line break

In addition, the direct (drag or impact) loads from water are also considered. These loads affect certain equipment located in or near the suppression pool. The vent clearing effects of a LOCA are small and therefore not considered in qualification.

The hydrodynamic loads result in significant magnitudes, frequency content beyond the seismic frequency range, and a large number of events for which the equipment must be qualified through its design life. They are postulated to combine with seismic and normal loads. The loading combinations for each service condition are presented in Tables 3.9A-6 and 3.9A-7. The method of combination is in accordance with Reference 3.

6A.17.2.2 Development of Response Spectra

The response spectra for the loads identified in Section 6A.17.2.1 are developed in three orthogonal directions by time-history analysis of the reactor building structural model. The radial and tangential spectra are enveloped for each load, and the enveloped response spectrum is generally used for qualification. The radial and tangential spectra are also used separately when equipment is qualified for a specific orientation. The response spectra of the hydrodynamic loads are peak broadened ± 15 percent in accordance with Regulatory Guide 1.122. They are then combined, as necessary, with the seismic spectra already peak broadened in accordance with Section 3.7.2.9.2A. Response spectra for four loading conditions are generated and generally are needed for qualification purposes. These conditions are SRV_{max} , Upset, Faulted, and Chugging. Equipment damping values conform to the values given in Regulatory Guide 1.61. For SRV_{max} and Upset condition, the values used correspond to that of OBE;^{max} and for Faulted condition and Chugging, the damping values of SSE are used.

6A.17.2.3 Magnitudes and Frequency Content

The spectra developed in Section 6A.17.2.2 are used as the Required Response Spectra (RRS) for qualifying floor- and wall-mounted equipment. For line-mounted equipment, the accelerations are obtained directly from the piping analysis. The magnitudes and the frequency content of the loading are addressed by using these RRS.

6A.17.2.4 Number of Events and Stress Cycles

The significant events associated with hydrodynamic loads that affect qualification are 1800 SRV actuations and 2600 chugs due to a LOCA as described in Reference 1. Each event produces several stress cycles. These stress cycles are determined by analyzing the responses of a number of single degree-of-freedom oscillators for representative time-histories. Since all events of the same load may not occur at the design amplitude, equivalent occurrence factors (EOF) are obtained by analyzing test pressure data. The total number of equivalent stress cycles due to a load is therefore a product of the number of events, the EOF, and the stress cycles per event.

6A.17.3 Qualification Acceptance Criteria

The acceptance criteria for qualification to the combined effects of seismic and hydrodynamic loads are the same as

those identified in Sections 3.9.2.2.1A, 3.9.2.2.2A, and 3.10.1A. The ability to perform a safety-related function is demonstrated during and after the Upset, Faulted, and LOCA plant conditions, as applicable. In addition, the cumulative usage factor due to the fatigue effects of the loads is maintained below unity.

6A.17.4 Qualification Procedures

Equipment qualification for the combined seismic and hydrodynamic loads is provided by either demonstrating the adequacy of the existing seismic qualification results through a reevaluation, or through new qualification. When reevaluation is performed, adequacy of functional operability and structural integrity of the equipment is demonstrated, as necessary. The methods of new qualification are the same as described in Section 3.7.3.1.1A. In addition, the frequency content and the number of events and stress cycles of the loads are a consideration in establishing the equipment adequacy.

6A.17.4.1 Qualification by Analysis

The static or dynamic analysis methods are used in qualification of equipment, as indicated in Sections 6A.17.4.1.1 and 6A.17.4.1.2. The maximum responses are computed in each of the three orthogonal directions and combined using the square root of the sum of squares (SRSS) method. Where reevaluation is performed, a comparison is made of the existing design margin with respect to the increased loads. In addition to determining the stress and deflections, an analysis is performed to calculate fatigue using factors for SRV, Upset condition, Faulted condition, and LOCA-Chugging. The cumulative usage factor is demonstrated to be less than unity.

6A.17.4.1.1 Static Analysis

For equipment that is qualified by analysis, the conservative and simple static analysis method is generally used. Equipment having a fundamental frequency in the resonant range of the response spectra is analyzed by using the peak resonant acceleration, increased by a static coefficient of 1.5.

6A.17.4.1.2 Dynamic Analysis

When dynamic analysis is performed for qualification, all significant modes of the equipment in the frequency range of

the loading are considered in the analysis. This accounts for the high frequency content of the hydrodynamic loads.

6A.17.4.2 Qualification by Testing

Testing is performed using random, multifrequency, multiaxis motions and single-frequency, single-axis motions as appropriate. Floor-mounted equipment is always qualified using the random, multifrequency motions in which the test response spectra (TRS) envelop the RRS. Line-mounted equipment, when installed close to supports, are also qualified using the random, multifrequency method. Single-frequency, single-axis tests are performed for line-mounted equipment when the input loading and the equipment dynamic characteristics conform to the provisions of Regulatory Guide 1.100.

For equipment already tested for seismic loads, the TRS are compared to the new RRS, which include the hydrodynamic loads. Test input motion time-histories are analyzed to determine the equivalent stress cycles at magnitudes representative of the equipment response. The equivalent stress cycles from all the dynamic loads are also obtained at the same magnitudes. If the TRS envelop the applicable portion of the RRS, and the test input motions yield higher cycles than those from the dynamic loads, no further testing is required.

When new testing is performed using the random, multifrequency, multiaxis method, the load cases considered are the SRV, Upset, Faulted, and LOCA (chugging), in that sequence. Five tests of a 30-sec duration each are used for the Upset condition. One 30-sec duration test is used for the Faulted condition loads. The durations for the SRV and LOCA (chugging) tests are based on the consideration that the expected stress cycles from these tests will exceed the stress cycles of the hydrodynamic load events. When single-frequency testing is used, the number and duration of the tests are based on the same consideration as above. The test frequencies in the single-frequency testing are representative of the frequency content of the dynamic loading. For line-mounted equipment, the input motions correspond to acceleration magnitudes obtained from the piping analysis.

6A.17.4.3 Pump and Valve Operability Program

No active pumps in the BOP scope of work are affected by the hydrodynamic loads. For the safety-related active valves, the operability program is the same as that stated in

Section 3.9.3.2.2A, and the qualification procedures of Section 6A.17.4 are followed. In addition, accelerations which keep the stresses and deflections within the allowable limits are established and reconciled with the accelerations from piping dynamic analysis, and an adequate margin of safety is demonstrated. The operability testing of the valve assembly and the dynamic testing of the actuator and other safety-related electric components are also performed using the accelerations determined from piping analyses, with adequate margins.

RBS USAR

ATTACHMENT A
(TO APPENDIX 6A)

NUMERICAL INFORMATION FOR
SAFETY/RELIEF VALVE DISCHARGE
LOADS

RBS USAR

ATTACHMENT A
(TO APPENDIX 6A)

TABLE OF CONTENTS

<u>Section</u>	<u>Title</u>	<u>Page</u>
A.6A.1	INTRODUCTION	A.6A.1-1
A.6A.2	SUMMARY AND CONCLUSIONS	A.6A.2-1
A.6A.3	DESCRIPTION OF THE PHENOMENA	A.6A.3-1
A.6A.4	ARRANGEMENT	A.6A.4-1
A.6A.4.1	Distribution in Pool (Quencher Arrangement)	A.6A.4-1
A.6A.4.2	SRVDL Routing	A.6A.4-1
A.6A.4.2.1	Line Lengths and Volume	A.6A.4-1
A.6A.4.2.2	Drywell Penetration Sleeve	A.6A.4-2
A.6A.4.2.3	SRVDL Vacuum Breaker	A.6A.4-2
A.6A.5	QUENCHER LOADS ON POOL BOUNDARY	A.6A.5-1
A.6A.5.1	Pressures on Drywell, Basemat, and Containment	A.6A.5-1
A.6A.5.1.1	Single S/R Valve Loads	A.6A.5-2
A.6A.5.1.2	Two Adjacent S/R Valve Loads	A.6A.5-2
A.6A.5.1.3	Nine S/R Valve Loads	A.6A.5-2
A.6A.5.1.4	Seven S/R Valve Loads (ADS)	A.6A.5-2
A.6A.5.1.5	All Sixteen S/R Valve Loads	A.6A.5-2
A.6A.5.2	Loads on Weir Wall	A.6A.5-2
A.6A.5.3	Loads on Submerged Structures	A.6A.5-3
A.6A.5.4	Normalized Pressure Time History (Theoretical Rayleigh Bubble)	A.6A.5-3
A.6A.5.5	Representative Pressure Time History	A.6A.5-3
A.6A.6	OTHER LOADS ON STRUCTURES IN THE POOL	A.6A.6-1
A.6A.6.1	LOCA and Pool Swell	A.6A.6-1
A.6A.6.2	Thermal Expansion Loads	A.6A.6-1
A.6A.6.3	Seismic Loads	A.6A.6-1

RBS USAR

ATTACHMENT A
(TO APPENDIX 6A)

TABLE OF CONTENTS

A.6A.6.4	Seismic Sloshing Loads	A.6A.6-1
A.6A.7	QUENCHER ARRANGEMENT	A.6A.7-1
A.6A.7.1	Quencher Arm/Strut Loads and Loading Application	A.6A.7-1
A.6A.7.1.1	Description of Discharge Event	A.6A.7-1
A.6A.7.1.2	Types of Load on Quencher Assembly	A.6A.7-1
A.6A.7.1.3	Application of Loads	A.6A.7-2
A.6A.7.1.4	Magnitude of Loads on Quencher and Struts	A.6A.7-3
A.6A.7.1.5	Quencher Allowable Loads	A.6A.7-3
A.6A.7.1.6	Quencher Load Combinations	A.6A.7-4
A.6A.7.2	Quencher Design Information	A.6A.7-4
A.6A.7.2.1	SRVDL Geometry	A.6A.7-6
A.6A.7.2.2	Quencher Design Criteria	A.6A.7-6
A.6A.8	S/R VALVE LOAD COMBINATIONS	A.6A.8-1
A.6A.8.1	S/R Valve Discharge Combinations	A.6A.8-1
A.6A.8.2	LOCA Considerations	A.6A.8-2
A.6A.8.2.1	Main Steam Line Break	A.6A.8-3
A.6A.8.2.2	Recirculation Line Break	A.6A.8-3
A.6A.8.3	Other SRV Conditions	A.6A.8-3
A.6A.8.3.1	Water-Clearing Pressure Spike for One SRV, First Actuation, Normal Operating Conditions	A.6A.8-3
A.6A.8.3.2	First Actuation of One SRV with a Pressurized Containment	A.6A.8-4
A.6A.8.3.3	Water-Clearing Pressure Spike for One SRV, Second Actuation, Normal Operating Conditions	A.6A.8-4
A.6A.8.3.4	Second Actuation of One SRV with a Pressurized Containment	A.6A.8-5
A.6A.8.3.5	First Actuation of One SRV, Leaking Valve Condition	A.6A.8-5
A.6A.8.3.6	SRV Steam Condensation	A.6A.8-5
A.6A.8.4	Design Load Summation	A.6A.8-6
A.6A.9	FATIGUE CYCLES	A.6A.9-1

RBS USAR

ATTACHMENT A
(TO APPENDIX 6A)

TABLE OF CONTENTS

A.6A.10	CALCULATION PROCEDURES	A.6A.10-1
A.6A.10.1	Constraints	A.6A.10-1
A.6A.10.2	Determine SRVDL Design	A.6A.10-1
A.6A.10.3	S/R Valve Air Clearing Loads	A.6A.10-3
A.6A.10.3.1	Absolute Pressure on Basemat and Walls	A.6A.10-3
A.6A.10.3.2	How to Find the Attenuated Pressure on the Drywell Wall, Basemat, and Containment Wall	A.6A.10-4
A.6A.10.3.2.1	Development of Grid to Determine Values of (r)	A.6A.10-4
A.6A.10.3.2.2	Wall Pressure at Point "A" Single S/R Valve	A.6A.10-5
A.6A.10.3.2.3	Wall Pressure at Point "A" for Multiple S/R Valve	A.6A.10-5

RBS USAR

ATTACHMENT A
(TO APPENDIX 6A)

TABLE OF CONTENTS

A.6A.4-1	SAFETY/RELIEF VALVE DISCHARGE LINE SIZE
A.6A.5-1	QUENCHER BUBBLE PRESSURE RIVER BEND STATION (90-90% CONFIDENCE LEVEL)
A.6A.5-2	NORMALIZED DYNAMIC PEAK PRESSURE FIELD FOR SINGLE S/R VALVE
A.6A.5-3	NORMALIZED DYNAMIC PEAK PRESSURE FIELD FOR 2 ADJACENT S/R VALVES
A.6A.5-4	NORMALIZED DYNAMIC PEAK PRESSURE FIELD FOR 7 S/R VALVES (ADS)
A.6A.5-5	NORMALIZED DYNAMIC PEAK PRESSURE FIELD FOR 16 S/R VALVES
A.6A.7-1	DIRECT LOADS ON QUENCHER STRUTS
A.6A.7-2	QUENCHER ASSEMBLY REACTION LOADS AND QUENCHER/SRVDL INTERFACE LOADS
A.6A.9-1	SAFETY RELIEF VALVE ACTUATION
A.6A.10-1	RIVER BEND STATION SRVDL PIPE SPOOL DIMENSIONS
A.6A.10-2	DRYWELL AND SUPPRESSION POOL GEOMETRY

RBS USAR

ATTACHMENT A
(TO APPENDIX 6A)

TABLE OF CONTENTS

A.6A.3-1	SRVDL AIR VOLUME VERSUS FL/D WITH 625 PSID CONSTRAINT
A.6A.4-1	QUENCHER ARRANGEMENT ELEVATION
A.6A.4-2	QUENCHER ARRANGEMENT, PLAN VIEW
A.6A.4-3	SAFETY RELIEF VALVE AND QUENCHER LOCATIONS
A.6A.5-1	SINGLE SAFETY RELIEF VALVE DISCHARGE NORMALIZED WALL PRESSURE AT 347.44°
A.6A.5-2	SINGLE SAFETY RELIEF VALVE DISCHARGE REFERENCE POINT 4 (CIRCUMFERENTIAL DISTRIBUTION)
A.6A.5-3	SINGLE SAFETY RELIEF VALVE DISCHARGE REFERENCE POINT 10 (CIRCUMFERENTIAL DISTRIBUTION)
A.6A.5-4	TWO ADJACENT SAFETY RELIEF VALVE DISCHARGE NORMALIZED WALL PRESSURE AT 360°
A.6A.5-5	TWO ADJACENT SAFETY RELIEF VALVE DISCHARGE REFERENCE POINT 4 (CIRCUMFERENTIAL DISTRIBUTION)
A.6A.5-6	TWO ADJACENT SAFETY RELIEF VALVE DISCHARGE REFERENCE POINT 10 (CIRCUMFERENTIAL DISTRIBUTION)
A.6A.5-7	SEVEN SAFETY RELIEF VALVE DISCHARGE (ADS) NORMALIZED WALL PRESSURE AT 247°
A.6A.5-8	SEVEN SAFETY RELIEF VALVE DISCHARGE REFERENCE POINT 4 (CIRCUMFERENTIAL DISTRIBUTION)
A.6A.5-9	SEVEN SAFETY RELIEF VALVE DISCHARGE (ADS) REFERENCE POINT 10 (CIRCUMFERENTIAL DISTRIBUTION)
A.6A.5-10	SIXTEEN SAFETY RELIEF VALVE DISCHARGE NORMALIZED WALL PRESSURE AT 222°
A.6A.5-11	SIXTEEN SAFETY RELIEF VALVE DISCHARGE REFERENCE POINTS 2 TO 8

RBS USAR

ATTACHMENT A
(TO APPENDIX 6A)

TABLE OF CONTENTS

A.6A.5-12	SIXTEEN SAFETY RELIEF VALVE DISCHARGE REFERENCE POINTS 10 AND 12 (CIRCUMFERENTIAL DISTRIBUTION)
A.6A.5-13	IDEALIZED QUENCHER BUBBLE PRESSURE OSCILLATION IN SUPPRESSION POOL (RAYLEIGH BUBBLE)
A.6A.5-14	REPRESENTATIVE PRESSURE TIME HISTORY FOR QUENCHER DYNAMIC LOAD
A.6A.6-1	CALCULATED PRESSURE AND TEMPERATURE ALONG SAFETY RELIEF PIPING DURING STEADY DESIGN FLOW
A.6A.7-1	QUENCHER ARM AND STRUT LOADS
A.6A.7-2	DELETED
A.6A.7-3	QUENCHER AND STRUT ANCHOR LOAD SUMMARY
A.6A.7-4	SECTIONAL VIEW OF SPARGER LEG (TYPICAL EACH SIDE)
A.6A.8-1	PRESSURE TIME HISTORY FOR SRV-CO
A.6A.10-1	SAFETY RELIEF VALVE DISCHARGE PIPING DETAIL VALVE TO FIRST ANCHOR
A.6A.10-2	SAFETY RELIEF VALVE DISCHARGE PIPING ARRANGEMENT (5 SHEETS)
A.6A.10-3	SUPPRESSION POOL GRID SYSTEM AND QUENCHER PRESSURE INFLUENCE
A.6A.10-4	DRYWELL AND SUPPRESSION POOL GEOMETRY

RBS USAR

ATTACHMENT A
(TO APPENDIX 6A)

NUMERICAL INFORMATION FOR
SAFETY/RELIEF VALVE DISCHARGE LOADS

A.6A.1 INTRODUCTION

This Attachment provides the numerical information for thermal hydraulic dynamic loading conditions in the River Bend Station pressure suppression containment system resulting from the air clearing phenomenon in the safety relief valve discharge line (SRVDL).

This Attachment provides the following:

1. Quencher arrangement
2. Quencher distribution in the pool
3. Pool boundary loads
4. Definition of other loads, including quencher anchor loads
5. Combinations of safety relief (S/R) valve discharge and estimated valve cycles
6. Procedures for calculating pool boundary loads.

A.6A.2 SUMMARY AND CONCLUSIONS

Once the SRVDL routing is established, the detailed calculation of the pool boundary loads resulting from the quencher air clearing transient is performed (see Sections A.6A.5 and A.6A.10). The line air volume is the critical parameter. For the River Bend Station design, a series combination of both 10-in, 12-in, and 14-in pipe is utilized in the line design (Table A.6A.4-1). The SRVDL peak pressure differential is limited to 625 psid (S/R valve back pressure limit).

Table A.6A.4-1 lists the SRVDL air leg information. The maximum air volume is 50.01 cu ft. With this design, the maximum design quencher bubble pressures are given in Table A.6A.5-1 (see Section A.6A.10 for clarification). This design procedure is based on single, multiple, or consecutive actuations.

To assure that the initial water leg ($L < 18$ ft) is not exceeded following the initial actuation, vacuum breakers are used on the SRVDL. The water leg limit is a design objective for the River Bend Station containment.

The design procedure requires an optimization of the SRVDL air volume to assure the 625-psid peak pressure differential limit is not exceeded with a minimum air volume.

The following lists summarize the SRVDL design requirements and objectives necessary to obtain the S/R valve pressure loads for the River Bend Station containment identified in this Attachment.

SRVDL Design Requirements

1. Maximum SRVDL pipe pressure differential ≤ 625 psid. (Coordinates of (fL/D) and (SRVDL air volume) must be on or above the 625-psid line as plotted on Fig. A.6A.3-1.)
2. Two vacuum breakers in each are required in the drywell.

SRVDL Design Objectives

1. Water leg < 18 ft
2. S/R valve opening time > 0.02 sec
3. Minimize the SRVDL air leg volume

RBS USAR

4. Minimize length of longest SRVDL
5. Minimize the contribution of fL/D to the first half of the discharge line.
6. Start 12-in or 14-in pipe just below the first anchor point to meet Objective 5.
7. Ratio of the air legs (length of 10-in pipe/length of 12-in pipe = C) should be $0.33 < C < 5$.
8. Slope lines down toward pool to avoid condensate-water accumulation in line (no horizontal runs).
9. Both SRVDL vacuum breakers should be 10-in size. Locate one > 10 ft above the water level and the other just below the first anchor point at the SRV.

Wall pressures on pool boundary due to the S/R valve discharge are discussed in Section A.6A.5.

A.6A.3 DESCRIPTION OF THE PHENOMENA

A description of the phenomena is given in Section 2.4 of Appendix 6A.

Prior to the lifting of a S/R valve, the downstream piping between the S/R valve discharge and the water surface is filled with air at drywell pressure and temperature conditions. The discharge piping terminates at the top of the quencher. The water level inside the pipe is the same as the water level in the suppression pool.

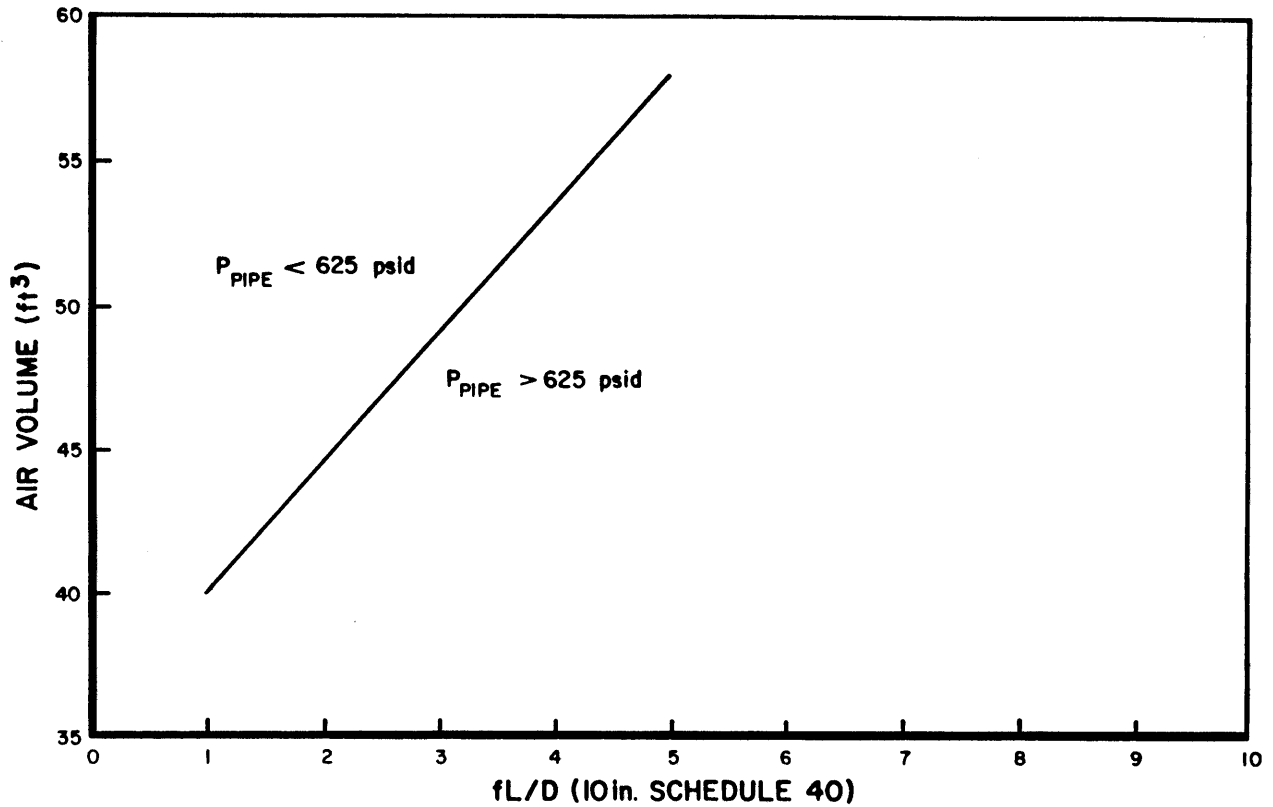
When a relief valve lifts, the effluent reactor steam causes a rapid pressure buildup in the discharge pipe. This rapid compression of the column of air in the pipe causes a subsequent acceleration of the water slug in the submerged portion of the pipe. During this blowout process, the pressure in the pipe builds to a peak as the last of the water is expelled. At this point, the highly compressed cushion of air between the water slug and the effluent vapor begins to leave the pipe. As the highly compressed air exits, it immediately begins to expand to the lower pressure of the suppression pool, displacing the water and propagating a pressure disturbance throughout the suppression pool. The dynamics of an expanding, highly compressed bubble of air are manifested in pressure oscillations (similar to that of a spring-mass system) arising from the bubble expansion coupled with inertial effects of the moving water mass. The air bubble-water mass system is capable of oscillating until all the air has left the pipe and is fully expanded. The sequence of expansion and contraction is repeated with an identifiable frequency until the bubbles reach the pool surface.

The magnitude of the pressure disturbance in the suppression pool decreases with increasing distance from the point of discharge, resulting in a damped oscillatory load at every point on structures below the water surface.

From an air-clearing standpoint, a decrease in the volume of air initially in the discharge pipe results in a decrease in the containment loads due to relief valve discharge. However, if the discharge pipes are shortened to reduce the initial volume of air, the peak pipe pressures inside the discharge lines increase. Since the design limit of the S/R valve is 625 psid*, the discharge pipe volume must be sized so this limit is not exceeded. There is a balance that must

*Based on back-pressure specifications to which valves are purchased.

be reached; pool boundary loads are optimized while the S/R valve line pressures are not exceeded. Fig. A.6A.3-1 demonstrates the effect of discharge pipe air volume on the peak pipe pressure and was developed for the specific parameters listed on the figure. The pipe pressures were calculated for first actuations or opening of a S/R valve.



NOTE: NOT TO BE EXTRAPOLATED
OR INTERPOLATED

SAFETY RELIEF VALVE SET PRESSURE = 1217 psid
SAFETY RELIEF VALVE FLOW RATE = 317.9 lb/sec

VALID ONLY FOR: $0.33 < C < 5.0$

WHERE $C = \frac{10 \text{ in. PIPE LENGTH (AIR)}}{12 \text{ in. PIPE LENGTH (AIR)}}$

WATER LEG = 18 ft

VALVE OPENING TIME > 0.02 sec

FIGURE A.6A.3-1

SRVDL AIR VOLUME
VERSUS FL/D WITH 625
psid CONSTRAINT.

RIVER BEND STATION
UPDATED SAFETY ANALYSIS REPORT

A.6A.4 ARRANGEMENT

A.6A.4.1 Distribution in Pool (Quencher Arrangement)

Fig. A.6A.4-1 and A.6A.4-2 show the elevation and plan views of the standard quencher arrangement. For River Bend Station, the quencher arm is located at 5.60 ft above the basemat, and the inclined penetration is 45 deg from horizontal. This results in a water-leg length of approximately 18 ft.

This arrangement meets the following objectives:

1. Minimize drywell structural interference.
2. Permit water circulation through top and bottom of the drywell sleeve penetration.
3. Locate quencher arms at an elevation between vent holes to minimize vent discharge loads on the quencher during LOCA.

Fig. A.6A.4-1 and A.6A.4-3 show the support arrangement of the quencher and the quencher azimuthal locations in the suppression pool, respectively. In Fig. A.6A.4-3, the low, intermediate, and high pressure-switch set valves are uniformly distributed around the pool to preclude concurrent adjacent valves operation.

A.6A.4.2 SRVDL Routing

The SRVDL is routed from the first pipe anchor point, just below the S/R valve, using 10-in, 12-in, and 14-in pipe to the drywell and 10-in pipe through the drywell wall, to and including the quencher. The SRVDL has sufficient slope in the air-leg section routing to prevent condensation accumulation in the line. Fig. A.6A.10-2, Sheets 1 through 5, illustrates the SRVDL routing layouts.

A.6A.4.2.1 Line Lengths and Volume

Line lengths and volumes are based on the layouts shown on Fig. A.6A.10-2 and the S/R valve constraint of 625 psid. These lengths and volumes are shown in Table A.6A.4-1. The layout design has been optimized to reduce pipe air volume and also to be within the 625-psid pipe pressure constraint. The design requirements for SRVDL are discussed in section A.6A.10.2.

The SRVDL from the elbow just above the pool to the quencher is a 10-in, Schedule 80 pipe (Fig. A.6A.4-1). The increase to Schedule 80 is necessary to increase the strength of the immersed portion of the SRVDL piping. This piping is subjected to pool hydrodynamic loads, such as vent air clearing and S/R valve loadings.

A.6A.4.2.2 Drywell Penetration Sleeve

The drywell penetration sleeve is a 14-in, Schedule 80 pipe at 45 deg with the horizontal, which acts as a conduit for the SRVDL. The sleeve is shown in Fig. A.6A.4-1, with the lower lip of the upper end just below the pool level and extending down 5 ft from the inside surface of the drywell wall. The sleeve is extended (as shown) to reduce pool hydrodynamic loads on the SRVDL.

Thermal Consideration

Studies by GE indicate that the 14-in, Schedule 80 pipe sleeve to concrete interface does not exceed the 200°F limit for normal S/R valve operation. The design temperature criteria from the ASME Boiler and Pressure Vessel Code Subsection CC-3440, Concrete Temperature, Section III, Division 2, is (quote):

1. The following temperature limitations are for normal operation or any other long-term period. The temperatures shall not exceed 150°F, except for local areas, such as around a penetration, which are allowed to have increased temperatures not to exceed 200°F.
2. The temperature limitations for accident or any other short-term period shall not exceed 350°F for the interior surface. However, local areas are allowed to reach 650°F from steam or water jets in the event of a pipe failure.

A.6A.4.2.3 SRVDL Vacuum Breaker

Vacuum breakers are provided for each of the S/R valve discharge lines to prevent excessive water rise in the SRVDL pipe above normal S/R pool level following valve actuations.

At the time of initial opening of the S/R valve, the water level in the SRVDL is at the normal suppression pool level. After the S/R valve closes, the steam remaining in the line condenses, creating a vacuum which draws the water to a higher than normal pool water level in the line. Higher

SRVDL peak pressure and thrust load occur if the SRV opens when the water is above the normal pool level. The purpose of the discharge line vacuum breakers is to prevent the water from rising substantially above its normal level when a subsequent S/R valve opening occurs; and thus, the SRVDL peak pressure is about the same as for the first opening.

The SRV vacuum breakers are located in the drywell above the expected level of water rise in the line subsequent to SRV closure. This eliminates the possibility of wetwell pressurization in the event of a stuck open vacuum breaker and ensures proper functioning of the vacuum breaker during the reflood transient.

The following parameters yield satisfactory performance for the River Bend Station SRVDL geometries and satisfy the preceding requirements.

1. Vacuum breaker effective area, (A/\sqrt{K}) (see the following explanation), is equal to or greater than 0.30 sq ft.

A/\sqrt{K} is used to calculate flow through the vacuum breaker as follows:

$$W = \sqrt{\Delta p (2\rho g_c) (144)} (A/\sqrt{K})$$

Where:

w = Flow rate through vacuum breaker in lbm/sec

P = Pressure differential across the vacuum breaker (psid)

ρ = Air or steam density in lbm/cu ft

$$g_c = 32.2 \frac{\text{lbm-ft}}{\text{lbf-sec}^2}$$

A/\sqrt{K} = Effective area of valve in sq ft

2. Vacuum breaker opens (fully closed to fully open) in 0.2 sec or less when an instantaneous ΔP of 0.5 psid is applied across it.
3. Minimum opening differential pressure to start the vacuum breaker to open is equal to or less than 2 psid.

4. Vacuum breaker must be fully open when pressure difference is equal to or less than 0.5 psid.
5. Vacuum breaker is located in the drywell at an elevation above the maximum water level rise in the line following an SRV closure.

TABLE A.6A.4-1

SAFETY/RELIEF VALVE DISCHARGE LINE SIZE*

Total S/R Valve	Length (ft)	Air Leg Length (ft)				Vol (ft ³)	fL/D**
		10 in.		12 in.	14 in.		
		Sch XS	Sch 80	Sch XS	Sch 60		
V-1	84.57	60.29	4.24	20.04	-	50.01	3.10
V-2	78.97	45.58	4.27	29.12	-	49.38	2.93
V-3	72.62	23.84	4.30	44.48	-	49.12	2.64
V-4	73.41	32.77	3.15	37.49	-	48.93	2.55
V-5	76.37	37.12	2.90	36.35	-	49.87	2.88
V-6	74.73	34.94	3.15	36.64	-	49.07	2.88
V-7	67.89	18.19	3.00	46.70	-	47.38	2.31
V-8	65.36	31.74	2.90	-	30.72	47.01	2.36
V-9	67.84	17.98	3.57	46.29	-	48.19	2.38
V-10	68.03	19.16	3.57	45.30	-	47.64	2.28
V-11	67.45	32.68	2.90	-	31.87	48.52	2.63
V-12	67.12	14.44	3.15	49.53	-	47.57	2.23
V-13	67.17	18.91	3.14	45.12	-	46.79	2.23
V-14	65.32	18.58	2.90	43.84	-	45.55	2.09
V-15	73.73	31.42	2.90	39.41	-	49.18	2.58
V-16	79.70	50.34	2.90	26.46	-	49.69	3.01

* Volumes calculated for suppression pool low water level of 89 ft - 6 in.

**fL/D is normalized to 10 in Sch 40 pipe.

NOTES:

1. $f = 0.015$
2. Design constraints are discussed in Section A.6A.10.
3. The values are based on Fig. A.6A.10-2.

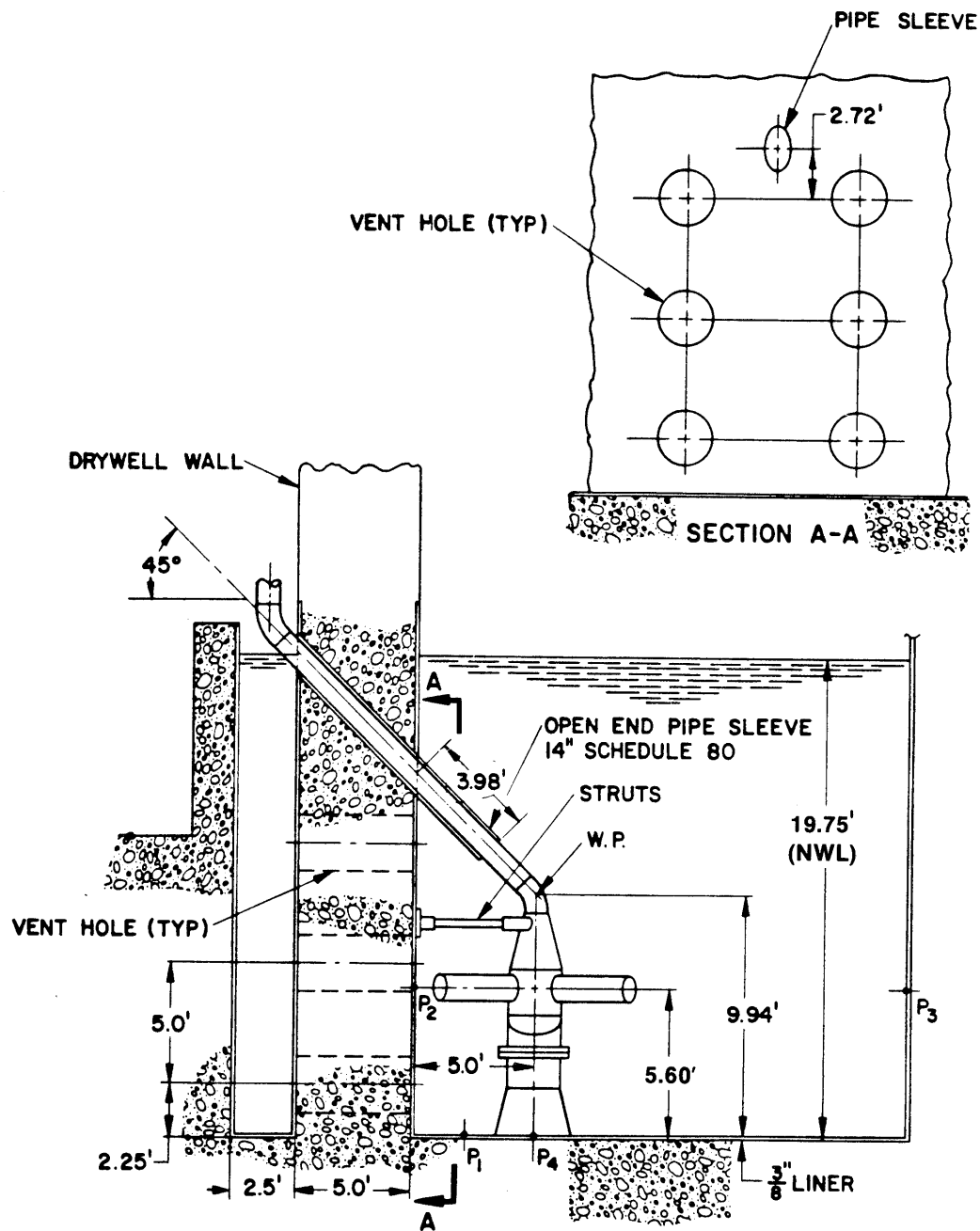


FIGURE A.6A.4-1

QUENCHER
ARRANGEMENT
ELEVATION

RIVER BEND STATION
UPDATED SAFETY ANALYSIS REPORT

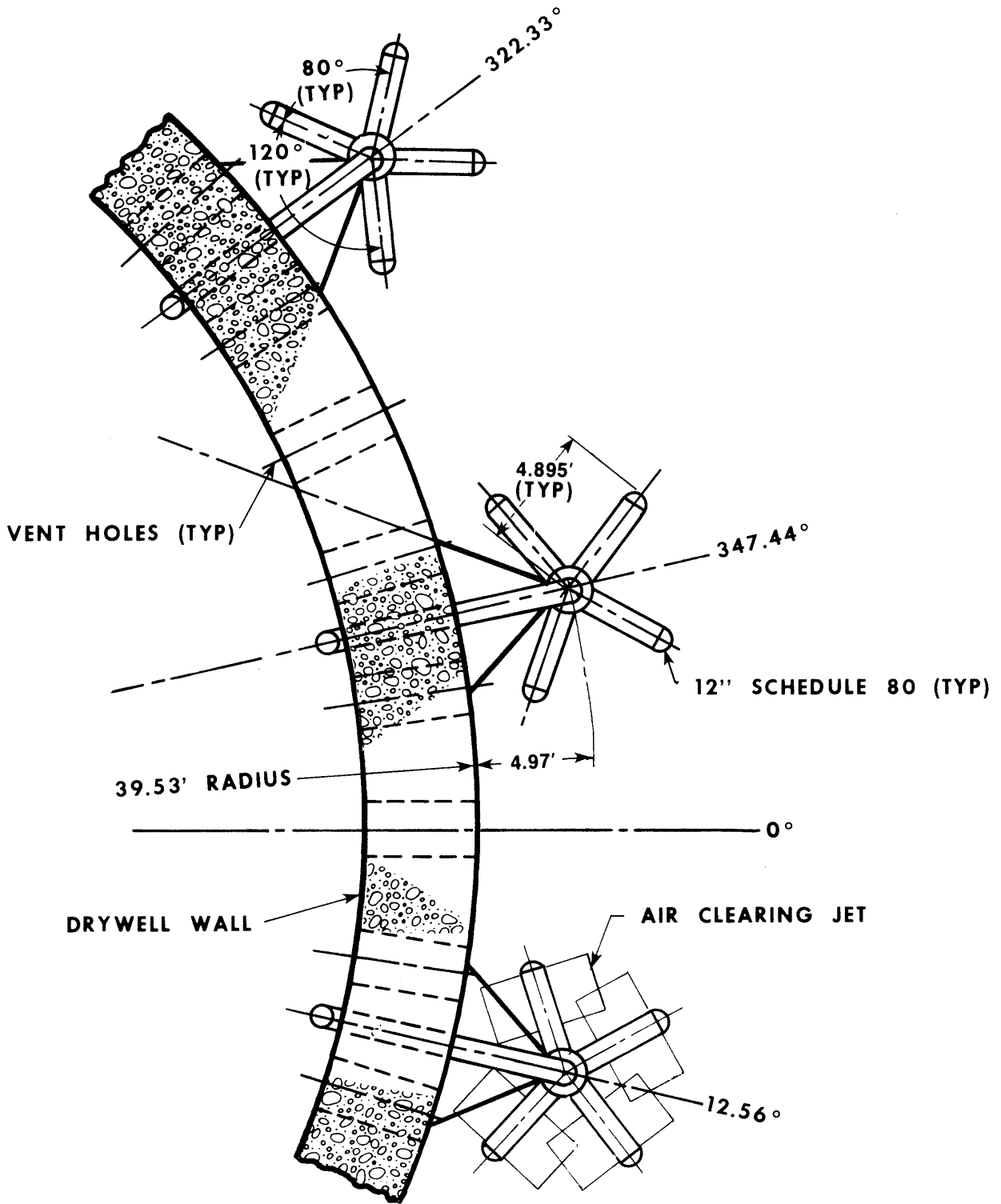
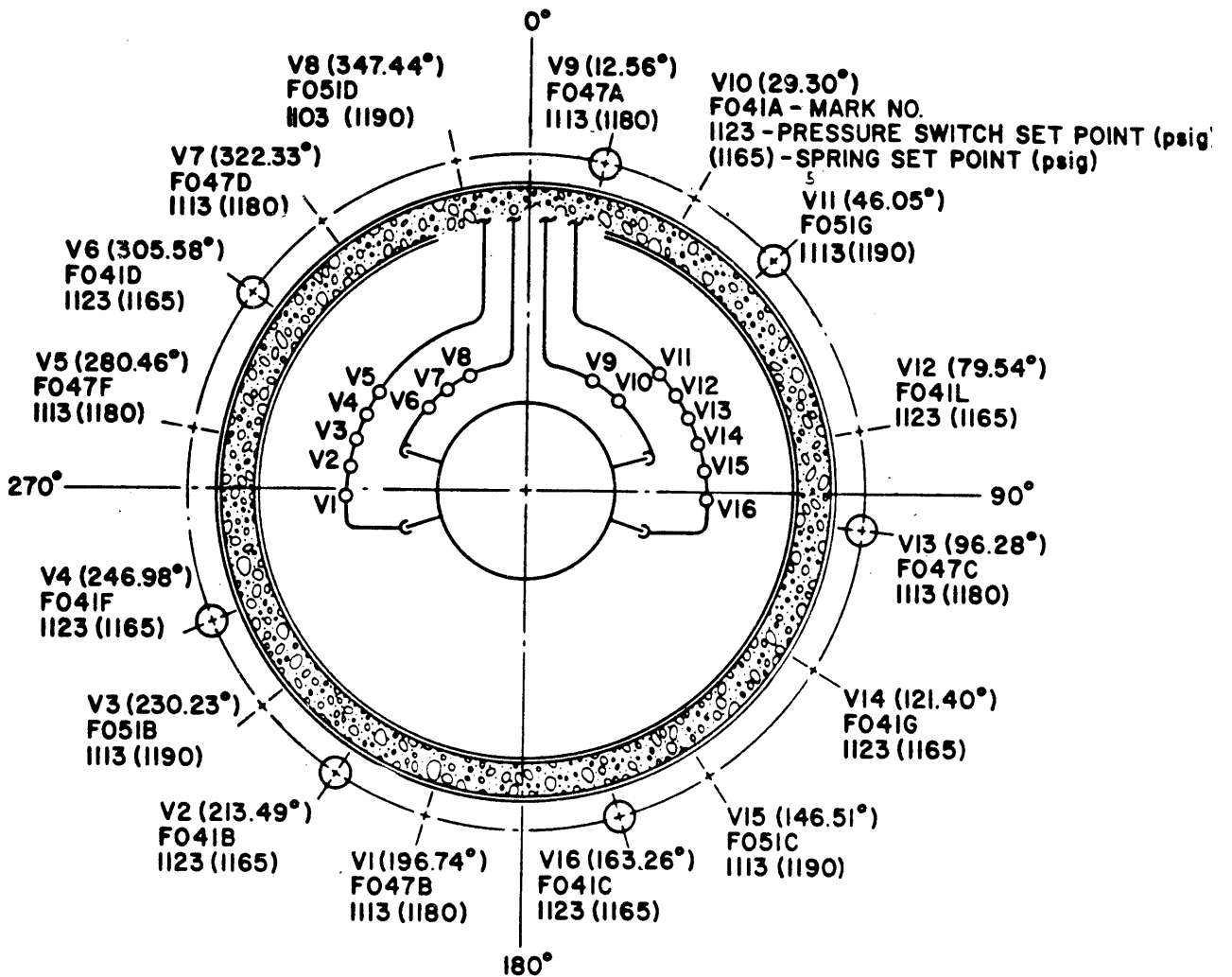


FIGURE A.6A.4-2

QUENCHER ARRANGEMENT,
PLAN VIEW

RIVER BEND STATION
UPDATED SAFETY ANALYSIS REPORT



NOTE:

PRESSURE SETPOINTS SHOWN ARE FOR INITIAL SET LOW-LOW RESET
LOGIC APPLIES FOR SUBSEQUENT ACTUATION

FIGURE A.6A.4-3

SAFETY RELIEF VALVE
AND QUENCHER LOCATIONS

RIVER BEND STATION
UPDATED SAFETY ANALYSIS REPORT

RBS USAR

A.6A.5 QUENCHER LOAD ON POOL BOUNDARY

A.6A.5.1 Pressures on Drywell, Basemat, and Containment

Pressures on drywell wall, basemat, and containment resulting from in-phase S/R valve discharge are calculated in Section A.6A.10. For River Bend Station, the maximum and minimum design bubble pressures below the quencher just after air clearing are shown in Table A.6A.5-1.

The absolute pressure on the pool walls can be calculated by the following equation:

$$P_{(a)} = P_{\text{containment}} + \frac{\rho h(a)}{144} + \Delta P(r)$$

where:

$P_{(a)}$ = Absolute pressure at point "a" (psia)

r = Distance from center of quencher to point "a" (ft)

$P_{\text{containment}}$ = Absolute pressure of containment atmosphere (psia)

$h(a)$ = Head of water acting at point "a" (ft)

ρ = Density of pool water 62.4 (lbm/cu ft)

$\Delta P(r)$ = Bubble pressure attenuated by distance, r to point "a", for multiple S/R valve actuations (psid).

The pressure decays with time as discussed in Section A.6A.5.4.

The following subsections discuss the dynamic pressure fields, at radial and circumferential locations of the pool for River Bend Station. The pressure fields are based on maximum bubble pressure, P_{BMAX} normalized to 1 psid. These dynamic peak pressure fields can be used to reflect the changes in the maximum and/or minimum bubble pressure. If for example, $P_{\text{BMAX}} = 25$ psid for another SRVDL layout, the normalized values of Tables A.6A.5-2 through A.6A.5-5 would be multiplied by 25 to obtain the design pressures. The P_{BMAX} values used for River Bend Station are the ones listed in Table A.6A.5-1.

RBS USAR

These distributions are based on all bubbles being "in phase." This assumption is made for evaluation of containment structures. For generation of amplified response spectra (ARS) for equipment and piping evaluation, the Monte Carlo approach described in Attachment N is used.

A.6A.5.1.1 Single S/R Valve Loads

The normalized dynamic peak pressures $\Delta P(r)$ for a single S/R valve discharge are given in Table A.6A.5-2, and the normalized radial and circumferential peak values are shown in Fig. A.6A.5-1 through A.6A.5-3.

This is the base case and this pressure field is used to develop any other S/R valve combination, as described in Section A.6A.10.

A.6A.5.1.2 Two Adjacent S/R Valve Loads

The normalized dynamic peak pressures $\Delta P(r)$ are given in Table A.6A.5-3 and the normalized radial and circumferential peak values are plotted in Fig. A.6A.5-4, A.6A.5-5, and A.6A.5-6 for the two adjacent S/R valves V-8 and V-9.

A.6A.5.1.3 Nine S/R Valve Loads

The 9 S/R valves load is not considered for design, because it is enveloped by other S/R valve conditions.

A.6A.5.1.4 Seven S/R Valve Loads (ADS)

Normalized $\Delta P(r)$ loads are given in Table A.6A.5-4, and the normalized values are shown in Fig. A.6A.5-7 through A.6A.5-9 for the 7 ADS valves V-2, V-4, V-6, V-9, V-11, V-13, and V-16.

A.6A.5.1.5 All Sixteen S/R Valve Loads

Normalized $\Delta P(r)$ loads are given in Table A.6A.5-5, and the normalized values are shown in Fig. A.6A.5-10 through A.6A.5-12 for all 16 valves V-1 to V-16.

A.6A.5.2 Loads on Weir Wall

The S/R valve loads on the weir wall are the same as those on the drywell wall, except that they act only on the projected area through the drywell wall vents.

A.6A.5.3 Loads on Submerged Structures

Loads on submerged structures due to the S/R valve loads are described in Attachment L of Appendix 6A.

A.6A.5.4 Normalized Pressure Time History (Theoretical Rayleigh Bubble)

The ideal Rayleigh bubble pressure is normalized for the maximum $P(r)$ positive value, as shown in Fig. A.6A.5-13. The oscillating frequency is 5 to 12 Hz as derived from the test data shown on Fig. A.6A.5-14, and the total time of oscillation is 0.75 sec (i.e., the time for the air bubbles to rise to the surface of the pool). Fig. A.6A.5-13 is used for determining pressure amplitudes with time and the number of pressure cycles (Section A.6A.9).

It should be noted that bubble pressure decays to $1/3 P$ within 5 cycles for any frequency between 5 and 12 Hz. For this linear attenuation rule, it is observed that the pressure amplitude is fully decayed ($P=0$ psig) in 7.5 pressure cycles after the peak. The justification of this amplification is from examination of full-scale plant data where most traces were observed to decay to a small fraction of their peak value in 2 or 3 cycles.

A.6A.5.5 Representative Pressure Time History

Fig. A.6A.5-14 depicts a representative pressure time history at points P through P as shown on Fig. A.6A.4-1. These curves provide a realistic picture of the pressure oscillations as opposed to the idealized Rayleigh bubbles.

RBS USAR

TABLE A.6A.5-1

QUENCHER BUBBLE PRESSURE
RIVER BEND STATION
(95-95% CONFIDENCE LEVEL)

Case Description	Design Value Bottom Maximum Pressure (psid)		Ratio of P(-) and P(+)
	P(+)	P(-)	
Single valve sub-sequent actuation, at 120°F pool temperature	16.56	-7.41	0.45
Two adjacent valves first actuation, at 100°F pool temperature	9.66	-6.10	0.63
16 valves (all valve case) first actuation, at 100°F pool temperature	11.12	-6.09	0.55
7 ADS valves first actuation at 120°F pool temperature	9.72	-6.14	0.63

RBS USAR

TABLE A.6A.5-2

NORMALIZED DYNAMIC PEAK PRESSURE FIELD FOR SINGLE S/R VALVE
(Fig. A.6A.5-1 through A.6A.5-3)

Time = 0.15 sec (Positive Pressure psid) P(r)
= 0.08 sec (Negative Pressure psid) P(r)

S/R Valves Angle (degrees) Reference Point	<u>257</u>	<u>266</u>	<u>275</u>	<u>284</u>	<u>293</u>	<u>302</u>	<u>311</u>	<u>320</u>	<u>329</u>	<u>338</u>	V-8 <u>347</u>	<u>356</u>
1							0.0	0.0	0.0	0.0	0.0	0.0
2							0.347	0.437	0.580	0.797	0.966	0.821
3							0.361	0.467	0.657	1.0	1.0	1.0
4							0.364	0.474	0.676	1.0	1.0	1.0
5				0.0	0.0	0.0	0.355	0.454	0.622	0.921	1.0	0.959
6			0.0	0.206	0.236	0.279	0.341	0.442	0.625	1.0	1.0	1.0
7		0.0	0.174	0.195	0.223	0.262	0.320	0.411	0.571	0.875	1.0	0.916
8		0.149	0.164	0.183	0.209	0.244	0.295	0.372	0.494	0.680	0.826	0.701
9		0.140	0.154	0.171	0.194	0.225	0.268	0.328	0.414	0.520	0.584	0.530
10		0.141	0.155	0.172	0.196	0.227	0.272	0.336	0.429	0.550	0.627	0.562
11		0.141	0.154	0.172	0.195	0.227	0.270	0.333	0.424	0.540	0.612	0.551
12		0.140	0.153	0.170	0.193	0.223	0.264	0.322	0.401	0.494	0.548	0.503
13	0.0	0.0	0.0	0.0	0.0	0.0	0.0	0.0	0.0	0.0	0.0	0.0

RBS USAR

TABLE A.6A.5-3

NORMALIZED DYNAMIC PEAK PRESSURE FIELD FOR TWO ADJACENT S/R VALVES
(Fig. A.6A.5-4 through A.6A.5-6)

Time = 0.15 sec (Positive Pressure) P(r)
= 0.08 sec (Negative Pressure) P(r)

S/R Valves Angle (degrees) Reference Point	<u>279</u>	<u>288</u>	<u>297</u>	<u>306</u>	<u>315</u>	<u>324</u>	<u>333</u>	<u>V-8</u>		<u>360</u>	<u>V-9</u>	
								<u>342</u>	<u>351</u>		<u>9</u>	<u>18</u>
1					0.0	0.0	0.0	0.0	0.0	0.0	0.0	0.0
2					0.382	0.492	0.668	0.984	1.0	1.0	1.0	0.984
3					0.401	0.536	0.794	1.0	1.0	1.0	1.0	1.0
4					0.406	0.547	0.830	1.0	1.0	1.0	1.0	1.0
5		0.0	0.0	0.0	0.393	0.517	0.736	1.0	1.0	1.0	1.0	1.0
6	0.0	0.218	0.253	0.303	0.441	0.572	0.823	1.0	1.0	1.0	1.0	1.0
7	0.182	0.206	0.292	0.341	0.414	0.532	0.745	1.0	1.0	1.0	1.0	1.0
8	0.172	0.194	0.274	0.318	0.381	0.478	0.633	0.840	0.915	0.862	0.915	0.840
9	0.161	0.226	0.255	0.293	0.346	0.421	0.525	0.638	0.689	0.683	0.689	0.638
10	0.162	0.228	0.257	0.296	0.351	0.431	0.544	0.674	0.729	0.717	0.729	0.674
11	0.162	0.227	0.256	0.295	0.349	0.427	0.537	0.661	0.715	0.705	0.715	0.661
12	0.160	0.225	0.253	0.290	0.341	0.412	0.507	0.607	0.655	0.654	0.655	0.607
13	0.0	0.0	0.0	0.0	0.0	0.0	0.0	0.0	0.0	0.0	0.0	0.0

RBS USAR

TABLE A.6A.5-4

NORMALIZED DYNAMIC PEAK PRESSURE FIELD FOR 7 S/R VALVES (ADS)
 (Fig. A.6A.5-7 through A.6A.5-9)

Time = 0.15 sec (Positive Pressure psid) P(r)
 = 0.08 sec (Negative Pressure psid) P(r)

S/R Valves Angle (degrees) Reference Point	0	V-9			V-11				V-13			
		9	18	27	36	45	54	63	72	81	90	99
1	0.0	0.0	0.0	0.0	0.0	0.0	0.0	0.0	0.0	0.0	0.0	0.0
2	0.714	0.996	0.996	0.876	0.923	1.0	0.837	0.716	0.661	0.741	0.879	0.948
3	0.877	1.0	1.0	1.0	1.0	1.0	1.0	0.805	0.715	0.849	1.0	1.0
4	0.925	1.0	1.0	1.0	1.0	1.0	1.0	0.828	0.728	0.879	1.0	1.0
5	0.800	1.0	1.0	0.954	1.0	1.0	0.984	0.765	0.692	0.799	1.0	1.0
6	0.916	1.0	1.0	0.973	1.0	1.0	1.0	0.807	0.712	0.809	1.0	1.0
7	0.822	1.0	1.0	0.900	0.992	1.0	1.0	0.741	0.662	0.758	1.0	1.0
8	0.688	0.870	0.880	0.781	0.810	0.912	0.805	0.650	0.596	0.671	0.823	0.857
9	0.566	0.668	0.680	0.651	0.659	0.683	0.635	0.557	0.524	0.570	0.635	0.648
10	0.588	0.705	0.716	0.674	0.682	0.723	0.666	0.574	0.536	0.588	0.669	0.687
11	0.581	0.692	0.703	0.666	0.672	0.709	0.655	0.568	0.532	0.581	0.657	0.673
12	0.547	0.637	0.651	0.630	0.629	0.650	0.609	0.543	0.513	0.554	0.608	0.616
13	0.0	0.0	0.0	0.0	0.0	0.0	0.0	0.0	0.0	0.0	0.0	0.0

RBS USAR

TABLE A.6A.5-4 (Cont)

S/R Valves Angle (degrees) Reference Point	V-16											
	<u>108</u>	<u>117</u>	<u>126</u>	<u>135</u>	<u>144</u>	<u>153</u>	<u>162</u>	<u>171</u>	<u>180</u>	<u>189</u>	<u>198</u>	<u>207</u>
1	0.0	0.0	0.0	0.0	0.0	0.0	0.0	0.0	0.0	0.0	0.0	0.0
2	0.736	0.537	0.533	0.539	0.564	0.775	0.962	0.843	0.719	0.661	0.737	0.874
3	0.918	0.596	0.560	0.569	0.634	0.997	1.0	1.0	0.810	0.715	0.834	1.0
4	0.974	0.611	0.567	0.575	0.651	1.0	1.10	1.0	0.834	0.727	0.871	1.0
5	0.831	0.570	0.599	0.556	0.603	0.888	1.0	0.993	0.769	0.692	0.795	1.0
6	0.937	0.629	0.530	0.538	0.650	1.0	1.0	1.0	0.771	0.713	0.844	1.0
7	0.834	0.608	0.496	0.503	0.633	0.890	1.0	1.0	0.729	0.663	0.771	1.0
8	0.687	0.543	0.478	0.484	0.561	0.718	0.870	0.797	0.637	0.597	0.669	0.834
9	0.557	0.475	0.451	0.436	0.486	0.572	0.653	0.625	0.561	0.526	0.568	0.648
10	0.581	0.486	0.458	0.443	0.499	0.599	0.693	0.656	0.577	0.538	0.586	0.681
11	0.573	0.483	0.456	0.440	0.495	0.590	0.679	0.645	0.572	0.533	0.580	0.669
12	0.537	0.465	0.495	0.429	0.475	0.550	0.621	0.600	0.547	0.515	0.552	0.620
13	0.0	0.0	0.0	0.0	0.0	0.0	0.0	0.0	0.0	0.0	0.0	0.0

RBS USAR

TABLE A.6A.5-4 (Cont)

S/R Valves Angle (degrees) Reference Point	V-2		V-4			V-6						
	<u>216</u>	<u>225</u>	<u>234</u>	<u>243</u>	<u>252</u>	<u>261</u>	<u>270</u>	<u>279</u>	<u>288</u>	<u>297</u>	<u>306</u>	<u>315</u>
1	0.0	0.0	0.0	0.0	0.0	0.0	0.0	0.0	0.0	0.0	0.0	0.0
2	1.0	0.903	0.887	1.00	0.966	0.678	0.611	0.591	0.597	0.820	0.966	0.798
3	1.0	1.0	1.0	1.0	1.0	0.812	0.658	0.629	0.683	1.0	1.0	1.0
4	1.0	1.0	1.0	1.0	1.0	0.850	0.669	0.638	0.705	1.0	1.0	1.0
5	1.0	1.0	0.973	1.0	1.0	0.749	0.638	0.613	0.694	0.957	1.0	0.922
6	1.0	1.0	1.0	1.0	1.0	0.869	0.664	0.628	0.719	1.0	1.0	1.0
7	1.0	0.953	0.953	0.935	1.0	1.0	0.787	0.618	0.586	0.960	1.0	0.920
8	0.906	0.807	0.743	0.900	0.852	0.672	0.559	0.534	0.597	0.752	0.866	0.730
9	0.682	0.662	0.657	0.688	0.650	0.562	0.495	0.477	0.530	0.604	0.633	0.576
10	0.722	0.689	0.681	0.725	0.686	0.582	0.505	0.486	0.544	0.633	0.674	0.604
11	0.708	0.680	0.673	0.712	0.673	0.575	0.501	0.483	0.539	0.623	0.659	0.594
12	0.650	0.640	0.635	0.658	0.620	0.545	0.485	0.468	0.517	0.580	0.600	0.552
13	0.0	0.0	0.0	0.0	0.0	0.0	0.0	0.0	0.0	0.0	0.0	0.0

TABLE A.6A.5-4 (Cont)

<u>S/R Valves</u> <u>Angle (degrees)</u> <u>Reference Point</u>	<u>324</u>	<u>333</u>	<u>342</u>	<u>351</u>
1	0.0	0.0	0.0	0.0
2	0.580	0.437	0.530	0.522
3	0.658	0.467	0.557	0.577
4	0.677	0.479	0.563	0.590
5	0.623	0.459	0.546	0.553
6	0.679	0.544	0.565	0.657
7	0.623	0.536	0.529	0.610
8	0.587	0.491	0.487	0.548
9	0.508	0.461	0.440	0.483
10	0.521	0.468	0.447	0.494
11	0.517	0.466	0.444	0.490
12	0.496	0.454	0.434	0.473
13	0.0	0.0	0.0	0.0

RBS USAR

TABLE A.6A.5-5

NORMALIZED DYNAMIC PEAK PRESSURE FIELD FOR 16 S/R VALVES (ADS)
 (Fig. A.6A.5-10 through A.6A.5-12)

Time = 0.15 sec (Positive Pressure psid) P(r)
 = 0.08 sec (Negative Pressure psid) P(r)

S/R Valves Angle (degrees) Reference Point	0	V-9		V-10		V-11		63	V-12		V-13	
		9	18	27	36	45	54		72	81	90	99
1	0.0	0.0	0.0	0.0	0.0	0.0	0.0	0.0	0.0	0.0	0.0	0.0
2	1.0	1.0	1.0	1.0	1.0	1.0	1.0	1.0	1.0	1.0	1.0	1.0
3	1.0	1.0	1.0	1.0	1.0	1.0	1.0	1.0	1.0	1.0	1.0	1.0
4	1.0	1.0	1.0	1.0	1.0	1.0	1.0	1.0	1.0	1.0	1.0	1.0
5	1.0	1.0	1.0	1.0	1.0	1.0	1.0	1.0	1.0	1.0	1.0	1.0
6	1.0	1.0	1.0	1.0	1.0	1.0	1.0	1.0	1.0	1.0	1.0	1.0
7	1.0	1.0	1.0	1.0	1.0	1.0	1.0	1.0	1.0	1.0	1.0	1.0
8	1.0	1.0	1.0	1.0	1.0	1.0	1.0	1.0	1.0	1.0	1.0	1.0
9	0.873	0.905	0.934	0.944	0.932	0.905	0.836	0.810	0.842	0.891	0.905	0.891
10	0.904	0.944	0.976	0.988	0.975	0.946	0.867	0.833	0.873	0.932	0.946	0.931
11	0.893	0.930	0.961	0.972	0.960	0.431	0.856	0.825	0.862	0.917	0.932	0.917
12	0.846	0.873	0.898	0.907	0.896	0.870	0.810	0.790	0.815	0.856	0.870	0.858
13	0.0	0.0	0.0	0.0	0.0	0.0	0.0	0.0	0.0	0.0	0.0	0.0

RBS USAR

TABLE A.6A.5-5 (Cont)

S/R Valves Angle (degrees) Reference Point	<u>108</u>	<u>V-14</u>		<u>135</u>	<u>V-15</u>		<u>162</u>	<u>V-16</u>		<u>189</u>	<u>V-1</u>	
		<u>117</u>	<u>126</u>		<u>144</u>	<u>153</u>		<u>171</u>	<u>180</u>		<u>198</u>	<u>207</u>
1	0.0	0.0	0.0	0.0	0.0	0.0	0.0	0.0	0.0	0.0	0.0	0.0
2	1.0	1.0	1.0	1.0	1.0	1.0	1.0	1.0	1.0	1.0	1.0	1.0
3	1.0	1.0	1.0	1.0	1.0	1.0	1.0	1.0	1.0	1.0	1.0	1.0
4	1.0	1.0	1.0	1.0	1.0	1.0	1.0	1.0	1.0	1.0	1.0	1.0
5	1.0	1.0	1.0	1.0	1.0	1.0	1.0	1.0	1.0	1.0	1.0	1.0
6	1.0	1.0	1.0	1.0	1.0	1.0	1.0	1.0	1.0	1.0	1.0	1.0
7	1.0	1.0	1.0	1.0	1.0	1.0	1.0	1.0	1.0	1.0	1.0	1.0
8	1.0	1.0	1.0	1.0	1.0	1.0	1.0	1.0	0.933	1.0	1.0	1.0
9	0.851	0.857	0.867	0.851	0.892	0.905	0.900	0.843	0.813	0.842	0.911	0.942
10	0.882	0.894	0.903	0.883	0.931	0.946	0.941	0.873	0.835	0.873	0.953	0.984
11	0.871	0.881	0.890	0.872	0.917	0.931	0.927	0.863	0.828	0.862	0.938	0.969
12	0.823	0.826	0.837	0.823	0.858	0.869	0.866	0.816	0.793	0.815	0.877	0.905
13	0.0	0.0	0.0	0.0	0.0	0.0	0.0	0.0	0.0	0.0	0.0	0.0

RBS USAR

TABLE A.6A.5-5 (Cont)

S/R Valves Angle (degrees) Reference Point	<u>V-2</u>	<u>V-3</u>		<u>V-4</u>		<u>261</u>	<u>270</u>	<u>V-5</u>		<u>297</u>	<u>V-6</u>	
	<u>216</u>	<u>225</u>	<u>234</u>	<u>243</u>	<u>252</u>			<u>279</u>	<u>288</u>		<u>306</u>	<u>315</u>
1	0.0	0.0	0.0	0.0	0.0	0.0	0.0	0.0	0.0	0.0	0.0	0.0
2	1.0	1.0	1.0	1.0	1.0	0.965	0.983	1.0	1.0	1.0	1.0	1.0
3	1.0	1.0	1.0	1.0	1.0	1.0	1.0	1.0	1.0	1.0	1.0	1.0
4	1.0	1.0	1.0	1.0	1.0	1.0	1.0	1.0	1.0	1.0	1.0	1.0
5	1.0	1.0	1.0	1.0	1.0	1.0	1.0	1.0	1.0	1.0	1.0	1.0
6	1.0	1.0	1.0	1.0	1.0	1.0	1.0	1.0	1.0	1.0	1.0	1.0
7	1.0	1.0	1.0	1.0	1.0	1.0	1.0	1.0	1.0	1.0	1.0	1.0
8	1.0	1.0	1.0	1.0	1.0	0.929	0.957	1.0	1.0	1.0	1.0	1.0
9	0.948	0.957	0.946	0.918	0.855	0.805	0.806	0.843	0.847	0.863	0.901	0.911
10	0.993	1.0	0.989	0.960	0.890	0.828	0.832	0.880	0.881	0.896	0.942	0.953
11	0.977	0.985	0.974	0.945	0.877	0.820	0.823	0.867	0.869	0.884	0.928	0.938
12	0.910	0.920	0.909	0.883	0.825	0.785	0.784	0.813	0.819	0.834	0.866	0.876
13	0.0	0.0	0.0	0.0	0.0	0.0	0.0	0.0	0.0	0.0	0.0	0.0

RBS USAR

TABLE A.6A.5-5 (Cont)

S/R Valves Angle (degrees) Reference Point	V-7		V-8	
	<u>324</u>	<u>333</u>	<u>342</u>	<u>351</u>
1	0.0	0.0	0.0	0.0
2	1.0	1.0	1.0	1.0
3	1.0	1.0	1.0	1.0
4	1.0	1.0	1.0	1.0
5	1.0	1.0	1.0	1.0
6	1.0	1.0	1.0	1.0
7	1.0	1.0	1.0	1.0
8	1.0	1.0	1.0	1.0
9	0.900	0.870	0.869	0.869
10	0.941	0.901	0.899	0.906
11	0.926	0.890	0.887	0.893
12	0.866	0.842	0.834	0.838
13	0.0	0.0	0.0	0.0

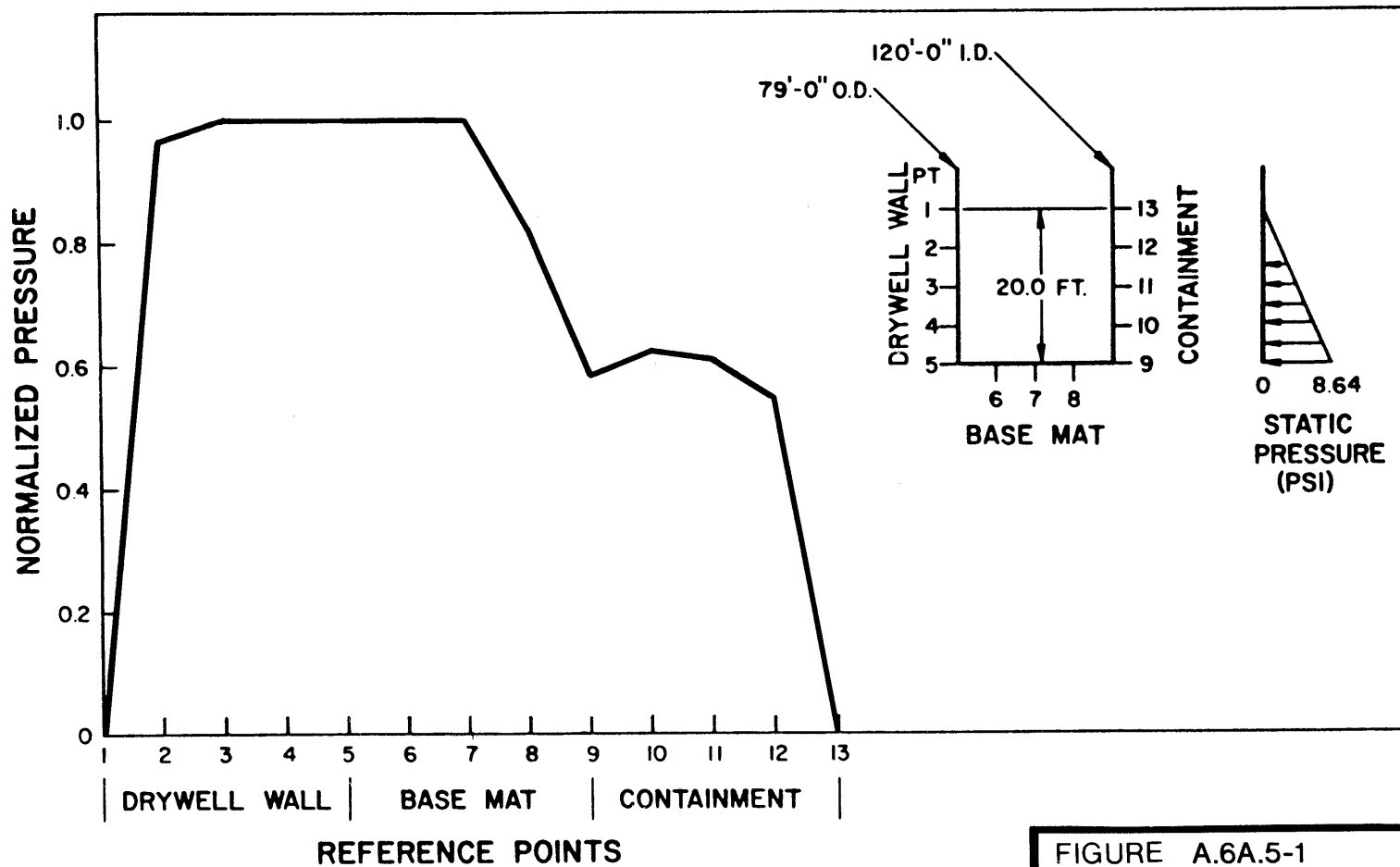


FIGURE A.6A.5-1

SINGLE SAFETY RELIEF VALVE
DISCHARGE NORMALIZED
WALL PRESSURE AT 347.44°

RIVER BEND STATION
UPDATED SAFETY ANALYSIS REPORT

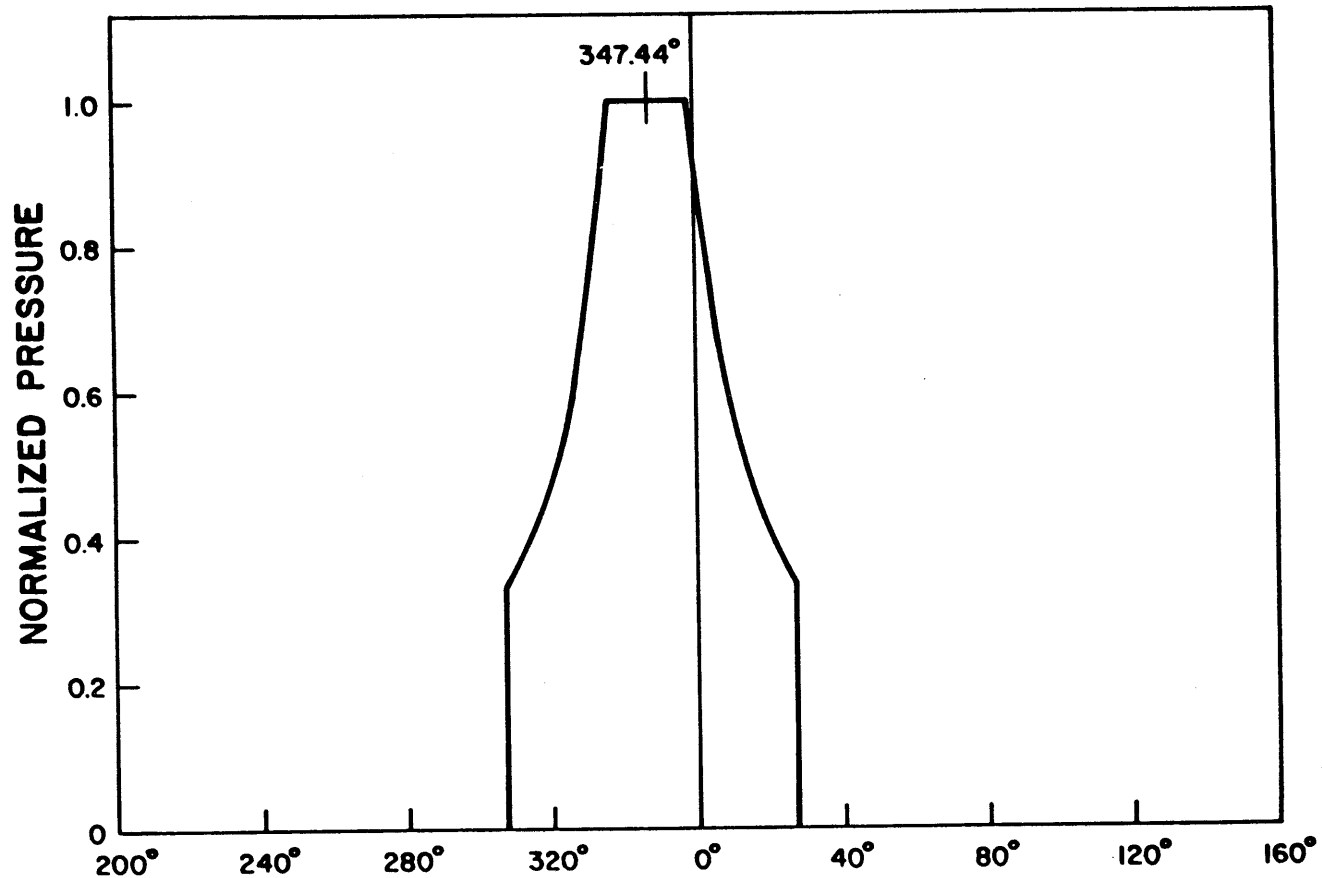


FIGURE A.6A.5-2

SINGLE SAFETY RELIEF VALVE
DISCHARGE REFERENCE POINT 4
(CIRCUMFERENTIAL DISTRIBUTION)

RIVER BEND STATION
UPDATED SAFETY ANALYSIS REPORT

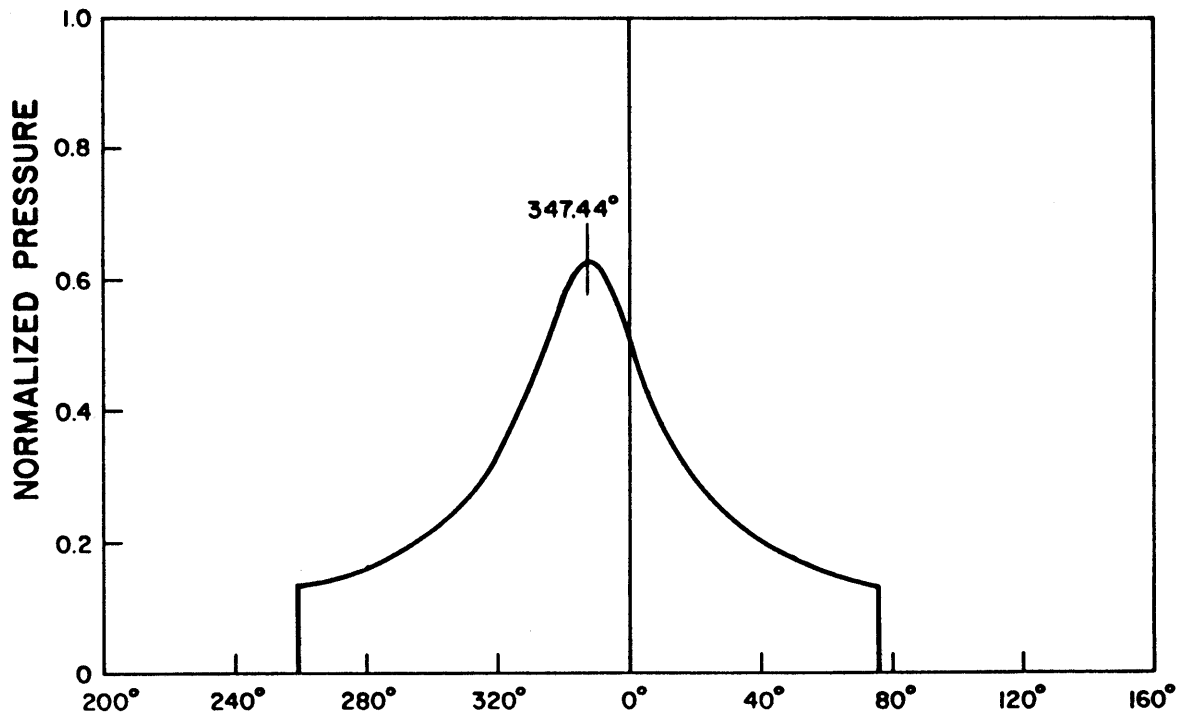


FIGURE A.6A.5-3

SINGLE SAFETY RELIEF VALVE
DISCHARGE REFERENCE POINT 10
(CIRCUMFERENTIAL DISTRIBUTION)

RIVER BEND STATION
UPDATED SAFETY ANALYSIS REPORT

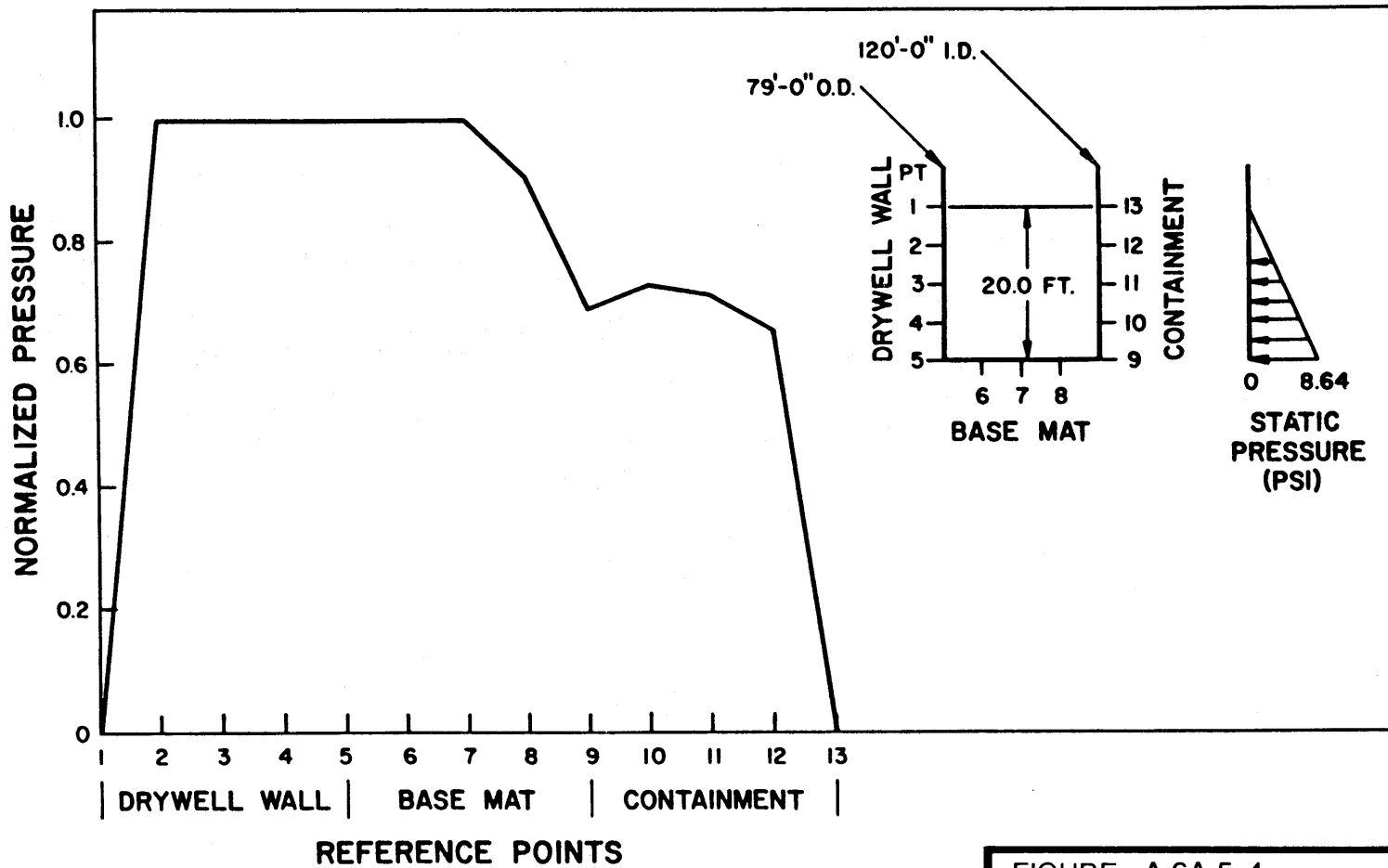


FIGURE A.6A.5-4

TWO ADJACENT SAFETY RELIEF VALVE DISCHARGE NORMALIZED WALL PRESSURE AT 360°

RIVER BEND STATION
 UPDATED SAFETY ANALYSIS REPORT

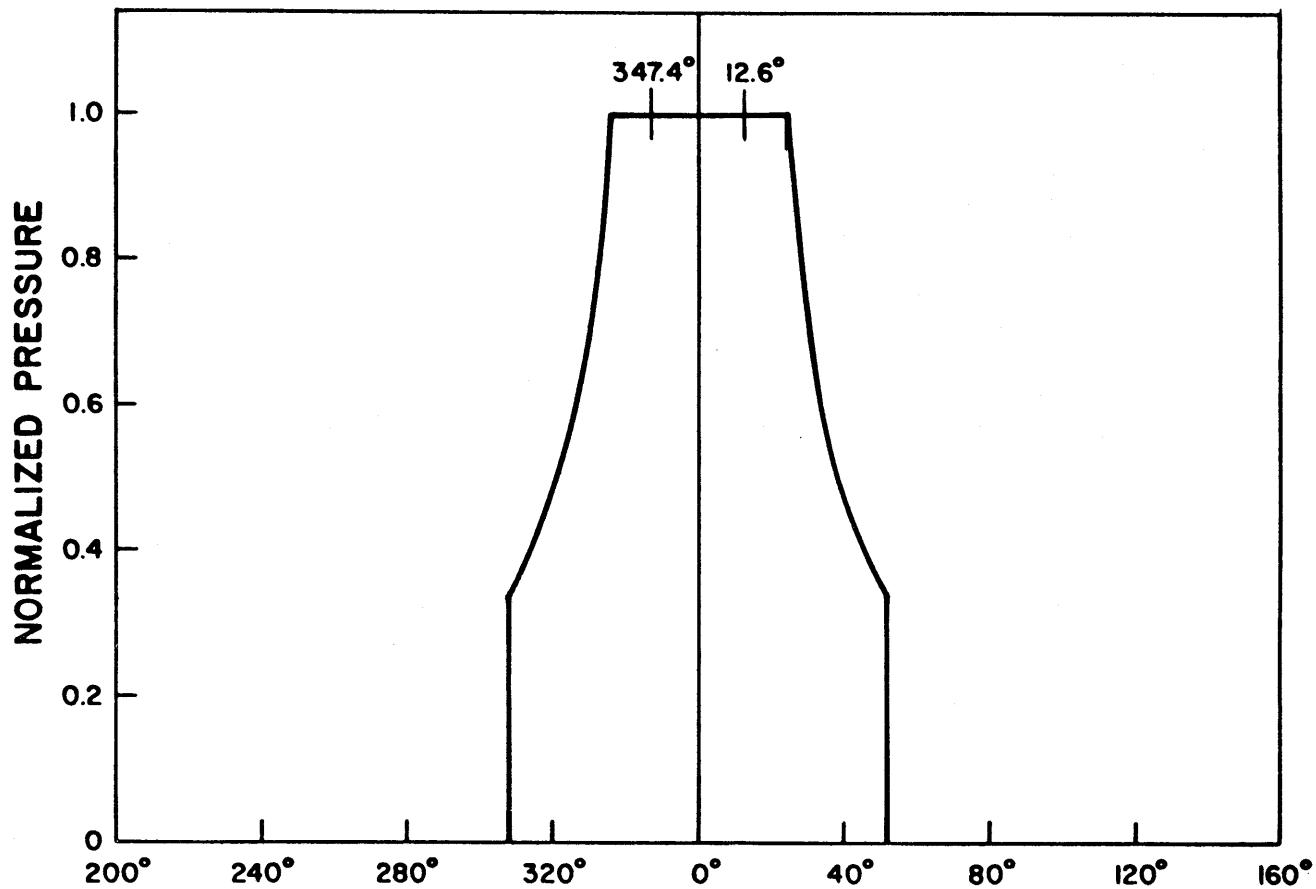


FIGURE A.6A.5-5

TWO ADJACENT SAFETY RELIEF
VALVE DISCHARGE REFERENCE
POINT 4 (CIRCUMFERENTIAL
DISTRIBUTION)

RIVER BEND STATION
UPDATED SAFETY ANALYSIS REPORT

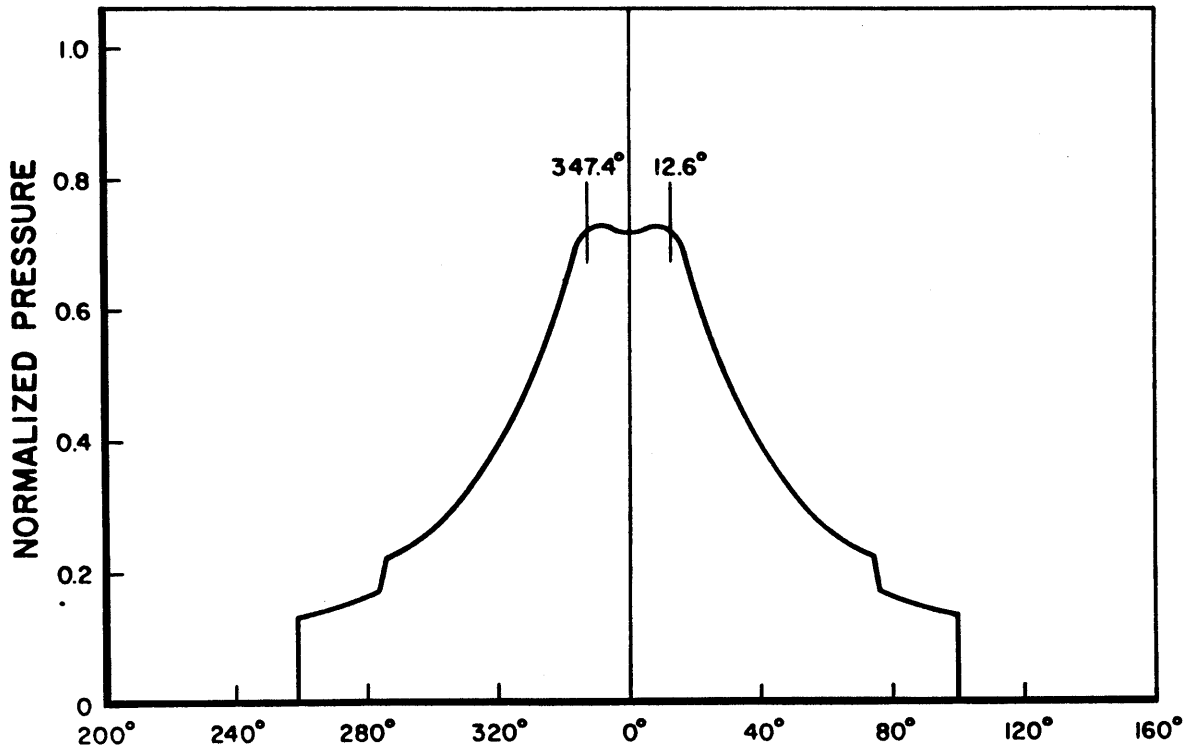


FIGURE A.6A.5-6

TWO ADJACENT SAFETY RELIEF
VALVE DISCHARGE REFERENCE POINT
10 (CIRCUMFERENTIAL DISTRIBUTION)

RIVER BEND STATION
UPDATED SAFETY ANALYSIS REPORT

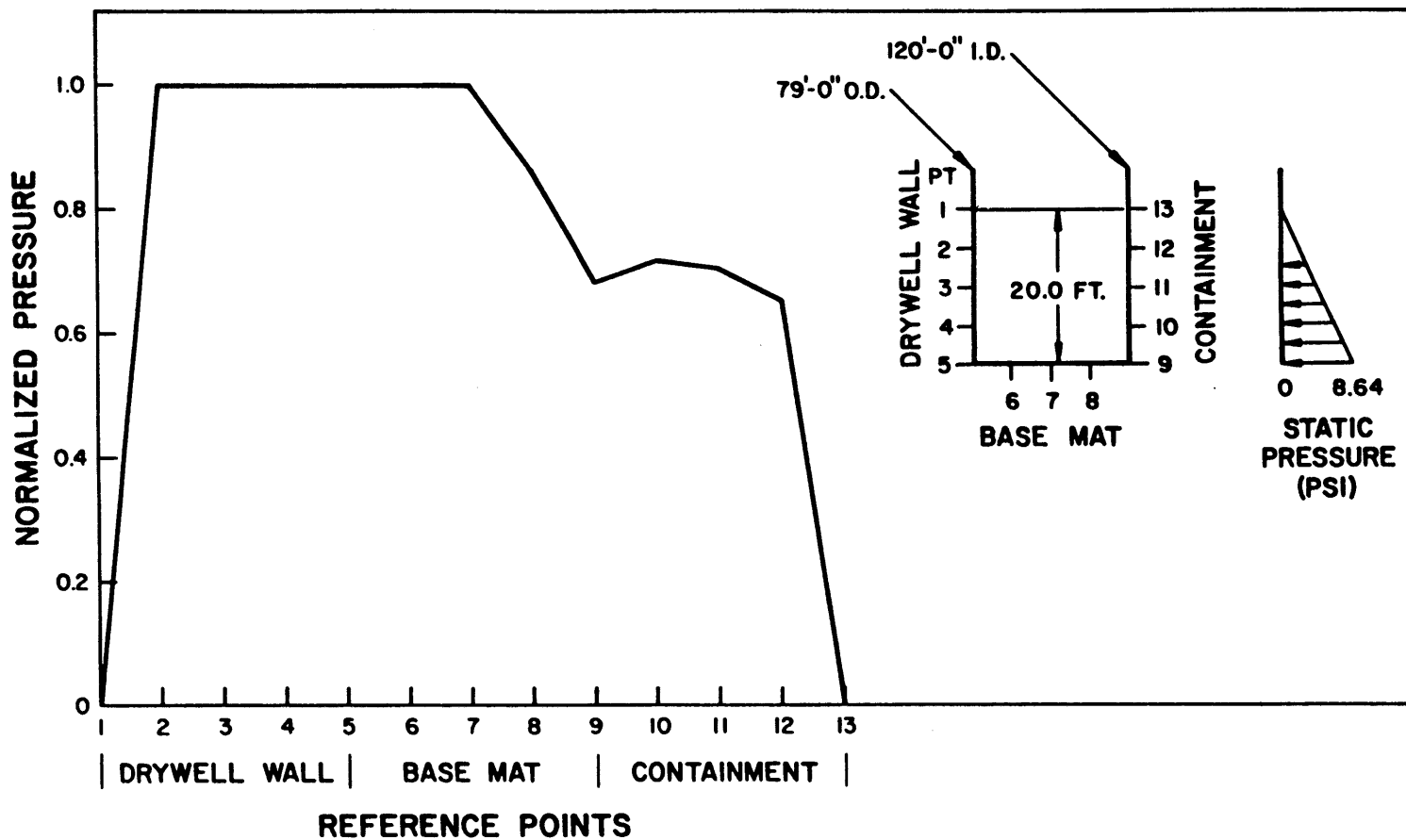


FIGURE A.6A.5-7

SEVEN SAFETY RELIEF VALVE DISCHARGE (ADS) NORMALIZED WALL PRESSURE AT 247°

RIVER BEND STATION
UPDATED SAFETY ANALYSIS REPORT

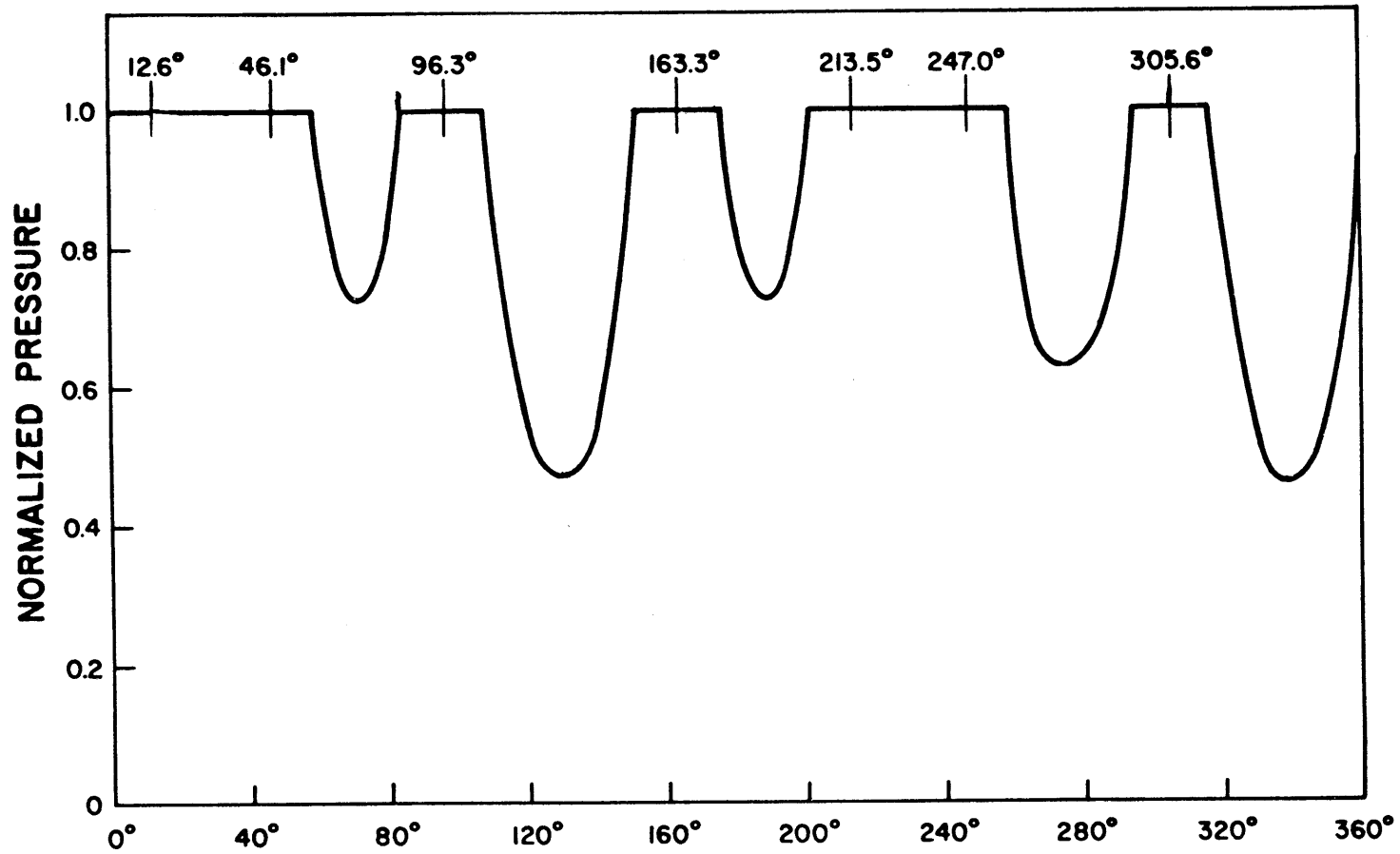


FIGURE A.6A.5-8

SEVEN SAFETY RELIEF VALVE
DISCHARGE REFERENCE POINT 4
(CIRCUMFERENTIAL DISTRIBUTION)

RIVER BEND STATION
UPDATED SAFETY ANALYSIS REPORT

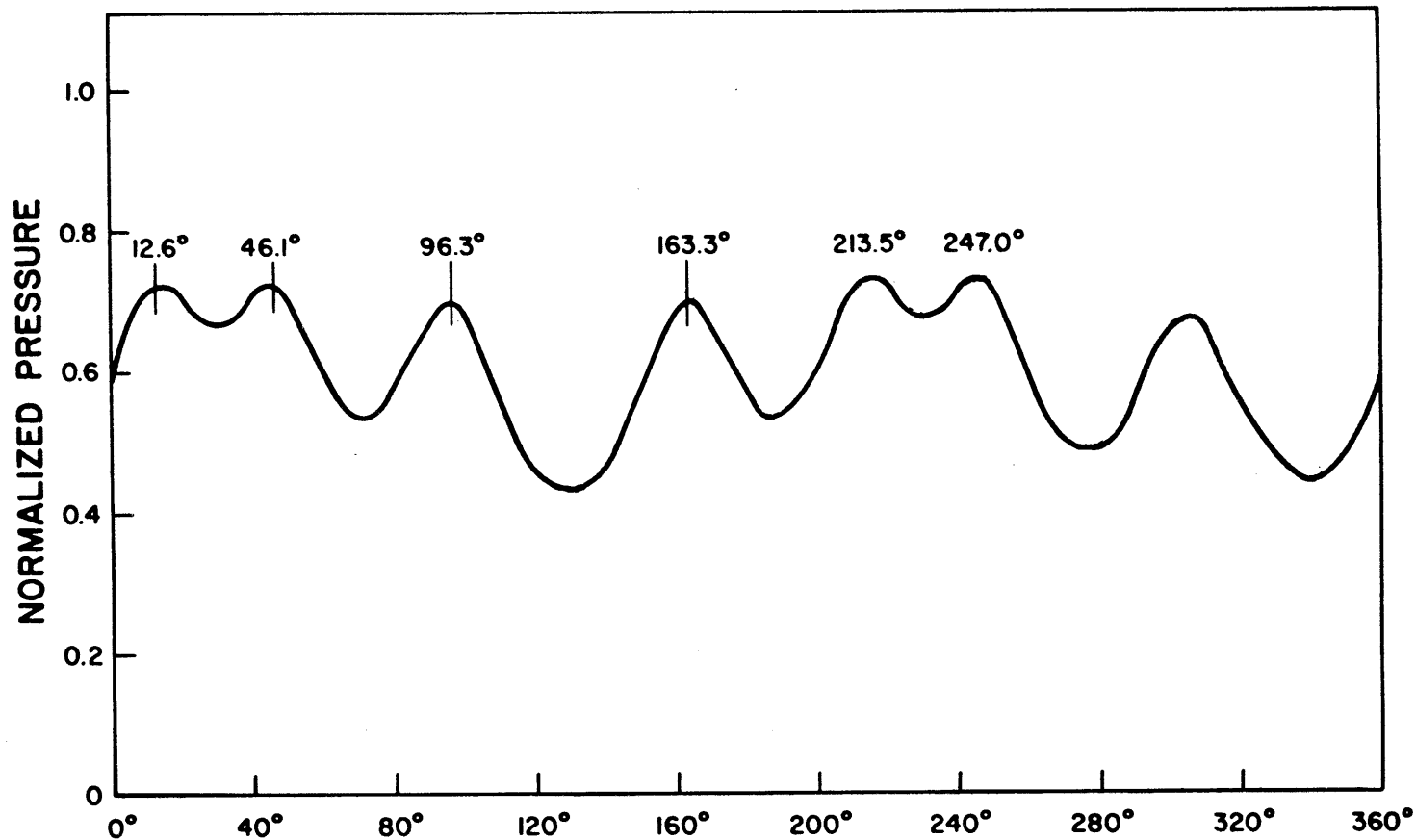
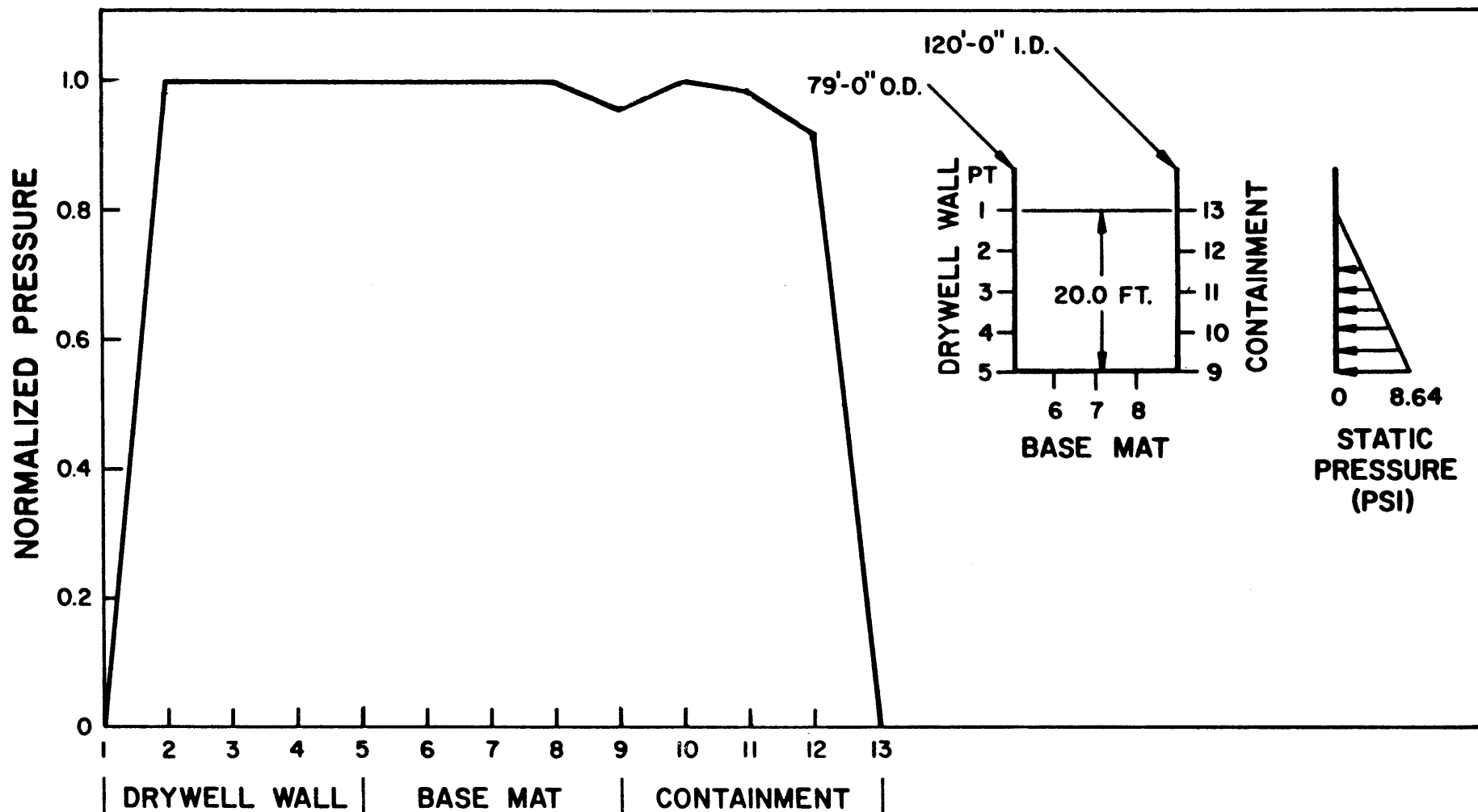


FIGURE A.6A.5-9

SEVEN SAFETY RELIEF VALVE
DISCHARGE (ADS) REFERENCE
POINT 10 (CIRCUMFERENTIAL
DISTRIBUTION)

RIVER BEND STATION
UPDATED SAFETY ANALYSIS REPORT



REFERENCE POINTS

FIGURE A.6A.5-10

SIXTEEN SAFETY RELIEF VALVE
DISCHARGE NORMALIZED
WALL PRESSURE AT 222°

RIVER BEND STATION
UPDATED SAFETY ANALYSIS REPORT

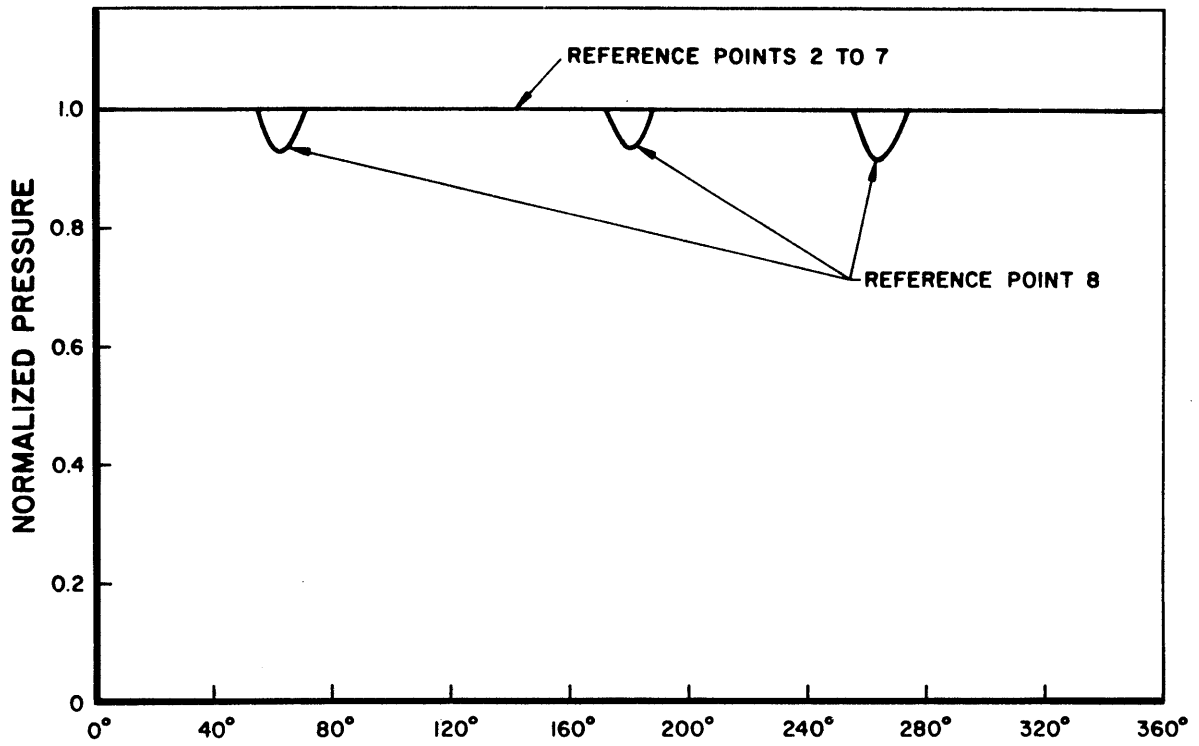


FIGURE A.6A.5-11

SIXTEEN SAFETY RELIEF VALVE
DISCHARGE REFERENCE POINTS
2 TO 8

RIVER BEND STATION
UPDATED SAFETY ANALYSIS REPORT

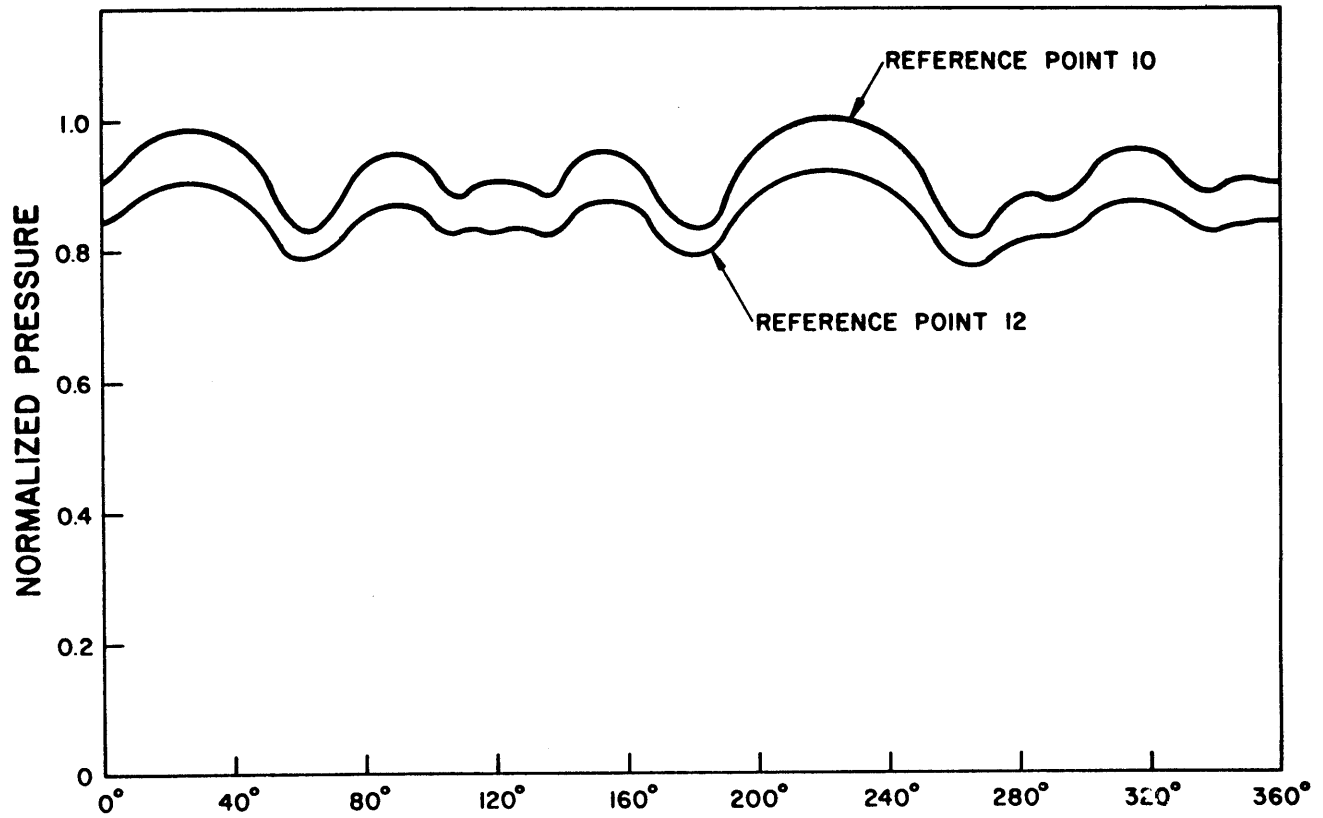
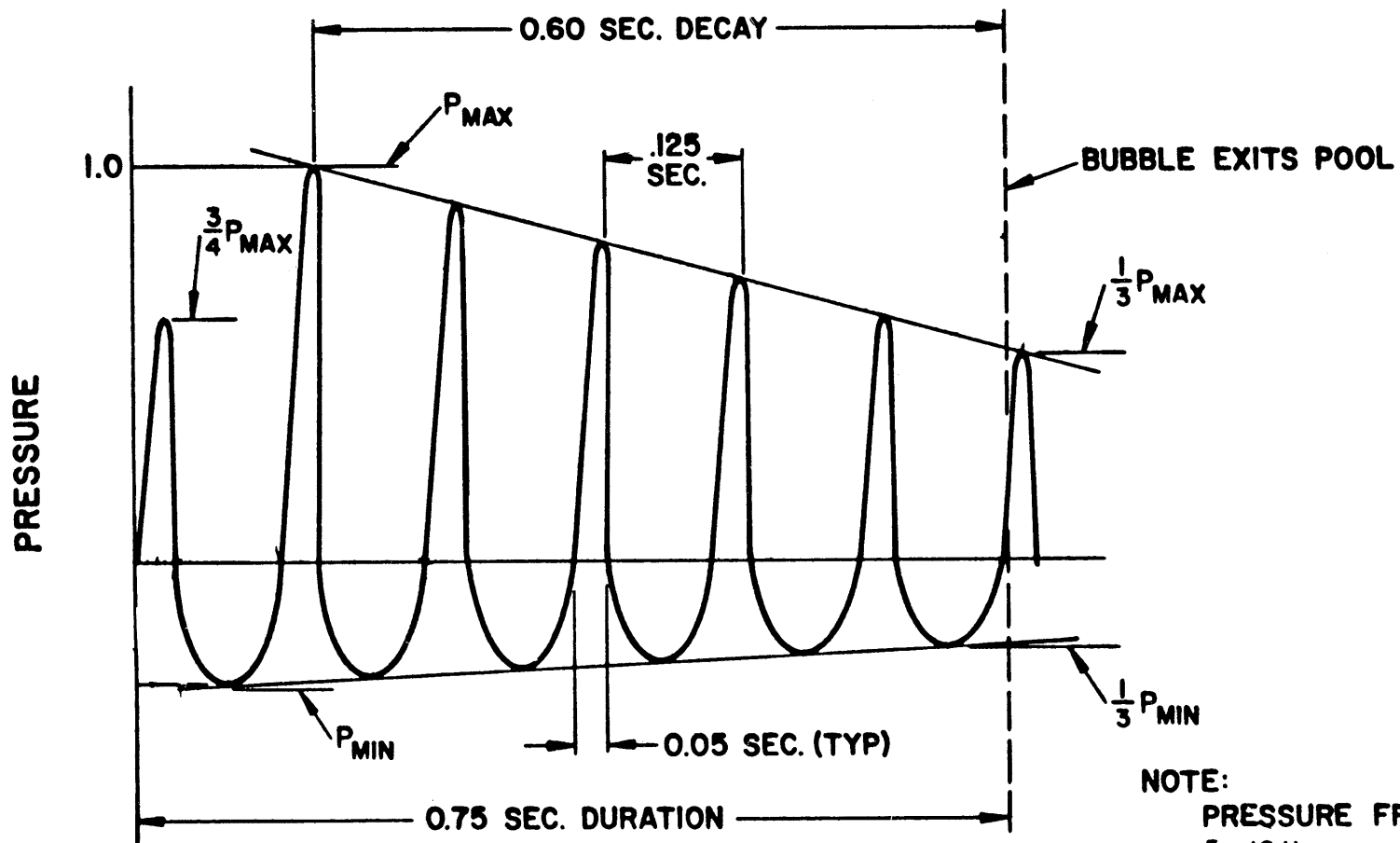


FIGURE A.6A.5-12

SIXTEEN SAFETY RELIEF VALVE
DISCHARGE REFERENCE POINTS
10 AND 12 (CIRCUMFERENTIAL
DISTRIBUTION)

RIVER BEND STATION
UPDATED SAFETY ANALYSIS REPORT

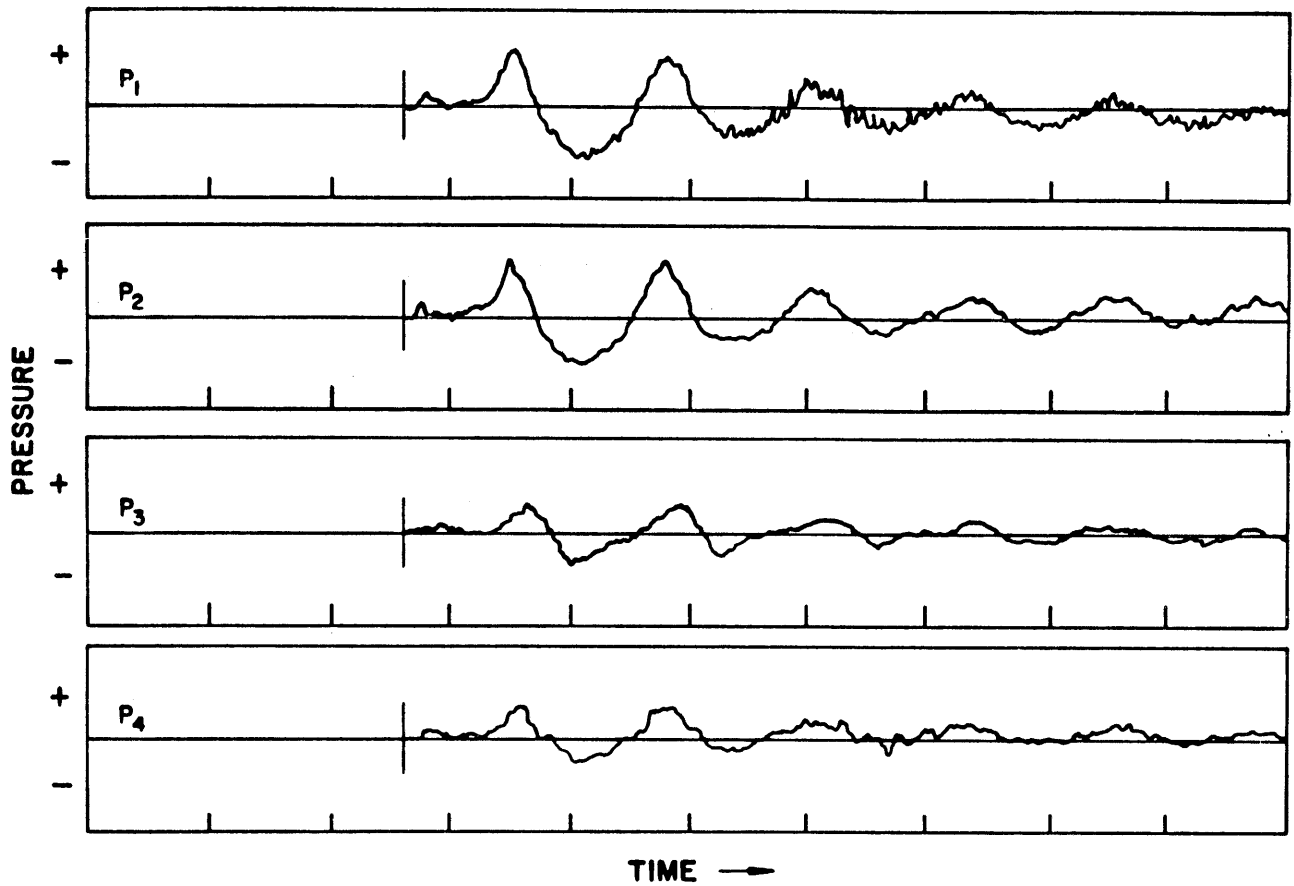


NOTE:
 PRESSURE FREQUENCY RANGE
 5-12 Hz

FIGURE A.6A.5-13

IDEALIZED QUENCHER BUBBLE
 PRESSURE OSCILLATION IN
 SUPPRESSION POOL
 (RAYLEIGH BUBBLE)

RIVER BEND STATION
 UPDATED SAFETY ANALYSIS REPORT



NOTE SEE FIGURE A.6A.4-1 FOR POINT LOCATION (P₁ THRU P₄)

(REPRODUCED FROM GESSAR, FIG. 3BA-2)

FIGURE A.6A.5-14

REPRESENTATIVE PRESSURE
TIME HISTORY FOR
QUENCHER DYNAMIC LOAD

RIVER BEND STATION
UPDATED SAFETY ANALYSIS REPORT

A.6A.6 OTHER LOADS ON STRUCTURES IN THE POOL

A.6A.6.1 LOCA and Pool Swell

See Sections 6A.2 and 6A.7.

Forces on Pipes Due to Vent-Clearing, Pool Swell, and Fallback

The loads on the quencher are evaluated as standard and acceleration drag forces on cylindrical bodies. The drag forces based on these velocities are applied normal to the cylindrical components of the quencher and to the projected SRVDL or sleeve areas to obtain the maximum design forces. The SRVDL loads transmitted to the quencher are given as F , M in Table A.6A.7-2 and are included in the quencher and strut anchor loads in Section A.6A.7.

A.6A.6.2 Thermal Expansion Loads

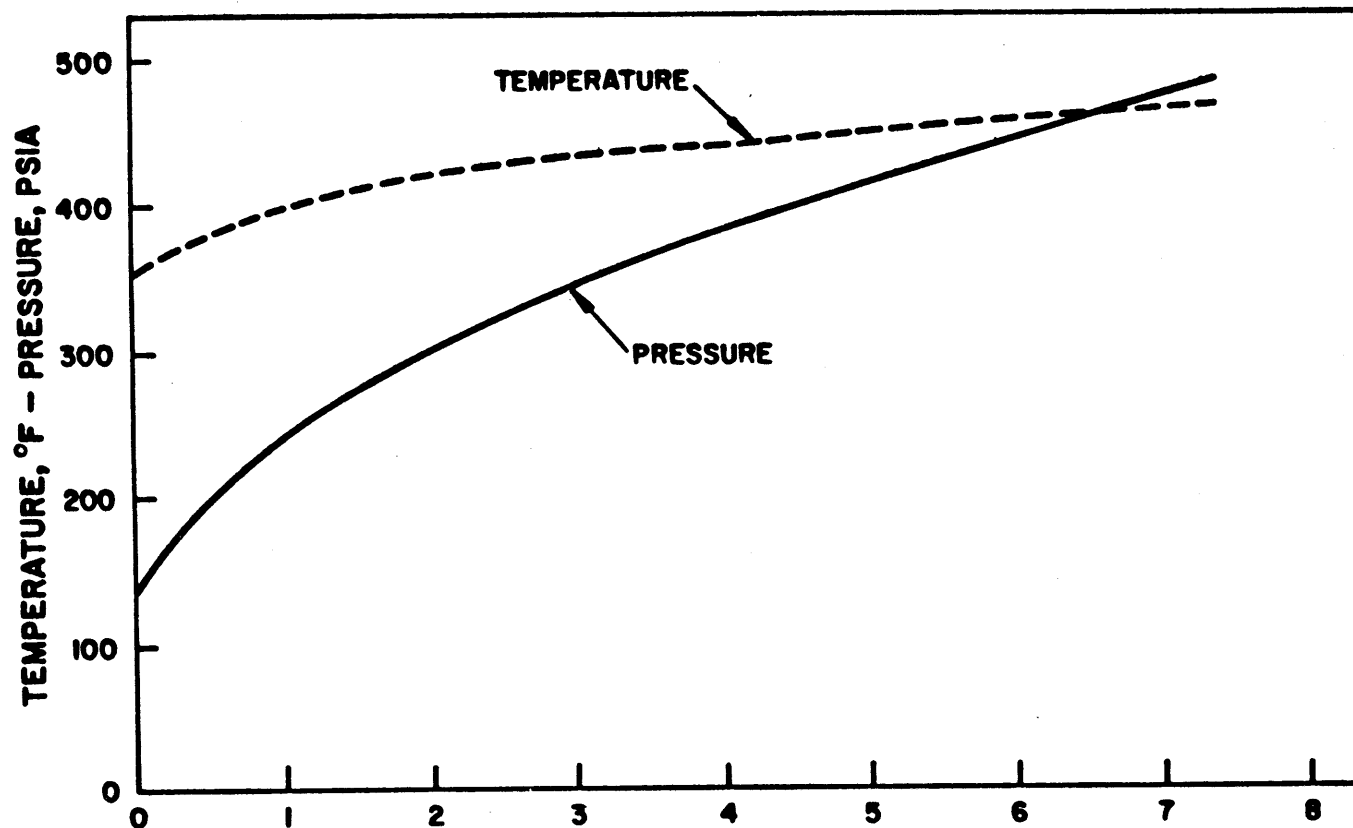
Fig. A.6A.6-1 gives the pressure and corresponding temperature for the SRVDL as a function of fl/D . The temperature is then applied to the SRVDL for determining thermal expansion loads.

A.6A.6.3 Seismic Loads

Seismic loads are considered as described in Section 3.7A and are included in Section A.6A.7.

A.6A.6.4 Seismic Sloshing Loads

See Attachment E.



BASES:
 $M = 0.907 \times 10^6$ lbm/hr
 PIPE 10in SCHEDULE 80

FIGURE A.6A.6-1

CALCULATED PRESSURE AND
 TEMPERATURE ALONG SAFETY RELIEF
 PIPING DURING STEADY DESIGN FLOW

RIVER BEND STATION
 UPDATED SAFETY ANALYSIS REPORT

A.6A.7 QUENCHER ARRANGEMENT

Fig. A.6A.4-1 and A.6A.4-2 show the general arrangement of the quencher in the suppression pool.

A.6A.7.1 Quencher Arm/Strut Loads and Loading Application

A.6A.7.1.1 Description of Discharge Event

Quenchers discharge steam upon actuation of the upstream safety/relief valve in a number of transient events, as given in Section A.6A.9. First a water slug, then the air column is expelled through the holes in the quencher arms, and then a steady steam expulsion follows.

The air being expelled forms initially one oscillating bubble at each quencher arm and eventually one so-called SRV bubble engulfing the quencher. Upon termination of air expulsion, this bubble separates and rises to the surface of the pool within about 1.5 sec from the onset of the bubble oscillation.

Associated with the expulsion of water and air is a flow transient in the SRV discharge line (SRVDL) and the quencher body. The momentum change caused by the water slug exiting the quencher body and arms produces vertical water expulsion loads in the quencher axis which are at their highest as the last portion of water turns 90 deg to enter the quencher arms.

Adjacent quencher, whether active or inactive, experience drag loads from the active quencher, identified as SRV bubble drag loads.

A.6A.7.1.2 Types of Load on Quencher Assembly

1. Quencher, Strut, SRVDL:
 - a. Weight and internal pressure
 - b. Thermal expansion
 - c. OBEI and OBE sloshing drag
 - d. SSEI and SSE sloshing drag
 - e. SRV inertia and SRV bubble drag
 - f. OBEA

- g. Loss of coolant accident (LOCA)
 - (1) Vent-clearing water jet - Strut only
 - (2) LOCA air bubble inertia and drag - DBA only
 - (3) Upward pool swell drag - DBA only
 - (4) Fallback drag - DBA only
 - (5) Chugging inertia and drag
 - (6) Condensation oscillation inertia and drag
 - (7) Lateral drag load associated with Chug and CO (insignificant)

2. Quencher Only:

- a. Flow transient loads - active quencher only
- b. Water expulsion load - active quencher only
- c. Self-actuating load on quencher, quencher arm, and quencher support struts - active quencher only

A.6A.7.1.3 Application of Loads

Quencher, strut, and SRVDL are one analytical model. The self-actuating loads imposed by the pool water on the active quencher are given in the form of quencher arm loads and quencher body loads. These loads are applied in different directions to form the following design load cases:

- Case A - Maximum torque about the quencher vertical axis due to uneven air or water clearing.
- Case B - Maximum load acting in the circumferential direction of the pool when uneven air or water clearing occurs in an adjacent pair of arms.
- Case C - Maximum load acting in the radial direction of the pool when uneven air or water clearing occurs in an adjacent pair of arms.
- Case D - Maximum vertical loads during air/water clearing.

The loads from active quenchers, i.e., the SRV bubble loads, on any quencher are applied as follows:

When all quenchers are active, the air bubbles of one may have any phase relationship with the air bubble of the other. The following two cases are analyzed and are considered bounding for all other cases for the loads on active and inactive quencher:

1. The bubbles of all quenchers oscillate in phase with each other.
2. The four bubbles per quencher oscillate in phase with each other, but the bubbles of the quenchers to the right of the affected quencher are expanding while the bubbles of the quenchers to the left are contracting. This is identified as the out-of-phase SRV bubble drag.

The drag loads from these two cases are also applied to the struts and the submerged SRV DL and sleeve in the analysis of active and inactive quencher. The quencher and the struts are represented by short pipe segments. The loads are applied as forces at the center of each segment.

A.6A.7.1.4 Magnitude of Loads on Quencher and Struts

The self-actuating load on the quencher arm, shown as F on Fig. A.6A.7-1, may act in any direction normal to the arm centerline. $F_a = \pm 16,460$ lb. The loads on the struts are listed in Table A.6A.7-1.

The water expulsion spike load on the quencher body cap depends on the SRV DL lengths and therefore varies among the quenchers.

A.6A.7.1.5 Quencher Allowable Loads

Allowable loads are specified at the following interface locations:

Quencher/SRV DL

Quencher pedestal adapter/pedestal

Quencher arm/header nozzle

Quencher arm at first row of holes from body

Strut attachments

A.6A.7.1.6 Quencher Load Combinations

Each quencher is analyzed twice: as active quencher and as inactive quencher. The drag loads are considered the same on all 16 quenchers. All groups of occasional drag loads in the local coordinate system as listed below are combined via the SRSS method. For the remainder of the load types (P, DW, inertia loads, thermal expansion, OBEA), Table 3.9A-3 applies.

1. Normal/Upset Condition:

a. Active quencher

- OBE sloshing
- Flow transient
- Self-actuating loads
- SRV bubble drag

b. Inactive quencher

- OBE sloshing
- SRV bubble drag

2. Emergency Condition (SBA, IBA):

In addition to the normal/upset occasional loads, the following loads apply:

Maximum drag (Chug, CO) on quencher, SRVDL, and struts

3. Faulted Condition (DBA):

In addition to the normal/upset occasional loads, with SSE replacing OBE, the following loads apply:

Maximum drag (LOCA bubble, pool swell, fallback, Chug, CO) on quencher, SRVDL, and struts

A.6A.7.2 Quencher Design Information

The quencher used in River Bend Station is designed as specified by GE in Section 3BA.7.2 of GESSAR, except as given in the following criteria.

The X-quencher was designed and analyzed as a Class 3 piping component in accordance with the requirements of Section ND-3600 of the ASME Boiler and Pressure Vessel Code. The evaluation included all required loads associated with safety relief valve operation including both mechanical and hydrodynamic loads. The quencher is capable of withstanding loading from connecting safety relief valve discharge piping for sustained, occasional, thermal expansion, emergency, and faulted conditions.

This section ND-3645 of the ASME Boiler and Pressure Vessel Code Section III-1983 Edition was considered during the design of the quencher. Cyclic loading was accounted for in the allowable stress of equations 10 and 11 of ND-3652.3 and found to be acceptable. Stress concentrations and the potential for local bending stresses and flattening were minimized during design.

Although ND-3645 does not require any separate analysis, the bracket-quencher interface connection was analyzed to the requirements of subsection NB-3600 of the ASME Code. The analysis consisted of calculating the fatigue usage factor for 40 years of plant life at the support bracket connection.

The analysis was restricted to the quencher bracket interface because this is the cross section which is most affected by the normal and upset condition loads. A fatigue usage factor was calculated using alternating stress S and peak stress S obtained from equations 11 and 14 of subsection NB-3600 respectively. Equation 11 was modified to include the stresses due to lug 1 effects by incorporating ASME Code Case N-122. To calculate the worst thermal gradients across the bracket connection, the most severe transient was used. The transient consisted of a step change from 70°F to 350°F. Appropriate heat transfer coefficients were calculated for the transient. Other normal and upset condition loads being transmitted by SRV piping were included in Equation 11.

The results of the analysis showed a usage factor of 0.47 at the support bracket connection. We can, therefore, safely conclude that the X-quencher for the River Bend Station can safely withstand the expected normal and upset condition loads.

The stresses at critical locations in the quencher configuration were determined to be within the ASME code allowables for quencher design. Thermal gradients and localized stresses are considered in the fatigue factor used

in the stress analysis for ASME Code Class 3 piping components. The requirements of ND-3645 have been satisfied.

A.6A.7.2.1 SRVDL Geometry

See Fig. A.6A.10-2a through A.6A.10-2e for River Bend Station SRVDL routing.

A.6A.7.2.2 Quencher Design Criteria

Forces - See Fig. A.6A.7-1 and A.6A.7-3 and
Tables A.6A.7-1 and A.6A.7-2

Fatigue - See Sections A.6A.9 and 6A.17.2.4, and
Fig. A.6A.5-13

Cycles of Operation - See Section A.6A.9.

RBS USAR

TABLE A.6A.7-1

DIRECT LOADS ON QUENCHER STRUTS
(Reference Fig. A.6A.7-1)

		<u>Max Load (lb)</u>
F _a	Drag in any direction normal to strut axis	
	SRV bubble drag - active or inactive quencher	2481.0
	Chug (SBA/IBA, DBA)	1200.4
	CO (SBA/IBA, DBA)	214.2
	LOCA bubble (DBA)	2727.0
	Vent clearing water jet (DBA)	2828.0
	Sloshing	73.0
F _c	Vertical drag load - active or inactive quencher	
	Pool swell (DBA)	5302.0
	Fall back (DBA)	5302.0

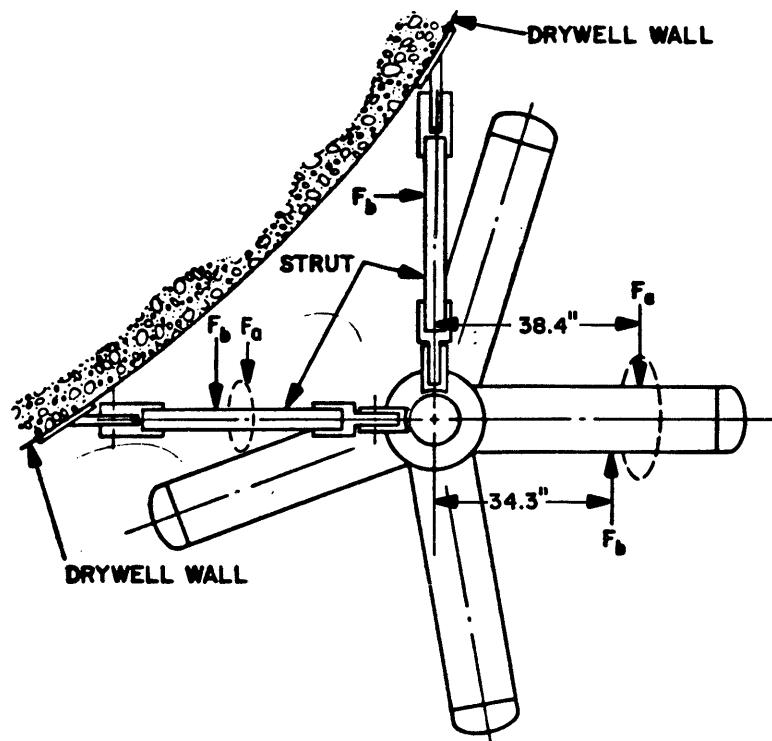
RBS USAR

TABLE A.6A.7-2

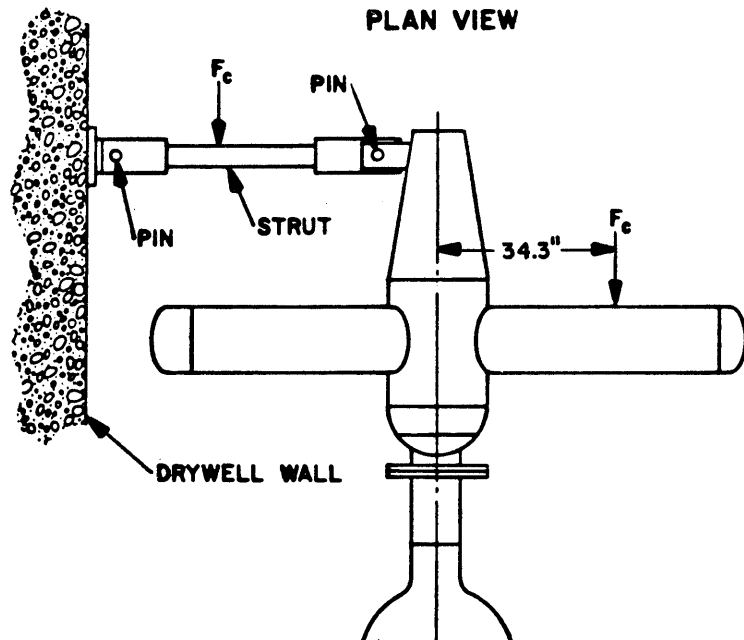
MAXIMUM QUENCHER ASSEMBLY REACTION LOADS AND
 MAXIMUM QUENCHER/SRVDL INTERFACE LOADS
 (Reference Fig. A.6A.73)

	Interface Loads (Node 1)	Reaction Loads (Node 2)	<u>Strut 1</u>	<u>Strut 2</u>
<u>THERMAL</u>				
F_1	6902	38736	28850	32241
F_v	10428	10428		
M_B	22323	324162		
M_T	8101	12793		
<u>SRSS (OBET, OCCU)</u>				
F_1	45286	63288	36778	40679
F_v	46561	181839		
M_B	17862	372324		
M_T	5019	105758		
<u>SRSS (OBET, OCCE)</u>				
F_1	45346	77923	35045	39586
F_v	46454	181856		
M_B	19448	389493		
M_T	5738	107556		
<u>SRSS (SSEI, OCCF)</u>				
F_1	45357	77944	35063	39613
F_v	46460	181858		
M_B	19468	389852		
M_T	5768	107568		

NOTE: Forces in lb, moments in ft lb.



PLAN VIEW



ELEVATION

FIGURE A.6A.7-1

QUENCHER ARM AND STRUT LOADS

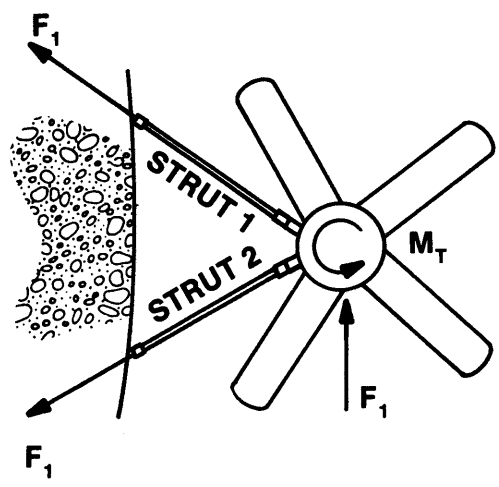
RIVER BEND STATION
 UPDATED SAFETY ANALYSIS REPORT

**(THIS FIGURE HAS
BEEN DELETED)**

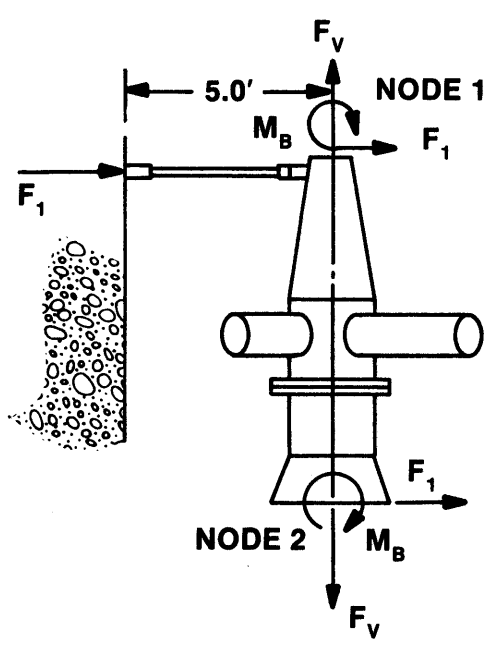
FIGURE A.6A.7-2

QUENCHER LOAD DIAGRAM

**RIVER BEND STATION
UPDATED SAFETY ANALYSIS REPORT**



PLAN VIEW



ELEVATION

FIGURE A.6A.7-3
QUENCHER AND STRUT ANCHOR LOADS
RIVER BEND STATION UPDATED SAFETY ANALYSIS REPORT

PROPRIETARY
(THIS FIGURE IS IDENTICAL TO THAT SUBMITTED
BY GENERAL ELECTRIC AS PROPRIETARY IN
APPENDIX 3B OF GESSAR-238, AM. 43)

FIGURE A.6A.7-4

SECTIONAL VIEW OF SPARGER LEG
(TYPICAL EACH SIDE)

RIVER BEND STATION
UPDATED SAFETY ANALYSIS REPORT

A.6A.8 S/R VALVE LOAD COMBINATIONS

S/R valve loads are combined with other design loads using the load combination tables presented for structures in Section 3.8 and for components in Section 3.9. Additional considerations are discussed in this Attachment.

A.6A.8.1 S/R Valve Discharge Combinations

S/R valve discharge piping routed to the suppression pool is arranged so that the points of discharge within the pool are distributed as shown in Fig. A.6A.4-3. The location of quenchers around the pool is for distribution of air clearing loads, as well as for consideration of pool thermal mixing.

The number of S/R valves that can open at one time is dependent on many variables. The following table shows several discrete cases where various numbers of open valves can be postulated for River Bend Station:

<u>Case</u>	<u>Number of Valves</u>	<u>Comment</u>
1	1	Single active failure, normal function, or operator action (first or subsequent actuation).
2	2	One normal plus single active failure of adjacent valve (first actuation).
3	7	ADS activation (first actuation).
4	16	All valves set pressure < 1,123 psi (first actuation).

The number of S/R valves that open during a reactor vessel pressure transient could be from 1 to 16 valves. This can be shown for situations where various reactor power levels are assumed when the transient event is initiated. Therefore, the containment must be able to withstand any number of valve combinations previously given, discharging at a given moment.

The following represent selected asymmetric cases for containment loads:

1. One S/R Valve - This situation can occur due to an operator action or a single active failure. Subsequent actuation of a S/R valve after an

initial pressure transient would be limited to the single 1,103 psi setpoint valve.

2. Two adjacent S/R Valves - This situation can occur due to a pressure transient at low power, which would lift one valve. Concurrent with this, the single active failure of an adjacent valve is assumed.

The probability of the simultaneous actuation of two adjacent valves would be very low. However, if the containment structural design requirements are satisfied under this asymmetric condition, subsequent analysis need not be performed for the multitude of other, more probable asymmetric load cases.

3. Seven ADS Valves - This situation can occur with an intermediate break, where ADS system is activated.

The following represents the symmetric case for containment loads:

Sixteen (All) Valves - This event can occur due to a high-power isolation transient.

For structural evaluation, the four preceding load cases will be used. From observation of Fig. A.6A.5-3, A.6A.5-6, A.6A.5-9, and A.6A.5-12, the 1- or 2-valve load case is the governing case for asymmetrical considerations. For River Bend Station, all four load cases are considered for the design.

A.6A.8.2 LOCA Considerations

In evaluating the River Bend Station structural loads and containment/drywell capability, it is necessary to properly account for the postulated accident related loads and their sequence of occurrence. In defining the loads for this evaluation, this Attachment addresses the design basis accident (pipe break) and the loads associated with the hypothetical concurrent earthquake, pool dynamics, and static loading. The ability of the design to accommodate these loadings, when properly sequenced, constitutes the design basis of the structure. This design basis includes the single-failure criterion.

This Attachment also addresses an additional consideration; namely, the inadvertent opening of a single S/R valve. The opening of a single valve is not a direct result of the LOCA

and furthermore, is not an expected occurrence during the accident sequence. For conservatism, it is considered in combination with LOCA loads to provide additional capacity.

A.6A.8.2.1 Main Steam Line Break

For the main steam line break, no valves lift due to rapid vessel depressurization.

A.6A.8.2.2 Recirculation Line Break

For a recirculation line break, no valves lift due to rapid vessel depressurization.

A.6A.8.3 Other SRV Conditions

Other SRV conditions have also been analyzed at the forcing function level, and their effect (except for SRV steam condensation) were found to be less controlling than the base case SRV loads. These other conditions result from a detailed analysis of pressure traces from Caorso SRV quencher plant tests and the postulation of an SRV discharge under LOCA conditions. These other SRV conditions are:

1. Water-clearing spike which precedes the air bubble pressure oscillation for the SRV quencher discharge
2. A leaking SRV
3. SRV steam condensation
4. SRV discharge for the LOCA-related conditions is postulated with a pressurized drywell and wetwell.

The conditions are identified, since the forcing function frequency range was generally broader, but with much lower pressure amplitude than the normal SRV base cases described in A.6A.8.0 and A.6A.8.1. Analyses showed that the effects from these additional cases were generally less than the major bubble effects from the base cases. Comparisons are discussed in the following subsections.

A.6A.8.3.1 Water-Clearing Pressure Spike For One SRV, First Actuation, Normal Operating Conditions

During Caorso SRV testing, a high-frequency (15 to 30 Hz) pressure spike was observed just prior to the air bubble oscillation. This spike occurs during the water-clearing portion of the SRV blowdown. Multipliers were applied to the predicted bubble pressure amplitude, such that the

Caorso data, including the spike, would be bounded at a 90-90, one-sided statistical tolerance limit and would account for Mark III design conditions.

A comparison was then made of Amplified Response Spectra (ARS) for the forcing function, including the water spike and the base-case SRV loads currently specified waveform (Fig. A.6A.5-13). The results show that the ARS for the base-case SRV discharge waveform bounds the ARS for the waveform which includes a water spike. In summary, the water spike observed in the Caorso data is not significant due to its short duration and limited number of cycles (one to three), and its effect is bounded by the waveform of Fig. A.6A.5-13.

A.6A.8.3.2 First Actuation of One SRV With a Pressurized Containment

For the case of an SRV actuation under small break accident LOCA conditions, when the drywell and containment are pressurized, the initial water level in the SRVDL is depressed below normal water level. This lower water level is due to pressurization of the SRV line through the SRV vacuum breaker. Using a simplified model, the predicted bubble pressure forcing function results in water spike pressures which are lower than predicted for normal operating conditions, and air bubble pressures which are slightly higher due to an increase in air mass from the pressurized drywell condition. This case was also found to be bounded by the waveform of Fig. A.6A.5-13 for single-valve, first-actuation loads when a comparison was made of the amplified response spectra generated from the bubble pressure forcing functions.

A.6A.8.3.3 Water-Clearing Pressure Spike for One SRV, Second Actuation, Normal Operating Conditions

Second-actuation, normal operating condition SRV blowdowns are also characterized by a high-frequency water spike followed by lower magnitude, lower frequency air clearing loads. Second actuations occur with higher initial SRV discharge line (SRVDL) temperature, higher pool temperature, and lower air mass in the SRVDL. Second-actuation forcing functions were obtained by applying multipliers to the predicted bubble pressure amplitude such that the Caorso data, including water spike, would be bounded at the 90-90 one-sided statistical tolerance limit and account for Mark III design conditions. Comparison of ARS for this pressure load to the waveform of Fig. A.6A.5-13 for one SRV,

second actuation, showed the base-case SRV load specification to be bounding.

A.6A.8.3.4 Second Actuation of One SRV With a Pressurized Containmentment

Subsequent actuation of SRVs under accident (LOCA) conditions are not predicted to occur; thus, no load specifications are required.

A.6A.8.3.5 First Actuation of One SRV, Leaking Valve Condition

During the Caorso test series, one SRV was found to be leaking. Several tests were conducted with this valve to determine the effect on bubble pressure. Results showed the typical water spike followed by low amplitude high frequency (20 to 30 Hz) random oscillatory behavior which was atypical of normal air bubble response. An evaluation of this effect was performed using a typical leaking SRV data trace from Caorso. The pressure amplitude was increased to account for design operating conditions. A comparison of amplified response spectra was made for this leaking valve trace and the Fig. A.6A.5-13 waveform for one SRV, subsequent actuation. The Fig. A.6A.5-13 waveform was found to be bounding.

The probability of leaky SRV actuation in combination with LOCA is sufficiently small, such that the leaky SRV is not specified in combination with LOCA loads (C.O. and chugging).

A.6A.8.3.6 SRV Steam Condensation

During the Caorso testing of the SRV blowdown, steam condensation effects were observed after the air bubble oscillation phase. Boundary pressure amplitudes of 0.5 to 3.3 psid with typical mean values of ≈ 2 psid, and frequency content of 40 to 110 Hz were noted. These values also apply to Mark III. An evaluation of the effect of these steam condensation loads was made by selecting a Caorso data trace with the highest RMS pressure value. This trace is shown in Fig. A.6A.8-1. The 2-valve and 16-valve cases were considered as the worst asymmetric and symmetric cases, respectively, for evaluation of structures and equipment.

A.6A.8.4 Design Load Summation

The design loads on structures are comprised of static (dead loads, live loads, hydro, etc) and alternating dynamic loads (seismic and S/R valve loads, etc).

The load combinations of hydrodynamic load cases with each other and with the other loads are given in the load combination tables in Section 3.8 for structures and are given and justified in Section 3.9 for components.

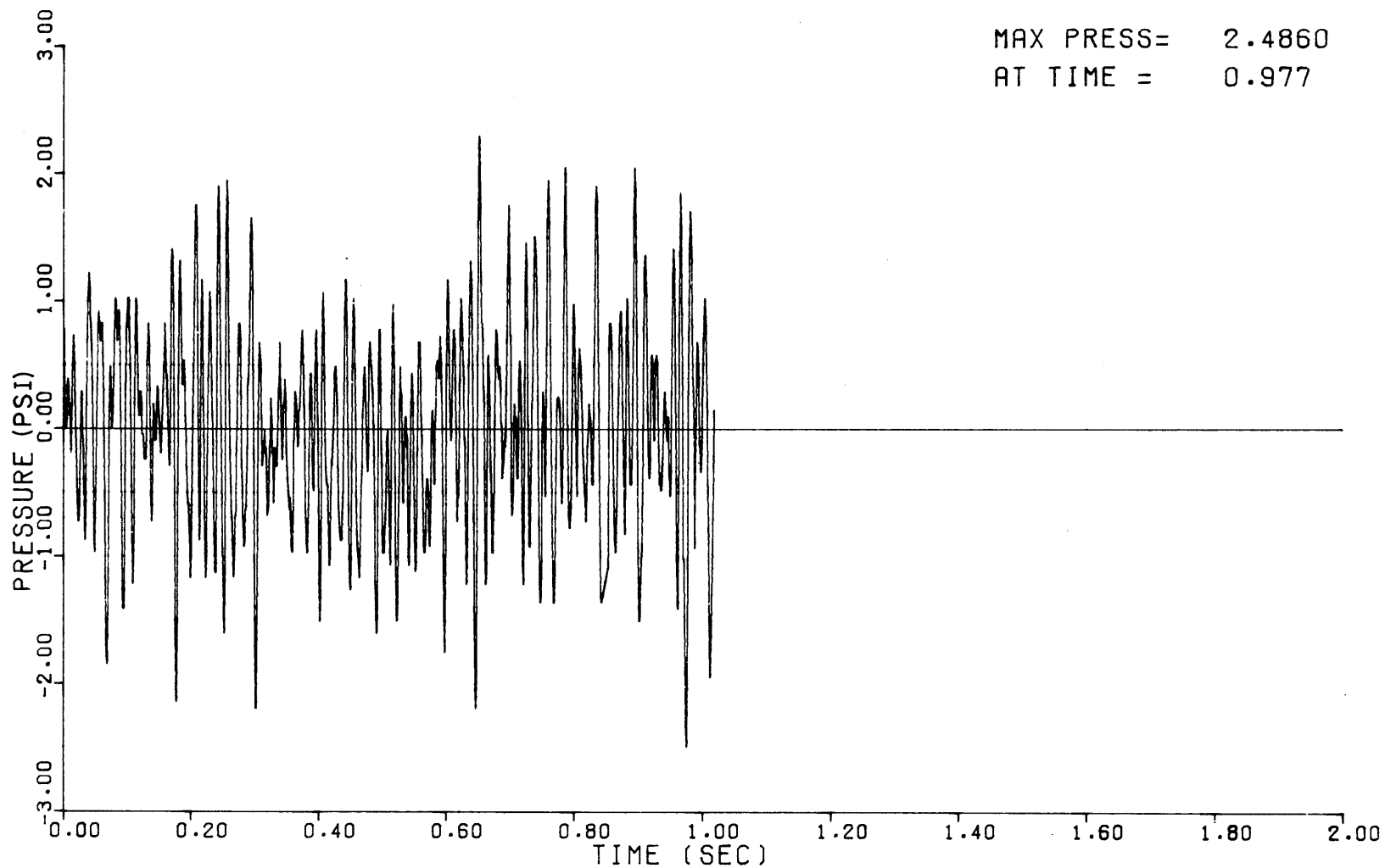


FIGURE A.6A.8-1

PRESSURE TIME HISTORY FOR SRV-CO

RIVER BEND STATION
UPDATED SAFETY ANALYSIS REPORT

A.6A.9 FATIGUE CYCLES

A number of safety relief valve (SRV) discharge events may occur during the 40-yr plant life. An analysis, based on many years of BWR plant operations, was performed to determine the mean frequency of occurrence of these potential events. Results of the study are summarized in Table A.6A.9-1.

•→10

The River Bend Station incorporates the low-low reset logic which automatically limits the cycling of relief valves to one valve subsequent to initial actuation during a main steam line isolation event. Transients which result in containment isolation are identified in the table. During isolation events, the decay heat is initially removed from the reactor vessel via the SRVs. As shown in Table A.6A.9-1, half to all of the valves are initially actuated. Subsequently, the low-low set valve cycles or the main condenser becomes available. The total actuations of the low-low set valve during an isolation event is 15 per event. The valve nominally remains open 80-90 sec following each opening actuation.

10←•

The nonisolation transients are also listed in Table A.6A.9-1. These events typically result in a single-opening actuation of several or all SRVs, but the low-low set SRV does not cycle. When all valves are actuated, the open duration is 5-10 sec.

Considering 15 actuations for each isolation event and all of the nonisolation events, the total number of SRV actuations is approximately 1,800. Each actuation results in certain pressure pulses in the suppression pool which are transmitted to the containment as discussed throughout this Attachment. For fatigue evaluation purposes, the most significant forcing function on the containment due to SRV actuation is the SRV bubble pressure.

The normal bubble frequency range and duration are provided in Fig. A.6A.5-13. Using this figure in conjunction with the SRV actuations provides the number of cycles affecting the containment due to the SRV air bubbles.

The SRV steam condensation pressure oscillation frequency is nominally specified as 80 cps. This value is based upon the pressure trace shown in Fig. A.6A.8-1. Utilizing this frequency, the noted durations per actuation, and the number of actuations provides the cycles in the event this load has significant stress effect on the containment. The

phenomenon creates a relatively high number of cycles, but the lower pressure amplitude forcing function typically results in low stress intensities. Hence, the containment fatigue factor due to this load is minor compared to the normal bubble effect.

TABLE A.6A.9-1

SAFETY RELIEF VALVE ACTUATION

Events	Mean Frequency Per yr	Mean Frequency /40 Years	Number of Valves Open for Initial Blow			Isolation Type Event
			(All- 2/3)	(1/3- 2/3)	(1/3 -0)	
Turbine Trip (w/BP) *	1.33	53	x			No
Load Rejection (w/BP)	0.75	30	x			No
Pressure Regulator Failure	0.65	26		x		Yes
Feedwater Controller Failure	0.50	20		x		No
Trip of Both Recirculation Pumps	0.33	13		x		No
Recirculation Controller Failure	0.33	13		x		No
Loss of Feedwater Flow	0.75	30			x	No
Loss of Auxiliary Power	0.375	15	x			Yes
Closure of All MSIVs	1.00	40.0	x			Yes
Loss of Condenser Vacuum	0.65	26	x			Yes
Inadvertent Relief Valve Opening	0.10	4.0			x	No
Turbine Trip (w/o BP)	0.013	0.5	x			Yes
Load Rejection (w/o BP)	0.013	0.5	x			Yes

*BP - Bypass

A.6A.10 CALCULATION PROCEDURES

The following information provides the procedures for predicting loads on the drywell wall, basemat, and containment wall associated with the air-clearing transient following the opening of a S/R valve for River Bend Station. The calculated bubble pressures are based on information in Section 3BA.12 of GESSAR.

A.6A.10.1 Constraints

The following constraints are not to be exceeded for the design of the SRVDL:

1. Peak pipe pressure < 625 psid
2. fL/D cannot exceed those values given in Fig. A.6A.3-1 at the corresponding pipe volume.
3. Water leg < 18.0 ft.

Constraints on routing the S/R valve discharge line are:

1. No more than one 90-deg long radius bend coming off the relief valve, and two 45-deg long radius bends entering the quencher in the 10-in piping. The remaining bends should be in the 12-in, Schd 40 piping as far down stream as possible, such that no more than 50 percent of the total fL/D of the system is in the first-half of the length of the discharge line.
2. The initial length of 10-in pipe be kept to a minimum.

A.6A.10.2 Determine SRVDL Design

The following steps were taken for designing the SRVDL within the preceding constraints and the design requirements in Section A.6A.2:

1. A layout drawing showing the SRVDL routing was prepared.
2. For each SRVDL length, the air volume and fL/D (see Item 5) values are calculated and plotted on Fig. A.6A.3-1. The piping size was then adjusted to minimize total air volume and fL/D for the 625-psi pipe balance of 10-in and

12-in or 14-in pipe was used. All the SRVDL air volume and fL/D from the SRV to the free water surface was included. Fig. A.6A.10-1 in conjunction with Table A.6A.10-1 shows the portion of SRVDL from the SRV to the first anchor.

3. For the portion of the SRVDL shown in Fig. A.6A.10-1, the loss coefficient, K, for each of the three flexible joints are shown on the figure.

4. The iterative process of Item 2 was repeated for each of the other SRVDL.

5. fL/D - The corresponding maximum values of fL/D were calculated in reference to the 10-in pipe velocities shown as follows. Pipe friction losses should be considered from the S/R valve to the surface of the water.

For reference to 10-in pipe velocities:

$$fL/D_{\text{Ref. 10in}} = \left[K_{\text{Total 10in}} + K_{\text{Total 12in}} \left(\frac{A_{10in}}{A_{12in}} \right)^2 + K_{\text{Total 14in}} \left(\frac{A_{10in}}{A_{14in}} \right)^2 \right]$$

Where:

$$K_{\text{Total 10in}} = fL/D_{10in} + K_{\text{Losses 10in}}$$

The preceding formula is valid when only Schedule 40 pipes are used. For other pipe schedules, the K value is modified in the following manner:

$$K_{10in} = K \times \left(\frac{A_{10in \text{ schedule 40}}}{A_{10in \text{ actual}}} \right)^2$$

$$K_{\text{Total 12in}} = fL/D_{12in} + K_{\text{Losses 12in}}$$

$$K_{\text{Total 14in}} = fL/D_{14in} + K_{\text{Losses 14in}}$$

Where:

A_{10in} = Hydraulic area of 10 in, Schedule 40 pipe (sq ft)

A_{12in} = Hydraulic area of 12 in, Schedule 40 pipe (sq ft)

A_{14in} = Hydraulic area of 14 in, Schedule 40 pipe (sq ft)

D_{10in} = Diameter of 10 in, Schedule 40 pipe (ft)

D_{12in} = Diameter of 12 in, Schedule 40 pipe (ft)

D_{14in} = Diameter of 14 in, Schedule 40 pipe (ft)

L = Length of segment (ft)

f = Friction factor 0.015

The preceding system fL/D calculation was entered into Fig. A.6A.3-1 with the corresponding air volume. The intersection must fall on or above the 625-psid curve.

6. The quencher bubble pressure was determined according to the procedure given in GESSAR Section 3BA.12.6.

A.6A.10.3 S/R Valve Air Clearing Loads

After the quencher bubble pressure was obtained, the next step was to calculate basemat and wall pressures based on the peak bubble pressure (+ and -).

A.6A.10.3.1 Absolute Pressure on Basemat and Walls

The absolute pressure anywhere on the drywell wall, basemat, and containment wall in the wetwell region can be calculated by the equation:

$$P(a) = P_{\text{containment}} + \frac{\rho h(a)}{144} + \Delta P(r) \quad (\text{A.6A.10-1})$$

Where:

$P(a)$ = Absolute pressure at Point "A" (psia)

r = Distance from quencher center to Point "A"
(ft)

$P_{\text{containment}}$ = Absolute pressure of containment atmosphere
(psia)

$h(a)$ = Water head acting at Point "A" (ft)

ρ = Water density (approximately 62.4 lbm/ft)

$\Delta P(r)$ = Bubble pressure attenuated by distance (r)
to Point "A".

The attenuated bubble pressure for one S/R valve, $P(r)$, can be calculated from the bubble pressure, P , using the following equations:

$$\Delta P(r) = 2 \Delta P_B (r_o/r) \text{ for } r > 2r_o \quad (\text{A.6A.10-2})$$

$$\Delta P(r) = \Delta P_B \text{ for } r \leq 2r_o \quad (\text{A.6A.10-3})$$

Where:

r_o = Quencher radius = 4.87 ft

A.6A.10.3.2 How to Find the Attenuated Pressure on the Drywell Wall, Basemat, and Containment Wall

A.6A.10.3.2.1 Development of Grid to Determine Values of (r)

1. Make a scaled layout of the pool with quencher (Fig. A.6A.10-3).
2. Divide wall distances by 4.
3. Arc distance every 9 degrees.
4. Draw line (Fig. A.6A.10-3) from bubble cloud extremity (i.e., quencher radius) tangent to drywell wall and project to containment. This gives the area of pressure influence for this quencher.
5. Point "A" is then selected and the distance (r) to "A" is obtained from the layout.

A.6A.10.3.2.2 Wall Pressure at Point "A" Single S/R Valve

The wall pressures are obtained from Section A.6A.10.3.1, Equations A.6A.10-2 and A.6A.10-3.

A.6A.10.3.2.3 Wall Pressure at Point "A" for Multiple S/R Valve

In the event of multiple S/R valve actuation, the attenuated bubble pressure, ΔP_B , must be calculated using the following equations:

$$\Delta P(r) = \left[\sum_{n=1} \Delta P_n^2 \right]^{1/2}$$

Where:

$$\Delta P_n = 2\Delta P_B (r_o/r_n) \text{ for } r_n > 2r_o$$

$$\Delta P_n = \Delta P_B \text{ for } r_n \leq 2r_o$$

If the calculated $\Delta P(r) > \Delta P_B$, set $\Delta P(r) = \Delta P_B$. Note that

r_n = the distance from the center of the quencher to Point "A".

For the cases where multiple valves are discharged due to a pressure transient, the valves in each set point group (1,103, 1,113, and 1,123 psi) are assumed to discharge simultaneously. The set point groups, however, discharge at different times, depending on the rate of reactor pressure increase associated with the event under consideration. The most severe pressure transient is the postulated "generator load rejection with failure of the turbine bypass valve" event which results in a calculated 132 psi-per-sec pressure increase at the beginning of the transient. This results in a 0.075-sec difference in time of discharge due to the 10-psi difference in pressure setpoints of the valve groups. Using the quencher bubble model presented in Fig. A.6A.5-13, it is seen that when P, from the 1,123-psi set point valves occurs, the bubble pressure from the 1,113-psi set point valves has dropped to 0.9175 P, and the bubble pressure from the 1,103-psi set point valve is 0.835 P. These values are used in determining the attenuated bubble pressure at Point "A" for the multiple S/R valve cases.

For local peak containment pressure loading, there is significant reduction in pressure at certain locations when considering the time-sequenced phasing approach. The most limiting position on the containment is not affected (i.e., the local peak pressure is equal to the maximum bubble pressure - see Table A.6A.5-1). In addition, the 95-95 confidence level statistical analysis for the individual valve is conservatively applied to the multiple valve cases without consideration of the number of valves being actuated. In reality, the 95-95 confidence total load for the 16-valve case is much lower than that used in the local pool boundary load calculation. These two factors (i.e., time phasing and the multiple valve statistical consideration) have not been included in the development of the local pressure distributions on the containment wall, because they do not affect the limiting local pressure. However, these factors are important to the structural response and are employed in the building response evaluation. Attachment N describes the methodology used in developing structural responses for equipment evaluation.

RBS USAR

TABLE A.6A.10-1

RIVER BEND STATION SRVDL PIPE SPOOL DIMENSIONS

<u>Valve No.</u>	<u>Dimension A* (in)</u>	<u>Dimension B (in)</u>	<u>Total Dimension (in)</u>	<u>(A+B) (ft)</u>
V-1	84.38	82.50	166.88	13.91
V-2	84.38	82.50	166.88	13.91
V-3	84.38	82.50	166.88	13.91
V-4	84.41	82.50	166.91	13.91
V-5	84.41	82.50	166.91	13.91
V-6	141.04	82.50	223.54	18.63
V-7	129.38	82.50	211.88	17.66
V-8	126.90	82.50	209.40	17.45
V-9	126.90	82.50	209.40	17.45
V-10	141.04	82.50	223.54	18.63
V-11	84.41	82.50	166.91	13.91
V-12	84.41	82.50	166.91	13.91
V-13	84.38	82.50	166.88	13.91
V-14	84.38	82.50	166.88	13.91
V-15	84.38	82.50	166.88	13.91
V-16	84.38	82.50	166.88	13.91

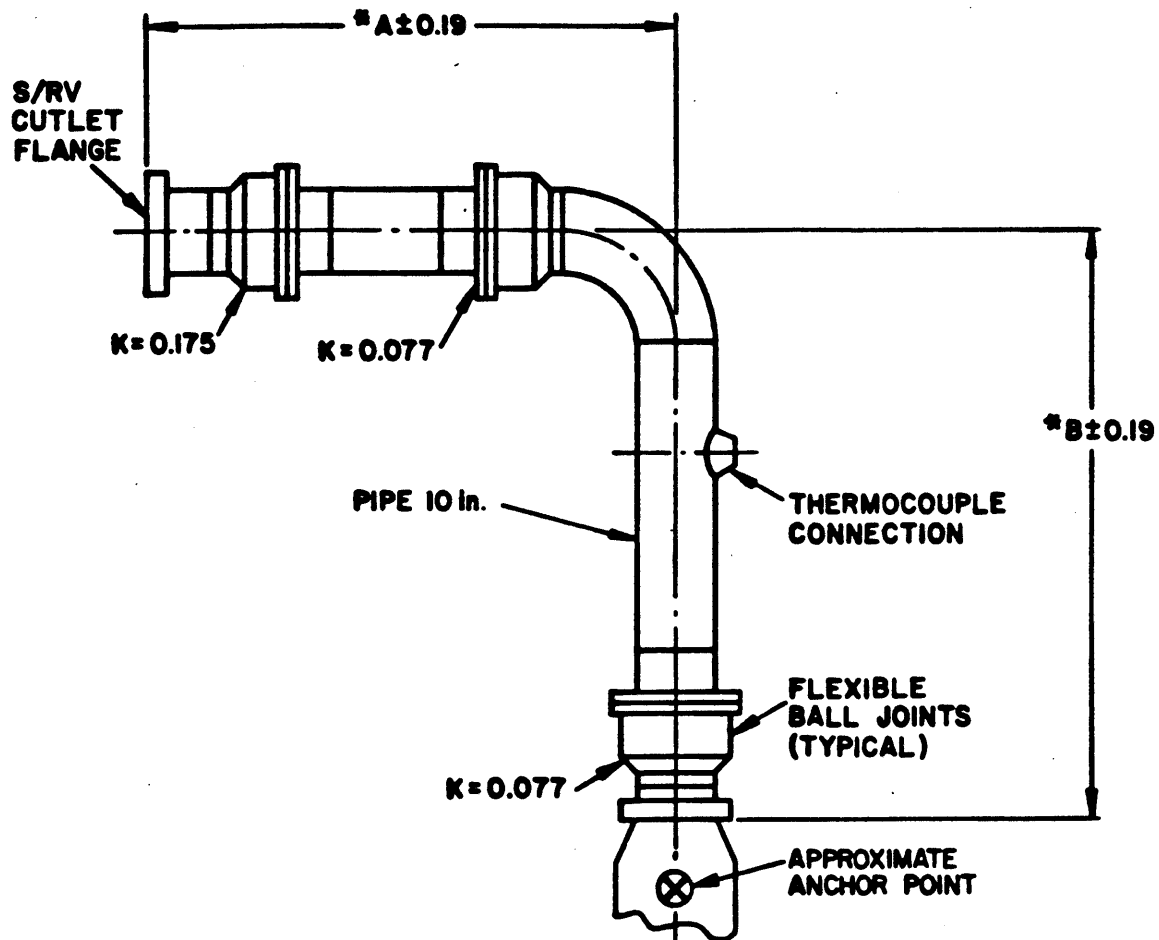
NOTE: The valve numbers are the same as those on Fig. A.6A.4-3.

* See Fig. A.6A.10-1.

TABLE A.6A.10-2

DRYWELL AND SUPPRESSION POOL GEOMETRY
(Figure A.6A.10-4)

<u>Description</u>	<u>Identification</u>	<u>Data</u>
Elevation high water level (ft)	HWL	90
Elevation bottom vents (ft)	J	72.25
Elevation top of basemat (ft)	F	70.03125
Number of vents	-	129
Vents/row	-	43
Number of safety/relief valves	-	16
Area (sq ft)	S	6,400
Radius (ft)	D	39.53
Radius (ft)	E	60



* SEE TABLE A.6A.10-1 FOR VALUES A&B

FIGURE A.6A.10-1
SAFETY RELIEF VALVE DISCHARGE PIPING DETAIL VALVE TO FIRST ANCHOR
RIVER BEND STATION UPDATED SAFETY ANALYSIS REPORT

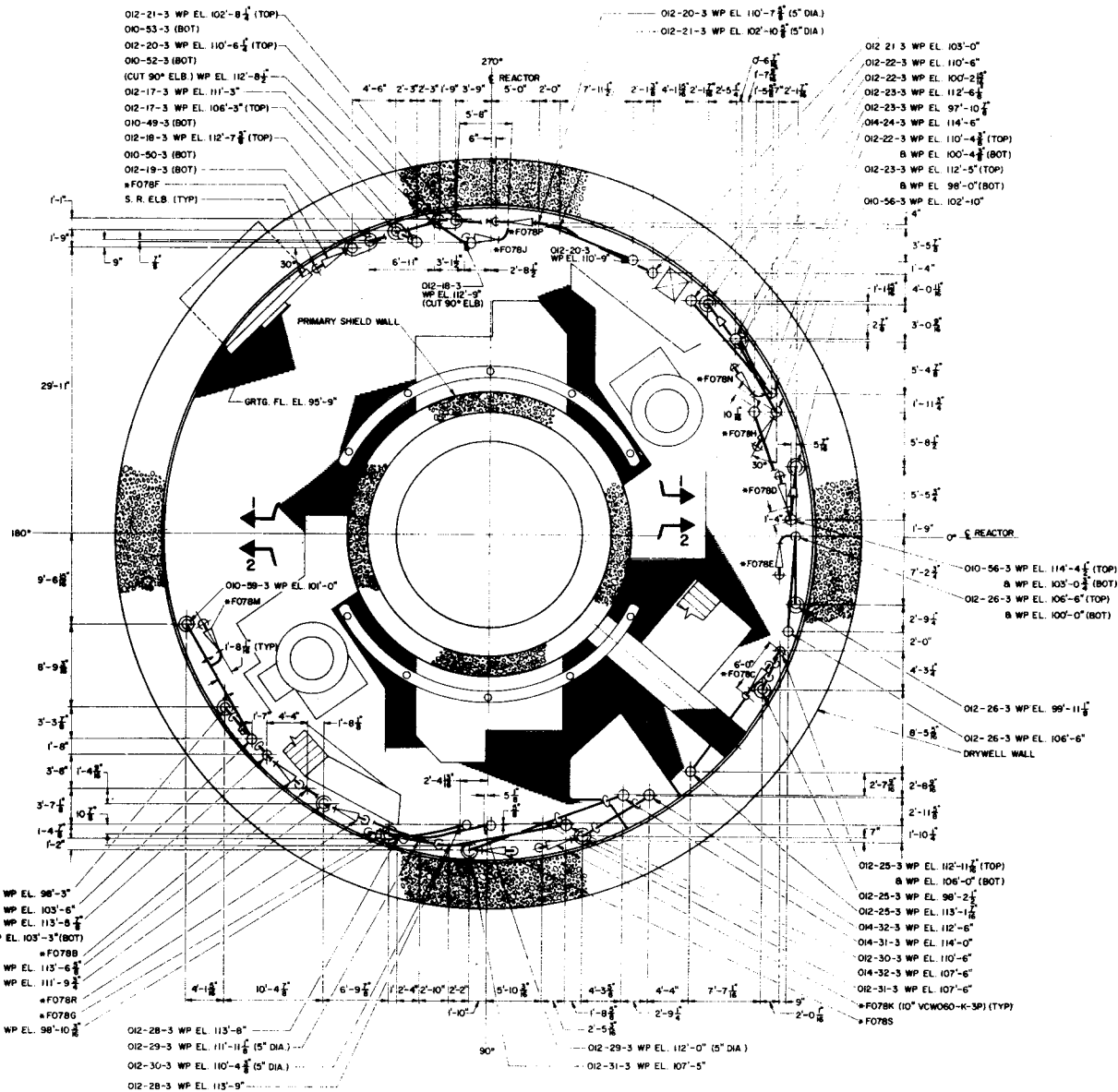


FIGURE A.6A.10-2

SAFETY RELIEF VALVE DISCHARGE
PIPING ARRANGEMENT (SHEET 2 OF 5)

RIVER BEND STATION
UPDATED SAFETY ANALYSIS REPORT

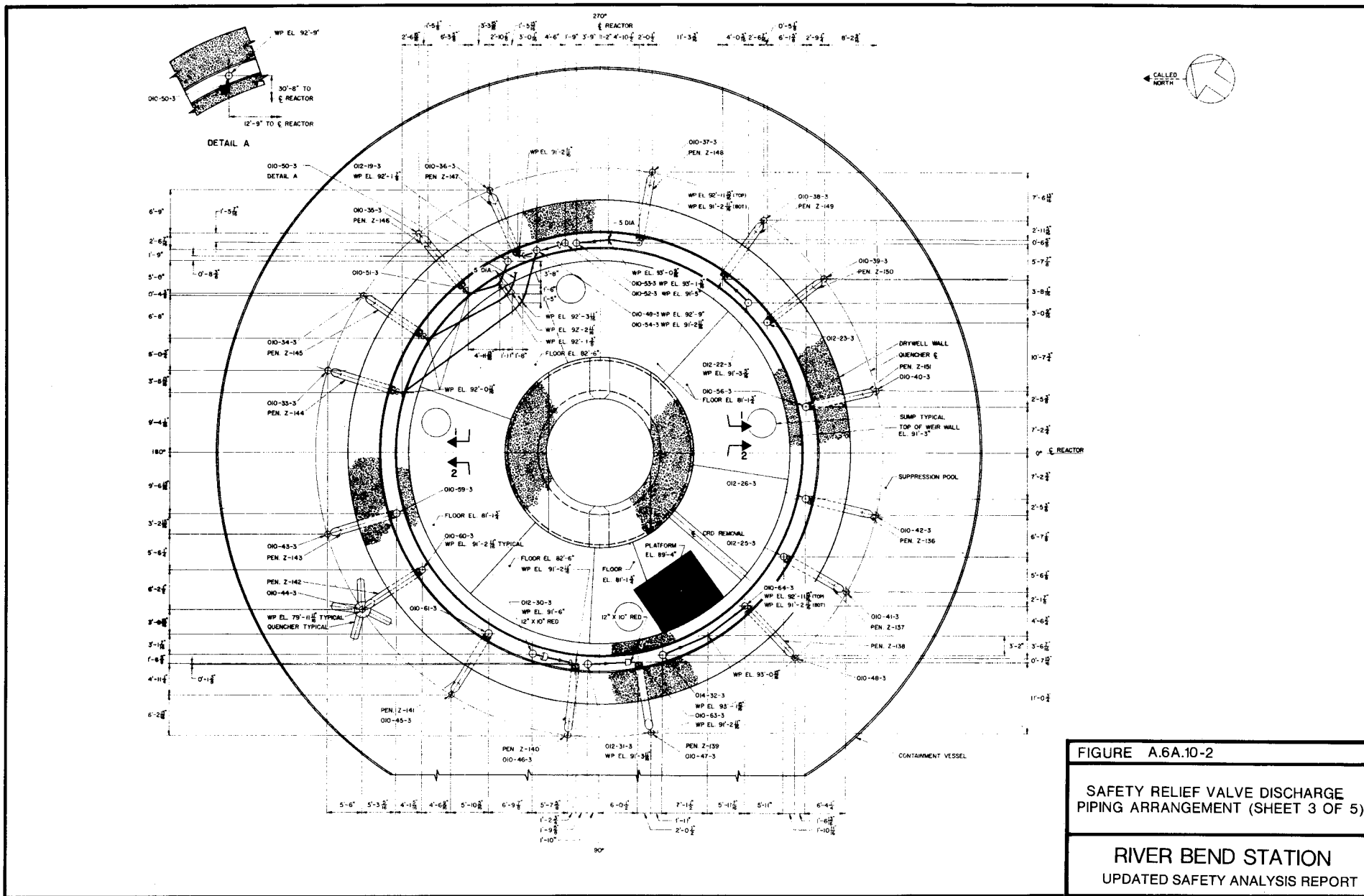
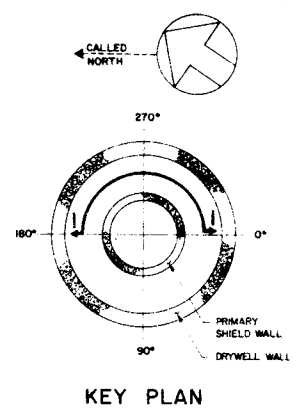
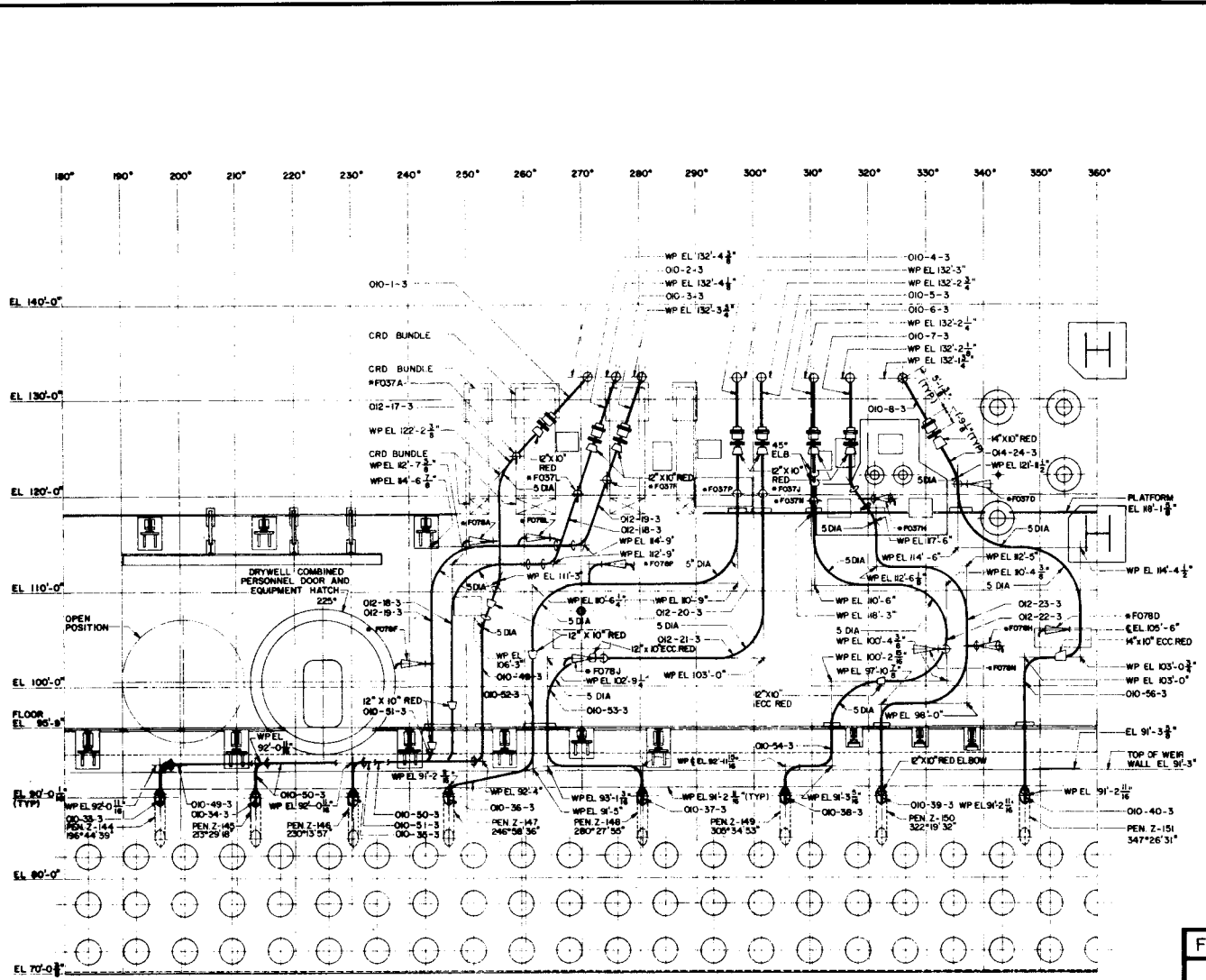
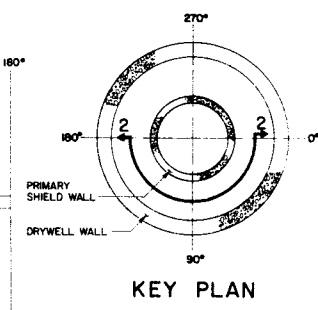
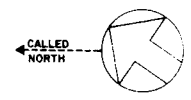
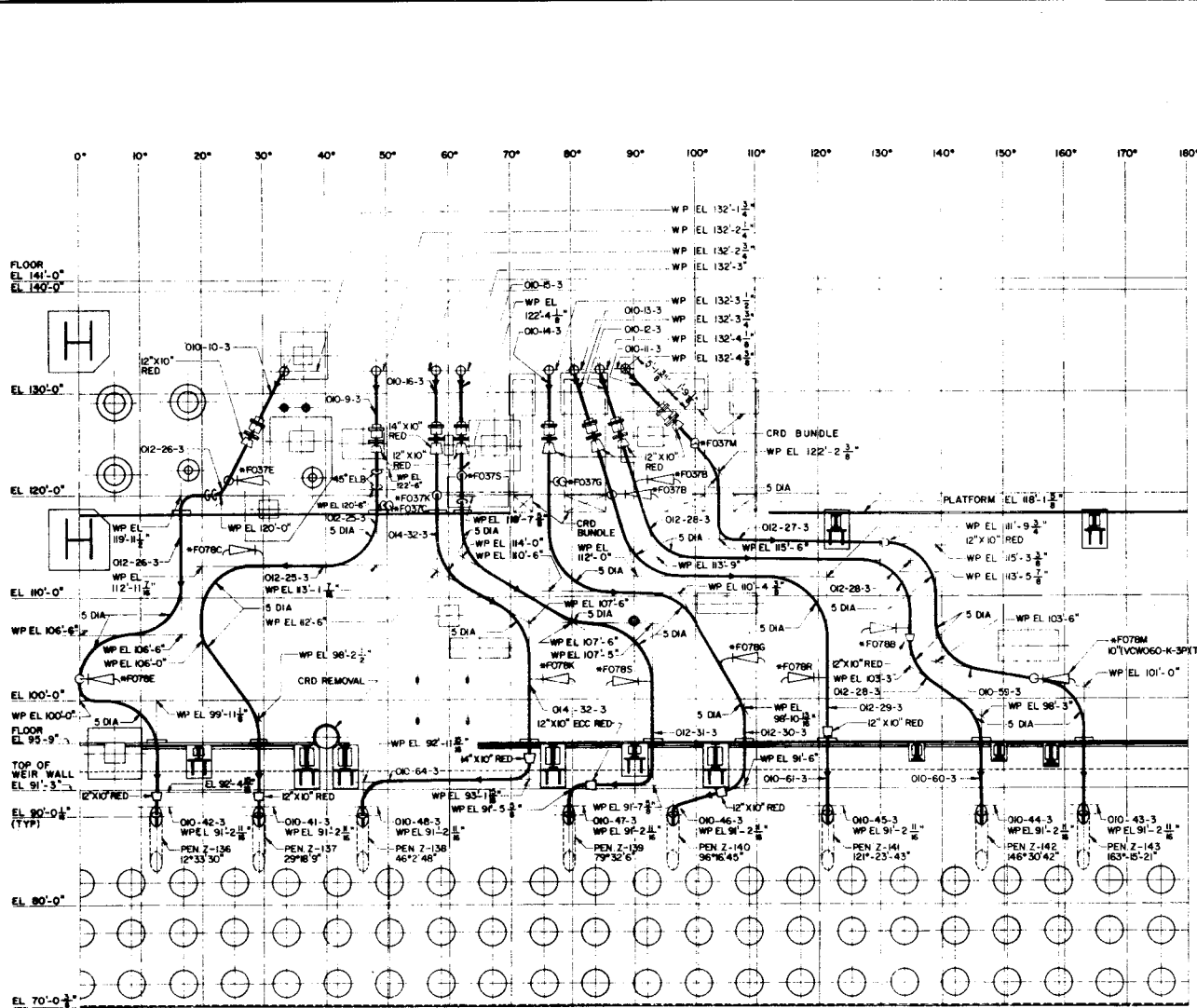


FIGURE A.6A.10-2
SAFETY RELIEF VALVE DISCHARGE PIPING ARRANGEMENT (SHEET 3 OF 5)
RIVER BEND STATION
UPDATED SAFETY ANALYSIS REPORT



SECTION I - I

FIGURE A.6A.10-2
 SAFETY RELIEF VALVE DISCHARGE
 PIPING ARRANGEMENT (SHEET 4 OF 5)
 RIVER BEND STATION
 UPDATED SAFETY ANALYSIS REPORT



SECTION 2-2

FIGURE A.6A.10-2
 SAFETY RELIEF VALVE DISCHARGE
 PIPING ARRANGEMENT (SHEET 5 OF 5)
 RIVER BEND STATION
 UPDATED SAFETY ANALYSIS REPORT

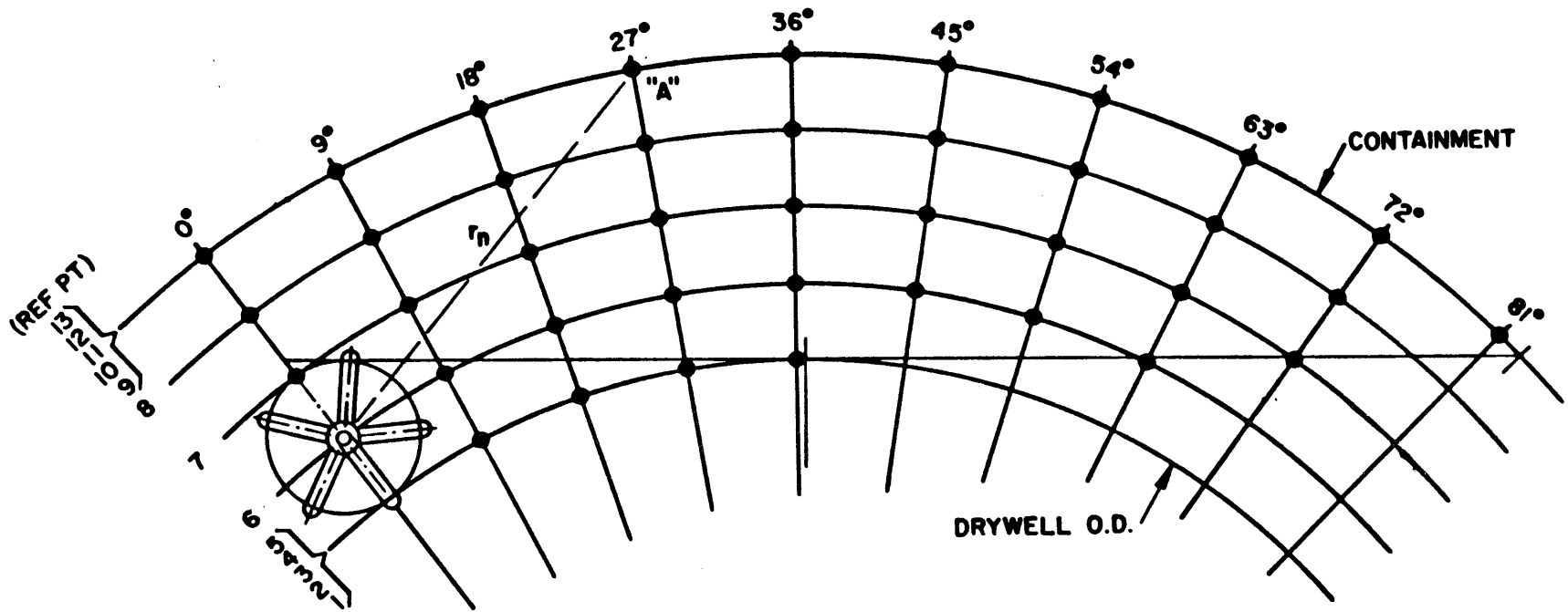


FIGURE A.6A.10-3
SUPPRESSION POOL GRID SYSTEM AND QUENCHER PRESSURE INFLUENCE
RIVER BEND STATION UPDATED SAFETY ANALYSIS REPORT

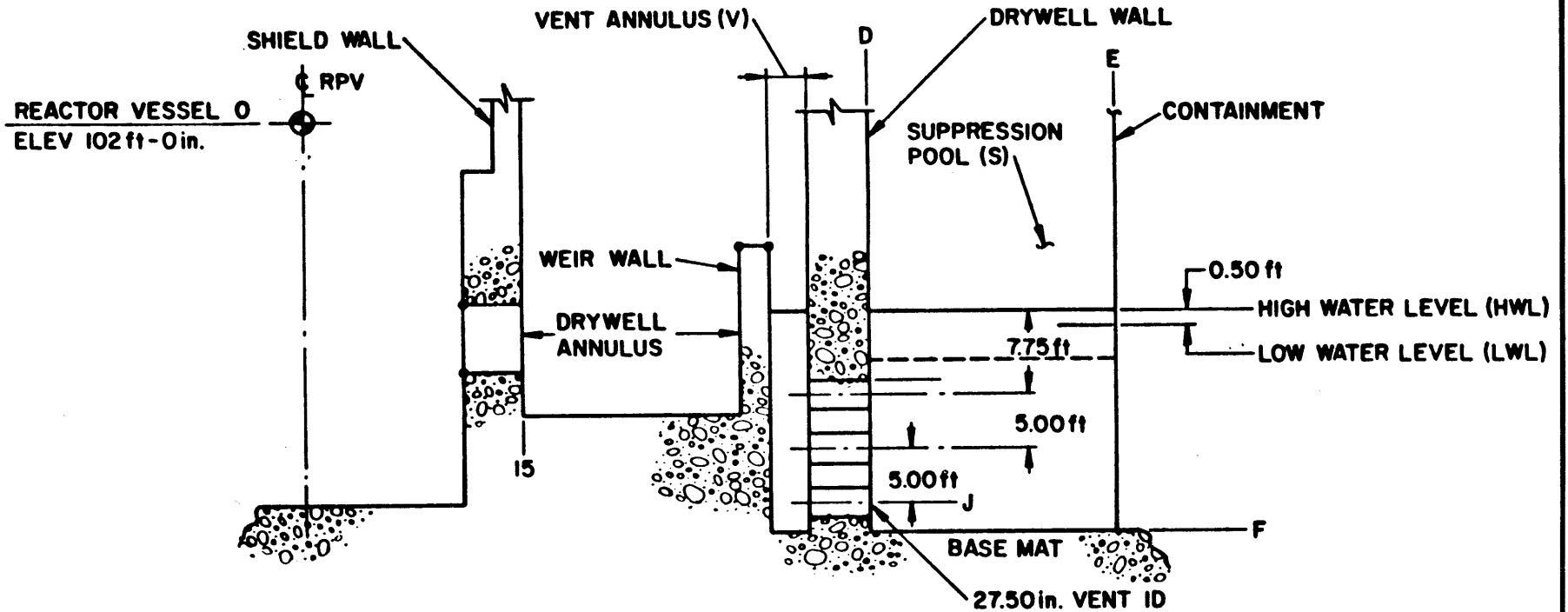


FIGURE A.6A.10-4

DRYWELL AND SUPPRESSION
POOL GEOMETRY

RIVER BEND STATION
UPDATED SAFETY ANALYSIS REPORT

RBS USAR

ATTACHMENT E
(TO APPENDIX 6A)

SUPPRESSION POOL SEISMIC INDUCED LOADS

LIST OF TABLES

<u>Table Number</u>	<u>Title</u>
E. 6A-1	PEAK DRAG LOAD VALVES FOR 1-ICS-012-52-2, SEGMENT 1
E. 6A-2	PEAK DYNAMIC PRESSURES (PSI)
E. 6A-3	PEAK FREE SURFACE DEFLECTIONS (FT)

LIST OF FIGURES

<u>Figure Number</u>	<u>Title</u>
E. 6A-1	SUPPRESSION POOL SYSTEM AND COORDINATE SYSTEM
E. 6A-2	HYDRODYNAMIC DRAG LOAD TIME HISTORY FOR SEGMENT 1 OF 1-ICS-012-52-2, X-DIRECTION
E. 6A-3	HYDRODYNAMIC DRAG LOAD TIME HISTORY FOR SEGMENT 1 OF 1-ICS-012-52-2, Y-DIRECTION
E. 6A-4	HYDRODYNAMIC DRAG LOAD TIME HISTORY FOR SEGMENT 1 OF 1-ICS-012-52-2, Z-DIRECTION
E. 6A-5	DESIGN/MODEL STRUCTURE 1-ICS-012-52-2

ATTACHMENT E
(TO APPENDIX 6A)

SUPPRESSION POOL SEISMIC-INDUCED LOADS

Movement of suppression pool boundaries due to seismic events will induce movement of suppression pool water. The response of the water, known as sloshing, will cause hydrodynamic pressure loads on the boundary walls and drag loads on structures submerged in the pool.

A mathematical model was developed to determine hydrodynamic pressure within the pool and drag loads on submerged structures. The suppression pool system is represented by the geometry presented in Fig. E.6A-1. Formulation of seismic sloshing problems in such an annular tank requires determination of the velocity potential function. This function can be solved from a three-dimensional Laplace equation. The flow in the suppression pool is assumed incompressible, irrotational and inviscid. Boundary conditions are based on rigid pool boundaries. The seismic ground motion is incorporated in the solution as a time-dependent boundary condition.

The Laplace solution for an annular pool is:

$$\begin{aligned} \phi(r, \theta, Z, t) = & rU_x(t) \cos \theta + rU_y(t) \sin \theta + \\ & \sum_{n=0}^k [E_n(t) \sin \theta + F_n(t) \cos \theta] \cosh(\lambda_n Z) * \\ & \left[\frac{J_1(\lambda_n r) - \frac{J_1(\lambda_n r_p)}{Y_1(\lambda_n r_p)} \cdot Y(\lambda_n r)}{Y_1(\lambda_n r_p)} \right] \end{aligned} \quad (1)$$

Where:

$U_x(t), U_y(t)$ = Horizontal seismic ground motions
(ft/sec)

$E_n(t), F_n(t)$ = Time dependent functions determined
from free surface boundary condition

r_p = Outer radius of drywell wall

r_c = Suppression pool containment radius
(ft+)

h = Depth of water in pool (ft)

$A_x(t), A_y(t)$ = Horizontal seismic ground motion
(ft/sec)

$A_z(t)$ = Vertical seismic ground motion
(ft/sec)

r = Radial coordinate (ft)

θ = Angular coordinate (deg)

Z = vertical coordinate (ft)

ρ = fluid density (slugs/ft)

J_1 = Bessel function of the first kind Order 1

Y_1 = Bessel function of the second kind Order 1

The eigenvalues (λ_n) are obtained from the solution of the following equation:

$$J_1'(\lambda_n r_p) \cdot Y_1'(\lambda_n r_c) - J_1'(\lambda_n r_c) \cdot Y_1'(\lambda_n r_p) = 0 \quad (2)$$

Solution of the eigenvalue problem allows for determination of the natural frequencies and mode shapes of the sloshing motions. In this analysis, surface sloshing motions are assumed to be of small amplitude and, therefore, linear theory is incorporated.

The fluid velocities and acceleration, free surface displacement, and dynamic pressures can be derived by determination of the velocity potential.

$$V_\theta = \frac{1}{r} \frac{\delta\phi}{\delta\theta} \quad (3)$$

$$V_\theta = \frac{\delta}{\delta t} \left(\frac{1}{r} \frac{\delta\phi}{\delta\theta} \right)$$

The free surface displacement is determined as follows:

$$\xi = \frac{-1}{[g + A_z(t)]} \cdot \frac{\delta\phi}{\delta t} \Big|_{z=h}$$

Where:

$$g = \text{gravitational acceleration} = 32.2 \text{ ft/sec}^2$$

The total dynamic pressure P_{DT} is based on a contribution due to vertical acceleration P_D and the dynamic pressure (P_{DV}).

$$P_{DT} = P_D + P_{DV} \quad (5)$$

Where:

$$P_D = -\rho \frac{\delta\phi}{\delta t} \quad (6)$$

$$P_{DV} = \rho A_z (h + \xi - z) \quad (7)$$

The drag loads on submerged structures are computed using Morrison's equation. This includes loads due to velocity and acceleration drag.

The seismic ground motion forcing function used in the sloshing analysis is the basemat excitation. The basemat excitation for a safe shutdown earthquake (SSE) event (Section 3.7A) was used for the analysis of submerged structures (Fig. 3.7A-5 through 3.7A-7).

Fig. E.6A-2, E.6A-3, and E.6A-4 show the hydrodynamic drag load time histories (x, y, z directions) for segment 1 of 1-ICS-012-52-2, shown in Fig. E.6A-5. Table E.6A-1 summarizes the peak drag loads on this pipe segment in each direction.

The dynamic pressure and free surface deflection were analyzed for a case assuming $h = 68 \text{ ft } 4 \frac{5}{8} \text{ in}$ (flooded pool water depth).

Table E.6A-2 summarizes the peak dynamic pressures along suppression pool surfaces. Note that the peak dynamic pressure values along the walls occur near their base, and the peak values for the basemats occur at the maximum distances from the center of the pool (at the inside of the drywell wall and at the inside of the containment wall). These pressures do not include atmospheric and hydrostatic pressure. Table E.6A-3 summarizes the peak surface deflections at the water free surfaces of the inner and outer tanks. These also occur at a maximum distance from the center of the pool.

TABLE E.6A-1

PEAK DRAG LOAD VALUES FOR
1-ICS-012-52-2, SEGMENT 1

	<u>Min Load</u> <u>(lbf)</u>	<u>T Min</u> <u>(sec)</u>	<u>Max Load</u> <u>(lbf)</u>	<u>T Max</u> <u>(sec)</u>
X direction	-66.53	10.6	50.66	3.2
Y direction	-35.77	4.7	43.68	10.6
Z direction	-1.01	4.7	1.36	12.0

TABLE E.6A-2

PEAK DYNAMIC PRESSURES (PSI)

	<u>Min</u>	<u>Max</u>
Basement (outer tank)	-4.78	4.57
Drywell wall (outer tank)	-3.50	3.88
Basement (inner tank)	-4.47	4.49
Drywell wall (inner tank)	-4.44	4.10
Containment wall	-4.66	4.17

RBS USAR

TABLE E.6A-3

PEAK FREE SURFACE DEFLECTIONS (FT)

<u>Surface</u>	<u>Min</u>	<u>Max</u>
Outer tank	-2.28	2.28
Inner tank	-1.85	1.85

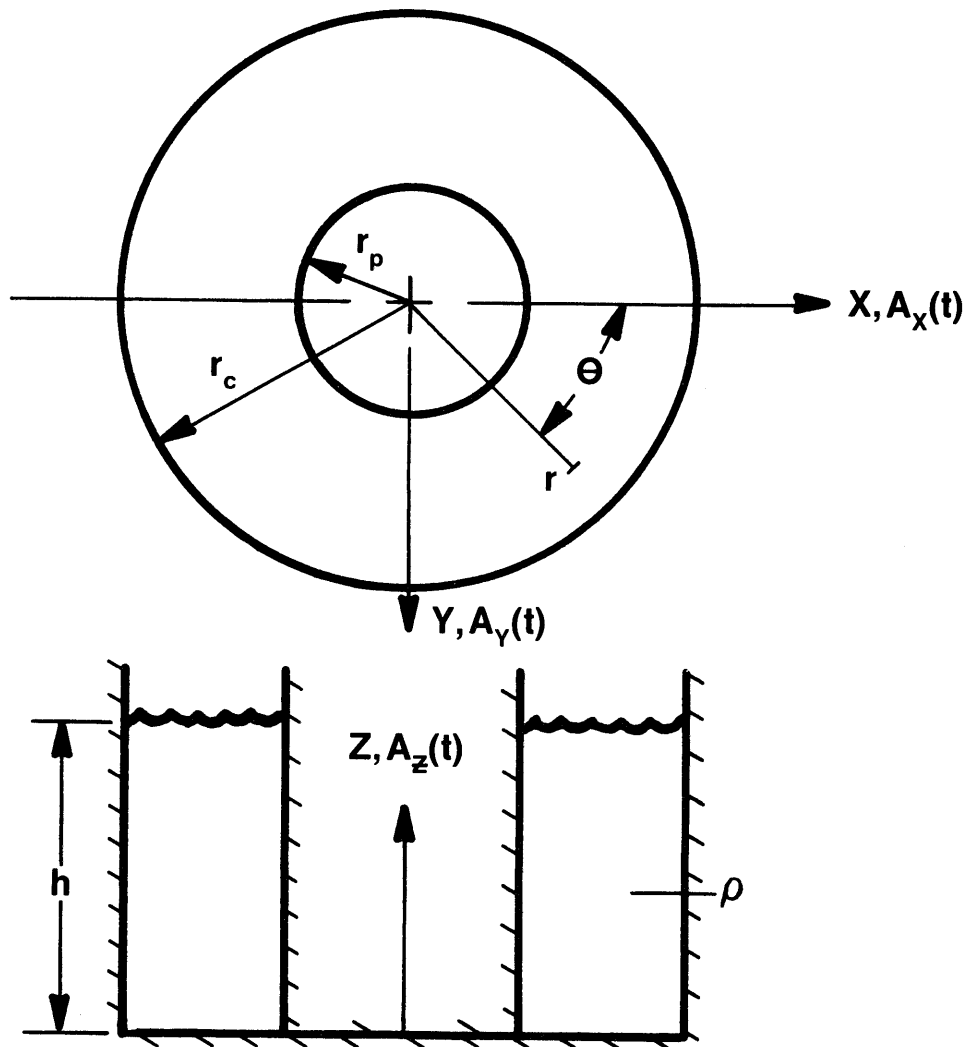


FIGURE E.6A-1

SUPPRESSION POOL SYSTEM AND
COORDINATE SYSTEM

RIVER BEND STATION
UPDATED SAFETY ANALYSIS REPORT

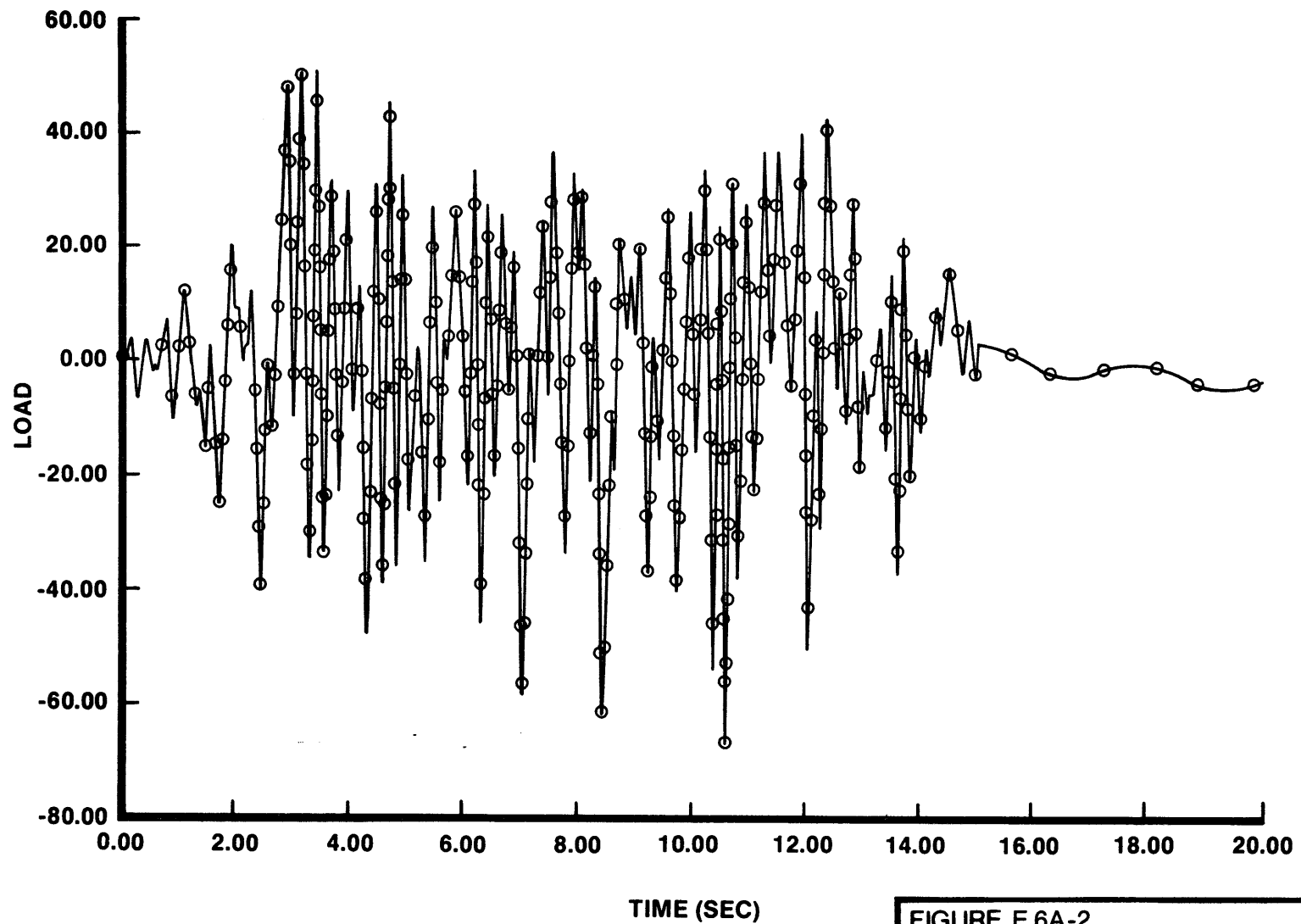


FIGURE E.6A-2

HYDRODYNAMIC DRAG LOAD TIME
HISTORY FOR SEGMENT 1 OF
1-ICS-012-52-2, X-DIRECTION

RIVER BEND STATION
UPDATED SAFETY ANALYSIS REPORT

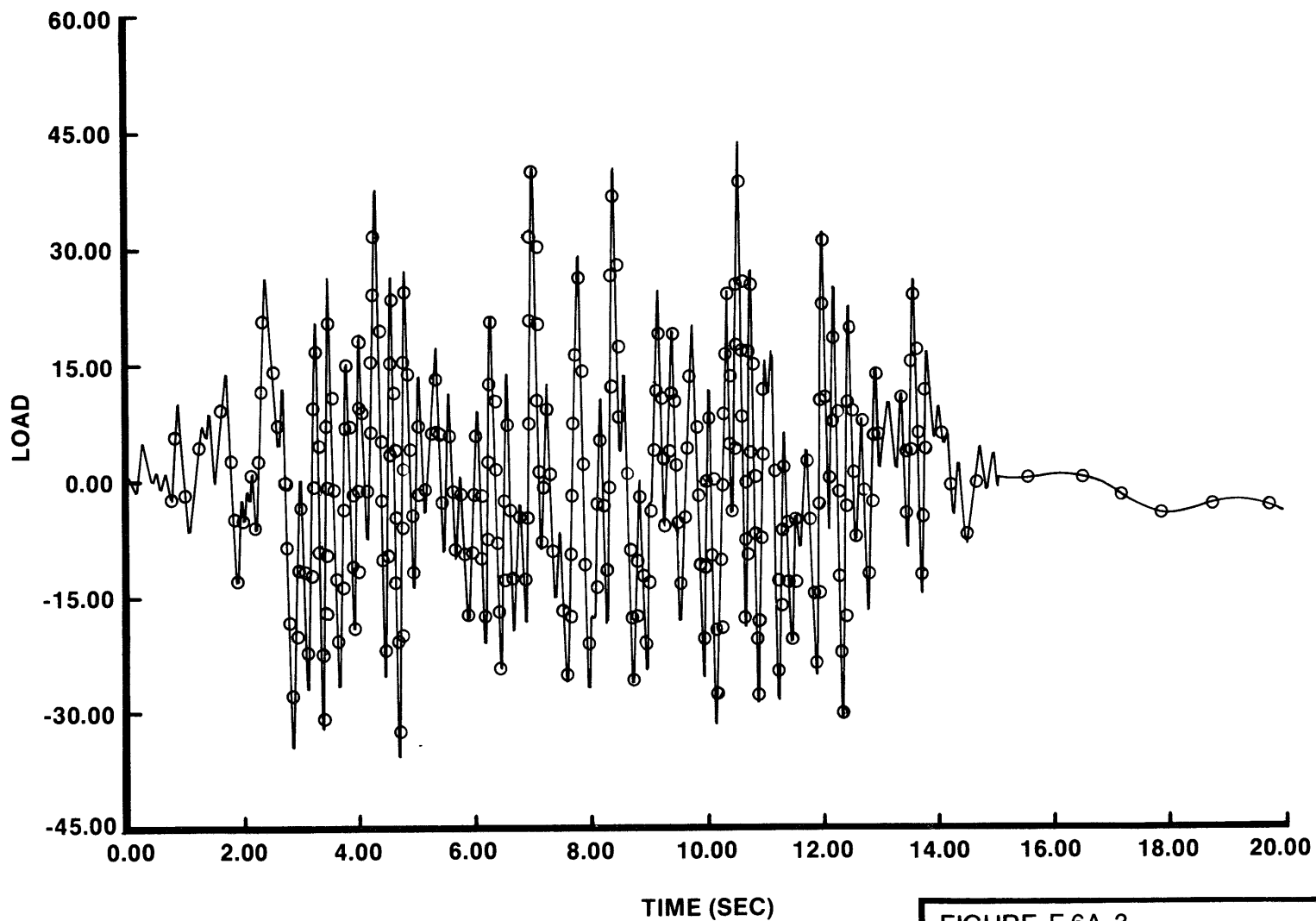


FIGURE E.6A-3

HYDRODYNAMIC DRAG LOAD TIME
HISTORY FOR SEGMENT 1 OF
1-ICS-012-52-2, Y-DIRECTION

RIVER BEND STATION
UPDATED SAFETY ANALYSIS REPORT

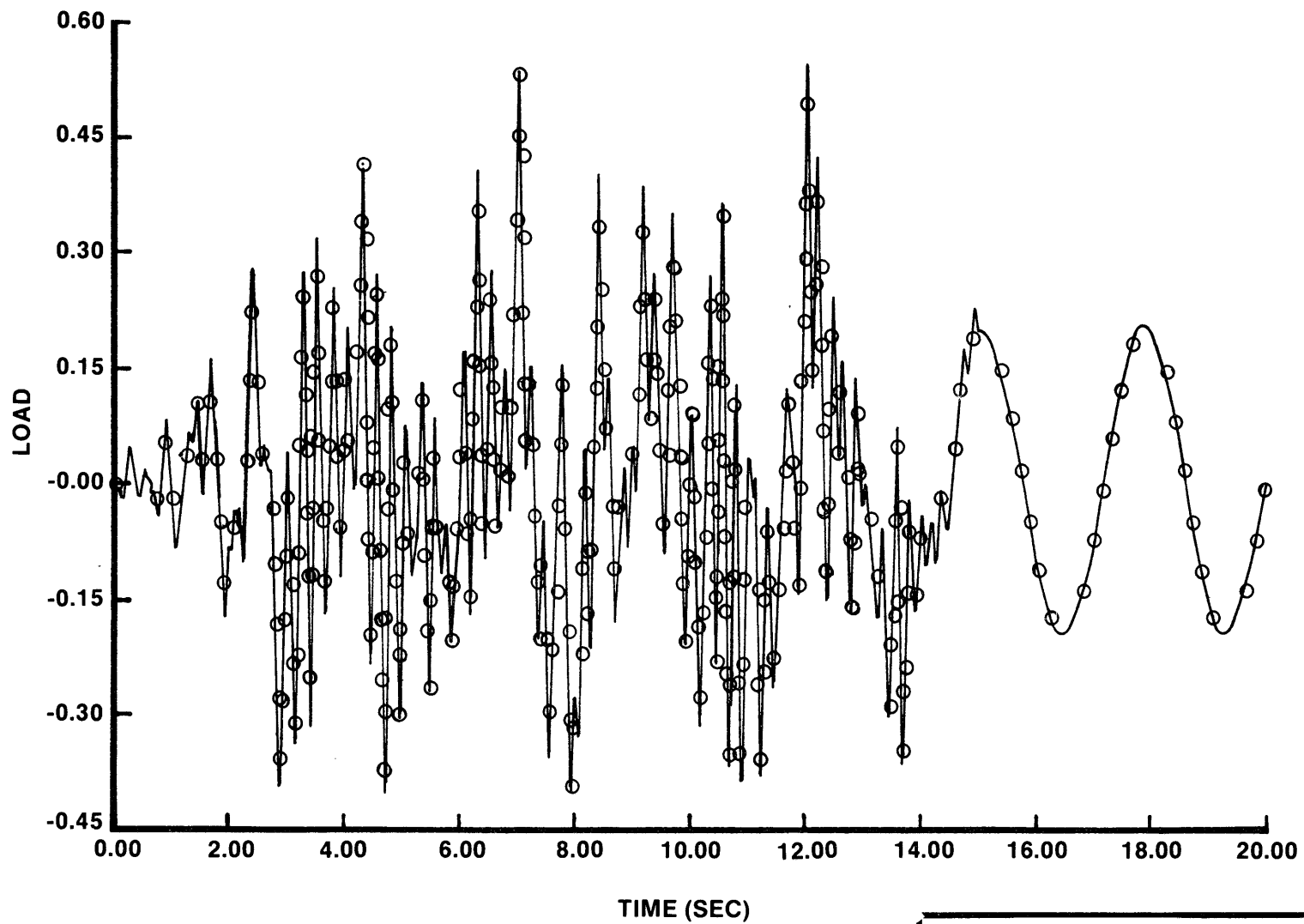


FIGURE E.6A-4

HYDRODYNAMIC DRAG LOAD TIME
HISTORY FOR SEGMENT 1 OF
1-ICS-012-52-2, Z-DIRECTION

RIVER BEND STATION
UPDATED SAFETY ANALYSIS REPORT

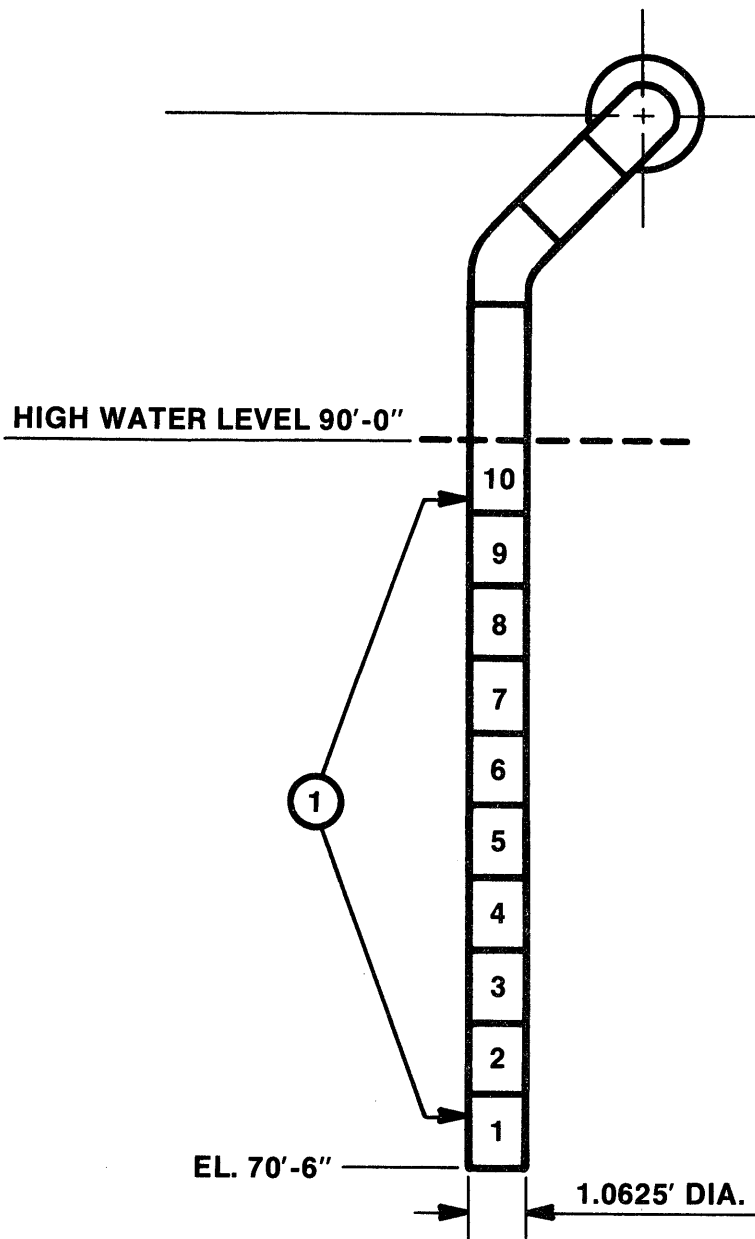


FIGURE E.6A-5

DESIGN/MODEL STRUCTURE
1-ICS-012-52-2

RIVER BEND STATION
UPDATED SAFETY ANALYSIS REPORT

RBS USAR

ATTACHMENT G
(TO APPENDIX 6A)

DRYWELL NEGATIVE PRESSURE CALCULATION

Refer to Section 6.2.1.1.3.3.1.

August 1987

RBS USAR

ATTACHMENT H
(TO APPENDIX 6A)

CONTAINMENT ASYMMETRIC LOADS

August 1987

RBS USAR

ATTACHMENT H
(TO APPENDIX 6A)

CONTAINMENT ASYMMETRIC LOADS

TABLE OF CONTENTS

<u>Section</u>	<u>Title</u>	<u>Page</u>
H.6A.1	CONTAINMENT ASYMMETRIC LOADS	H.6A-1
H.6A.2	ASYMMETRIC POOL SWELL	H.6A-1
H.6A.3	ASYMMETRIC CHUGGING	H.6A-2

LIST OF TABLES

<u>Table Number</u>	<u>Title</u>
H.6A-1	CONTAINMENT ASYMMETRIC LOADS

H.6A.1 CONTAINMENT ASYMMETRIC LOADS

This attachment discusses the potential for circumferential variations in the LOCA dynamic loads and SRV loads. The asymmetric loads are identified and the data being used for containment design evaluation is presented. Table H.6A-1 is a tabulation of the postulated phenomena which could cause loading asymmetries. The table either provides a reference for the asymmetric loads that are significant and should be considered, or provides a reference that justifies the assumption that a particular phenomenon does not lead to asymmetric loads of significance.

H.6A.2 ASYMMETRIC POOL SWELL

As discussed in Section 6A.6, the maximum containment pressure increase associated with the bubble formation that follows vent clearing is specified as 10 psi. The basis for this specification is data from the large scale air blowdown tests that were conducted as part of the Mark III test program. Circumferential variations in this relatively small pressure increase could result from either seismically induced submergence variations or variations in the vent flow composition (i.e., air/steam mixture variations). Increased submergence could lead to an increase in the load. However, PSTF data show a very weak relationship between submergence and the containment pressure increase caused by bubble information. The survey of the PSTF data shown in GESSAR Fig. 3B-56 shows that for tests having the same drywell pressure at vent clearing, variations of up to 6 ft in submergence lead to variations in the bubble load of 2 to 3 psi; it is concluded that variations in suppression pool depth due to seismically induced waves do not lead to significant asymmetric containment bubble loads.

The bubble loading specification of 10 psi being used for Mark III design was derived from an air test and is thus the most conservative in terms of vent flow composition. Any steam in the vent flow would be condensed and this would lead to a less rapid pool acceleration and thus a reduced pressure load on the containment wall. It should be noted that PSTF data show that the high degree of turbulent mixing in the drywell during a LOCA leads to a uniform mixture of

air and steam in the vent flow. This condition also exists in the full scale Mark III and this uniform vent flow composition will preclude any significant circumferential variations in the containment bubble formation loads. In addition, Attachment D shows no significant circumferential variations in drywell pressure that could lead to variations in vent flow rates and thus pool swell. Despite strong evidence that circumferential variation in the containment bubble load does not occur, an arbitrary loading combination of 0 psid on one side of the containment with a 10 psid load on the other side is considered to account for any uncertainties about asymmetric loading conditions. The conservative asymmetric condition assumes that all air is vented on half of the drywell periphery and steam is vented on the other half.

The large scale PSTF test data is the basis for specifying the maximum asymmetric load of 10 psi. The 10 psi asymmetric pressure condition applied in a worst case distribution as a bounding specification is used for containment evaluation.

H.6A.3 ASYMMETRIC CHUGGING

An analysis was performed to determine the possible asymmetric chugging effects. It was assumed that all of the vents chugged simultaneously, but all vents on one half of the drywell were at a maximum 90 to 90 percent tolerance limit pressure while the other half of the vents in the opposite 180° sector were at a minimum 90 to 90 percent tolerance limit pressure. The resulting differential forces were then applied to the pool boundaries and weir annulus. Overturning moments were calculated and compared to the currently specified asymmetric pool swell load (Section 6A.4.1.9 and 6A.6.1.3). The current specification loads (from asymmetric pool swell) result in moments twice as large as the asymmetric chugging moments. Since the current asymmetric pool swell specification bounds the conservatively calculated asymmetric chugging results by a large margin, asymmetric chugging is not a design basis load.

TABLE H.6A-1
CONTAINMENT ASYMMETRIC LOADS

<u>Phenomena</u>	<u>Potential for Significant Asymmetric Containment Loads</u>	<u>Asymmetric Loads Being Used for Design Evaluation</u>	<u>Comments</u>
1. Seismic induced pool surface waves	No	See Attachment E	of Appendix 6A
2. Seismic induced changes in the pool hydrostatic pressure	Yes	See Attachment E of Appendix 6A	
3. Relief valve actuation	Yes	See Attachment A of Appendix 6A	
4. Jet loads during vent cleaning	No	0	Loads are of negligible magnitude (6A.6.1.2)
5. Sonic and compressive waves	No	Both 0	Loads are of negligible magnitude (6A.4.1.1 and 6A.6.1.1)
6. Bubble pressure load	Yes	0-10 psi	See discussion (H.6A.2)
7. HCU floor flow pressure differential	No	0	See Attachment K of Appendix 6A
8. Fall back		No	0 Loads on the containment are of negligible magnitude (6A.6.1.7)
9. Post-LOCA waves	No	0	Loads on the containment are of negligible magnitude (6A.6.1.8)
10. Containment pressurization	No	0	This is a relatively slow charging process (Figure 6A.4-4)
11. Condensation oscillation	No	0	Loads are small (6A.6.1.9)
12. Chugging	No	0	See discussion (H.6A.3)
13. Pool swell loads with seismic induced waves present	No	0	See Section 6A.10.1 and discussion (H.6A)

RBS USAR

ATTACHMENT L
(TO APPENDIX 6A)

SUBMERGED STRUCTURE LOADS DUE TO LOCA
AND SRV ACTUATIONS

August 1987

RBS USAR

ATTACHMENT L
(TO APPENDIX 6A)

SUBMERGED STRUCTURE LOADS DUE TO LOCA
AND SRV ACTUATIONS

TABLE OF CONTENTS

<u>Section</u>	<u>Title</u>	<u>Page</u>
L.6A.1	INTRODUCTION	L.6A-1
L.6A.2	SUBMERGED STRUCTURE LOADS DUE TO LOCA	L.6A-2
L.6A.2.1	Compressive Wave Loading	L.6A-2
L.6A.2.2	LOCA Water Jet Load	L.6A-2
L.6A.2.3	LOCA Bubble Loads	L.6A-3
L.6A.2.4	Fallback Loads	L.6A-10
L.6A.2.5	LOCA Condensation Oscillations Loads	L.6A-10
L.6A.2.6	LOCA Chugging Loads	L.6A-10
L.6A.3	SUBMERGED STRUCTURE LOADS DUE TO SRV ACTUATIONS	L.6A-12
L.6A.3.1	Quencher Water Jet Load	L.6A-12
L.6A.3.2	Quencher Bubble Load	L.6A-13

RBS USAR

ATTACHMENT L
(TO APPENDIX 6A)

LIST OF TABLES

<u>Table Number</u>	<u>Title</u>
L.6A-1	K VS TIME
L.6A-2	MAXIMUM CONDENSATION OSCILLATION VELOCITIES IN THE SUPPRESSION POOL

RBS USAR

ATTACHMENT L
(TO APPENDIX 6A)

LIST OF FIGURES

<u>Figure Number</u>	<u>Title</u>
L.6A-1	STRUT LOCATIONS (2 Sheets)
L.6A-2	LOADING ON THE STRUT WITH RADIUS - 0.276 FT
L.6A-3	SUPPRESSION POOL MODEL FOR MO1 (2 Sheets)
L.6A-4	LOCA BUBBLE RADIUS GROWTH
L.6A-5	ARRANGEMENT OF IMAGES
L.6A-6	MARK III HORIZONTAL VENT CHUGGING
L.6A-7	FOUR-BUBBLE MODEL FOR QUENCHER AIR DISCHARGE

ATTACHMENT L
TO APPENDIX 6ASUBMERGED STRUCTURE LOADS DUE TO LOCA
AND SRV ACTUATIONS

L.6A.1 INTRODUCTION

In the following two sections, the flow-induced loads on structures submerged in the suppression pool due to LOCA and SRV actuations are discussed. During LOCA, steam rapidly escapes from the break and creates a compressive wave in the drywell air space. This wave is transmitted from the weir wall water surface to the suppression pool and finally to the submerged structure. This compressive wave loading is negligible (Section L.6A.2.1). Following this compressive wave, the drywell is rapidly pressurized. The water in the weir annulus and drywell vents is expelled to the suppression pool. A highly localized induced flow field is created in the pool, and a dynamic loading is then induced on submerged structures (Section L.6A.2.2). After the water is expelled from the vent system, the air in the drywell air space, prior to the LOCA event, is forced from the top vents and forms expanding bubbles which create moderate dynamic loads on submerged structures (Section L.6A.2.3). These air bubbles cause the pool water surface to rise until they break through the pool water surface. The pool surface slug decelerates and falls back to the original pool level (fallback loads are discussed in Section L.6A.2.4). At this point, steam from the break fills the drywell space and is channeled to the pool via the vent system. Steam condensation oscillation starts, and the vibratory nature of pool water motion causes an oscillatory load on submerged structures (Section L.6A.2.5).

This condensation oscillation continues until pressure in the drywell decays. This is followed by a somewhat regular but less persistent vibration called chugging. During this chugging period, a high wave propagation spike is observed which causes an acoustic load on submerged structures (Section L.6A.2.6).

During SRV actuations, the dynamic process of the steam blowdown is quite similar to LOCA but the load is mitigated by the X-quencher device attached at the end of each SRV discharge line. Two types of loads are important: one due to the water jet formed at the confluence of the X-quencher arm discharges (Section L.6A.3.1); and another due to the four air bubbles formed between the arms of the X-quencher.

These air bubbles are smaller in size than the LOCA air bubbles, reside longer in the pool, and oscillate as they rise to the pool surface. The load created by these bubbles is discussed in Section L.6A.3.2.

The material in this attachment is organized as follows:

1. The specific analytical model, and
2. A load calculation procedure that summarizes the ———
———engineering process.

L.6A.2 SUBMERGED STRUCTURE LOADS DUE TO LOCA

L.6A.2.1 Compressive Wave Loading

As discussed in Section 6A.6.1.1, the very rapid compression of the drywell air theoretically generates a compressive wave; but, as pointed out in Sections 6A.6.1.1 and 6A.6.1.2, there were no loads recorded on the containment wall in PSTF for this phenomena. Therefore, it can be concluded that compression wave loads on structures in the suppression pool are significantly smaller than loads caused by the water jet for structures close to drywell. For structures near the containment, neither compressive nor jet loads are significant.

L.6A.2.2 LOCA Water Jet Load

During the initial phase of the DBA, the drywell air space is pressurized and the water in the weir annulus vents is expelled to the pool and induces a flow field throughout the suppression pool. This induced flow field is not limited to direct jet contact and creates a dynamic load on structures submerged in the pool.

●→10

GESSAR-II gives the zone of influence of these jets as a cylindrical region whose diameter is 1.5 times the diameter of the weir vent and extends 5 times the vent diameter into the pool. Individual zones of influence varies from the top vent elevation to the bottom vent elevation (Detailed analysis in Reference 7). X-quencher struts are located in this zone (see Figure L.6A-1), and jet impact and drag loads are calculated for these struts. Impact loads are based on the empirical methods of Reference 1, and drag loads include both standard and acceleration drags.

10←●

Jet velocities, accelerations, and frontal displacements needed for the impact and drag load analysis are calculated based on one-dimensional mass and momentum equations and assume inviscid flow⁽²⁾. The GESSAR II vent clearing water jet velocities were evaluated and determined to be

applicable for RBS based on sensitivity studies performed with the SWEC LOCTVS containment analysis code. For RBS load definition, the GESSAR II vent clearing velocity time history for the middle vent (GESSAR II, Figure 3BL-3) is multiplied by the factor 1.2 and used as input to the jet load analysis.

A typical load time history is shown in Fig. L.6A-2.

L.6A.2.3 LOCA Bubble Loads

During the initial phase of the DBA, pressurized drywell air is purged into the suppression pool through the submerged vents. After vent clearing, a single bubble is formed around each top vent. It is during the bubble growth period that unsteady fluid motion is created within the suppression pool. During this period, all submerged structures below the pool surface will be exposed to transient hydrodynamic loads.

The bases of the flow model and load evaluation for the LOCA bubble-induced submerged structure load definition are derived from the model of Reference 3. The following procedure is recommended for calculating loads on submerged structures:

1. Pool Dimensions and Bubble Data

Specific data that must be obtained are:

- R_i - Initial bubble radius, assumed to be the same as the vent radius (1.146 ft)
- P_o - Drywell transient pressure obtained from Fig. 6.2-5 (psia) (from plant unique analysis of Section 6.2.1.1.3.1)
- ρ_o - Air density corresponding to drywell conditions when the drywell pressure is P_o (lb_m/ft^3)
- ρ - Pool liquid density ($62.4 \text{ lb}_m/\text{ft}^3$)
- P_c - Containment air space pressure assumed to be constant at 14.7 psia
- P_∞ - Initial pool pressure at the top vent centerline submergence (psia)
- H - Pool depth (20 ft)

- L - Pool length (20.5 ft)
- D - Pool width (Fig. L.6A-3) (312.6 ft)
- y_0 - Initial bubble location from bottom of pool, same as top vent centerline (12.25 ft)

2. Duration of Loads

Loads on submerged structures due to LOCA air clearing begin when an air bubble forms at each vent exit immediately following air clearing and end when a bubble engulfs the structure or when breakthrough occurs if a bubble does not engulf the structures.

3. Initial Bubble Location

Initially, a bubble center (x_0 , y_0 , z_0) is assumed to be located on each vent axis at a distance equal to one vent radius from the vent exit.

4. Movement of Bubble Center

The bubble center movement is used only to calculate bubble engulfment time. The effects of bubble movement on the predicted load are accounted for conservatively by a factor of 2 (step 13).

5. Bubble Dynamics

The following bubble dynamics equations can be solved for:

$R(t)$ - Bubble radius at time t

$\dot{R}(t)$ - Bubble growth rate at time t

$\ddot{R}(t)$ - Rate of change of bubble growth rate
rate at time t

Bubble Dynamics Equations

$$R = \frac{1}{R} \left[\frac{g_C}{\rho} (P_B - P_\infty) - \frac{3}{2} \dot{R}^2 \right] \quad (\text{L.6A-1})$$

$$\dot{P}_B = 3k \left[\frac{1}{4\pi R^3} \frac{P_o \dot{m}_B}{\rho_o} - \frac{P_B \dot{R}}{R} \right] \quad (\text{L.6A-2})$$

$$P_\infty = P_C + \rho (H - y_o) \quad (\text{L.6A-3})$$

Where:

P_B = Bubble pressure at time t (psia)

\dot{m}_B = Bubble charging rate (lb /sec)
(Equation A46, Reference 4)

k = Ratio of specific heats for air (1.4)

Initial Conditions

$R(0) = R_i$ = vent radius = 1.146 ft

$\dot{R}(0) = V_i / 4 = 18.25$ ft/sec

Where:

V_i = Top vent water jet velocity at vent clearing = 73 ft/sec (from plant unique analysis described in Section 6.2.1.1.3.1)

$P_B(0) = P_o$ at top vent clearing = 32.2 psia (from plant unique analysis described in Section 6.2.1.1.3.1)

$m_B(0) = 4/3 \pi R_i^3 \rho_o$

A plot of bubble radius versus time has been obtained from the bubble dynamics equations (Fig. L.6A-4).

6. Structure Data

Locate structure and identify elevation and distances from drywell and containment walls.

Identify dimensions, shape, and orientation of structure. Long structures should be divided into smaller segments (with each segment approximately 2 ft long) for more precise evaluation.

7. Distance to Structure

Determine the following at time t :

D_s = The cross-sectional dimension of structures or structure segment in the direction of the bubble center. (The bubble center is assumed to be displaced horizontally a distance equal to $R(t)$.)

8. Check Structure/Bubble Contact

At any time t , using the value of bubble radius $R(t)$ from step 5, check if:

$$R(t) \geq \sqrt{[x-R(t)]^2 + (y-y_0)^2 + (z-z_0)^2} - d_s/2$$

If true, then end loading calculations for the structure or structure segment under consideration since it is inside the bubble and the drag forces are zero. If not true, proceed with step 9 until the bubble breaks through the pool surface.

9. Pool Boundary Effects

To account for the effects of pool walls, floor, and free surface, use the method of images described in Section 4.10 of Reference 3. First, determine r_{ijk} , which is the distance from the center of the structure or structure segment (x, y, z) to the source or sink image at (x_i, y_j, z_k) .

$$r_{ijk} = \sqrt{(x-x_i)^2 + (y-y_j)^2 + (z-z_k)^2} \quad (\text{L.6A-4})$$

$r_{0'0'0}$ corresponds to the real source. Then evaluate functions X, Y, Z as given by Equation A80 of Reference 3. Using the notations adopted here, these functions may be written as:

$$\begin{aligned}
 X &= \sum_{\ell=1}^M \left[K_{\ell} \sum_{k=-N}^N \sum_{j=-N}^N \sum_{i=-N}^N \frac{(-1)^j (x-x_i^{(\ell)})}{r^3 ijk} \right] \\
 Y &= \sum_{\ell=1}^M \left[K_{\ell} \sum_{k=-N}^N \sum_{j=-N}^N \sum_{i=-N}^N \frac{(-1)^j (y-y_j^{(\ell)})}{r^3 ijk} \right] \\
 Z &= \sum_{\ell=1}^M \left[K_{\ell} \sum_{k=-N}^N \sum_{j=-N}^N \sum_{i=-N}^N \frac{(-1)^j (z-z_k^{(\ell)})}{r^3 ijk} \right]
 \end{aligned}
 \tag{L.6A-5}$$

Where:

M = The number of sources in the pool (i.e., 43 air bubbles)

N = The total number of images considered for each source

K = Factor used for finite bubbles to satisfy the local pressure boundary condition at the real bubble surface (i.e., the pressure at the real bubble surface equals the independently calculated bubble pressure P_B).

The K factor is not a function of the structure location in the pool; it is a function of bubble radius and the bubble image function. The calculation of K is based on Reference 3, which is the same method as used in GESSAR (see GESSAR Reference 24). Calculated values of K as a function of time for RBS are shown in Table L.6A-1.

10. Number of Images

The results of a sensitivity study show that 7, 10, and 2 images in the vertical, radial, and circumferential directions, respectively, will provide adequate convergence.

A

typical

arrangement of image sets in the vertical plane is shown on Fig. L.6A-5.

11. Direction of the Flow Field

The direction of the flow field, at time t is determined by the unit vector \vec{n} where:

$$\vec{n} = \frac{X n_x + Y n_y + Z n_z}{\sqrt{X^2 + Y^2 + Z^2}} \quad (\text{L.6A-6})$$

12. Acceleration and Velocity

Using the results from steps 5 and 11, the equivalent uniform acceleration at time t at the structure location in a finite containment is:

$$\dot{U}_\infty(t) = s \sqrt{x^2 + y^2 + z^2} \quad (\text{L.6A-7})$$

Where:

$$\dot{S} = R^2(t) \ddot{R}(t) + 2R(t) \dot{R}^2(t)$$

The corresponding velocity $U_\infty(t)$ may be obtained by numerically integrating $\dot{U}_\infty(t)$.

$$\dot{U}_\infty(t) = s \sqrt{x^2 + y^2 + z^2} \quad (\text{L.6A-8})$$

Where:

$$S = R^2(t) \dot{R}(t)$$

13. Drag Forces

The acceleration drag is calculated from:

$$F_A(t) = \frac{\dot{U}_{\infty n}(t) V_A \rho}{g_c} \quad (\text{L.6A-9})$$

Where:

$\dot{U}_{\infty n}$ = Acceleration component normal to the structure

V_A = Acceleration drag volume

The standard drag force is calculated from

$$F_s(t) = C_D A_n \frac{\rho U_{\infty n}^2(t)}{2 g_c}$$

(L.6A-10)

Where:

C_D = Drag coefficient for flow normal to the structure

A_n = Projected structure area normal to $U_{\infty n}(t)$

Add F_A and F_s at any time t to get the total load on the structure segment.

In accordance with NUREG-0978 acceptance criteria, noncylindrical structures are modeled as circumscribed cylinders. To determine standard drag, Morrison's equation is used with a standard drag coefficient of not less than 1.2. If structures are found in the vicinity of each other, interference effects are evaluated and the drag coefficient increased accordingly.

The loads predicted by this procedure agree with the Mark III submerged structures test data (Reference 5). For additional conservatism, the final load is multiplied by a factor of 2 to cover the effects of a moving source.

The direction of total drag is normal to the submerged structures.

L.6A.2.4 Fallback Loads

There is no pressure increase on the suppression pool boundary during pool fallback (Section 6A.4.1.6). Structures within the containment suppression pool that are above the bottom vent elevation will experience drag loads as the water level subsides to its initial level. For design purposes, it is assumed that these structures will experience drag forces associated with water flowing at 35 ft/sec; this is the terminal velocity for a 20-ft freefall and is a conservative bounding number. Freefall height is limited by the HCU floor. The load computation procedure is the same as for calculating standard drag load in step 13 (Section L.6A.2.3) and will not be repeated here.

L.6A.2.5 LOCA Condensation Oscillations Loads

Steam condensation begins after the vent is cleared of water and the drywell air has been carried over into the wetwell. This condensation oscillation phase induces bulk water motion and therefore creates drag loads on structures submerged in the pool.

The basis of the flow model for condensation oscillation load definition is derived from the work of Reference 4. The load calculation procedure is the same as for LOCA bubble loads given in Section L.6A.2.3 except for source strength and locations.

The condensation oscillation disturbances are modeled as phase point sources centered at the exit of each top vent. The source strength for calculating acceleration drag (S) is determined from the Mark III $1/\sqrt{3}$ scale test data to be $188 \text{ ft}^3/\text{sec}^2$. The time history follows the wall pressure time history presented in Section 6A.4.1.5 which produces a frequency range of 2 to 3.5 Hz. The source strength for the velocity drag (S) is determined from the time integration of S time history. Since the sources are considered points, no adjustment for finite bubbles is required so the K factor of Equation L.6A-5 is set equal to 1.

L.6A.2.6 LOCA Chugging Loads

Chugging occurs after drywell air has been purged and the vent mass flux falls below a critical value. Chugging then induces acoustic pressure loads on structures submerged in the pool.

In accordance with NUREG-0978 acceptance criteria (Appendix C, Section 2.0), circumscribed cylinders are used

for noncylindrical structures. In addition, standard drag is calculated and combined with the acceleration drag for all structures. The standard drag is calculated using Morrison's equation, with a drag coefficient of not less than 1.2. Structural interference effects are also evaluated when structures are found in the vicinity of each other. Table L.6A-2 provides the maximum velocity in the suppression pool. In accordance with Criteria 2.14.2 (2a) of the Mark I acceptance criteria, a standard drag coefficient of 3.6 is used for structures that do not satisfy the condition:

$$\frac{U_m T}{D} \leq 2.74$$

Where:

U_m = Maximum velocity

T = Period of condensation oscillation

D = Cylinder diameter

A 2-in RCIC minimum flow line is the only structure which does not satisfy the exclusion condition. A standard drag coefficient of 3.6 is used in the submerged structure load evaluation for this line.

The basis of the flow model for chugging load definition is derived from the work of Reference 4.

The loads on submerged structures due to chugging are calculated from the following procedure:

1. Locate the bubble center at 2.0 ft above the top vent centerline.
2. Determine location of structure (x, y, z) relative to bubble center (Fig. L.6A-6).
3. Calculate distance r from chugging center to a structure from

$$r = \sqrt{x^2 + y^2 + z^2}$$

4. Evaluate angle (θ) between structure axis and \vec{r} from

$$\cos \theta = \cos \alpha_s \cos \alpha_b + \cos \beta_s \cos \beta_b + \cos \gamma_s \cos \gamma_b$$

Where $\cos \alpha_s$, $\cos \beta_s$, $\cos \gamma_s$ are the direction cosines of the structure axis, while $\cos \alpha_b$, $\cos \beta_b$, $\cos \gamma_b$ are the direction cosines of the vector r from the bubble center to the structure.

5. Calculate chugging load from

Where:

A = Projected area of the structure normal to its own axis

ΔP_{or_0} = 2.53 psi-ft as the pulse strength.

6. Include the effect of another vent by repeating steps 1 through 5. The pulse width is 0.002 sec. Include those vents for which the signals arrive at the submerged structure within 0.002 sec of each other. Use 4,000 ft/sec for the acoustic velocity in water.

7. Add the two forces linearly.

8. Obtain time history as follows:

Load duration is 2 msec.

Period between individual chugs is 1 to 5 sec.

9. For long structures, the structure is broken into separate sections, and the load on each section is calculated.

L.6A.3 SUBMERGED STRUCTURE LOADS DUE TO SRV ACTUATIONS

L.6A.3.1 Quencher Water Jet Load

Following the actuation of an SRV, water is rapidly discharged through the X-quencher device attached at the end of the SRV line. A highly localized water jet is formed around the X-quencher arms. The load induced outside a sphere circumscribed around the quencher arms by the quencher water jet is small. There are no submerged structures located within the sphere in the RBS arrangement. The induced load for submerged structures located outside a

sphere circumscribed by the quencher arm is negligible and is ignored.

L.6A.3.2 Quencher Bubble Load

The analytical model for quencher air bubble loads on submerged structures is presented in References 5 and 6. The following procedure is used to apply the analytical model for calculating loads on submerged structures due to quencher air bubbles.

1. Determine the location, dimensions, shape, and orientation of the submerged structure. For more precise evaluation, long structures are divided into smaller segments, with each segment being approximately 2-ft long.
2. Determine the initial location of the four bubbles. Each bubble is assumed to form at the intersection of hole pattern centerlines from adjacent arms (Fig. L.6A-7). If the presence of pool boundaries or other structures prevent bubble formation at the location thus determined, the bubble is assumed to be located along the bisector between adjacent arms and is tangent to the boundaries or structures.
3. Obtain values of the following parameters from Attachment A to Appendix 6A.

P_{\max} = Maximum bubble pressure (psia)

P_{\min} = Minimum bubble pressure (psia)

T_{pool} = Initial pool temperature ($^{\circ}\text{R}$)

H_q = Quencher arm submergence (ft)

V_i = Initial air volume in the safety/relief valve discharge line (SRVDL) (ft)

P_i = Initial air pressure in SRVDL (psia)

T_i = Initial air temperature in SRVDL ($^{\circ}\text{R}$)

P_c = Containment air space pressure (psia)

k = Specific heat ratio of air

ρ = Water density at T_{pool} (lb /ft³)

4. Assume that the maximum volume of each bubble occurs when the pressure is at its minimum and the air in the bubble attains the surrounding pool water temperature and calculate the maximum bubble radius from

$$V_{\max} = \frac{V_i}{4} \frac{T_{\text{pool}}}{T_i} \frac{P_i}{P_{\min}} \text{ ft}^3 \quad (\text{L.6A-11})$$

and

$$R_{\max} = (3/4\pi V_{\max})^{1/3} , \text{ ft} \quad (\text{L.6A-12})$$

5. To account for the vertical motion of the bubbles, the following bubble rise equation must be solved simultaneously with the bubble dynamics equations for $R(t)$, $R_1(t)$, $R_2(t)$, and $Z_b(t)$,

Where:

$R(t)$ = Bubble radius at time t

$R_1(t)$ = Bubble growth rate at time t

$R_2(t)$ = Rate of change of the bubble growth rate at time t

C_D = Drag coefficient

$Z_b(t)$ = Submergence of bubble center at time t

Bubble Dynamics Equations

$$R(t) = \frac{1}{R} \left(\frac{g_c}{\rho} (P_B - P_\infty) - \frac{3}{2} \dot{R}^2 \right) \quad (\text{L.6A-13})$$

$$\dot{P}_B = -3kP_B \dot{R}/R \quad (\text{L.6A-14})$$

$$P_{\infty} = P_c + \rho Z_b \quad (\text{L.6A-15})$$

Bubble Rise Equations

$$\ddot{z}_b = \frac{-\frac{1}{2} \pi \rho C_D R^2 \dot{z}_b |\dot{z}_b| - \frac{4}{3} \pi \rho g R^3 + m_B g}{m_B + \frac{2}{3} \pi \rho R^3} \quad (\text{L.6A-16})$$

..

$$m_b = 1/4 \frac{P_i V_i}{R_{\text{air}} T_i} = \text{bubble air mass} \quad (\text{L.6A-17})$$

R_{air} = Gas constant of air

Initial Conditions

$$R(0) = R$$

$$\dot{R}(0) = 0$$

$$Z_b(0) = H$$

$$\dot{Z}_b(0) = 0$$

$$P_B(0) = P$$

6. Determine the location of images of the four source bubbles to account for the effects of pool walls, floor, and free surface. Then calculate parameters X, Y, and Z, which are defined by Equation A67 of Reference 3.
7. For multiple quencher, use Equation A79⁽³⁾ to evaluate parameters X, Y, and Z. Note that Heaviside step functions $H(t-t_1)$ and $H(s_1-t)$ are introduced to account for phasing relations among the quencher of interest. The bubbles from a quencher are assumed to be in phase, but quencher are phased to maximize the load on the structure.

8. Using the results from steps 5 through 7, calculate the equivalent uniform acceleration, $U_{\infty}(t)$, at time t at the structure location from

$$U_{\infty}(t) = \dot{S} \sqrt{x^2 + y^2 + z^2} \quad (\text{L.6A-18})$$

Where:

$$\dot{S} = R^2(t)\ddot{R}(t) + 2R(t)\dot{R}^2(t)$$

The corresponding velocity, $U(t)$, may be obtained by numerically integrating $U(t)$. As a first approximation, $U(t)$ can also be evaluated from

$$U_{\infty}(t) = S \sqrt{x^2 + y^2 + z^2} \quad (\text{L.6A-19})$$

Where:

$$S = R^2(t)\dot{R}(t)$$

9. The acceleration drag is calculated from

$$F_A(t) = \frac{\dot{U}_{\infty n}(t) V_A \rho}{g_c} \quad (\text{L.6A-20})$$

Where:

$\dot{U}_{\infty n}$ = Acceleration component normal to the structure

V_A = Acceleration drag volume for flow normal to the structure

The standard drag force is calculated from

$$F_s(t) = C_D A_n \frac{\rho U_{\infty n}(t) |U_{\infty n}(t)|}{2 g_c} \quad (\text{L.6A-21})$$

Where:

C_D = Drag coefficient for flow normal to the structure

A_n = Projected structure area normal to $U_{\infty n}(t)$

Add F_A and F_s at any time to get the total force on the structure or structure segment. The direction of the total force is normal to the submerged structure.

References - L.6A

1. U.S Nuclear Regulatory Commission Staff Report, "NRC Acceptance Criteria for Mark I Containment Long Term Program," Appendix A to Safety Evaluation Report, NUREG-0661, Washington, DC, 1980.
 2. Moody, F.J. Analytical Model for Liquid Jet Properties for Predicting Forces on Rigid Submerged Structures, NEDE-21472, September 1977, General Electric Company.
 3. Moody, F.J. Analytical Model for Estimating Drag Forces on Rigid Submerged Structures Caused by LOCA and Safety/Relief Valve Ramshead Air Discharges, NEDE-21471, revised by L.C. Chow and L.E. Lasher, September 1977, General Electric Company.
 4. Lasher, L.E. Analytical Model for Estimating Drag Forces on Rigid Submerged Structures Caused by Steam Condensation Oscillations and Chugging, Mark III Containments, NEDO-25153, July 1979.
 5. Chuang, F.H. Mark III One-Third Area Scaled Submerged Structure Tests, NEDE-21606-P, October 1977, General Electric Company.
 6. Lasher, L.E. Analytical Model for Estimating Drag Forces on Rigid Submerged Structures Caused by LOCA and Safety Relief Valve Ramshead Air Discharges, Supplement for X-Quencher Air Discharge, NEDO-21471-01 (Supplement 1), October 1979.
- 10
7. G13.18.14.1*026, "Determination of Jet Influence Zone", Dated 10-1-97
- 10←●

TABLE L.6A-1

K VS TIME

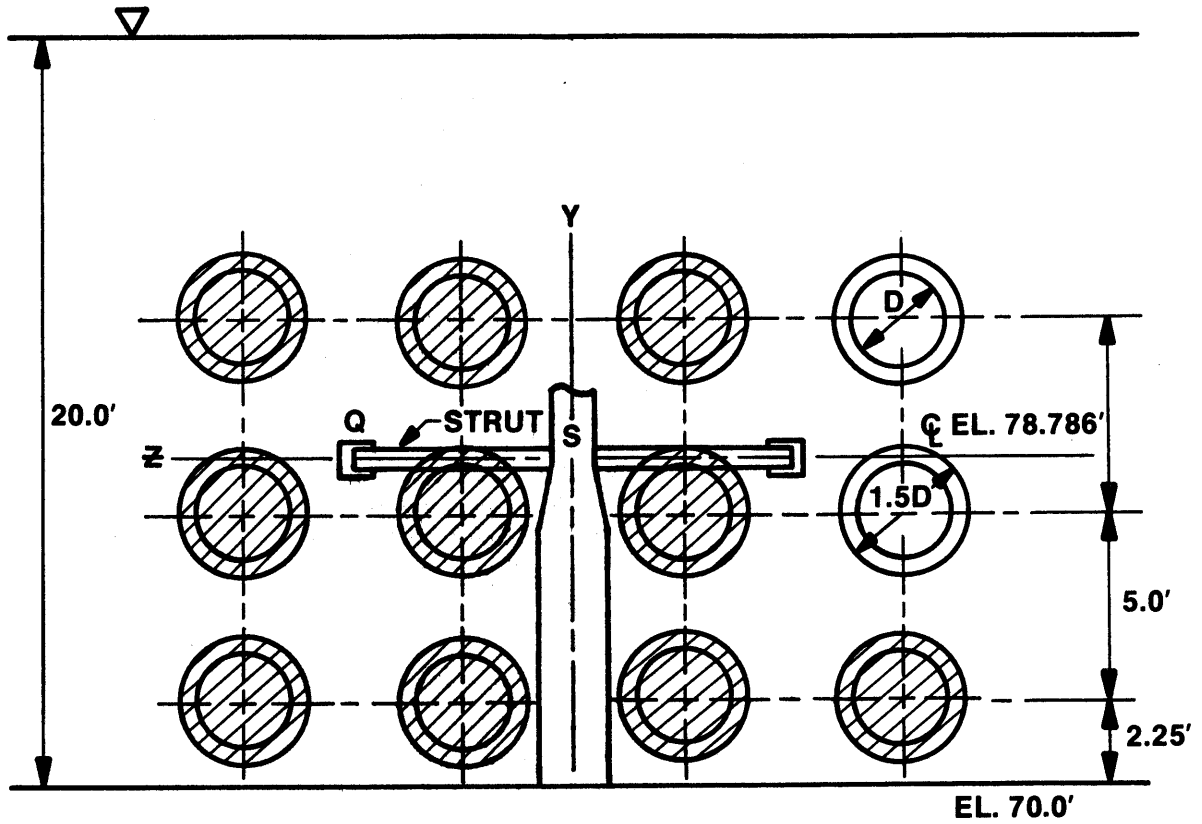
<u>Time (sec)</u>	<u>K</u>
0.0	0.6887
0.05	0.5232
0.085	0.4440
0.090	0.4350
0.098	0.4222
0.102	0.4155
0.110	0.4026
0.115	0.3917
0.119	0.3905
0.152	0.3529
0.200	0.3147
0.230	0.2972
0.295	0.2697
0.340	0.2566
0.395	0.2447
0.429	0.2389
0.555	0.2239
0.600	0.2200
0.793	0.2065
0.911	0.1987
1.040	0.1908
1.091	0.1881

TABLE L.6A-2

MAXIMUM CONDENSATION OSCILLATION VELOCITIES
IN THE SUPPRESSION POOL

<u>Distance From Drywell Wall (ft)</u>	<u>Maximum Velocity, U_m (ft/sec)</u>	<u>$D = \frac{U_{mT}}{2.74}$ (ft)</u>
3.0	2.6	0.5
5.0	1.58	0.3
18.0	0.96	0.175

Period = 0.5 sec
Frequency = 2 Hz



SECTION A-A

FIGURE L.6A-1 SHEET 2 OF 2
STRUT LOCATIONS
RIVER BEND STATION UPDATED SAFETY ANALYSIS REPORT

FIGURE L.6A-2

THE LOCA WATER JET LOAD ON THE STRUT IS SHOWN IN FIG.5. THE LOADING F IS NORMAL TO THE AXIS OF THE STRUT, HOWEVER ITS ORIENTATION CAN BE ARBITRARY. THE TIME HISTORY OF THE LOADING LEADING TO F IS SHOWN IN FIG.6.

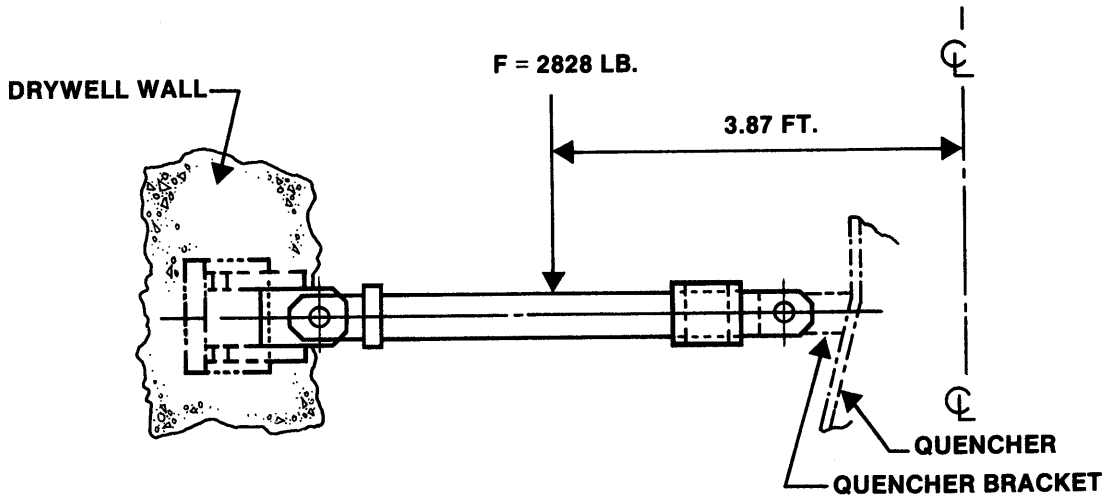


FIGURE 5

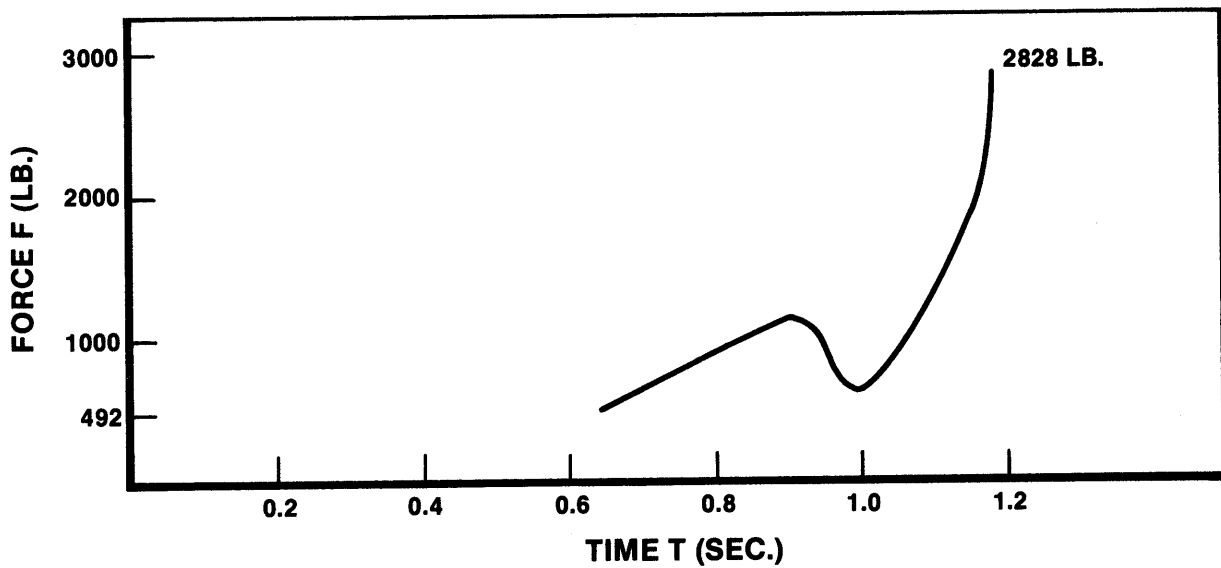


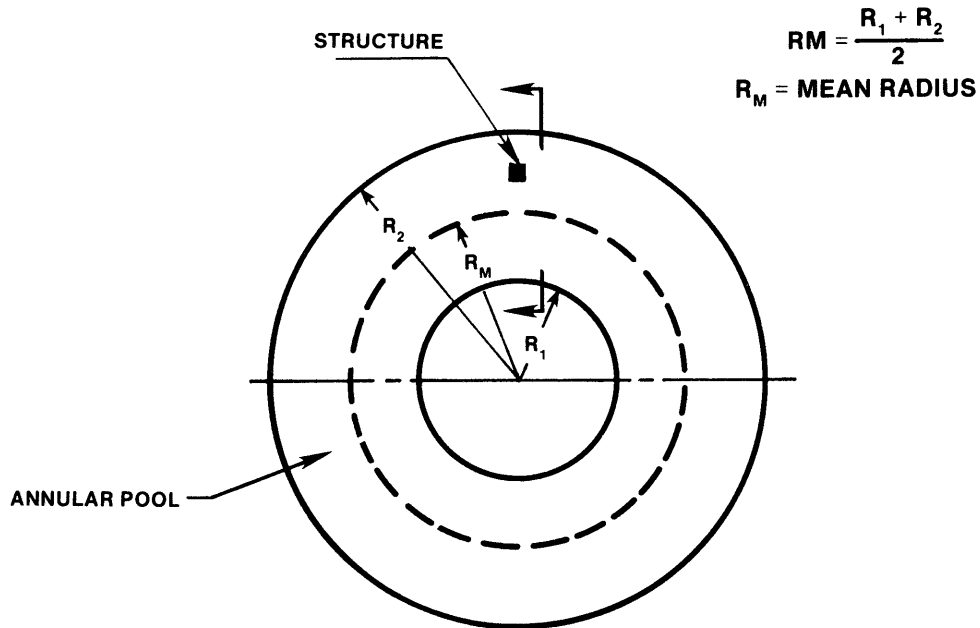
FIGURE 6

FIGURE L.6A-2

LOADING ON THE STRUT
WITH RADIUS = 0.276 FT.

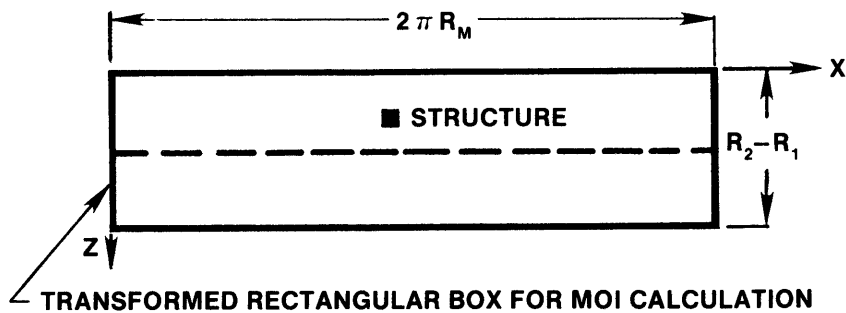
RIVER BEND STATION
UPDATED SAFETY ANALYSIS REPORT

THE POOL IS APPROXIMATED BY UNWRAPPING THE ANNULAR POOL AND TRANSFORMING IT INTO A RECTANGULAR BOX WITH THE SHOWN DIMENSIONS. THE LOCAL X COORDINATE AXIS OF THE TRANSFORMED POOL IS CENTERED WITH RESPECT TO THE STRUCTURE.



$$R_M = \frac{R_1 + R_2}{2}$$

$R_M = \text{MEAN RADIUS}$



LOCAL MOI COORDINATES:

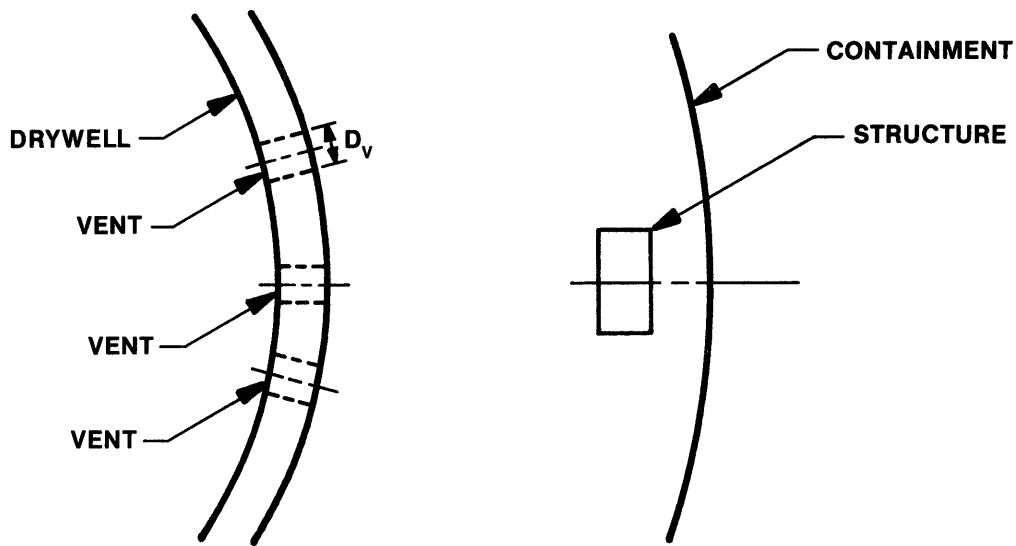
X IS IN THE DRAWING AZIMUTHAL DIRECTION
 Y IS IN THE VERTICAL UP DIRECTION
 Z IS IN THE NEGATIVE RADIAL DIRECTION

$K_1 = 39.5 \text{ FT}$
 $R_2 = 60.0 \text{ FT}$

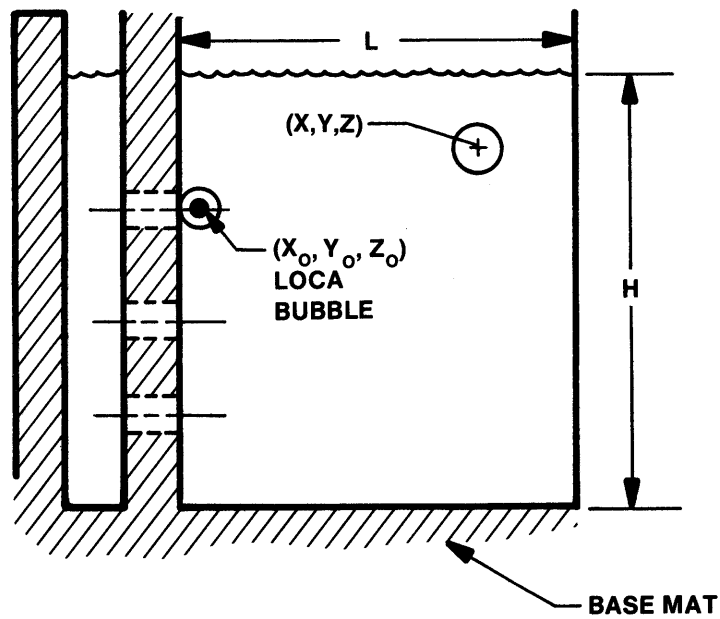
FIGURE L.6A-3 SHEET 1 OF 2

SUPPRESSION POOL MODEL FOR MOI

RIVER BEND STATION
 UPDATED SAFETY ANALYSIS REPORT



(a) PLAN VIEW OF POOL SEGMENT



(b) ELEVATION VIEW

REF: GESSAR FIG. 3BL-8

FIGURE L.6A-3 SHEET 2 OF 2

SUPPRESSION POOL MODEL FOR MOI

RIVER BEND STATION
 UPDATED SAFETY ANALYSIS REPORT

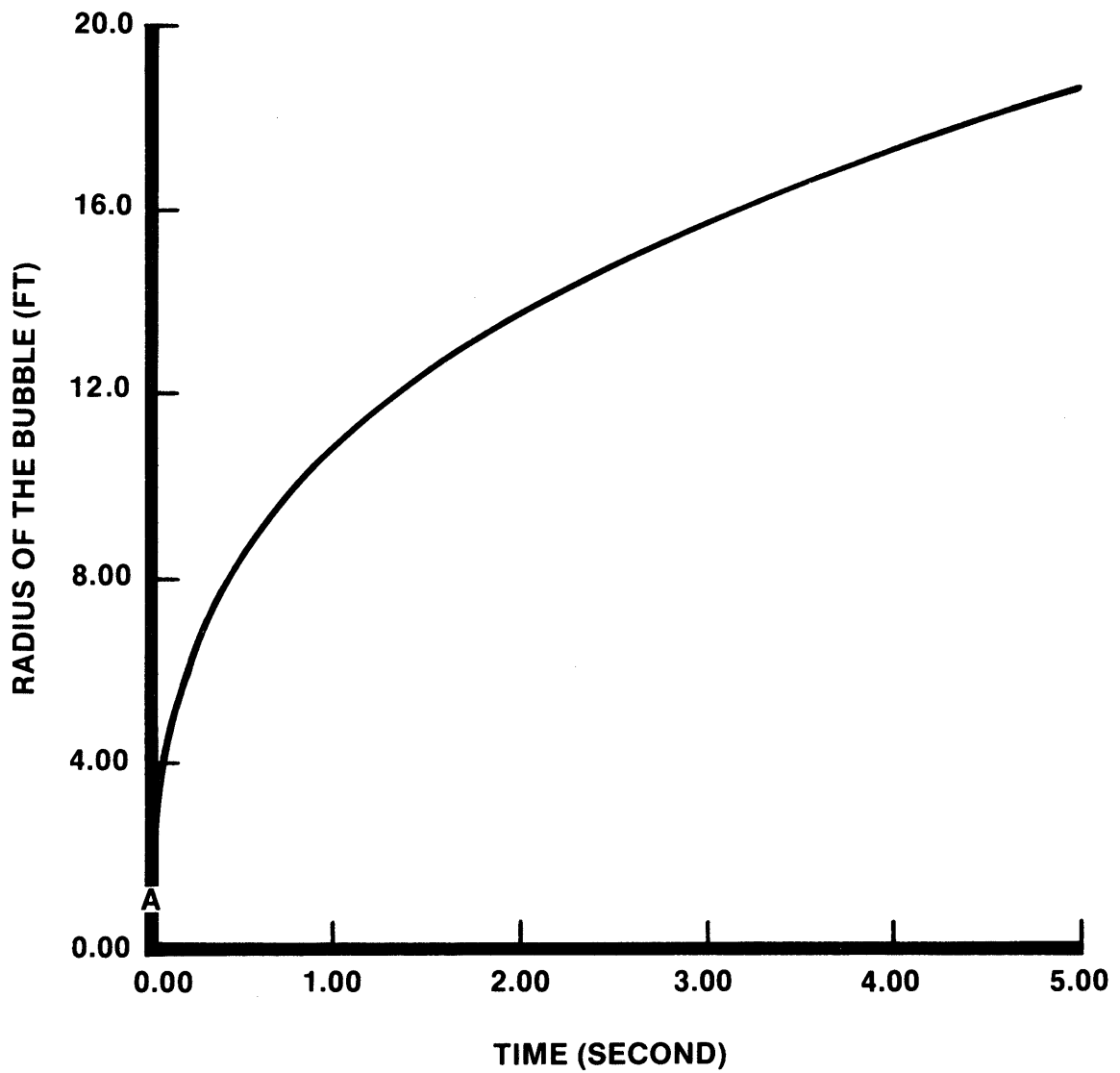
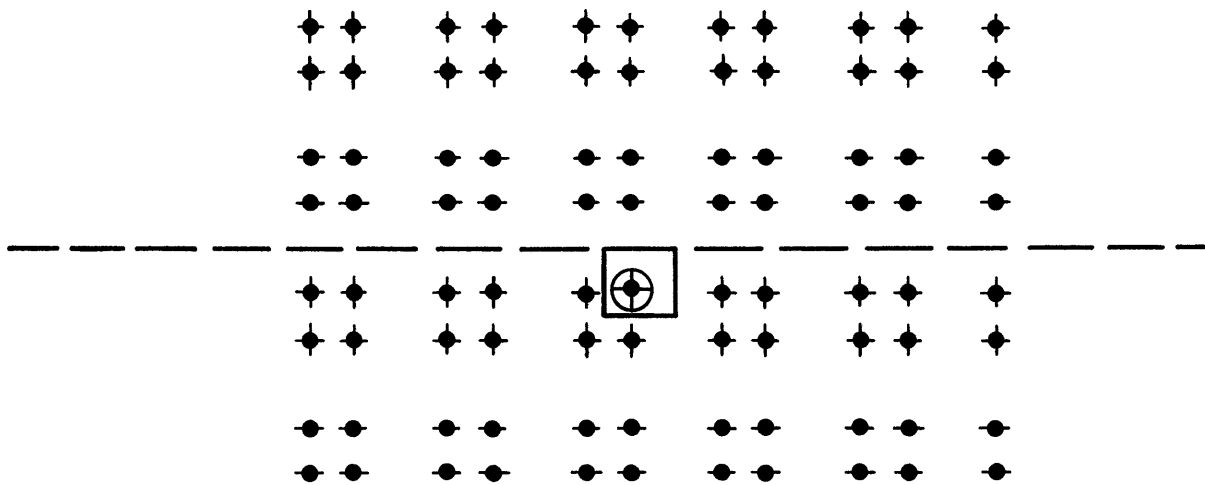


FIGURE L.6A-4

LOCA BUBBLE RADIUS GROWTH

RIVER BEND STATION

UPDATED SAFETY ANALYSIS REPORT



LEGEND:

-  REAL SOURCE (BUBBLE)
-  IMAGINARY SOURCE
-  IMAGINARY SINK

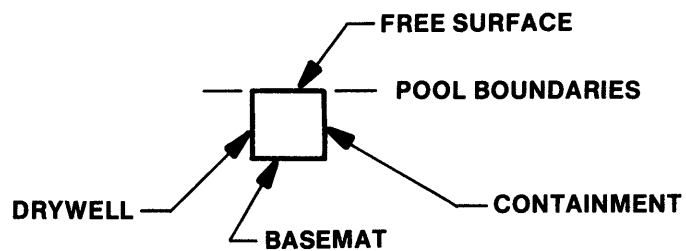
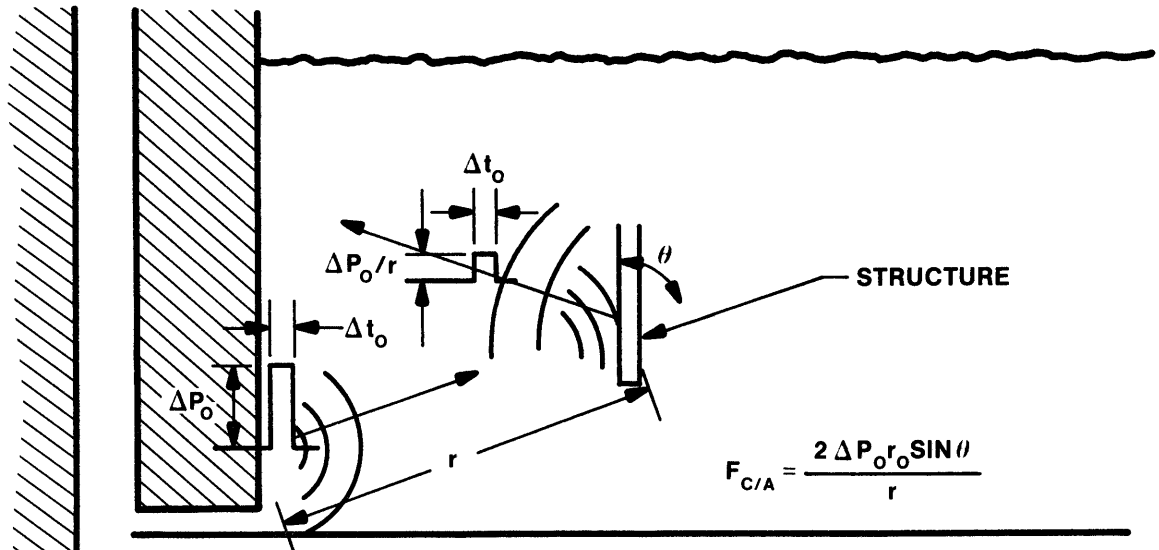


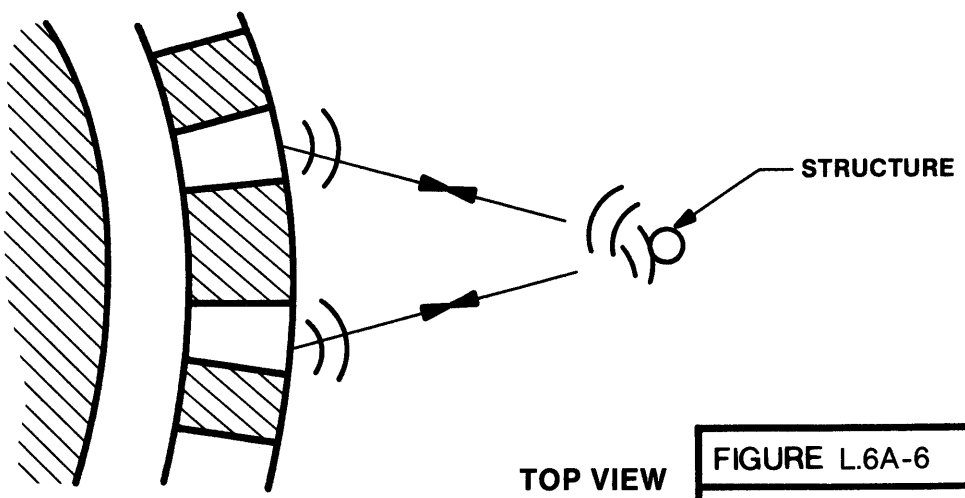
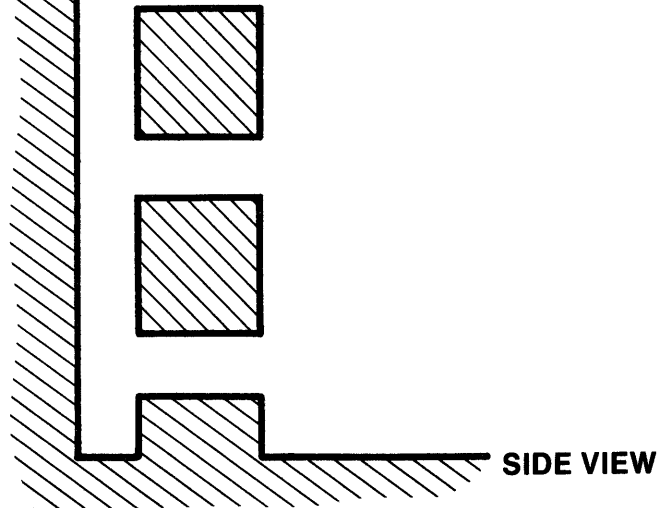
FIGURE L.6A-5

ARRANGEMENT OF IMAGES

RIVER BEND STATION
 UPDATED SAFETY ANALYSIS REPORT



$$F_{C/A} = \frac{2 \Delta P_0 r_0 \sin \theta}{r}$$



TOP VIEW

REF: GESSAR FIG. 3BL-9

FIGURE L.6A-6
MARK III HORIZONTAL VENT CHUGGING
RIVER BEND STATION
UPDATED SAFETY ANALYSIS REPORT

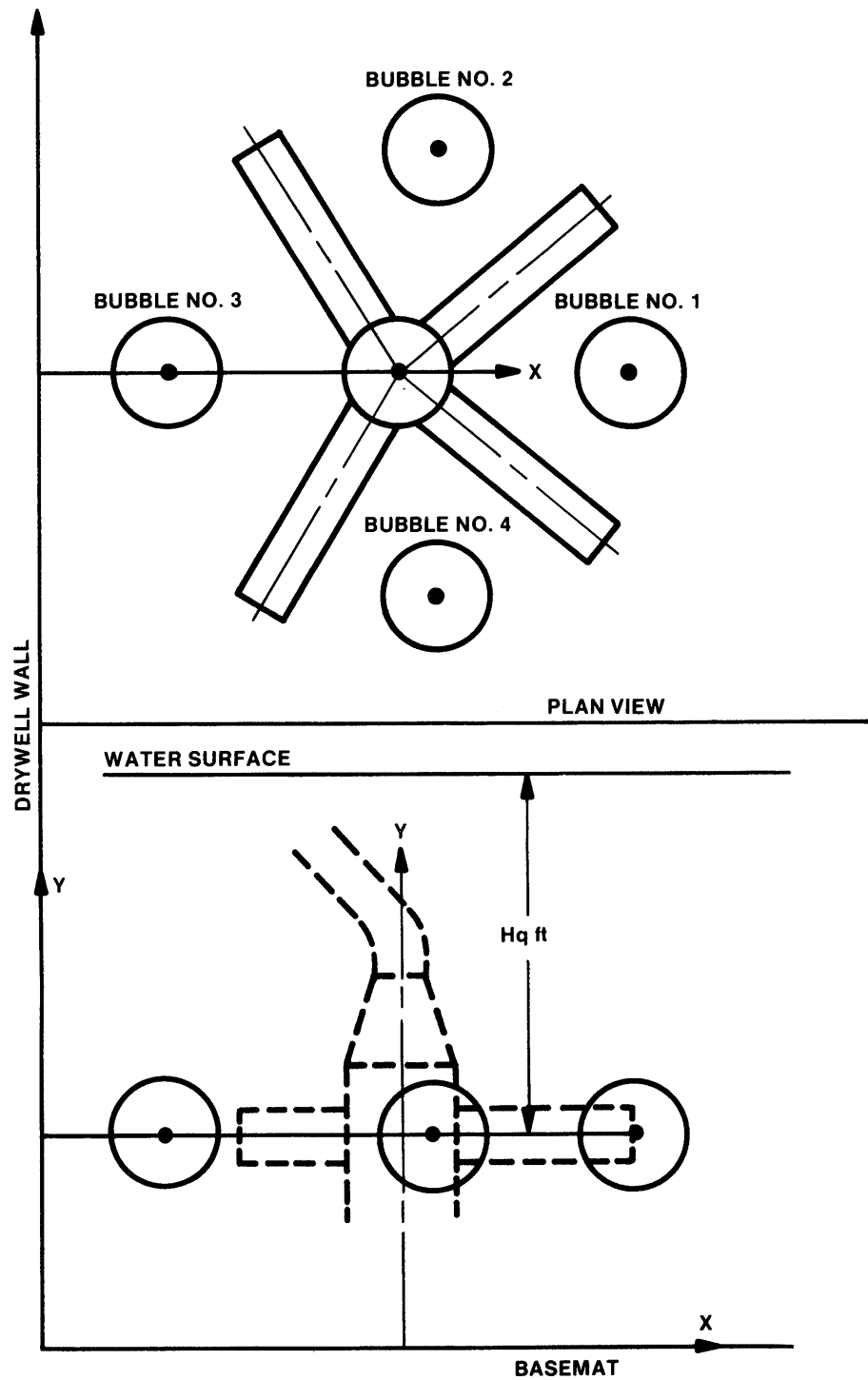


FIGURE L.6A-7

FOUR-BUBBLE MODEL FOR QUENCHER
AIR DISCHARGE

RIVER BEND STATION
UPDATED SAFETY ANALYSIS REPORT

RBS USAR

ATTACHMENT M
(TO APPENDIX 6A)

POOL SWELL VELOCITY

August 1987

RBS USAR

ATTACHMENT M
(TO APPENDIX 6A)

POOL SWELL VELOCITY

The pool swell velocity used to evaluate loads on structures in the pool swell zone for RBS is defined as a function of height above the initial pool surface in Section 6A.10.2. The velocity is specified to increase from zero to the maximum value of 50 ft/sec in the first 10 ft above the initial surface elevation. Between 10 ft and 20 ft above the initial surface, the velocity is assumed to be constant at 50 ft/sec and from 20 ft to 30 ft the velocity is reduced due to deceleration by gravity. Section 6A.10 provides equations for calculating the velocity to be used in design.

RBS USAR

ATTACHMENT N
(TO APPENDIX 6A)

MULTIPLE SAFETY/RELIEF VALVE ACTUATION
FORCING FUNCTION METHODS

August 1987

RBS USAR

ATTACHMENT N
(TO APPENDIX 6A)

MULTIPLE SAFETY/RELIEF VALVE ACTUATION
FORCING FUNCTION METHODS

TABLE OF CONTENTS		
<u>Section</u>	<u>Title</u>	<u>Page</u>
N.6A.1	INTRODUCTION	N.6A-1
N.6A.2	RANDOM PARAMETERS	N.6A-2
N.6A.2.1	Reactor Vessel Pressure Rise Rate (PRR)	N.6A-2
N.6A.2.2	Valve Setpoint Tolerance (VST)	N.6A-2
N.6A.2.3	Valve Opening Time (VOT)	N.6A-2
N.6A.2.4	Quencher Bubble Frequency Distribution (QBF)	N.6A-3
N.6A.3	MONTE CARLO TRIAL SIMULATIONS	N.6A-4
N.6A.3.1	Basis for Using 59 Monte Carlo Trial Simulations	N.6A-4
N.6A.3.2	Sensitivity of Forcing Function to Valve Setpoint Standard Deviation	N.6A-5
N.6A.3.2.1	Analysis of Time Between Actuation of Valve Groups	N.6A-5
N.6A.3.2.2	Effect on Forcing Function	N.6A-6
N.6A.3.3	Monte Carlo Trial Simulation Analysis	N.6A-7
N.6A.3.4	Bubble Arrival Time	N.6A-8
N.6A.3.4.1	Calculation of Reference Arrival Time	N.6A-8
N.6A.3.4.2	Adjustment of Bubble Arrival Time for Pressure Setpoint Variations	N.6A-8
N.6A.3.4.3	Adjustment of Bubble Arrival Time for Valve Opening Time Variations	N.6A-8
N.6A.3.5	Quencher Bubble Frequency Variation	N.6A-9
N.6A.4	FACTORS AFFECTING PRESSURE DISTRI- BUTION ON THE SUPPRESSION POOL BOUNDARY	N.6A-9
N.6A.4.1	Bubble Pressure Attenuation	N.6A-9
N.6A.4.2	Line-of-Sight Influence	N.6A-9

RBS USAR

ATTACHMENT N
(TO APPENDIX 6A)

TABLE OF CONTENTS (Cont)

<u>Section</u>	<u>Title</u>	<u>Page</u>
N.6A.4.3	Combination of Multiple SRV Pressure Time Histories	N.6A-9
N.6A.5	FORCING FUNCTIONS FOR NSSS EQUIPMENT EVALUATION	N.6A-9
N.6A.5.1	Time Sequencing	N.6A-9
N.6A.5.2	Pressure Time Histories	N.6A-10
N.6A.5.3	Vertical Basemat Force and Overturning Moment	N.6A-10
N.6A.5.4	Fourier Spectra	N.6A-10
N.6A.6	STRUCTURAL RESPONSE ANALYSIS	N.6A-11
N.6A.7	EXAMPLE OF TYPICAL TIME SEQUENCING APPLICATION	N. 6A-11
N.6A.8	COMPARISON OF SELECTED TRIALS WITH THE FOURIER SPECTRA OF THE 59 MONTE CARLO SIMULATIONS	N. 6A-11
N.6A.9	CONSERVATISM OF SRVA METHODOLOGY	N.6A-11

RBS USAR

ATTACHMENT N
(TO APPENDIX 6A)

LIST OF TABLES

<u>Table Number</u>	<u>Title</u>
N.6A-1	CRITICAL TRIAL SELECTION
N.6A-2	INPUT DATA UNCERTAINTY
N.6A-3	SENSITIVITY RESULTS

RBS USAR

ATTACHMENT N
(TO APPENDIX 6A)

LIST OF FIGURES

<u>Figure Number</u>	<u>Title</u>
N.6A-1	PROBABILITY DENSITY FUNCTION VERSUS PRESSURE RISE RATE
N.6A-2	PROBABILITY DENSITY FUNCTION VERSUS VALVE GROUP SETPOINT VARIATION
N.6A-3	PROBABILITY DENSITY FUNCTION VERSUS VALVE OPENING TIME VARIATION (CROSBY AND DIKKERS VALVES)
N.6A-4	BUBBLE PRESSURE TIME HISTORY $F = 9$ Hz
N.6A-5	PROBABILITY DENSITY FUNCTION VERSUS BUBBLE FREQUENCY
N.6A-6	EFFECT OF VALVE SETPOINT TOLERANCE ON VALVE OPENING TIME

RBS USAR

ATTACHMENT N
(TO APPENDIX 6A)

MULTIPLE SAFETY/RELIEF VALVE
ACTUATION FORCING FUNCTION METHODS

N.6A.1 INTRODUCTION

This attachment describes the procedure for determining the safety/relief valve (SRV) discharge 95-95 percent confidence level forcing functions that are imposed on the containment structure to obtain structural responses which are used as input for the evaluation of equipment located within the containment. The procedure utilizes the random nature of several parameters that significantly influence the phase relationship of the individual air bubbles formed in the suppression pool during multiple SRV discharge events. The random variables that are utilized in this procedure are: 1) SRV setpoint tolerance, 2) valve opening time, 3) reactor vessel pressure rise rate, and 4) quencher bubble frequency.

The maximum positive and negative bubble pressures for each individual discharge location are determined by using the method described in Section A.6A.12.6. Test data indicated randomness in the peak pressure amplitude which could also be used for determining structural response. However, this is not being used at RBS.

Of the SRV cases identified for consideration in containment structural design, the expected bounding vertical response at equipment locations is based on the all-valve case. The expected bounding horizontal response is based on either the single-valve subsequent actuation, two adjacent valves, or the all-valve case. The ADS case is also evaluated. From each of these four cases, the Fourier spectra of the forcing functions for 59 Monte Carlo simulations of the event are plotted. A forcing function is then selected in each of the frequency ranges of interest for use in developing the dynamic responses at a selected location on the containment structure (i.e., basemat, drywell, and containment). These dynamic responses are then employed for RBS equipment evaluations. A dynamic time-history analysis is performed to determine the acceleration time histories, response spectra, and displacements needed. Dynamic responses for equipment evaluations are made by enveloping the results from the selected trial cases with the largest Fourier spectra magnitude in each frequency interval. For clarification, an example is presented in Section N.6A.7.

N.6A.2 RANDOM PARAMETERS

N.6A.2.1 Reactor Vessel Pressure Rise Rate (PRR)

The PRR distribution for RBS is shown in Fig. N.6A-1. The distribution is determined from an evaluation of BWR/6 transient events. The figure represents the probability density function for pressure rise rates for events opening more than two-thirds of the SRVs weighted by the relative occurrence of the events and averaged overall reactor conditions anticipated during the last 40 percent of an operating cycle. The lower limit of 40 psi/sec is the minimum pressure rise rate expected to open two-thirds of the SRVs. The upper limit of 140 psi/sec has a high probability of not being exceeded for any operating condition.

GESSAR Section 3BP.1 demonstrates that no unique PRR can be identified that will yield a maximum forcing function. Therefore, the PRR should be included as a variable in the Monte Carlo method. It should be noted that the PRR variable is only used in the all-valve case Monte Carlo event simulations.

N.6A.2.2 Valve Setpoint Tolerance (VST)

The setpoints for SRVs on RBS are arranged in three groups with redundant logic trains consisting of a pressure transducer and three pressure switches. The logic for RBS design consists of one pressure switch set at 1103 psi, eight on a pressure switch set at 1113 psi, and the remaining seven on a pressure switch at 1123 psi. A testability feature is also included which utilizes pressure trip instrumentation. The tolerance on the pressure switch setpoints with this testability feature is based on a normal (Gaussian) distribution with a standard deviation of 2 psi as shown in Fig. N.6A-2. For the grouped arrangement, the standard deviation is applied to the group setpoints; thus, the valves within the group will have the same adjustment.

The SRV arrangement and pressure setpoints for RBS are identified in Fig. A.6A.4-3.

N.6A.2.3 Valve Opening Time (VOT)

Test data indicate that there is a normal distribution for the VOT with a standard deviation of 0.009 sec, as shown in Fig. N.6A-3.

N.6A.2.4 Quencher Bubble Frequency Distribution (QBF)

A typical forcing function for a quencher SRV bubble is shown in Fig. A.6A.5-13. The bubble lasts effectively 0.75 sec in the suppression pool. In the 8-Hz bubble, the pressure decays to one-third of the peak value over five cycles and a complete pressure cycle oscillation period lasts 0.125 sec, 0.05 sec for the positive pulse, and 0.075 sec for the negative pulse. For other frequencies, the same damping definition applies (i.e., two-thirds decay over five cycles or 0.133 decay per cycle).

The quencher bubble pressure time history in Fig. A.6A.5-13 is an idealized bubble model. This pressure trace is digitized for use in this procedure. Rather than truncating the pressure time history at 0.75 sec, when the bubble leaves the pool, the pressure is reduced from the last peak before $t=0.75$ sec to zero over a time equal to $1/2$ of the period, using the relationship

$$A = A_{LP} \left[\frac{1 + \cos(2\pi f)(t - t_0)}{2} \right]^4$$

where:

- A_{LP} = Pressure at last peak (+ or -)
- f = Bubble frequency
- t = Time
- t_0 = Time of last peak before 0.75 sec

Fig. N.6A-4 shows the bubble pressure time history for $f=9$ Hz. This smoothing at the end of the bubble pressure time history is more realistic and eliminates unnecessary noise in the loading.

Quencher test data show that the frequency of the air bubble is a function of the SRV discharge line air volume. The distribution of bubble frequencies for a discharge line air volume of 50 cu ft is shown in Fig. N.6A-5 and is used as the reference for this procedure. This reference value is the SRV line volume from the operating plants from which the quencher bubble frequency data were obtained. The normal distribution for the curve has a mean frequency of 1.8 Hz with a standard deviation of 1.7 Hz. It is truncated at the minimum and maximum bounds of 5 and 12 Hz.

N.6A.3 MONTE CARLO TRIAL SIMULATIONS

N.6A.3.1 Basis for Using 59 Monte Carlo Trial Simulations

The method used to develop the overall forcing function from the 59 Monte Carlo trials begins with selecting critical trials. Those trials giving peak spectral values in vertical forces and overturning moments in three frequency ranges as described in Section N.6A.5.4 are selected from Fourier transforms of the 59 trials. Each critical trial is selected independently to obtain one of the nine spectral peaks used (one vertical force and two rocking moments in each of three frequency ranges). The 95-95 percent confidence level is for the calculated spectral peaks and is based on the input probability distributions.

Since calculated forces and moments are used in the selection process, using the forcing function to calculate these loads does not decrease the final confidence level.

The data base used to develop the input probability distributions was reviewed to evaluate the uncertainty in input means and standard deviations. The results are summarized in Table N.6A-2.

Sensitivity results are summarized in Table N.6A-3. The sensitivity of -1 percent per psi for valve setpoint tolerance is based on the analysis in Section N.6A.3.2. Examination of these sensitivity results shows that uncertainties in the valve setpoint tolerance and in the shape of the valve opening time distribution have negligible effects on calculated peak spectral values. Variations in the mean quencher bubble frequency can cause a shift in the envelope of spectral peaks, while variations in the shape of the bubble frequency distribution can affect the amplitude and distribution of spectral values. This later variation preserves the energy content under the spectral peaks, however, so that the response spectrum is insensitive. It is concluded that uncertainties in the shape of the input probability distribution are not important to the overall process.

The overall confidence level in the loads is much better than the 95-95 percent level in the spectral peaks. The reason for this is that design bubble pressures are used in the simulations instead of nominal bubble pressures. Consequently, the spatial and time attenuation of actual bubbles are bounded, and calculated peak bubble pressures bound measured bubble pressures with ample margin. The time attenuation curve currently used is compared with measured

attenuation in GESSAR Figure 3BN-6. Calculated and measured pressures are compared in Section N.6A.9. Additional margin is provided in the structural analysis, where peak broadening of the response spectrum by 15 percent is done. Low damping factors, used in the structural analysis, also add margin by magnifying peaks in the spectrum of the forcing function.

GESSAR Section 3BP.4 shows that quencher bubble frequency is the only random variable for which uncertainties in the input probability distribution have a significant effect on the calculated peak spectral values. A shift in the mean bubble frequency induces a one-for-one shift in the envelope of spectral peaks. Reduction in the standard deviation increases peak spectral values, but preserves the energy under the peak. These effects do not significantly affect design margins.

Section N.6A.9 shows that local pressure loads produced by any of the 59 trials will bound the in-plant Caorso measured pressure after peak broadening is applied to an amplified response spectrum (ARS) analysis. GESSAR Section 3BN.8 shows that the procedure for selection of critical trials gives coverage of the spectrum comparable to using all 59 trials. These results confirm that the overall forcing function has adequate margin for design of piping and equipment.

N.6A.3.2 Sensitivity of Forcing Function to Valve Setpoint Standard Deviation

The sensitivity of the forcing function to valve setpoint tolerance is estimated and shown to be small. In Section N.6A.3.2.1, the probability distribution for the time interval between valve actuations is determined. In Section N.6A.3.2.2, the sensitivity of the forcing function to errors in the input value of the setpoint standard deviation is estimated.

N.6A.3.2.1 Analysis of Time Between Actuation of Valve Groups

River Bend Station has 16 valves. The lowest setpoint valve is actuated individually, and the remaining valves are actuated in two groups of eight and seven valves each with nominal setpoints 10 and 20 psi, respectively, above that of the lowest setpoint valve. Variation in the setpoint affects the time interval between actuation of valve groups as shown on Fig. N.6A-6. The following analysis provides an estimate of the effect on forcing function.

Let:

t = Time between actuation of valve groups
 t_0 = Nominal time of Group 1 actuation
 t_1 = Actual time of Group 1 actuation
 t_2 = Time of Group 2 actuation
s = Nominal setpoint difference
r = Pressure rise rate
 e_1 = Random component of Group 1 opening time
 e_2 = Random component of Group 2 opening time

desire $p(t > X)$ = probability that the time interval between valve actuations is greater than some value, X.

By definition,

$$t_1 = t_0 + e_1$$

$$t_2 = t_0 + s/r + e_2.$$

Then

$$t = t_2 - t_1 = s/r + e_2 - e_1.$$

The desired probability is

$$\begin{aligned} p(t > X) &= p(s/r + e_2 - e_1 > X) \\ &= p(e_2 - e_1 > X - s/r). \end{aligned}$$

Now, e_1 and e_2 are independent random variables with zero mean, and variance $\sigma^2 = (2.1)^2/r^2$. The linear combination of e_1 and e_2 has zero mean and variance $2\sigma^2 = 2(2.1)^2/r^2$. The distribution of $e = e_2 - e_1$ has zero mean and standard deviation:

$$\overline{\sigma} = \left[\frac{2(2.1)^2}{r^2} \right]^{1/2} \approx \frac{3.0}{r}$$

The time interval between actuation of valve groups is $t = s/r + e$. The mean time is s/r and the minimum time (90 percent confidence) is $s - 3.85/r$.

N.6A.3.2.2 Effect on Forcing Function

By the time the second valve group is actuated, the contribution to the forcing function from the first group is decaying at a fractional rate of 2/15 per bubble cycle (using the waveform of Fig. A.6A.5-13). Thus, if the time

interval for valve actuation is reduced from s/r to $s/r - 1.282 \bar{\sigma}$ (90 percent confidence level), the contribution to the forcing function from the first valve group will increase by a fractional amount:

$$\phi = 2/15 (\bar{f}) 1.282 \bar{\sigma}$$

Where \bar{f} is the average bubble frequency. Nominal values for \bar{f} and $\bar{\sigma}$ are:

$$\bar{f} = 8.1 \text{ cycles/sec}$$

$$\bar{\sigma} = 0.33 \text{ sec (assuming } r = 90 \text{ psi/sec)}$$

The effect of this change is to increase the Group 1 contribution by 4.6 percent of its maximum value. For two groups of nine valves, the contribution of Group 1 to the forcing function is less than half of the total amplitude on the average. Thus, the estimated effect of a 100-percent error in the standard deviation of the valve setpoint is less than a 2.3-percent change in the forcing function with 90-percent confidence.

N.6A.3.3 Monte Carlo Trial Simulation Analysis

There are four SRV cases that are considered to get bounding forcing function for the equipment evaluations. They are:

1. Single valve subsequent actuation
2. Two adjacent valves
3. ADS valves
4. All valves

In each of these cases, 59 Monte Carlo trials are performed in which appropriate random variable adjustments are selected for the parameters listed in Section N.6A.2. For the single-valve subsequent actuation case, only the quencher bubble frequency is varied. For the ADS and two adjacent valve cases, the valve setpoint tolerance and pressure rise rate considerations are not incorporated for obtaining the forcing function because the entire group of ADS valves is simultaneously activated by a single signal. For the all-valve case, all variables are considered.

The all-valve trials each consist of selecting a random pressure rise rate from Fig. N.6A-1 and a random pressure

switch setpoint for each group of SRVs using Fig. N.6A-2. This information is used to compute the bubble arrival time difference or separation between each group of valves. These bubble arrival times are adjusted for each individual valve by randomly selecting a time variation due to valve opening time (VOT) using Fig. N.6A-3.

Once the bubbles are in the suppression pool, each bubble frequency is randomly varied by selecting a frequency from a unique distribution for the discharge line volume involved. Fig. N.6A-5 is used. The bubble time history for each valve location is then used to determine the forcing function on the suppression pool boundary by utilizing the methods described in Section A.6A.10.3.1.

For the ADS and two adjacent valve cases, each trial assumed that all valves are actuated together and then bubble phasing is adjusted by randomly selecting a time variation due to VOT for each valve. Each bubble frequency is then randomly selected as for the multiple valve trials. For the single-valve case, only the bubble frequency is varied.

N.6A.3.4 Bubble Arrival Time

N.6A.3.4.1 Calculation of Reference Arrival Time

The arrival time for each air bubble in the suppression pool relative to the lowest set SRV is a function of the SRV setpoint arrangement and the reactor pressure rise rate. Assuming no tolerance on setpoints, no variation in VOT, and randomly selecting a pressure rise rate (PRR), the arrival times of the bubbles in the suppression pool are computed by dividing the nominal setpoint differences (i.e., $\Delta p = 10$ and 20 psi) by the PRR. SRV discharge line lengths are not considered. For nominal setpoints at 1103, 1113, and 1123 psi, the time separation is 0.077 and 0.154 seconds based upon PRR = 130 psi/sec.

N.6A.3.4.2 Adjustment of Bubble Arrival Time for Pressure Setpoint Variations

As described in Reference 1 (Section 3BN.3.4.2).

N.6A.3.4.3 Adjustment of Bubble Arrival Time for Valve Opening Time Variations

As described in Reference 1 (Section 3BN.3.4.3).

N.6A.3.5 Quencher Bubble Frequency Variation

As described in Reference 1 (Section 3BN.3.5).

N.6A.4 FACTORS AFFECTING PRESSURE DISTRIBUTION ON THE SUPPRESSION POOL BOUNDARY

N.6A.4.1 Bubble Pressure Attenuation

The attenuation of the bubble pressure with distance r from the quencher is $2r_0 / r$, where r_0 = radius of the quencher (4.87 ft), $r \geq 2r_0$ (Section A.6A.10.3.1), and r = the true spatial distance from the quencher center to the node.

N.6A.4.2 Line-of-Sight Influence

The line-of-sight criterion for the bubble pressure states that points which cannot be seen through a direct line from the outer radius of the quencher arms to the location in question will not be affected by the pressure from that quencher (Section A.6A.10.3.2.1).

N.6A.4.3 Combination of Multiple SRV Pressure Time Histories

The time sequencing application provides a given phase relationship between quencher bubbles. The pressure at each node point and time step is calculated by combining the contribution from each valve (in the line of sight) using algebraic summation. At each node where the total calculated pressure at any time step exceeds the maximum pressure (positive or negative) from any of the contributing valves, the calculated pressure at the specific time step is set equal to the maximum bubble pressure at the same instant in time.

N.6A.5 FORCING FUNCTIONS FOR NSSS EQUIPMENT EVALUATION

N.6A.5.1 Time Sequencing

Time sequencing with random parameters is used to arrive at the forcing function for the multiple SRV air-clearing events referenced in Section N.6A.3.3.

A Monte Carlo technique is used to generate the building forcing function for equipment evaluations. The bounding forcing function from 59 trials will result in a 95-percent confidence level that 95 percent of the time the actual forcing function will be less than the forcing function determined by the Monte Carlo technique.

N.6A.5.2 Pressure Time Histories

Fifty-nine cases of pressure distribution on the pool boundary are calculated using the random parameters delineated in Section N.6A.2.

N.6A.5.3 Vertical Basemat Force and Overturning Moment

The total basemat force is calculated as a function of time by integrating the node pressures over the suppression pool basemat incremental areas. The overturning moments (about two perpendicular horizontal axes through the basemat center upper surface) are calculated as a function of time by integrating the product (node pressure times the incremental area moment arm times the incremental area) over the suppression pool boundary (containment, basemat, and drywell wall).

N.6A.5.4 Fourier Spectra

Fourier spectra of the vertical basemat force and overturning moment for the 59 cases are developed for selecting the cases used to determine dynamic responses for equipment evaluations. The significant frequency range is divided into three frequency intervals determined as follows:

- Step 1. Adjust the mean frequency of each safety/relief valve discharge line for air volume differences (Section N.6A.3.5.1).
- Step 2. Calculate the mean frequency (f) for all applicable safety/relief valve discharge lines.
- Step 3. Establish the frequency intervals based on $0.5 f_m$ to $1.5 f_m$, $1.5 f_m$ to $2.5 f_m$, and $2.5 f_m$ to $3.5 f_m$

Where:

$$f_m = 1/N \sum f_i$$

$$i = 1, \dots, N$$

N = total number of valves actuated

The loading cases with the largest spectral value within each frequency interval (from the 59 cases) are selected for determination of equipment responses. A maximum of nine load trials is possible for each loading type.

N.6A.6 STRUCTURAL RESPONSE ANALYSIS

Forcing functions corresponding to the case selected in each frequency range (selected in Section N.6A.5.4) are used as input to the structural analysis. Structural dynamic analysis is then performed for these selected cases. Only the 16 valve discharge load cases produce a full nine trials. For other load cases the same trial appears as the dominant trial in more than one of the nine selection ranges. The resulting dynamic responses are then enveloped for RBS equipment evaluations.

The ADS case was found to be bounded by the 16 valve cases in each of the nine ranges. For this reason the ADS case was not analyzed, and the 16 valve results were used in place of ADS results.

N.6A.7 EXAMPLE OF TYPICAL TIME SEQUENCING APPLICATION

As described in Reference 1 (Section 3BN.7).

N.6A.8 COMPARISON OF SELECTED TRIALS WITH THE FOURIER SPECTRA OF THE 59 MONTE CARLO SIMULATIONS

As described in Reference 1 (Section 3BN.8).

N.6A.9 CONSERVATISM OF SRVA METHODOLOGY

As described in Reference 1 (Section 3BN.9).

RBS USAR

TABLE N.6A-1

CRITICAL TRIAL SELECTION

Example of one load case

<u>Frequency</u>	<u>Vertical</u>	<u>Rocking</u>	
		<u>Mx</u>	<u>My</u>
4-12	39*	57*	51
12-20	54*	27*	57
20-28	29*	47	9*

* Critical trials giving highest spectral value for either vertical force or rocking moment. For moments, the cases giving the highest values for either Mx or My are selected and the loads applied in both directions.

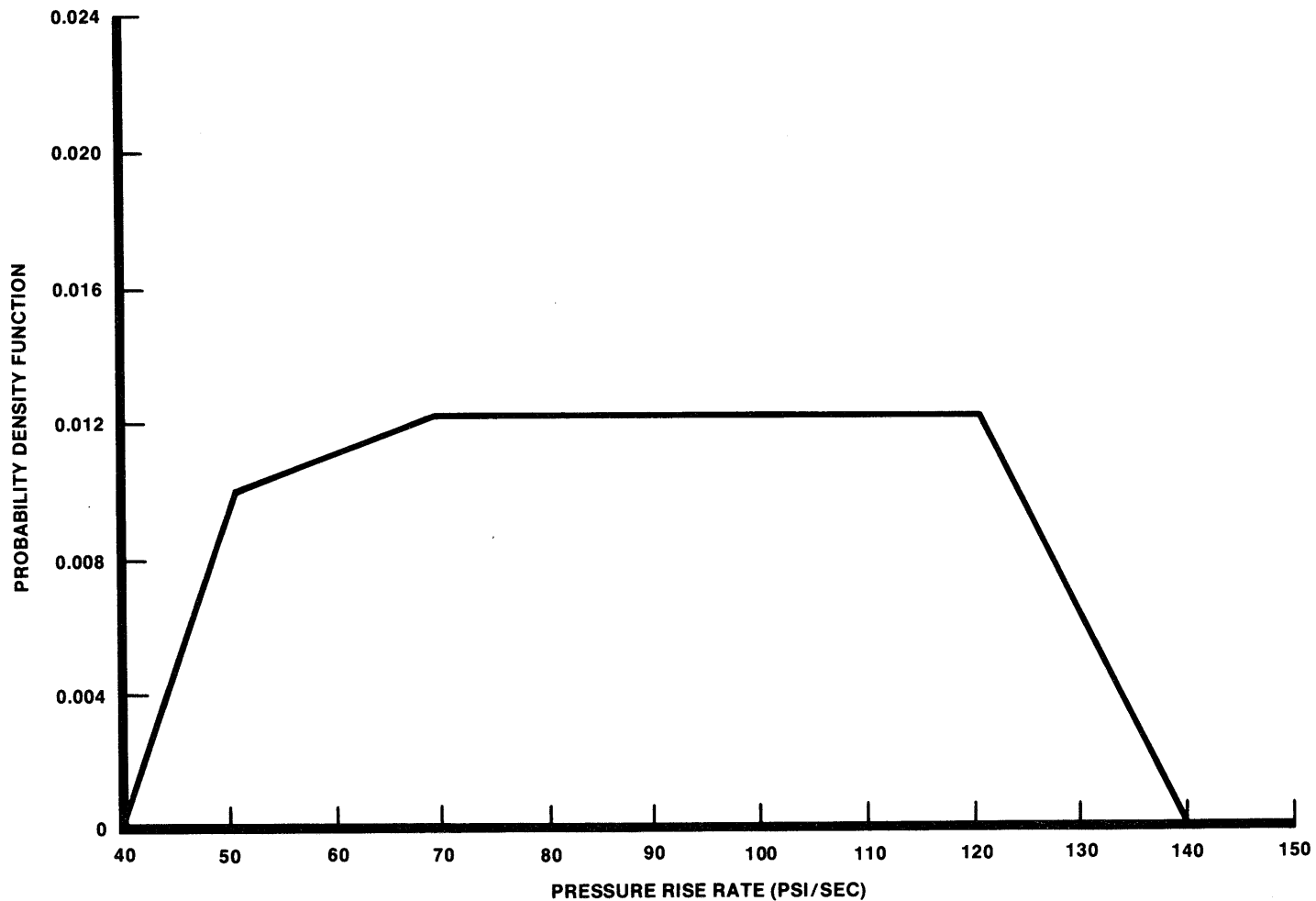
RBS USAR

TABLE N.6A-2

INPUT DATA UNCERTAINTY

<u>Measurement</u>	<u>σ</u>	<u>n</u>	<u>$2\sigma/\sqrt{n}$</u>	<u>% Uncertainty*</u>	
<u>Valve Opening Time</u>	<u>(msec)</u>	<u>(Samples)</u>	<u>(msec)</u>	<u>μ</u>	<u>σ</u>
Crosby	9.2	408	0.91	1.6	10
Dijkers	9.7	50	2.7	4.7	28
MK III Input	9.0	NA	NA	NA	NA
<u>Valve Setpoint Tolerance</u>	<u>(psi)</u>	<u>(Samples)</u>	<u>(psi)</u>		
Crosby } Dijkers }	2.1	NA	NA	NA	NA
MK III Input	2.0	NA	NA	NA	NA
<u>Bubble Frequency</u>	<u>(Hz)</u>	<u>(Samples)</u>	<u>(Hz)</u>		
	1.74	132	0.30	3.7	17

 * Indicates 2σ uncertainty for mean and standard deviation of indicated variable.

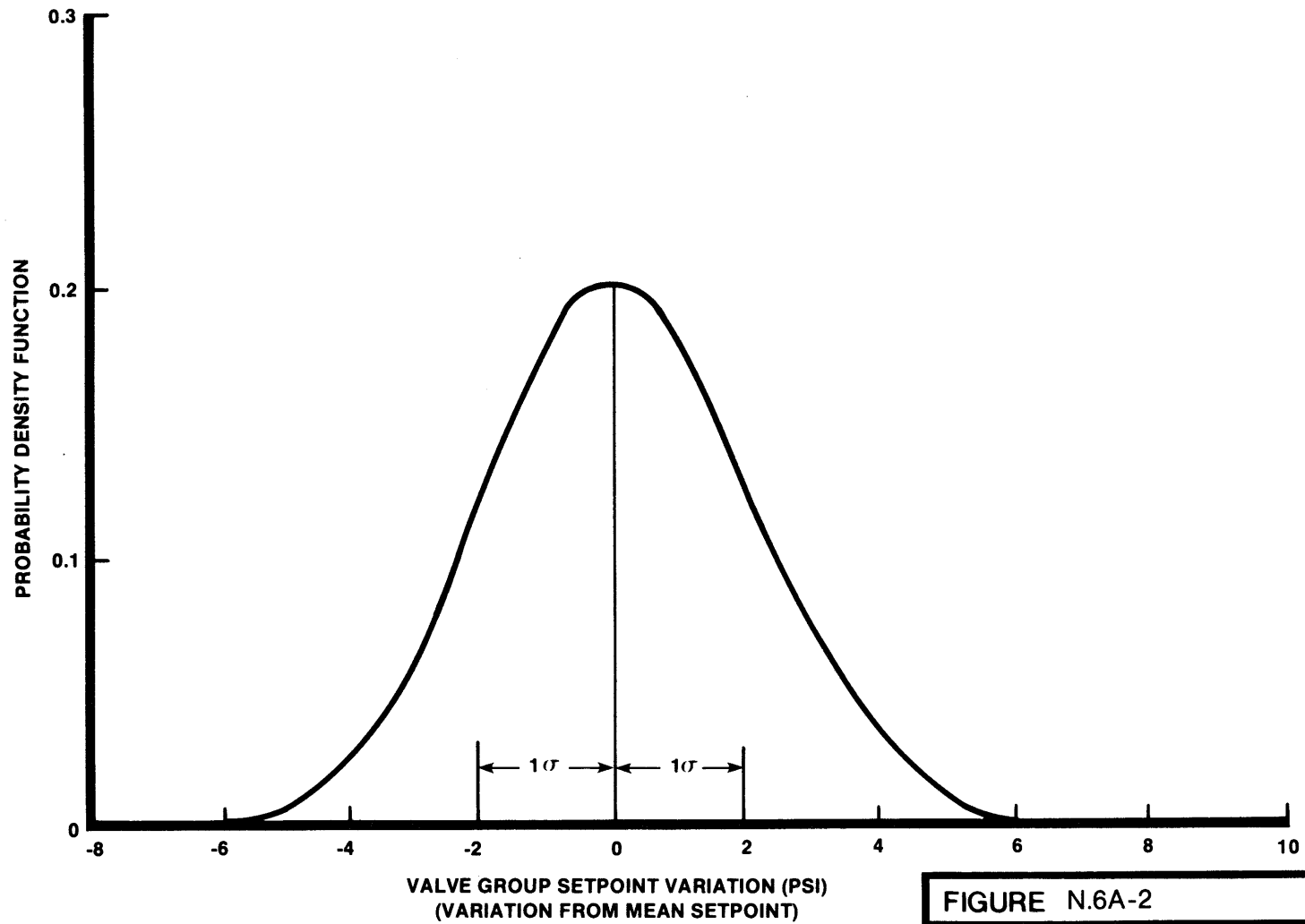


REF: GESSAR FIG. 3BN-1

FIGURE N.6A-1

PROBABILITY DENSITY FUNCTION VERSUS
PRESSURE RISE RATE

RIVER BEND STATION
UPDATED SAFETY ANALYSIS REPORT

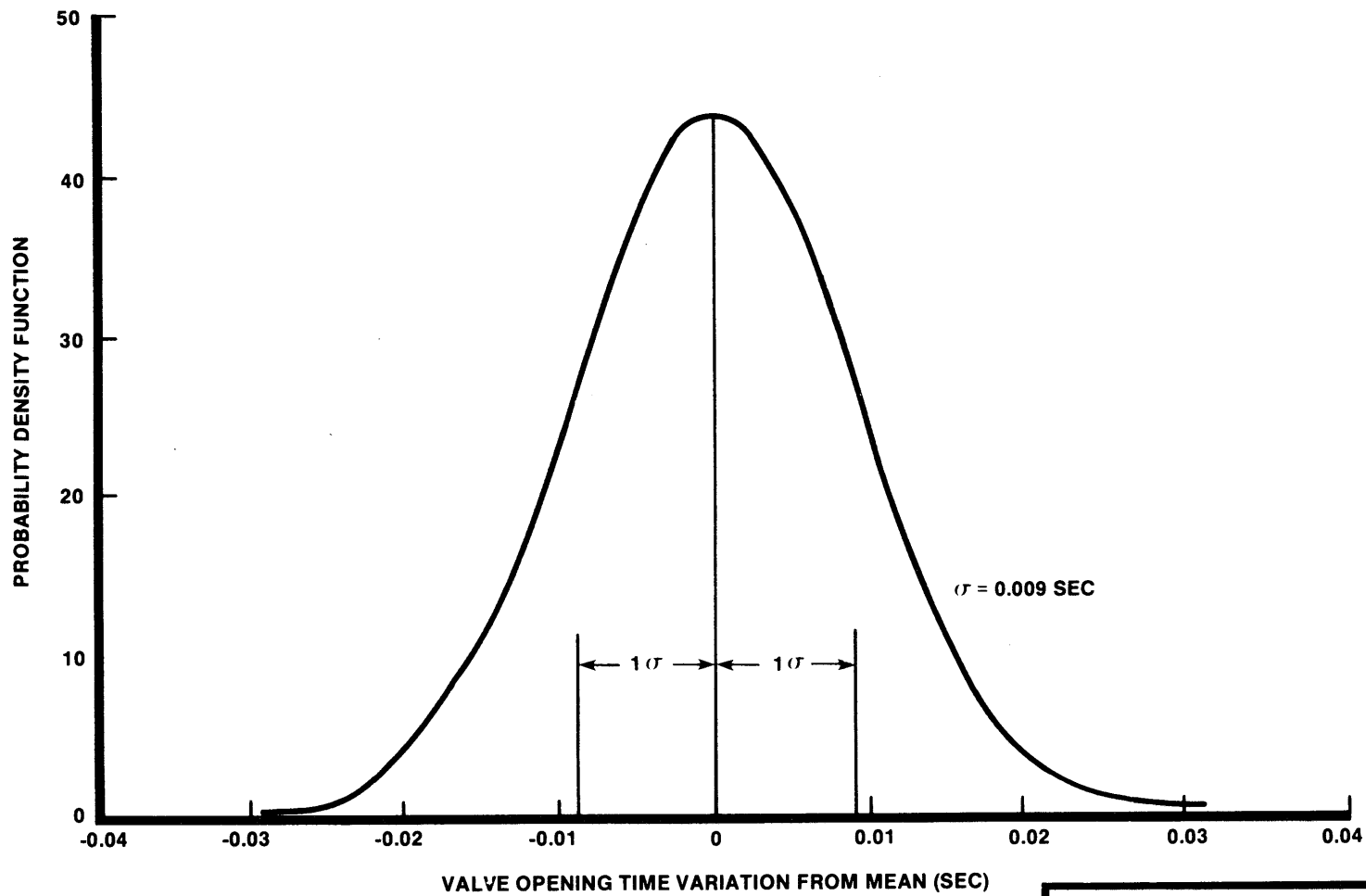


REF: GESSAR FIG. 3BN-2

FIGURE N.6A-2

PROBABILITY DENSITY FUNCTION VERSUS
VALVE GROUP SETPOINT VARIATION

RIVER BEND STATION
UPDATED SAFETY ANALYSIS REPORT



REF: GESSAR FIG. 3BN-3

FIGURE N.6A-3

PROBABILITY DENSITY FUNCTION VERSUS
VALVE OPENING TIME VARIATION
(CROSBY AND DIKKERS VALVES)

RIVER BEND STATION
UPDATED SAFETY ANALYSIS REPORT

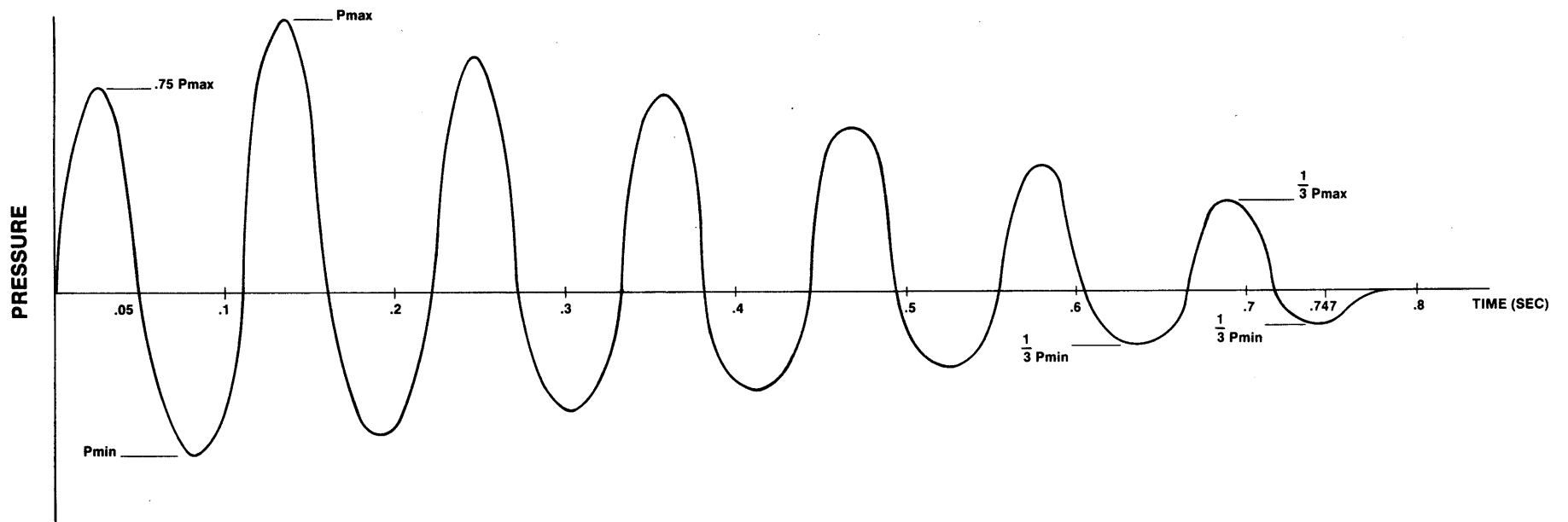
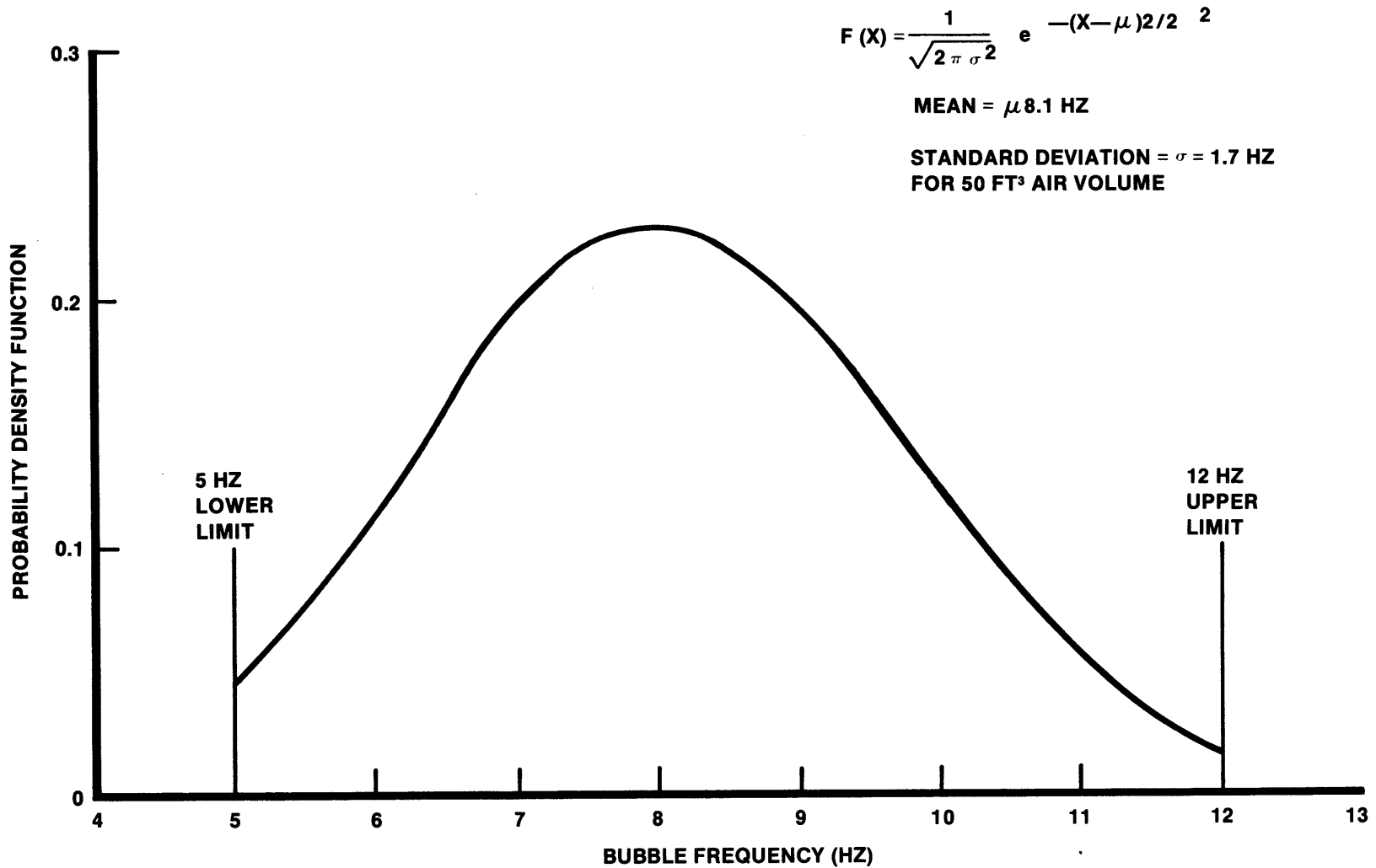


FIGURE N.6A-4

BUBBLE PRESSURE TIME HISTORY
 $f = 9 \text{ Hz}$

RIVER BEND STATION
 UPDATED SAFETY ANALYSIS REPORT



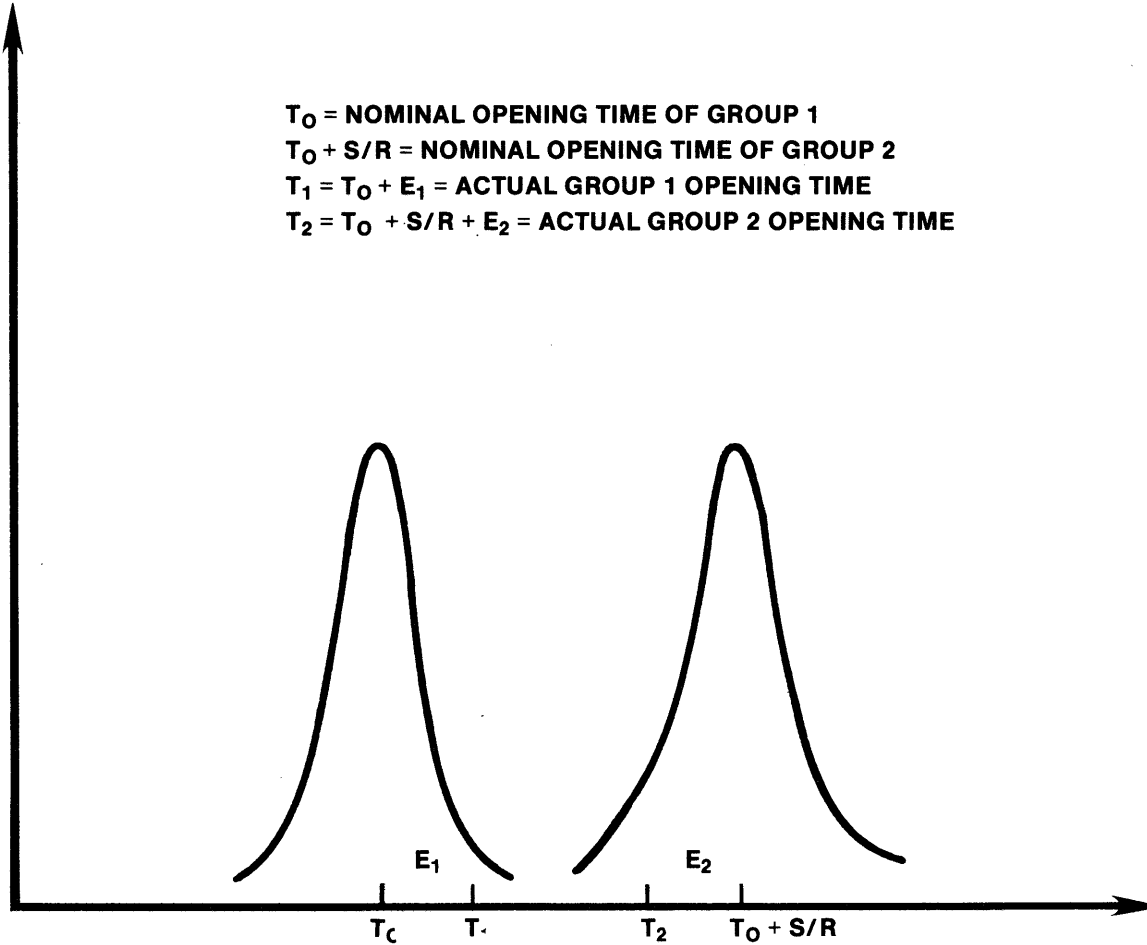
REF: GESSAR FIG. 3BN-5

FIGURE N.6A-5

PROBABILITY DENSITY FUNCTION VERSUS
BUBBLE FREQUENCY

RIVER BEND STATION
UPDATED SAFETY ANALYSIS REPORT

T_0 = NOMINAL OPENING TIME OF GROUP 1
 $T_0 + S/R$ = NOMINAL OPENING TIME OF GROUP 2
 $T_1 = T_0 + E_1$ = ACTUAL GROUP 1 OPENING TIME
 $T_2 = T_0 + S/R + E_2$ = ACTUAL GROUP 2 OPENING TIME



REF: GESSAR FIG. 3BN-7

FIGURE N.6A-6

EFFECT OF VALVE SETPOINT TOLERANCE
ON VALVE OPENING TIME

RIVER BEND STATION
UPDATED SAFETY ANALYSIS REPORT

RBS USAR

ATTACHMENT O
(TO APPENDIX 6A)

SUPPRESSION POOL TEMPERATURE RESPONSE TO
SAFETY RELIEF VALVE DISCHARGE EVENTS

August 1987

RBS USAR

ATTACHMENT O
(TO APPENDIX 6A)

SUPPRESSION POOL TEMPERATURE RESPONSE TO
SAFETY RELIEF VALVE DISCHARGE EVENTS

TABLE OF CONTENTS

<u>Section</u>	<u>Title</u>	<u>Page</u>
O.6A.1	INTRODUCTION	O.6A-1
O.6A.2	CONDENSATION TEMPERATURE LIMIT	O.6A-1
O.6A.3	PLANT TRANSIENT EVENTS	O.6A-3
O.6A.4	ASSUMPTIONS USED IN THE ANALYSIS	O.6A-4
O.6A.4.1	General Assumptions	O.6A-4
O.6A.4.2	Assumptions for Specific Events	O.6A-5
O.6A.4.2.1	Stuck-Open Relief Valve (SORV)	O.6A-5
O.6A.4.2.2	Primary System Isolation	O.6A-6
O.6A.4.2.3	ADS Actuation	O.6A-7
O.6A.5	RESULTS OF TRANSIENT ANALYSES	O.6A-7

RBS USAR

ATTACHMENT O
(TO APPENDIX 6A)

LIST OF TABLES

Table
Number

Title

O.6A-1 SUPPRESSION POOL TEMPERATURE TRANSIENT SUMMARY

O.6A-2 FEEDWATER SYSTEM INVENTORY

RBS USAR

ATTACHMENT O
(TO APPENDIX 6A)

LIST OF FIGURES

<u>Figure Number</u>	<u>Title</u>
O.6A-1	REACTOR VESSEL PRESSURE CASE 1, STUCK OPEN RELIEF VALVE
O.6A-2	SUPPRESSION POOL TEMPERATURE CASE 1, STUCK OPEN RELIEF VALVE
O.6A-3	REACTOR VESSEL PRESSURE CASE 2, STUCK OPEN RELIEF VALVE
●→14	
O.6A-3a	REACTOR VESSEL PRESSURE CASE 2A, STUCK OPEN RELIEF VALVE (3100 MWt)
O.6A-4	SUPPRESSION POOL TEMPERATURE CASE 2, STUCK OPEN RELIEF VALVE
O.6A-4a	SUPPRESSION POOL TEMPERATURE CASE 2A, STUCK OPEN RELIEF VALVE (3100 MWt)
14←●	
O.6A-5	REACTOR VESSEL PRESSURE CASE 3, STUCK OPEN RELIEF VALVE
O.6A-6	SUPPRESSION POOL TEMPERATURE CASE 3, STUCK OPEN RELIEF VALVE
O.6A-7	REACTOR VESSEL PRESSURE CASE 4, ISOLATION AND DEPRESSURIZATION
O.6A-8	SUPPRESSION POOL TEMPERATURE CASE 4, ISOLATION AND DEPRESSURIZATION
O.6A-9	REACTOR VESSEL PRESSURE CASE 5, ISOLATION AND DEPRESSURIZATION
O.6A-10	SUPPRESSION POOL TEMPERATURE CASE 5, ISOLATION AND DEPRESSURIZATION
O.6A-11	REACTOR VESSEL PRESSURE CASE 6, ADS ACTUATION
O.6A-12	SUPPRESSION POOL TEMPERATURE CASE 6, ADS ACTUATION
O.6A-13	REACTOR VESSEL PRESSURE CASE 7, ADS ACTUATION
O.6A-14	SUPPRESSION POOL TEMPERATURE CASE 7, ADS ACTUATION

O.6A.1 INTRODUCTION

BWR plants take advantage of the large thermal capacitance of the suppression pool during plant transients requiring safety relief valve (SRV) actuation. Discharge of each relief valve is piped to the suppression pool where the steam is condensed, resulting in a temperature increase of the pool water, but a negligible increase in the bulk containment pressure. Most transients that result in relief valve actuation are of very short duration and have a small effect on the suppression pool temperature. However, there are some events which present the potential for substantial energy releases to the suppression pool that could result in undesirable high pool temperatures if timely corrective action is not taken.

The possibility of encountering unstable steam condensation is unlikely due to the condensation performance of the SRV discharge quencher device, rigid technical specifications on the pool temperature during power operation, and the large capacity for heat absorption. However, since the possibility does exist when assuming limiting situations of peak service water temperature, technical specification pool temperatures, etc, it is important that potential situations leading to this phenomenon be recognized and procedural controls, temperature limits, and instrumentation be utilized to avoid it.

O.6A.2 CONDENSATION TEMPERATURE LIMIT

●→14

The local suppression pool temperature is defined as the fluid temperature in the vicinity of the safety relief valve (SRV) discharge line quencher device. The local pool temperature controls the condensation process. Without quencher devices, unstable steam condensation may occur with conditions of high suppression pool temperature and high SRV steam mass flux to the suppression pool. With quencher devices, such as X-quenchers used in River Bend, these loads are mitigated. However, due to the lack of available SRV test data at the time, the NRC imposed local pool temperature limits in NUREG-0783 (Reference A) for plants with quencher devices to ensure stable condensation is ensured even with local pool temperature approaching saturation conditions. GE documented these findings in Reference B, which was provided to the NRC for review and approval. Reference B, which was approved by the NRC, provides justification for elimination of the local pool temperature limit for plants with X-quenchers, stable steam without the imposition of significant loads on the containment. After NUREG-0783 was issued, GE compiled X-quencher test data which was used to confirm that with X-quenchers, stable condensation is ensured even with local pool temperatures approaching saturation conditions. GE documented

14←●

•→14

these finding in Reference B, which was provided to the NRC for review and approval. Reference B, which was approved by the NRC, provides justification for elimination of the local pool temperature limit for plants with X-quenchers. However in the NCR's safety evaluation of Reference B, Reference C, the NRC raised an additional concern with regard to the transfer of noncondensed SRV steam to the ECCS suction strainer if the ECCS suction strainer is at an elevation which is higher than the SRV quencher. The NRC stated in Reference C that the local pool temperature limits can be eliminated if the plant has emergency pump inlets located below the elevation of the quencher elevation. If the quencher centerline is at an elevation above the pump suction elevation the results of Reference B would be applicable to River Bend. However, to address this concern the analysis was performed to demonstrate continued compliance with the NUREG-0783 local suppression pool temperature limits.

14←•

1. For all plant transients involving SRV operations during which the steam flux through the quencher perforations exceeds 94 lbm/sq ft-sec, the suppression pool local temperature will not exceed 200°F.
2. For all plant transients involving SRV operations during which the steam flux through the quencher perforations is less than 42 lbm/sq ft-sec, the suppression pool local temperature will be at least 20°F subcooled. For RBS, this is equivalent to a local temperature of 209°F with quencher submergence of 13.9 ft.

RBS USAR

THIS PAGE LEFT INTENTIONALLY BLANK

3. For plant transients involving SRV operations during which the steam flux through the quencher perforations exceeds 42 lbm/sq ft-sec, but is less than 94 lbm/sq ft-sec, the suppression pool local temperature limit will be determined by linearly interpolating the local temperature limits under Items 1 and 2.

However, bulk average suppression pool temperature, rather than local, is the best indicator of the available heat sink capacity of the pool. Therefore, technical specification limits are placed on bulk pool temperature, and a pool temperature monitoring system is incorporated to provide bulk temperature indication and alarms inside the main control room.

The local pool temperature limits for stable quencher condensation performance are converted to equivalent bulk pool temperature limits assuming a worst case local-to-bulk temperature difference of 20°F based on proprietary Kuosheng inplant test results. The RBS bulk limits are determined on this basis to be as follows:

	Quencher Steam Flux, lbm/sq ft-sec	
	<u>>94</u>	<u><42</u>
Local Pool Temperature Limit, °F	200	209
Maximum Local-to-Bulk T, °F	<u>20</u>	<u>20</u>
Bulk Pool Temperature Limit, °F	180	189

Stable quencher steam condensation is ensured for RBS by showing that the predicted bulk pool temperature after any SRV discharge event is less than the applicable limit defined above. The steam flux limits are directly related to the reactor pressure, with 500 psia and 200 psia corresponding to 94 lbm/sq ft-sec and 42 lbm/sq ft-sec, respectively. Thus, reactor pressure and suppression pool bulk temperature transients for each SRV discharge event are compared to these limits.

O.6A.3 PLANT TRANSIENT EVENTS

Since the discharge of the safety relief valves is piped directly to the suppression pool, any SRV actuation will result in some temperature rise in the pool. Most SRV actuations are of short duration (seconds) and result in negligible temperature increase. Three events, however, present the potential for substantial energy addition to the

suppression pool via the relief valves. These events are 1) stuck-open relief valve (SORV), 2) system isolation, and 3) automatic depressurization. A brief description of each of these events is given in the following paragraphs.

1. Stuck-Open Relief Valve

In the event of a stuck-open relief valve, the suppression pool temperature increases at a rate dependent on the SORV flow rate, pool size, and heat removal system capability. The only means of terminating the energy input to the pool is to scram the reactor and depressurize the RPV (assuming that the SORV cannot be closed).

2. Primary System Isolation

•→12

Whenever the primary system is isolated from the main condenser for any reason, the reactor is scrammed automatically and fuel relaxation and decay heat energy is removed automatically from the RPV via vessel pressure actuation of the safety relief valves. The water level in the RPV is controlled by the feedwater system, RCIC, or HPCS. River Bend Station employs heat exchangers that are utilized to remove energy directly from the RPV or from the suppression pool after primary system isolation.

12←•

3. Auto Depressurization System (ADS) Actuation

Actuation of the ADS results in rapid depressurization of the primary system due to simultaneous opening of seven preselected relief valves. This system is automatic but can also be actuated manually. Typically the RPV is depressurized to 150 psi or less in approximately 10 minutes. During this transient, the bulk suppression pool temperature rises approximately 40°F. Uniformly spaced ADS relief valve discharges in the suppression pool will result in near uniform mixing of the pool during this depressurization transient. It should be noted that the RBS pool temperature transients were evaluated prior to the publication of NUREG-0783. In addition to the SORV and isolation/scram events, NUREG-0783 defines the event of a SORV following a small break accident inside the drywell. Although this case was not included in the RBS analysis, the RBS pool temperature transient results are considered to be more limiting because a significant amount of energy will be stored in the drywell atmosphere and structural heat sinks as a result of a break in the drywell. This

energy will not be available for pool heatup; thus the resulting pool temperature transient will be less severe than the limiting case identified herein for RBS.

O.6A.4 ASSUMPTIONS USED IN THE ANALYSIS

The suppression pool temperature transients predicted in this analysis are based on certain general and specific assumptions. The following two sections describe the general assumptions which apply to all cases and the specific assumptions which are case dependent.

•→14

The analyses performed in the following sections are performed with an initial reactor thermal power of 2952 MWt and use analysis methods developed by Stone and Webster Engineering Corporation. The limiting event analysis, Case 2, is also performed with an initial reactor power of 3100 MWt (100.3% of current rated power). The additional case analysis, Case 2a, is performed using the GE SHEX code.

O.6A.4.1 General Assumptions

1. The service water temperature, RHR heat exchanger capability, and suppression pool initial temperature are consistent with those used in the analysis of containment pressure and temperature response to a loss-of-coolant accident. These values are specified in Section 6.2-1 and Tables 6.2-2 and 6.2-3. For Cases 1 through 7, an initial reactor power of 2952 MWt was used in the analyses with the decay heat shown in Figure 0.6A-15. For Case 2a an initial reactor power of 3100 MWt was used with the normalized core power curve shown Figure 6.2-11a.
2. The initial water level of the suppression pool is at the low water level (el 89 ft 6 in) corresponding to the initial water volume of 124,726 cu ft. This volume does not include the water in the weir annulus or in the horizontal vents.

For Case 2a, the initial water volume is consistent with the value of 122,846 ft³ given in Table 6.2-1.

14←•

3. Primary system isolation for all cases, except Case 6, is assumed to be instantaneous closure of the turbine control valves and opening of the steam bypass valves resulting in bypass of 9.5 percent of rated steam flow to the main condenser. This bypass flow is assumed to continue until

the MSIV closure is complete 5.5 seconds after the MSIV closure signal based on low reactor pressure equal to 865 psia.

4. Feedwater pumps supply water to the reactor until the entire inventory of feedwater including the condenser hotwell is exhausted. The feedwater flow is assumed to be periodic at the full power rate as required to restore reactor water level from level 4 to level 8 (normal range). The feedwater inventory is divided into seven nodes as listed in Table O.6A-2 with the fluid enthalpy increased to reflect the addition of the piping sensible heat to the feedwater flow.

●→14

For Case 2a, the feedwater inventory is lumped into four nodes as shown in Table O.6A-2A. Enthalpy values include metal sensible heat and are based on feedwater system conditions at 100.3% of current rated thermal power.

14←●

5. Offsite power is available to support the assumption of continued feedwater flow.

THIS PAGE LEFT INTENTIONALLY BLANK

6. The RHR shutdown cooling mode is not utilized.
7. The SRV flow rate is assumed to be approximately 110 percent of the ASME rated flow.
8. There are no heat losses to the containment atmosphere and structures.

O.6A.4.2 Assumptions for Specific Events

The specific assumptions applicable to each of the seven cases (three SORV, two isolation, and two ADS events) analyzed for the River Bend Station pool temperature response are listed below.

O.6A.4.2.1 Stuck-Open Relief Valve (SORV)

Case 1

1. SORV occurs with the reactor operating at full power.
2. The analysis begins at $t=0$ when suppression pool temperature reaches 110°F (TS3* limit).
3. Operator initiates manual scram at $t=0$, assuming high pool temperature alarm at $\text{TS3}=110^{\circ}\text{F}$. Prior to this action, the operator will be alerted to the increasing pool temperature condition by an alarm at $\text{TS1}=95^{\circ}\text{F}$.
4. Reactor scram causes the turbine control valves to close and bypass valves to open.
5. Suppression pool cooling with two RHR heat exchanger loops is initiated at $t=10$ minutes.

Case 2

The assumptions for this case are identical to Case 1 except that only one RHR heat exchange loop is utilized in the pool cooling mode beginning at $t=10$ minutes.

●→14

Case 2a

The assumptions for this case are identical to Case 2. However, for this case the GE SHEX code is used with an initial reactor power of 3100 MWt. In addition, an initial suppression pool volume of 122,846 ft³, the feedwater inventory shown in Table O.6A-2 and the core power curve in Figure 6.2-11a are used.

14←●

Case 3

1. Reactor scrams, turbine control valves close, and steam bypass valves open at t=0.
2. Initial suppression pool temperature is 100°F.
3. SRVs cycle on pressure setpoints to control reactor pressure.
4. Pool temperature increases due to SRV discharge, and at T(pool)=120°F (TS4 limit), one relief valve sticks open as the operator attempts to initiate controlled depressurization.
5. Suppression pool cooling with two RHR heat exchange loops is initiated at t=30 minutes.

O.6A.4.2.2 Primary System Isolation

Case 4

1. Isolation (turbine control valve closure) and scram occur with the reactor initially at full power.
2. Initial suppression pool temperature is 100°F.
3. SRVs cycle on pressure setpoints to control reactor pressure.
4. At T(pool)=120°F (TS4 limit) the operator initiates controlled (100°F/hr) cooldown by manually operating the required number of SRVs.
5. Suppression pool cooling with two RHR heat exchange loops is initiated at t=30 minutes.

Case 5

1. Same as Case 4
2. Same as Case 4.
3. Same as Case 4.
4. Operator initiates controlled (100°F/hr) cooldown at t=10 minutes.

5. Suppression pool cooling with only one RHR heat exchange loop is initiated at t=30 minutes.

0.6A.4.2.3 ADS Actuation

Case 6

1. Scram occurs at full power at t=30.
2. The ADS is actuated at t=0.
3. Initial suppression pool temperature is 100°F.
4. MSIV closure signal occurs at t=0, and MSIVs are fully closed at t=5.5 seconds.
5. Suppression pool cooling with one RHR heat exchange loop is initiated at t=30 minutes.

Case 7

1. Same as Case 3.
2. Same as Case 3.
3. Same as Case 3.
4. The ADS is actuated by the operator when pool temperature reaches 120°F (TS4 limit).
5. Suppression pool cooling with two RHR heat exchange loops is initiated 10 minutes after ADS actuation.

0.6A.5 RESULTS OF TRANSIENT ANALYSES

The specific cases analyzed, initial conditions, and results are summarized in Table O.6A-1. Fig. O.6A-1 through O.6A-14 show the transient response of the suppression pool and reactor pressure for the seven cases. Table O.6A-1 shows that a stuck-open relief valve occurring at full-power initial conditions with only one RHR pool cooling heat exchanger operating (Case 2) is the limiting case for which a peak bulk pool temperature of 185°F is predicted. This result is conservative and acceptable from the standpoint of steam condensation stability because it is less than the previously defined limit of 189°F for RBS. For this same case, Fig. O.6A-3 and O.6A-4 show that pool temperature increases to only 139°F during the period when reactor pressure exceeds 500 psia. This result compares favorably to the limit of 180°F under high mass flux conditions.

●→14

The reactor pressure and suppression pool temperature response curves for Case 2a are shown in figures O.6A-3a and O.6A-4a. For Case 2a, the maximum bulk suppression pool temperature is 181.1 °F. The maximum bulk pool temperature with the reactor pressure

14←●

•→14

above 500 psia is 134.5 °F. These temperatures are approximately 4 degrees lower than the values obtained for Case 2. This reduction is attributed to the use of a more realistic decay heat curve (ANS 5.1 + two sigma, Figure 6.2-11a) than used for Case 2 (figure O.6A-15), which offsets the effect of the higher initial reactor thermal power assumed for Case 2A.

14←•

RBS USAR

TABLE O.6A-1

SUPPRESSION POOL TEMPERATURE TRANSCRIPT SUMMARY

Case No.	Event	At Time of Event		Initial Pool Temp (°F)	Scram Time (Sec)	RPV Depressurization	RHR HX's (Pool Cooling)	Service Water Temp (°F)	Peak Pool Temp (°F)	Time of Peak Pool Temp (Sec)
		Reactor	Pool Temp (°F)							
1	SORV	Full Power	110	110	0	Uncontrolled	2 at 10 min	95	163	8,760
2	SORV	Full Power	110	110	0	Uncontrolled	1 at 10 min	95	185	10,760
•→14 2a	SORV	Full Power	110	110	0	Uncontrolled	1 at 10 min	95	181	11,940
3	SORV	Isolated	120	100	0	Uncontrolled	2 at 30 min	95	158	12,950
4	Isolation/ Depressurization	Full Power	100/120	100	0	100°F/hr at T _{pool} = 120°F	2 at 30 min	95	160	13,370
5	Isolation/ Depressurization	Full Power	100/109	100	0	100°F/hr at 10 min	1 at 30 min	95	182	12,120
6	ADS	Full Power	100	100	0	Uncontrolled	1 at 30 min	95	179	10,880
7	ADS	Isolated	120	100	0	Uncontrolled	2 at 10 min after ADS	95	165	4,270

*Cases 1, and 3 through 7 are performed with an initial reactor thermal power of 2952 MWt. Case 2 is performed with an initial reactor thermal power of 3100 MWt with the GE SHEX code.

14←•

RBS USAR

TABLE O.6A-2

FEEDWATER SYSTEM INVENTORY

<u>Node No.</u>	<u>Components Included</u>	<u>Fluid Mass (lbm)</u>	<u>Fluid Enthalpy* (Btu/lbm)</u>
1	Piping, 1st point heater, and feed pumps	318,624	382.0
2	Piping and 2nd point heater	95,725	360.6
3	Piping and 3rd point heater	53,590	345.1
4	Piping and 4th and 5th point heaters	128,143	289.3
5	Piping and 6th point heater	91,843	214.5
6	Piping and 4th and 5th point drain coolers	104,751	174.2
7	Piping and condenser hotwell	864,921	105.7

 ●→14

*Includes associated metal sensible heat above 120°F
 Based on reactor thermal power of 2952 MWt.

14←●

RBS USAR

TABLE O.6A-2a

FEEDWATER SYSTEM INVENTORY (Case 2a)

<u>Node No.</u>	<u>Components Included</u>	<u>Fluid Mass (lbm)</u>	<u>Fluid Enthalpy* (Btu/lbm)</u>
1	Piping, 1st point heater, and feed pumps	318,624	387.8
2	Piping and 2nd point heater and 3rd point point heater	149,315	360.5
3	Piping, 4th, 5th and 6th point heaters	219,986	262.0
4	Piping and 4th and 5th point drain coolers	104,751	176.0
5	Piping and condenser hotwell	864,921	107.3

*Includes associated metal sensible heat above 120°F
Based on reactor thermal power of 3100 MWt.

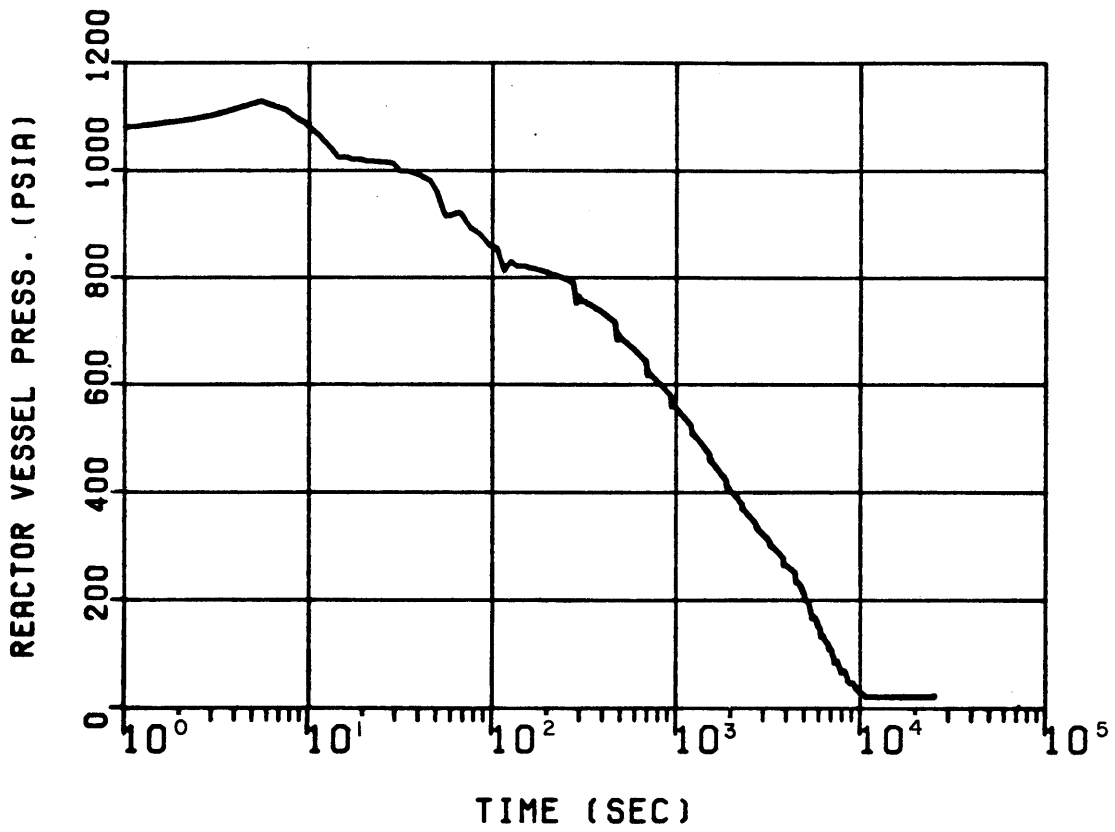


FIGURE Q6A-1

REACTOR VESSEL PRESSURE
CASE 1
STUCK OPEN RELIEF VALVE

RIVER BEND STATION
UPDATED SAFETY ANALYSIS REPORT

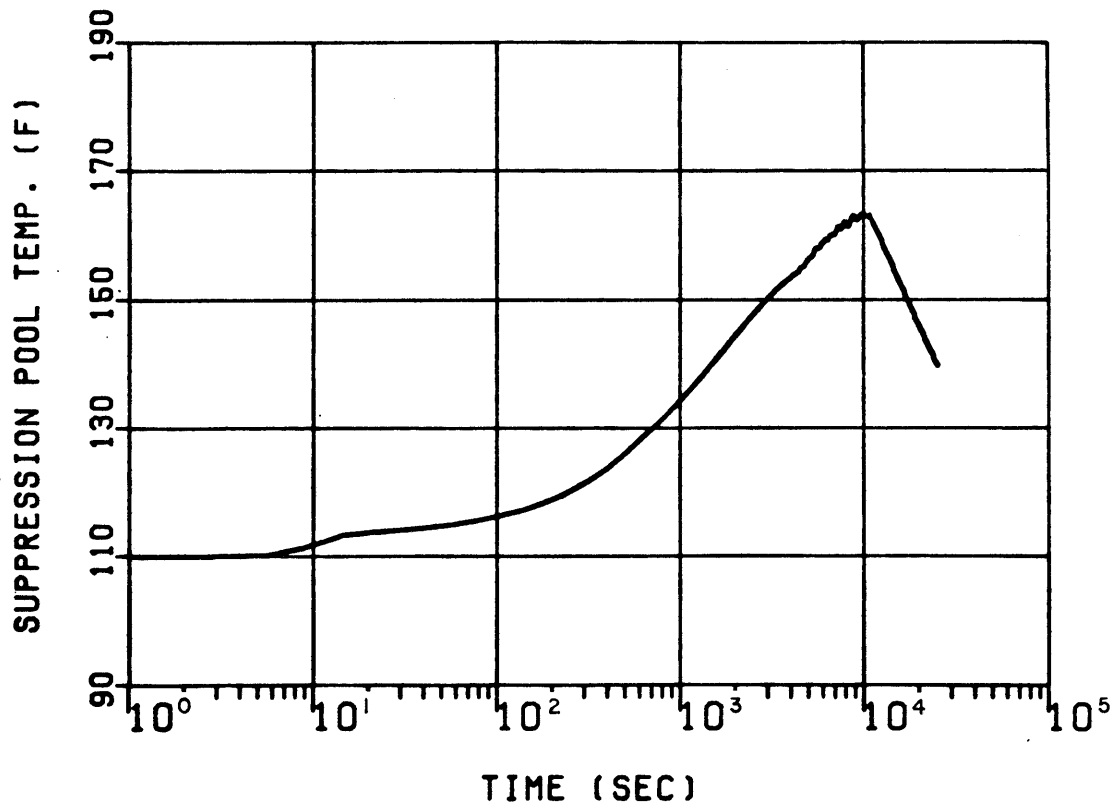


FIGURE O6A-2

SUPPRESSION POOL TEMPERATURE
CASE 1
STUCK OPEN RELIEF VALVE

RIVER BEND STATION
UPDATED SAFETY ANALYSIS REPORT

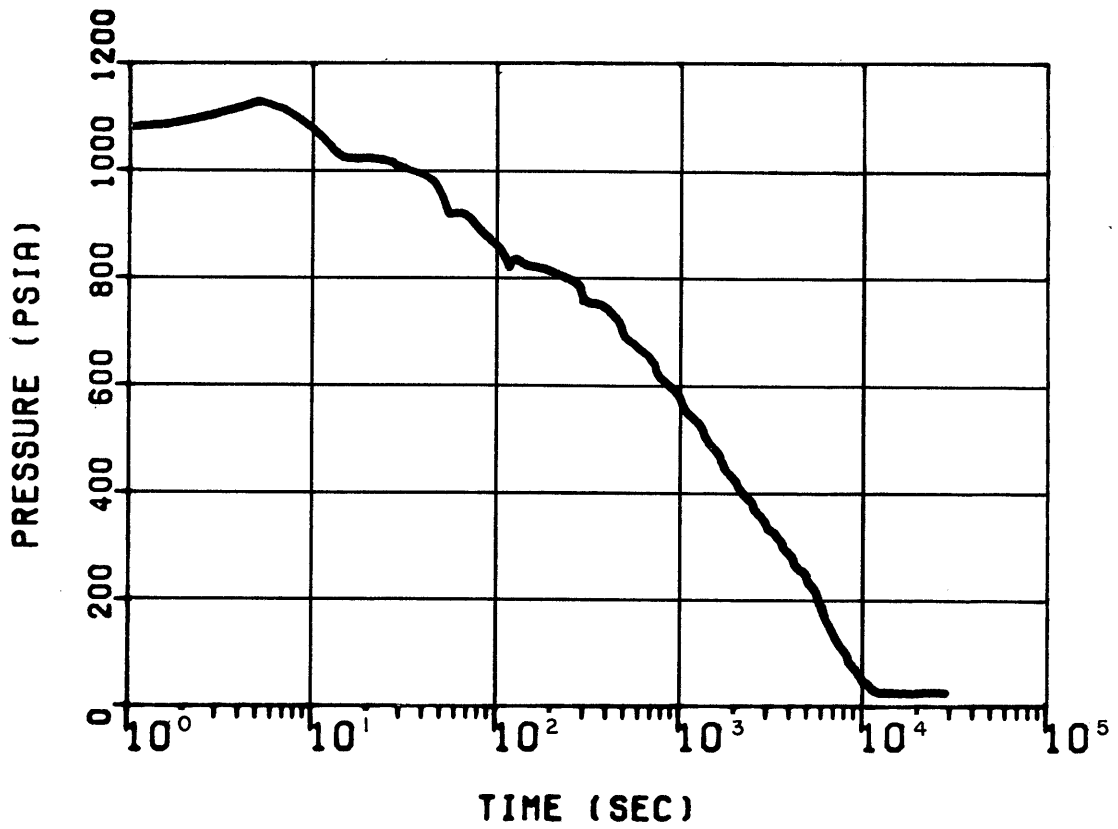


FIGURE Q6A-3
REACTOR VESSEL PRESSURE CASE 2 STUCK OPEN RELIEF VALVE
RIVER BEND STATION UPDATED SAFETY ANALYSIS REPORT

(3100 MWT, SHEX)

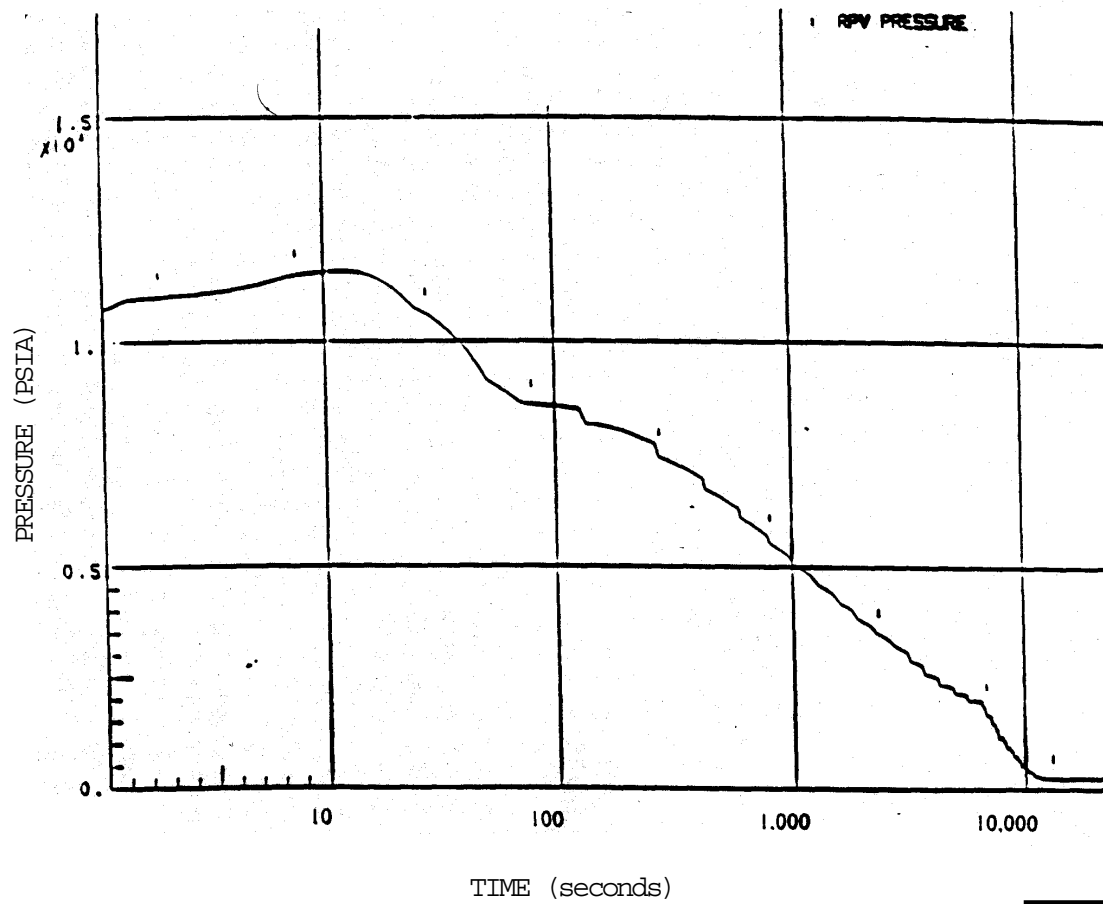


FIGURE 0.6A-3a

REACTOR VESSEL PRESSURE, CASE 2a
STUCK OPEN RELIEF VALVE

RIVER BEND STATION
UPDATED SAFETY ANALYSIS REPORT

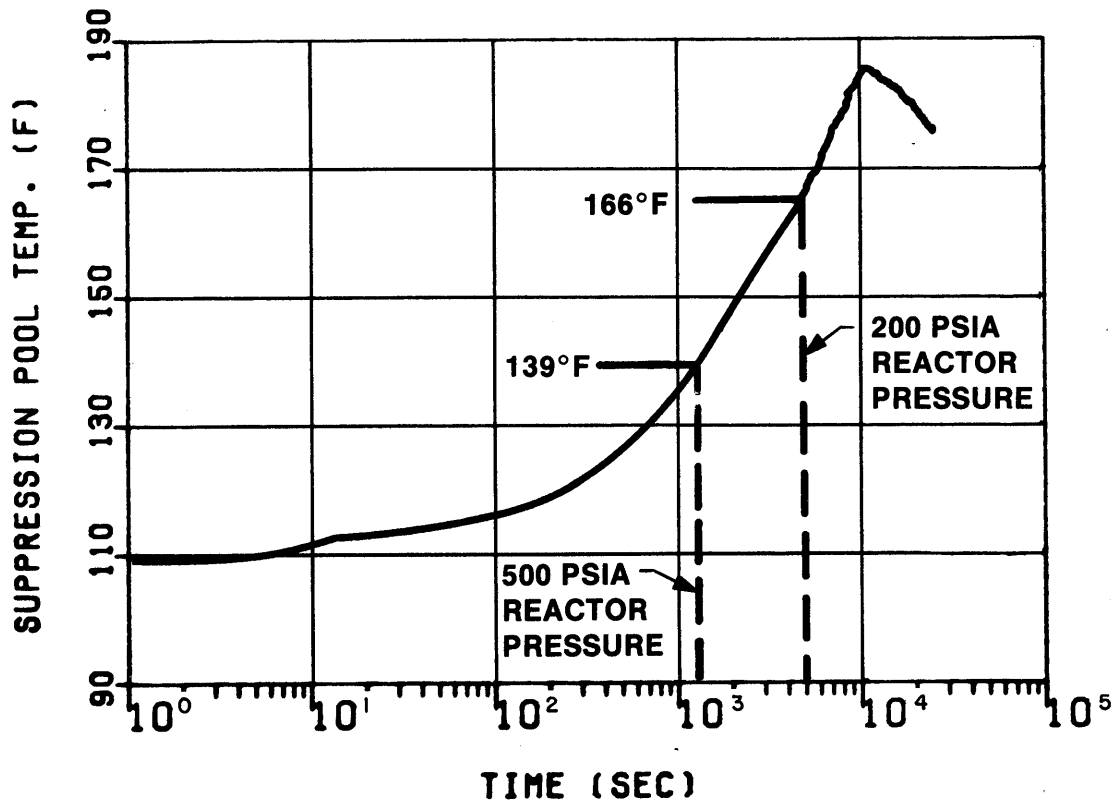


FIGURE O6A-4

SUPPRESSION POOL TEMPERATURE
CASE 2
STUCK OPEN RELIEF VALVE

RIVER BEND STATION
UPDATED SAFETY ANALYSIS REPORT

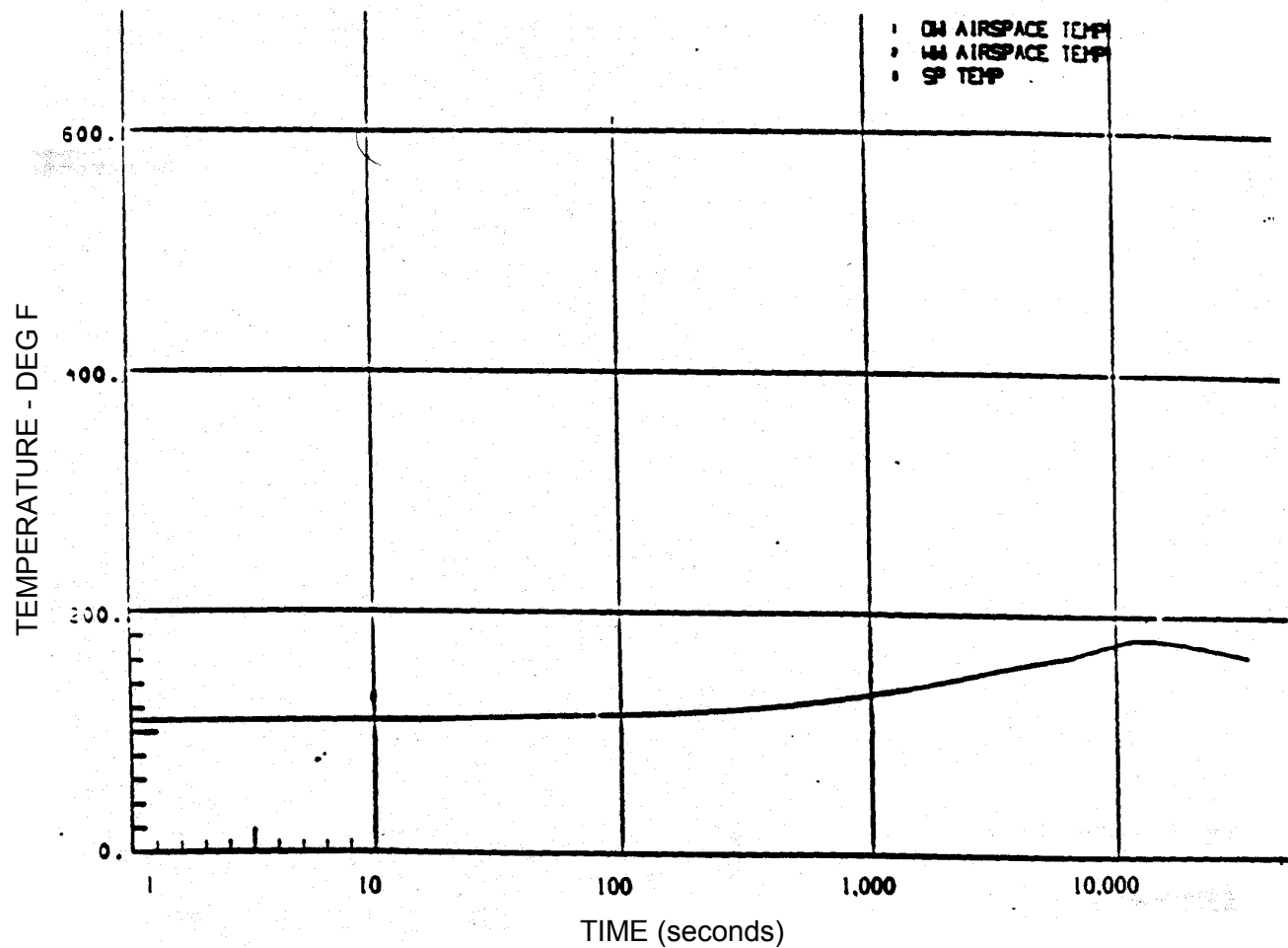


FIGURE 0.6A-4a

SUPPRESSION POOL TEMPERATURE
CASE 2a
STUCK OPEN RELIEF VALVE

RIVER BEND STATION
UPDATED SAFETY ANALYSIS REPORT

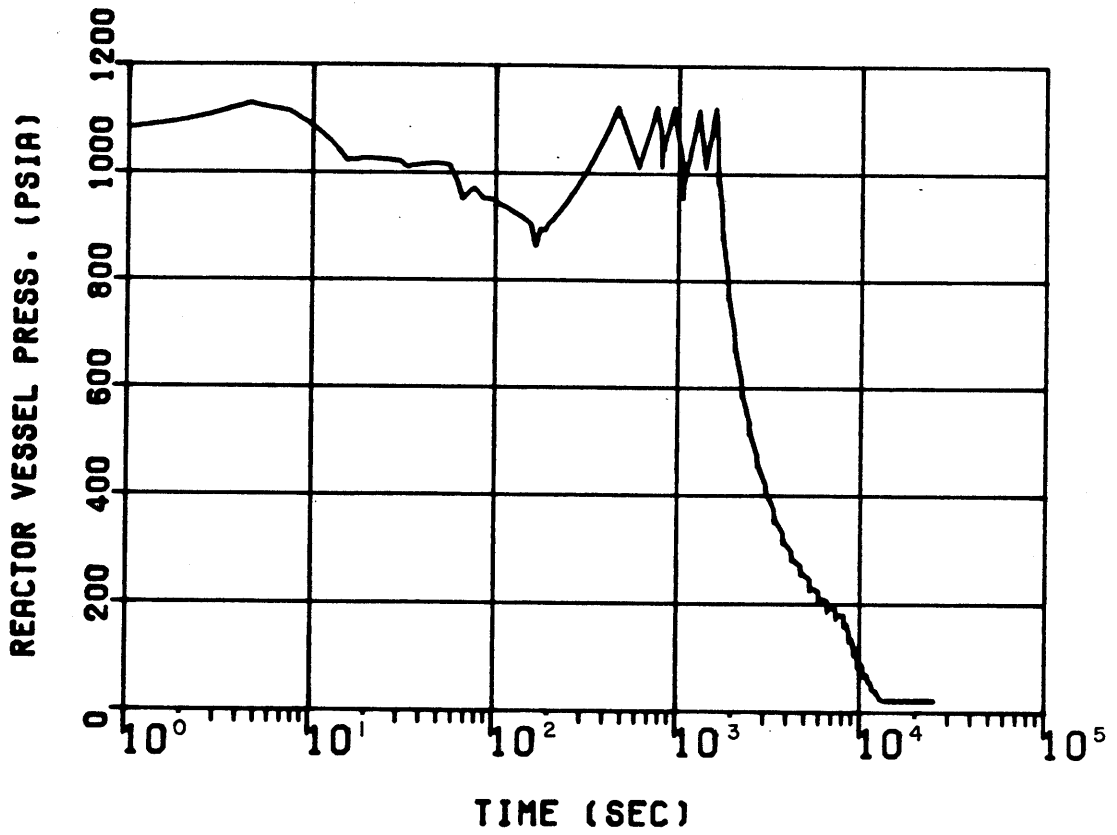


FIGURE O6A-5

REACTOR VESSEL PRESSURE
CASE 3
STUCK OPEN RELIEF VALVE

RIVER BEND STATION
UPDATED SAFETY ANALYSIS REPORT

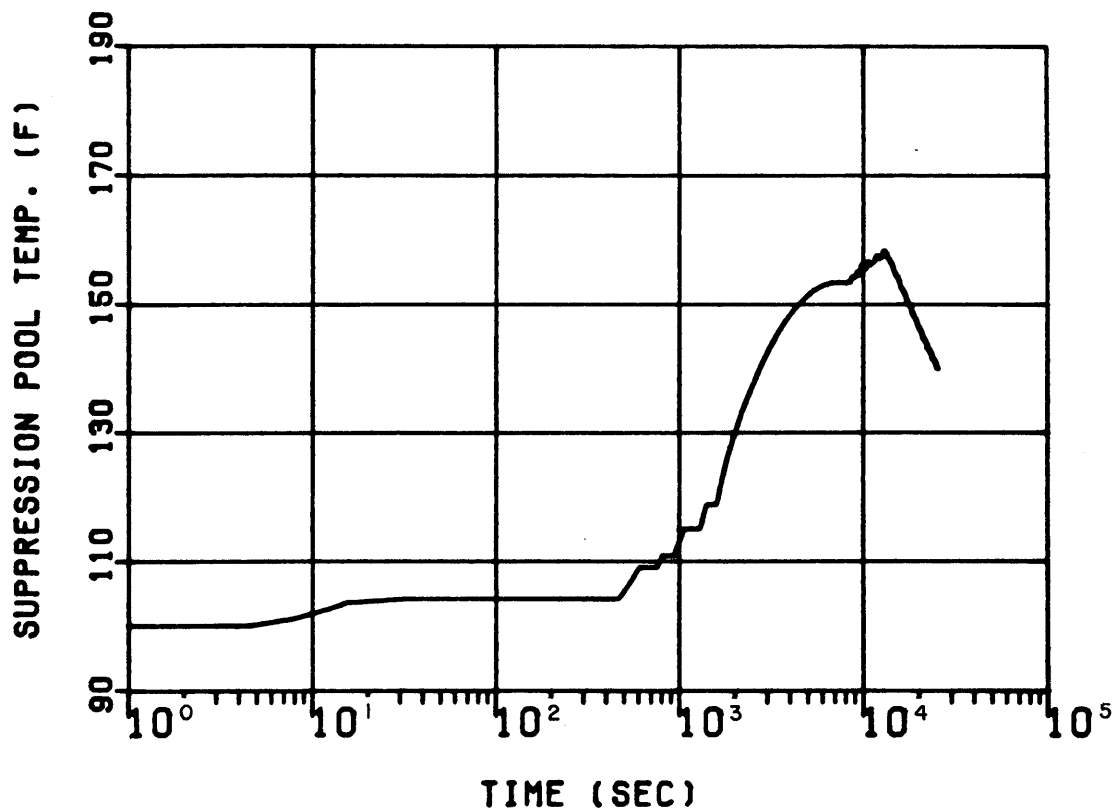


FIGURE O6A-6

SUPPRESSION POOL TEMPERATURE
CASE 3
STUCK OPEN RELIEF VALVE

RIVER BEND STATION
UPDATED SAFETY ANALYSIS REPORT

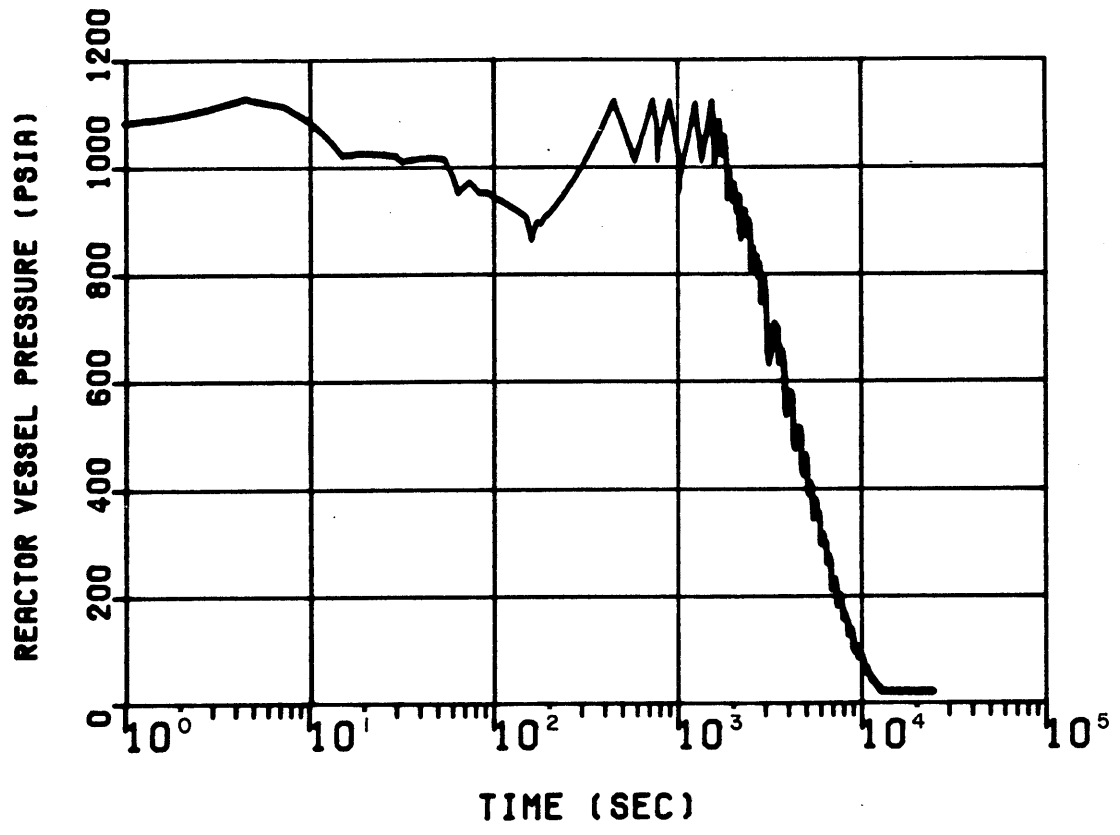


FIGURE Q6A-7
REACTOR VESSEL PRESSURE CASE 4 ISOLATION AND DEPRESSURIZATION
RIVER BEND STATION UPDATED SAFETY ANALYSIS REPORT

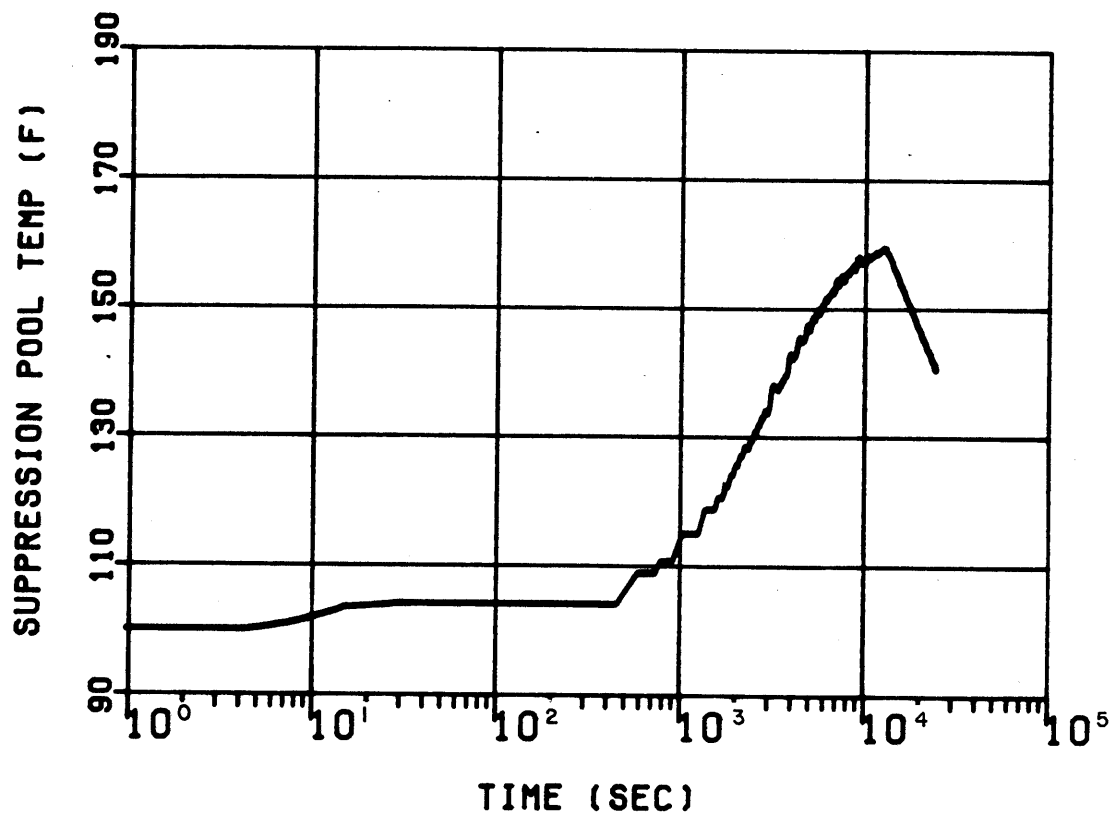


FIGURE Q6A-8

SUPPRESSION POOL TEMPERATURE
CASE 4
ISOLATION AND DEPRESSURIZATION

RIVER BEND STATION
UPDATED SAFETY ANALYSIS REPORT

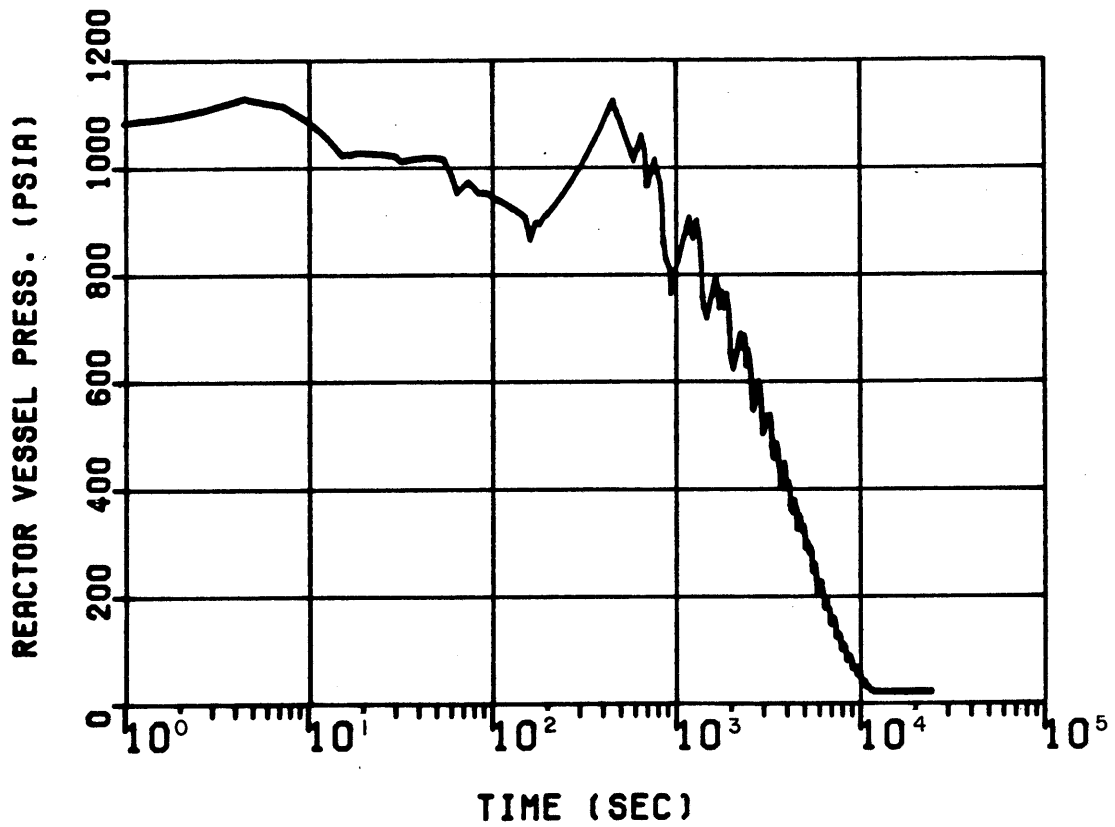


FIGURE Q6A-9

REACTOR VESSEL PRESSURE
CASE 5
ISOLATION AND DEPRESSURIZATION

RIVER BEND STATION
UPDATED SAFETY ANALYSIS REPORT

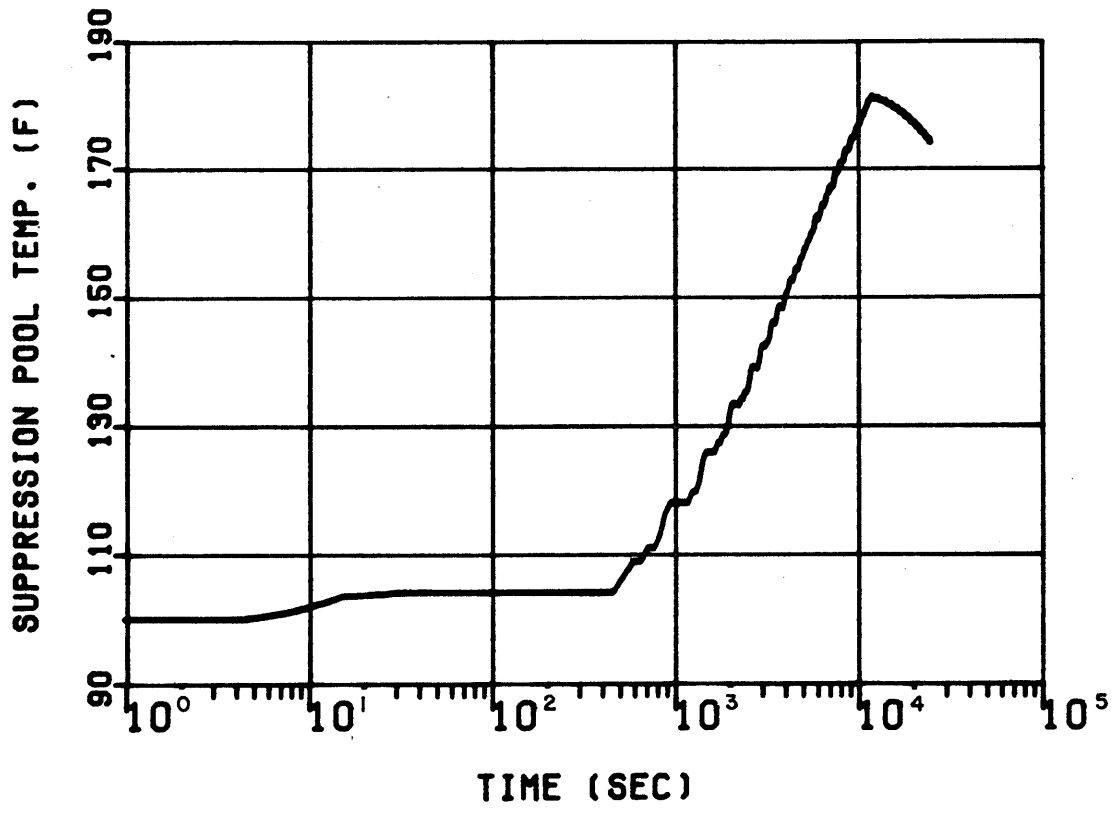


FIGURE Q6A-10
 SUPPRESSION POOL TEMPERATURE
 CASE 5
 ISOLATION AND DEPRESSURIZATION
 RIVER BEND STATION
 UPDATED SAFETY ANALYSIS REPORT

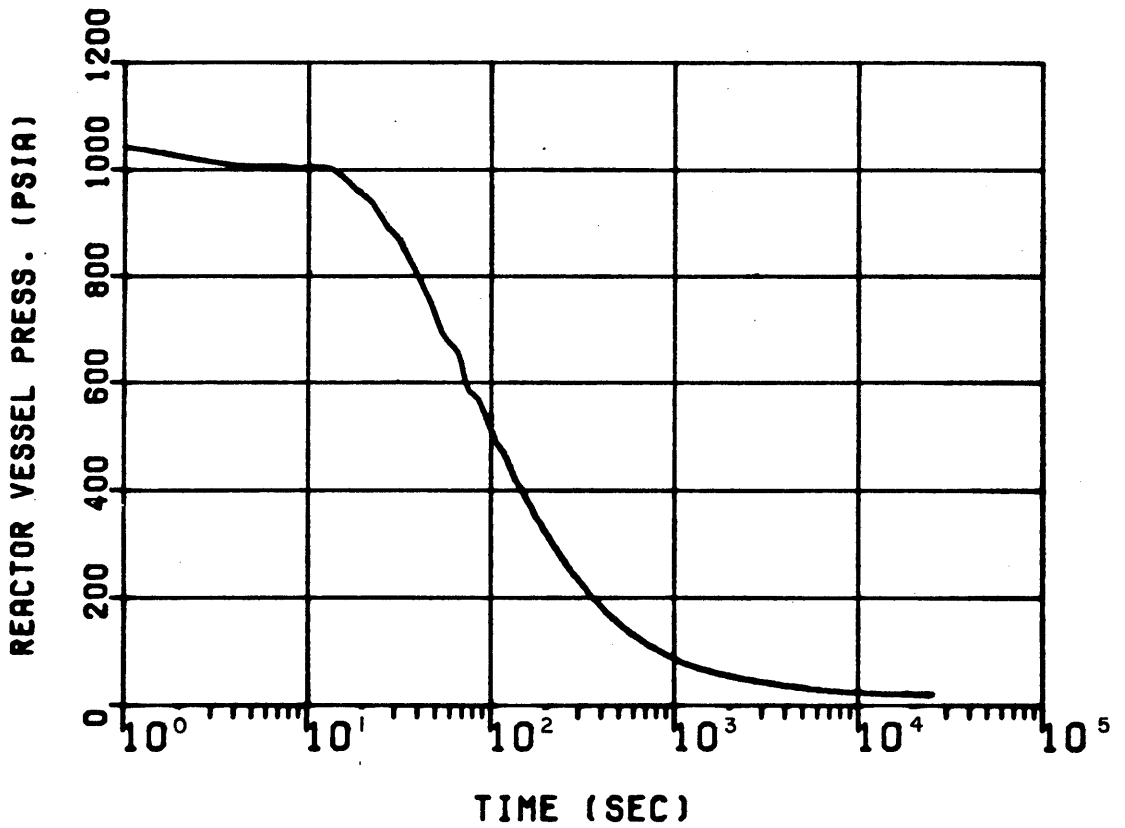


FIGURE O6A-11

REACTOR VESSEL PRESSURE
CASE 6
ADS ACTUATION

RIVER BEND STATION
UPDATED SAFETY ANALYSIS REPORT

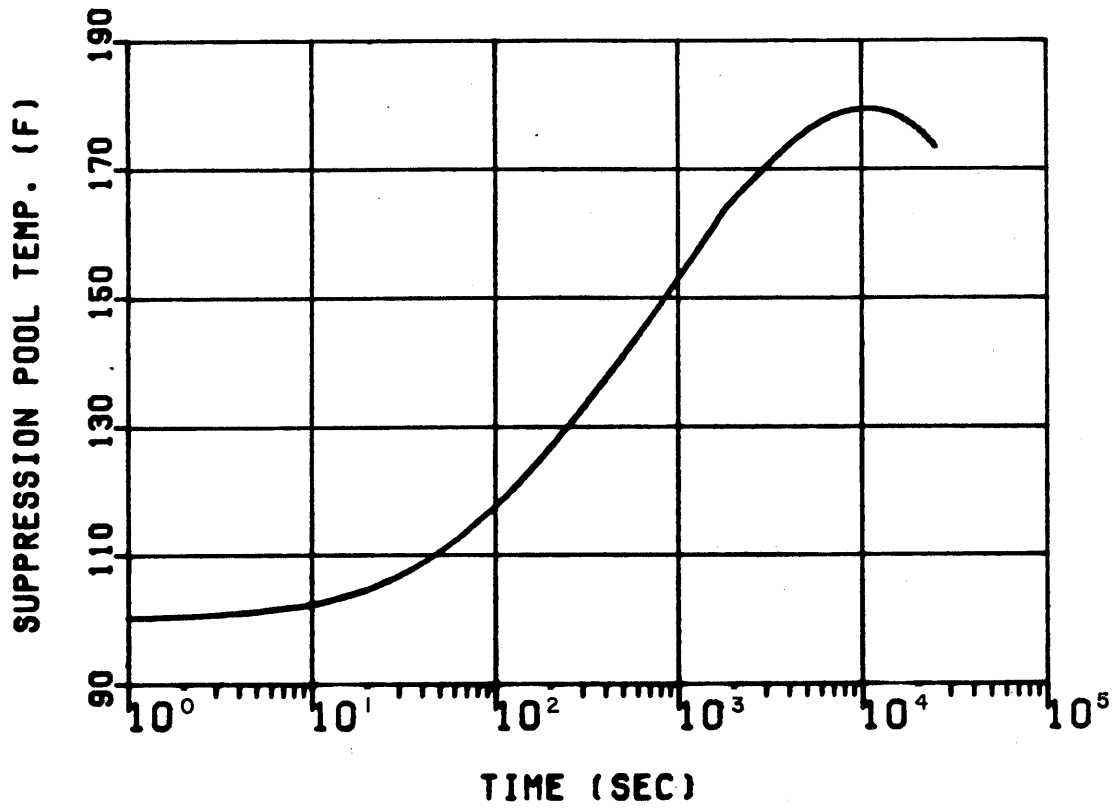


FIGURE Q6A-12
SUPPRESSION POOL TEMPERATURE
CASE 6
ADS ACTUATION
RIVER BEND STATION
UPDATED SAFETY ANALYSIS REPORT

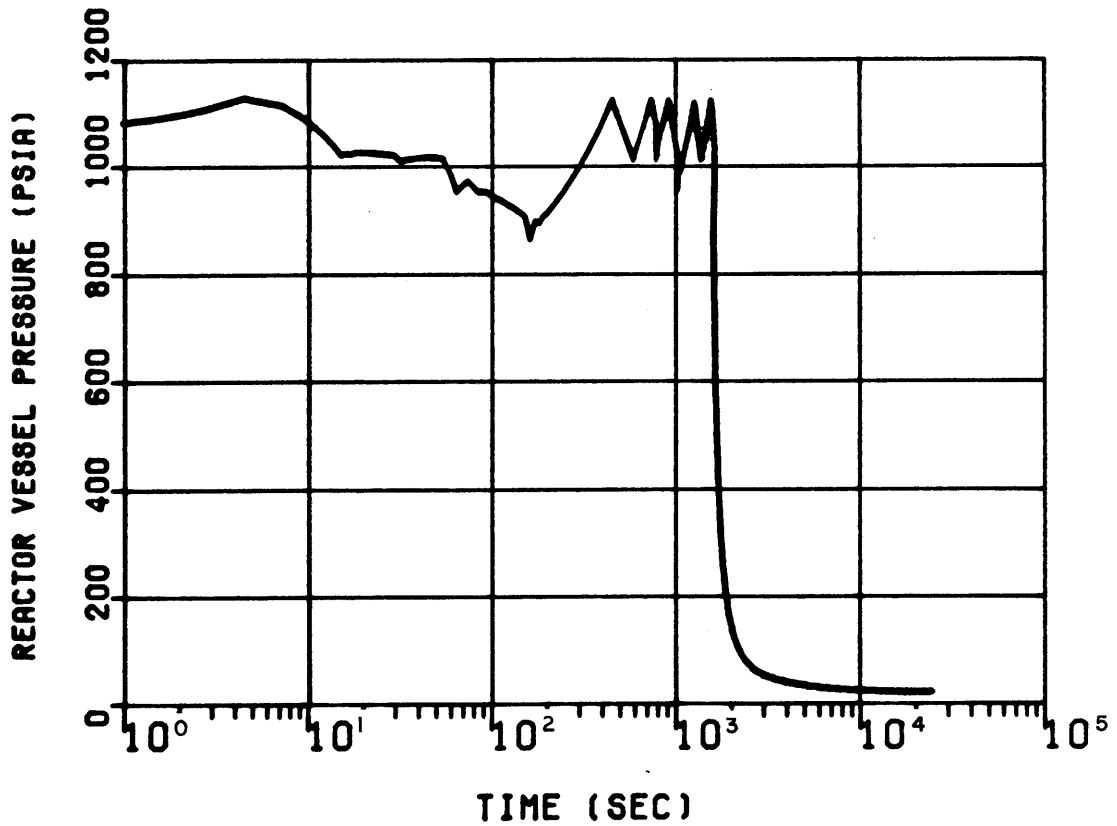


FIGURE O6A-13

REACTOR VESSEL PRESSURE
CASE 7
ADS ACTUATION

RIVER BEND STATION
UPDATED SAFETY ANALYSIS REPORT

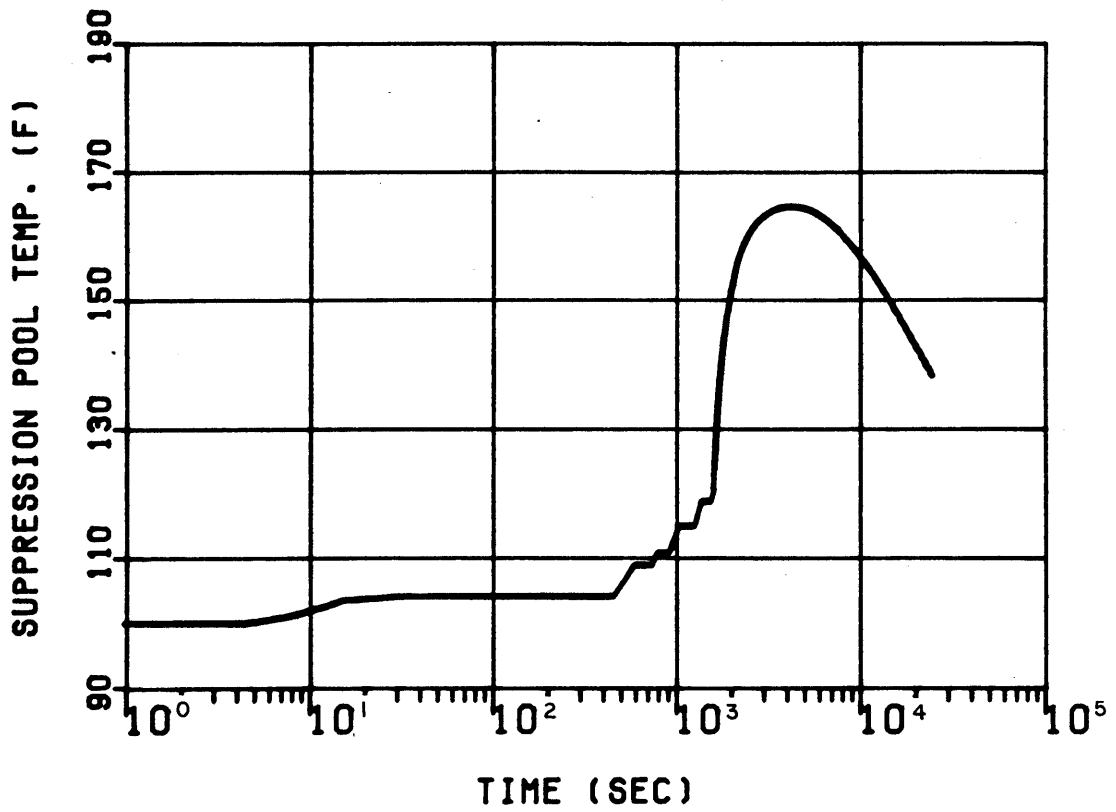


FIGURE Q6A-14

SUPPRESSION POOL TEMPERATURE
CASE 7
ADS ACTUATION

RIVER BEND STATION
UPDATED SAFETY ANALYSIS REPORT

RBS USAR

APPENDIX 6B

THREED SUBCOMPARTMENT ANALYTICAL MODEL

TABLE OF CONTENTS

Section	<u>Title</u>	<u>Page</u>
6B.1	FUNCTIONAL DESCRIPTION OF THREED CODE	6B-1
6B.2	DESCRIPTION OF THE MODEL	6B-1
6B.3	ASSUMPTIONS EMPLOYED IN THREED	6B-8

LIST OF FIGURES

<u>Figure Number</u>	<u>Title</u>
6B-1	STAGGERED MESH CONTROL VOLUME APPROXIMATION FOR THREED
6B-2	COMPUTATIONAL BLOCK DIAGRAM FOR THREED

APPENDIX 6B

THREED SUBCOMPARTMENT ANALYTICAL MODEL

6B.1 FUNCTIONAL DESCRIPTION OF THREED CODE

The THREED computer program is used to calculate the transient conditions of pressure, temperature, and humidity in various subcompartments following a postulated rupture in a moderate- or high-energy pipeline. The results obtained from THREED analyses are used to calculate loads on structures and to define environmental conditions for equipment qualification.

The THREED computer program is similar to RELAP4 and will give the same results as RELAP4 if similar options are chosen^(1, 2). THREED was formulated to perform subcompartment analyses with capabilities and options extended beyond those available in RELAP4. A significant improvement in THREED is that the homogeneous equilibrium model (HEM) has been extended to include two-phase, two-component flow which is encountered in subcompartment analysis.

6B.2 DESCRIPTION OF THE MODEL

The THREED computer code can be viewed as a numerical integrator for the macroscopic form of the basic field equations describing the conservation of mass, energy, and momentum. The conservation equations, along with the equation of state for the fluid, give a complete solution to the fluid flow phenomena. THREED solves a stream tube form of the field equations based on the assumptions of one-dimensional, homogeneous, thermal-equilibrium flow. Although THREED does not prohibit the use of multidimensional flow paths, the flow paths are modeled to approximate a one-dimensional equation.

Subcompartments are modeled in THREED as an hydraulic network which consists of a series of interconnecting, user-defined nodes (mass and energy control volumes). Nodes are connected by internal junctions (momentum control volumes) with the internodal flow rates determined by the solution of the momentum equation. An internal junction control volume is defined as the composite volume between the centers of adjacent nodes. This inconsistency in control volumes (i.e., a different control volume for momentum than for mass and energy) is illustrated on Fig. 6B-1. This "staggered mesh" approximation is necessary for purposes of solving the equations.

Fill junctions are dissimilar to internal junctions in that they have no initial node, and their flow rate is dependent only on

the junction area and time. These junctions are used to simulate flow originating external to the network (i.e., blowdown). Mathematically, they are treated as boundary conditions.

THREED numerically solves finite difference equations which account for mass and energy flows into and out of a node. Fig. 6B-2 summarizes the computational approach used in THREED.

The fluid conservation equations used by THREED can be obtained by integrating the stream tube equations over a fixed volume, V . The mass and energy equations are developed for the generalized i^{th} node, while the momentum equation is developed for the generalized j^{th} internal junction connecting nodes K and L . Neglecting kinetic energy effects, the resulting equations are as follows.

Conservation of Mass - The mass equation is ⁽¹⁾:

$$\frac{dM_i}{dt} = \sum_j w_{ij}$$

where:

M_{wi} = Total mass of water in node i

M_{ai} = Total mass of air in node i

W_j = Mass flow rate into node i from junction j

Conservation of Energy - The energy equation for homogeneous flow is ⁽¹⁾:

$$\frac{dU_i}{dt} = \sum_j w_{ij} (h_{ij} + z_{ij} - \bar{z}_i) \quad (6B-2)$$

where:

U_i = Total fluid internal energy of water in node i

h_{ij} = Local enthalpy at junction j of the fluid entering
or leaving node i

$Z_{ij} - \bar{Z}_i$ = Elevation change from the center of mass in node i
at \bar{Z}_i to junction j

Conservation of Momentum - The incompressible equation for
homogeneous flow is⁽¹⁾:

$$I_j \frac{dW_j}{dt} = (P_K + P_{Kg_j}) - (P_L + P_{Lg_j}) - F_j \quad (6B-3)$$

where:

I_j = Geometric "inertia" for junction j

W_j = Mass flow rate in junction j

P_K = Total static pressure in node K (at center)

P_{Kg_j} = Gravity pressure differential from the center of
node K to junction j

P_L = Total static pressure in node L (at center)

P_{Lg_j} = Gravity pressure differential from junction j to
the center of node L

F_j = Static pressure change term

Equation of State - The functional form of the equation of state is:

$$P_i = f (U_i, M_{wi}, M_{ai}) \quad (6B-4)$$

where:

P_i = Total static pressure in node i

The following assumptions are made in deriving the equation of state:

1. The components of water and air form an homogeneous mixture at a uniform temperature.
2. Water, if present, occupies the entire volume. Air, if present, occupies the same volume as the water vapor according to the Gibbs-Dalton Law. Air is assumed to be insoluble in water, and there can be no air present if the volume is filled with liquid water.
3. Air is treated as a perfect gas.
4. If air and liquid water are present, the water vapor is saturated (relative humidity of 100 percent).
5. If air is present, the liquid water conditions are the saturated conditions for P_{wi} . A more accurate model would have liquid water at the subcooled conditions corresponding to P_i and T_i . This assumption is made to limit calls to the water property routines to one per iteration.

If no water is present in the volume ($M = 0$), the detailed form of the equation of state is:

$$U_i = M_{ai} C_{va} T_i \quad (6B-5)$$

$$P_i = \frac{M_{ai} R_a T_i}{V_i} \quad (6B-6)$$

where:

C_{va} = Constant volume heat capacity of air

T_i = Temperature in node i

R_a = Gas constant of air

V_i = Volume of node i

If water is present in the volume ($M \neq 0$), the detailed form of the equation of state is:

$$V_{wi} = M_{wi}/V_i \quad (6B-7)$$

$$U_i = M_{wi}U_{wi}(T_i, V_{wi}) + M_{ai}Cv_aT_i \quad (6B-8)$$

$$P_{ai} = \frac{M_{ai}R_aT_i}{X_iM_{wi}V_{gi}(T_i, V_{wi})} \quad (6B-9)$$

$$P_i = P_{wi}(T_i, V_{wi}) + P_{ai} \quad (6B-10)$$

where:

V_{wi} = Specific volume of water in node i

U_{wi} = Specific internal energy of water in node i

P_{ai} = Partial pressure of air in node i

X_i = Quality in node i

V_{ai} = Specific volume of water vapor in node i

P_{wi} = Partial pressure of water in node i

It should be noted that the internal code calculations are done in SI units. The reference temperature used for the calculation of the internal energy of air is zero degrees Kelvin. The properties of steam are based on the 1967 ASME formulation of the properties of steam.

Fill Junctions - These are normally used to input blowdown (mass and energy release) into a node(s). Their functional form is:

$$W_j = f(t) \quad (6B-11)$$

$$h_{ij} = f(t) \quad (6B-12)$$

Fan Junctions - These junctions may be used to model ventilation fan operation in situations where such modeling is appropriate. Their functional form is:

$$W_j = f(H_j) \quad (6B-13)$$

where:

$$H_j = \text{Head difference across the fan junction}$$

Choked Flow Options For Internal Junctions - Since an incompressible flow model has no mechanism to restrict flow through a junction to the maximum allowable (choked) flow rate, it is necessary to use a separate calculation to restrict the flow rate. To determine if the flow is choked, momentum equation 6B-3 is solved using a forward finite difference approximation and compared with a calculated choked flow (HEM or Moody). The lesser flow is selected as the junction flow rate for the time step.

Both the HEM and the Moody flow model are based on stagnation properties. Since it is not usually possible to calculate the velocity in a node, it is assumed that the static and stagnation properties in a node are the same (i.e., neglect kinetic energy effects). This may result in an underprediction of the choked flow rate, which is conservative in most cases.

Homogeneous Equilibrium Model - The HEM is approximated in THREED using an "ideal gas" approximation. That is, the choked isentropic ideal gas flow equation is utilized and the isentropic exponent is modified to accommodate two-phase, two-component flow. The isentropic exponent is defined as:

$$\gamma_i = -\frac{V_{wi} \left[\frac{\delta P_i}{P_i} \right]}{\left[\delta V_{wi} \right]_s} \quad (6B-14)$$

where:

$$\gamma_i = \text{Isentropic exponent in node } i$$

The equation utilized by THREEED to calculate the HEM is:

$$W_j = 12 A_j (2/\gamma_i - 1)^b (g_c \gamma_i \frac{P_{ai}}{V_{ai}})^{1/2} \quad (6B-15)$$

where:

$$b = (\gamma_i + 1) / 2 (\gamma_i - 1)$$

$$A_j = \text{Flow area of junction } j \text{ (sq ft)}$$

$$\gamma_i = \text{Isentropic exponent of source node } i$$

$$g_c = \text{Proportionality constant} - 32.2 \text{ (ft-lbm/lbf-sec}^2\text{)}$$

$$P_{ai} = \text{Stagnation pressure in source node } i \text{ (psia)}$$

$$V_{ai} = \text{Stagnation specific volume of air in source node } i \text{ (cu ft/lbm)}$$

$$W_j = \text{Mass flow in junction } j \text{ (lbm/sec)}$$

Moody Choked Flow Model - The Moody flow model, used in THREEED, is based on the interpolation of tables from RELAP4/MOD5^(1,3). The model is for one-component flow and, when air is present, the tables are accessed with the total pressure and average enthalpy of the node.

Junction Check Valves - A valve may be modeled in any nonfan internal junction as follows:

Normally closed - trips open instantaneously
 Normally open - trips closed instantaneously

Time Step Control - If the automatic time step control option is selected, the maximum time step will be limited by the following calculation, based on the nodal conditions⁽¹⁾:

$$DT = \min \left\{ 0.01 \left| \frac{P_i}{\dot{P}_i} \right| \right\} \quad (6B-16)$$

where:

$$i = 1, \dots, n$$

DT = Time step size

$$P_i = \alpha P / \alpha t$$

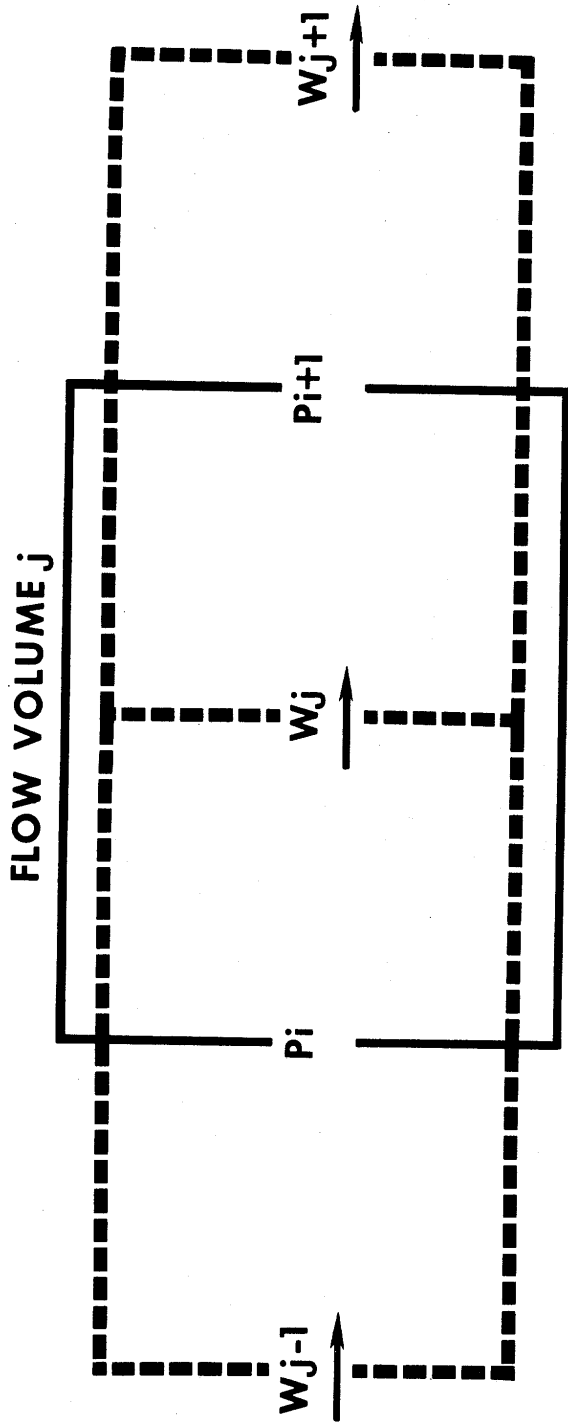
6B.3 ASSUMPTIONS EMPLOYED IN THREED

The following assumptions are employed in THREED:

1. Lumped parameter (control volume) approach utilized
2. Adiabatic process
3. Independent inflow (blowdown)
4. Thermodynamic equilibrium in each node
5. One-dimensional formulation
6. Staggered mesh for the conservation equations
7. Homogeneous flow, unless the Moody choking option is chosen
8. Incompressible form of the momentum equation
9. Kinetic energy effects neglected
10. For choked flow models, static properties in the nodes considered to be stagnation properties
11. Valves open or close instantaneously.

References - Appendix 6B

1. RELAP4/MOD5: A Computer Program for Transient Thermal Hydraulic Analysis of Nuclear Reactors and Related Systems. User's Manual Vol I-III, Report ANCR-NUREG-1335. Aerojet Nuclear Company, September 1976.
2. Moore, K. V. and Rettig, W. H. RELAP4 - A Computer Program for Thermal Hydraulic Analysis. Report ANCR-1127 Aerojet Nuclear Company, August 1974.
3. Moody, L. J. Maximum Flow Rate of a Single Component, Two-Phase Mixture. Journal of Heat Transfer, Trans ASME Vol 87, 1965, p 134-142.



NOTE:
 DASHED LINES INDICATE NODE BOUNDARIES OR MASS AND ENERGY CONTROL VOLUMES
 SOLID LINES INDICATE INTERNAL JUNCTION OR MOMENTUM CONTROL VOLUMES

FIGURE 6B-1

STAGGERED MESH CONTROL VOLUME APPROXIMATION FOR THREE

RIVER BEND STATION
 UPDATED SAFETY ANALYSIS REPORT

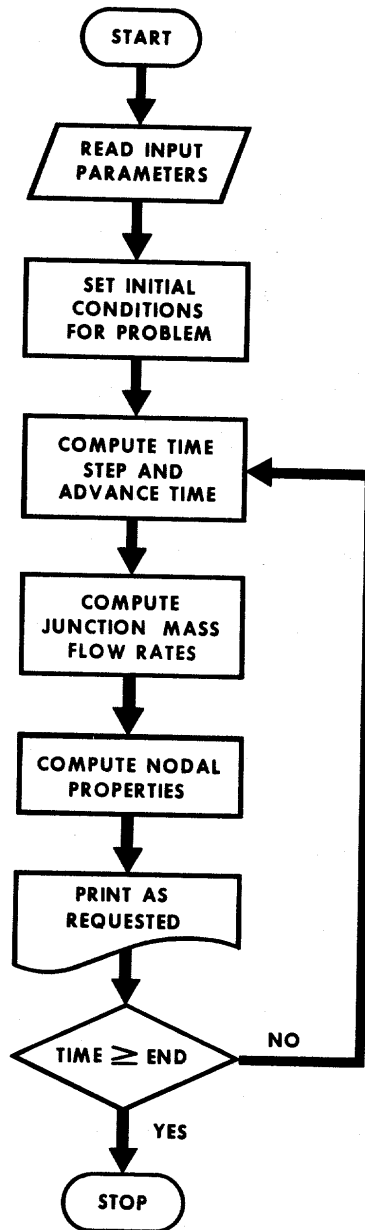


FIGURE 6B-2

COMPUTATIONAL BLOCK
DIAGRAM FOR THREE

RIVER BEND STATION
UPDATED SAFETY ANALYSIS REPORT